INTERNATIONAL COUNCIL FOR BUILDING RESEARCH STUDIES AND DOCUMENTATION

WORKING COMMISSION W18A - TIMBER STRUCTURES

CIB - W18 A

MEETING TWENTY
DUBLIN
IRELAND
SEPTEMBER 1987

CONTENTS

1. LIST OF PARTICIPANTS

AUSTRALIA

D R	Syme	Wentworthville

CANADA

I	Smith	University of New Brunswick
C K A	Stieda	Forintek Canada Corp., Vancouver

DENMARK

T	Feldborg	Danish Building Research Institute, Horsholm
P	Hoffmeyer	Technical University of Denmark, Lyngby
H J	Larsen	Danish Building Research Institute, Horsholm
H	Riberholt	Technical University of Denmark, Lyngby

FEDERAL REPUBLIC OF GERMANY

H J	Blass	University of Karlsruhe
H	Brüninghoff	University of Wuppertal
J	Ehlbeck	University of Karlsruhe
P	Glos	University of München

FINLAND

R	Kytomaki	Tampere
T	Poutanen	Tampere Technical University
A	Ranta-Maunus	Technical Research Centre of Finland, Espoo
U	Saarelainen	Technical Research Centre of Finland, Espoo

FRANCE

P	Crubilé	Centre Technique du Bois et de l'Ameublement, Paris

IRELAND

P R	Colclough	Institute for Ind. Res. + Stand., Dublin
V	Picardo	Institute for Ind. Res. + Stand., Dublin
W J	Robinson	Institute for Ind. Res. + Stand., Dublin

ISRAEL

U	Korin	Building Research Station, Technion, Haifa

ITALY

A	Ceccotti	University of Florence
L	Uzielli	University of Florence
A	Vignoli	University of Florence

JAPAN

M	Yasumura	Building Research Institute, Tsukuba

NETHERLANDS

J	Kuipers	Technical University, Delft

NORWAY

E	Aasheim	Norwegian Inst. of Wood Techn., Oslo
O A	Brynildsen	Oslo

PORTUGAL

P M	Pontifice de Sousa	Building Performance Division, Lisbon

SWEDEN

B	Källsner	Swedish Inst. for Wood Techn. Res., Stockholm
J	König	Swedish Inst. for Wood Techn. Res., Stockholm
A	Martensson	Lund Institute of Technology, Lund
S	Mohager	Department of Building Materials, Stockholm
S	Thelandersson	Lund Institute of Technology, Lund

SWITZERLAND

U A	Meierhofer	EMPA, Dübendorf

UNITED KINGDOM

H J	Burgess	TRADA, High Wycombe
Y H	Chui	TRADA, High Wycombe
A R	Egerup	Tubney, Abingdon
A R	Fewell	Princes Risborough Laboratory, Aylesbury
R	Marsh	Ove Arup, London
C J	Mettem	TRADA, High Wycombe
J G	Sunley	TRADA, High Wycombe
L	Whale	Brighton Polytechnic, Brighton

UNITED STATES OF AMERICA

E G	Elias	American Plywood Association, Tacoma
M R	H'Halloran	American Plywood Association, Tacoma
E G	Stern	Virginia Polytechnic Inst. + State University, Blacksburg

ZIMBABWE

W R	Mackechnie	University of Zimbabwe

2.   CHAIRMAN'S INTRODUCTION

Welcoming the participants, DR. STIEDA said the work of the group had led to the production of a model code of practice for structural timber which had provided a basis for Eurocode 5. He went on to outline the programme of the present meeting which would propose work towards the revision of the CIB Code which was published in 1983.

3.   COOPERATION WITH OTHER ORGANISATIONS

ISO/TC 165:   MR.LARSEN said draft International Standards had been prepared for nail plate testing and for stress grading, the latter based on the ECE document.   Further drafts were being prepared on the grouping of structural timbers and on test methods for nails.

A design standard based on the CIB code was to be produced but this work was suspended pending the completion of Eurocode 5, which was expected to be ready for comment at the end of the year.

A future standard on the testing of wood-based sheet materials would be developed from the work of RILEM, and a system of European standards was to be built up for use in parallel with national codes;   these might be transformed subsequently to ISO standards.

RILEM: DR. CECCOTTI said RILEM had agreed to two proposals he had made, one related to seismic effects and one on the long term behaviour of composite structures which include timber. Following a request that he should contact potential chairmen, he had put forward the name of MR. RIBERHOLT for the group on long term behaviour.

MR. SUNLEY asked whether the collaboration between W18A and RILEM would continue. PROFESSOR KUIPERS said this was the intention, which would be achieved as long as a group chairman shared the aim; otherwise there would be a danger of divergence.

EUROCODE: MR. LARSEN said Eurocode 5 would soon be available in English, French and German, and later in Italian, Dutch and Portuguese. There would be a year allowed for comments through national representatives, including those of EFTA countries, before finalising about 1991.

PROFESSOR KUIPERS said a conference in Luxemburg on the 7 - 9 March 1988 would describe the background to Eurocode 5 but would have a wider scope including recent timber projects and means of improving education in the design of timber structures.   The conference was not so much for research people, but rather to give practising engineers information on future requirements. The cooperation of timber promotion agencies had been sought in ensuring the desired attendance.

After a discussion of CEN standards and grading standards the Chairman and PROFESSOR GLOS suggested W18A should discuss whether they ought to take an interest in grading in future, as this influenced the derivation of characteristic values.

CEI-Bois/FEMIB: DR. BRUNINGHOFF said Sous-Commission GLULAM had produced a production standard which had been incorporated in the Eurocode as Annex 3 and had been accepted by the industry. New material on quality control in relation to test standards would be put forward for inclusion in Annex 3.

IUFRO S5.02: PROFESSOR HOFFMEYER gave advance notice of the next meeting on 13-17 June 1988, for which Finland had kindly agreed to act as host country. He thought the 1990 meeting would probably be in Canada.

CIB-W18B: The Chairman said the first meeting of the recently established working commission on tropical and hardwood timber structures would take place in Singapore at the end of October 1987. PROFESSOR GLOS asked if there was a link between W18 and MR. METTEM's ISO sub-group on the grading of tropical hardwoods. MR. METTEM thought his sub-group was mainly concerned with the European use of tropical hardwoods.

A discussion of the functions of W18A and W18B concluded that there was no narrowing of scope for W18A. The Chairman expressed the hope that there would be cooperation between the two working commissions, and suggested a joint meeting could be held at the next meeting to be planned for W18A.

SEATTLE CONFERENCE, 1988: MR. O'HALLORAN gave details of the conference, to take place on 19 - 22 September 1988, and added that he thought it would be an appropriate occasion for a joint meeting of W18A & B.

BERLIN SYMPOSIUM, 1989: Attention was drawn to paper 20-105-1 giving information on this symposium to be held in the German Democratic Republic in September 1989.

CIB-W18A MEETINGS: An invitation from Canada for a 1988 meeting was read out. For 1989 an invitation from Germany (GDR) had been received, to coincide with their symposium. Portugal was mentioned as a possible alternative for the 1989 meeting and the Chairman asked members to consider the possibilities before making a decision later in the meeting.

4.   TRUSSED RAFTER SUB-GROUP

MR. RIBERHOLT said he had become Chairman of the sub-group and had prepared a statement of proposed objectives. A paper on simple design had been completed previously and he suggested concentration on frame models and on reliability effects including defect location. He was in touch with the industry and would hold a meeting of the sub-group during the Dublin meeting.

5.   SUB-GROUP ON DERIVATION OF CHARACTERISTIC VALUES

PROFESSOR GLOS said he hoped that three papers would be available for next year's meeting: one on solid timber species and grades by himself and A.R.Fewell, one condensed from a Seattle paper on the North American sampling programme and one on board materials by the APA. He asked whether the proposed Annex should deal only with the present population or should also provide for future changes by means of quality control. A discussion concluded that only the first of these tasks should be attempted, at least for the present.

Following further questions to establish what was wanted by the group, PROFESSOR GLOS said the discussion had been helpful and he would try to produce a paper stating exactly how characteristic values should be decided by simplified methods.

6.   MECHANICAL JOINTS

Paper 20-7-1 'Design of nailed and bolted joints - proposals for the revision of existing formulae in draft Eurocode 5 and the CIB code' by L.R.J. Whale, I. Smith and H.J.Larsen was presented by MR. WHALE.

PROFESSOR EHLBECK said work at Karlsruhe had tested drift bolts up to 30mm diameter and the formula given in the paper was not satisfactory for diameters over about 25mm. The values would have to be reduced, and for the next meeting he would produce a paper giving recommendations.

Answering a question by PROFESSOR KUIPERS, MR. WHALE said the apparent discontinuity in Figure 1 arose from different failure mechanisms as there was a greater tendency to splitting with bolts. MR. LARSEN said the diagram compared prebored hardwoods with softwoods that had not been prebored, and thought it would be better to consider the complete range of wood prebored and the complete range without preboring.

DR. STIEDA asked if a standard could be drafted for embedding tests and MR. WHALE said a proposal to RILEM had been made at the Israel meeting. MR. LARSEN said he would draft an ISO standard based on the Israel paper.

PROFESSOR STERN said allowance should be made for nails of higher yield strength, and MR. LARSEN said this could be done using a Nordic method which he would include. Answering the Chairman, he said the draft standard would be shown to W18A at a future meeting.

MR. WHALE said research was continuing to establish modification factors allowing for long term behaviour. During a subsequent discussion of testing methods, PROFESSOR EHLBECK said a substantial difference between tests in compression and tension had been found for large diameters.

Presenting paper 20-7-2 'Slip in joints under long-term loading' by T.Feldborg and M. Johansen, MR. FELDBORG said it was supplementary to Florence paper 19-7-5. He added that the conclusions referred only to the joint types tested; with short teeth, there was a considerable loss of strength arising from varying humidity.

PROFESSOR KUIPERS drew attention to the fact that the standard short-duration (SSD) strength of the joints after the period of loading showed mostly slightly higher values than the SSD-strength of joints that had not been preloaded. This was in accordance with the results of his W18-paper presented in Florence. He thought the phenomenon of damage due to load or stress should be further investigated in connection with the whole aspect of safety.

Several participants felt that some indication should be given to designers regarding the effect of humidity variation, but that it was difficult to do this because of differing climates, and MR. LARSEN said he would find out which CIB group deals with environmental factors.

Paper 20-7-3 'Ultimate properties of bolted joints in glued-laminated timber' by M. Yasumura, T. Murota and H. Sakai was introduced by DR. YASUMURA.

Referring to Figure 20, DR. SMITH asked how the maximum tension stress perpendicular to grain was estimated. DR. YASUMURA replied that the value was obtained from the experimental results for the bulk of the joints. Answering questions by MR. LARSEN he said formula (6) had been discovered in previous work and that the results were not valid for design practice as they were derived from tests using steel side plates. MR. LARSEN said the drop between one bolt and two bolts in Figure 13, for example, was misleading because a different mode of failure arose. DR. YASUMURA displayed Figure 8 again, saying that the end distance was too low in the region at the left, but at the right there was a different failure mode.

DR. SMITH presented his paper 20-7-4 ' Modelling the load-deflection behaviour of connections with pin-type fasteners under combined moment, thrust and shear forces'.

MR. RIBERHOLT commented that the equation made use of displacement data for directions parallel and perpendicular to the grain and suggested data for different angles to the grain would be preferable. MR. LARSEN was doubtful whether knowledge of the entire load-deflection behaviour was needed for design. The Chairman suggested there were different approaches to the problem, and MR. POUTANEN said the one adopted was valuable for sensitivity analysis, adding that contact of the timber members in a joint might have a large influence. DR. SMITH replied that this could be taken into account, but the present work was concerned with serviceability rather than ultimate behaviour, which would be considered when test results were available.

DR. EGERUP thought a detailed knowledge of load-slip behaviour was necessary as some parts of a structure under ultimate load would be in the intermediate range, and the Chairman concluded that there was evidently scope for further discussion.

7.   GLUED JOINTS

Ms. MARTENSSON drew attention to the conclusions of paper 20-18-1 'Wood materials under combined mechanical and hygral loading' by herself and S. Thelandersson and stressed that mechano-moisture effects cannot be neglected in design.

PROFESSOR RANTA-MAUNUS said the work confirmed earlier findings that relaxation cannot be predicted accurately from creep. DR. SMITH wondered if changes in the cross-section dimensions had much influence, but Ms. MARTENSSON and DR. THELANDERSSEN thought the influence was small. PROFESSOR HOFFMEYER said that clear wood in bending showed opposite effects, with creep during the drying-out stage tending to be restored upon re-wetting. He asked whether the reported behaviour was obtained because hardboard was used, but Ms. MARTENSSON suggested it arose from using tension rather than bending specimens.

Two papers on glued joints were presented by DR. THELANDERSSON, the first being 20-18-2 'Analysis of generalized Volkersen-joints in terms of non-linear fracture mechanics' by P.J. GUSTAFSSON. The second paper was 20-18-3 'The complete stress-slip curve of wood-adhesives in pure shear" by H. Wernersson and P.J. Gustafsson.

MR. LARSEN said the strength of overlap joints had been found in the past to be too small for practical use, and enquired whether improved adhesives now made them worthwhile. DR. THELANDERSSEN said the theory provided a basis, analogous to the Euler theory for columns. It was useful for mechanical joints and the aircraft industry were interested in the work. MR. RIBERHOLT said a double lap joint was frequently used. He thought the Volkersen joint was very simple but was unsure whether perpendicular stresses could be disregarded; if tests confirmed this, the theory provided a good tool for design.

MR. RIBERHOLT added that an analysis existed which took account of perpendicular stresses. DR. THELANDERSSON suggested an important application could be finding the optimal joint shape for attaching windmill blades to their hub as described in an address given to the group by MR. LARSEN and MR. RIBERHOLT on the previous day.

PROFESSOR GLOS thought the papers were of a type more suitable for IUFRO S5.02 The Chairman agreed that W18 concentrated on code matters while more basic studies were covered by S5.02, but he felt occasional research papers were valuable and thanked the authors for their contribution.

8.   STRESSES FOR SOLID TIMBER

DR. KORIN dealt with his paper 20-6-1 'A comparative investigation of the engineering properties of "whitewoods" imported to Israel from various origins'.

DR. STEIDA said the paper illustrated the need for recommendations on how design stresses should be derived. Some countries could undertake large-scale testing of timbers, but others could test only a few samples. DR. KORIN said the project had arisen because some timber suppliers wanted to know what design stresses to ascribe to their material, but he now found it difficult to suggest values. The design engineer would specify a size such as 50 x 100 but did not know what size would actually be used on site. PROFESSOR GLOS said the material was sized when green and the densest timber would have the highest shrinkage, but MR. LARSEN pointed out that shrinkage could not account for the large undersize often seen in the paper.

Introducing his paper 20-6-2 'Effects of yield class, tree section, forest and size on strength of home grown Sitka spruce', MR. PICARDO referred to a previous paper 17-17-2 which had described the sampling plan.

MR. FEWELL said the depth factor he applied had now been modified from the value stated in the paper, and his data had been reanalysed taking into account small sizes down to 35 x 35mm. A more conservative depth factor was applied in BS 5268.

MR. SUNLEY wondered if enough consideration was given to similar work in the United Kingdom. MR. PICARDO replied that a different management system and different yield classes were concerned in his paper. He had spoken to the Princes Risborough Laboratory staff, who would be comparing their results with his.

Paper 20-6-3 'Determination of shear strength and strength perpendicular to grain' by H.J. Larsen was introduced by the author who said it seemed desirable for test methods to use specimen volumes comparable with those used in structures, but enormous test forces were sometimes needed.

The test for strength perpendicular to grain was discussed with reference to the manner of application of load and the specimen size, concluding with a suggestion by PROFESSOR EHLBECK that more research was needed on these topics.

Regarding the test for compression perpendicular to grain, MR. METTEM said he had found no volume effect in compression parallel to grain tests on a wide range of sizes in two hardwoods. (IUFRO S5.02, Boras, Sweden, May 1982). MR. RIBERHOLT asked if the test should incorporate the failure mechanism arising in practice, where combined stresses may cause failure at a beam support. In the detailed discussion that followed, DR. KORIN mentioned having South African literature on tests of mining timbers and agreed to produce a paper for the next meeting.

A supplementary page on shear testing was added to the paper. Answering a question by DR. KORIN, MR. LARSEN said PVAC glue had been used to attach the steel flanges. PROFESSOR GLOS suggested testing laminations instead of glulam, but MR. LARSEN said there was a pronounced volume effect; on the other hand small specimens could be used if research was done to correlate their behaviour with that of large ones, and this would help to reduce the stress concentrations and perpendicular forces mentioned by MR. RIBERHOLT. Extensive further discussion followed.

9.   STRUCTURAL CODES

EUROCODE 5:   A description of the draft was given by MR. SUNLEY, MR. LARSEN, MR. EHLBECK and DR. BRUNINGHOFF.

MR. FEWELL clarified a point by saying that for visually graded and machine graded material, both the strength value and the dividing factor would be different. The lower variability of the machine graded timber justified use of a lower dividing factor so that the same design value was reached for both materials. PROFESSOR GLOS said his working group needed to define the derivation of characteristic values for both machine and visually graded timber, and at present only the Princes Risborough Laboratory had a clear understanding of the procedure. He thought some revision of the strength class boundaries might be needed and this was supported by others. DR. MEIERHOFER emphasised the need to allow for future changes, and PROFESSOR EHLBECK replied that provision was made for this.

CIB CODE: After a discussion of the desirability of including material on safety in the CIB code, the Chairman said a position paper was needed on the reliability of timber structures. MR. O'HALLORAN said a paper had been prepared for the ASCE and could be shown to the next meeting of W18A. MR. LARSEN suggested that MR. O'HALLORAN and DR. STIEDA could then arrange a discussion with other members concerned with the subject.

Answering a question by MR. METTEM, PROFESSOR EHLBECK said finger joints occurring in weak areas with low elasticity might have a higher strength than needed. However, if they appeared in stiff sections they would be more heavily loaded. He offered a paper on the subject for the next meeting and this was accepted by the Chairman.

PROFESSOR EHLBECK said there were anomalies in the design of pitched cambered beams and further research was now being undertaken to resolve them. He thought the CIB code should give basic design rules for glued-in rods, and an offer by MR. RIBERHOLT to translate the Danish design paper was accepted.

MR. SYME asked if the CIB code would still be needed when Eurocode 5 became available. MR. LARSEN said the CIB code gave guidelines for world-wide unification. The Eurocode was related to European materials and safety considerations and would not have political force outside the EEC. PROFESSOR KUIPERS added that the ISO code would develop in parallel with the CIB code.

The Chairman concluded the discussion of the CIB code by saying that a need could be foreseen for continuing work over the next several years.

GDR CODE: Paper 20-102-1 'Development of a GDR limit states design code for timber structures (report 1987) by W. Rug and M. Badstube was introduced in the proceedings but could not be presented by the writers in person.

10.   TIMBER BEAMS

MR. POUTANEN presented his paper 20-10-3 ' Composite structure of timber joists and concrete slab', saying this type of construction started in Sweden and later spread to Finland. The connections formed a relatively cheap part of the construction and could be over-designed with little extra expense. The effect of loss of composite behaviour was shown on page 7.

The Chairman asked if provision for this form of composite construction was appropriate for the CIB code, but the general feeling was that the code should concentrate exclusively on timber for the present.

Paper 20-10-2 'Space joists in Irish timber' by W.J. Robinson was presented by the author.

MR. POUTANEN asked if any point load had been applied. MR ROBINSON replied that the members were regarded as joists to carry uniform design load and only uniform test loading was used. DR. SMITH said similar tests had been done at Brighton Polytechnic and thought liaison would be advantageous. DR. EGERUP asked why traditional theory could not be applied to find the deflection caused by bending moments and shear forces. MR. ROBINSON said that calculations found negligible shear deflection. Answering MR. POUTANEN he said no tests had been done to find the long-term effect of moisture variation when plates with short teeth are used.

11.   STABILITY

Presenting his paper 20-2-1 'Lateral buckling theory for rectangular section
deep beam-columns', MR. BURGESS said his paper at the previous meeting
(19-10-1) had considered the lateral buckling of beams, reaching a formula
which was also obtained as a special case in a paper by Dr. Leicester at the
same meeting (19-2-1).   The new paper allowed for end forces as well as
moments.

He then went on to describe 20-10-1, 'Draft clause for CIB code for beams
with initial imperfections'. This arose following Dr. Leicester's suggestion
at the Florence meeting that calculations for lateral instability in beams
should cater for initial imperfections just as the column formulae did.

MR. LARSEN suggested the design chart in the draft clause should show further
curves in the region for lower l/b values. He asked why the formulae in the
first part of paper 20-2-1 differed from Nylander's results, developed in the
second part of the same paper.   MR. BURGESS drew attention to page 13,
explaining that Nylander applied a reducing initial twist as the end moment
decreased. Answering a further question by MR. LARSEN he said the middle
term on the left of equation (6) came from the introductory section on
page 2, and represented the effect of the end load on the initial twist.

Replying to MR. MARSH he said that setting the initial imperfections too
large for a well-made section such as glulam would result in a penalty in
comparison with the Hooley and Madsen method which had given good service
over many years.

The Chairman agreed that departure from an Euler type of calculation should
not introduce excessive conservatism, and said the clause could be accepted
for incorporation in the CIB code.

DR. BLASS introduced his paper 20-2-2 'Design of timber columns', showing
the more conservative buckling curves from EC5 in comparison with the results
plotted in his diagrams.

DR. THELANDERSSON commented that he would have expected a greater variation
in moisture content but DR. BLASS said this was not found with glulam and
went on to answer questions from DR. EGERUP on the variability of the
properties used in the simulations.

MR. LARSEN said that transformation of the curves for glulam and solid timber
would lead to different values for their transformed ordinates. He asked if
it was possible to have the same design curve for both using different
'kappa' values for the two and DR. BLASS thought this could be investigated.
DR. SMITH asked how the results would relate to those of Buchanan, Johns and
Madsen (paper 18-2-1). DR.BLASS and MR. LARSEN said the comparison was
difficult, the latter adding that it would be an advantage if MR. BUCHANAN
could supply normalised curves.

The Chairman asked if the results by DR. BLASS could be codified and
MR. LARSEN said he would discuss possible simplification with DR. BLASS.

Paper 20-15-1 'Behaviour factor of timber structures in seismic zones' by A. Ceccotti and A. Vignoli was introduced by DR. CECCOTTI, who said it continued the work shown in a paper at the previous meeting (19-15-1) and mentioned the punitive values that were ascribed to timber in Eurocode 8 pending the acquisition of test data.

A discussion followed on the need to secure more favourable treatment for timber, and DR. CECCOTTI confirmed that he was in touch with work in Japan and New Zealand. The Chairman concluded with the hope that the adverse coefficients in Eurocode 8 would be changed.

12.   VIBRATION

MR. CHUI presented paper 20-8-1 'Proposed code requirements for vibrational serviceability of timber floors' by Y.H. Chui and I. Smith making reference to a paper at the previous meeting (19-8-1).

A long discussion took place, on whether the equations for calculating fundamental frequency and r.m.s. acceleration should be incorporated in an Annex of the CIB code and, if so, whether acceptance limits for these should also be stated.

Some members felt that the acceptance limits which had been recommended in the light of an ISO document were not universally acceptable, that some countries were more tolerant or that different tolerances were applied to different materials. Others doubted whether the recommendations took sufficient account of research elsewhere, mentioning in particular the work of S. Ohlsson in Sweden.

The authors with backing from MR. METTEM and MR. WHALE insisted that the equations gave a satisfactory calculation of the two effects, that literature surveys and constant contact with other countries (in particular Sweden) ensured world-wide research had been taken into account, and that the best available information on tolerance levels had been used. They felt that the existing EC5 draft limitation, based upon frequency alone, was insufficient.

It was concluded that for the next meeting another paper would be produced in the light of the comments made, including a comparison with Swedish recommendations.

13.   WOOD-BASED PANELS

Paper 20-13-1 'Classification of sheet materials' by V.C. Kearley and A.R. Abbott was presented by MR. METTEM.

PROFESSOR GLOS obtained confirmation that the current project would extend to the derivation of characteristic values, and asked if a paper could be produced for the next meeting. MR. METTEM believed this would be possible.

MR. RIBERHOLT said a strength classification was almost impossible and the essential factors were durability and moisture effects. MR. O'HALLORAN and MR. ELIAS emphasised the value of performance standards. PROFESSOR GLOS suggested stating what classes a given board fell into for strength, durability, fastener values etc., but MR. FEWELL thought it better to start by saying what boards were suitable for different end uses.

MR. SUNLEY said boards could be separated initially into types suitable or not suitable for high-moisture applications. DR. KORIN said performance criteria were given by W60 which dealt with performance in building.

The Chairman concluded that some useful suggestions had been made, and that thought should be given to the nomenclature of different boards.

14. TRUSSED RAFTERS

MR. POUTANEN presented his paper 20-14-1 'Some notes about testing nail plates subjected to moment load'.

After some questions by MR. RIBERHOLT were answered, PROFESSOR EHLBECK asked if a proposal for modification of the testing methods should go to RILEM. Following discussions it was agreed that a group comprising Ehlbeck, Aasheim and Brynildsen from W18A could consider proposals for the meeting after next when MR. POUTANEN's project would be completed, and their conclusions could go to RILEM and the ISO.

MR. POUTANEN went on to his paper 20-14-2 'Moment distribution in trussed rafters', showing some tentative conclusions which would be confirmed in a future paper.

MR. RIBERHOLT asked some questions on the strain measurements, concluding that mechanical gauging verified under known moments and forces provided a very good tool for the work concerned. MR. POUTANEN said he did not attempt measurements beyond the linear state but went up to twice the serviceability loading.

Introducing his paper 20-14-3 'Practical design methods for trussed rafters', DR. EGERUP hoped that it would make a contribution to the work of the re-formed trussed rafter group.

After a comment by PROFESSOR EHLBECK that the paper indicated the goal of simple design rules was still far away despite years of work, the Chairman expressed the hope that the trussed rafter group would provide recommendations for the next meeting. DR. EGERUP suggested a conservative model could be provided for future refinement but MR. SUNLEY said there was little to refine when only three timber sizes were in common use. Regarding a suggestion by MR. POUTANEN that there was a potential gain by refinement, PROFESSOR STERN said it would only be achieved in borderline cases.

DR. EGERUP concluded that simplified methods did work and a successful industry had been based on them.

15.   OTHER BUSINESS

FUTURE MEETINGS: It was agreed that the next meeting would be held in
British Columbia after the Seattle conference, on Sat. - Tues., 24 - 27
September 1988.

An invitation to East Berlin for 1989 was accepted, on dates fitting in with
the GDR international symposium on timber engineering, September 1989.

Subjects mentioned for the British   Columbia meeting were reliability,
wood-based panels, trussed rafters, the derivation of characteristic values,
Eurocode 5, test methods, mechanical joints (Ehlbeck paper), glulam general
(Ehlbeck paper on Eurocode background), columns - Blas/Buchanan comparison,
CIB-W18B, code simplification and strength class systems.

The Chairman said care should be taken to avoid overcrowding the agenda, and
only advance papers could be accepted.

JOINT SESSION, W18A and W18B: The Chairman said Dr. Leicester had written
asking him to consider a joint meeting of the two working commissions.
MR.   METTEM proposed this should take the form of a report from W18B and a
joint session, and MR. SYME thought the joint session should last at least a
whole day. MR. SUNLEY suggested all W18B members might be invited to the
W18A meeting.

CONCLUSION: The Chairman   expressed the   thanks of those present to
MR.   COLCLOUGH for the highly successful meeting, and to the Irish timber
trade and Messrs. WOODFAB for their hospitality.   He also thanked those
present for their contributions in papers and in the discussions, and hoped
to see them in British Columbia in 1988.

MR. SUNLEY expressed appreciation to DR. STIEDA for his orderly conduct of
the meeting and associated arrangements.

16. List of CIB-W18A Papers
    Dublin 1987

16. LIST OF CIB-W18A PAPERS
   DUBLIN 1987

20-2-1   Lateral Buckling Theory for Rectangular Section
          Deep Beam-Columns - H J Burgess

20-2-2   Design of Timber Columns - H J Blaß

20-4-1   Considerations of Reliability - Based Design for Structural
          Composite Products - M R O'Halloran, J A Johnson, E G Elias
          and T P Cunningham

20-6-1   A Comparative Investigation of the Engineering Properties of
          "Whitewoods" Imported to Israel from Various Origins
          - U Korin

20-6-2   Effects of Yield Class, Tree Section, Forest and Size on
          Strength of Home Grown Sitka Spruce - V Picardo

20-6-3   Determination of Shear Strength and Strength Perpendicular
          to Grain - H J Larsen

20-7-1   Design of Nailed and Bolted Joints-Proposals for the
          Revision of Existing Formulae in Draft Eurocode 5 and the
          CIB Code - L R J Whale, I Smith and H J Larsen

20-7-2   Slip in Joints under Long Term Loading - T Feldborg and
          M Johansen

20-7-3   Ultimate Properties of Bolted Joints in Glued-Laminated
          Timber - M Yasumura, T Murota and H Sakai

20-7-4   Modelling the Load-Deformation Behaviour of Connections with
          Pin-Type Fasteners under Combined Moment, Thrust and Shear
          Forces - I Smith

20-8-1   Proposed Code Requirements for Vibrational Serviceability of
          Timber Floors - Y H Chui and I Smith

20-10-1   Draft Clause for CIB Code for Beams with Initial
          Imperfections - H J Burgess

20-10-2   Space Joists in Irish Timber - W J Robinson

20-10-3   Composite Structure of Timber Joists and Concrete Slab
          - T Poutanen

20-13-1   Classification Systems for Structural Wood-Based Sheet
          Materials - V C Kearley and A R Abbott

17. Current List of CIB-W18A Papers

17. CURRENT LIST OF CIB-W18A PAPERS

Technical papers presented to CIB-W18A are identified by a code
CIB-W18A/a-b-c, where:

a   denotes the meeting at which the paper was presented. Meetings
        are classified in chronological order:

    1   Princes Risborough, England; March 1973
    2   Copenhagen, Denmark; October 1973
    3   Delft, Netherlands; June 1974
    4   Paris, France; February 1975
    5   Karlsruhe, Federal Republic of Germany; October 1975
    6   Aalborg, Denmark; June 1976
    7   Stockholm, Sweden; February/March 1977
    8   Brussels, Belgium; October 1977
    9   Perth, Scotland; June 1978
   10   Vancouver, Canada; August 1978
   11   Vienna, Austria; March 1979
   12   Bordeaux, France; October 1979
   13   Otaniemi, Finland; June 1980
   14   Warsaw, Poland; May 1981
   15   Karlsruhe, Federal Republic of Germany; June 1982
   16   Lillehammer, Norway; May/June 1983
   17   Rapperswil, Switzerland; May 1984
   18   Beit Oren, Israel; June 1985
   19   Florence, Italy; September 1986
   20   Dublin, Ireland; September 1987

b   denotes the subject:

    1   Limit State Design   7   Timber Joints and Fasteners
    2   Timber Columns   8   Load Sharing
    3   Symbols   9   Duration of Load
    4   Plywood   10   Timber Beams
    5   Stress Grading   11   Environmental Conditions
    6   Stresses for Solid Timber   12   Laminated Members

   13   Particle and Fibre Building Boards
   14   Trussed Rafters
   15   Structural Stability
   16   Fire
   17   Statistics and Data Analysis
   18   Glued Joints
  100   CIB Timber Code
  101   Loading Codes
  102   Structural Design Codes
  103   International Standards Organisation
  104   Joint Committee on Structural Safety
  105   CIB Programme, Policy and Meetings
  106   International Union of Forestry Research Organisations

c   is simply a number given to the papers in the order in which they
        appear:

Example: CIB-W18/4-102-5 refers to paper 5 on subject 102 presented
             at the fourth meeting of W18.

Listed below, by subjects, are all papers that have to date been
presented to W18. When appropriate some papers are listed under more
than one subject heading.

LIMIT STATE DESIGN

1-1-1   Limit State Design - H J Larsen

1-1-2   The Use of Partial Safety Factors in the New Norwegian
            Design Code for Timber Structures - O Brynildsen

1-1-3   Swedish Code Revision Concerning Timber Structures - B Norén

1-1-4   Working Stresses Report to British Standards Institution
            Committee BLCP/17/2

6-1-1   On the Application of the Uncertainty Theoretical Methods
            for the Definition of the Fundamental Concepts of Structural
            Safety - K Skov and O Ditlevsen

11-1-1   Safety Design of Timber Structures - H J Larsen

18-1-1   Notes on the Development of a UK Limit States Design Code
            for Timber - A R Fewell and C B Pierce

18-1-2   Eurocode 5, Timber Structures - H J Larsen

19-1-1   Duration of Load Effects and Reliability Based Design
            (Single Member) - R O Foschi and Z C Yao

TIMBER COLUMNS

2-2-1   The Design of Solid Timber Columns - H J Larsen

3-2-1   The Design of Built-Up Timber Columns - H J Larsen

4-2-1   Tests with Centrally Loaded Timber Columns - H J Larsen and
            S S Pedersen

4-2-2   Lateral-Torsional Buckling of Eccentrically Loaded Timber
            Columns - B Johansson

5-9-1   Strength of a Wood Column in Combined Compression and
            Bending with Respect to Creep - B Källsner and B Norén

5-100-1   Design of Solid Timber Columns (First Draft) - H J Larsen

6-100-1   Comments on Document 5-100-1, Design of Solid Timber Columns
            - H J Larsen and E Theilgaard

6-2-1   Lattice Columns - H J Larsen

TIMBER JOINTS AND FASTENERS

LOAD SHARING

ENVIRONMENTAL CONDITIONS

LAMINATED MEMBERS

18-14-1   Simplified Calculation Method for W-Trusses (Part 2) -
           B Källsner

18-14-2   Model for Trussed Rafter Design - T Poutanen

19-14-1   Annex on Simplified Design of W-Trusses - H J Larsen

19-14-2   Simplified Static Analysis and Dimensioning of Trussed
           Rafters - Part 2 - H Riberholt

19-14-3   Joint Eccentricity in Trussed Rafters - T Poutanen

20-14-1   Some Notes about Testing Nail Plates Subjected to Moment
           Load - T Poutanen

20-14-2   Moment Distribution in Trussed Rafters - T Poutanen

20-14-3   Practical Design Methods for Trussed Rafters - A R Egerup

STRUCTURAL STABILITY

8-15-1   Laterally Loaded Timber Columns: Tests and Theory
           - H J Larsen

13-15-1   Timber and Wood-Based Products Structures. Panels for Roof
           Coverings. Methods of Testing and Strength Assessment
           Criteria. Polish Standard BN-78/7159-03

16-15-1   Determination of Bracing Structures for Compression Members
           and Beams - H Brüninghoff

17-15-1   Proposal for Chapter 7.4 Bracing - H Brüninghoff

17-15-2   Seismic Design of Small Wood Framed Houses - K F Hansen

18-15-1   Full-Scale Structures in Glued Laminated Timber,
           Dynamic Tests: Theoretical and Experimental Studies -
           A Ceccotti and A Vignoli

18-15-2   Stabilizing Bracings - H Brüninghoff

19-15-1   Connections Deformability in Timber Structures: a
           Theoretical Evaluation of its Influence on Seismic Effects -
           A Ceccotti and A Vignoli

19-15-2   The Bracing of Trussed Beams - M H Kessel and J Natterer

19-15-3   Racking Resistance of Wooden Frame Walls with Various
           Openings - M Yasumura

19-15-4   Some Experiences of Restoration of Timber Structures for
           Country Buildings - G Cardinale and P Spinelli

19-15-5   Non-Destructive Vibration Tests on Existing Wooden Dwellings
           - Y Hirashima

20-15-1   Behaviour Factor of Timber Structures in Seismic Zones
A Ceccotti and A Vignoli

FIRE

12-16-1   British Standard BS 5268 the Structural Use of Timber:
Part 4 Fire Resistance of Timber Structures

13-100-2   CIB Structural Timber Design Code. Chapter 9. Performance in
Fire

19-16-1   Simulation of Fire in Tests of Axially Loaded
Wood Wall Studs - J König

STATISTICS AND DATA ANALYSIS

13-17-1   On Testing Whether a Prescribed Exclusion Limit is Attained
- W G Warren

16-17-1   Notes on Sampling and Strength Prediction of Stress Graded
Structural Timber - P Glos

16-17-2   Sampling to Predict by Testing the Capacity of Joints,
Components and Structures - B Norén

16-17-3   Discussion of Sampling and Analysis Procedures - P W Post

17-17-1   Sampling of Wood for Joint Tests on the Basis of Density
- I Smith, L R J Whale

17-17-2   Sampling Strategy for Physical and Mechanical Properties of
Irish Grown Sitka Spruce - V Picardo

18-17-1   Sampling of Timber in Structural Sizes - P Glos

18-6-3   Notes on Sampling Factors for Characteristic Values -
R H Leicester

19-17-1   Load Factors for Proof and Prototype Testing - R H Leicester

19-6-2   Confidence in Estimates of Characteristic Values
- R H Leicester

GLUED JOINTS

20-18-1   Wood Materials under Combined Mechanical and Hygral Loading
- A Martensson and S Thelandersson

20-18-2   Analysis of Generalized Volkersen - Joints in Terms of
Non-Linear Fracture Mechanics - P J Gustafsson

20-18-3   The Complete Stress-Slip Curve of Wood-Adhesives in Pure
Shear - H Wernersson and P J Gustafsson

CIB TIMBER CODE

13-100-4 CIB Structural Timber Design Code. Proposal for Section 6.1.5 Nail Plates - N I Bovim

14-103-2 Comments on the CIB Structural Timber Design Code - R H Leicester

15-103-1 Resolutions of TC 165-meeting in Athens 1981-10-12/13

LOADING CODES

4-101-1 Loading Regulations - Nordic Committee for Building Regulations

4-101-2 Comments on the Loading Regulations - Nordic Committee for Building Regulations

STRUCTURAL DESIGN CODES

1-102-1 Survey of Status of Building Codes, Specifications etc., in USA - E G Stern

1-102-2 Australian Codes for Use of Timber in Structures - R H Leicester

1-102-3 Contemporary Concepts for Structural Timber Codes - R H Leicester

1-102-4 Revision of CP 112 - First Draft, July 1972 - British Standards Institution

4-102-1 Comparsion of Codes and Safety Requirements for Timber Structures in EEC Countries - Timber Research and Development Association

4-102-2 Nordic Proposals for Safety Code for Structures and Loading Code for Design of Structures - O A Brynildsen

4-102-3 Proposal for Safety Codes for Load-Carrying Structures - Nordic Committee for Building Regulations

4-102-4 Comments to Proposal for Safety Codes for Load-Carrying Structures - Nordic Committee for Building Regulations

4-102-5 Extract from Norwegian Standard NS 3470 "Timber Structures"

4-102-6 Draft for Revision of CP 112 "The Structural Use of Timber" - W T Curry

8-102-1 Polish Standard PN-73/B-03150: Timber Structures; Statistical Calculations and Designing

8-102-2 The Russian Timber Code: Summary of Contents

9-102-1 Svensk Byggnorm 1975 (2nd Edition); Chapter 27: Timber Construction

11-102-1   Eurocodes - H J Larsen

13-102-1   Program of Standardisation Work Involving Timber
Structures and Wood-Based Products in Poland

17-102-1   Safety Principles - H J Larsen and H Riberholt

17-102-2   Partial Coefficients Limit States Design Codes for
Structural Timberwork - I Smith

18-102-1   Antiseismic Rules for Timber Structures: an Italian
Proposal - G Augusti and A Ceccotti

18-1-2   Eurocode 5, Timber Structures - H J Larsen

19-102-1   Eurocode 5 - Requirements to Timber - Drafting Panel
Eurocode 5

19-102-2   Eurocode 5 and CIB Structural Timber Design Code
- H J Larsen

19-102-3   Comments on the Format of Eurocode 5 - A R Fewell

19-102-4   New Developments of Limit States Design for the New GDR
Timber Design Code - W Rug and M Badstube

19-7-3   Effectiveness of Multiple Fastener Joints According to
National Codes and Eurocode 5 (Draft) - G Steck

19-7-6   The Derivation of Design Clauses for Nailed and Bolted
Joints in Eurocode 5 - L R J Whale and I Smith

19-14-1   Annex on Simplified Design of W-Trusses - H J Larsen

20-102-1   Development of a GDR Limit States Design Code for Timber
Structures - W Rug and M Badstube

INTERNATIONAL STANDARDS ORGANISATION

3-103-1   Method for the Preparation of Standards Concerning the
Safety of Structures (ISO/DIS 3250) - International
Standards Organisation ISO/TC98

4-103-1   A Proposal for Undertaking the Preparation of an
International Standard on Timber Structures
- International Standards Organisation

5-103-1   Comments on the Report of the Consultion with Member Bodies
Concerning ISO/TC/P129 - Timber Structures - Dansk
Ingeniorforening

7-103-1   ISO Technical Committees and Membership of ISO/TC 165

8-103-1   Draft Resolutions of ISO/TC 165

12-103-1   ISO/TC 165 Ottawa, September 1979

13-103-1   Report from ISO/TC 165 - A Sorensen

14-103-1   Comments on ISO/TC 165 N52 "Timber Structures;
Solid Timber in Structural Sizes; Determination of Some
Physical and Mechanical Properties"

14-103-2   Comments on the CIB Structural Timber Design Code
- R H Leicester

JOINT COMMITTEE ON STRUCTURAL SAFETY

3-104-1   International System on Unified Standard Codes of Practice
for Structures - Comité Européen du Béton (CEB)

7-104-1   Volume 1: Common Unified Rules for Different Types of
Construction and Material - CEB

CIB PROGRAMME, POLICY AND MEETINGS

1-105-1   A Note on International Organisations Active in the Field of
Utilisation of Timber - P Sonnemans

5-105-1   The Work and Objectives of CIB-W18-Timber Structures
- J G Sunley

10-105-1   The Work of CIB-W18 Timber Structures - J G Sunley

15-105-1   Terms of Reference for Timber - Framed Housing Sub-Group
of CIB-W18

19-105-1   Tropical and Hardwood Timbers Structures - R H Leicester

INTERNATIONAL UNION OF FORESTRY RESEARCH ORGANISATIONS

7-106-1   Time and Moisture Effects - CIB W18/IUFRO 55.02-03
Working Party

INTERNATIONAL COUNCIL FOR BUILDING RESEARCH STUDIES AND DOCUMENTATION

WORKING COMMISSION W18A - TIMBER STRUCTURES

LATERAL BUCKLING THEORY FOR
RECTANGULAR SECTION DEEP BEAM-COLUMNS

by

H J Burgess
Timber Research and Development Association
United Kingdom

MEETING TWENTY
DUBLIN
IRELAND
SEPTEMBER 1987

CONTENTS

Lateral buckling theory for
rectangular section deep beam-columns

When end loads parallel to the beam axis are added to the equal end moments considered in a previous paper (Burgess,1986), the effect of torsional buckling under the end load (called 'twist buckling' by Leicester) is to be considered in addition to the lateral-torsional buckling arising from the combination of thrust and end moments.

The differential equations given by Larsen and Theilgaard (1979), with small changes to the signs and symbols to agree with the previous paper, are as follows:-

$$EI \frac{d^2 v_1}{dz^2} + P(v_1 + v_0) + M = 0 \tag{1}$$

$$EI \frac{d^2 u_1}{dz^2} - \gamma M (\phi_1 + \phi_0) + P(u_1 + u_0) = 0 \tag{2}$$

$$\left(C - P\frac{I_0}{A}\right) \frac{d\phi_1}{dz} + M \frac{d(u_1 + u_0)}{dz} = 0 \tag{3}$$

in which C = GJ is the torsional stiffness.

Leicester (1986) presents the same equations but with $\left(C - P\frac{I_0}{A}\right)$ replaced by GJ, pointing out that the effects of warping and twist buckling may be included by using an effective torsional stiffness which for a tall rectangular section will correspond to the term $\left(C - P\frac{I_0}{A}\right)$. However, the following work will show that if this term is shown explicitly and a further term is added to allow for the effect of the initial twist ϕ_0 on the twist buckling under the end load, then a simpler design formula may be obtained for the particular case of the tall rectangular section.

When considering this type of section without an end load, the deflection in the stiff direction is small compared with the lateral deflection. Equations (1) to (3) with P=0 are applicable but no use is made of equation (1) for bending in the stiff direction. With vertical deflection approximated as zero in this customary manner of deriving design equations for deep sections under end moments only, the different cross-sections of the beam rotate about the point 0 in Figure 1, which refers to the case without initial imperfections. With lateral deflections assumed to be small, the radius of rotation R is given by

$$R = \frac{u}{\phi}$$

where u and ϕ are the deflection and rotation of any cross-section when buckling takes place under the action of the critical end moments M_{cr}.

Torsional buckling under end load only

Similar behaviour can be assumed for a preliminary examination of torsional buckling in isolation, under the action of end load only. If the deflection in the stiff direction is negligible, the behaviour of the buckling member will be similar to that of a portion of one fin of the cruciform member illustrated in Figure 2. Its position in the fin will depend on the value of R, the distance of the centre line of the chosen portion from the stationary line represented by the axis of the cruciform section.

Timoshenko and Gere (1961) consider the case with no initial imperfection, obtaining the expression

$$P_\phi = \frac{A\,C}{I_o}$$

for the critical value of the compressive stress for the cruciform column, where $C = GJ$ and I_o is the polar second moment of area of the entire cross-section about the central axis. When only the shaded portion in Figure 2 is considered, the same expression is obtained but it has to be remembered that I_o is the polar second moment of the cross-section of this portion only, about the axis at a distance R from its centroid.

Without fixing a value for R at the present stage, the object will be to find the solution for the shaded portion when there is an initial imperfection appearing as a twist $\phi_o \sin\frac{\pi}{\ell}\gamma$ along the length ℓ of the member, its ends remaining untwisted. This initial twist is shown in Figure 3 for the central cross-section where $\gamma = \frac{\ell}{2}$.

The case with an initial twist of this kind was considered by Goodier (1941) who states that the axial moment he found for the cruciform section would change from

$$\frac{P}{A} I_o \frac{d\phi}{d\gamma} \qquad t_o \qquad \frac{P}{A} I_o \left(\frac{d\phi_1}{d\gamma} + \frac{d\phi_o}{d\gamma}\right)$$

leading to an equation which with the warping term omitted becomes

$$C\left(1 - \frac{P}{P_\phi}\right)\frac{d\phi_1}{d\gamma} - C\frac{P}{P_\phi}\frac{d\phi_o}{d\gamma} = 0$$

Integrating and applying the end conditions gives

$$\phi_1 = \frac{\frac{P}{P_\phi}}{1 - \frac{P}{P_\phi}} \phi_o \sin\frac{\pi}{\ell}\gamma \qquad\qquad (4)$$

where $P_\phi = \frac{A\,C}{I_o}$ is the critical torsional buckling stress for the shaded portion in Figure 2, with no initial imperfection, when constrained to buckle in the manner described. The total angle of twist at any cross-section is

$$\phi = \phi_e + \phi_1 = \frac{\phi_o}{1 - \frac{P}{P_\phi}} \sin\frac{\pi}{\ell}\gamma$$

COMBINED EFFECT OF MOMENTS AND END FORCES

The differential equations for the beam in Figure 4 with equal end moments and a longitudinal force P will be:

$$EI \frac{d^2 u_1}{dz^2} - \gamma M (\phi_1 + \phi_o) + P(u_1 + u_o) = 0 \tag{5}$$

$$C \left(1 - \frac{P}{P_\phi}\right) \frac{d\phi_1}{dz} - C \frac{P}{P_\phi} \frac{d\phi_o}{dz} + M \frac{d(u_1 + u_o)}{dz} = 0 \tag{6}$$

giving the solution

$$u_1 = \frac{\left\{\frac{M^2}{M_{cr}^2} + \frac{P}{P_e}\left(1 - \frac{P}{P_\phi}\right)\right\} u_o - \frac{C}{M} \frac{M^2}{M_{cr}^2} \phi_o}{\left(1 - \frac{P}{P_e}\right)\left(1 - \frac{P}{P_\phi}\right) - \frac{M^2}{M_{cr}^2}} \sin \frac{\pi}{\ell} z \tag{7}$$

The total central deflection of the centre-line is

$$u = u_o + u_1 = \frac{\left(1 - \frac{P}{P_\phi}\right) u_o - \frac{C}{M} \frac{M^2}{M_{cr}^2} \phi_o}{\left(1 - \frac{P}{P_e}\right)\left(1 - \frac{P}{P_\phi}\right) - \frac{M^2}{M_{cr}^2}} \tag{8}$$

The solution for ϕ_1 is

$$\phi_1 = \frac{-\frac{M}{C} u_o + \left\{\frac{M^2}{M_{cr}^2} + \frac{P}{P_\phi}\left(1 - \frac{P}{P_e}\right)\right\} \phi_o}{\left(1 - \frac{P}{P_e}\right)\left(1 - \frac{P}{P_\phi}\right) - \frac{M^2}{M_{cr}^2}} \sin \frac{\pi}{\ell} z \tag{9}$$

The total central twist is given by

$$\phi = \phi_o + \phi_1 = \frac{-\frac{M}{C} u_o + \left(1 - \frac{P}{P_e}\right) \phi_o}{\left(1 - \frac{P}{P_e}\right)\left(1 - \frac{P}{P_\phi}\right) - \frac{M^2}{M_{cr}^2}} \tag{10}$$

BEAM-COLUMN WITH RELATED TWIST AND CURVATURE

The previous paper (Burgess, 1986) developed a simplification of the formulas for lateral buckling caused by equal end moments, by relating the initial imperfections u_o and ϕ_o in the same way that u and ϕ are related in the buckling of a beam without initial imperfections. The same relationship will now be applied to the expressions derived above, but this implies a certain value for I_c which as stated earlier is the second moment of area about the centre of rotation 0 in Figure 3. The value of R in the diagram will be

$$R = \frac{u_o}{\phi_o} = \frac{\ell}{\pi}\sqrt{\frac{C\gamma}{EI}}$$

– this being the relationship between u and ϕ in the ideal beam after buckling, with a negative sign removed.

About 0,
$$I_c = I_x + I_y + AR^2$$

$$= \frac{b\ell^3}{12} + \frac{\ell_1 b^3}{12} + A\frac{\ell^2}{\pi^2}\frac{C\gamma}{EI}$$

$$\frac{I_c}{A} = \frac{\ell^2 + b^2}{12} + \frac{\ell^2}{\pi^2}\frac{C\gamma}{EI} \tag{11}$$

This value will be adopted when plotting the results of the following work, and at a later stage an approximation will be applied to obtain expressions which are simplified still further.

Expressions for u and ϕ with related values of u_o and ϕ_o

Putting $\phi_o = -\frac{\pi}{\ell}\sqrt{\frac{EI}{C\gamma}}u_o$ in (8) gives

$$u = \frac{\left(1-\frac{P}{P_\phi}\right) + \frac{M}{M_{cr}}}{\left(1-\frac{P}{P_e}\right)\left(1-\frac{P}{P_\phi}\right) - \frac{M^2}{M_{cr}^2}}\, u_o \tag{12}$$

and putting $u_o = -\frac{\ell}{\pi}\sqrt{\frac{C\gamma}{EI}}\phi_o$ in (10) gives

$$\phi = \frac{\frac{M}{M_{cr}} + \left(1-\frac{P}{P_e}\right)}{\left(1-\frac{P}{P_e}\right)\left(1-\frac{P}{P_\phi}\right) - \frac{M^2}{M_{cr}^2}}\, \phi_o \tag{13}$$

Deflection

Similarly the additional central deflection u_1 when u_o and ϕ_o are related is found from (7) to be

$$u_1 = \frac{\frac{M}{M_{cr}}\left(1 + \frac{M}{M_{cr}}\right) + \frac{P}{P_e}\left(1-\frac{P}{P_\phi}\right)}{\left(1-\frac{P}{P_e}\right)\left(1-\frac{P}{P_\phi}\right) - \frac{M^2}{M_{cr}^2}}\, u_o$$

Combined stress

The maximum combined stress is obtained in the manner described in the previous paper, but expanded to allow for the addition of end loads. The sum of the stresses due to vertical and horizontal bending with torsion neglected is

$$\sigma_{max} = \frac{M}{Z} + \frac{P}{A} + \frac{Eb}{2} \frac{d^2 u_1}{dz^2} \tag{14}$$

From equation (5)

$$EI \frac{d^2 u_1}{dz^2} = \gamma M \phi - Pu$$

The combined stress could be found using equations (8) and (10) for independent values of u_o and ϕ_o , but here the special relationship described above will be assumed, and the central values of u and ϕ are inserted from equations (12) and (13) to give

$$EI \frac{d^2 u_1}{dz^2} = \frac{\gamma M \left(1 - \frac{P}{P_e} + \frac{M}{M_{cr}}\right) \phi_o - P \left(1 - \frac{P}{P_\phi} + \frac{M}{M_{cr}}\right) u_o}{\left(1 - \frac{P}{P_e}\right)\left(1 - \frac{P}{P_\phi}\right) - \frac{M^2}{M_{cr}^2}}$$

Inserting this in (14) gives

$$\sigma_{max} = \frac{M}{Z} + \frac{P}{A} + \frac{\frac{b}{2}\gamma \frac{M}{Z} \phi_o \left(1 - \frac{P}{P_e} + \frac{M}{M_{cr}}\right) - \frac{P}{A} \cdot \frac{bu_o}{b}\left(1 - \frac{P}{P_\phi} + \frac{M}{M_{cr}}\right)}{\left(1 - \frac{P}{P_e}\right)\left(1 - \frac{P}{P_\phi}\right) - \frac{M^2}{M_{cr}^2}}$$

The term $\frac{bu_o}{b}$ is identical to the term η used for columns, but of course relates to buckling in the lateral direction, and $\frac{b}{2}\gamma\phi_o$ was given the symbol η' in the previous paper. Inserting these and limiting the combination of stresses in the manner applied for columns,

$$1 = \frac{\sigma_m}{f_m} + \frac{\sigma_c}{f_c} + \frac{\frac{\sigma_m}{f_m}\eta'\left(1 - \frac{\sigma_c}{\sigma_{eu}} + \frac{\sigma_m}{\sigma_{cr}}\right) + \frac{\sigma_c}{f_c}\frac{f_c}{f_m}\eta\left(1 - \frac{\sigma_c}{\sigma_{tor}} + \frac{\sigma_m}{\sigma_{cr}}\right)}{\left(1 - \frac{\sigma_c}{\sigma_{eu}}\right)\left(1 - \frac{\sigma_c}{\sigma_{tor}}\right) - \left(\frac{\sigma_m}{\sigma_{cr}}\right)^2} \tag{15}$$

SIMPLIFICATION BY APPROXIMATING I_o

An expression for $\frac{I_e}{A}$ was shown in equation (11). For tall sections the following approximations may be made when u_o and ϕ_o are related:

$$\frac{I_o}{A} \simeq \frac{\ell^2}{\pi^2} \frac{C\gamma}{EI} \tag{16}$$

and

$$\gamma = 1 - \left(\frac{b}{h}\right)^2 \simeq 1$$

giving

$$P_\phi = \frac{AC}{I_o} = \frac{\pi^2 EI}{\ell^2} \qquad i.e. \quad P_\phi = P_e$$

Then (12) becomes

$$u = \frac{u_o}{1 - \frac{P}{P_e} - \frac{M}{M_{cr}}} \tag{17}$$

(13) becomes

$$\phi = \frac{\phi_o}{1 - \frac{P}{P_e} - \frac{M}{M_{cr}}} \tag{18}$$

and making the approximation $\frac{\sigma_c}{\sigma_{tor}} = \frac{\sigma_c}{\sigma_{eu}}$ in (15) yields

$$1 = \frac{\sigma_m}{f_m} + \frac{\sigma_c}{f_c} + \frac{\frac{\sigma_m}{f_m}\eta' + \frac{\sigma_c}{f_c}\frac{f_c}{f_m}\eta}{1 - \frac{\sigma_c}{\sigma_{eu}} - \frac{\sigma_m}{\sigma_{cr}}} \tag{19}$$

From either (15) or (19)

when $\sigma_m = 0$,

$$1 = \frac{\sigma_c}{f_c}\left(1 + \frac{\frac{f_c}{f_m}\eta}{1 - \frac{\sigma_c}{\sigma_{eu}}}\right) \tag{20}$$

when $\sigma_c = 0$,

$$1 = \frac{\sigma_m}{f_m}\left(1 + \frac{\eta'}{1 - \frac{\sigma_m}{\sigma_{cr}}}\right) \tag{21}$$

in agreement with expressions found for a column without lateral load and for a beam with end moments only.

Deflection

The same approximation applied to the additional central deflection u_1 gives

$$u_1 = \frac{\frac{P}{P_e} + \frac{M}{M_{cr}}}{1 - \frac{P}{P_e} - \frac{M}{M_{cr}}} u_o$$

Plotted relationships

By overlaying computer-plotted curves it is confirmed that equation (19) is a good approximation to equation (15) for tall sections. The values incorporated in the calculations were shown in the previous paper except for $\frac{\sigma_c}{\sigma_{tor}}$ which is obtained as

$$\frac{\sigma_c}{\sigma_{tor}} = \sigma_c \frac{I_o}{G \, J}$$

$$= \frac{\sigma_c}{E}\left[4 \cdot \frac{\left(\frac{h}{b}\right)^2 + 1}{1 - 0.63\frac{b}{h}} + \frac{12\chi}{\pi^2}\left(\frac{\ell}{b}\right)^2\right]$$

The graphs shown in the previous paper for a beam without end load were drawn by fixing the value $\phi_o = 0.0001\,\ell/b$, and this determined the related value of u_o. When extending the study to beam-columns it becomes evident that u_o must be fixed as a constant times the ℓ/b ratio if the graphs are to reduce to appropriate values for columns without lateral load when $\sigma_m = 0$.

A set of curves drawn with this basis will be shown as Figure 8 to compare with Nylander's design method in a later section of this paper. If the solutions of (20) and (21) are expressed as $k_c f_c$ and $k_m f_m$ it can be seen from the shape of the curves that

$$\frac{\sigma_m}{k_m f_m} + \frac{\sigma_c}{k_c f_c} = 1 \tag{22}$$

is always a conservative approximation, and is a very close approximation for high values of ℓ/b. It must be remembered that $\frac{\sigma_m}{k_m f_m}$ relates to bending in the vertical plane, while $k_c f_c$ is the value for a column buckling in the weak direction. This expression was adopted for BS 5268: Part 3, applying equation (39) of Larsen and Theilgaard (1979) but with a reduced effective length to make allowance for partial lateral restraint (Burgess, 1982).

It is found later that with u_o = constant x ℓ/b, the related value of ϕ_o is independent of ℓ/b. In equation (21) for values on the vertical axis, η' does not vanish when $\ell/b = 0$, so when $\sigma_{cr} \rightarrow \infty$

$$\frac{\sigma_m}{f_m} = \frac{1}{1+\eta'} \simeq 0.87 \text{ for } \frac{h}{b} = 8$$

For smaller $\frac{h}{b}$ ratios the terminating value is higher than 0.87.

If equation (21) is used to plot permissible $\frac{\sigma_m}{f_m}$ values against ℓ/b for deep beams, then $\frac{\sigma_m}{f_m}$ will not be unity when $\ell/b = 0$. This is a consequence of the value of u_o applied for columns, coupled with the relationship between u_o and ϕ_o. It can be overcome artificially by plotting

$$1 = \frac{\sigma_m}{f_m}\left(1 + \frac{\eta'}{1 - \frac{\sigma_m}{\sigma_{cr}}}\right) - \eta'$$

which gives good correspondence with the graphs in the previous report for $h/b = 8$ (Burgess,1982), and with graphs plotted for $\phi_0 = 0.05 b/h$ as suggested by the Larsen and Theilgaard paper (1979).

ADDITIONAL TERM FOR VERTICAL BUCKLING

Going back to the opening paragraphs of this paper, it will be realised that the calculations have so far been limited to the case of beam-columns of such a depth that the vertical deflection is small compared with the lateral deflection and no use has been made of the differential equation for vertical deflection.

To add to (15) a term allowing for the effect of end thrust on the vertical deflection, an approximation by Larsen and Theilgaard (1979) will be adopted, giving the following equation instead of (15):

$$1 = \frac{\sigma_c}{f_c} + \frac{\frac{\sigma_c}{f_c}\frac{f_c}{f_m}\frac{b}{d}\eta + \frac{\sigma_m}{f_m}}{1 - \frac{\sigma_c}{\sigma_{eu,x}}} + \frac{\frac{\sigma_m}{f_m}\eta'\left(1 - \frac{\sigma_c}{\sigma_{eu}} + \frac{\sigma_m}{\sigma_{cr}}\right) + \frac{\sigma_c}{f_c}\frac{f_c}{f_m}\eta\left(1 - \frac{\sigma_c}{\sigma_{tcr}} + \frac{\sigma_m}{\sigma_{cr}}\right)}{\left(1 - \frac{\sigma_c}{\sigma_{eu}}\right)\left(1 - \frac{\sigma_c}{\sigma_{tcr}}\right) - \left(\frac{\sigma_m}{\sigma_{cr}}\right)^2} \quad (23)$$

where $\sigma_{eu,x}$ is the Euler stress for bending in the stiff direction.

RANGE OF VALIDITY OF THE APPROXIMATION $P_e = P_\phi$.

With the initial imperfections related as indicated by equation (11), the value of P_ϕ will be

$$P_\phi = \frac{AC}{I_o} = \frac{\frac{E}{16}\frac{h b^3}{3}\left(1 - 0.63\frac{b}{h}\right)}{\frac{h^2 + b^2}{12} + \frac{\ell^2}{4\pi^2}\left(1 - 0.63\frac{b}{h}\right)\left\{1 - \left(\frac{b}{h}\right)^2\right\}}$$

and $$P_e = \frac{\pi^2 EI}{\ell^2} = \frac{\pi^2 E h b^3}{12\ell^2}$$

leading to

$$\frac{P_e}{P_\phi} = \frac{\pi^2\left(\frac{b}{\ell}\right)^2\left\{\left(\frac{h}{b}\right)^2 + 1\right\}}{3\left(1 - 0.63\frac{b}{h}\right)} + 1 - \left(\frac{b}{h}\right)^2 \quad (24)$$

$\frac{P_e}{P_\phi}$ is plotted against $\frac{\ell}{b}$ in Figure 5, for values $\frac{h}{b}$ equal to 8, 6, 4, and 2. For the deeper beam-columns with $\frac{h}{b}$ from 4 to 8, $P_e = P_\phi$ is seen to be a reasonable approximation for design purposes for $\frac{\ell}{b}$ ratios more than about 50. In these cases, equation (19) may be applied.

For $\frac{h}{b} < 4$ or $\frac{\ell}{b} < 50$, equation (15) may be used but equation (23) is preferred for smaller $\frac{h}{b}$ values.

NYLANDER'S METHOD

Nylander (1949) gives a design method for monosymmetrical I sections with eccentric end load, which should provide also for beam-columns with equal end moments and central end forces (Leicester, 1986). The following outline is simplified by restricting it to tall rectangular sections, and is developed in a manner making the results comparable with those above.

Behaviour with no initial imperfections

The eccentrically loaded column is first examined as a 'perfect' member having no initial imperfections, and in Figure 6 the end load P_k is the critical load that causes buckling.

The relevant differential equations are

$$EI\frac{d^2u}{dz^2} + Pu + \gamma Pe\phi = 0 \tag{25}$$

and

$$C\left(1-\frac{P}{P_\phi}\right)\frac{d\phi}{dz} - Pe\frac{du}{dz} = 0 \tag{26}$$

leading to

$$\frac{P_k}{P_e} = \frac{1}{2\left\{1-\gamma\left(\frac{e}{i_p}\right)^2\right\}}\left(1+\frac{P_\phi}{P_e}\right) \pm \sqrt{\left(1-\frac{P_\phi}{P_e}\right)^2+4\gamma\left(\frac{e}{i_p}\right)^2\frac{P_\phi}{P_e}} \tag{27}$$

The radius of rotation about the point 'O' in Figure 6 is obtained as

$$a = \frac{u}{\phi} = -\frac{P_k e}{P_k - P_e} = \frac{e}{\frac{P_e}{P_k} - 1} \tag{28}$$

and this relationship is established between the initial imperfections in the next stage of the work. The relationship is variable, and 'a' becomes infinite when the load is applied centrally so that $P_k = P_e$.

When e = ∞, that is when the column is subjected to two equal moments $P_k e$, equation (28) becomes

$$a = \frac{P_k e}{P_e} = \frac{M_k}{P_e} \tag{29}$$

where M_k is the critical value of the moment. Taking this as

$$M_k = \frac{\pi}{\ell}\sqrt{\frac{C E I}{\gamma}}$$

gives

$$a = \frac{u_o}{\phi_o} = \frac{\ell}{\pi}\sqrt{\frac{C\gamma}{E I}} \tag{30}$$

for a beam with equal end moments and no end load. This relationship between initial imperfections is the same as in the first part of this paper but applies only along the vertical axis where P = 0.

Behaviour with initial imperfections

The equations to be solved for any value of eccentricity 'e', and making allowance for imperfections are

$$EI\frac{d^2 u_1}{d\gamma^2} + P(u_1 + u_o) + Pe(\phi_1 + \phi_o) = 0 \tag{31}$$

$$C\left(1 - \frac{P}{P_\phi}\right)\frac{d\phi_1}{d\gamma} - C\frac{P}{P_\phi}\frac{d\phi_o}{d\gamma} - Pe\frac{d(u_1 + u_o)}{d\gamma} = 0 \tag{32}$$

Apart from sign differences these equations with Pe replaced by M correspond closely to equations (5) and (6) above. However, there is a fundamental difference because Nylander's $P_\phi = \frac{AC}{I_p}$ contains I_p the polar second moment of area about the shear centre (coinciding with the centre of area in the rectangular section considered here) whereas the work above has $P_\phi = \frac{AC}{I_o}$ where I_o is the polar second moment about the centre of rotation 0 in Figure 1.

Combined stress expression

The equations are solved to give the central values

$$\phi = \frac{\phi_o}{1 - \frac{P}{P_k}}$$

and

$$u = \frac{u_o}{1 - \frac{P}{P_k}}$$

From (31),

$$-EI\frac{d^2u_1}{dy^2} = Pe\phi + Pu = \frac{Pe\phi_o + Pu_c}{1 - \frac{P}{P_k}}$$

Then following the development above leads to

$$\sigma_{max} = \frac{Pe}{Z} + \frac{P}{A} + \frac{1}{1 - \frac{P}{P_k}}\left[\frac{h}{b}\gamma\frac{Pe}{Z}\phi_o + \frac{P}{A}\frac{6u_c}{b}\right] \tag{33}$$

or

$$1 = \frac{\sigma_m}{f_m} + \frac{\sigma_c}{f_c} + \frac{\frac{\sigma_m}{f_m}n' + \frac{\sigma_c}{f_c}\frac{f_c}{f_m}n}{1 - \frac{P}{P_k}} \tag{34}$$

n' and n are related, so that

$$\frac{n'}{n} = \frac{h}{b}\gamma\phi_o \cdot \frac{b}{6u_o} = \gamma\frac{h}{6}\frac{\phi_o}{u_o} \quad where \quad \frac{\phi_o}{u_o} = \frac{1}{a} \tag{35}$$

so

$$n' = n\gamma\frac{h}{6}\frac{\frac{P_e}{P_k} - 1}{e} \tag{36}$$

Plotting of curves for Nylander method (Figure 7)

For use in equation (27), with C = GJ and G = E/16,

Nylander's
$$P_\phi = \frac{AC}{I_p} = \frac{Ehb^3\left(1 - 0.63\frac{b}{h}\right)}{4(h^2 + b^2)} \tag{37}$$

$$P_e = \frac{\pi^2 EI}{\ell^2} = \frac{\pi^2 E}{\ell^2}\frac{hb^3}{12} \tag{38}$$

hence
$$\frac{P_\phi}{P_e} = \frac{3\left(1 - 0.63\frac{b}{h}\right)}{\pi^2\left(\frac{b}{\ell}\right)^2\left\{\left(\frac{h}{b}\right)^2 + 1\right\}} \tag{39}$$

Values on the vertical axis in Figure 7 are found from equation (34) with $\sigma_c = 0$ and with P_k having the special value considered in equation (29), while initial imperfections are related as shown by equation (30), i.e. from

$$1 = \frac{\sigma_m}{f_m}\left(1 + \frac{\eta'}{1 - \frac{\sigma_m}{\sigma_{cr}}}\right) \tag{40}$$

which is the same as equation (21) above

For values on the horizontal axis, (34) with $\sigma_m = 0$ reduces to

$$1 = \frac{\sigma_c}{f_c}\left(1 + \frac{\frac{f_c}{f_m}\eta}{1 - \frac{\sigma_c}{\sigma_{cu}}}\right) \tag{41}$$

as equation (20) above.

The value $\eta = 0.005\,\ell/r = 0.01732\,\ell/b$ is adopted for Figure 7. For intermediate values of $\frac{\sigma_c}{f_c}$, $\frac{\sigma_m}{f_m}$ is incremented until the stress ratio summation in equation (34) reaches unity. From the set value of $\frac{\sigma_m}{f_m}$

$$\frac{\sigma_m}{f_m} = \frac{Pe}{Z f_m} = \frac{6 b h \sigma_c e}{b h^2 f_m} = 6\frac{\sigma_c}{f_m}\frac{e}{h}$$

so

$$\frac{e}{h} = \frac{\sigma_m}{f_m}\frac{f_m}{6\sigma_c}$$

$$= \frac{\sigma_m}{f_m} \times \frac{1}{6}\frac{f_m}{f_c}\frac{f_c}{\sigma_c} \tag{42}$$

This is the incremented value of eccentricity required to produce the set value of $\frac{\sigma_m}{f_m}$.

Then for use in working out $\frac{P_k}{P_e}$ from (27)

$$\left(\frac{e}{i_p}\right)^2 = \frac{12 e^2}{b^2 + h^2} = \frac{12\left(\frac{e}{h}\right)^2}{1 + \frac{b^2}{h^2}} \tag{43}$$

From (35) the value of η' on the vertical axis is found as

$$\eta' = \eta\gamma\frac{h}{6}\frac{\sigma_c}{u_o} = \eta\gamma\frac{h}{6}\frac{\pi}{\ell}\sqrt{\frac{EI}{C\gamma}} \qquad \text{using (30)} \tag{44}$$

$$= 0.01732\frac{\ell}{b}\gamma\frac{h}{6b}\frac{b}{\ell}\pi\sqrt{\frac{EI}{C\gamma}}$$

$$= 0.01732\,\gamma\frac{h}{b}\;\frac{2\pi}{6\sqrt{\left(1 - 0.63\frac{b}{h}\right)\left\{1 - \left(\frac{b}{h}\right)^2\right\}}} \tag{45}$$

-independent of ℓ/b for values on the vertical axis only.

For η' at non-zero values of $\frac{\sigma_c}{f_c}$

$$\eta' = \eta\gamma\frac{h}{6}\frac{\frac{P_e}{P_k}-1}{e}$$ from (36)

$$= \frac{\eta\gamma}{6\frac{e}{h}}\left(\frac{P_e}{P_k}-1\right)$$ (46)

tending to zero when the horizontal axis is approached.

The curves plotted from equation (34) are shown in Figure 7 for values of ℓ/b ranging from 50 to 200 in steps of 10.

Curves for simplified equation (19)

For comparison, Figure 8 shows curves plotted using equation (19) above, which is the same as (34) except that $1-\frac{P}{P_k}$ is replaced by $1-\frac{\sigma_c}{\sigma_{eu}}-\frac{\sigma_m}{\sigma_{cr}}$ where σ_{eu} is the Euler stress for lateral bending as a column and σ_{cr} is the critical bending stress that causes buckling of a 'perfect' beam under equal end moments only.

For Figure 8, the value of $\eta = 0.005\frac{\ell}{r}$ is again adopted and the curves have the same values along the vertical and horizontal axes as those of Figure 7, but the intermediate values differ greatly. With $\ell/b = 80$ and $\frac{\sigma_c}{f_c} = 0.12$, the computed permissible value of $\frac{\sigma_m}{f_m}$ in Figure 8 is 0.1068 while that from Figure 7 is 0.2411, more than twice as great.

In Nylander's method, the value of the initial twist ϕ_o in $\eta' = \frac{h}{b}\gamma\phi_o$, see equation (33), changes from

$$\phi_o = \frac{\eta'b}{\gamma h} = \frac{0.1500}{0.9844\text{x}8} = 0.01905 \text{ radian} = 1.091 \text{ degrees}$$

at the vertical axis for $\ell/b = 80$

to $$\phi_o = \frac{0.03508}{0.9844\text{x}8} = 0.004455 \text{ radian} = 0.2553 \text{ degrees}$$

when $\frac{\sigma_c}{f_c} = 0.12$, and of course tends to zero as the horizontal axis is approached for any given ℓ/b value. In Figure 8 the value of ϕ_o remains constant with $\eta' = 0.1500$ throughout the range of ℓ/b .

DIFFERENCE BETWEEN THE TWO METHODS

A fundamental difference between the two methods was mentioned earlier. In Nylander's $P_\phi = \frac{AC}{I_p}$, I_p is the polar second moment of area about the shear centre which coincides with the centre of area for the rectangular section. I_o used in $P_\phi = \frac{AC}{I_o}$ of the first part of this paper means the polar second moment about the point 0 in Figure 1.

A second important difference is that the earlier work adopted a fixed relationship between u_o and ϕ_o for a given ℓ/b value as shown by equation (44). Nylander's method applies a varying relationship, ranging from that in equation (44) when $\frac{\phi_o}{f_c} = 0$, and tending to $\frac{\phi_o}{u_o} = 0$ as the horizontal axis is approached.

The diminishing initial twist ϕ_o of Nylander's method is difficult to accept as it implies that the shape of a piece of timber will change depending on the eccentricity of the end load that is going to be applied to it. The method is actually difficult to apply in practice, and equation (19) is preferred for design because of its easier use, logical appearance and more reasonable results.

References

Burgess, H.J.(1982) - A rafter design method matching UK test results
          for trussed rafters. CIB-W18 paper No. 15-14-5,
          Karlsruhe, June 1982.

Burgess, H.J.(1986) - Possible code approaches to lateral buckling in
          beams. CIB-W18 paper No. 19-10-1, Florence, September 1986.

Goodier, J.N.(1941) - The buckling of compressed bars by torsion and
          flexure. Bulletin 27, Cornell University Engineering
          Experiment Station.

Larsen, H.J. and Theilgaard, E.(1979) - Laterally loaded timber
          columns. Jl Structural Div. ASCE, Vol.105 No.ST7,
          July 1979.

Leicester, R.H.(1986) - Creep buckling strength of timber beams and
          columns. CIB-W18 paper No.19-2-1, Florence, September 1986.

Nylander, H. (1949) - Torsional and lateral buckling of eccentrically
          compressed I and T columns. Trans. Royal Institution of
          Technology, Stockholm, No.28, 1949.

Timoshenko, S.P. and Gere, J.M. (1961) - Theory of elastic stability,
          2nd edition, McGraw-Hill, London 1961.

Fig 1.

M_{cr} M_{cr}

PERFECT
BEAM

TORSIONAL BUCKLING
UNDER END LOAD ONLY

z

ℓ

y

R

x   Fig. 2

Fig. 3

ϕ_0 ϕ_1

M   BEAM − COLUMN   M

P   P
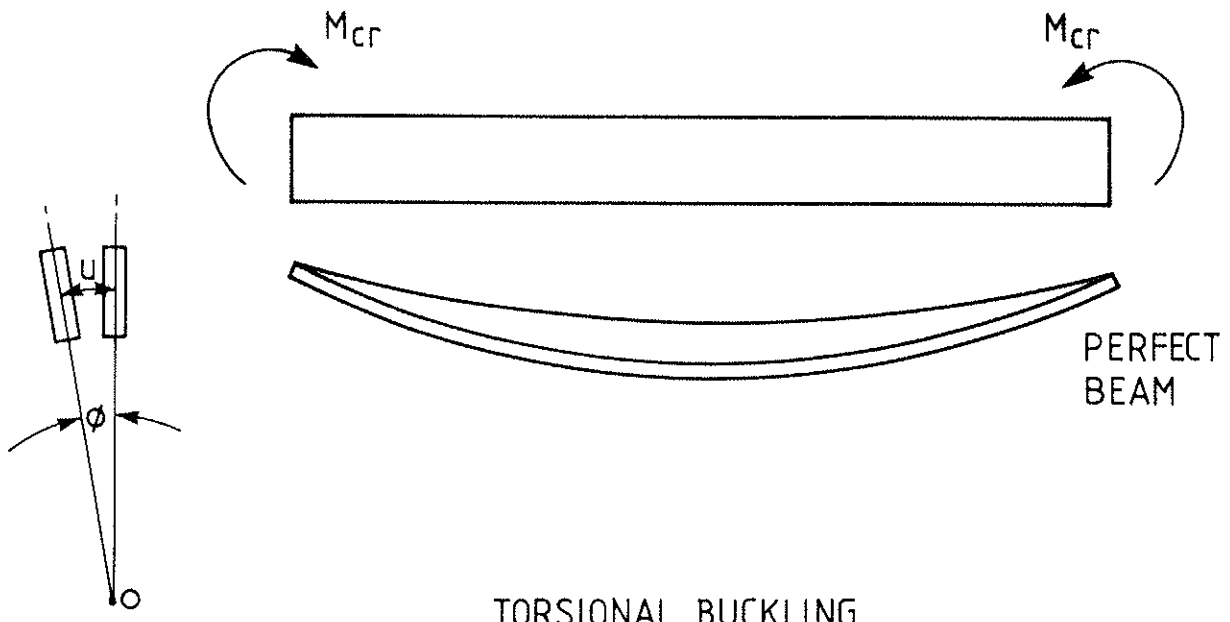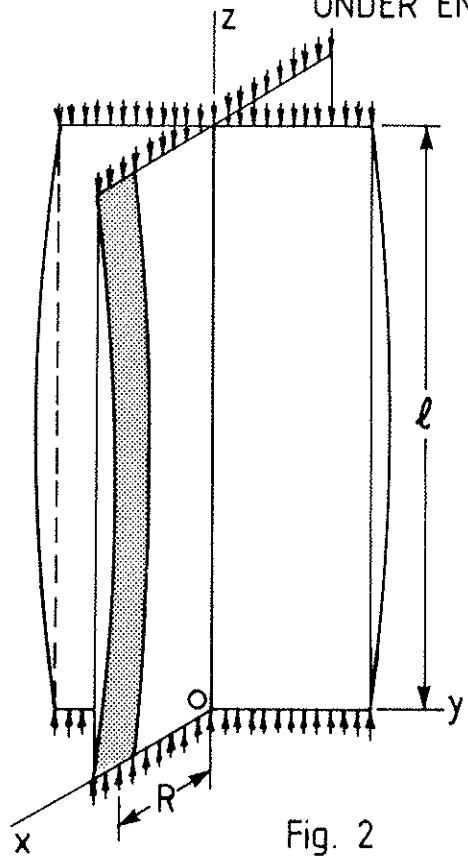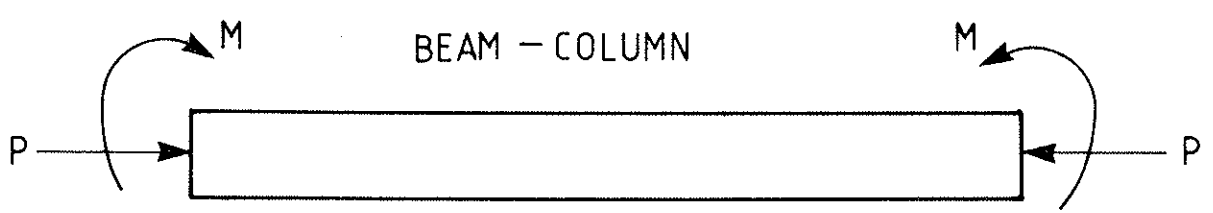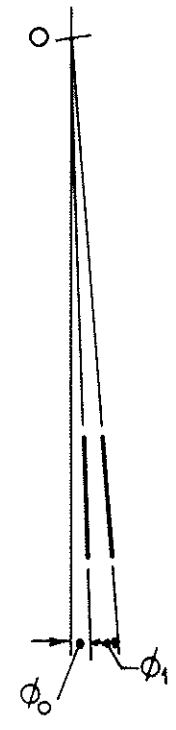
Fig. 4
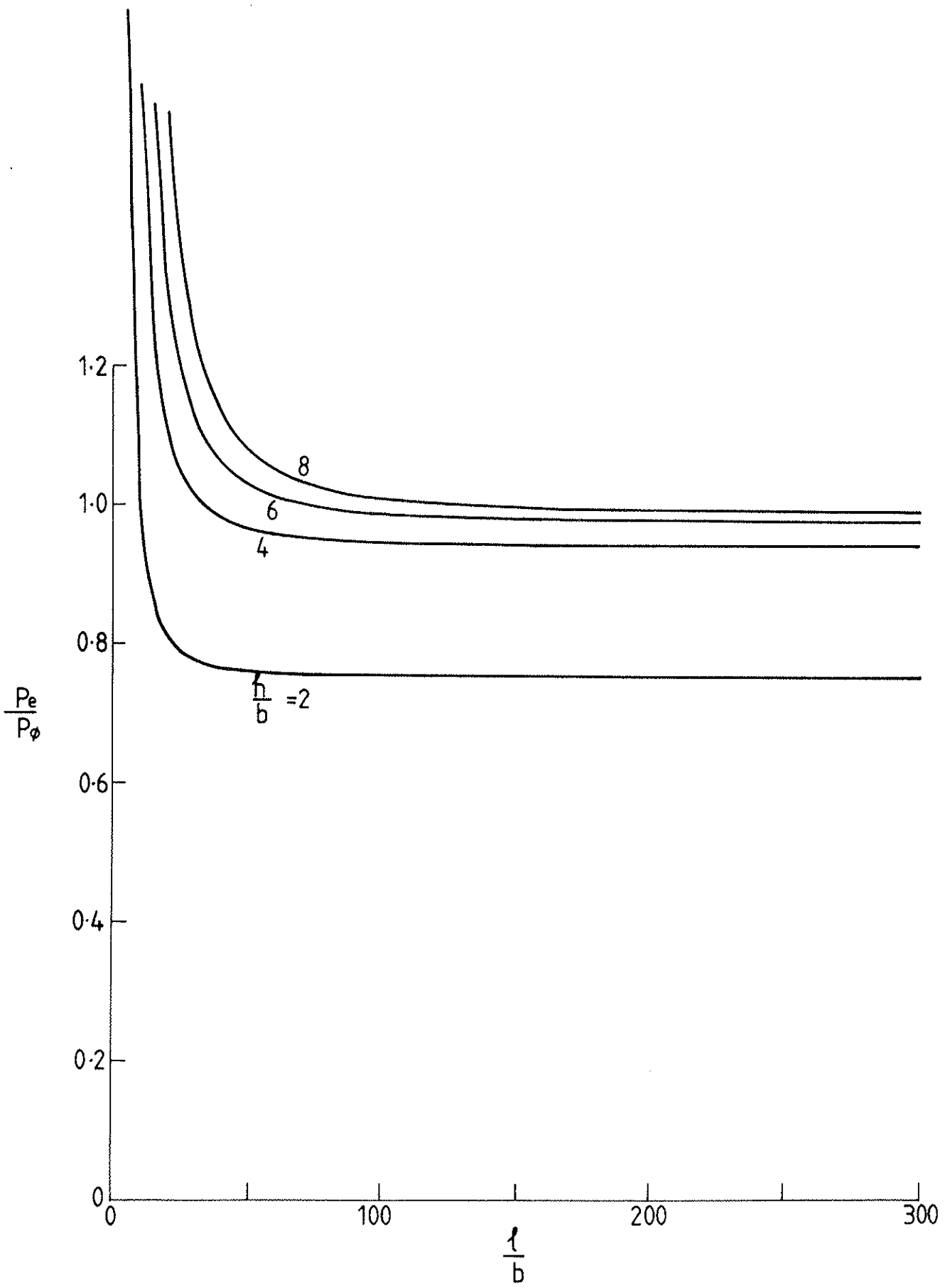
Fig. 5
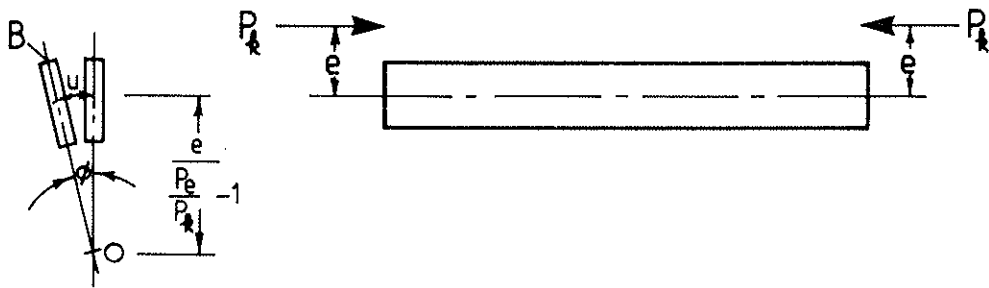
Fig. 6
Without imperfections
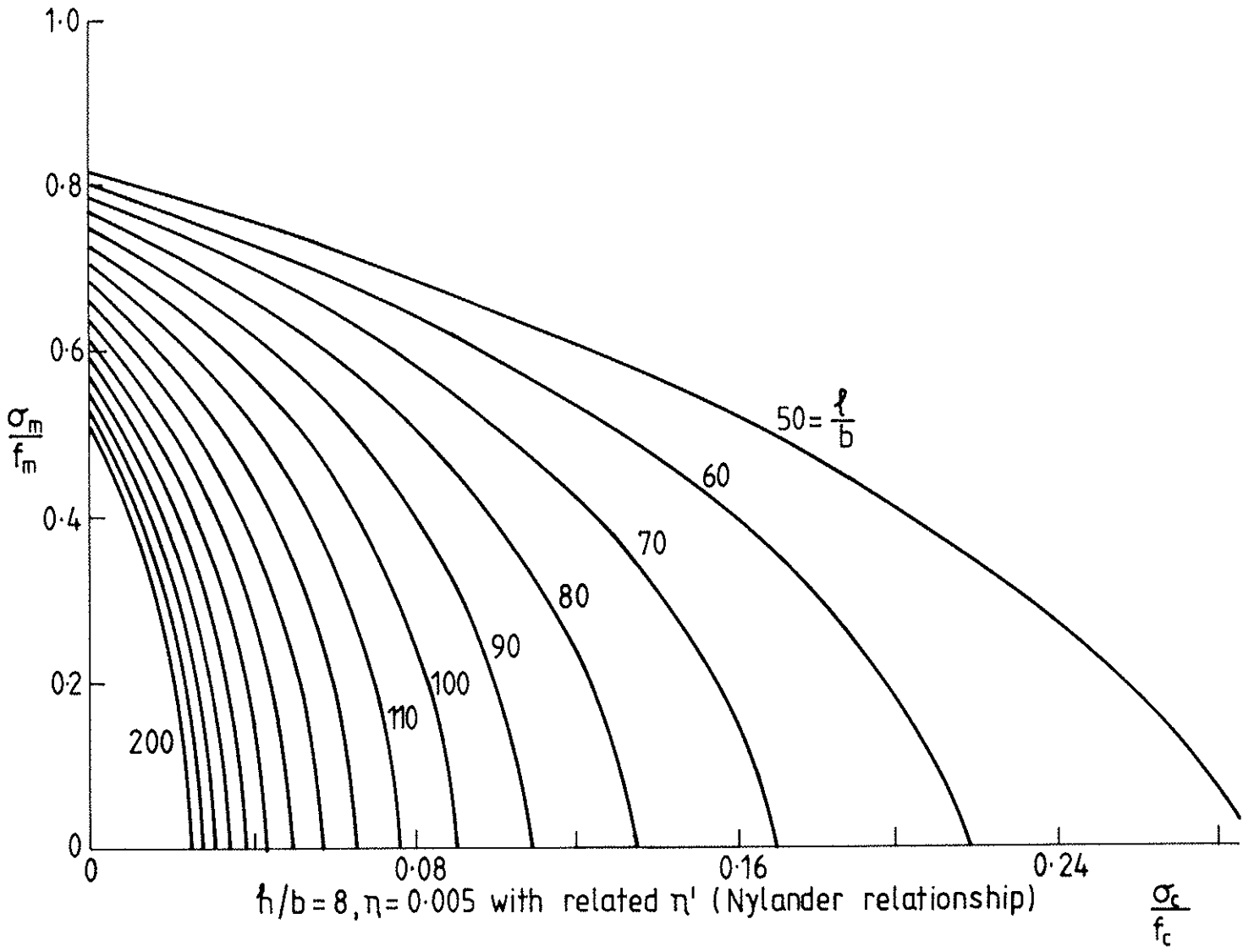
Fig. 7
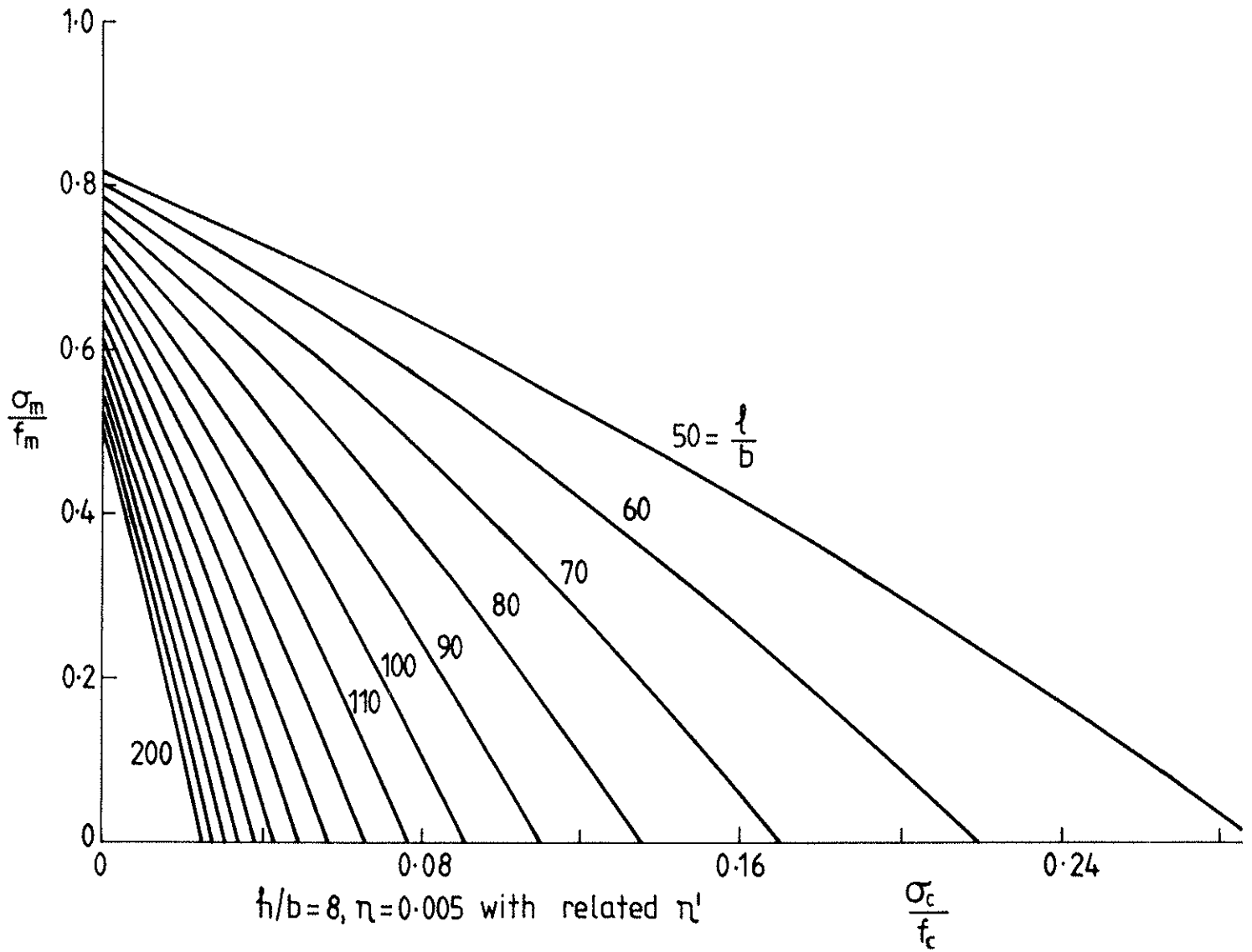
Fig. 8

INTERNATIONAL COUNCIL FOR BUILDING RESEARCH STUDIES AND DOCUMENTATION

WORKING COMMISSION W18A - TIMBER STRUCTURES

DESIGN OF TIMBER COLUMNS

by

H J Blaß
University of Karlsruhe
Federal Republic of Germany

MEETING TWENTY
DUBLIN
IRELAND
SEPTEMBER 1987

DESIGN OF TIMBER COLUMNS

H.J. Blaß

Lehrstuhl für Ingenieurholzbau und Baukonstruktionen
Universität (TH) Karlsruhe

1 INTRODUCTION

The design of timber columns in the draft Eurocode 5 (1986) and in the CIB Structural timber design code (1983) is based on the elastic theory with a linear failure criterion of the cross section: collapse of the column occurs when in the critical cross section an elastic limit stress is reached.

Some research results during the last years |1, 2| show that this is a conservative failure criterion. Taking into account the plastic deformations of the timber when subjected to compression parallel to grain, the ultimate loads of timber compression members are considerably higher than under assumption of the elastic theory.

It is the objective of this paper to provide approximate functions for the characteristic strength of centrically and eccentrically loaded timber columns.

2 STRENGTH MODEL

A computer model for calculating the ultimate loads of glued laminated columns was presented in |3| and is used to determine characteristic values of the load-carrying capacity of timber compression members. Monte-Carlo-simulations are used for calculating the ultimate load by a second order plastic analysis.

The principal run of the stress-strain-diagram (fig. 1) applies to
both glued laminated and solid timber columns. In case of glulam
columns the stress-strain-relationship of the cross section of each
lamination with a length of 150 mm may be verified by using the
following decisive structural attributes: density, knot area ratio,
moisture content, portion of compression wood and finger-joint. Such
detailed relations are unknown for timber sections in structural
sizes. A great number of test results concerning the material proper-
ties of timber are, however, available. GLOS |4| presented for Euro-
pean softwood under normal climate (20/65) conditions statistic
distribution functions of the elastic and the strength properties and
their mutual correlations. The results of this study are based on
values summarized in table 1 and 2. For the so-called asymptotic
compressive strength $f_{c,a}$ and the ultimate compressive strain at
failure $\varepsilon_{c,u}$ the following approximate values are assumed:

$$f_{c,a} = 0,85 \cdot f_{c,u} \qquad |N/mm^2| \qquad\qquad (1)$$

$$\varepsilon_{c,u} = 1250 \cdot f_{c,u}/E_{0,c} \qquad |‰| \qquad\qquad (2)$$

The influence of the moisture content ω on the stress-strain behaviour
is taken into account by modifying the characteristic values of the
stress-strain-relationship corresponding to table 3.

Based on these material data it is possible to simulate the stress-
strain-relationship of solid timber members and to use this relations-
hip in a realistic mechanical model.

The stochastic model of the glulam column includes the statistic
distribution functions of the prevailing structural properties i.e.
the density, the knot area ratio, the moisture content, the portion of

compression wood and the finger joints. These structural properties
determine the stress-strain curve of lamination sections. Further-
more, the geometric imperfections, such as curvature of the member
axis and deviations of the cross-sectional dimensions from the nominal
values, are included in the stochastic model. Simulating the structu-
ral properties in each lamination at an equal distance of 150 mm leads
to elements with changing properties in longitudinal and transverse
direction. The corresponding ultimate loads are a sample of the resi-
stance of the element.

The basic variables of the stochastic model of the solid timber column
are the elastic and the strength properties under normal climate
(20/65) conditions as well as the moisture content. The probabilistic
density of the moisture content of timber columns was determined in
situ in a measuring series |5|. Furthermore, the statistic distribu-
tion functions of the geometric imperfections are used in the stocha-
stic model of the solid timber columns. The resulting material proper-
ties within the timber column are, in analogy to |1|, assumed to be
constant. The ultimate loads of a great number of members simulated in
this way provide the resistance of European softwood timber columns.
Fig. 2 shows the flow diagram of the simulation calculations for
glulam and solid timber columns.

3 BUCKLING CURVES FOR CENTRICALLY LOADED COLUMNS

The evaluation of the calculation of the ultimate load is shown in
Fig. 3 to 5. The 3-parameter Weibull distribution, fitted to the
samples, is used to calculate the characteristic values of the failure
stress, $f_{c,u}$, i.e. the buckling strength. The sample size amounts to
400 for high slenderness ratios and up to 1000 for low slenderness
ratios. The simulation calculation for the glulam columns was realized
with members of seven laminations.

Fig. 3 presents the characteristic values of the buckling strength depending on the slenderness ratio for glulam columns made from laminations of quality grade II according to the german standard DIN 4074. The single points represent the 5-percentiles resulting from the Monte-Carlo-simulations, the solid line describes a fitting approximate function. The approximating curve depends on the characteristic compressive strength $f_{c,o,k}$ and on the ratio $E_{o,k}/f_{c,o,k}$. Equation (3) is the function of the approximate curve:

$$g_c \ (f_{c,o,k}, \ E_{o,k}) \ = \ \varkappa \cdot f_{c,o,k} \qquad (3)$$

with

$$\varkappa \ = \ \begin{cases} 1 & \text{for } \bar{\lambda} \leqq 0,5 \\[2ex] \dfrac{1}{k + \sqrt{k^2 + \bar{\lambda}^2}} & \text{for } \bar{\lambda} > 0,5 \end{cases}$$

$$k \ = \ 0,5 \ (1 + 0,13 \ (\bar{\lambda} - 0,5) + \bar{\lambda}^2)$$

$$\bar{\lambda} \ = \ \lambda / \lambda_f$$

$$\lambda_f \ = \ \sqrt{\dfrac{E_{o,k}}{f_{c,o,k}}} \cdot \pi$$

Fig. 3a belongs to glulam columns with an equilibrium moisture content for normal climate conditions, whereas Fig. 3b was calculated on the basis of a moisture content distribution, which was determined in buildings with a mean value of 14,8 % and a standard deviation of 1,2 %.

Due to a low moisture content the buckling strength of columns with low slenderness increases more than that of high slender columns. This may be explained by the distinct influence of the moisture content on the compressive strength, whereas the moisture content is of less influence on the modulus of elasticity.

Fig. 4 gives the characteristic buckling strengths for glulam columns from laminations of quality grade I (DIN 4074). Differences between the grades I and II are only based on different knot area ratios, as long as the laminations are graded only visually. COLLING and DINORT |7| found, however, that there are only small differences between the knot area ratios of the two quality classes. This explains the fact, that there is nearly no difference between the buckling strength of columns grade I and II (see Fig. 3b and 4b). A significant increase of the buckling strength is possible when an additional machine grading is applied, e.g. for density grading. Fig. 4a was calculated for glulam columns of grade I with an additional assumption of a minimum oven-dry density of 420 kg/m³. This leads to an increase of the characteristic values of about 15 % for all slenderness ratios.

The buckling strengths of solid timber columns, quality grade II, as shown in Fig. 5, are considerably lower than the corresponding data for glulam columns. This can be explained by the considerable higher variation of the material properties of solid timber compared to those of glulam as well as the higher moisture content of solid timber columns in situ (mean = 17,6 %, standard deviation = 3,0 %), the greater inital curvature of the member axis and the more unfavourable ratio of existing to nominal cross section area.

4 MOMENT-NORMAL FORCE-INTERACTION

The results of ultimate load calculations for eccentrically loaded columns are described as moment-normal force-interaction diagrams for glulam columns grade II (DIN 4074). The curves shown in Fig. 6 were computed for columns with different end eccentricities and slenderness ratios between $\lambda = 10$ and $\lambda = 200$. The values on the abscissa represent the end moments of the columns, i.e. the first order moments. The values on the normal force axis for $M/M_u = 0$ correspond to the buckling stresses for centrically loaded columns.

5 DESIGN PROPOSAL

For the design of timber and glulam columns the following design
method is proposed:

Approximated curves for centrically loaded columns are shown in Figs.
3 to 5, whereas approximations for the moment-normal force-interaction
are given as dashed lines in Fig. 7 for the slenderness ratios $\lambda = 10$,
60 and 120.

For columns the stresses should satisfy the following condition:

$$(\frac{\sigma_{c,o,d}}{\varkappa \cdot f_{c,o,d}})^m + \frac{\sigma_{m,d}}{f_{m,d}} \leq 1 \qquad (4)$$

$\sigma_{m,d}$ is the bending stress caused by the first order bending moments.

$$\varkappa = \begin{cases} 1 & \text{for } \bar{\lambda} \leq 0,5 \\[2ex] \dfrac{1}{k + \sqrt{k^2 - \bar{\lambda}^2}} & \text{for } \bar{\lambda} > 0,5 \end{cases}$$

$$m = \begin{cases} 2 & \text{for } \bar{\lambda} \leq 0,5 \\[2ex] 1 & \text{for } \bar{\lambda} > 0,5 \end{cases}$$

with k and $\bar{\lambda}$ as defined in equation (3).

Using equation (4) the design of columns on the basis of a second
order plastic analysis is reduced to a simple function depending only

on the compressive strength $f_{c,o,k}$ and the modulus of elasticity $E_{o,k}$
of the timber used. The approximate equation (4) contains the influ-
ence of all structural and geometric imperfections, such as the ini-
tial curvature of the member axis.

Creep effects are not yet taken into account, but the influence of
long duration loads is being investigated with a sophisticated
computer program.

6 SUMMARY

For the design of timber compression members a new method is sub-
mitted, based on a non linear moment - normal force - interaction of
the cross section. The method is derived from the results of extensive
simulation calculations and applies to European spruce glulam and to
European softwood timber columns. The material behaviour is taken into
account better than in former methods. Whith this method a more econo-
mic design of columns is possible. The influence of moisture content
and grading is shown for centrically loaded columns.

7 LITERATURE CITED

|1| Buchanan, A.H.; Johns, K.C.; Madsen, B.: Column design
       methods for timber engineering. Canadian Journal of Civil
       Engineering 12 (1985) No. 4, pp 731-744.

|2| Blaß, H.J.: Strength model for glulam columns. Proc. Joint
       meeting CIB-W18/IUFRO S 5.02, Sept. 1986, Florence, Italy,
       14 pp.

|3| Blaß, H.J.: Tragfähigkeit von Druckstäben aus Brettschicht-
       holz unter Berücksichtigung streuender Einflußgrößen.
       Dissertation Universität Karlsruhe, 1987, 192 pp.

|4| Glos, P.: Zur Modellierung des Festigkeitsverhaltens von
       Bauholz bei Druck-, Zug- und Biegebeanspruchung.
       Arbeitsberichte zur Zuverlässigkeitstheorie der Bauwerke 61,
       Technische Universität München 1981, 58 pp.

|5| Ehlbeck, J.; Blaß, H.J.: Imperfektionsannahmen für
       Holzdruckstäbe. Holz als Roh- und Werkstoff 45 (1987)
       pp 231-235.

|6| Glos, P.: Zur Bestimmung des Festigkeitsverhaltens von
       Brettschichtholz bei Druckbeanspruchung aus Werkstoff- und
       Einwirkungskenngrößen. Arbeitsberichte zur Zuverlässigkeits-
       theorie der Bauwerke 35, Technische Universität München 1978,
       335 pp.

|7| Colling, F.; Dinort, R.: Die Ästigkeit des in den
       Leimbaubetrieben verwendeten Schnittholzes. Holz als Roh- und
       Werkstoff 45 (1987) pp 23-26.
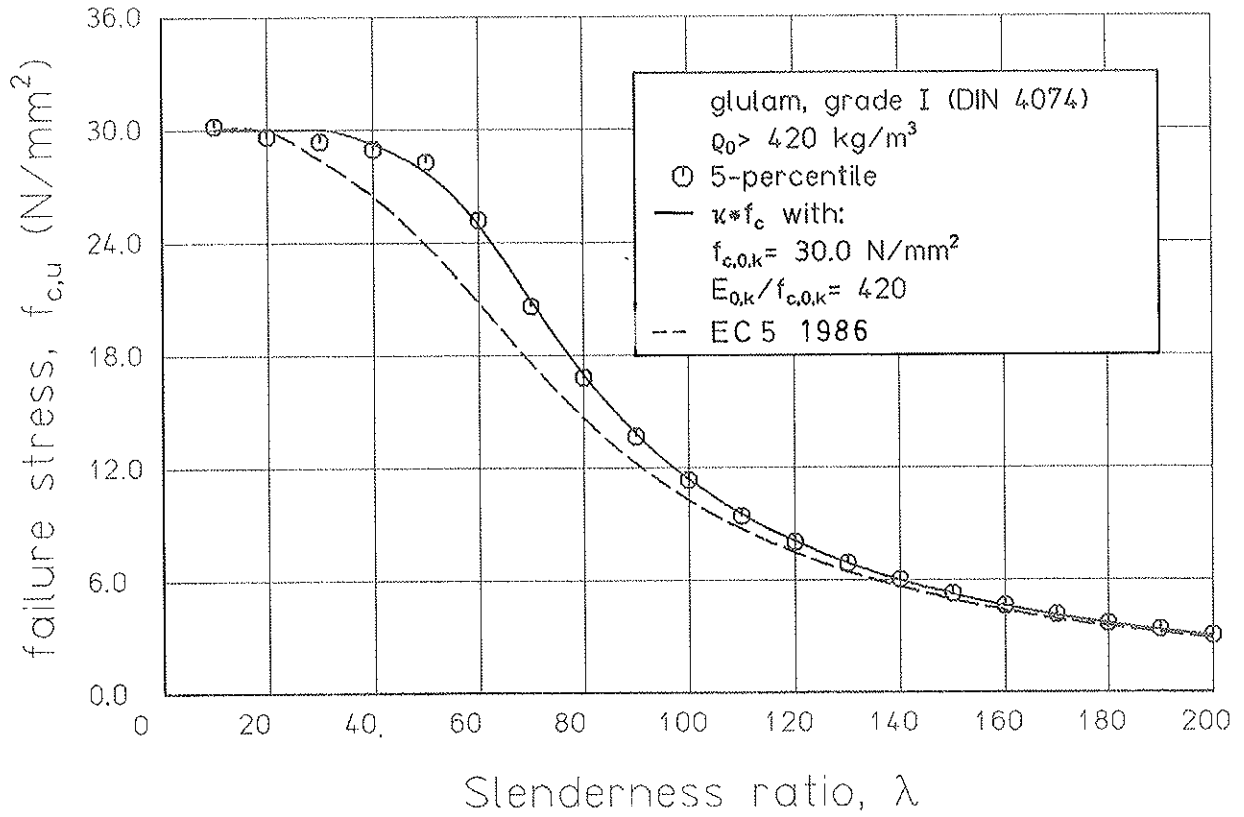
a) Compressive strength $f_{c,o,k}$ = 30,0 N/mm^2
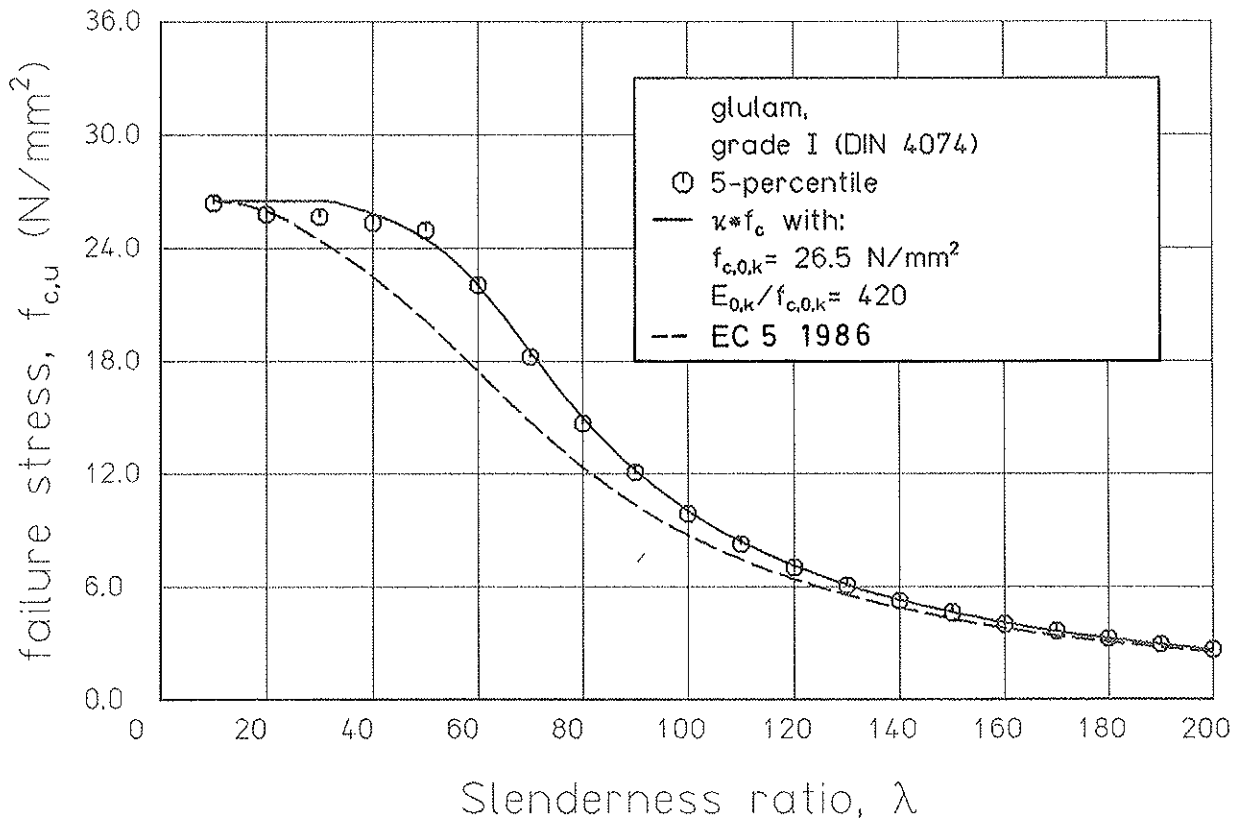
b) Compressive strength $f_{c,o,k}$ = 26,5 N/mm^2

Fig. 4 Characteristic buckling strengths (failure stresses) for glulam
columns grade I (DIN 4074) assuming different compressive strengths
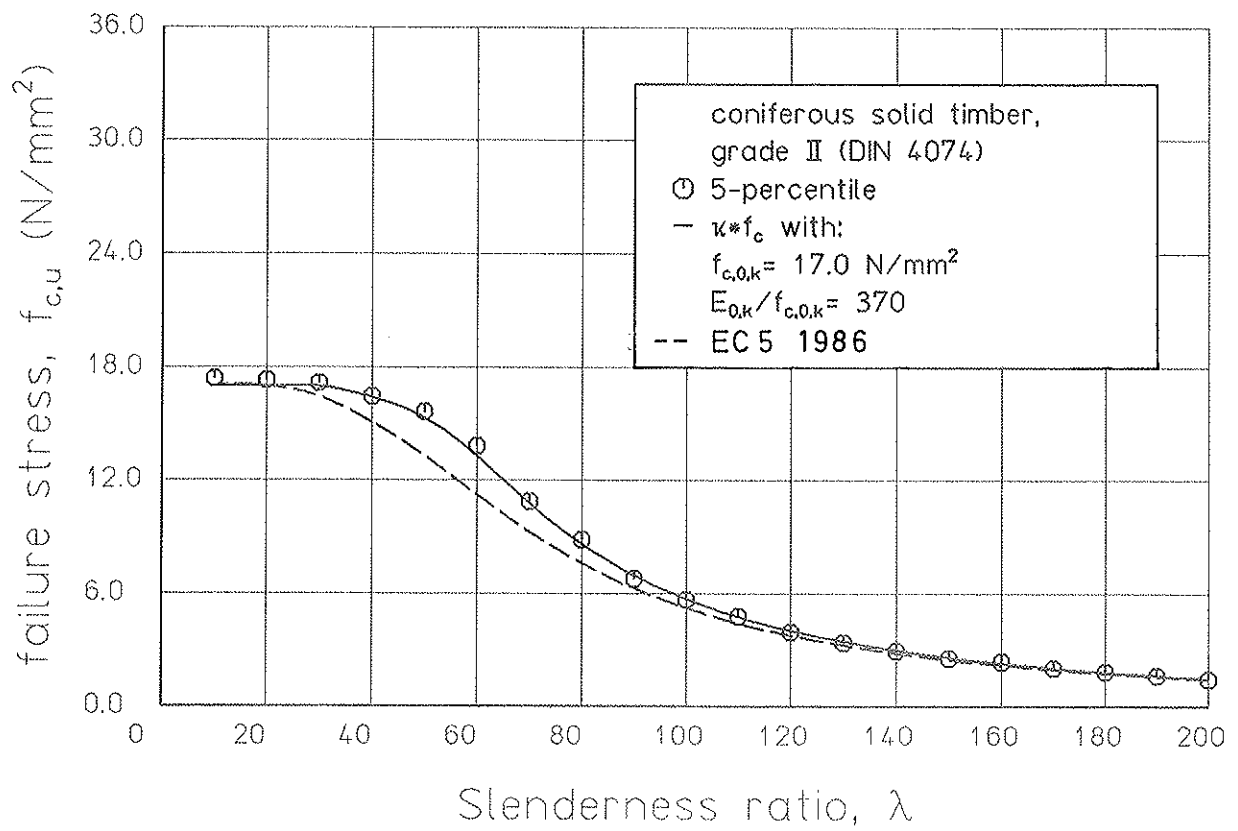
Fig. 5 Characteristic buckling strengths (failure stresses)
for solid timber columns
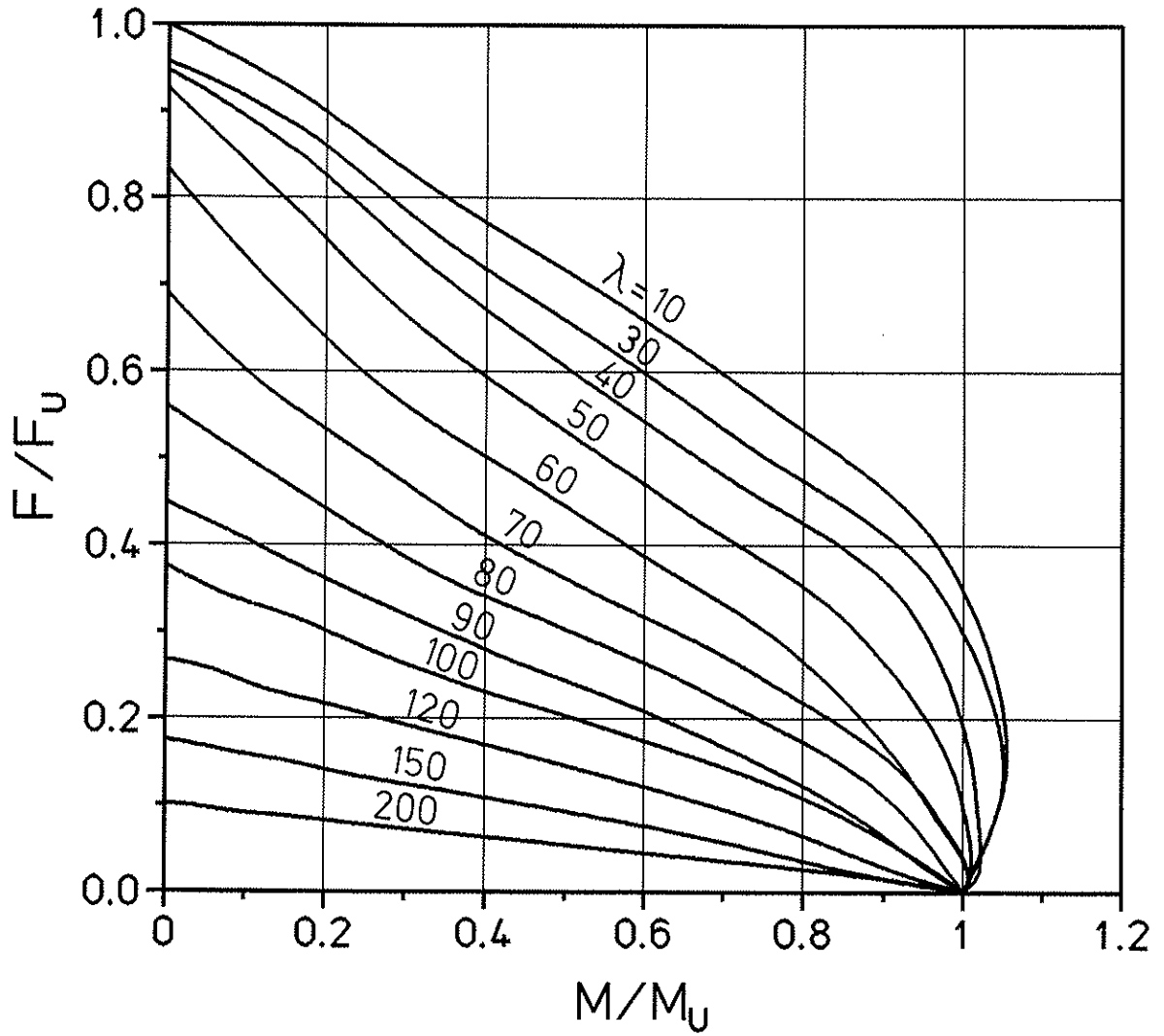
Fig. 6   Moment - normal force - interaction for glulam
         columns grade II
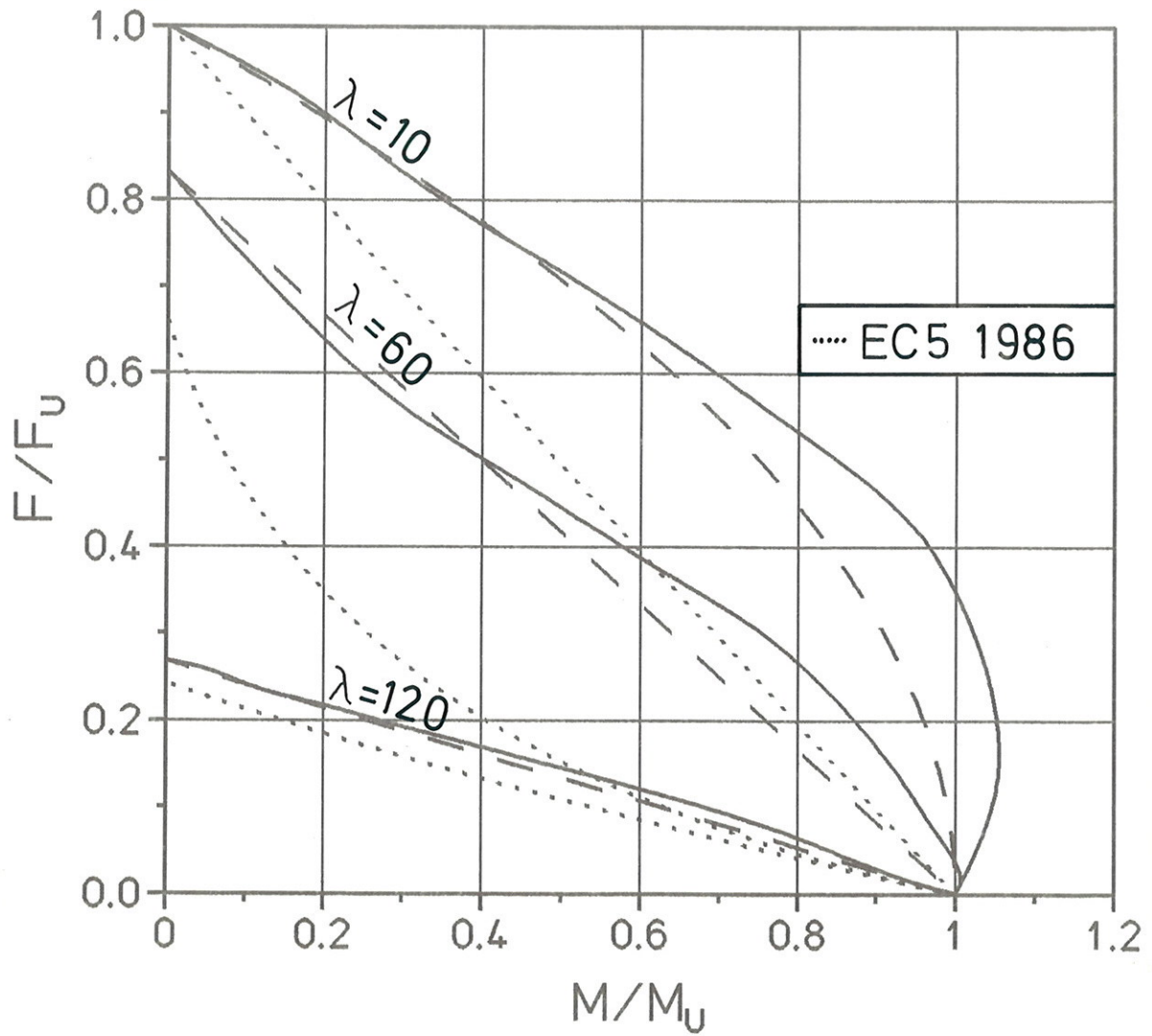
Fig. 7 Approximations for eccentrically loaded columns
as basis for a new column design proposal

Table 1: Elastic and strength properties in Mpa and parameters of the
3-parameter Weibull distribution of European softwood in
normal climate according to GLOS |4|

		compressive strength	bending strength	modulus of elasticity
Mean	|Mpa|	32	37	11500
Coefficient of Variation		0,18	0,27	0,22
5-percentile	|Mpa|	21	24	7000
Parameters of the 3-parameter Weibull distribution				
location	|Mpa|	14	15	3500
Scale	|Mpa|	20	26	9000
shape		2,6	2,5	3,1

Table 2: Relationship between compressive strength, bending strength
and modulus of elasticity according to GLOS |4|

	compressive strength	bending strength	modulus of elasticity
compressive strength	1	0,8	0,75
bending strength	0,8	1	0,75
modulus of elasticity	0,75	0,75	1

Table 3: Modification of timber properties in % related to change of
moisture content of $\Delta\omega$ = 1 %, based on ω = 12 % and
applicable in the range of ω from 5 to 25 %, according
to GLOS |4|

timber quality	compressive strength	bending strength	modulus of elasticity
low (5 percentile)	- 1	0	- 1
mean (50 percentile)	- 4	- 2	- 2
high (95 percentile)	- 6	- 3,5	- 3,5

INTERNATIONAL COUNCIL FOR BUILDING RESEARCH STUDIES AND DOCUMENTATION

WORKING COMMISSION W18A - TIMBER STRUCTURES

CONSIDERATIONS OF RELIABILITY-BASED DESIGN
FOR STRUCTURAL COMPOSITE PRODUCTS

by

M R O'Halloran, E G Elias and T P Cunningham
American Plywood Association
USA

J A Johnson
University of Washington
USA

MEETING TWENTY
DUBLIN
IRELAND
SEPTEMBER 19876

TECHNOLOGY TRANSFER ABSTRACT

CONSIDERATIONS OF RELIABILILITY-BASED DESIGN
FOR STRUCTURAL COMPOSITE PRODUCTS

The concepts of reliability-based design are reviewed as they might

be applied to structural composite products such as panels or

lumber substitutes. The paper reviews the current method of

qualifying products and the subsequent impact on gathering reliable

mechanical characteristics information. Example data sets are dis-

cussed, along with the analysis of the sets by distribution fitting

techniques. The data sets are then used to compute the reliability

as measured by beta for the simple case of dead plus live load.

The results indicate that for panels, a significant margin of

safety exists for both strength and serviceability reliability.

ABSTRACT

CONSIDERATIONS OF RELIABILITY-BASED DESIGN
FOR STRUCTURAL COMPOSITE PRODUCTS

Structural composite products, such as panels and lumber substitutes, are being certified under performance-based standards. These standards provide use classifications for a vast array of product types under a uniform system of trademarking.

The performance standards are briefly reviewed along with the ongoing in-grade testing program. This review forms the basis for accessing the character of the products so certified.

Two data sets, extracted from the APA in-grade testing program are presented. Each set is fit with various probability density functions and the results discussed. Finally, the data sets are evaluated for the reliability index, using transformation techniques. This analysis is run for strength and the serviceability limit state of deflection for both dead and live load situations. The first assessment indicates good levels of safety exist for structural panel products.

CONSIDERATIONS OF RELIABILITY BASED DESIGN
FOR STRUCTURAL COMPOSITE PRODUCTS

By M. R. O'Halloran (1)
J. A. Johnson (2)
E. G. Elias (3)
T. P. Cunningham (3)

INTRODUCTION

Concepts of structural design have undergone radical philosophical changes in recent years. As a result of major research efforts devoted to the applications of reliability analysis concepts to structural design, new reliability-based design (RBD) codes are emerging. Reliability-based design is the method by which the reliability of a structure or permanent component is controlled through appropriate recognition of the means, variabilities, and uncertainties of loads and material resistance (9, 11, 12, 14, 15, 16, 20, 21, 22, 25, 26, 28, 29, 30, 31, 45, 46, 47, 48, 50). The loads are specified by regulatory agencies while the material resistance information is supplied by material advocate groups.

Procedures using RBD for steel and concrete building structures have been developed in the United States, Canada and Europe (1, 11, 12, 14, 15). A summary review of these developments can be found in the paper by Goodman (29) and more details can be obtained from the references provided.

---

(1) Manager, Research & Development Department, American Plywood Association, Tacoma, Washington.
(2) Associate Professor, College of Forest Resources, University of Washington, Seattle, Washington.
(3) Senior Scientist, Research & Development Department, American Plywood Association, Tacoma, Washington.

The use of RBD methodology for timber is beginning to appear in Europe and Canada (11, 15). Of special interest in Europe is Euro Code 5, a set of common unified rules for timber structures (15) which uses RBD concepts. The draft code has been undertaken by members of the Commission of the European Communities and is expected to have significant influence in Western Europe. In Canada, a new Canadian standard has been devoted to the engineering design in wood (limit states design) (11).

In the U.S., the 1982 American National Standards Institute (ANSI) document "Minimum Design Loads for Buildings and Other Structures" (22) provides RBD methodology to establish the loads. This activity is primarily the result of work by the National Bureau of Standards with support from the concrete and steel interests.

The level of RBD technical activity for timber design in the U.S. is quite low. A task group of the ASCE (American Society of Civil Engineers) Committee on Wood is working on a preliminary design aid, but there is no major research effort underway at the present.

Portions of this paper were presented at a workshop on Reliability-Based Wood Design, held at Purdue University, April 21-23, 1986.

Current design methods and engineering data for structural wood panels are given in the Plywood Design Specification (4) and in other APA technical literature specified to end-use requirements. Currently engineering properties are derived from small clear wood specimen data based on limiting species characteristics in each species grouping. This technical foundation, while adequate in the 1960s, is badly outdated in the 1980s due to addition of species (over 70 in use) and rapid changes in production technology.

Innovative glued composite products are being introduced in increasing frequency which enhance the potential for full utilization of the wood resource.

The objective of this paper is to provide an overview of one approach being considered by American Plywood Association (APA) staff to develop a rationale for characterizing mechanical properties of structural-use panels and structural composite lumber. Ideally, the program will be compatible with emerging reliability based design (RBD) procedures.

Before reviewing the characterizing procedures and discussing example data sets, the framework established for trademarking and sampling of production will be discussed. This background information is necessary if we are to assess the potential usefulness of the new system as a design aid for engineers and architects. Accordingly, our discussion will consider the task ahead by examining the following:

-- Products

A brief review of product classification.

-- Standards

Review the major changes for evaluation and certification of product performance.

-- Sampling & Testing

Overview of the APA "in-grade" testing program.

-- Resistance

For two sample data sets, examine methods of characterizing strength and stiffness data.

-- Reliability

A snapshot of the relative reliability of the sample data as measured by computing a beta using the Rackwitz-Fiessler algorithm.

-- Design Factor

A brief commentary on the need for procedures to establish design influencing factors.

BACKGROUND

The primary market for structural panels and structural composite lumber is light-frame construction (low-rise and residential structures). These products tend to be long-lived, durable goods which are manufactured and distributed in standard sizes and grades. In the case of panels, these "standard" grades are manufactured in over 170 facilities, yielding over 25 billion square feet (3/8" based) in 1986. Thirty-four percent of this is produced in the Western U.S., 48 percent in the South, 10 percent in the Inland Empire, and 8 percent in the northern tier of states (7). The resulting product is a broad mix of species and production technology which is marketed under a unified system.

Structural composite lumber is an industry which is in the developing stages. It is expected that a performance based system will also be implemented yielding a structure similar to that which

exists for panels, e.g., an array of species and production technology being certified under a system which unifies the trademarking process.

To better understand the existing system, a discussion of the product types and their standards will follow.

The Products

Structural panel products include plywood, oriented strand board, waferboard, COMPLY*, and structural particleboard. Structural composite lumber includes laminated veneer lumber (LVL), and parallel strand lumber (PSL). Each product is discussed briefly, reviewing the raw material resource and basic product structure.

COMPLY Panels and Lumber. Since 1976 several manufacturers have produced COMPLY, which features face veneers bonded to a structural wood core. The panel product looks much like plywood because the veneer used for the face and back is identical to that used in standard plywood production. While plywood utilizes veneer in its interior laminations, COMPLY utilizes structural composite boards made from strands, flakes or wafers. Cross alignment of the particle core considerably enhances overall panel dimensional stability and improves cross-panel strength and stiffness.

The panel manufacturing procedures used are either a one- or two-step process. In a two-step manufacturing process the core is made separately and transferred to a conventional plywood plant for processing to the finished composite product. In a one-step process where the wood particles composing the core are laid directly

*Comply is a registered mark of the American Plywood Association

on the veneer sheets, the top sheets are then placed and the entire panel pressed in a single-step operation.

Composite studs and joists have been prepared utilizing structural particleboard cores and veneers to produce lumber substitutes (19, 35, 41). Again, the basic components are derived from structural panel plants, and have the advantages of consistent strength and stiffness in unlimited lengths. Size limitations (cross section) appear to be consistent with ordinary commodity lumber.

At one time five composite panel plants were in production. As of the first quarter 1986 only one plant is operating. One further announcement has been made for construction of a plant to produce COMPLY lumber.

Laminated Veneer Lumber. Since the late 1950s a variety of researchers have reported on various "super strength" beams manufactured from rotary peeled veneer. The products have come to be known as parallel laminated veneer (PLV) or laminated veneer lumber (LVL) (10, 33, 34, 36, 37). Generally, the products are manufactured from continuously laminating rotary peeled veneer into panels or billets in which all the veneer sheets are oriented in the same direction. The economics of these structural products is exemplified by the significant manufacturing facilities operated by the Trus Joist Corporation of Boise, Idaho (36).

Primary advantages of LVL are the dispersement of defects by utilizing veneer, and the attainment of very high stresses consistent with the highest grades of solid sawn lumber.

As of the first quarter of 1986, two companies were in production and two additional companies have announced plans to construct a plant.

Oriented Strand Board. Oriented strand board is a panel product composed of three to five layers of strands or rectangular shaped flakes. The flakes are typically three to five times longer than they are wide. Strands are produced (by a variety of flaking machines) from round wood, which are logs transferred directly from the forest (18, 24, 27, 49).

The product gets its name from the fact that the strands are oriented; that is, strands within a layer are aligned in the same general direction. Each layer is oriented perpendicular to the next, much as the veneers in plywood are perpendicular to one another in alternating layers. Strand alignment on the faces is typically parallel to the long or 8-foot direction, with cross-alignment of one or more layers in the interior of the product.

Orientation is perceived to provide considerable product flexibility in that it may be designed with stiffness and strength characteristics in particular panel directions.

Oriented strand board is typically manufactured with liquid phenolic resin and wax applied just prior to pressing. The use of liquid phenolic resin typically results in slightly darker appearance to the board. The strand or rectangular wafer geometry provides a somewhat different surface appearance than other flake-board products.

As of the first quarter 1986, there are eight oriented strand board plants in production with several others announced.

Particleboard. Particleboards typically differ from other struc-
tural products such as waferboard or oriented strand board in that
the raw material source is typically the residue of other solid
wood processing operations. Consequently, the particles from which
the board is manufactured tend to be very small and have short par-
ticles. Certain of these products can be used structurally in
light frame construction. Such products typically will gain their
additional strength and stiffness from either higher resin content
and/or additional product thickness along with increased density
(2, 13). Because of the resulting cost differential the percentage
of product manufactured under these constraints is very small. One
plant was currently producing such a product in the first quarter
of 1986 (42).

Parallel Strand Lumber. Another more recent proposal has been to
produce structural lumber substitutes using parallel strand lumber
(PSL). Such schemes would develop cross sections in a continuous
process using strands developed either from veneer or other
processes utilizing round wood as the basic raw material source.
Again, the perceived advantages are unlimited sizes and lengths,
consistent properties and very high mechanical properties.

As of the first quarter of 1986, one plant is in production.

Plywood. The first production runs of softwood plywood took place
in the U.S. West Coast in the early 1900s. Production capacity
continued to build on the West Coast until the early 1960s when
southern pine plywood was introduced. Currently nearly half the
construction plywood industry (capacity basis) exists in the
southeastern United States with the remaining plants in the Inland
Empire and West Coast of the United States (7, 18).

Plywood is produced from veneers which are laid up in alternate layers, each layer being perpendicular to the other. By altering veneer thickness, ply orientation and species, plywood has demonstrated considerable versatility in being useful for a wide variety of industrial and residential construction market areas. Continuing research over the past twenty years has enabled plywood to enter many diversified markets, primarily due to a sound data base. Currently, approximately 56 percent of plywood's markets are tied directly to new residential construction or construction activities associated with repair and remodeling (7). The remaining material finds its way into a variety of end uses such as products made for sale; materials handling; plant repair and maintenance; and the transportation market. Additional uses include concrete forming, farm buildings and a wide variety of miscellaneous applications. As of the first quarter 1986 approximately 170 individual plywood mills were producing. Their total in-plant capacity exceeds 22 billion square feet on a 3/8" basis.

Waferboard. Waferboard is a structural panel first produced in Canada in 1966. Since then it has spread to several Canadian and U.S. manufacturing locations. Plant locations, as for OSB, are taking advantage of low raw material costs in central and eastern Canada, and central and upper midwestern U.S.

Waferboard is generally manufactured from low density hardwoods (most predominantly aspen), although other manufacturers are considering the utilization of spruce, southern pine and western softwoods.

The product is composed of a rather large squarish (2" x 2" to 3-1/2" x 3-1/2") wafers. These wafers are flaked from roundwood

and are generally bonded together with a powdered phenolic resin
(24, 42).

Waferboards are typically produced in three random layers. The
largest flakes possessing the best mechanical properties, are laid
on the faces of the panel, and the fines and other smaller flakes
being utilized as core material. More recently, most manufacturers
have begun orientation of the panel faces using more rectangular
wafers -- thus approaching the OSB concept.

As of first quarter 1986, twelve waferboard (and oriented wafer-
board) plants existed in the Continental United States. There are
eleven similar plants in the Canadian provinces.

The Standards

Product Standards. Historical standards, against which wood based
panel products have been manufactured, have been product standards
such as PS 1-83 for Construction and Industrial Plywood, or ANSI
208.1 (2) for Mat-Formed Wood Particleboard. National consensus or
product standards are most frequently promulgated through organiza-
tions such as the American National Standards Institute (ANSI), or
the U.S. Department of Commerce.

Review of the product or commodity standards reveal that they are
essentially manufacturing prescriptions for minimum product.
Requirements are centered around the specific manufacturing
process, and typically do not address the question of product
application nor how well the product is suited for any particular
application.

<u>Performance Standards</u>. A performance standard, such as that promulgated by the American Plywood Association for APA Rat d Sheathing and APA Rated Sturd-I-Floor (4), reverses the standards process by defining the end use of the product and does not prescribe how the product will be made. The objective of a performance standard is to assure for a particular end use that the product will satisfy the requirements of the application for which it is intended. To do this the performance standard must define performance criteria and test methods. Performance standards are limited in application to the intended end use.

In the case of the two standards currently promulgated by APA, that for single layer floors (APA Rated Sturd-I-Floor) and that for sheathing (APA Rated Sheathing), the intended end use is light-frame wood construction as practiced in the United States. Panels so rated are intended for combination subfloor-underlayment and sheathing intended for roofs, walls and subfloors. The products are span rated for their particular end use. The standards cover supports spaced 16 to 48 inches o.c. (400 to 1220mm) for floor and roofs. Provisions are also made for wall bracing when the studs (vertical framing elements) are spaced 16 or 24 inches o.c. (400 or 600mm).

The system results in a simple span index, which rates the panel for a single floor use, or a sheathing application where the index indicates its possible use at a maximum rafter or floor joist spacing.

The performance concept is being applied to structural composite lumber (LVL and PSL) but in this case for mechanical performance. A document under development by the APA will rate the product by

testing and follow up verification, as with panels. Other standards activity includes a subcommittee of ASTM D07 and an AITC Standard (3).

Requirements. Panel performance is evaluated through testing under a qualification procedure for three basic areas of investigation: structural adequacy, dimensional stability, and bond performance.

Testing for structural adequacy includes:

1. Verification of the ability to sustain concentrated loads, both static and following impact at the rated span.

2. Uniform loads testing demonstrates the ability of the product to sustain wind or snow loads at the rated span.

3. Fastener holding ability is tested to assure that the panel has the ability to hold covering materials in place and to develop lateral load capacity in mechanically fastened connections to lumber or other framing.

4. Wall sheathing panels must demonstrate shear resistance for wall bracing at the rated stud spacing.

Physical properties include measure of the expansion of the panels when exposed to moisture conditions. A performance test was developed which measures linear expansion when wetting on one side for a period of 14 days. This test approximates severe exposure conditions as might occur during construction and serves as a relative measure of linear expansion conditions that might be expected in service.

Finally, the bond durability of the panel must be demonstrated for site-built construction, since panels will be called upon to resist wetting and drying and still be able to perform following exposure in these conditions (43). Research indicates that large-scale specimens exposed to hot water soaking and oven-drying and then subjected to the same structural performance criteria is adequate evidence of the ability of the product to remain intact during exposure to weathering. These tests are equivalent to several years permanent exposure to the weather.

Qualification. Certification of performance is a straight-forward procedure under a performance-based system. To begin, a sampling of the candidate product is tested according to the individual performance criteria previously discussed. After completing the performance requirements a span rating can then be assigned.

Concurrent with performance-oriented tests, a "product evaluation" is also performed. Product evaluation provides for measuring properties unique to the product and suitable for quality assurance measurements. Such data includes bending strength and stiffness, thickness, density, and other manufacturing data which may prove useful in monitoring quality under a third-party basis.

A mill specification (4, 44) is drawn up following this intensive product evaluation. This individualized mill production specification is unique to the mill and product qualified under the performance standard. It pertains only to the mill and product qualified and is not a constraint on other mills or similar products.

The mill specification serves as the quality assurance document for future evaluation. The APA quality program provides for sampling

from each mill's production each day with testing and reporting at one of seven regional facilities. In addition, a quarterly sampling program requires ten panels (4 x 8 ft or 1.2 x 2.4m) per mill per quarter to be shipped to the APA Research Center in Tacoma. These panels are tested for conformance to the mill specification and will form the data base discussed later in the paper.

Acceptance. The Council of American Building Officials (CABO) is a joint venture of the Building Officials and Code Administrators International, Inc. (BOCA), the International Conference of Building Officials (ICBO) and the Southern Building Code Congress International (SBCCI). CABO has recognized the APA Performance Standards under their National Evaluation Report NER-108 (17). This research report constitutes approval by the sponsoring model code agencies and subsequent regional acceptances have since been secured by the APA technical staff.

PRODUCT CHARACTERIZATION

In anticipation of the need for new technical data, APA has been in the process of a significant product characterization study. This "in-grade" study is conducted under the provisions of the performance standard, and will lead to development of significant technical data on the characteristics of products produced by members of APA under the performance based standards. The program covers sampling, mechanical properties, physical properties, and data base management. While the example data used in this paper is for structural panels, the same basic concept and techniques are being used for LVL and PSL products trademarked by the APA.

Panel Sampling

Sampling of product occurs at two stages. First, during the product qualification stage previously discussed, a significant sample of product is taken under carefully supervised conditions. That is, the panel product is sampled at minimum manufacturing conditions such that minimum acceptable performance is evaluated. This initial bias provides a measure of the minimum product against the performance criteria, and is an indication of minimum lot performance. Products which satisfy the established performance criteria under these conditions are certified for production at manufacturing specifications at or above the levels sampled. Thus, the data leading to the development of the individual product manufacturing specifications becomes the baseline for future evaluation of the product.

The second level of data collection is a quarterly production sampling program. Under the provisions of the performance standard, a minimum of 10 panels per plant per quarter are tested by APA against the product's individual manufacturing specification. This evaluation provides an ongoing measure of product performance and continuing confirmation that the products are conforming to the provisions of the performance standard.

The panel sampling plan provides two significant opportunities. First, the initial biased sample provides an opportunity to evaluate minimum lot performance. The qualification sample is a snapshot of minimum product performance as produced by individual mills and products distributed over the country. Secondly, the quarterly sampling program provides an ongoing evaluation of products "as

produced" and can then be used to establish any trends in product performance.

Mechanical Properties

Panels sampled under the Performance-Rated Panel program are full-sized panels (4 ft x 8 ft or 1.2m x 2.4m). Properties collected under both the qualification or initial bias sample scheme and ongoing quarterly sampling include the following:

- Full-sized bending strength and stiffness.

- Tensile strength.

- Shear strength through the thickness.

- Shear strength in the plane of the product.

- Compression strength and stiffness.

- Bearing strength through the thickness.

- Modulus of rigidity.

Each of these basic mechanical properties are collected with stress along and across the major of the product when appropriate. Products are tested in the dry, as-received condition.

Data Base Management

To accommodate such a comprehensive sampling plan, encompassing a large number of products, constructions and geographic manufacturing regions of the country, a computer data base management system is utilized. Data base management schemes are most often firmware and software based systems which provide for easy assemblage of

complicated data schemes providing for quick ad hoc reporting as well as routine data manipulation and updating.

The computer-based data system is utilized for ongoing evaluation of quarterly sampling programs via control chart and statistical anaylsis schemes, as well as providing overall statistical analysis of mechanical and physical property data.

RESISTANCE CHARACTERIZATION

To illustrate the difficulties associated with characterizing the material properties of panels, two example data sets referenced as A and B, will be used. These example data sets are extracted from the APA data base and represent two classes of production, each class with the same span rating. The data are short-term panel bending capacities for strength (maximum moment) and stiffness (EI). The subsets were constructed from each class by placing them in ascending order and selecting data at equal intervals. The values shown have been normalized to illustrate the shape of the distribution and to minimize accidental misinterpretation. The data sets are intended for illustration of actual performance but should not be interpreted as representing the entire production population.

Distribution Fitting

The parent distribution for material resistance is usually an unknown entity. The approach generally followed in establishing distributional form is to "fit" recognized statistical distributions to data sampled from the parent population of interest. This is accomplished by using the sample data in estimating parameters

for each selected distribution. The distributional form which provides the "best fit" is chosen to represent the distribution of the parent population. Basis for "best fit" may vary for unique purposes. For example, the "best fit" estimator may be quantitative, qualitative (visual comparison of observed versus theoretical probability density functions (pdf)), or a blend of both. In addition, the entire range of sample data may be studied or a subset (e.g., lower range of strength capacity) of the range may be considered as most important. In development of RBD procedures, an objective is to determine a "reliability index" which relates the overlap of the high end of one distribution (e.g., load) over the low end of another distribution (e.g., load capacity). In RBD, specific ranges of distributions are of paramount importance. On the other hand, if the purpose in distribution fitting is for simulation applications, the entire range of data is important. Visual comparison of the observed and theoretical pdfs provides a useful measure of fit which allows study over an entire range or specific subsets of ranges.

Example cumulative distributions for stiffness and maximum moment capacity are shown in Figures 1 and 2, respectively.

Data sets A and B may be considered to represent a class of production within a span index classification. Recall that the span index is the basis for trademarking and is established by test. The sets A and B reflect the differences that we might experience between product types, between mills for the same product type, or between geographic production regions. These sets reflect a problem common to characterizing data which represents

commodity production, e.g., where there is little economic incentive to create many categories of use.

Four probability density functions were used to characterize the measured values. The four pdf's used were:

1. Normal (two parameters)

2. Lognormal (two parameters)

3. Weibull (three parameters)

4. Johnson Sb (four parameters)

The mathematical forms have not been reproduced here but may be found in the statistical references listed (32). The parameters were determined via computer software which used a maximum likelihood technique to determine the respective pdf parameters (23).

The resulting best fit densities for stiffness are shown in Figure 3 for classes A and B. Similar fits are shown for strength in Figure 4. The statistical analysis revealed that of the four, the lognormal distribution best fit the data as measured by the log-likelihood value. Table 1 notes the log-likelihood values for each class property combination. Note that in some cases the three parameter Weibull may provide a slightly better fit as determined by this measure. Note also in Table 1 that the difference between some of the distributions is not great.

Figure 5 illustrates the relationship between the pdf's estimates and the actual data. We note for this case as much as 4.8 percent error in estimating what might be taken as the design point (5th percentile level).

Reliability

The objective of characterizing test results in terms of probability distributions is to assess the reliability of the products in actual use. The reliability index, β, is a statistical parameter which serves as a measure of the uncertainty in the variables that are involved in the design of a structure or component of a structure (20, 21, 22, 25). The following discussion indicates how reliability can be estimated for typical panel strength and deflection limit states. The reliability index is determined using a first order second moment procedure. A linear failure surface is assumed with live and dead loads only and the reliability is calibrated to current practice. The calculations are based on short term strength and stiffness data which does not include the affects of damage accumulation which in fact takes place over time.

Ultimate Strength Reliability. The conventional design equation for panels can be expressed as:

$$R_n > L_n + D_n \qquad\qquad\qquad\qquad\qquad\qquad [1]$$

where:

R_n = Nominal bending capacity (moment)

L_n = Nominal maximum live load (moment)

D_n = Nominal maximum dead load (moment)

The equation, [1], is sustained from strength of materials arguments and serves as the basis for a general equation defining the failure surface, g(R, L, D):

$$g = R-L-D \qquad\qquad\qquad\qquad\qquad\qquad\qquad [2]$$

where:

R, L, D are random variables representing moment capacity

for resistance, live and dead loads.

Clearly, if the panel capacity is exceeded by the sum of the

applied moments (g becomes negative) the system will be considered

unsafe. The reliability of the panel underload is related to the

probability that the failure surface will be negative.

The failure surface can be rearranged as follows:

$$g = (\frac{R}{R_n} - W_1 \frac{L}{L_n} - W_d \frac{D}{D_n}) R_n \quad \ldots \ldots \ldots \ldots \ldots \ldots \text{[3]}$$

where:

$$W_1 = L_n/R_n$$
$$W_d = D_n/R_n$$

Furthermore, using the current design formulae, $R_n = L_n + D_n$, the

failure surface can then be expressed in terms of currently used

nominal values, resulting in:

$$W_1 = (L_n/D_n)/(1 + L_n/D_n)$$

and

$$Wd - 1/(1 + L_n/D_n) \quad \ldots \ldots \ldots \ldots \ldots \ldots \ldots \text{[4]}$$

If R, L, and D are attributed normally, then it can be shown that g

is normally distributed with mean, μg:

$$g = \frac{R}{R_n} - W_1 \frac{L}{L_n} - W_d \frac{D}{D_n} \quad \ldots \ldots \ldots \ldots \ldots \ldots \text{[5]}$$

and standard deviation, σg:

$$g = [(\frac{R}{R_n} CV_r)^2 + (W_1 \frac{L}{L_n} CV_1)^2 + (W_d \frac{D}{D_n} CV_d)^2]^{1/2} \quad \ldots \text{[6]}$$

where:

  X/X_n = Mean of random variable, R, L, or D

  CV_x = Coefficient of variation for the random variables, R, L, or D

The probability that g is negative (g $<$ 0) can be found from a standard normal probability table using $Z = -\beta$

 where:

$$\beta = \mu_g / \sigma_g \quad . \quad . \quad . \quad . \quad . \quad . \quad . \quad . \quad . \quad . \quad . \quad . \quad . \quad . \quad . \quad . \quad [7]$$

The quantity, β, is referred to as the reliability index. In general, the variables R, L, and D are not normally distributed but a modification of the calculation procedure can be made to retain the second moment approach. The modification involves replacing X/X_n and CV_x by corresponding values characterizing normal distributions in the appropriate extreme regions of the original distributions. This resulting reliability index, defined by Hasofen and Lind (48) results in the shortest distance between the origin and the failure surface in this now normalized system.

Using the traditional (deterministic) design values published by APA (5), a calculation was made for the reliability index, beta, associated with the short-term moment capacity distributions of A & B class panels. The procedures for this calculation have been discussed elsewhere (20, 21, 22), but the specific program used was developed by Dr. Joseph Murphy at the Forest Products Laboratory, Madison, WI (40). The reliability index is shown as a function of a live to dead load ratio (Lo/Dn) in Figure 6 for both A and B classes. A lognormal distribution was used for both classes in this example. Since traditional design is based on a Lo/Dn ratio in the region of 6, an estimate of the reliability index for A and

B classes is 3.45 and 3.56, respectively. Clearly, the use of these panels is associated with high levels of reliability.

Serviceability Reliability. Most discussions on the reliability index have considered strength as the primary limit state (9, 21, 29, 30, 45, 46, 47). For many wooden structures, the controlling design parameter is deflection rather than strength. A recent effort by Galambos and Ellingwood (26) provides some insight into this subject, as well as a methodology for computing the reliability index.

Galambos and Ellingwood (26) provide ratios of mean/nominal load with corresponding coefficients of variation (CV). They suggest that loading criteria for ultimate limit states, based upon 50-year mean recurrence intervals, are too severe for most serviceability needs. An eight-year reference is used with consideration given to a one-year reference when the serviceability limit state is recoverable. Ratios of mean/nominal snow loads of 0.45 and 0.20 are presented for eight-and one-year reference periods, respectively. The corresponding CV for the eight-year reference period is 0.35 with a CV of 0.75 for the one-year reference period.

Assuming a log-normal distribution of snow loads, these statistics allowed simulation of snow loads in concert with simulation of load capacities. Load capacities were generated using design criteria consistent with the span rating of the example data sets and by assuming a log-normal distribution of panel stiffness. This simulation study provides a preliminary performance index for each

of example Sets A and B. For the eight-year reference period the serviceability reliability indices range from about 3.0 to 3.2 and increase to an average of about 3.3 for the one-year referenece period.

Since the deterministic methodology considers average deflection performance, this again appears to result in high levels of reliability for deformation.

Commentary on Reliability

Given that an initial first "cut" at estimating reliability of panel strength (moment capacity) indicates a very reliable situation, are there any problems associated with this calculation? If so, what are they and what are the consequences? One problem has to do with the data sets themselves. The data set of moment capacities of A may be a collection from many manufacturers using different species, adhesives, production techniques, showing change in operating characteristics over time. Thus, the data set is not a homogeneous collection of values. Many underlying frequency distributions are possible; consequently, it seems that no one theoretical distribution will characterize the distribution (see Figure 4). Moreover, there is a large coefficient of variation due to the wide range of property values being produced by the many different manufacturers. Since the data set is large, the characterization is undoubtedly adequate to assure safety for the particular span rating analyzed. It will be noted that both panel types are rated for the same end-use. Does it make sense to combine the A and B class data? The whole question of combining for products destined for identical end-uses needs to be studied since it could impact the practical needs of marketing and distribution.

Another concern is associated with the criteria for selecting the most appropriate form of probability density function to characterize the data set. Basically, the shape of the lower tail of the distribution influences the value of the safety index. The tails of the four distributions used in this study are quite different (Figure 5). If very large data sets are available, it may be possible to use a relatively large subset consisting of values in the lower tail to make more accurate determinations of the safety index.

We have found that the distribution type significantly impacts the calculated reliability index, beta. We suspect that if selection of the pdf is made on the basis of a statistic which measures the "global" goodness of fit, that greater errors could be encountered as the tail of the resistance distribution determines beta for strength limit states.

Finally, it should be mentioned that although the moment capacity distribution of Class A is greater than Class B (Fig. 1), which of course leads to a higher reliability index, there is a dynamic component to this industrial segment whereby manufacturers are changing their operations by equipment, species or new technology. Consequently, the distributions are changing and thus so is the reliability index for this set of panels. However, since the safety index appears to be large there is the possibility of setting a fixed level of the safety index and allowing manufacturers to produce panel products that will satisfy this level of safety.

FACTORS INFLUENCING ENGINEERING DESIGN PROPERTIES

A product characterization study will provide insight to performance of products as produced and tested under laboratory conditions. Clearly, there is a myriad of factors which influence the performance of mechanical properties and, consequently, structural design. A few of the most important structural properties will be addressed here in the hopes of stimulating thought toward solutions.

In-Service Performance

A variety of techniques have been used to address the in-service load performance of wood structural systems. These include creep studies, creep rupture studies, and evaluation of product after long-term in-service use. Given the time-consuming factors of creep and creep-rupture studies, it appears that some potential alternative means to identify the peformance of these products is needed. In conjunction with that, a North American duration of load committee of interested industry principals has been established in cooperation with the Forest Products Laboratory in Madison, Wisconsin and Forintek's western lab. These deliberations may provide a structured approach to providing short-term conservative answers and development of data which will give us longer term information.

Environmental Effects

A variety of environmental factors must be assessed and their influence determined. Such areas include moisture effects, temperature, corrosive chemical environments and the like. A

priorities list needs to be developed and assessed so these factors may be included in any design format.

Fasteners

Standardized methods of fastener evaluation for both lateral load-slip modulus and ultimate lateral loads need to be established. With the significant variation in fastener size and stock stiffness, better methods of grading and identification are needed for engineering design.

Effect of Treatments

Little data exists on the effect of pressure treatments for preservatives and fire retardants on mechanical properties of structural-use panel products. Basic impacts of these procedures is needed as volumes of treated material grows.

Commentary on Factors

This brief discussion indicates that there are many strength and stiffness reducing factors which must be considered by the design engineer. A preliminary review of the existing literature and discussions for determining factored resistance have shown that these procedures and techniques are not well established. Consequently, establishing factors which could have great influence on the resulting design and the economics of the use of the product should be carefully contemplated by the architects of an RBD format. Sample sizes, study designs, requirements for establishing these factors and the reliability of those factors needs to be addressed by the proponents of this design format.

SUMMARY

Our discussion has reviewed the commercial "facts of life" that a significantly different set of generic product types is being manufactured and marketed under a uniform span rating system for use in light-frame construction. The system represents a vast production volume, inclusion of over 70 some species and many product types enhancing the complexities of implementation of a reliability based design format.

In reviewing the performance based standards under which these products are rated, it was indicated that a significant in-grade sampling and testing procedure is underway. This data will provide the ability to characterize minimum product as well product as produced over time. This is providing a significant data base from which the resistance of products rated under this system can be characterized.

Two example data sets were extracted from the APA in-grade testing program representing two hypothetical production classes A and B. For each production class we noted differences in the distribution shapes, tails and their locations. When evaluated for the reliability index, we obtained different results for the production classes and their respective assumed distributions.

Additionally, it was pointed out that to successfully characterize products for engineering design factored resistance data needs to be developed to indicate strength reducing and/or stiffness reducing criteria. It was pointed out that while the physical studies to determine these factors can be undertaken, that no good solutions to determining these factors and their reliability in the

overall RBD based code format currently exist. It seems that the influence of each of these individual factors on the reliability of the entire design system needs to be evaluated by a rational process.

CONCLUSIONS/RECOMMENDATIONS

From examination of material characteristics and reliability analysis for structural panel products, we have determined that preliminary data indicates a high overall reliability. However, in examining the requirements for implementing an entire system for the structural composite products the need for additional research in the following areas seems to be warranted.

1. Numerical solutions. The validity of using numerical solutions to characterize the lower tail distributions for implementation of an RBD procedure seems appropriate when large data sets are available.

2. Combined or composite distributions. The impact of combining or otherwise providing overall evaluations of reliability for very large production based systems such as structural composite panels needs to be assessed.

3. Reliability index. The computed beta seems to be very sensitive to distribution types. Interpretation of the variability of beta, given different sampling schemes, seems very important, especially in light of new products entering a market with no service history.

4. <u>Resistance factors</u>. It appears that assessment and
    development of evaluation schemes from the mathematical
    viewpoint needs to be developed.

SELECTED BIBLIOGRAPHY

1. American Institute of Steel Construction. 1983. Proposed
   Load and Resistance Factor Design Specifications for
   Structural Steel Buildings. AISC, Chicago, IL.

2. American National Standard Institute. 1979. Mat-formed wood
   particleboard. American National Standard ANSI A208.1.

3. American Institute of Timber Construction. 1982. Standard
   for laminated veneer lumber (LVL) used in structural glued
   laminated timber. AITC 402-83. Englewood, CO.

4. American Plywood Association. 1980. Performance standards
   and policies for APA structural-use panels. American Plywood
   Association, Tacoma, WA.

5. _____. 1973. Plywood Design Specification Form
   Y510J/Revised Dec. 1983. American Plywood Association,
   Tacoma, WA.

6. American Society for Testing and Materials. 1978.
   Performance of wood and wood-based floor and roof sheathing
   under concentrated static and impact loads. ASTM Standard
   E661-78. ASTM, Philadelphia, PA.

7. Anderson, R. G. and J. J. Hutton. 1985. Regional production
   and distribution patterns of the structural panel industry.
   Economics Report E39. American Plywood Association, Tacoma,
   WA.

8.   Bodig, J. and B. A. Jayne. 1982. Mechanics of wood and wood composites. Van Nostrand Reinhold Co., New York, NY.

9.   Bulleit, W. M. 1985. Relative Reliability of Dimension Lumber in Bending. Journal of Structural Engineering, VIII, U9, pg. 1984.

10. Bohlen, N. C. 1972. LVL-development and economics. Forest Products Journal 22(1):18.

11. Canadian Standards Association. 1984. Engineered Design in Wood (Limits States Design). National Standard of Canada CAN3-086. 10M84. CSA, Toronto, Ontario, Canada.

12. _____. 1974. Steel Structures for Buildings - limit states design, CSA Standard S16.1. CSA, Toronto, Ontario, Canada.

13. Carll, Charles G., H. Edward Dickerhoof and John A. Youngquist. 1982. U.S. wood-based panel industry: standards for panel products. Forest Products Journal 32(7):12.

14. Committee European du Beton. 1976. First order reiability concepts for design codes, Bulletin d'Information No. 112, Munich, West Germany.

15. Commission of the European Communities. 1985. EURO Code 5. Common Unified Rules for Timber. Draft of October 1985.

16. Cornell, C. A. 1969. A probability-based structural code. Journal of the American Concrete Institute, V66, N12.

17. Council of American Building Officials. 1980. Report No. NRB-108. APA structural-use panels. Whittier, CA.

18. Dickerhoof, H. Edward, J. A. Youngquist and C. G. Carll. 1982. U.S. wood-based panel industry: production trends and changing markets. Forest Products Journal 32(16):14.

19. Duff, J. E. and G. A. Koenigshof, D. C. Wittenburg. 1978. Performance standards for COMPLY floor joists. USDA Forest Service Research Paper SE-192. Southeastern Forest Experiment Station, Athens, GA.

20. Ellingwood, B. 1983. Probability-based load criteria for Codified design. Fourth International Conference on Application of Statistics and Probability in Soil and Structural Engineering. University di Frenze (Italy).

21. _____ and T. Galambos, J. MacGregor, C. A. Cornell. 1981. Probability-based Load Criterion for Structural Design. Civil Engineering - ASCE, July p. 74.

22. _____. 1980. Development of a probability-based load criterion for American National Standard A58. NBS Special Publication 577, U.S. Department of Commerce, NBS.

23. Engineering Data Management. 1984. Statistical Data Management Software EDM, 736 Whalers Way, Ft. Collins, CO.

24. Ethington, R. L. (Editor). 1978. Structural flakeboard from forest residues. USDA Forest Service. General Technical Report WO-5. Washington, DC.

25. Galambos, T. V. and M. K. Ravindra. 1976. Load and resistance factor design criteria for steel beams, Research Report No. 27, Civil Engineering Department, Washington University, St. Louis, MO.

26.   _____ and B. Ellingwood. 1986. Serviceability Limit States: Deflection. Journal of Structural Engineering. Vol. 112, No. 1, Paper 20286.

27.   Geimer, R. L. 1976. Flake alignment in particleboard. USDA Forest Service Research Paper FPL275, Madison, WI.

28.   Goodman, J. R. 1983. Developments and potentials in timber engineering. International Union of Forestry Research Organizations, Plenary Paper. Madison, WI.

29.   _____. Z. Kovacs and J. Bodig. 1981. Code comparisons of factor design for wood. Journal of the Structural Division, ASCE 107, No. ST8, prov. paper 16423.

30.   _____ _____, M. D. Vanderbilt, M. E. Criswell, and J. Bodig. 1981. Probability based design of wood transmission structures, Research Institute of Colorado, Ft. Collins, CO. Final report (three volumes) to Electric Power Research Institute.

31.   Goodman, J. R., Chairman. 1979. Important research needs in wood as a structural material. Journal of the Structural Division, ASCE Vol. 105 No. ST10, prov. paper 14893.

32.   Hahn, G. J. and S. S. Shapiro. 1967. Statistical Models in Engineering. John Wiley and Sons, New York, NY.

33.   Jung, J. 1982. Properties of parallel-laminated veneer from stress-wave-tested veneers. Forest Products Journal. 32(7):30.

34. Koch, P. 1967. Super-strength beams laminated from rotary-cut southern pine veneer. Forest Products Journal. 17(6):42.

35. Koenigshof, G. A. and D. C. Wittenburg. 1978. Structural performance standards for COMPLY partition studs. USDA Forest Research Paper SE-181. Southeastern Forest Experiment Station, Athens, GA.

36. Kunesh, R. H. 1978. Micro-Lam: structural laminated veneer lumber. Forest Products Journal. 28(7):41.

37. Laufenberg, T. 1982. Exposure effects upon performance of laminated veneer lumber and glulam materials. Forest Products Journal. 32(5):42.

38. Marra, G. G. and John A. Youngquist. 1981. Wood composites. Chemtech, July, p. 418-421.

39. Marra, G. G. The future of wood as an engineered material. 1972. Forest Products Journal 22(9):43-51.

40. Murphy, J. 1984. Personal Communication and Beta Calculation Software. Forest Products Laboratory, Madison, WI.

41. McAlister, R. H. 1978. Structural properties of COMPLY studs. USDA Forest Service Research Paper SE-180. Southeastern Forest Experiment Station, Athens, GA.

42. O'Halloran, M. R. and J. A. Youngquist. 1983. An Overview of Structural Composite Products. Proceedings of Structural Wood Research. State-of-the-Art and Research Needs Workshop. Milwaukee, WI. American Society of Civil Engineers.

43. _____ and C. M. Erb. 1981. Performance-based testing for durability. Proceedings, Fifteenth International Particleboard Symposium, Washington State University, Pullman, WA.

44. _____. 1980. The performance approach to acceptance of building products. Proceedings, Fourteenth International Particleboard Symposium, Washington State University, Pullman, WA.

45. Ravinda, M. K. and T. Galambos. 1978. Load and resistance factor design for steel. Journal of the Structural Division, ASCE Vol. 104, NST9, p. 1337-1353.

46. Sexsmith, R. G. and S. P. Fox. 1978. Limit states design concepts for timber engineering. Forest Products Journal. 28(5).

47. Suddarth, S. K., F. Woeste and W. L. Galligan. 1978. Differential reliability: probabilistic engineering applied for wood members in bending/tension. U.S. Forest Products Laboratory Research Paper FPL 302.

48. Thoft-Christensen, P. and M. Baker. 1982. Structural Reliability Theory and its Application. Springer-Valley, New York.

49. Youngquist, John A., Charles G. Carll and H. E. Dickerhoof. 1982. U.S. wood-based panel industry: research and technological innovations. Forest Products Journal 32(8):14-24.

50. Zahn, J. J. 1977. Reliability based design procedures for wood structures. Forest Products Journal. 27(3):21.

Table 1. Log-likelihood indicator (maximum logarithm of the likelihood function) of distribution goodness-of-fit.

Distribution	Class			
	A		B	
	Stiffness	Strength	Stiffness	Strength
Normal	-398.2	-519.5	-387.1	-497.2
Lognormal	-388.9	-494.9	-379.5	-481.6
Weibull	-394.6	-501.6	-378.9	-483.4
Sb	-394.0	-498.0	-394.0	-481.7

* Maximum of log-likelihood indicator

CUMULATIVE FREQUENCY (%)

STIFFNESS (EI) ALONG

+ Population "A"
o Population "B"
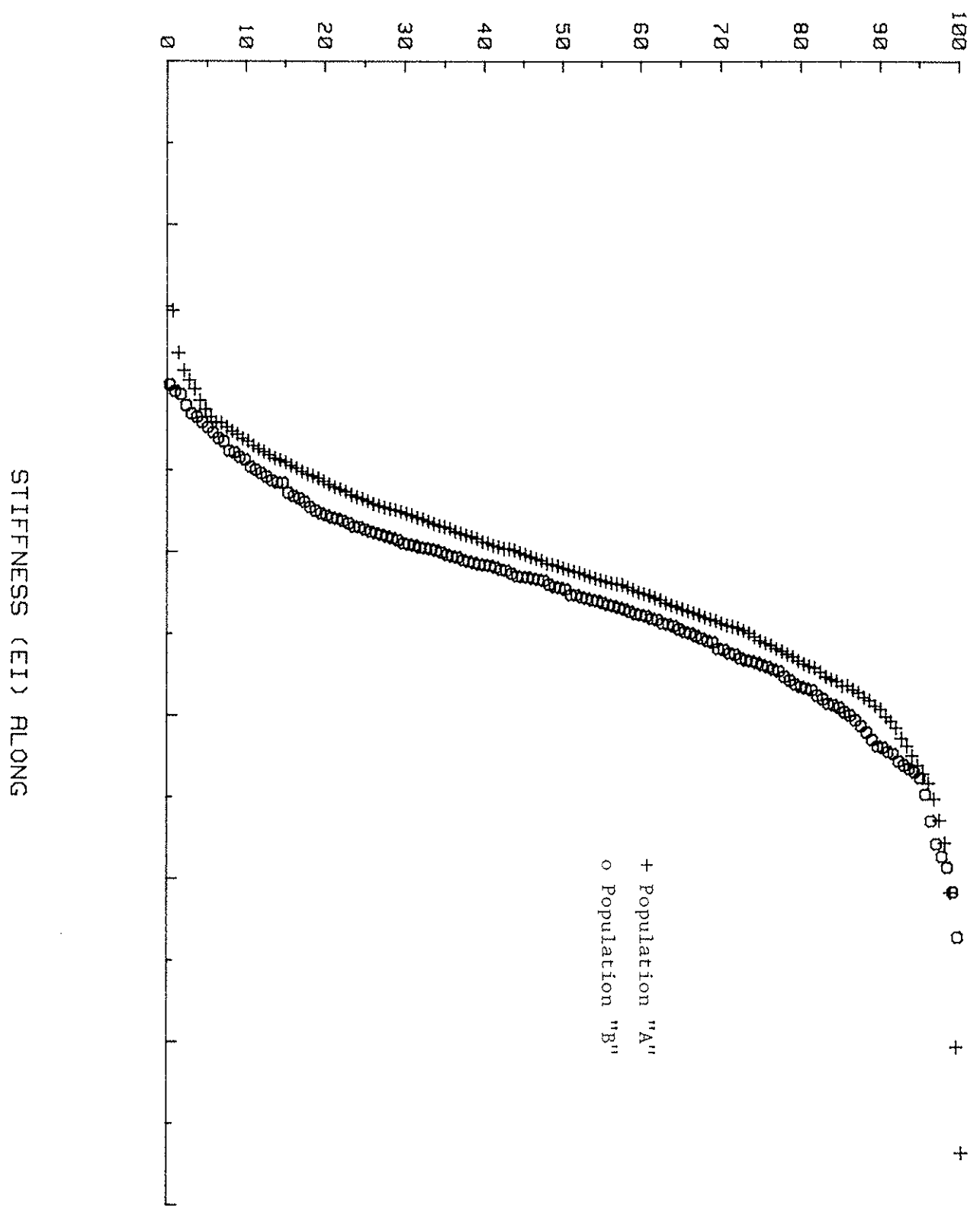
FIGURE 1. CUMULATIVE DISTRIBUTION FOR STIFFNESS (EI) ON TEST POPULATIONS "A" AND "B".

CUMULATIVE FREQUENCY (%)

MAXIMUM MOMENT ALONG

+ Population "A"
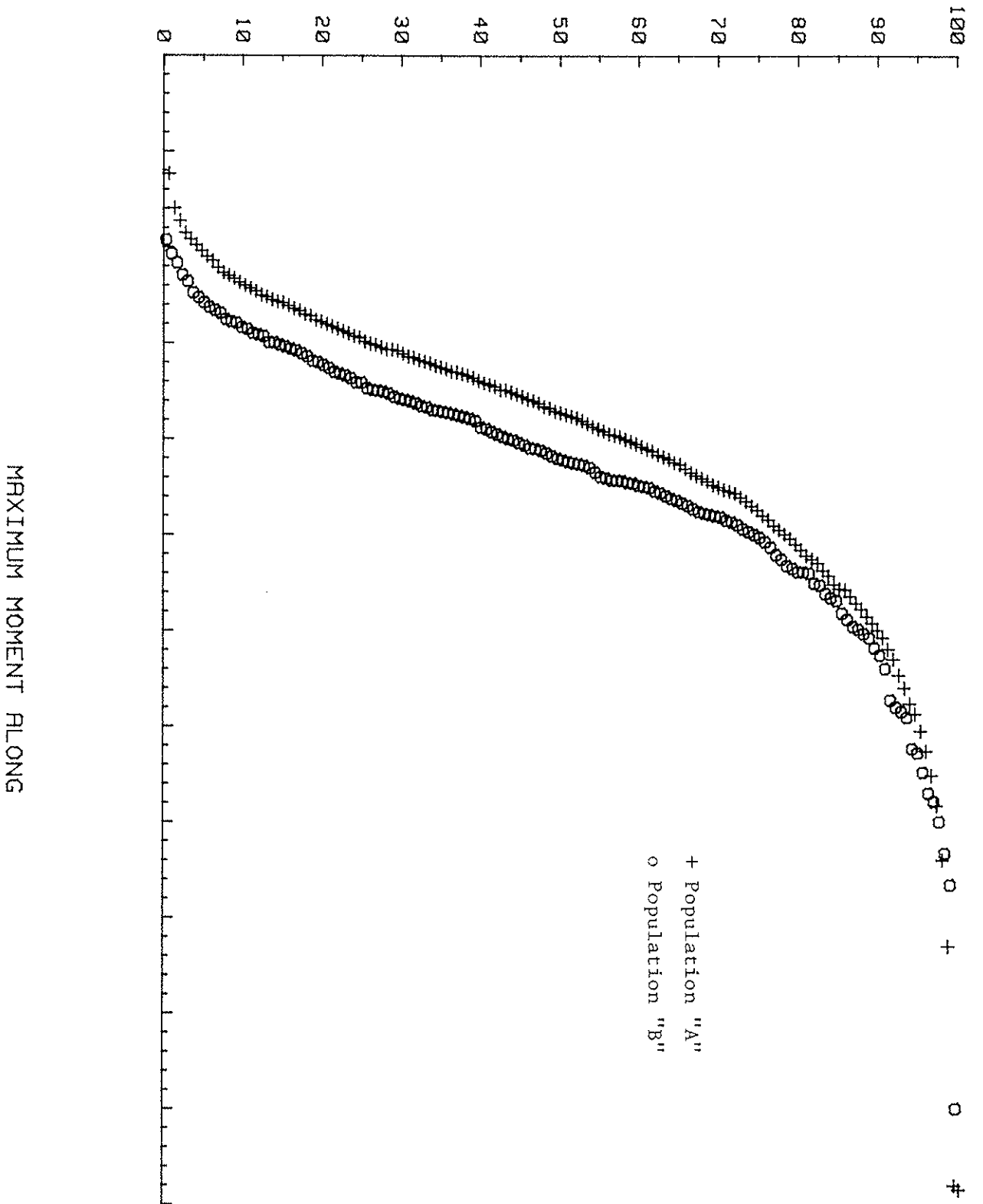
o Population "B"

FIGURE 2. CUMULATIVE DISTRIBUTION FOR STRENGTH (MAXIMUM MOMENT) ON TEST POPULATIONS "A" AND "B".
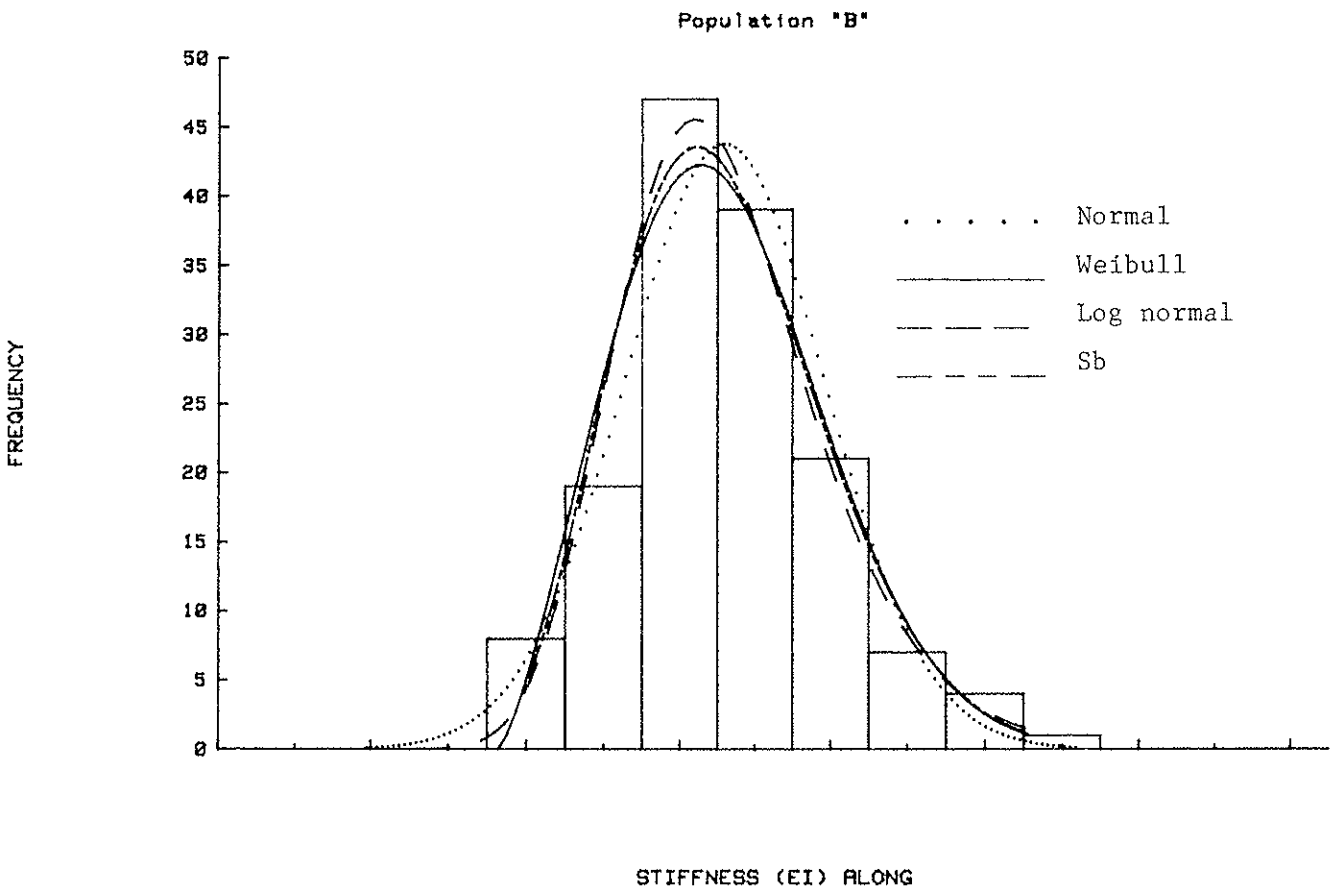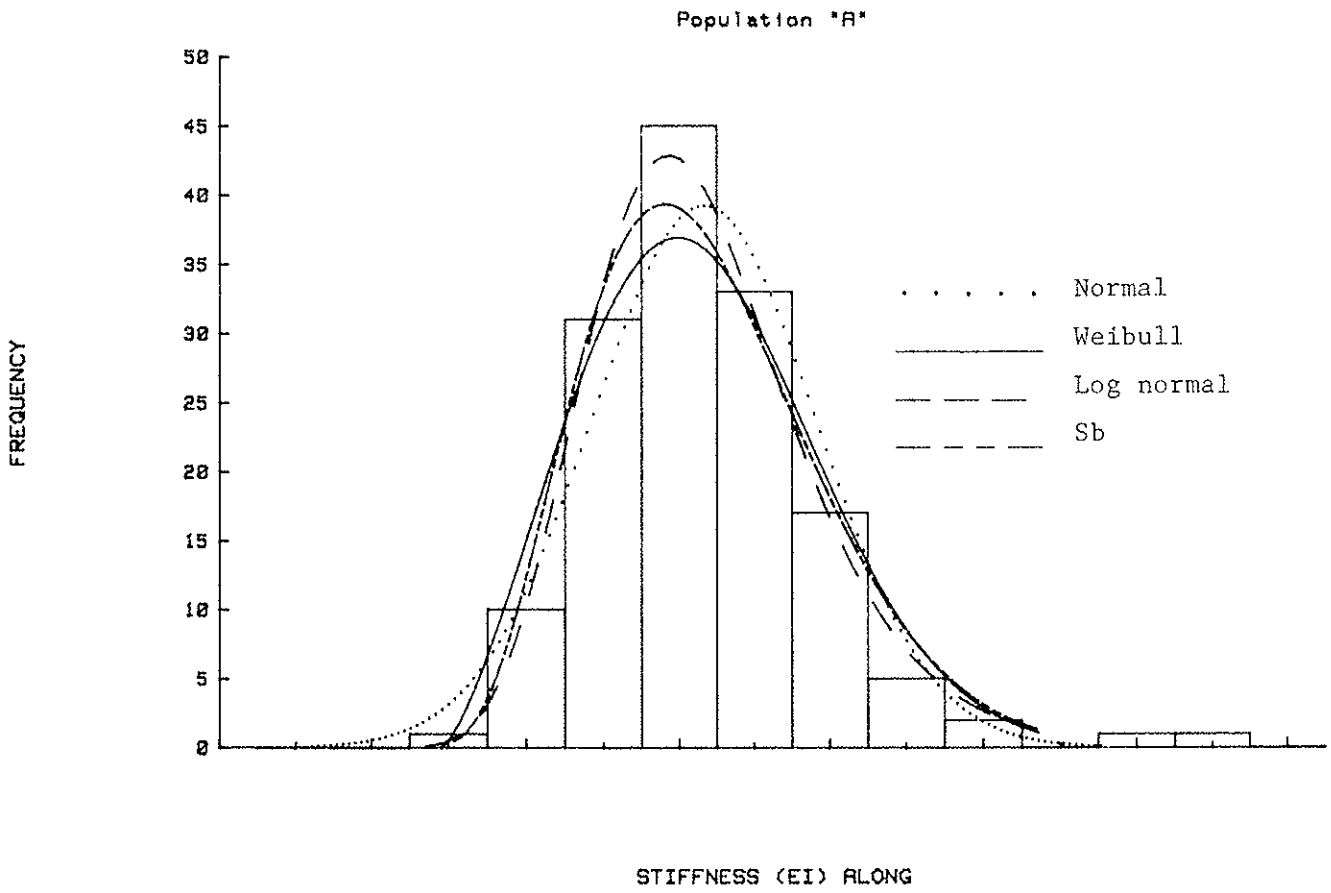
FIGURE 3.   PROBABILITY DENSITY FUNCTIONS FOR STIFFNESS (EI) ON
TEST POPULATIONS "A" AND "B".
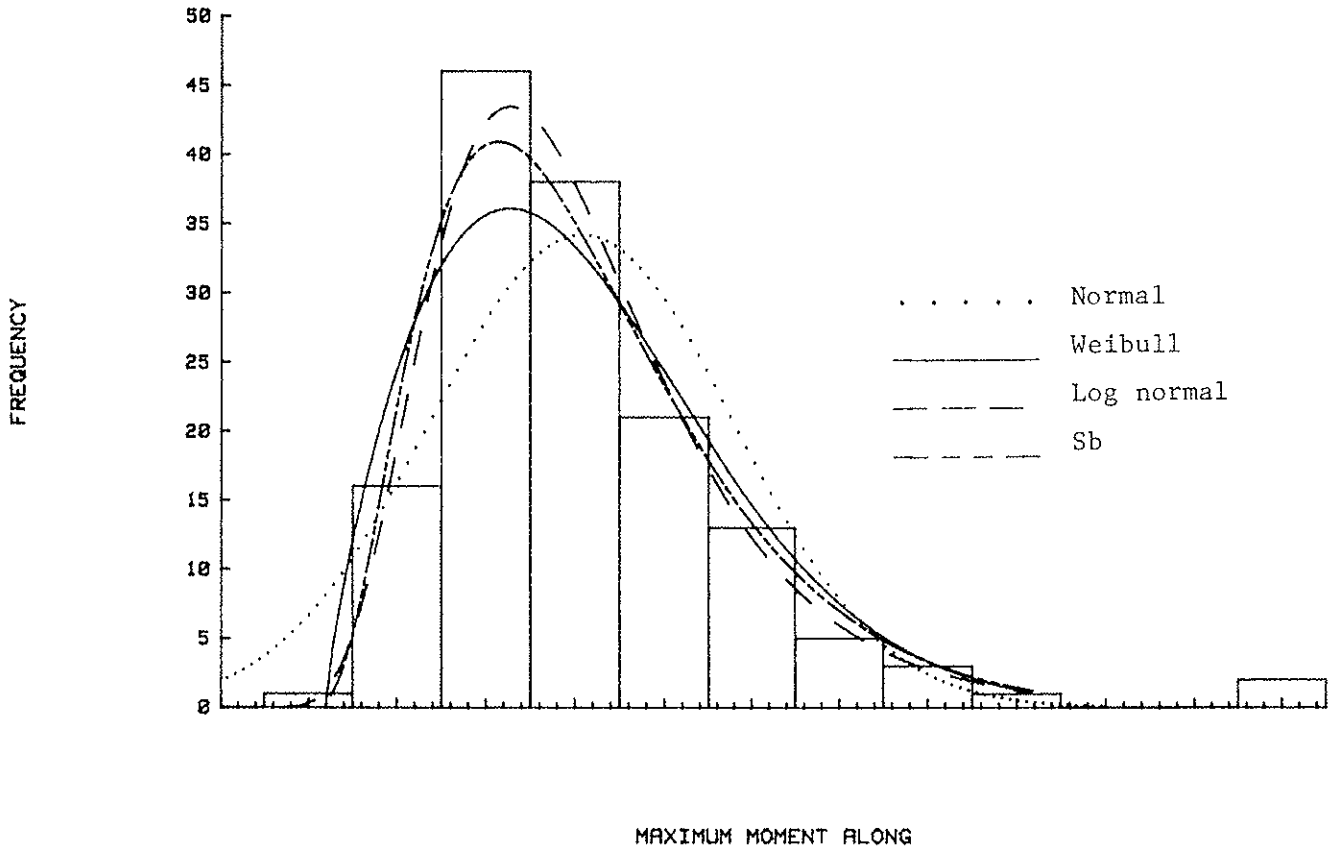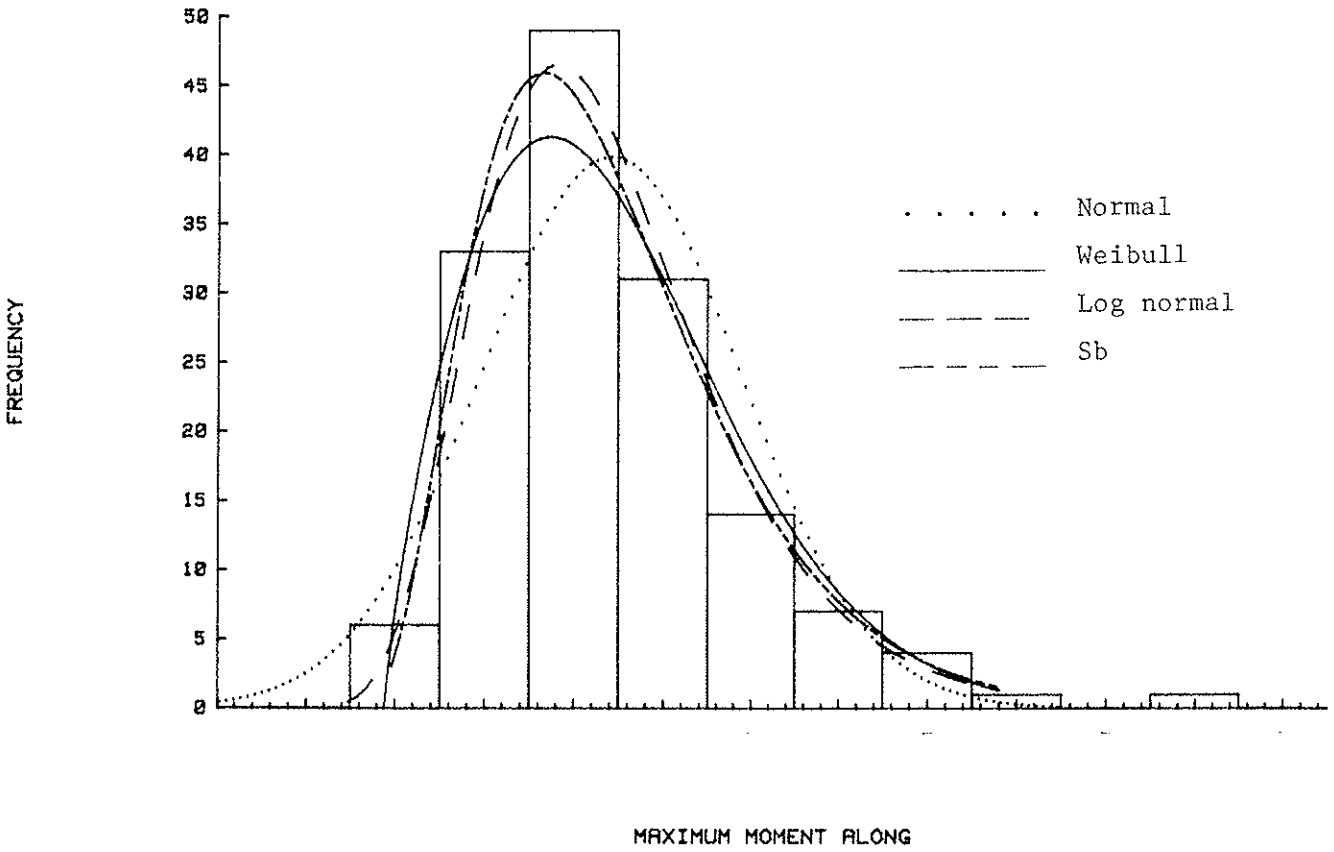
FIGURE 4. PROBABILITY DENSITY FUNCTIONS FOR STRENGTH (MAXIMUM MOMENT) ON TEST POPULATIONS "A" AND "B".

CUM. FREQUENCY (%)

POPULATION "B" — LOWER 8%

MAXIMUM MOMENT ALONG

4.77%

LEGEND

+ — Normal
* — Log Normal
O — Sb
X — Weibull
▲ — Actual
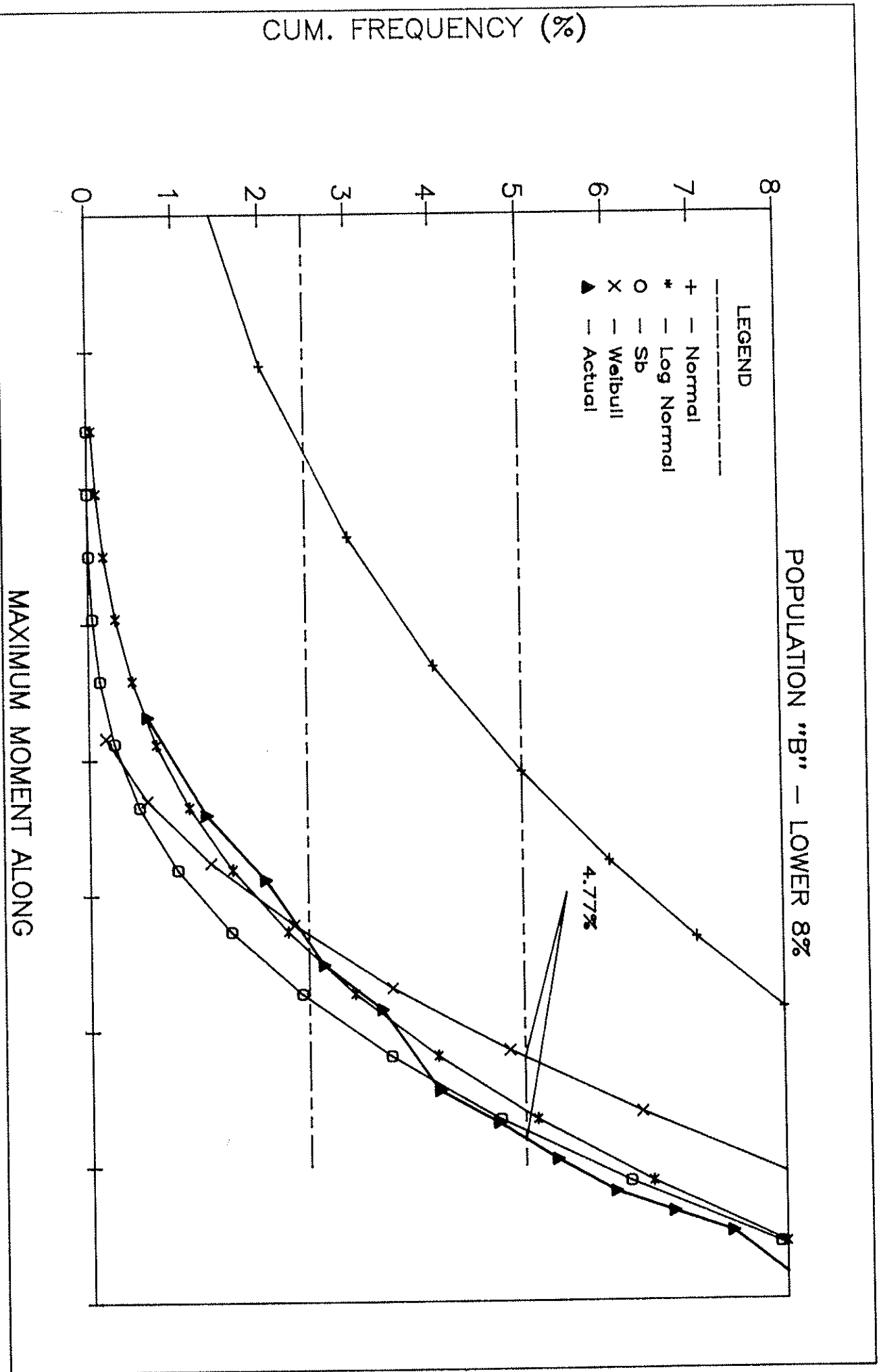
FIGURE 5.   COMPARISON OF PROBABILITY DENSITY FUNCTIONS VERSUS ACTUAL TEST DATA FOR
THE LOWER 8% OF STRENGTH ON TEST POPULATION "B".
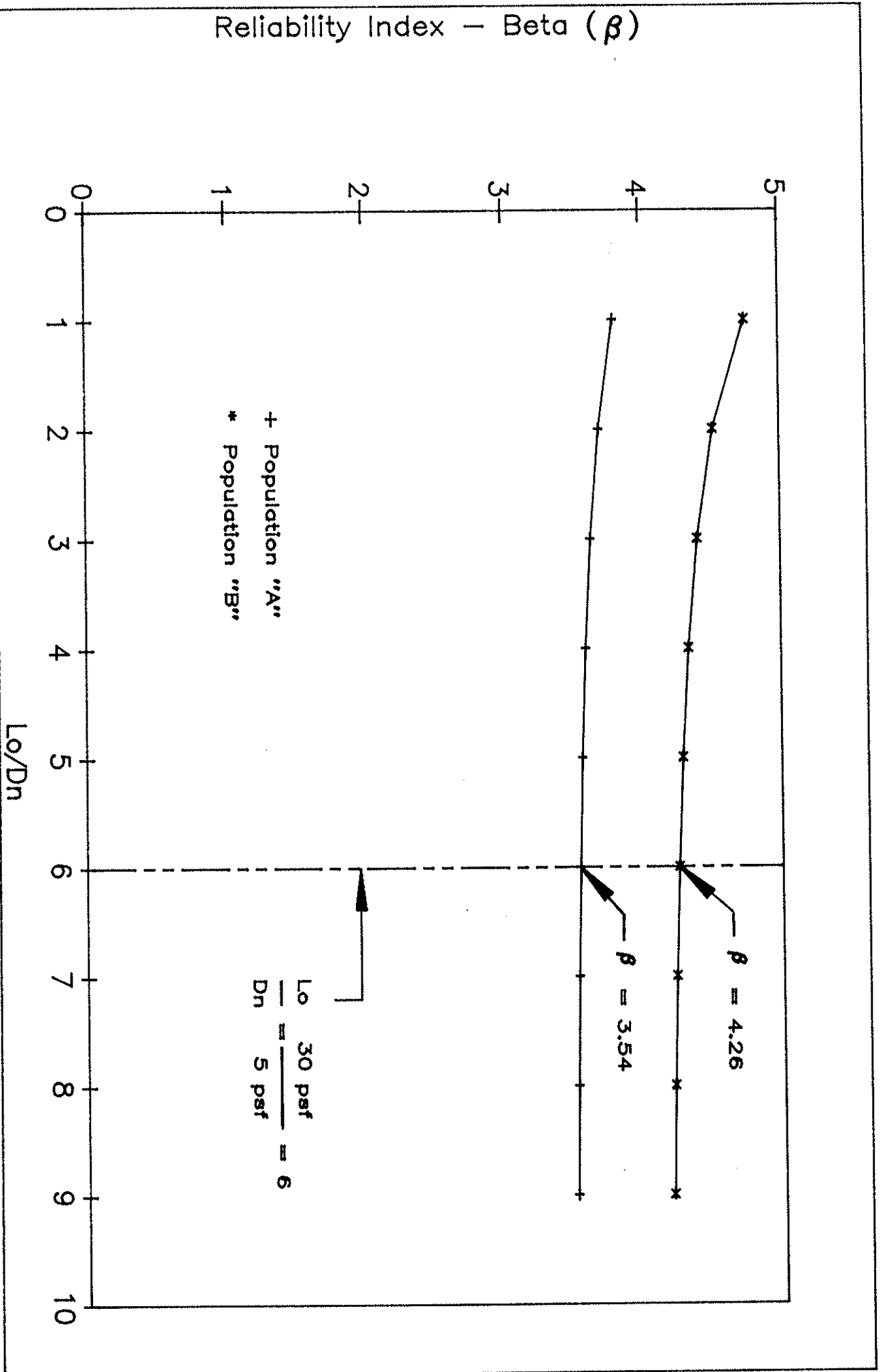
FIGURE 6. COMPARISON OF BETAS BETWEEN TEST POPULATIONS "A" AND "B".

INTERNATIONAL COUNCIL FOR BUILDING RESEARCH STUDIES AND DOCUMENTATION

WORKING COMMISSION W18A - TIMBER STRUCTURES

A COMPARATIVE INVESTIGATION OF THE ENGINEERING PROPERTIES
OF 'WHITEWOODS' IMPORTED TO ISRAEL FROM VARIOUS ORIGINS

by

U Korin
Timber Center, Building Research Station
Technion, Israel Institute of Technology
Israel

MEETING TWENTY
DUBLIN
IRELAND
SEPTEMBER 1987

A Comparative Investigation of the Engineering Properties
of "Whitewoods" Imported to Israel From Various Origins

Dr. U. Korin

Summary

The physical and natural characteristics, and the engineering properties
of "whitewoods" imported to Israel from seven origins, were investigated.
The data will be used as an initial layer of a "Timber data bank"
established at the "Timber Center" of "The Building Research Station" of
the Technion, Israel Institute of Technology.

The paper presents the experimental data and compares between the timber
from the different origins, according to quality level and uniformity
considerations.

The structural efficiency of the use of the different timber as bending or
compression members is examined.

1. Scope

Whitewood timber in structural sizes is imported to Israel from different
origins. The timber is used for various purposes such as construction of
roofs covered with tiles or other lighweight coverings, agricultural
buildings, formwork and shoring in civil engineering works and many other
purposes. The timber is usually supplied according to the commercial
gradings of the exporting countries, or even without any reliable grading.

During the structural use of the timber there is usually a significant
waste of the material caused mainly by the fact that the whitewood is
related to as one general group without any consideration to the origin of
the timber, its commercial grading and actual quality. This treatment of
the whitewood is a cause for uncertainties regarding the real safety
cooeficients of timber structures.

The timber center of the B.R.S. performed a comparative investigation of the engineering properties of whitewoods from various origins. This investigation was carried out with very limited funds and thus comprised only a limited number of individual samples from each origin. It is planned to used the accumulated data as a basic data bank to which future data will be added from further investigations.

It is planned to submit to the potential user data about the characteristic properties of the timber from the different origins inorder to achieve a safe and economical use of the imported timber, and a tool for consideration of the relative advantage of any one of the whitewoods.

2. Origins of the investigated timber

This stage of the investigation comprised whitewood from seven origins according to the following list:

group 1 - Canada, SPF timber, No. 2 commercial grading

group 2 - Sweden, whitewood (spruce, hemlock, fir) No. 5, commercial grading

group 3 - Yugoslavia whiteweed (spruce, hemlock, fir)

group 4 - Canada - SPF timber, No. 2 structural grading

group 5 - Finland - whitweood (spruce, hemlock, fir) No. 5, commercial grding

group 6 - South Africa - Radiata pine

group 7 - Romania - whitewood (spruce, hemlock, fir)

The material selected for the investigation was rectangular 5 cm x 10 cm planks. It is common in the local practice to relate to the lumber nominal cross section of 50 mm x 100 mm as a basis for structural design and engineering utilization.

From each one of the groups five different planks were randomly selected from stocks at timber yards. The test samples required for the investigation were prepared from the selected planks.

3. <u>The tests</u>

The samples brought to the laboratory, were air dried until of a moisture content in the range of 14%-16% was attained.

The following tests were performed on each one of the samples:
a) Measurement of the plank dimensions.
b) Listing of growth and other defects.
c) Measurement of annual ring widths.
d) Defining of the type of log cutting.
e) Electronic measurement of the moisture content (during the mechanical tests of the timber).
f) Density of the timber.
g) Modulus of elasticity in bending (1800mm span, 1/3-2/3 span loading).
h) Modulus of rupture (1800mm span, 1/3-2/3 span loading).
i) Modulus of elasticity in compression (200mm long specimens).
j) Compressive strength (200mm long specimens).

The mechanical tests of the timber were performed according to RILEM 3TT-3 recommendation (1). Test results are submitted in tables 1-7.

4. <u>Characteristic Properties of the timber</u>

Considering the average values and standard deviations obtained for each one of the measured properties, and assuming a normal distribution of the timber population, the characteristic property for 95% proof were calculated according to equation 1.

$$K_k = \bar{X} - 1.65s \tag{1}$$

where K_k - any characteristic property. $\bar{X}$ - the average value of the tested group and s - the standard deviation of the same.

Table 8, summarizes the characteristic values of the various investigated properties as well as the average values of the elastic moduli (Em aver., Ec aver.) of the timber (the average elastic moduli are required for

structural movement calculations). Table 8 also presents values of critical bending moments (M_{crit}) calculated according to the characteristic bending strength (f_m) and characteristic section modulus (W_x) according to equation 2[2] and critical axial compression load for a strut having an effective length of 1000mm (equation 3)[3].

$$M_{crit} = W_x \cdot f_m \tag{2}$$

$$N_{c\ crit} = A \cdot f_c \cdot k_{10} \tag{3}$$

where A is the characteristic cross section area, f_c, the characteristic compressive strength and k_{10}, the modification factor for compression members according to B.S. 5268, Part 2[3].

5. Discussion and conclusions

It must be emphasized that the samples population of this investigation is quite small. The main reason for that is the very limited funds allocated for the program. Some of the samples were supplied by clients interested in the testing of timber from their stock. Some of the samples were simply purchased from timber yards, that were not particularly interested in the test results. However, inspite of the small size of the tested population, the obtained results serve as an important foundation for a data bank of engineering properties of timber. This bank may later be enlarged to include timber of more origins and grades, and larger populations of timber from the investigated origins.

Israel imports the major part of timber for construction purposes. The timber market is dominated by the suppliers. The timber is imported for general use, and there is almost no import of timber according to structural grades. The commercial grading is based mainly on the dimensions of the knots, and their frequency, and on other natural defects in the timber. The average user must comply with the stock offered by the market.

There are almost no engineering data concerning the basic properties of timber from different origins, and of characteristic properties of timber of each one of the grades from each origin. A support from timber exporting countries towards expansion of the investigation may contribute to the increase of the size of this data bank and to its reliability.

The economical question of the relative advantage of the use of timber also arises from each on of the origins depending on the price of the timber and their potential use. This question has not been considered at this stage in the investigation. It must be stressed, that the Israeli engineering community is expecting to obtain data not only about technological aspects but also about the economics of the use of different timber, and in the future, attention should be given to that question.

In addition to the mechanical properties of the timber, other features of the timber such as width of annual rings, type of conversion of the timber, density and knot size and frequency were also examined. The small population of the research cannot at this stage present distinct relations between the measured properties and the natural and conversion features. However there are some indications worth further consideration:
a) Within each one of the timber groups, specimens having higher densities possessed superior mechanical properties.
b) Within each one of the timber groups knot size and knot frequency adversly affect the mechanical properties.
c) Within each group, the smaller the width of the annual ring, the better are the mechanical properties.

The uniformity of the different properties attained within a single timber group was uneven. If we accept the coefficient variation as a scale for assessment of the uniformity of each group, it may be said that the most even uniformities were attained in group No. 4, Canada b (coefficients of variations range 0.103 to 0.165) and the most uneven uniformities were attained in group 3, Yugoslavia (coefficients of variations range 0.177 to 0.310).

One of the reasons for the uneven uniformities of the different mechanical properties of the timber of each group could be the small number of specimens comprising the group. The results may have a clearer image when more samples are tested.

The uniformity obtained during the examination of each property in the group, expressed by the standard deviation(s) has a high impact on the characteristic value ($K_k = \bar{X} - 1.65s$), and on the economic utilization of the timber.

Tables 9 and 10 present the relations between the different mechanical properties in each of the groups. The average values are shown in table 9 and the characteristic values in table 10. Table 10 also shows a comparison with the relations reported in the CIB Code [2]. The values obtained in this investigation do not comply with those reported in the Code, and it is quite clear that many more samples should be tested in order to obtain safe engineering values.

The dimensional uniformity has also a high impact on the efficient use of the tiber. In each one of the groups the dimensional uniformity was satisfactory. But when the different groups were compared, it was clear that we were dealing with differently converted timber. Practically, each one of the groups has its one combination of width and height of the cross section. These dimensional differences, are expressed through the calculations of the cross section area, the section modulus, and the second moment of inertia around the two axis. (table 8). It is necessary to compare these values with the theoretical cross section of 50mm x 100mm ($A = 5.0$ x 10^3mm^3, $W_x = 8.33$ x 10^4 mm^3, $I_x = 4.17$ x 10^6 mm^4 and $I_y = 1.0^4$ x 10^6 mm^4), which is used for calculation and design purposes by the engineering community. One of the targets of this investigation is to try to adopt a section with uniform dimensions for the whitewood, to distribut this information among the engineering community, and to convince the suppliers to comply with the recommended timber sizes.

The most perceptible comparison between the timber from the various
origins is presented in table 8 in the lines relating to the critical
bending moments and critical axial compression load (for a strut having
1000mm equivalent length). The ratio between the maximum and minimum
bending capacities was 2.85 and ratio between the respective axial
compression capacities was 2.00.

The impacts of these results are, that when the actual engineering
properties and actual sizes of a particular consignment of timber are not
accounted for, we may find ourselves beyond the critical capacity on the
one hand or to waste good timber on the other hand.

References

1. Testing methods for timber is structural sizes, Recommendation,
    RILEM/CIB 3TT-3, Materials and Structures, Volume 11, No. 66, pp.
    445-452.

2. CIB Structural timber design code, CIB Report 1983, Publication 66.

3. British standard, BS 5268 Part 2, "The structural use of timber",
    April 1982.

Table 1 - Individual test results - group 1 - Canada SPF - No. 2 commercial (a)

specimen property	1	2	3	4	5	average X	standard deviation s	cooficient of variation s/X = v
annual ring width (mm)	1.2	1.8	1.4	1.2	1.3			
type of cutting	through and through							
moisture content (%)	14.0	14.5	14.0	14.0	14.0	14.1	0.22	0.016
width of section (mm)	47.5	47.6	48.1	47.1	47.8	47.62	0.37	0.008
height of section (mm)	97.5	97.0	98.0	97.8	18.2	97.70	0.47	0.005
density (kgm-3)	405	452	448	441	473	463.6	25.5	0.055
largest knot (mm)	10	25	25	25	20			
knots - 10-20mm (m-1)	2	1	2	2	3			
knots - 20mm up (m-1)	--	1	1	1.5	-			
modulus of elasticity in bending (mPa)	12,048	8,951	10,603	9,309	10,572	10,333	1,240	0.120
modulus of rupture (mPa)	57.8	35.3	51.4	39.9	25.4	42.0	12.9	0.306
modulus of elasticity in compression (mPa)	12,387	9,211	8,421	8,371	11,111	9,900	1,779	0.180
comperssive strength (mPa)	39.4	34.4	36.8	33.6	39.8	36.8	2.82	0.078

Table 2 - Individual test results - group 2 - Sweden - No. 5 commercial

specimen / property	1	2	3	4	5	average X	standard deviation s	cooficient of variation s/X = v
annual ring width (mm)	2.3	2.3	1.6	1.8	1.8			
type of cutting	half			sawn				
moisture content (%)	16.0	16.0	15.5	15.0	15.0	15.5	0.5	0.032
width of section (mm)	46.2	47.6	45.5	47.5	46.2	46.6	0.91	0.020
height of section (mm)	102.0	103.3	102.0	101.9	101.5	102.1	0.68	0.007
density (kgm-3)	472	471	496	434	524	479.4	33.4	0.070
largest knot (mm)	10	15	10	10	20			
knots - 10-20mm (m-1)	1	3	2	2	2			
knots - 20mm up (m-1)	-	-	-	-	-			
modulus of elasticity in bending (mPa)	15,137	13,940	15,667	10,949	12,947	13,728	1,879	0.137
modulus of rupture (mPa)	58.4	51.1	66.9	54.0	54.5	57.0	6.12	0.107
modulus of elasticity in compression (mPa)	11,924	9,412	19,337	12,200	15,983	13,771	3,897	0.283
comperssive strength (mPa)	35.7	35.6	37.2	40.1	44.2	38.6	3.64	0.094

Table 3 - individual test results - group 3 - Yugoslavia

specimen property	1	2	3	4	5	average X	standard deviation s	cooficient of variation s/X = v
annual ring width (mm)	3.7	2.0	2.9	1.3	2.5			
type of cutting	half		sawn					
moisture content (%)	16.0	15.0	15.5	15.0	15.0	15.3	0.45	0.029
width of section (mm)	49.0	51.0	46.5	46.5	47.0	48.0	1.97	0.041
height of section (mm)	98.1	98.8	99.9	96.0	98.0	98.16	1.43	0.015
density (kgm-3)	443	448	462	498	440	458	23.8	0.052
largest knot (mm)	15	20	25	20	25			
knots - 10-20mm (m-1)	1	3	1	2	2			
knots - 20mm up (m-1)	-	1	2	1	1			
modulus of elasticity in bending (mPa)	8,866	9,265	8,036	15,203	6,490	9,572	2,972	0.310
modulus of rupture (mPa)	43.0	38.4	29.3	61.9	37.1	41.9	12.2	0.291
modulus of elasticity in compression (mPa)	10,000	10,435	10,903	15,123	6,356	10,563	3,120	0.295
comperssive strength (mPa)	32.2	36.0	34.1	41.5	25.1	33.8	6.0	0.172

Table 4 - Individual test results - group 4 - Canda SPF structural grade 2 (b)

specimen property	1	2	3	4	5	average X	standard deviation s	cooficient of variation s/X = v
annual ring width (mm)	2.0	1.5	2.4	2.7	2.4			
type of cutting		half		sawn				
moisture content (%)	16.0	16.0	16.0	15.5	16.0	15.9	0.22	0.014
width of section (mm)	47.5	47.5	47.2	46.3	46.7	47.0	0.53	0.011
height of section (mm)	100.1	100.3	100.7	99.9	101.7	100.5	0.71	0.007
density (kgm-3)	502	436	412	487	469	461	36.9	0.080
largest knot (mm)	27	15	22	20	17			
knots - 10-20mm (m-1)	3	2	3	5	2			
knots - 20mm up (m-1)	2	-	1.5	0.5	-			
modulus of elasticity in bending (mPa)	9,068	10,432	10,017	12,490	10,417	10,485	1,250	0.119
modulus of rupture (mPa)	48.2	50.8	35.9	57.3	53.0	49.0	8.1	0.165
modulus of elasticity in compression (mPa)	11,265	8,685	10,399	10,601	11,363	10,457	1,071	0.103
comperssive strength (mPa)	31.4	31.1	29.1	38.8	39.3	33.9	4.8	0.140

Table 5 - Individual test results - group 5 - Finland No. 5 commercial

specimen property	1	2	3	4	5	average X	standard deviation s	cooficient of variation s/X = v
annual ring width (mm)	1.5	1.4	1.4	1.5	1.0			
type of cutting	half		sawn					
moisture content (%)	14.0	15.0	14.0	15.0	15.0	14.6	0.55	0.038
width of section (mm)	45.0	44.7	43.0	47.5	44.0	44.8	1.7	0.037
height of section (mm)	100.0	102.0	99.0	101.0	99.6	100.3	1.2	0.012
density (kgm-3)	515	467	583	539	564	534	452	0.085
largest knot (mm)	10	15	10	10	10			
knots - 10-20mm (m-1)	-	2.5	-	-	-			
knots - 20mm up (m-1)	-	-	-	-	-			
modulus of elasticity in bending (mPa)	19,292	13,113	17,203	15,484	15,881	16,195	2,275	0.141
modulus of rupture (mPa)	78.4	55.4	72.8	80.1	71.1	71.6	9.8	0.137
modulus of elasticity in compression (mPa)	15,680	8,411	13,727	11,490	19,490	13,812	4,281	0.310
comperssive strength (mPa)	52.5	33.7	46.6	46.8	44.4	44.8	6.9	0.154

Table 6 - Individual test results - group 6 - South Africa

specimen property	1	2	3	4	5	average X	standard deviation s	cooficient of variation s/X = v
annual ring width (mm)	8.6	8.4	11.2	6.0	8.7			
type of cutting	through	and	through					
moisture content (%)	15.0	14.0	15.5	15.5	15.5	15.1	0.65	0.043
width of section (mm)	43.5	45.0	47.4	46.0	46.6	45.7	1.51	0.033
height of section (mm)	107.0	105.5	105.6	105.7	105.8	105.9	0.61	0.006
density (kgm-3)	437	397	420	465	412	425	25.6	0.060
largest knot (mm)	25	30	27	25	24			
knots - 10-20mm (m-1)	3	2.5	3	2	2			
knots - 20mm up (m-1)	1	2	1	1	1			
modulus of elasticity in bending (mPa)	8,261	8,238	7,544	13,550	7,471	9,013	256	0.284
modulus of rupture (mPa)	25.7	35.2	27.4	36.4	21.4	29.2	6.4	0.219
modulus of elasticity in compression (mPa)	6,580	4,691	5,152	9,162	5,846	6,286	1,759	0.280
comperssive strength (mPa)	27.6	21.9	24.5	34.9	28.0	27.4	4.9	0.178

Table 7 - Individual test results - group 7 - Romania

specimen property	1	2	3	4	5	average X	standard deviation s	cooficient of variation s/X = v
annual ring width (mm)	3.1	4.0	3.0	2.7	4.3			
type of cutting		half		sawn				
moisture content (%)	14.0	14.0	15.5	17.5	15.0	15.2	1.44	0.095
width of section (mm)	50.1	47.2	46.7	47.9	50.7	48.52	1.78	0.037
height of section (mm)	93.7	95.2	96.1	97.8	93.5	95.26	1.78	0.019
density (kgm-3)	427	424	382	426	366	405	28.9	0.071
largest knot (mm)	14	12	10	25	12			
knots - 10-20mm (m-1)	2	2	1	2.5	1			
knots - 20mm up (m-1)	-	-	-	2	-			
modulus of elasticity in bending (mPa)	8,511	12,335	10,273	6,503	6,918	8,908	2,724	0.306
modulus of rupture (mPa)	31.7	52.0	43.2	32.9	25.9	37.1	10.4	0.280
modulus of elasticity in compression (mPa)	13,800	12,850	13,550	13,700	12,800	13,340	479	0.036
coperssive strength (mPa)	29.0	28.0	29.0	28.1	26.5	28.1	1.0	0.036

Table 8 - Characteristic properties the timber groups
_____

group and origin characteristic properties	1 Canada (a)	2 Sweden	3 Yugo- slavia	4 Canada (b)	5 Finland	6 South Africa	7 Romania
width of section (b) (mm)	47	45	45	46	42	43	46
height of section (h) (mm)	97	101	96	99	98	105	92
cross section (A) $(10^3 \times mm^2)$	4.60	4.55	4.32	4.55	4.12	4.52	4.23
modulus of section (Wx) $(10^4 \times mm^3)$	7.37	7.65	7.20	7.58	6.72	7.90	6.48
moment of inertia (Ix) $(10^6 \times mm^4)$	3.58	3.87	3.32	3.72	3.29	4.15	2.98
moment of inertia (Iy) $(10^6 \times mm^4)$	0.839	0.767	0.729	0.803	0.605	0.696	0.746
modulus of elasticity in bending (Em) (mPa)	8,300	10,600	4,700	8,400	12,400	4,800	4,400
modulus of elasticity in bending (Em aver) (mPa)	10,300	13,700	9,600	10,500	16,200	9,000	8,900
modulus of rupture (fm) (mPa)	21	47	22	36	55	19	20
modulus of elasticity in compression (Ec) (mPa)	7,000	7,300	5,400	8,700	6,700	3,400	12,500
modulus of elasticity in compression (Ec aver)(mPa)	9,900	13,800	10,600	10,500	13,800	6,300	13,300
compressive strength (fc) (mPa)	32	33	24	26	33	19	26
critical bending moment (Mcrit) (Nm)	1,548	3,600	1,584	2,792	3,696	1,501	1,296
critical axial compression (Leq = 1000mm)(Ncrit) (KN)	55.5	53.0	36.6	43.7	42.4	27.8	40.6

Table 9 - Relation between averge different mechanical properties

group and origin average properties	1 Canada (a)	2 Sweden	3 Yugo- slavia	4 Canada (b)	5 Finland	6 South Africa	7 Romania
modulus of rupture (fm aver)	1.0	1.0	1.0	1.0	1.0	1.0	1.0
modulus of elasticity in bending (Em aver)	246	241	228	214	226	309	240
compressive strength (fc aver)	0.88	0.68	0.81	0.69	0.62	0.94	0.76
modulus of elasticity in compression (Ec aver)	236	242	252	213	193	215	360

Table 10 - Relations between characteristic different mechanical properties

group and origin average properties	1 Canada (a)	2 Sweden	3 Yugo- slavia	4 Canada (b)	5 Finland	6 South Africa	7 Romania
modulus of rupture (fm)	1.0	1.0	1.0	1.0	1.0	1.0	1.0
modulus of elasticity in bending (Em)	395 (279)	225 (194)	214 (254)	233 (245)	225 (194)	253 (279)	220 (279)
compressive strength (fc)	1.52 (0.92)	0.70 (0.75)	1.09 (0.88)	0.72 (0.79)	0.60 (0.75)	1.0 (1.16)	1.3 (1.16)
modulus of elasticity in compression (Ec)	333	155	245	242	122	179	625

Note: the values in brackets are the relations calculated according to (2) CIB
structural design code, annex 42, for the respective rupture noduli.

INTERNATIONAL COUNCIL FOR BUILDING RESEARCH STUDIES AND DOCUMENTATION

WORKING COMMISSION W18A - TIMBER STRUCTURES

EFFECTS OF YIELD CLASS, TREE SECTION, FOREST AND SIZE
ON STRENGTH OF HOME GROWN SITKA SPRUCE

by

V   Picardo
Forest Products Department
Institute for Industrial Research and Standards
Ireland

MEETING TWENTY
DUBLIN
IRELAND
SEPTEMBER 1987

ABSTRACT

Data was collected from tests and measurements made on 1487 planks in three different sizes. The sampling strategy was described in CIB-W18 Paper 17-17-2. Twenty eight different items of data were collected which were grouped into five groups one of which contained what was called the CLASSIFYING VARIABLES. This group consisted of data on Yield class, forest, size, tree, and section of tree.

Although the primary aim of the project was to obtain estimates of the bending strength of Sitka Spruce grown in Ireland a separate analyses was carried out to examine the effects of the classifying variables on the strength properties measured. Yield class and section were found to be interrelated. From the practical view point Section had the greatest effect. Tree effects were too complicated to analyse. The size effect followed the well established pattern.

ABBREVIATIONS

MOR   Modulus of rupture or ultimate stress in bending

MOE   Modulus of elasticity measured using 900mm gauge
also referred to as Grade MOE

EFFECTS OF YIELD CLASS, TREE SECTION, FOREST & SIZE
ON STRENGTH OF HOME-GROWN SITKA SPRUCE

INTRODUCTION

In Ireland as in many other countries there is a growing awareness of the potential and need for encouraging the use of home produced materials. However, the use of a material requires its properties to be known and this is particularly so in the case of timber which is to be used in a load carrying capacity such as in floor joists. This sort of information has been singularly lacking in the case of timber grown in Ireland. With a greater amount of timber now reaching maturity and ready for conversion to sawn timber it became an urgent requirement to determine the quality of timber that is at present reaching the market and to obtain enough data in order that analyses could be carried out to give some indication of future quality. For the latter objective analyses was required to determine the effects of the classifying variables namely, Yield class, tree section, size and forest.

EXPERIMENTAL DESIGN

The selection of samples was described in a paper "Sampling Strategy for Physical and Mechanical Properties of Irish Grown Sitka Spruce" submitted to the CIB-W18 group (Paper no. 17-17-2). The sampling plan was subseqently altered during the course of the project by increasing the number of planks tested and reducing the number of Yield Classes by one.
Samples were obtained in 3 sizes from each of 5 forests selected from each of 4 Yield classes i.e. a total of twenty forests were sampled. The basic unit (of which there were 60 i.e 20 forests x 3 sizes) consisted of a minimum of between 25 and 30 samples except for YC16 for which the minimumm was 12.
Figure 1 shows a schematic diagram of the various groupings for statistical analyses.Figure 2 shows the locations of the forests from which samples were obtained from around the country.

DATA COLLECTION

Most of the measurements involved routine procedures described in ISO documents or British Standards and are not described here. The data consisted of measurements on 1487 planks and consisted of 28 items grouped as follows :

1. General classification (Yield class, forest, size, tree section) also called
CLASSIFYING VARIABLES
2. Density (gross, at m.c., dry and nominal)
3. Moduli of Elasticity (simulation, computermatic, fpg, grade and 5h)
4. Modulus of rupture in bending
5. Grading - mechanical and visual

STATISTICAL ANALYSES

The basic objectives of the statistical analyses of the data were to obtain:-

a) a general description of the data
b) examine the interrelationships between the variables
c) a detailed investigation of the strength properties

This paper is confined to the analyses regarding the classifying variables only. The basic statistics i.e. means, standard deviations, coefficient of variation etc. were determined for each variable.
The sampling design was unbalanced with regard to the classifying variables. This was not unexpected as the main aim of the project was to obtain a reliable estimate of the Sitka Spruce grown in Ireland. However, this unbalance created some problems with the interpretation of the results of the analyses on the effects of the classifying variables in that it was not possible to attribute an effect uniquely to a particular factor. It was also found that due to this unbalance the effects of yield class and section were to some extent confounded but there was virtually no confounding between size and the other two factors. In order to quantify the effects of the classifying variables the approach adopted was to analyse the data using one variable at a time and in the presence of the

3

other factors. The random effects of 'forest' and 'tree' were too complicated to take account of in this part of the analyses and were ignored. It was thus possible to produce interpretable estimates of means for each of the other three factors. The means by which the effects were measured was to determine the mean square defined as

$$\frac{\text{sum of squares attributable to factor}}{\text{degrees of freedom}}$$

The maximum (MS_{max}) and minimum $MS(_{min})$ values were obtained by considering all the possible models ($2^3=8$) involving three main effects only i.e. yield class, section and size. These effects were only considered for MOR and MOE.

A more detailed analyses to assess the practical influence of each classifying variable on the MOR in bending and Grade MOE was carried out by doing an Analyses of Variance using one factor at a time. A parallel analyses was done on a sub grouping of SS grade planks only.

RESULTS & DISCUSSION

Table 1 shows the population statistics cross-tabulated by yield class and section.

A summary of the influence of the three main classifying variables on MOR and MOE using mean squares as described above are shown in Tables 2 and 3 respectively. The effects of yield class and section were statistically significant at a very high level (0.1%). As can be seen from the Tables, of the three factors considered Section made the highest contribution. The influence of size was quite small for both properties.

The details of the analyses of variance for the following discussion are shown in Tables 4 and 5. The MOR values were all corrected to a common depth of 200mm using the depth factor from Fewell and Curry

$$k=(200/h)^{0.4}$$

and MOE values were corrected to 18% moisture content using the following :

$$E_1 = \log [\log E_2 + C (M_2 - M_1)]$$

4

where

E_1 = MOE at 18% moisture content

E_2 = MOE at test moisture content

C = constant = 5.01×10^{-3} for Sitka Spruce

M_1 = 18% moisture content

M_2 = moisture content at time of test.

Effect of Yield Class

MOR : YC16 had the highest mean. This was significantly higher than the means for YCs 12 and 20. YC24 was significantly weaker. The pattern was the same when only SS planks were considered although the means were higher.

MOE : YC20 had the highest mean followed by 16 and 12. YC24 had the lowest mean. The range of means was 650 N/mm^2. Within the SS grade the means of YCs 20 and 12 were 700 N/mm^2 than the other two means.

Effect of Section

The data contained planks from four sections of the tree depending on how big the trees were :

A = Butt section

B = Middle section

C,D = Top section

However, as there were only 11 planks from the D section (i.e. trees from which 4 logs were obtained) conclusions about the properties of this section are dubious.

MOR : There were clear differences here. The means decreased the higher the tree level. Section A was about 12 % higher than section B which in turn was 15 % higher than section C. Within the SS grade the differences were marginally smaller.

MOE : The pattern was similar to MOR. Section A was 8% higher than section B which in turn was 15% higher than section C. The range of means was 1800 N/mm^2. The differences were halved when only SS planks were considered.

Effect of Size

MOR : It is a recognised fact that MOR increases with decreasing depth which is why depth factor corrections are used. In this analyses when the uncorrected values of MOR were analysed they followed this known pattern. The corrected MOR values however, followed the opposite pattern suggesting that the correction factor used overcorrected although it must be stated that the difference between the big and small sizes was only 2.3 N/mm^2.

MOE : The effect of size was found to be only marginally statistically significant. The range of means was only 300 N/mm^2.

Effect of Forests

MOR : The differences between forests were statistically significant with the means ranging from 24 to 36 N/mm^2. It was also found that the means could be divided into three groups - top, middle and low. The top group consisted of 4 forests with values between 32 and 36 N/mm^2 and these forests came mainly from one particular region in the south of the country. The middle group consisted of eight forests with means between 27.5 and 29.5 N/mm^2 and the remaining eight forests had means in the region of 25 N/mm^2. When only the SS grade was analysed The differences were less and there were no distinct groups although three of the forest with the highest means were also the highest in the overall sample.

MOE : There were also three distinct groups for this property. There were five forests in the top group with values ranging from 9500 to 10900 N/mm^2 and not surprisingly four pf the five were also in the top group for MOR. Within the SS grade the pattern was similar although the differences were larger.

6

CONCLUSIONS

Yield class, section and forest influenced MOR and MOE significantly although, only section appeared to have practical significance.
The effect of forest was appeared to be confined to a particular region which appeared to produce better timber than the rest of the country but further analyses would be required to determine the reasons for this.
  It was found that the effects of yield class and section were to some extent interrelated. The higher yield classes would tend to produce more of the higher sections. This means that some corrections to the means would be required if the mix of yield classes reaching the market at any time showed a significantly high proportion of the higher yield classes.
The effects of size on bending strength (MOR) followed the recognised pattern i.e. higher ultimate strength for smaller section sizes. However, the correction formula tended to overcoorect slightly. Size had no effect on MOE.

ACKNOWLEDGMENTS

REFERENCES

1. V.Picardo : Data base on Physical and Mechanical Properties of Irish Sitka Spruce - Final report for FWS ,1986.

2. ISO 8375 : Solid timber in structural sizes - Determination of some Physical and Mechanical Properties (1984)

3. ISO 3130 : Determination of moisture content for physical and mechanical tests

4. ISO 3131 : Determination of density for physical and mechanical tests (1975)

5   BS 5820 : Determination of certain physical and mechanical of timber in structural sizes (1979)

6. BS 4978 : Timber grades for structural use (1973)

7. Fewell A R : Size factors for timber bending and tension stresses - CIB W18 paper no.16-6-1

8. Fewell & Curry : Depth factor adjustments in the determination of characteristic bending stresses for visually stress graded timber - BRE Information sheet IP 1/83.

9. Covington & Fewell : The effect of change in moisture content on the geometrical properties, modulus of elasticity and stiffness of timber - BRE Current paper CP21/75

YC	SECTION	N	MOR				MOE			
			Mean	max	min	s.d.	Mean	max	min	s.d.
12	A	261	28.9	47.4	8.0	8.0	8890	17030	2580	2350
	B	118	24.6	55.3	10.3	7.5	7950	14250	3690	1830
	C	7	20.5	24.8	10.7	5.5	7500	9470	4270	2000
	ALL	*390	27.4	55.3	8.0	8.1	8570	17030	2580	2230
16	A	161	30.0	46.2	11.6	7.0	9210	16400	4400	2240
	B	58	25.8	40.9	7.4	7.4	8140	14500	1850	2350
	C	9	20.2	30.4	13.8	5.6	6505	11450	3870	2290
	ALL	228	28.6	46.2	7.4	7.5	8830	16400	1850	2350
20	A	223	29.2	55.1	10.0	7.2	9630	18320	3420	2370
	B	148	26.9	56.1	10.5	7.7	9100	21820	2900	2500
	C	58	23.3	38.2	7.3	6.4	7590	11960	3400	1730
	ALL	*433	27.5	56.1	7.3	7.6	9150	21820	2900	2430
24	A	204	27.0	45.9	12.1	6.1	8860	13920	4820	1850
	B	139	24.6	44.9	8.8	5.9	8520	14130	4820	1680
	C	77	21.8	34.5	7.4	6.0	7190	12080	3570	1760
	ALL	*436	25.1	45.9	7.4	6.4	8400	14130	3570	1890

* includes planks with unknown tree section   All units in N/mm²

TABLE 1 : POPULATION STATISTICS

Factor	d.f.	MS_{max}	MS_{min}	R_{max}
Yield Class	3	118	51	4.1%
Section	3	272	177	9.4%
Size	2	154	41	3.6%

MSE = 5.2 based on model including all factors

TABLE 2 : Effective Contribution of Classifying variables to MOR value

Factor	d.f.	MS_{max}	MS_{min}	R_{max}
Yield Class	3	35	27	1.5%
Section	3	183	164	7.8%
Size	2	30	4	0.8%

MSE = 4.3 based on model including all factors

TABLE 3 : Effective Contribution of Classifying variables to MOE value

Source	d.f.	MS	F
Bet. YCs	3	839.5	14.3
error	1483	58.8	
Bet. Sections	3	2713	49.8
error	1448	54.4	
Bet. Sizes	2	1402	23.9
error	1484	58.6	
Bet. Forests	19	608	11.4
error	1467	53.3	

TABLE 4 : ANOVA ON MOR

Source	d.f.	MS	F
Bet. YCs	3	31.3E6	6.48
error	1478	4.83E6	
Bet. Sections	3	16.9E4	37.5
error	1443	4.5E6	
Bet. Sizes	2	6.85E6	1.4
error	1479	4.88E6	
Bet. Forests	19	61.9E6	14.9
error	1462	4.14E6	

TABLE 5 : ANOVA ON MOE
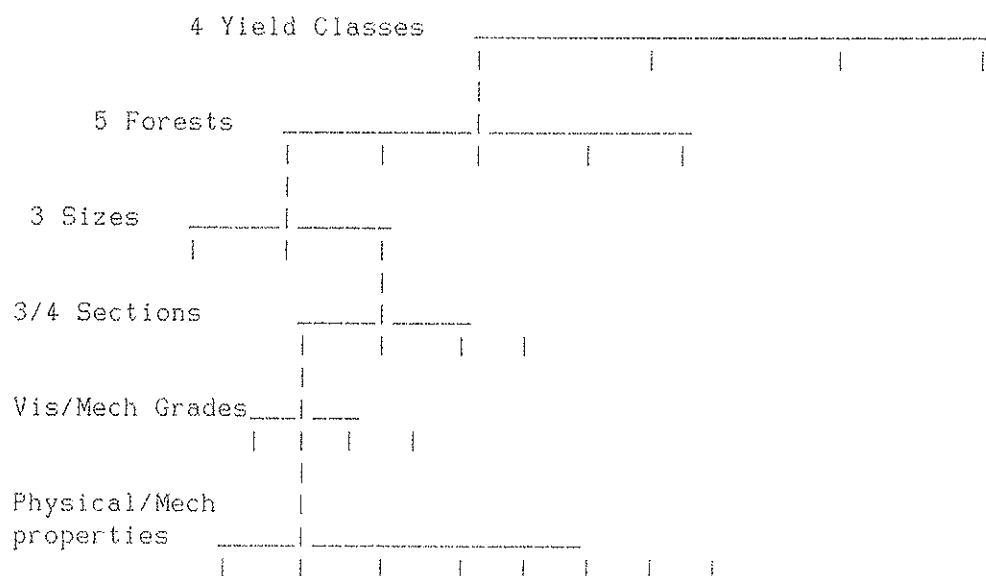
FIGURE 1 : Schematic of Heirachy for Analyses

FIGURE 2

Location of Forests
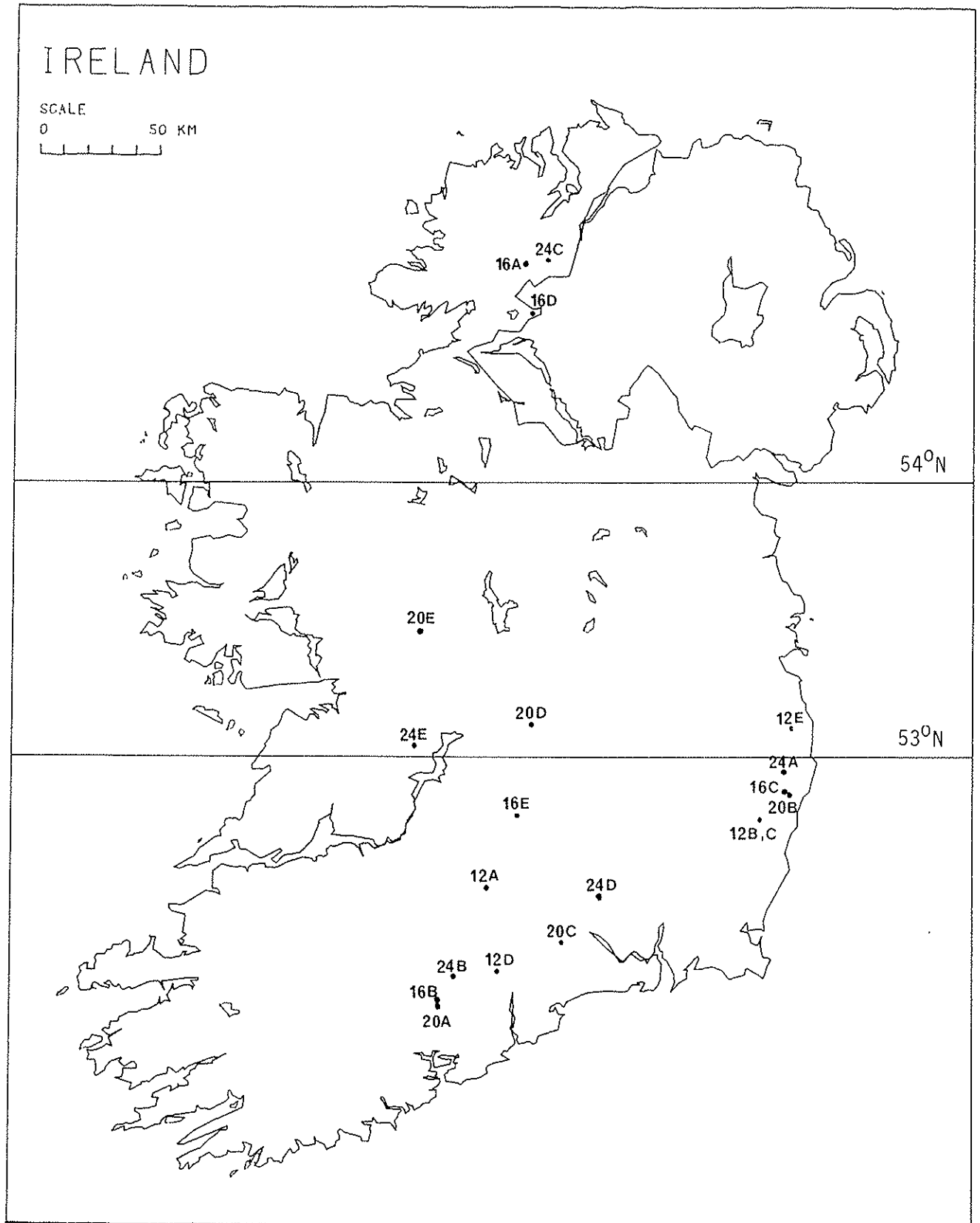
IRELAND

SCALE
0   50 KM

24C
16A•   •
      16D
     •

54°N

20E
•

20D   12E
•   •

24E   53°N
•

24A
16C• •
   •20B
12B,C

16E
•

12A   24D
•   •

20C
•

24B 12D
•   •
16B
•
20A

INTERNATIONAL COUNCIL FOR BUILDING RESEARCH STUDIES AND DOCUMENTATION

WORKING COMMISSION W18A - TIMBER STRUCTURES

DETERMINATION OF SHEAR STRENGTH AND STRENGTH PERPENDICULAR TO GRAIN

by

H J Larsen
Danish Building Research Institute
Denmark

MEETING TWENTY
DUBLIN
IRELAND
SEPTEMBER 1987

1. INTRODUCTION

In ISO 8375 (Solid Timber in Structural Sizes - Determination of Some Physical and Mechanical Properties) methods for the determination of tension and compression perpendicular to the grain and the shear strength parallel to the grain are missing.

The following is intended as background for a discussion of appropriate test methods for these properties.

2. TENSION PERPENDICULAR TO THE GRAIN

An appropriate test specimen and test method is shown in figure 1.
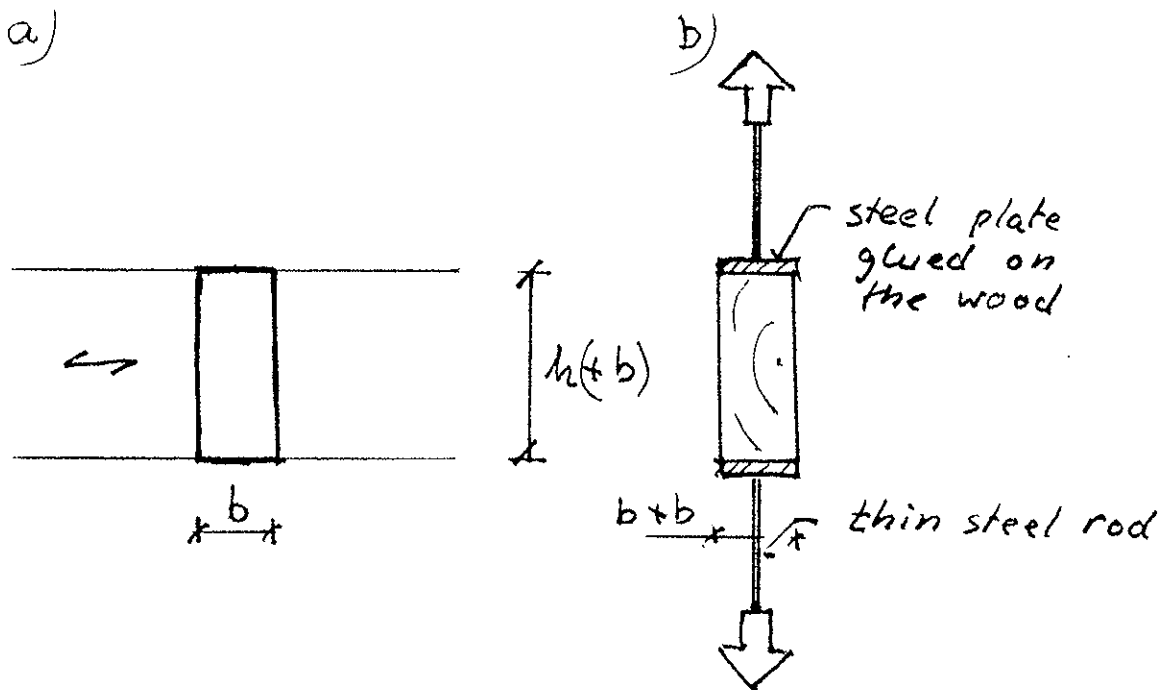
Figure 1. a) Specimen with square cross-section b x b is cut from a beam with depth h and width b

b) Steel plates are glued to the wood, and the load transferred through thin steel rods.

The steel plates can easily be glued to the wood; almost any good PVAC glue will ensure failure in the specimen, not in the glue-line.

Yielding in the thin steel rods will ensure a uniform distribution of the stresses.

In most cases it will also be possible to determine the modulus of elasticity.

The only problem is that the volume for solid timber always will be much smaller than the reference volume – $V_o = 0.02 \text{ m}^3$ – used in Eurocode 5. It will, therefore, be neccessary to use correction factors either determined experimentally or given directly in the standard. This may be a small problem, sice tension perpendicular normally will be of interest only for glued laminated timber, and for this it will be possible to let the test specimen have the reference volume.

3. COMPRESSION PERPENDICULAR TO THE GRAIN

There are no technical problems in introducing the forces; it can e.g. be done as shown in figure 2.
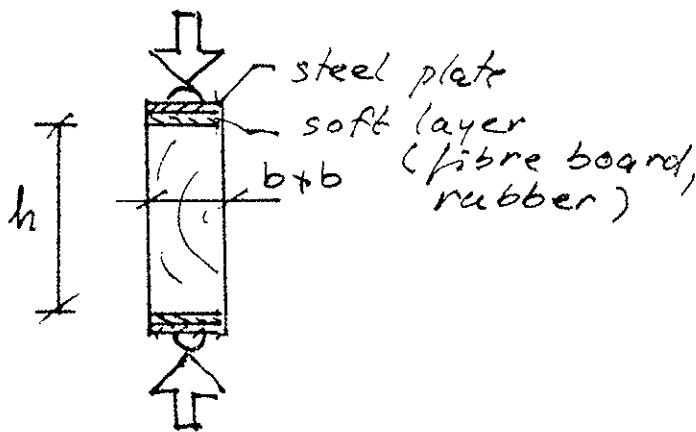
Figure 2. Full cross-section compression test

The following questions should, however, be answered:

- Should also the modulus of elasticity be determined?

- What should the depth of the specimen be for glued laminated timber?

- Should there also be a test method corresponding to figure 3, and what should the distances a and c then be?
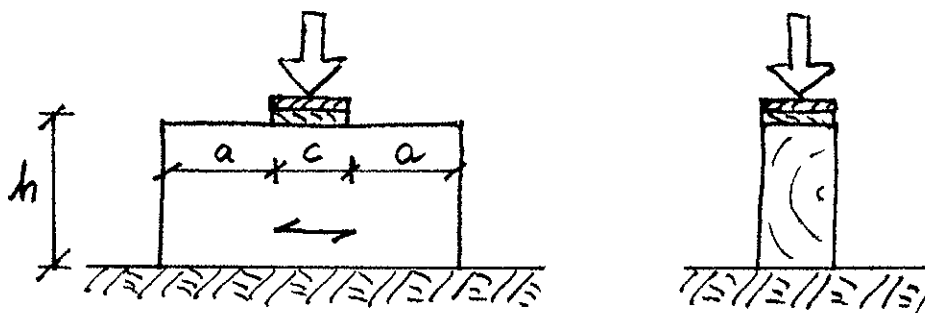
Figure 3. "Sleeper" compression test

4. SHEAR

4.1 Block Shear Tests

A block shear test - figure 4 a - as used for routine testing in connection with production control of glued laminated timber or for performance testing of adhesives is not suited for determining the shear strength of beams: The shear stress distribution is very uneven, and it is in practice impossible to avoid large stresses perpendicular to the grain.

For the same reasons test specimens as those used for plywood testing - figure 4 b - are disregarded.
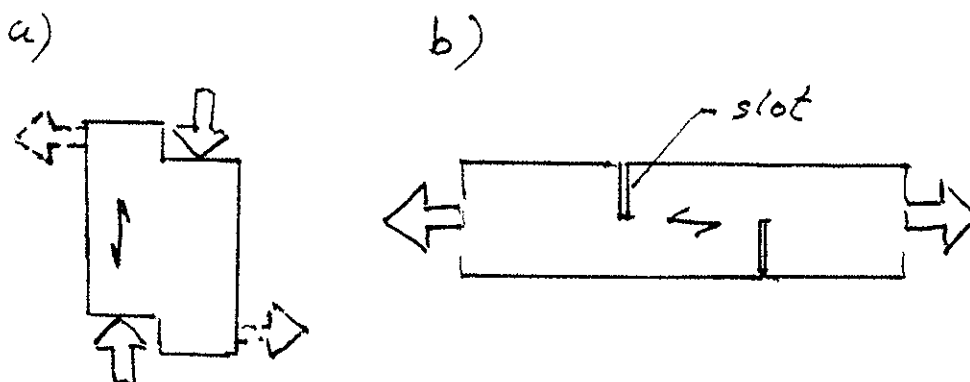
Figure 4. a) Block shear test
    b) Plywood test specimen

4.2 <u>Beam Test</u>

For the specimen shown in figure 5 a the shear stress τ according to the simple beam theory is

$$\tau = 1.5 \ F/bh$$

the bending stress σ_m at mid-span:

$$\sigma_m = 15 \ F/bh = 10 \ \tau$$

and the stress perpendicular to the grain $\sigma_{c,90}$:

$$\sigma_c = 2 \ F/bh = 1.33 \ \tau$$

According to Eurocode 5 the ratio between the characteristic values of the bending strength and the shear strength is about 10. There should therefore be a reasonable chance of getting shear failures.
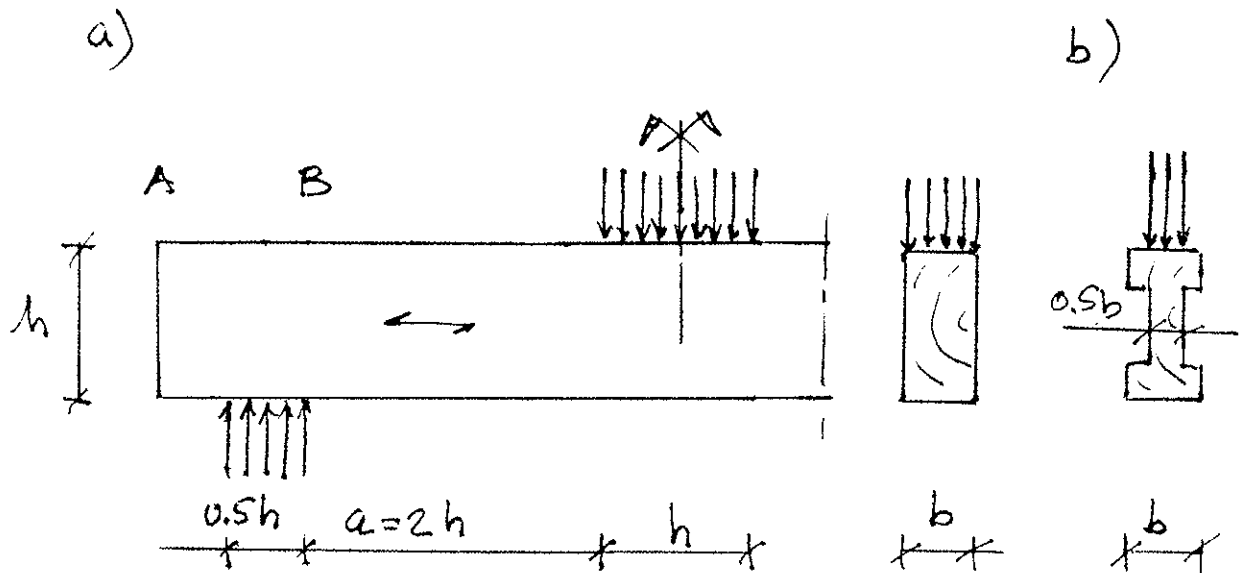
Figure 5. a) Test specimen with rectangular cross-section
         b) I-shaped cross-section

There are, however, two problems: The beam is so short that the stress distribution will probably deviate from the assumed, and the overhang A-B will hinder the development of the shear failure.

The first problem could be overcome by a more rigorous calculation of the stresses, or by using a cross-section as shown in figur 5 b, or by both. For the I-shaped cross-section shown in figure 5 b the bending strength is reduced by a factor of 0.94, the shear strength by 0.94 · 0.57 = 0.53. This means that the free length a could be increased to about 3.5 h.

4.3 Torsion Test

It is very easy to establish a pure torsional action, see figur 6.
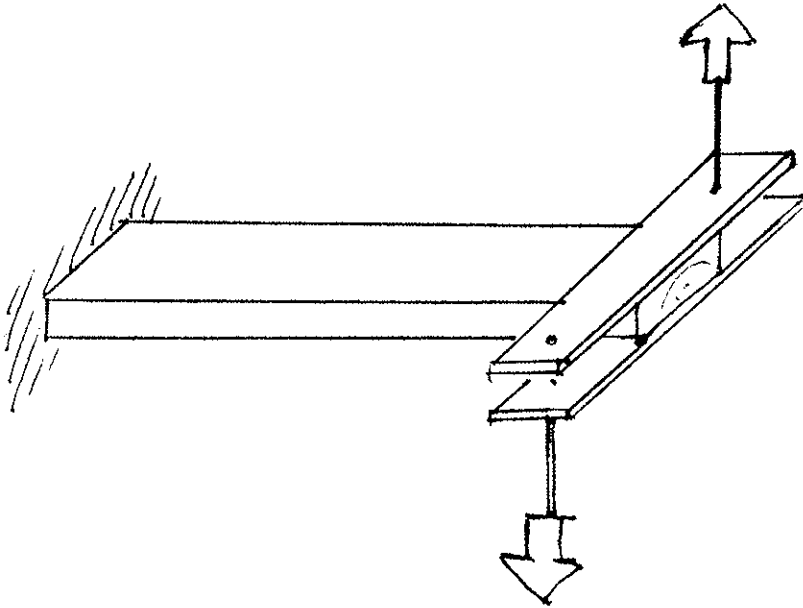
Figure 6. Torsion test

Also here the free failure is hindered by the cramping, but by making the specimen rather long, it is possible to reduce this effect.

The only problem is that for getting a statically determinated stress distribution, the specimen should be formed as a thin-walled cylinder. It is, however, possible to determine the stresses in a rectangular cross-section with an acceptable accuracy.

INTERNATIONAL COUNCIL FOR BUILDING RESEARCH STUDIES AND DOCUMENTATION

WORKING COMMISSION W18A - TIMBER STRUCTURES

DESIGN OF NAILED AND BOLTED JOINTS
PROPOSALS FOR THE REVISION OF EXISTING FORMULAE
IN DRAFT EUROCODE 5 AND THE CIB CODE

by

L R J Whale
Brighton Polytechnic
United Kingdom

I Smith
University of New Brunswick
Canada

H J Larsen
Danish Building Research Institute
Denmark

MEETING TWENTY
DUBLIN
IRELAND
SEPTEMBER 1987

Symbols

$f_h ; f_H$	=	General term for embedding strength
$f_{h,m} ; f_{h,mean}$	=	Mean embedding strength
$f_{h,K}$	=	Characteristic embedding strength
$f_{h,0} ; f_{h,mean,0}$	=	Mean embedding strength
$f_{h,\Theta} ; f_{h,mean,\Theta}$	=	Mean embedding strength at angle Θ to the grain
$f_{h,1} ; f_1$	=	Joint side member embedding strength
$f_{h,2} ; f_2$	=	Joint middle member embedding strength
β	=	Constant or ratio between middle member embedding strength and side member embedding strength (f_2/f_1)
ρ_m, ρ_{mean}	=	Mean density
ρ_K	=	Characteristic density
$\rho_{effective}$	=	Effective density for board materials
f_y	=	General term for yield strength of fastener
$f_{y,K}$	=	Characteristic yield strength of fastener
$M_{y,K}$	=	Characteristic yield moment
R_K	=	Characteristic load-carrying capacity of joint
t_1	=	Joint side member thickness
t_2	=	Joint middle member thickness
α	=	Ratio between middle member thickness and side member thickness (t_2/t_1)
d	=	Fastener diameter
u	=	Joint slip
l_2	=	Nail penetration depth

Introduction

At the joint CIB-W18/IUFRO Wood Engineering Group meeting in Florence in 1986, papers were presented which described the results of a comprehensive investigation by TRADA on short-term properties of nailed and bolted joints (Whale, Smith and Hilson, 1986) and the application of that data in deriving design equations for Eurocode 5 (Whale and Smith, 1986a).

In accordance with discussions on these papers at the meeting, slight modifications are now made to the design approaches which had originally been put forward. Results from over 400 joint tests, carried out as part of the TRADA investigation, are also now presented as a testament to the accuracy of the design equations which are proposed.

Furthermore, the results of tests on nailed plywood and tempered hardboard specimens, which through lack of time had been precluded from the previous analysis, are now presented. These are used in an assessment of the design approaches to board material-to-timber joints which currently exist in the (CIB code, 1983) and the draft (Eurocode 5, 1986). As a result, modifications are proposed which extend the range of design possibilities for these types of joint.

Embedding Strength of Wood

The basic wood strength parameter determining the lateral load carrying capacity of joints with nails, bolts, screws and other dowel-type fasteners is the embedding strength f_h.

The results of TRADA's recent research on these types of joint, in (Smith, 1983) and (Whale and Smith, 1986b, 1986c) are summarized in Figure 1, where also the values assumed in the draft (Eurocode 5, 1986) are shown.

In the TRADA work, embedding strengths were found for plain round nails with a diameter, d, between 2.65 and 6.0mm loaded parallel and perpendicular to the grain in softwoods (mean density, ρ_{mean} about 400-500 kg/m^3) and in dense hardwoods (ρ_{mean} about 700-1000 kg/m^3). In softwoods no preboring was used. In hardwoods holes were prebored to 80% of the nail diameter.

The embedding strength was also found for bolts with a diameter between 8 and 20mm loaded parallel and perpendicular to the grain. The holes were

Figure 1

$\dfrac{f_h \text{ mean}}{\rho \text{ mean}}$ as a function of diameter d for nails or bolts in solid timber

-2-
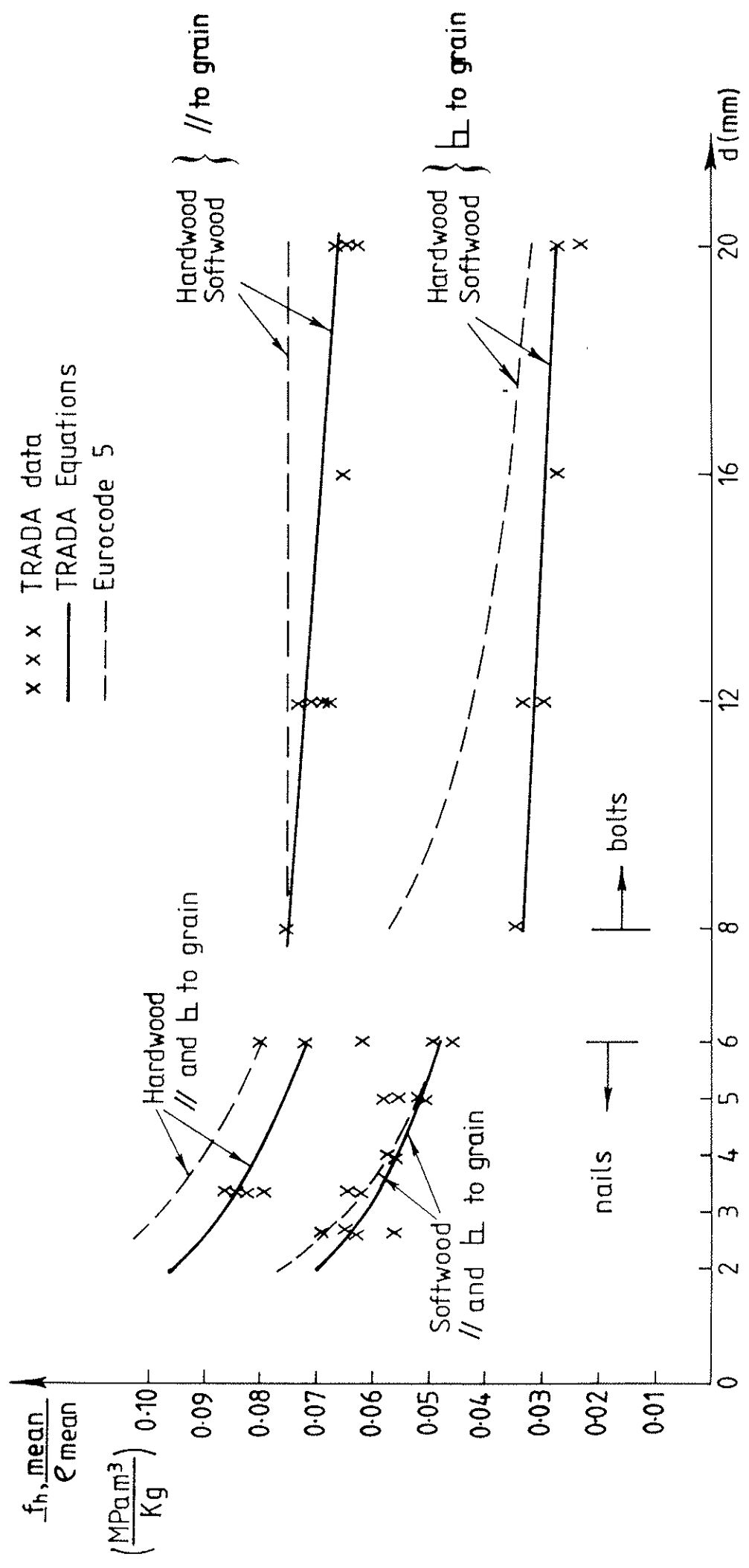
approximately 1.5mm oversized. This followed ealier work by (Smith, 1983) in which embedding strengths were determined in European whitewood for plain steel dowels in close-fitting holes.

For bolts, no difference was found between the softwood and dense hardwood specimens in respect of their embedding strength density trends.

It is conceivable therefore, that the difference between nails in softwood and hardwoods is attributable to the effect of preboring, rather than to inherent differences in the behaviour of the wood species as had previously been assumed in (Whale and Smith, 1986a). This approach is certainly more appealing from the codification viewpoint, and is supported by the fact that the differences found in Figure 1 compare well with those reported by (Wilkinson, 1973) for the effects of lead holes in softwoods.

The curve in Figure 1 for nails in softwood corresponds to (see Whale and Smith, 1986a):-

$$f_{h,mean} = 0.09 \, \varrho_{mean} \, d^{-0.36} \qquad \ldots\ldots (1)$$

where ϱ_{mean} is defined by volume and mass at 20°C/65% RH

and in the absence of contradictory data, this relationship will be assumed for all nails without preboring irrespective of timber species.

In Figure 1 the ratio for a given nail diameter between f_h/ϱ for hardwood and f_h/ϱ for softwood varies between 1.40 for $d = 2.65mm$ and 1.48 for $d = 6.0mm$. Hereinafter a constant value of 1.44 will be assumed.

The curve in Figure 1 for bolts loaded parallel to the grain corresponds to (see Whale and Smith, 1986a):-

$$f_{h,mean} = 0.082 \, (1-0.01d) \, \varrho_{mean} \qquad \ldots\ldots (2)$$

For the load acting at an angle Θ to the grain the following will be assumed:-

$$f_{h,mean} \, \theta = \frac{f_{h,mean,o}}{(2.3 \, Sin^2\theta + Cos^2\theta)} \qquad \ldots\ldots (3)$$

ie. a 'Hankinson' expression. As seen from Figure 1 this is an approximation for $\Theta = 90°$ by disregarding the slight diameter influence on $f_{h,\Theta}/f_{h,o}$ for the purposes of code presentation.

The values given above are valid for the mean values. In the following it will be assumed that the same relationship can be used between the characteristic values $f_{h,K}$ and ϱ_K.

Lateral Capacity of Nailed Timber Joints

Theoretically the characteristic load carrying capacity of nailed joints with typical nail slenderness ratios and members of equal embedding strength see (Larsen, 1973), is:-

$$R_K = \sqrt{2\, M_{y,k}\ f_{h,k}\ d}$$
$$\ldots\ldots (4)$$

where $M_{y,K}$ is the characteristic yield moment.

This can be found as:-

$$M_{y,k} = f_{y,k}\ d^3\!/6$$
$$\ldots\ldots (5)$$

where $f_{y,K}$ is the characteristic yield strength of the nail.

According to (Smith and Whale, 1985a, 1985b) a minimum value of $f_{y,K}$ can be taken as:-

$$f_{y,k} = 50\,(16-d)\qquad (MP_a)\qquad \ldots\ldots (6)$$

with d in mm. In the present draft (Eurocode 5, 1986) a minimum value of 600 Mpa has been assumed.

Nailed Joints with no Preboring

Inserting (1), (5) and (6) into (4) gives:-

$$R_K = 4\cdot90\ \sqrt{1-d/16}\ d^{1\cdot82}\sqrt{\varrho_k}\quad (N)\qquad \ldots\ldots (7)$$

In Table 1 $\sqrt{1-d/16}\,d^{1\cdot82}$ and $d^{1\cdot6}$ are compared. It can be seen that (7) can reasonably well be replaced by the similar expression:-

$$R_K = 4.90 \times 1.16d^{1.6}\sqrt{\rho k}$$
$$\text{or} \quad R_K = 5.7d^{1.6}\sqrt{\rho k} \qquad \qquad \ldots\ldots (8)$$

Table 1

d (mm)	2·5	3	4	5	6
$\dfrac{\sqrt{1-\frac{d}{16}}\; d^{1.82}}{d^{1.6}}$	1·12	1·15	1·17	1·17	1·17

Although an approximation slightly better than formula (8) is $R_K = 5.3d^{1.65}\sqrt{\rho k}$ the second decimal on the exponent seems an unnecessary complication.

Nailed Joints with Preboring

For nailed joints with preboring (8) can be multiplied by $\sqrt{1.44} = 1.2$.

Comparisons and Experimental Validation

In order to check the validity of expressions such as that in equation (8) and to verify the predictive ability of the finite element model for joints which had previously been developed by (Smith, 1983), a series of tests on nailed and bolted joints was planned and conducted. The joints were dimensioned purposely to exhibit a variety of failure modes according to the yield theory. The schedule of joint tests carried out is given in Table 2.

The joints were fabricated from the same source material which had provided the embedment test specimens. The nailed joints were fabricated with small gaps between the joint members, and the nail heads were not driven -home into the side members. This was to provide a lower-bound estimate of their strength and stiffness properties which did not rely upon partial restraints provided by the nail heads, or frictional interactions between the members. The results of the nailed timber-to-timber joint tests are summarized in Table 3 along with predictions from the 'yield theory' due to (Johansen, 1949) and the FE model due to (Smith, 1983), using the embedment properties which had been determined previously. The failure modes and equations relating to the yield theory are given in Figure 2.

Table 2 Programme of validatory joint tests (All 3-piece joints)

KEY

REF	CONNECTOR SPECIFICATION			SIDE MEMBER		MIDDLE MEMBER		JOINT SPECIFICATION		EXPECTED FAILURE MODE	NUMBER REPLICATIONS
	TYPE	DIAMETER	NO./JOINT	MATERIAL	THICKNESS	MATERIAL	THICKNESS	SHEAR PLANES	TYPE		
SS1	Wire Nail	3·35	1	Sitka Spruce	20mm	Sitka Spruce	20mm	2	PTC	1B/2	20
SS2	Wire Nail	3·35	1	Sitka Spruce	20mm	Sitka Spruce	20mm	2	PPC	2	30
SS3	Wire Nail	3·35	1	Sitka Spruce	20mm	Sitka Spruce	20mm	2	PPT	2	30
HH1	Wire Nail	3·35	1	Keruing	30mm	Keruing	30mm	2	PTC	3	20
HH2	Wire Nail	3·35	1	Keruing	30mm	Keruing	30mm	2	PTT	3	20
HH3	Wire Nail	3·35	1	Keruing	30mm	Keruing	30mm	2	PPC	3	20
SS4	Black Bolt	M12	1	Redwood	15mm	Redwood	30mm	2	PTC	1A	20
SS5	Black Bolt	M12	1	Redwood	20mm	Redwood	20mm	2	PPC	1B	20
SS6	Black Bolt	M12	1	Redwood	20mm	Redwood	20mm	2	PPT	1B	20
HH4	Black Bolt	M20	1	Keruing	20mm	Keruing	20mm	2	PPC	1B	20
HH5	Black Bolt	M20	1	Keruing	15mm	Keruing	30mm	2	PTC	1A	20
BS1	Wire Nail	3·35	4	Redwood	27·6mm	Redwood	37mm	1	PTC	3	10
BS2	Wire Nail	3·35	4	Redwood	27·6mm	Redwood	37mm	1	PPC	3	10
SP1	Wire Nail	3·35	2	Finish birch Plywood	Nominal 6·75mm	Sitka Spruce	35mm	1	PPC	1	20
SP2	Wire Nail	3·35	2	Finish birch Plywood	Nominal 6·75mm	Sitka Spruce	35mm	1	PPT	1	20
SP3	Wire Nail	3·35	2	Douglas fir Plywood	Nominal 6·00mm	Redwood	50mm	1	PTT	2A	30
SP4	Wire Nail	3·35	2	Douglas fir Plywood	Nominal 6·00mm	Redwood	50mm	1	PTC	2A	30
SHb1	Wire Nail	3·35	2	Tempered Hardboard	Nominal 8mm	Sitka Spruce	50mm	1	PPC	1	20
SHb2	Wire Nail	3·35	2	Tempered Hardboard	Nominal 4·8mm	Sitka Spruce	50mm	1	PPC	1A	20
SHb3	Wire Nail	3·35	2	Tempered Hardboard	Nominal 4·8mm	Sitka Spruce	50mm	1	PPT	1	20
										TOTAL	420
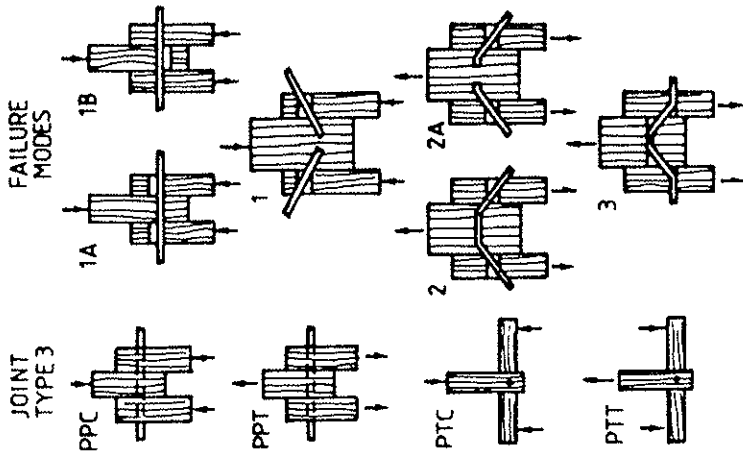
Figure 2 – Yield theory equations and their associated failure modes

Two-member joints

Arrangement

Three-member joints

Arrangement

$$P_y = \min \begin{cases}
f_M d t_1 & \text{(a)} \\
f_M d t_1 \, \alpha\beta \quad \text{(only for two-member joints)} & \text{(b)} \\
f_M d t_1 \, \alpha\beta/2 \quad \text{(only for three-member joints)} & \text{(c)} \\
f_M d t_1 \dfrac{\left[\sqrt{2\beta(1+\beta)+4\beta(2+\beta)d^3 f_y/(6 f_M d t_1^2)} - \beta\right]}{2+\beta} & \text{(d)} \\
f_M d t_1 \, \alpha \dfrac{\left[\sqrt{2\beta^2(1+\beta)+4\beta(1+2\beta)d^3 f_y/(6 f_M d \alpha^2 t_1^2)} - \beta\right]}{2\beta+1} & \text{(e)} \\
\hspace{3cm}\text{(only for two-member joints)} \\
f_M d t_1 \, \alpha \dfrac{\left[\sqrt{\beta+2\beta^2(1+\alpha+\alpha^2)+(\beta^3\alpha^2)} - \beta(1+\alpha)\right]}{1+\alpha} & \text{(f)} \\
\hspace{3cm}\text{(only for two member joints)} \\
4d^2 \sqrt{\dfrac{10\beta f_M}{1+\beta}} \sqrt{\dfrac{f_y}{240}} & \text{(g)}
\end{cases}$$

Failure Modes

Mode:	1a	1b	2	3
Equation:	(f)	(a) (b)	(d) (e)	(g)

Failure Modes

Mode:	1b	1b	3	2	3
Equation:	(a)	(c)	(g)	(d)	(g)

Table 3

Joint Ref.	Yield Theory		Experimental			F.E. Model		Comparisons			
	Failure Load(kN) (a)	Failure Mode (b)	Failure Load R_K (c)	Failure Mode(%) (d)	Slip at $R_K/3$ (mm) (e)	Failure Load(kN) (f)	Slip at $R_K/3$ (g)	Yield Theory VS. Experiment		F.E. Model VS.Experiment	
								$(a)/(c)$	% Mode Correct	$(f)/(c)$	$(g)/(e)$
SS1	1.63	1b/2	1.46	2(95) 1b(5)	0.32	1.47	0.29	1.12	1.00	1.01	0.91
SS2	1.55	2	1.34	2(100)	0.32	1.49	0.32	1.16	1.00	1.11	1.00
SS3	1.59	2	1.32	2(100)	0.35	1.49	0.32	1.20	1.00	1.13	0.91
BS1	4.21	3	4.46	3(100)	0.31	4.93	0.21	0.94	1.00	1.11	0.68
BS2	4.13	3	3.98	3(70) 2(30)	0.38	4.73	0.19	1.04	0.70	1.19	0.50
HH1	2.78	3	3.04	3(100)	0.40	2.87	0.27	0.91	1.00	0.94	0.68
HH2	2.77	3	2.86	3(100)	0.35	2.88	0.27	0.97	1.00	1.01	0.77
HH3	2.95	3	2.94	3(78) 2(22)	0.23	2.96	0.25	1.00	0.78	1.01	1.09
Average Error (+/-)								8.8%	/	7.8%	20.5%

Table 3 demonstrates that both the yield theory and the FE model can predict the failure load of nailed joints to an average accuracy of within 10%, and that the FE model can predict displacements to an average accuracy of around 20%. However, since both of these methods are impractical for design, simplified expressions of the type in equation (8) must be used.

In Table 4, a comparison is made between the nailed joint design formulae proposed in equation (8) of this paper, the existing draft Eurocode 5, and the CIB code, with the experimental joint test values and the yield theory predictions. Since the simplified expressions derive from the assumption that a mode 3 failure occurs, comparisons with the yield theory are confined to the mode 3 expression, irrespective of whether this was the governing failure mode.

Also since these code expressions assume a minimum nail yield stress (50(16-d) in this paper; or 600Mpa in the existing draft EC 5 and CIB code)), for the purposes of this comparitive exercise, each expression is adjusted for the true yield stress of the nails used in the joint tests.

In sets SS1, SS2 and SS3 failure occurred by modes other than mode 3, and so comparisons with the experimental failure loads in these cases can be expected to be poor. This eventuality is guarded against in the draft EC 5 and CIB code, by stipulating that member thicknesses should be at least 7d. A verification of this rule is made in the next section.

Table 4

Joint Ref	Load – Carrying Capacity, R_k						Slip at $R_k/3$
	Proposal in this paper $R_k=5.7d^{1.6}\sqrt{\rho}$		Existing draft EC5 $R_k=6.0d^{1.6}\sqrt{\rho}$		CIB Code $6.32d^{1.7}\sqrt{\rho}$ [1]		EC5 & CIB code $u=0.5d\ K_{creep}(P/R_k)^{1.5}$ [2]
	Versus		Versus		Versus		Versus
	Yield (Mode 3)	Experiment	Yield (Mode 3)	Experiment	Yield (Mode 3)	Experiment	Experiment
SS1 [4]	0·96	1·23	1·03	1·33	1·15	1·49	1·03
SS2 [4]	0·98	1·34	1·05	1·44	1·18	1·62	1·03
SS3 [4]	0·97	1·37	1·04	1·48	1·17	1·65	0·94
BS1	0·90	0·85	0·97	0·92	1·09	1·03	1·06
BS2	0·89	0·93	0·96	1·00	1·08	1·12	0·84
HH1	1·06	0·97	1·19	1·09	1·07	0·97	0·83
HH2	1·08	1·04	1·12	1·17	1·08	1·05	0·94
HH3	1·01	1·01	1·13	1·14	1·01	1·02	1·43
Average Error(+/-)	5·6 %	15·5% (4·0%) [3]	9 %	21·6% (9·6%) [3]	10·4%	25·1% (5·0%) [3]	12·5%

Footnotes :

[1] For the CIB code calculations, ρ was adjusted to oven dry mass/volume at 20°C/65% RH as the CIB code requires.

[2] K_{creep} is assumed to be 1.0.

[3] Percentage erros in parenthesis are values which related purely to joints which exhibited mode 3 failures.

[4] Joints in sets SS1, SS2 and SS3 violate the requirement in draft EC5 and the CIB code that the thinnest member should be a minimum of 7d thick (actual = 6d).

It can be seen from Table 4 that equation (8) in this paper, and its hardwood equivalent, models the yield theory expression for mode 3 failures to an average accuracy of around 5%, and the experimental results from joints with mode 3 type failures to around 4%. The existing expressions in draft Eurocode 5 and the CIB code provide slightly poorer predictions of observed behaviour.

The existing empirical expression for estimating slip in nailed joints at loads less than $R_K/3$ is seen however to provide extremely good predictions of observed values in short-term tests. Work is currently underway at TRADA which will provide the information necessary to check the accuracy of the K_{creep} factors proposed for longer time-scales.

Dimensioning Rules

In order to verify the ascertion in the draft Eurocode 5 and CIB code, that a mode 3 type failure can be assured if the t_1/d ratio of the joint has a minimum value of 7, Figures 3 and 4 trace the yield theory predictions for failure modes in various types of joint as the t_1/d ratio varies. Joints are postulated with high strength members typical of the high density hardwoods, and low strength membrs such as those produced from a low density softwood, and with various f_y/f_h ratios and α values. For both two and three joints it is clear that for the worst scenario when low strength timbers are jointed using small diameter nails, the $t_1 = 7d$ rule is an extremely accurate one. It would seem this could be reduced to $t_1 = 5d$ for the dense hardwoods, although this extra complication is of doubtful worth.

Figure 3

3—Member joints

Case 4 $\left.\begin{array}{l}f_h = 60 \text{ N/mm}^2 \\ d = 6\text{mm}(f_y = 500 \text{ N/mm}^2) \\ \beta = 1\end{array}\right\}$

Case 2 $\left.\begin{array}{l}f_h = 25 \text{ N/mm}^2 \\ d = 6\text{mm}(f_y = 500 \text{ N/mm}^2) \\ \beta = 1\end{array}\right\}$

Case 3 $\left.\begin{array}{l}f_h = 60 \text{ N/mm}^2 \\ d = 2\cdot5\text{mm}(f_y = 675 \text{ N/mm}^2) \\ \beta = 1\end{array}\right\}$

Case 1 $\left.\begin{array}{l}f_h = 25 \text{ N/mm}^2 \\ d = 2\cdot5\text{mm}(f_y = 675 \text{ N/mm}^2) \\ \beta = 1\end{array}\right\}$

Note :—
$\propto = \dfrac{t_2}{t_1}$

R_K (kN)

t_1/d

Figure 4

2 — Member joints

Note :—
$\alpha \equiv \dfrac{t_2}{t_1}$

Case 4 $\left\{\begin{array}{l} f_h = 60 \ N/mm^2 \\ d = 6mm \ (f_y = 500 N/mm^2) \\ \beta = 1 \end{array}\right.$

Case 2 $\left\{\begin{array}{l} f_h = 25 N/mm^2 \\ d = 6mm \ (f_y = 500 \ N/mm^2) \\ \beta = 1 \end{array}\right.$

Case 3 $\left\{\begin{array}{l} f_h = 60 \ N/mm^2 \\ d = 2.5mm \ (f_y = 675 \ N/mm^2) \\ \beta = 1 \end{array}\right.$

Case 1 $\left\{\begin{array}{l} f_h = 25 \ N/mm^2 \\ d = 2.5mm \ (f_y = 675 /mm^2) \\ \beta = 1 \end{array}\right.$

R_k (kN)

3·6
3·4
3·2
3·0
2·8
2·6
2·4
2·2
2·0
1·8
1·6
1·4
1·2
1·0
0·8
0·6
0·4
0·2
0

1·0 2·0 3·0 4·0 5·0 6·0 7·0 8·0 t_4/d

$\alpha = 5$
$\alpha = 1$
$\alpha = 5$
$\alpha = 1$
$\alpha = 5$
$\alpha = 1$
$\alpha = 5$
$\alpha = 1$

Figure 5.   Geometry and strength values for
a) symmetrical 3-member joints
b) 2-member joints

Theoretically, see (Larsen, 1973), the characteristic load-carrying capacity of a symmetrical 3-member joint is determined by:-

$$\frac{R_K}{f_1 d^2} = \min \begin{cases} \dfrac{t_1}{d} & \cdots\cdots (9) \\[2ex] 0\cdot5\ \dfrac{f_2}{f_1}\ \dfrac{t_2}{t_1}\ \dfrac{t_1}{d} & \cdots\cdots (10) \\[2ex] \sqrt{\left(\dfrac{2(f_1+f_2)}{f_2} + \dfrac{2}{3}\ \left(\dfrac{2f_1+f_2}{f_1\,f_2}\right)\dfrac{d^2}{t_1^2}f_y-1\right)\dfrac{f_2}{(2f_1+f_2)}}\ \dfrac{t_1}{d} & \cdots\cdots (11) \\[2ex] \sqrt{\dfrac{2}{3}\ \dfrac{f_2}{f_1+f_2}\ \dfrac{f_y}{f_1}} & \cdots\cdots (12) \end{cases}$$

These expressions are formally equivalent to those relating to 3-member joints in Figure 2.

In (Eurocode 5, 1986), formula (11) is approximated by :-

$$\frac{R_K}{f_1 d^2} = 0.5 \sqrt{\frac{2}{3} \frac{f_2}{f_1 + f_2} \frac{f_y}{f_1}} + 0.2 \, t_1/d \qquad \ldots\ldots (13)$$

Further simplifications are then made, by assuming $f_1 = f_2$ and $f_y = 240$. In Figures 6-8 the expressions (9)-(12) and the approximation (13) are shown for different joint configurations with f_y/f_h values of 4, 12 and 24. This covers the range of values found in practice.

For a 2-member joint, see figure 5b, equations (10), (11) and (12) - but not (9) - are valid and the following three conditions are added:-

$$\frac{R_K}{f_1 d^2} = \min \begin{cases} \dfrac{f_2}{f_1} \dfrac{t_2}{t_1} \dfrac{t_1}{d} & \ldots\ldots (14) \\[3ex] \left[\sqrt{\dfrac{2(f_1 + f_2)}{f_1} + \dfrac{2}{3} \dfrac{f_1 + 2f_2}{f_1 \, f_2} \dfrac{d^2}{t_2^2} f_y} - 1 \right] \dfrac{f_2}{f_1 + 2f_2} \dfrac{t_2}{t_1} \dfrac{t_1}{d} & \ldots\ldots (15) \\[3ex] \left[\sqrt{\dfrac{f_1}{f_2} + 2 + 2\dfrac{t_2}{t_1} + \left(\dfrac{t_2}{t_1}\right)^2 \left(2 + \dfrac{f_2}{f_1}\right)} - \left(1 + \dfrac{t_2}{t_1}\right) \right] \dfrac{f_2}{f_1 + f_2} \times \dfrac{t_1}{d} & \ldots\ldots (16) \end{cases}$$

These expressions are formally equivalent to those relating to 2-member joints in figure 2.

In (Eurocode 5, 1986) formula (15) is approximated by:-

$$\frac{R_K}{f_1 d^2} = 0.5 \sqrt{\frac{2}{3} \frac{f_2}{f_1 + f_2} \frac{f_y}{f_1}} + 0.2 \frac{t_2}{t_1} \frac{t_1}{d} \qquad \ldots\ldots (17)$$

before the further assumptions of $f_1 = f_2$ and $f_y = 240$ are added, and (16) is approximated by:-

$$R_K = 0.2 \, (f_1 \, t_1 + f_2 \, t_2) \, d \qquad \ldots\ldots (18)$$

The approximation in (18) is compared to (16) in Table 5.

Figure 6

-15-
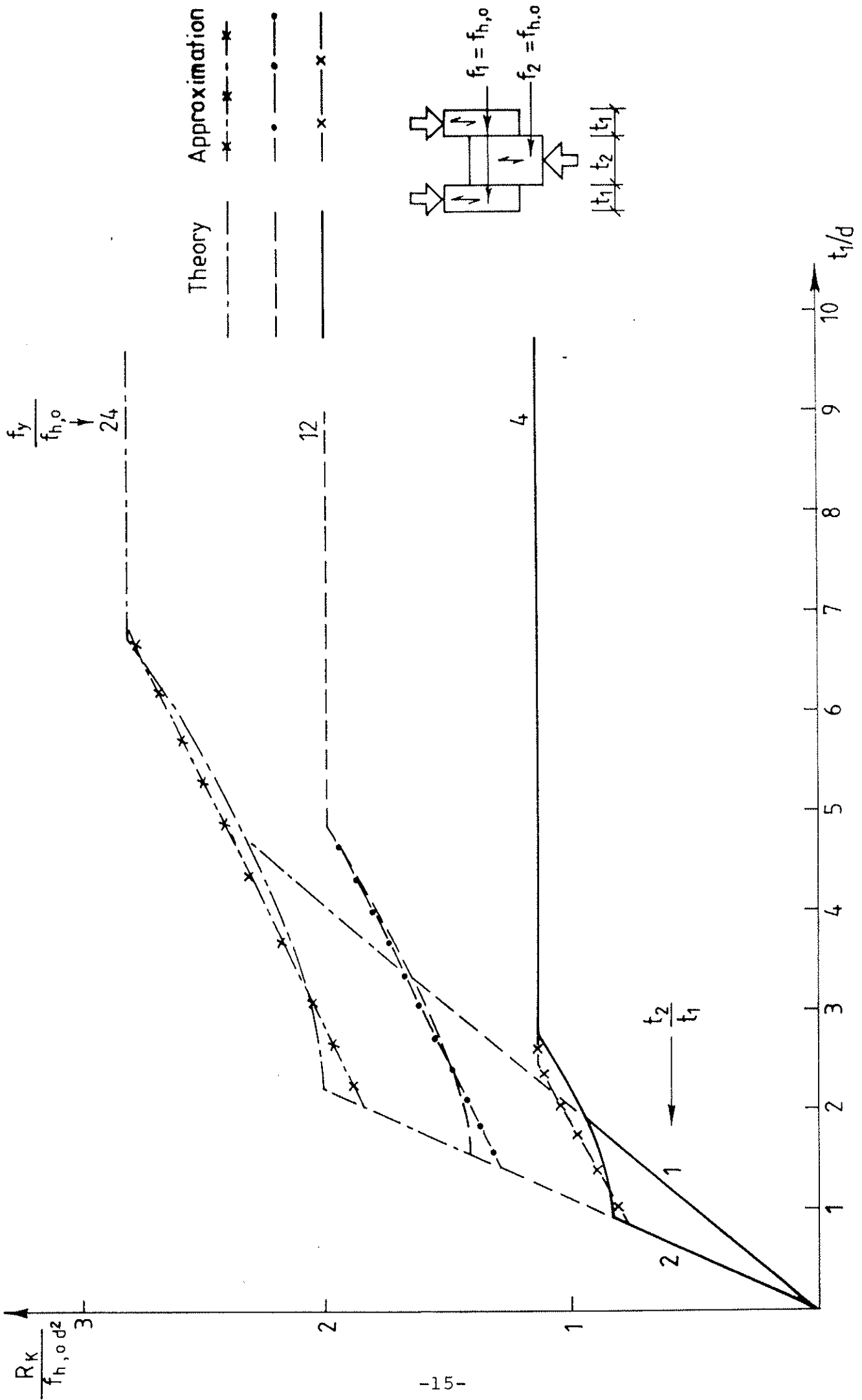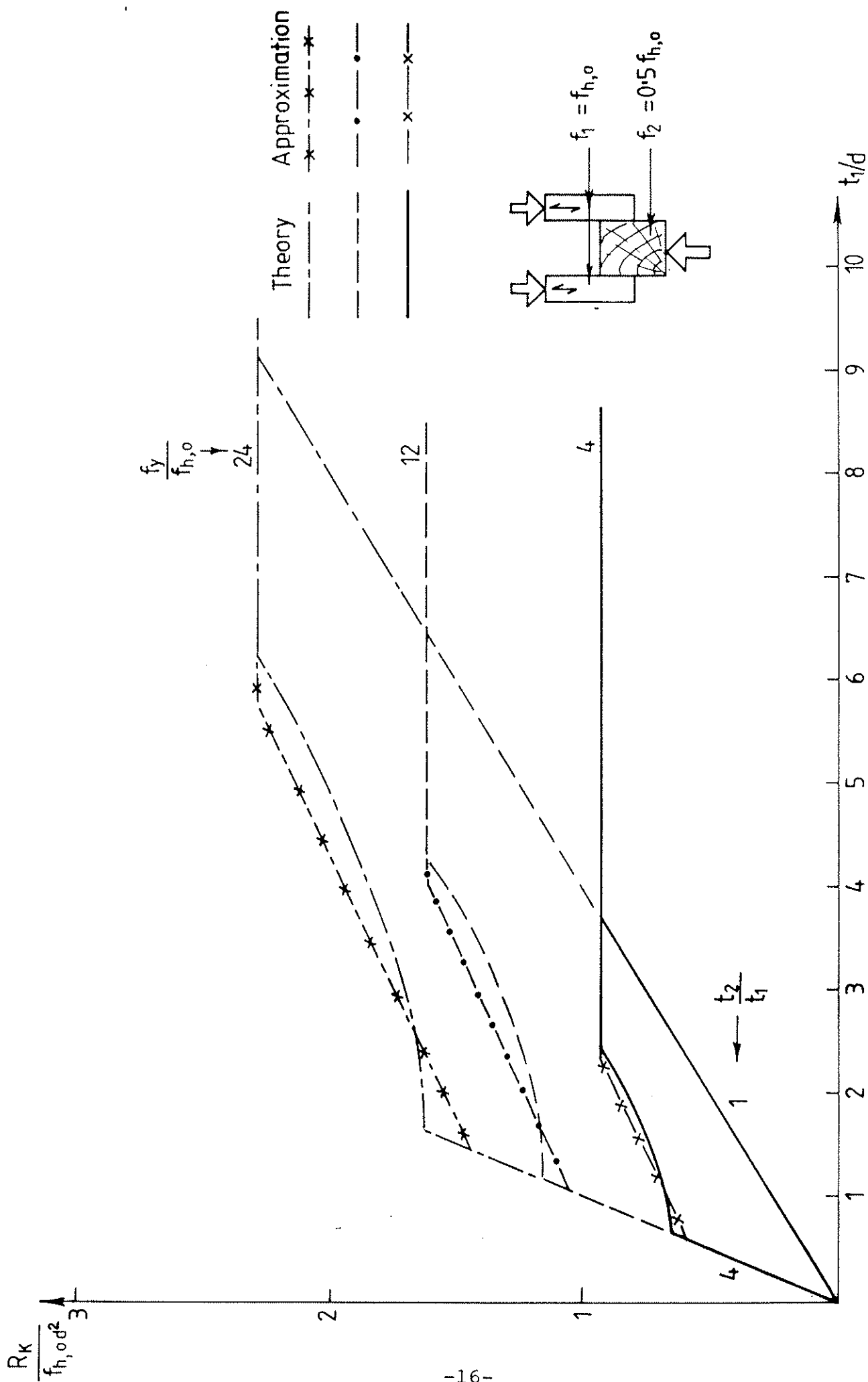
Figure 7

Figure 8
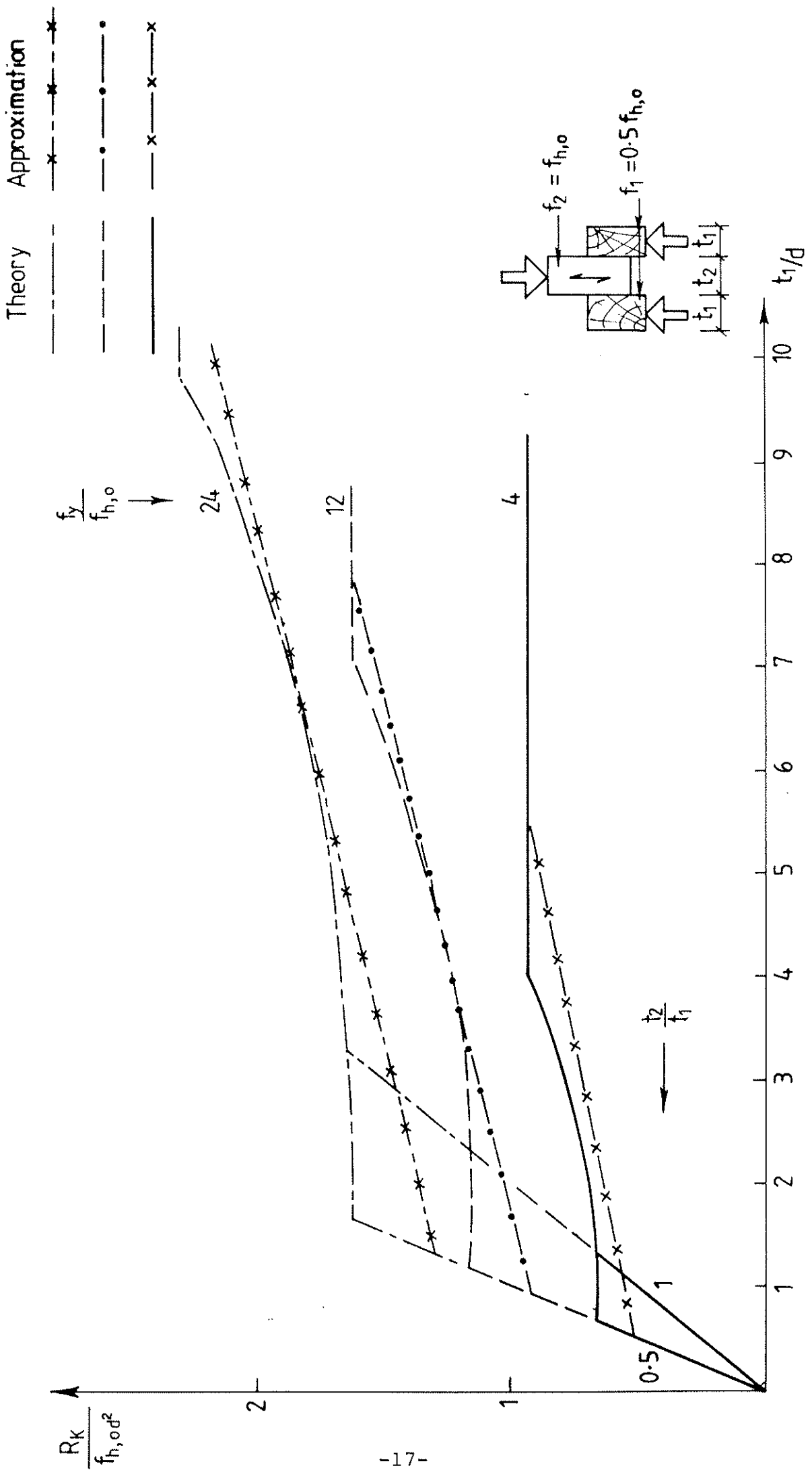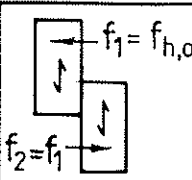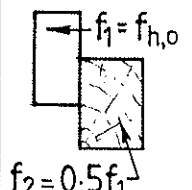
Table 5

	t_2/t_1	0.5	1	2	3	4	5
$\dfrac{R_K}{f_{h,o,t,d}}$	Theory (Eq. 16)		0.41	0.68	1.00		
	Approx (Eq. 18)		0.40	0.60	0.80		
$\dfrac{R_K}{f_{h,o,t,d}}$	Theory (Eq. 16)	0.29	0.31	0.41	0.57	0.74	0.92
	Approx (Eq. 18)	0.25	0.30	0.40	0.50	0.60	0.70

Comparisons and Experimental Validation

Once again, in order to check the validity of the expressions proposed for bolt embedding strengths in equations (2) and (3) and of the bolted joint design formulae in equations (9)-(13), a series of tests on bolted softwood and hardwood joints were carried out (see Table 2). Due to a shortage of material from which the joints had to be fabricated, only mode 1b type failures could be investigated in the programme. A complete verification of each of equations (9)-(13) is therefore not possible, although the results do provide a basis upon which to compare the various proposals for bolt embedding strengths.

The joints were fabricated with a single bolt in holes drilled 1.5mm oversize. No gaps were provided between the members of the bolted joints although soft springs were inserted between the bolt heads and nuts adjacent to the outer timber members, to prevent the introduction of undue lateral restraint provided via the washers. If bolts are not re-tightened in practice, this restraint cannot be relied upon in design.

The results of the bolted timber-to-timber joint tests are summarised in Table 6 along with the predictions from equations (9)-(13) and the FE model due to (Smith, 1983), using the true embedment properties of the joint members.

Table 6

Joint Ref.	Yield Theory		Experimental			F.E. Model		Yield Theory VS. Experiment		F.E. Model VS. Experiment	
	Failure Load(kN) (a)	Failure Mode (b)	Failure Load R_K (c)	Failure Mode(%) (d)	Slip at $R_K/3$ (mm) (e)	Failure Load(kN) (f)	Slip at $R_K/3$ [1/] (g)	(a)/(c)	% Mode Correct	(f)/(c)	(g)/(e)
SS4	5·19	1b Eq(9)	7·18	1b(100)	0·92	6·71	0·56 2·06	0·72	1·00	0·93	0·61 2·24
SS5	8·11	1b Eq(10)	9·26	1b(100)	0·77	8·75	0·47 1·97	0·88	1·00	0·94	0·61 2·56
SS6	10·45	1b Eq(10)	9·64	1b(100)	0·94	10·31	0·32 1·82	1·08	1·00	1·07	0·34 1·94
HH4	19·48	1b Eq(10)	19·69	1b(100)	1·16	19·43	0·31 1·81	0·99	1·00	0·99	0·27 1·56
HH5	13·31	1b Eq(9)	18·20	1b(100)	1·15	17·90	0·25 1·75	0·73	1·00	0·98	0·22 1·52
Average Error (+/-)								15·2%	\	4·6%	−59% +96%

Footnotes:

1/   Values for slip at $R_K/3$ from the FE Model represent upper and lower bound predictions, depending upon the amount of bolt-hole tolerence take-up.

It can be seen that equations (9) and (10) in this paper, when provided with embedding strength data from specimens matched with those in the joints, predicted the experimental failure loads to an average accuracy of around 15%. The finite element model is capable of substantially improving on this accuracy and is able to successfully predict the range of joint slip values expected at one third failure load.

A comparison of the experimental results with the design equations for bolted joints proposed in the existing draft Eurocode 5, the CIB code, and in this paper, is given in Table 7. This incorporates the different expressions for bolt bearing strengths which exist in each of these publications, in the basic design equations which are reproduced as Equations (9) and (10) in this paper.

Table 7

| Joint Ref. | Calculated versus Experimental Load-carrying capacities R_K | | | Calculated slip at $R_K/3$ EC5+CIB Code $u = 0.1d + 1mm$ versus Experiment (%) |
	Proposals in this paper $f_{h,o} = 0.082(1-0.01d)\varrho$ $f_{h,\theta} = \dfrac{f_{h,o}}{2.3Sin^2\theta + Cos^2\theta}$	Existing draft EC5 $f_{h,o} = 0.075\varrho$ $f_{h,\theta} = \dfrac{f_{h,o}(0.32+10d^{-1.5})}{(0.32+10d^{-1.5})Cos^2\theta + Sin^2\theta}$	CIB Code $f_{h,o} = 0.070\varrho$ [1] $f_{h,\theta} = \dfrac{f_{h,o}(0.45+8d^{-1.5})}{(0.45+8d^{-1.5})Cos^2\theta + Sin^2\theta}$	
SS4	0·68	0·90	0·85	2·40
SS5	0·88	0·92	0·76	2·87
SS6	0·83	0·86	0·71	2·36
HH4	0·89	1·01	0·84	2·59
HH5	0·60	0·68	0·70	2·62
Average Error (%)	22·4 %	13%	22·8%	≈+150%

Footnotes:

1/ For the CIB code calculations, ϱ is adjusted to oven dry mass/volume at $20°C/65\%$ RH as the CIB code requires.

The basic error of 15.2% brought about by the (yield theory) Equations (9) and (10) in this paper, increases to 22.4% when the approximative bolt embedding strength formulae in Equations (2) and (3) are used. Although the CIB code expressions result in a similar overall error, the existing draft Eurocode 5 expressions provide a much better model of the true embedding strengths of the joint members in this instance. When contrasted with the basic errors attributable to the yield theory itself (viz table 6), the existing draft EC5 expressions are seen to overestimate the embedding strength of the joint membes by an average of 2%. The formulae proposed in this paper and in the CIB code, underestimate their embedding strengths by an average of 6.5%. However, the authors feel the expressions in Equations (2) and (3) will provide a better model of bolt embedding strengths in the majority of cases which lie outside the scope of this particular comparative exercise.

Although the expressions in draft EC5 and the CIB code for calculating slip in bolted joints overestimated joint slip by a factor of 1.5, the majority of this was attributable to the 1mm allowance made for bolt tolerance take-up. The fact that this was not included in the experimental joints explains the major part of this error.

Embedding Strength of Sheet Materials

As part of TRADA's materials test programme, embedment characteristics for a wide range of nails and sheet materials were gathered. These included Finnish birch, Finnish birch faced, Finnish spruce, French pine, Canadian Douglas fir and Canadian Douglas fir faced plywoods, as well as 4.8mm and 8mm tempered hardboards, tested with nails ranging from 2.65 to 4mm diameter. In all,1600 such tests were carried out.

Twenty test replications were used throughout, with individual test samples from separate boards. Specimens were pre-conditioned in an environment of 20°C/65% RH before being tested in directions parallel and perpendicular to the face grain/board direction for durations up to 15 minutes.

Details and results from these tests are fully documented in (Whale and Smith, 1986b, 1986c). These may be summarized in terms of linear regression analyses between mean maximum embedding strength and mean density of the sheet material, as in Table 8. All regression lines have been fitted through zero, and sheet material densities have been adjusted to the draft (Eurocode 5, 1986) definition using mass and volume at 20°C/65% rh, assuming an average moisture content in the plywoods of 12% and in the tempered hardboards of 8%.

Table 8 — Results of Linear Regression Analysis of Maximum Nail Embedding Strength Against Mean Sheet Material Density at 20°C/65% rh

	Nail diameter	Mean maximum embedding strength (N/mm²)				Combined regression
		Comp. parallel to face grain/ Lengthways	Comp.perp. to face grain / Widthways	Tension parallel to face grain/ Lengthways	Tension perp. to face grain/ Widthways	
Plywoods	2·65	0·088e	0·089e	—	—	0·088e
	3·00	0·081e	0·085e	—	—	0·083e
	3·35	0·084e	0·081e	0·076e	0·077e	0·079e
	3·75	0·076e	0·077e	—	—	0·076e
	4·00	0·070e	0·072e	—	—	0·071e
4·8mm Tempered hardboard	2·65	0·061e	0·062e	0·057e	0·061e	0·059e
	3·00			0·054e	0·056e	0·055e
	3·35			0·051e	0·051e	0·056e
	3·75			0·052e	0·049e	0·050e
	4·00			0·045e	0·047e	0·046e
8mm Tempered hardboard	2·65	0·076e	0·077e	0·078e	0·077e	0·077e
	3·00			0·074e	0·075e	0·075e
	3·35			0·062e	0·060e	0·069e
	3·75			0·068e	0·066e	0·067e
	4·00			0·062e	0·060e	0·061e

It is clear from Table 8 that the density relationships illustrated, also show a distinct diameter trend. In the case of tempered hardboards this is also seen to depend upon board thickness, probably due to surface 'skin' effects. Variations between the strength properties of specimens determined in different directions, or in a tensile or compressive mode seem very small. Indeed, no significant differences could be detected between the contributions of parallel and perpendicular veneers in plywood specimens when the results from tests in mutually perpendicular directions were solved simultaneously in an attempt to establish these individual properties. All subsequent analyses are therefore based upon the combined regression values in Table 8.

The diameter trends illustrated in Table 8 were best described by a straight relationship. Figure 9 shows the nature of these trends and the linear relationships which were fitted to them. These may be written as follows:-

$$\text{Plywood}: \quad \frac{f_{h,mean}}{\varrho_{mean}} = 0 \cdot 119 - 0 \cdot 012 d \quad (r = -0 \cdot 88) \qquad \cdots \cdots (19)$$
$$\text{Approx} \; [0 \cdot 012 \; (10 - d)]$$

$$\begin{array}{l}\text{4·8mm (nom.)} \\ \text{Tempered} \\ \text{Hardboard}: \end{array} \quad \frac{f_{h,mean}}{\varrho_{mean}} = 0 \cdot 083 - 0 \cdot 0086 d \quad (r = -0 \cdot 70) \qquad \cdots \cdots (20)$$
$$\text{Approx} \; [0 \cdot 0084 \; (10 - d)]$$

$$\begin{array}{l}\text{8mm (nom.)} \\ \text{Tempered} \\ \text{Hardboard}: \end{array} \quad \frac{f_{h,mean}}{\varrho_{mean}} = 0 \cdot 11 - 0 \cdot 0125 d \quad (r = -0 \cdot 73) \qquad \cdots \cdots (21)$$
$$\text{Approx} \; [0 \cdot 011 \; (10 - d)]$$

For the purposes of comparison, the embedding strength data for nailed timber specimens illustrated in Figure 1 and expressed in Equation (1) can be re-analysed on the same basis as the board material specimens to yield the following:-

$$\begin{array}{l}\text{Softwoods} \\ \text{(no pre-boring)} \end{array} \quad \frac{f_{h,mean}}{\varrho_{mean}} = 0 \cdot 0755 - 0 \cdot 0045 d \quad (r = -0 \cdot 85) \qquad \cdots \cdots (22)$$
$$\text{Approx} \; [0 \cdot 004 \; (19 - d)]$$

$$\begin{array}{l}\text{Tropical} \\ \text{Hardwoods} \\ \text{(pre-bored)} \end{array} \quad \frac{f_{h,mean}}{\varrho_{mean}} = 0 \cdot 0978 - 0 \cdot 0044 d \quad (r = -0 \cdot 72) \qquad \cdots \cdots (23)$$
$$\text{Approx} \; [0 \cdot 005 \; (19 - d)]$$

Figure 9 $\underline{\dfrac{f_{h,\,mean}\,/\varrho\,mean}{}}$ as a function of diameter d for nails in **sheet** materials

$$\dfrac{\text{Nail embedding strength}}{\text{Timber density}} = \dfrac{f_{h,mean}}{\varrho_{mean}}\left(\dfrac{MPa\ m^3}{Kg}\right)$$

Plywood $\dfrac{f_{h,mean}}{\varrho_{mean}} = 0.119 - 0.012d$
$(r = -0.88)$

8mm Tempered hardboard $\dfrac{f_{h,mean}}{\varrho_{mean}} = 0.11 - 0.0125d$
$(r = -0.73)$

4·8mm Tempered hardboard $\dfrac{f_{h,mean}}{\varrho_{mean}} = 0.083 - 0.0086d$
$(r = -0.70)$

Nail diameter (mm)

1·0   2·0   2·65   3·0   3·35   3·75   4·0

0   0·01   0·02   0·03   0·04   0·05   0·06   0·07   0·08   0·09   0·10   0·11   0·12   0·13   0·14

-23-
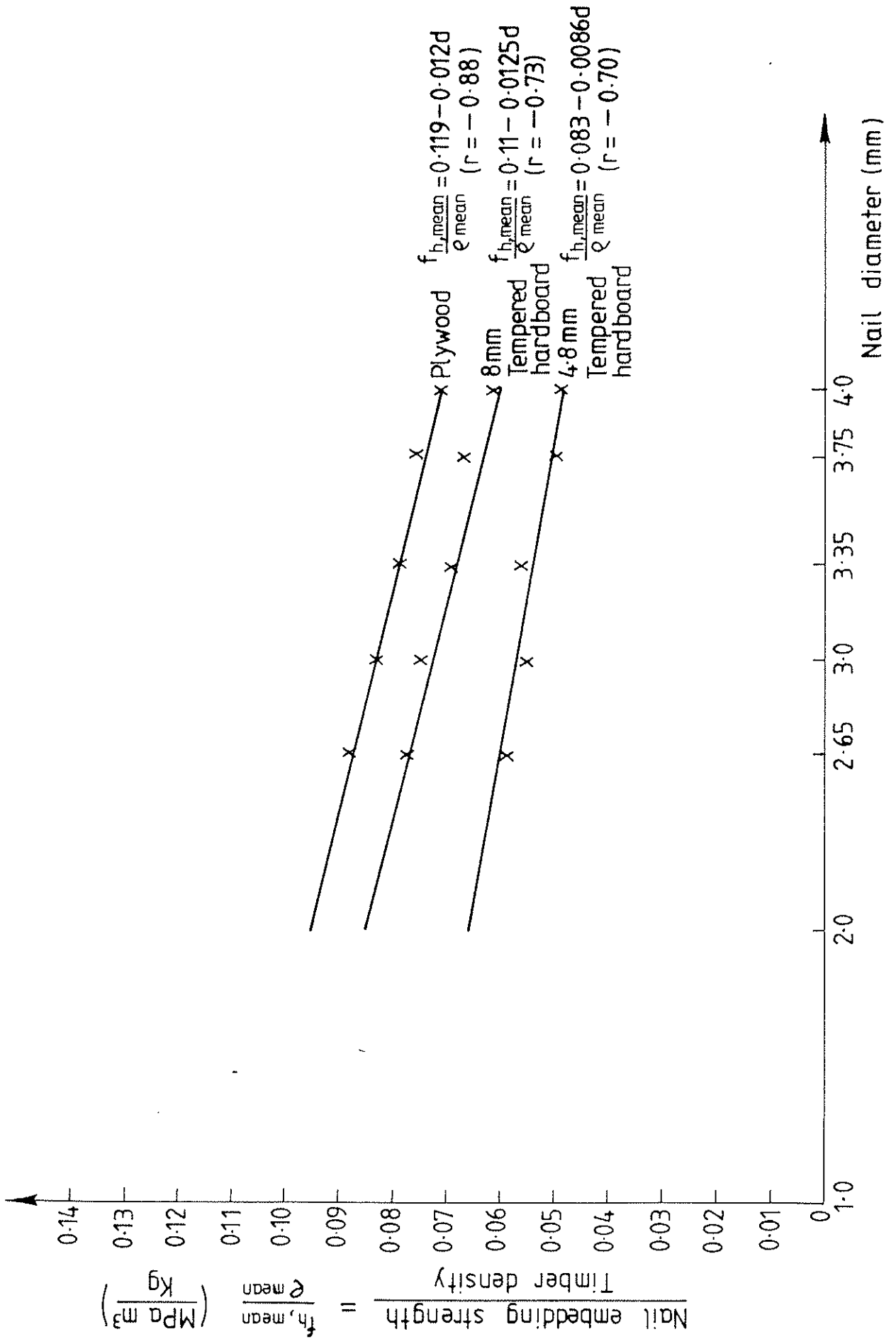
If we were to postulate that the thickness effect manifested in Equations (20) and (21) for tempered hardboard specimens, could be described by a power law relationship, for example, then:-

$$\frac{\left[\dfrac{f_h}{\varrho}\right]_{t_1}}{\left[\dfrac{f_h}{\varrho}\right]_{t_2}} = \left[\frac{t_1}{t_2}\right]^{\beta} \qquad \cdots\cdots (24)$$

Putting in the mean measured thicknesses of the two tempered hardboards, rather than the nominal values, we obtain:-

$$\frac{0\cdot 011 \,(10-d)}{0\cdot 0084\,(10-d)} = \left(\frac{8\cdot 0}{5\cdot 1}\right)^{\beta} \qquad \Rightarrow \quad \beta \doteq 0\cdot 6$$

The embedding strength of tempered hardboards could therefore be expressed by:-

Tempered
Hardboards :

$$\frac{f_h \text{ mean}}{\varrho \text{ mean}} = 0\cdot 0084 \,(10-d)\left(\frac{t}{5\cdot 1}\right)^{0\cdot 6}$$

$$\frac{f_h \text{ mean}}{\varrho \text{ mean}} = 0\cdot 00316 \,(10-d)\,t^{0\cdot 6} \qquad \cdots\cdots (25)$$

Since only two thicknesses of tempered hardboard were tested, the form of the thickness effect expressed in Equation (25) should only be regarded as tentative.

Density measurements on the 480 tempered hardboard specimens tested indicated that the particular brand involved had a mean density of 962kg/m^3 with a standard deviation of 26.1kg/m^3. Assuming the density variation was normally distributed, a 5% characteristic density value for tempered hardboard could then be taken as 920kg/m^3.

Comparisons between the sheet material embedding strength relationships in Equations (19) to (21) with those of the solid timber species, Equations (22) and (23), indicates that sheet material side members will often have greater bearing strengths than timber side plates of equivalent thickness. They will certainly almost always differ from those of the framing timber. This invalidates an assumption made in deriving Equation (4) used for solid timber nailed joints, and means that the full yield theory expression for mode 3 type failures in Equation (12) would need be solved. Given the fact that the ratio f_2/f_1 will vary according to the particular combination of sheathing material, framing material and nail diameter chosen, a considerable simplification is needed for the purposes of codification.

The approach which is adopted in the current (draft Eurocode 5, 1986) is to calculate the lateral capacity of board material to timber joints on the basis that the members were of equivalent strength to that of a timber with a density of 400kg/m^3, but that thinner side plates can be used in these types of joint than would otherwise be necessary. This latter statement, recognises the fact that where the sheet material has a bearing strength in excess of that assumed, thinner members can still develop the requisite resistance to enforce a mode 3 failure. The proposals in (draft Eurocode 5, 1986) for establishing minimum member thicknesses are given in Table 9:

Table 9

Side member material	Minimum Ratio t/d (d ≤ 5mm)
Timber	7
Particleboard	7
Softwood plywood	4·67
Mixed softwood/ hardwood plywood	3·5
Hardwood plywood	2·8
Tempered hardboard	2·8

By postulating joints which embrace the range of practical combinations of joint member materials and nail diameters which are possible, the yield theory equations in Figure 2 can be used to illustrate the relationship between the expected behaviour of these joints, and the assumptions which have been proposed. Reference to the basic embedding strength relationships derived in Equations (19) to (23), leads to the selection of possible joint configurations defined in Table 10:

Table 10

Case	Member Combination Outside	Centre	f_2/f_1	t_2/t_1	d	f_y
1	Softwood plywood ($\rho m = 550 Kg/m^3$)	Softwood ($\rho m = 400 Kg/m^3$)	0·55	1, 12	6	500
2		Hardwood ($\rho m = 750 Kg/m^3$)	1·45		2·5	675
3	Hardwood plywood ($\rho m = 700 Kg/m^3$)	Softwood ($\rho m = 400 Kg/m^3$)	0·4	1, 12	6	500
4		Hardwood ($\rho m = 750 Kg/m^3$)	1·1		2·5	675
5	Thin Hardboard ($\rho m = 960 Kg/m^3$)	Softwood ($\rho m = 400 Kg/m^3$)	0·5	1, 12	6	500
6		Hardwood ($\rho m = 750 Kg/m^3$)	2·0		2·5	675
7	Thick Hardboard ($\rho m = 960 Kg/m^3$)	Softwood ($\rho m = 400 Kg/m^3$)	0·35	1, 12	6	500
8		Hardwood ($\rho m = 750 Kg/m^3$)	1·3		2·5	675

The predicted behaviour of these joints based on the yield theory is compared with that of the approximative (draft Eurocode 5, 1986) expressions in Figures 10 to 13 for 2- and 3-member joints. These figures show that for joints made with softwood plywood the draft Eurocode 5 approach is safe and introduces only slight conservatism. For hardwood plywood joints the degree of conservatism introduced on the true mode 3 failure load is again quite small and at practical values of $\propto$ (say $\geqslant 4$) the expressions are almost always safe. The same can be said for the hardboard in Figures 12 and 13, although for side members with strengths similar to those of the thinner hardboards, at low t_1/d ratios the expressions can lead to gross overestimates of true load carrying capacities. For practical nail sizes this would not occur however, since the imposition of a limit on the t_1/d ratio of 2.8, means that only tempered hardboards with thicknesses in excess of 7mm could be used.

Although the existing proposals are seen to provide acceptable estimates of the true load-bearing capacity of sheet material-to-timber joints, the fact that they effectively preclude the use of many commercially available thicknesses, is a limitation. This is illustrated in Table 11.

Figure 10

3 — Member joints

Figure 11

2 — Member joints

Softwood ply→Hardwood
d = 2·5mm (Case 2)

Hardwood ply→Hardwood
d = 2·5mm (Case 4)

Softwood ply→Softwood
d = 6mm (Case 1)

Hardwood ply→Softwood
d = 6mm (Case 3)

Yield theory $\alpha = t_2/t_1 = 12$
Yield theory $\alpha = t_2/t_1 = 1$
Existing draft Eurocode 5
Proposals in this paper

$\dfrac{R_K}{f_H d^2}$

t/d

-28-

Figure 12

3—Member joints

Figure 13

2 — Member joints
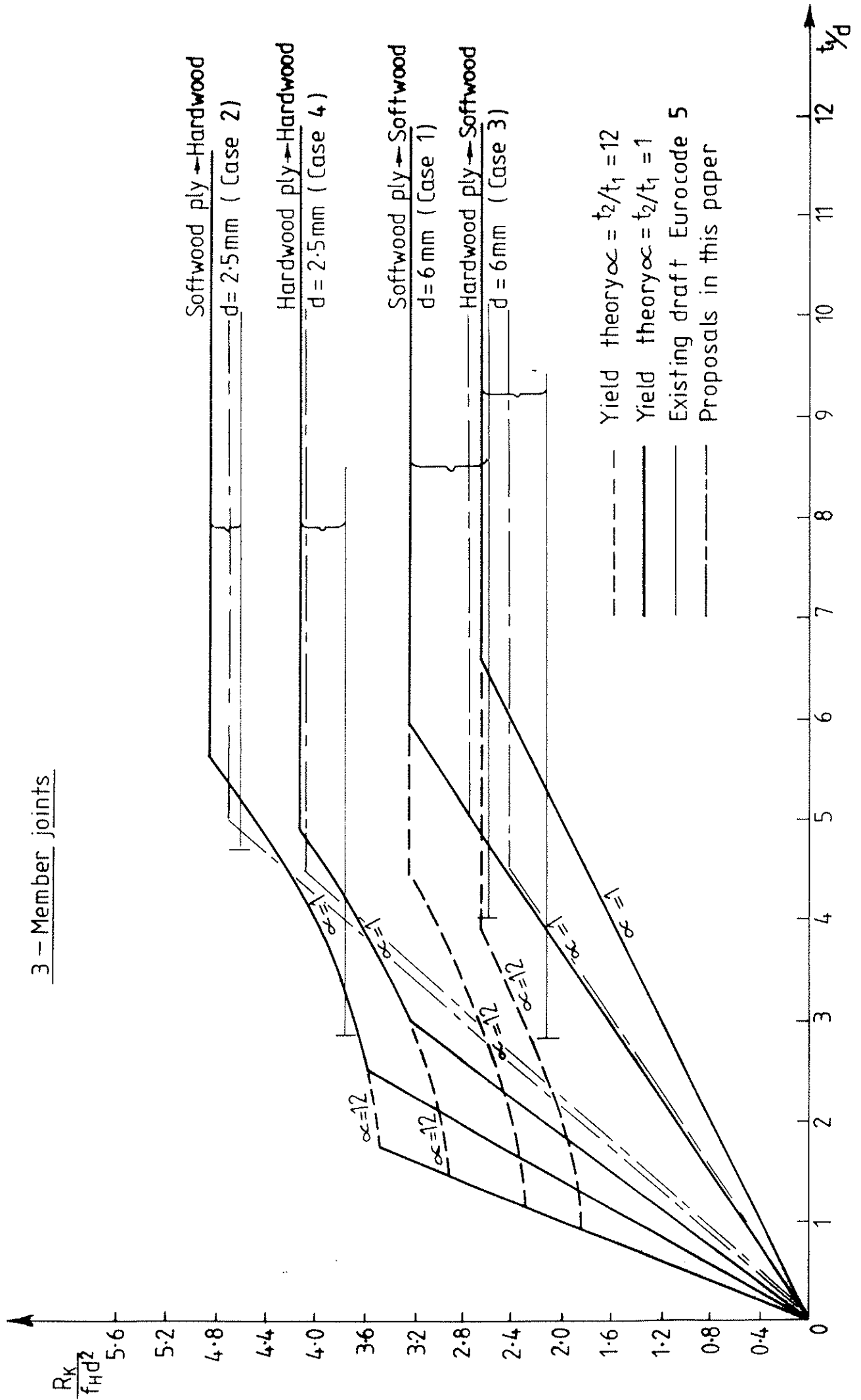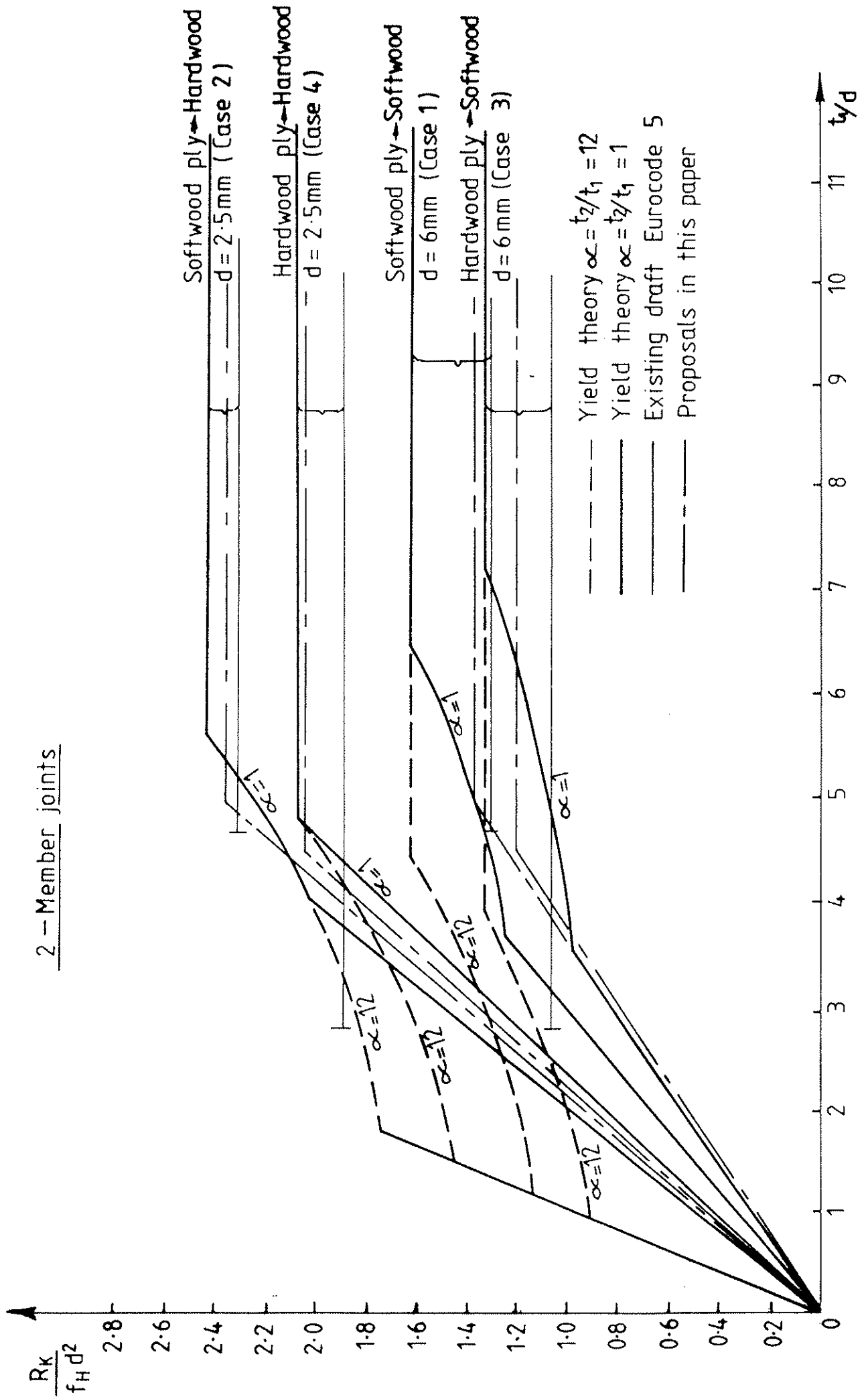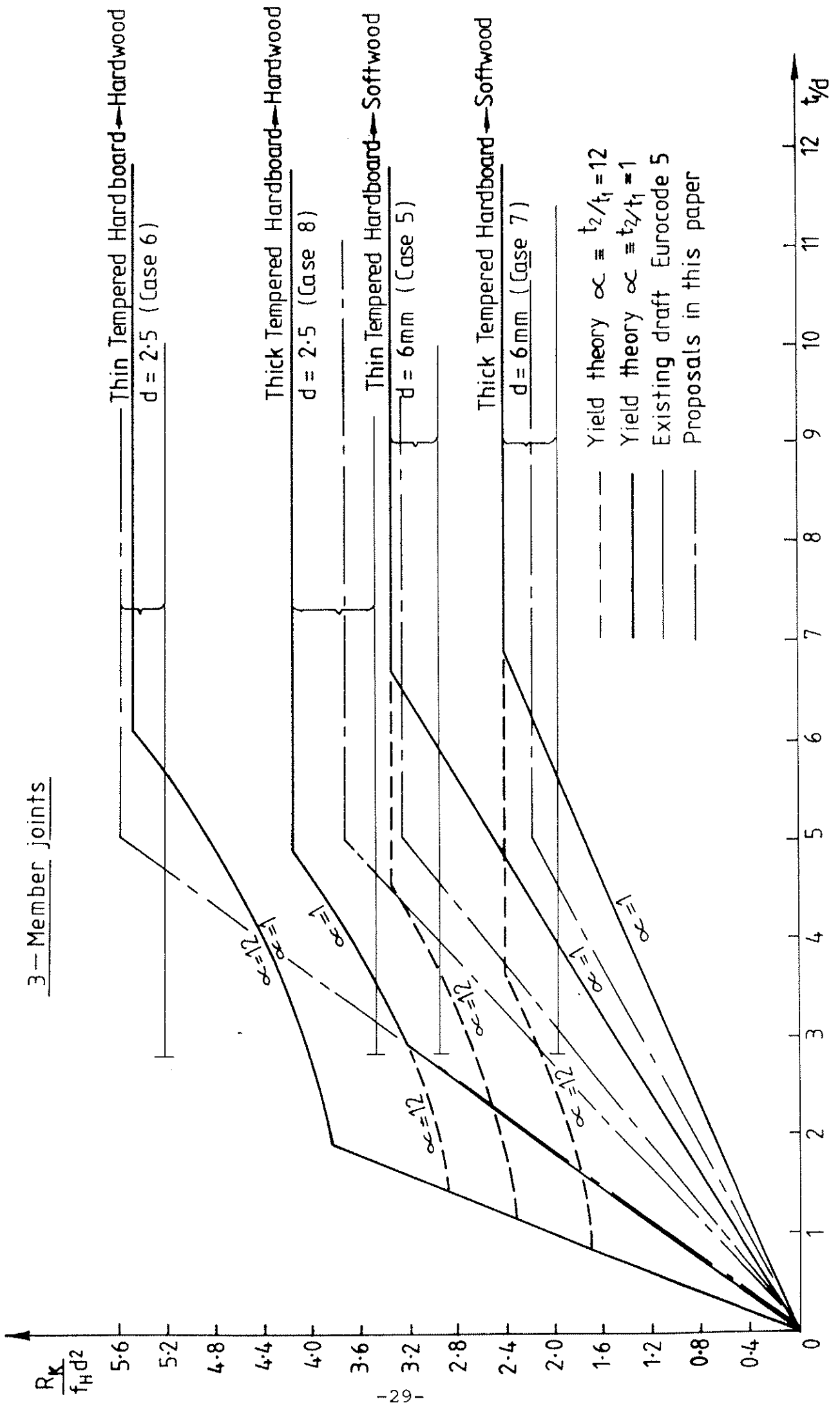
Figure 13
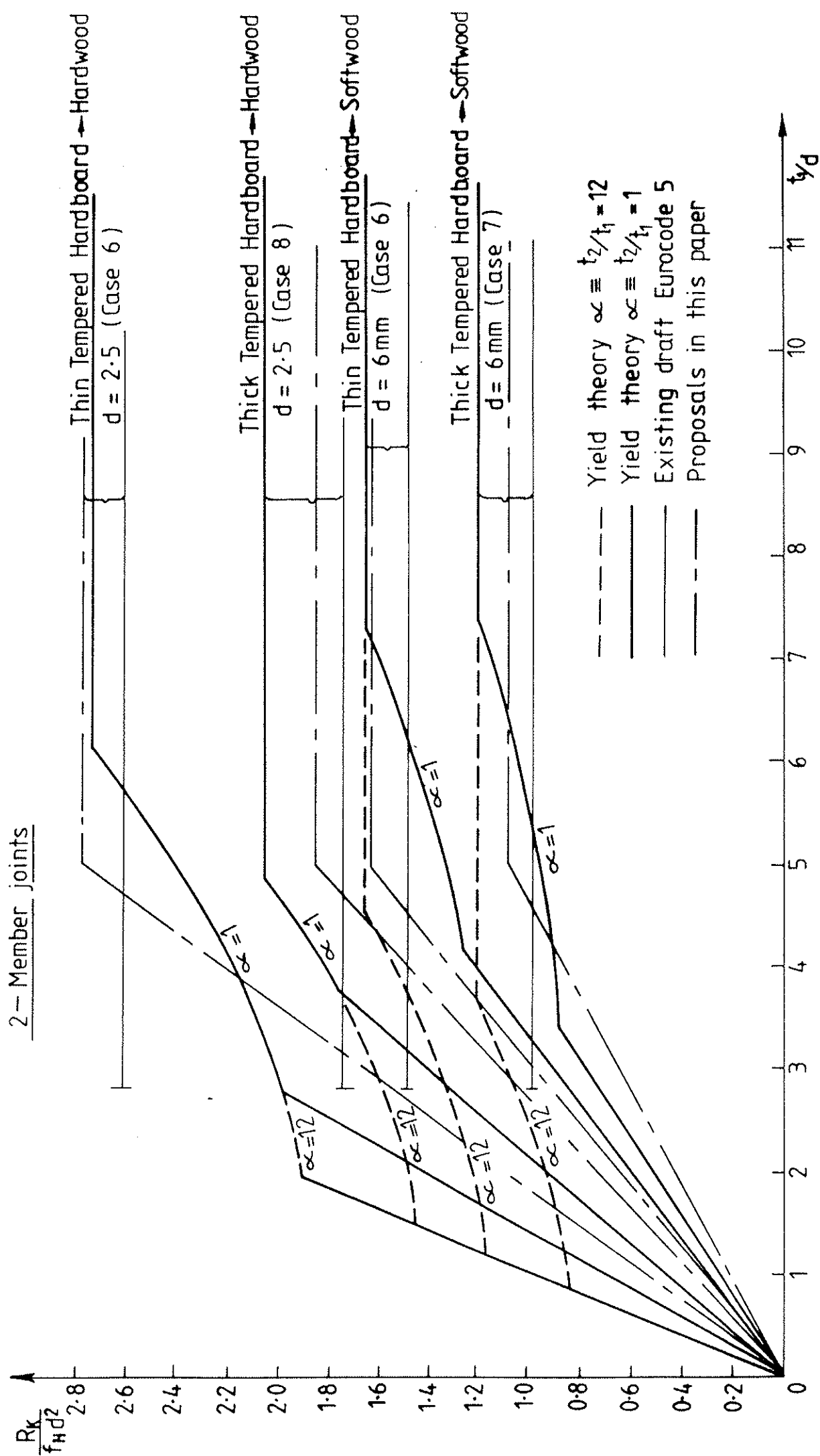
Table 11

Nail Diameter	Limiting sheet material thickness in (draft EC5, 1986)				
	Softwood plywood	Mixed hardwood/ Softwood plywood	Hardwood plywood	Tempered hardboard	Particleboard
2·5	$\geqslant 11\cdot7$ mm	$\geqslant 8\cdot75$mm	$\geqslant 7$ mm	$\geqslant 7$ mm	$\geqslant 17\cdot5$mm
4	$\geqslant 18\cdot7$ mm	$\geqslant 14$ mm	$\geqslant 11\cdot2$ mm	$\geqslant 11\cdot2$mm	$\geqslant 28$ mm
6	$\geqslant 28$ mm	$\geqslant 21$ mm	$\geqslant 16\cdot8$ mm	$\geqslant 16\cdot8$mm	$\geqslant 42$mm

One way of increasing the range of sheet material thicknesses permitted in timber joint design is to specify a sliding scale of equivalent timber densities depending upon the t_1/d ratio of the joint. This would allow the failure load diagrams in Figures 10 to 13 to be approximated by a bi-linear trend, rather than the single horizontal line which is currently used.

Analysis of the diagrams in Figures 10 to 13 suggest the following approximations:-

Hardwood plywoods:

$$\rho \text{ effective} = 28\left(\frac{t_1}{d}\right)^2 \qquad \frac{t_1}{d} \leqslant 4\cdot5 \qquad \dots\dots (26)$$

Softwood plywoods:

$$\rho \text{ effective} = 20\left(\frac{t_1}{d}\right)^2 \qquad \frac{t_1}{d} \leqslant 5 \qquad \dots\dots (27)$$

Tempered Hardboard: (all thicknesses)

$$\rho \text{ effective} = 22\left(\frac{t_1}{d}\right)^2 \qquad \frac{t_1}{d} \leqslant 5 \qquad \dots\dots (28)$$

By inserting these effective ρ values in Equation (8) the approximations to the true failure load diagrams which these expressions yield are plotted in Figures 10 to 13. It can be seen that these allow the use of all commercially available sheet material thicknesses in joints, albeit with reduced design values when t_1/d ratios become small.

For plywoods with alternating softwood and hardwood veneers, which would have density values intermediate between the two cases highlighted in Figures 10 and 11, the following expression is recommended:-

Mixed hardwood/
Softwood plywoods:
$$\rho\ \text{effective} = 26\left(\frac{t_1}{d}\right)^2 \quad \frac{t_1}{d} \leqslant 4\cdot5 \qquad \cdots\cdots (29)$$

To fall in line with the recommendations currently made for particleboard to timber joints in (draft Eurocode 5, 1986) an equivalent expression would be:-

Particleboards:
$$\rho\ \text{effective} = 8\left(\frac{t_1}{d}\right)^2 \quad \frac{t_1}{d} \leqslant 7 \qquad \cdots\cdots (30)$$

In the absence of any embedding strength data no other expression can be put forward. The results from a project currently underway at TRADA should provide the data necessary to allow an appraisal of this expression.

Comparisons and Experimental Validation

From Table 2 it can be seen that 160 board material to timber joints were included in TRADA's programme of joint tests. These can be used in a similar manner to the nailed and bolted joint tests discussed earlier, to compare theoretical and design code predictions with experimental results. Tables 12 and 13 provide these comparisons.

Table 12

| Joint Ref. | Yield Theory | | Experimental | | | F.E. Model | | Comparisons | | | |
| | | | | | | | | Yield Theory VS. Experiment | | F.E. Model VS.Experiment | |
	Failure Load(kN) (a)	Failure Mode (b)	Failure Load R_K (c)	Failure Mode(%) (d)	Slip at $R_K/3$(mm) (e)	Failure Load(kN) (f)	Slip at $R_K/3$ (g)	(a)/(c)	% Mode Correct	(f)/(c)	(g)/(e)
SP1	1·05	1a	1·01	1a(100)	0·47	1·07	0·38	1·04	1·00	1·06	0·81
SP2	1·05	1a	0·90	1a(100)	0·43	1·04	0·41	1·17	1·00	1·16	0·95
SP3	1·68	2	1·30	2(90) 1a(10)	0·67	1·72	0·41	1·29	0·90	1·32	0·61
SP4	1·74	2	1·39	2(100)	0·69	1·79	0·34	1·25	1·00	1·29	0·49
SHb1	1·66	1a	1·51	1a(90) 2(10)	0·75	1·54	0·40	1·10	0·90	1·02	0·53
SHb2	1·51	1a	1·15	1a(70) 1b(15) 2(15)	0·60	1·51	0·45	1·31	0·70	1·31	0·75
SHb3	1·26	1a	0·96	1a(95) 2(5)	0·49	1·28	0·45	1·31	0·95	1·33	0·92
Absolute Average error								21%	—	21·3%	27·7%

The joints were fabricated from single nails driven from each side of the joint in single shear. Small gaps (0.5mm) were left between the joint members to avoid any frictional forces, and the nail heads were left protruding from the face of the side members. The embedded length of the nails (which did not overlap) in the centre member was 15mm for sets SP1, SP2 and SP3, 24mm for sets SP4, SHb1, and SHb2 and 20mm for set SHb3. The joints with a 15mm nail penetration do not conform with the minimum requirements of (draft Eurocode 5, 1986) and the (CIB code, 1983) for nail penetration, and linear interpolation would be required for below standard penetration depths in the other joints. All of the sheet material thicknesses used to fabricate the joints were below the minimum required in the (CIB code) and (draft Eurocode 5, 1986). In calculating the EC 5 and CIB values in Table 13, this latter fact is ignored, although linear interpolation for sub-standard nail penetrations are applied to both the EC 5 and CIB values and those arising from the formulae in this paper.

Table 13.

Set Ref.	Experimental failure load (kN)	Calculated failure load (kN)		Calculated vs Experiment	
		Draft Eurocode 5 and CIB Code [1]	Proposals in this paper	EC5 + CIB Code	Proposals in this paper
SP1	1·01	1·688 (0·63)	0·828 (0·309)	1·67 (0·62)	0·82 (0·31)
SP2	0·90	1·688 (0·63)	0·831 (0·310)	1·88 (0·70)	0·92 (0·34)
SP3	1·30	1·675 (1·00)	0·687 (0·410)	1·29 (0·77)	0·53 (0·32)
SP4	1·39	1·675 (1·00)	0·683 (0·408)	1·21 (0·72)	0·49 (0·29)
SHb1	1·51	1·675 (1·00)	0·869 (0·519)	1·11 (0·66)	0·58 (0·34)
SHb2	1·15	1·675 (1·00)	0·554 (0·331)	1·46 (0·87)	0·48 (0·29)
SHb3	0·96	1·688 (0·84)	0·551 (0·274)	1·76 (0·88)	0·57 (0·29)
			Average Error	+48% (-25%)	-37% (-68%)

Footnotes:

[1] Strictly speaking, none of the joints conform with the requirements of draft Eurocode 5 and the CIB code for minimum joint member thickness.

Values in parenthesis are interpolated values for sub-standard nail penetration l_2.

It must be remembered that the comparisons in Table 13 relate to joints which violate the minimum member thickness requirements of the existing draft Eurocode and the CIB code, and which failed with either a mode 1 or mode 2 type configuration. The 48% average overestimate made by the EC5/CIB expressions is therefore not surprising, contrasting with the 37% underestimate which is brought about through the use of Equations (26) to (28). When reductions are made for sub-standard nail penetrations (l_2), this conservatism is increased and the EC5/CIB expressions would have become a better predictor if they had applied to such joints.

Clearly the expressions proposed for designing board-material to timber joints with failure modes other than mode 3 are extremely conservative. However, they do permit the use of joints which would otherwise have been excluded. For the more conventional, heavier-duty type board material to timber joints the proposals made in this paper permit a slight enhancement in design strengths, over the existing formulae in draft Eurocode 5, 1986 and the CIB code.

It is a matter for discussion, how, and indeed if the existing rules in draft Eurocode 5 and the CIB Code, should be modified for slender nails in board material to timber joints. The proposals made in this paper, for introducing an effective ϱ , is only one possible solution. Alternative solutions can also be envisaged, such as the incorporation of a general rule permitting linear interpolation down to e.g. half the minimum thickness for mode 3, when using sub-standard thicknesses.

Conclusions and Recommendations

Based upon an extensive programme of research at TRADA over the past seven years, proposals are made for the revision of the existing timber-to-timber and board material-to-timber joint formulae, in the draft Eurocode 5, 1986 and the CIB code.

Equation (8) is recommended for the design of nailed timber-to-timber joints without pre-boring. When pre-boring is used this should be multiplied by 1.2. Comparisons with experimental test results suggest these expressions predict failure loads of joints exhibiting mode 3 type failures to within 4%. The existing dimensioning rules in both codes, and the expressions for calculating nailed joint slip, are verified as being accurate.

For bolted joints the existing design equations in draft Euroecode 5 and the CIB code are advocated, but Equations (2) and (3) are recommended for the calculation of bolt embedding strengths. Comparisons with experimental test data suggests the design equations model actual joint failure loads to an accuracy of around 15% with the expressions for bolt bearing strengths adding a further 6% error.

For nailed board material-to-timber joints, it is suggested that the existing approaches in draft Eurocode 5 and the CIB code of specifying an equivalent timber density, could be extended to incorporate a range of effective timber densities, depending upon the joint slenderness ratio. Equations (26) to (30) are suitable for this purpose.

These give approximately the same result as the existing expressions for joints with high slenderness ratios, but unlike these existing rules, allow design strengths to be calculated for joints with sheet materials much thinner than can presently be used. Comparisons with experimental test results on joints of this type, show that a satisfactory degree of conservatism is in-built into this new range of design possibilities. Other means of acheiving this extension in design possibilities could also be found, such as permitting linear interpolation of design strengths for joints with sub-standard thicknesses for mode 3 type failures.

The selection of the best such solution to this problem, should be a matter for discussion.

References

1)   CIB, 1983 - Structural timber design code. 6th Edition. Publication 66. CIB-W18, 1983.

2)   EUROCODE 5, 1986 - Draft for comment. Common unified ruels for timber structures. Commission of the European Communities. October 1986.

3)   JOHANSEN, K.W., 1949 - Theory of timber connectors. Publication 9, Bern. International Association of Bridge and Structural Engineering, 1949.

4)   LARSEN, H.J., 1973 - The yield load of bolted and nailed joints. Proceedings IUFRO - 5 Congress, 1973.

5)   SMITH, I., 1983 - Short-term load-deformation relationships for joints with dowel type connectors. Ph.D. Thesis, CNAA, 1983.

6)   SMITH, I. and WHALE, L.R.J., 1985a - Mechanical properties of nails and their influence on mechanical properties of nailed timber joints subjected to lateral load. Part 1: Background and tests on nails of UK origin. TRADA Research Report 4/85. TRADA, Hughenden Valley, Buckinghamshire. January 1985.

7)   SMITH, I. and WHALE, L.R.J., 1985b - Mechanical properties of nails and their influence on mechanical properties of nailed timber joints subjected to lateral load. Part 2: Tests on nails of mainland Europe origin, comparisons of results with those of UK origin and conclusions. TRADA Research Report 9/85. TRADA, Hughenden Valley, Buckinghamshire. July 1985.

8)   WHALE, L.R.J., SMITH, I. and HILSON, B.O., 1986 - Behaviour of nailed and bolted joints under short-term lateral load - Conclusions from some recent research. Proceedings joints CIB-W18/IUFRO S5.02 meeting, Florence, Italy. September 1986.

9)   WHALE, L.R.J. and SMITH, I., 1986a - The derivation of design clauses for nailed and bolted joints in Eurocode 5. CIB-W18 Paper 19-7-6, Florence, Italy. September 1986.

10)   WHALE, L.R.J. and SMITH, I., 1986b - Mechanical timber joints. TRADA Research Report 18/86, Hughenden Valley, TRADA, 1986.

11)   WHALE, L.R.J. and SMITH, I., 1986c - Mechanical joints in structural timber - Information for probabilistic design. TRADA Research Report 17/86, Hughenden Valley, TRADA, 1986.

12)   WILKINSON, T.L., 1973 - Effect of deformed shanks, prebored lead holes, and grain orientation on the elastic bearing constant of laterally loaded nailed joints. USFPL Research Report FPL 192, 1973.

INTERNATIONAL COUNCIL FOR BUILDING RESEARCH STUDIES AND DOCUMENTATION

WORKING COMMISSION W18A - TIMBER STRUCTURES

SLIP IN JOINTS UNDER LONG-TERM LOADING

by

T Feldborg and M Johansen
Danish Building Research Institute
Denmark

MEETING TWENTY
DUBLIN
IRELAND
SEPTEMBER 1987

Introduction

A paper on timber joints under long-term loading was presented (paper 19-7-5) at the CIB-W18 meeting in 1986.

The paper to which reference is made described the test programme, the specimens, the test performance and the slip development during approx. 600 days of loading and 7 cycles of alternating relative humidity (RH).

The tests have been continued until 784 days (2.15 years) of loading and $9\frac{1}{2}$ cycles of alternating RH. After the unloading the stiffness and maximum strength of all joints were determined in a standard short-term test. The experimental work was finished in the spring of 1987 and the main results are reported below.

Slip caused by long-term loading

Figure 6a[1] shows joint slip development with time for the joints exposed to constant RH (series 1, 2 and 3) or alternating RH (series 4 and 5), together with the corresponding moisture content of the series in question. The slip measurements during the recovery were carried out for four weeks.

Figure 7a shows the same slip-time curves as in figure 6a, but with the time in logaritmic scale. In this scale the curves are close to straight lines for the first month.

It is seen that the main part of the slip-increase came in the drying-out periods.

Slip values are shown in figure 9a. The results from series 2 and 3 are pooled and so are the results from series 4 and 5.

The slip after $9\frac{1}{2}$ cycles of alternating humidity (the entire long-term loading period) was approx. 4 to 9 times higher than the slip v_{t10} (the slip after 10 minutes of full load). Compared to the slip under constant 85 per cent RH, the corresponding factors were approx. 3 to 4.

---

1) The numbering of figures is linked to the ones used in paper 19-7-5.
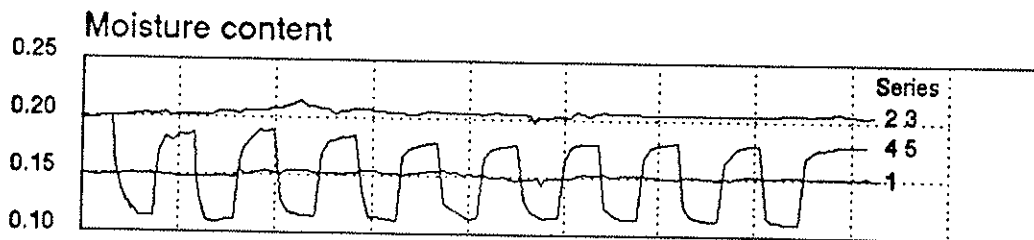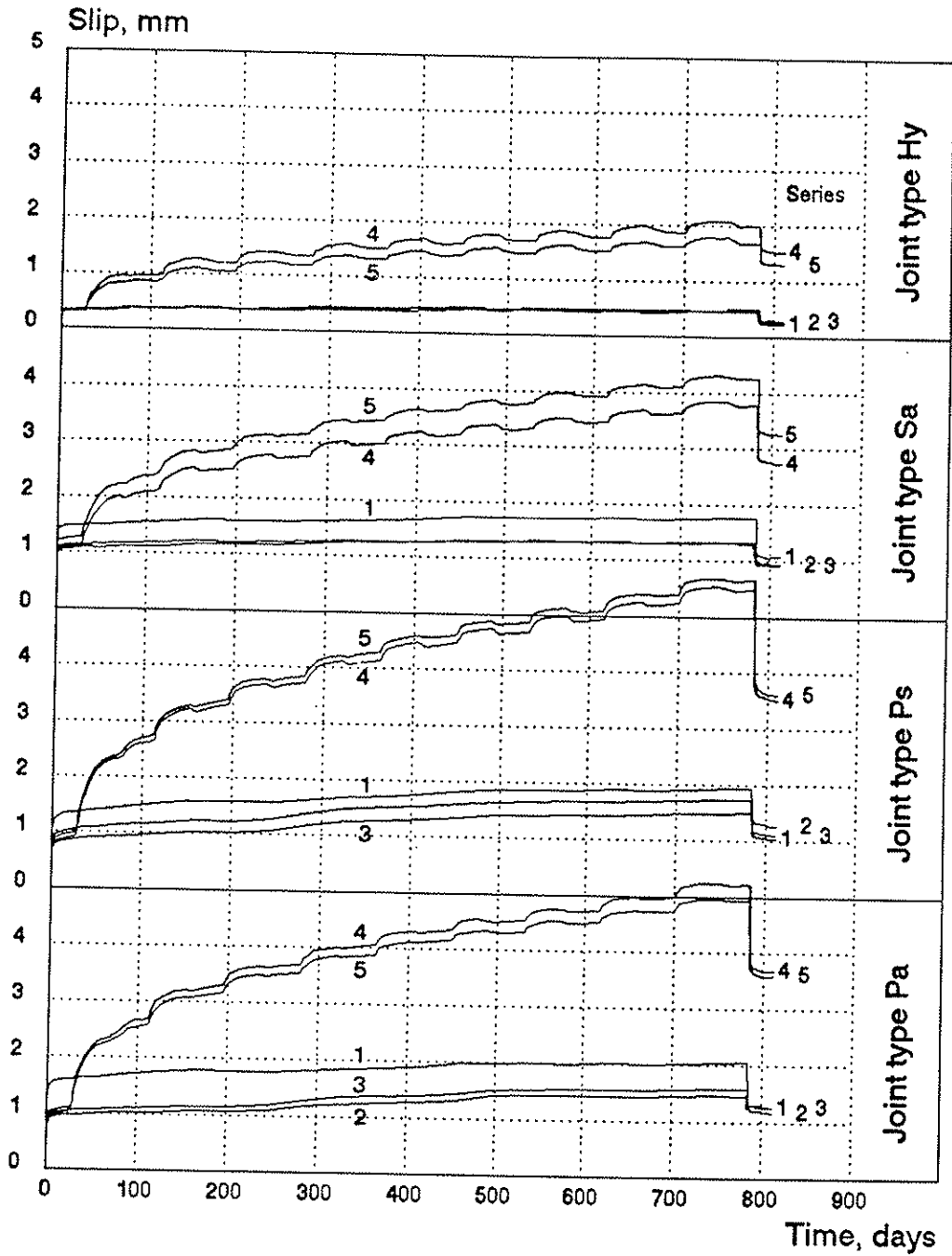
Figure 6a Slip in long-term loaded joints.

Series 1:   Constant load F = 10.0 kN. Constant rel.hum. 65 p.c.
Series 2 and 3: Constant load F = 8.6 kN. Constant rel.hum. 85 p.c.
Series 4 and 5: Constant load F = 8.6 kN. Alternating rel.hum. 85-50 p.c.

Joint type Hy: Nail plates.
Joint type Sa: Steel plates with annularly threaded nails.
Joint type Ps: Plywood gussets with square plain-shank nails.
Joint type Pa: Plywood gussets with annularly threaded nails.

Each curve represents the average from 6 joints.
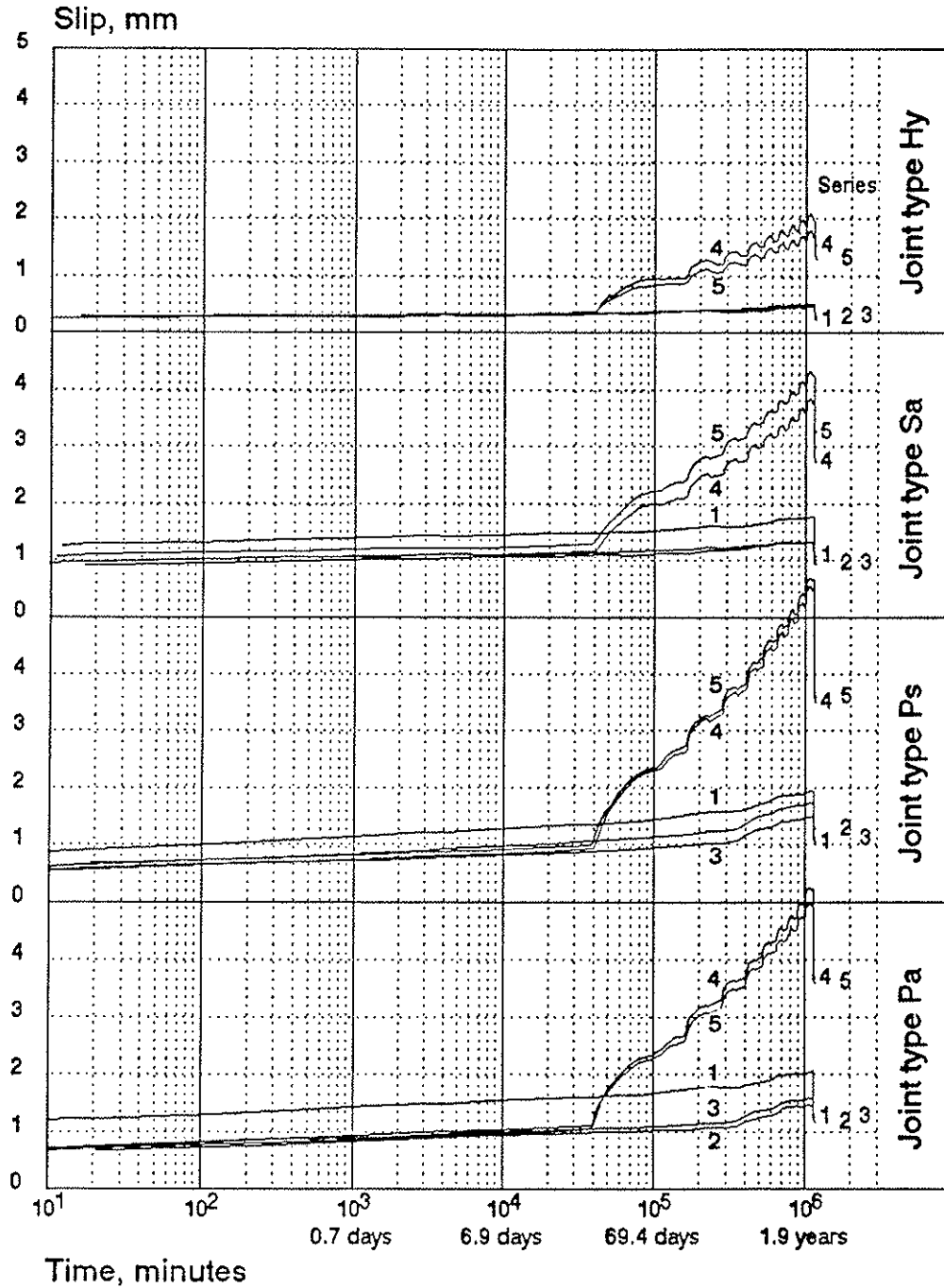
Figure 7a Slip in long-term loaded joints.

Series 1:   Constant load F = 10.0 kN. Constant rel.hum. 65 p.c.
Series 2 and 3: Constant load F = 8.6 kN. Constant rel.hum. 85 p.c.
Series 4 and 5: Constant load F = 8.6 kN. Alternating rel.hum. 85-50 p.c.

Joint type Hy: Nail plates.
Joint type Sa: Steel plates with annularly threaded nails.
Joint type Ps: Plywood gussets with square plain-shank nails.
Joint type Pa: Plywood gussets with annularly threaded nails.

Each curve represents the average from 6 joints.

Series	Number of specimens	Load F kN	Relative humidity RH per cent	Slip 10 min. v_{t10} mm	Load time days	Slip before unloading v mm	δ	Rel. slip v/v_{t10}	Slip 4 weeks after unloading v mm	δ
1LHy	6	10.0	65	0.27	784	0.44	0.08	1.6	0.22	0.13
1LSa	6	10.0	65	1.25	784	1.75	0.08	1.4	1.05	0.16
1LPs	6	10.0	65	0.90	784	1.95	0.11	2.2	1.05	0.12
1LPa	6	10.0	65	1.20	784	2.05	0.08	1.7	1.25	0.11
2+3LHy	12	8.6	85	0.28	784	0.48	0.10	1.7	0.29	0.11
2+3LSa	12	8.6	85	0.95	784	1.35	0.15	1.4	0.95	0.15
2+3LPs	12	8.6	85	0.60	784	1.60	0.12	2.7	1.20	0.12
2+3LPa	12	8.6	85	0.65	784	1.50	0.08	2.3	1.20	0.09
4+5LHy	12	8.6	85 (50)	0.25	784	1.80	0.09	7.2	1.40	0.11
4+5LSa	12	8.6	85 (50)	1.00	784	4.00	0.09	4.0	3.00	0.12
4+5LPs	12	8.6	85 (50)	0.60	784	5.60	0.07	9.3	3.60	0.08
4+5LPa	12	8.6	85 (50)	0.70	784	5.10	0.06	7.3	3.60	0.06

Figure 9a   Average values of slip in long-term loaded joints. Series 4 and 5 were run through 9½ cycles of alternating relative humidity. v_{t10} is the average slip after 10 minutes of full load. δ is the coefficient of variation.

Stiffness and strength determined by short-term testing

All specimens, non-preloaded (series N) and long-term loaded (series L), were tested according to ISO 6891 (Timber structures - Joints made with mechanical fasteners) from which the symbols used in the following are taken.

Stiffness values in the serviceability range are given as the initial slip v_i and the slip modulus k_e which are defined in figure 10.
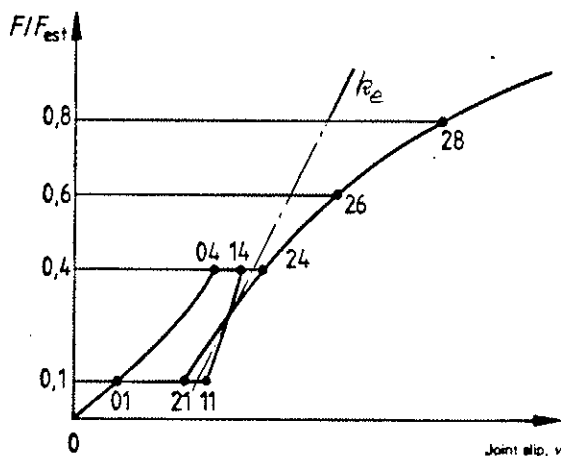
$$v_i = v_{04}$$

$$k_e = \frac{0.4\ F_{est}}{\frac{4}{3}(v_{14} + v_{24} - v_{11} - v_{21})/2}$$

Figure 10   Definition of the initial slip v_i and the slip modules k_e. The estimated maximum load F_{est} was 25.0 kN for series 1, and 20.4 kN for series 2, 3, 4 and 5.

Strength values, F_{max} , are defined as the highest load with a slip not more than 15 mm. The average values of F at a slip of v = 5 mm are indicated where relevant.

The types of failure were:

Series Hy and Ps: Tooth or nail withdrawal.

Series Sa: Nail withdrawal or splitting of wood in nail rows.

Series Pa: Combined nail withdrawal and pull-through of nail heads in plywood gussets.

Main results of some essential stiffness and strength characteristics are given in the figures 11 and 12. Examples of load-slip curves are shown in figure 13.

Figure 11   Stiffness and strength from short-term testing of (N) non-preloaded and (L) long-term loaded joints with nail plates and steel plates. Average values and 95 p.c. confidence intervals from 6 specimens.
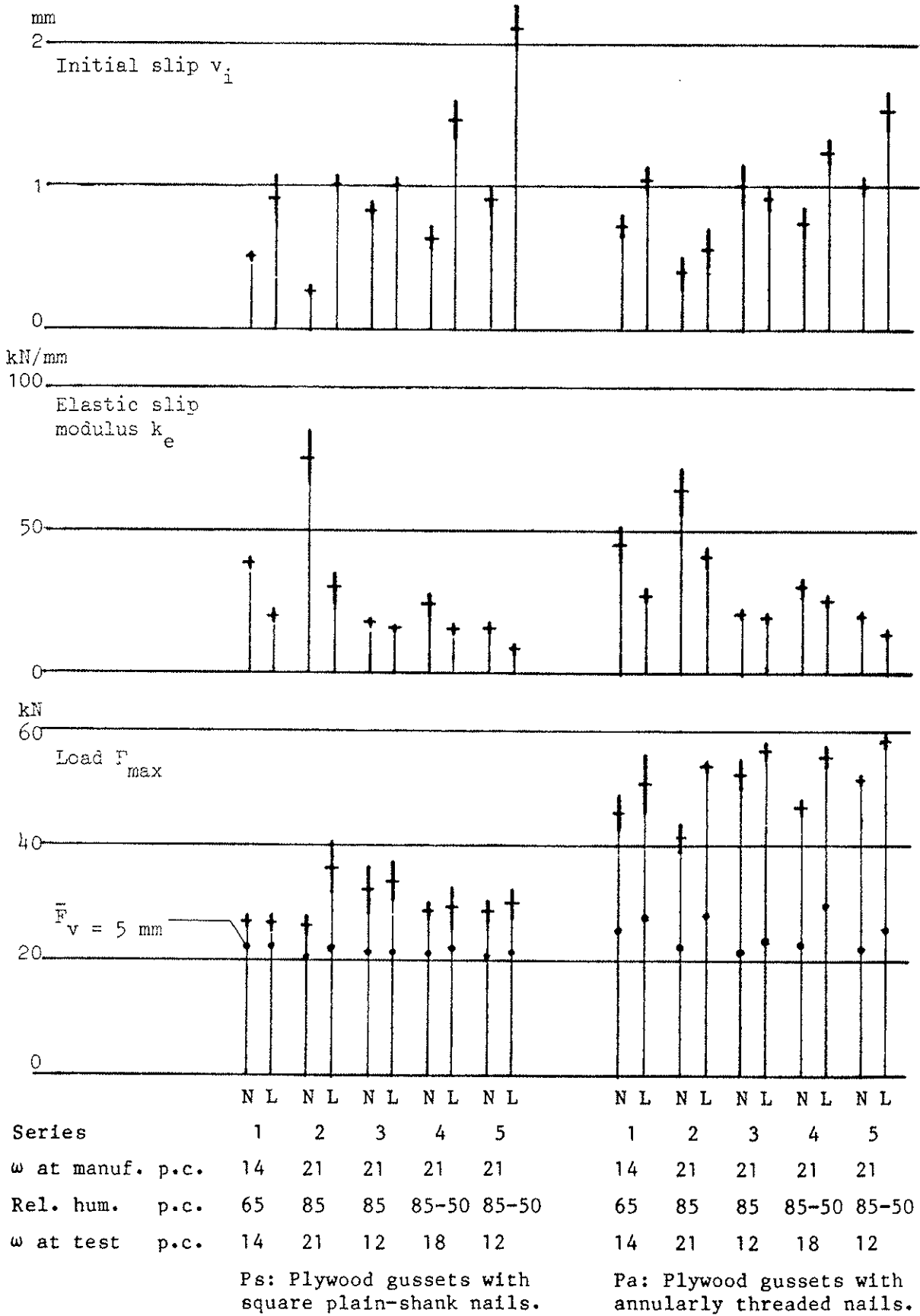
Figure 12 Stiffness and strength from short-term testing of (N) non-preloaded and (L) long-term loaded joints with plywood gussets. Average values and 95 p.c. confidence intervals from 6 specimens.

Load, kN

Slip, mm
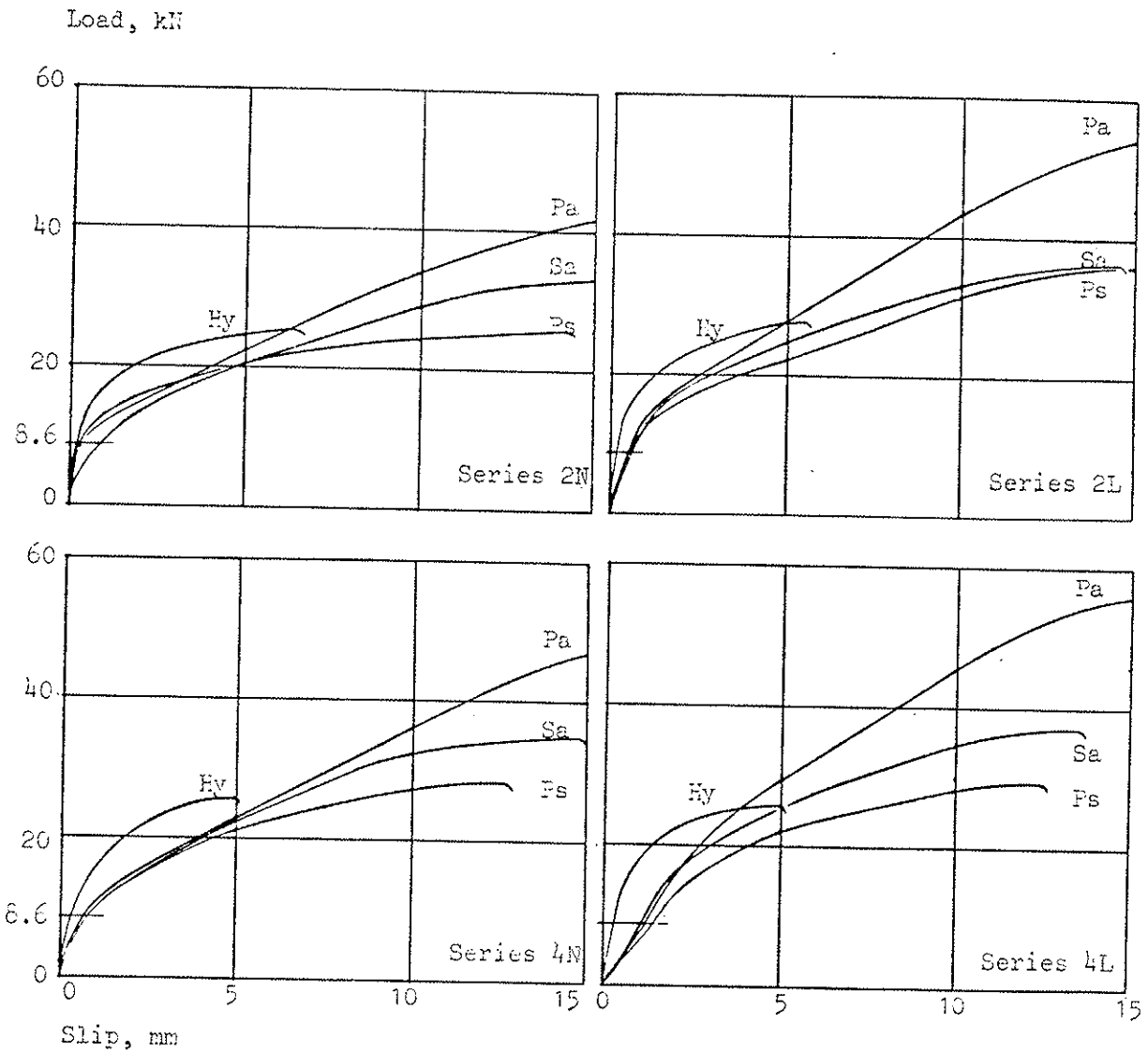
Figure 13 Examples of load-slip curves from short-term testing of (N) non-preloaded and (L) long-term loaded joints.

Conditioning of series 2: 85 p.c. RH constant.
Conditioning of series 4: 85 p.c. RH at manufacture and at test, alternating between 85 and 50 p.c. RH in the period of long-term loading.

Each curve represents the average from 6 specimens.

Relative_values_of_stiffness_and_strength. The effect of long-term
loading and alternating RH in the same period is shown in figure 14 as
relative values which should be seen together with the absolute values in
the figures 11 and 12.

Joint	Initial slip		Elastic slip modulus		Max. load	
	$\dfrac{v_i(4L)}{v_i(2N)}$	$\dfrac{v_i(5L)}{v_i(3N)}$	$\dfrac{k_e(4L)}{k_e(2N)}$	$\dfrac{k_e(5L)}{k_e(3N)}$	$\dfrac{F(4L)}{F(2N)}$	$\dfrac{F(5L)}{F(3N)}$
Nail plates	1.8	1.3	0.6	0.8	1.0	1.0
Steel plates	1.2	1.4	0.8	0.9	1.1	1.0
Plywood, square nails	5.7	2.5	0.2	0.5	1.1	0.9
Plywood, ann. thr. nails	3.1	1.5	0.4	0.7	1.3	1.1

Figure 14   Average values from long-term loaded specimens under alternating
RH divided by the corresponding average values from non-preloaded specimens
under constant RH. Series 4L and 2N were tested at 85 p.c. RH; 5L and 3N at
50 p.c. RH.

Conclusions

Slip_caused_by_long-term_loading_and_alternating_RH

Alternating humidity is a dominant factor for the long-term development of
slip in joints with mechanical fasteners.

The absolute slip values (listed in figure 9a) are rather high for the
joint types other than the joint with nail plates. For joints with nailed
steel plates and plywood gussets the slip will often be decisive for the
design of the joint.

From the values of relative slip it appears that stiffness of joints
based on slip measurements from short-term loading does not give sufficient
information about the development of the slip due to long-term loading. The
relative slip varies considerably for the different types of joints.

Stiffness_and_strength_determined_from_short-term_testing

Regarding joint stiffness the effect of long-term loading together with
alternating RH in relation to non-preloading together with constant RH was
considerable. Regarding joint strength the effect was negligible. The most
unfavorable factors found for the investigated joints were:

Joint	Initial slip	Elastic slip modulus	Max. load
Nail plates	1.8	0.6	1.0
Steel plates	1.4	0.8	1.0
Plywood, square nails	5.7	0.2	0.9
Plywood, ann. thr. nails	3.1	0.4	1.1

As a basis for the determination of design values for splice joints in tension a standardized short-term testing with specimens conditioned at 85 per cent RH at manufacture and at test will therefore be satisfatory as regards the strength but quite inadequate as regards stiffness.

INTERNATIONAL COUNCIL FOR BUILDING RESEARCH STUDIES AND DOCUMENTATION

WORKING COMMISSION W18A - TIMBER STRUCTURES

ULTIMATE PROPERTIES OF
BOLTED JOINTS IN GLUED-LAMINATED TIMBER

by

M Yasumura, T Murota and H Sakai
Structural Engineering Department
Building Research Institute
Ministry of Construction
Japan

MEETING TWENTY
DUBLIN
IRELAND
SEPTEMBER 1987

The wooden members were the glued-laminated wood of spruce and douglas fir of JAS-type-1 whose density was respectively 0.44 and 0.54 in average. The ratio of the thickness of a main member to the diameter of a bolt varied two, four and eight, and the end distance and the edge distance were seven times and two and a half times as large as the diameter of a bolt respectively. In the specimen having the steel side plates, the end distance varied from two and a half times to ten times as large as the diameter of a bolt. The diameter of a bolt was sixteen millimeters and twenty millimeters, and the diameter of a pre-drilled hole in wooden member was the same as that of a bolt, and that in a steel member was one millimeter greater than that of a bolt.

2) SPECIMEN HAVING MULTIPLE SHEAR BOLTS

Fig.2 shows the specimens having multiple shear bolts. The specimen included a main member of glued-laminated wood of spruce and ezomatu-todomatu of JAS-type-1, steel side plates of twelve millimeters thick and the multiple bolts of the diameter of sixteen millimeters. The number of bolts varied from two to twelve, and the number of rows varied from one to three. The ratio of the thickness of a main member to the diameter of a bolt was four, six and eight, and the spacing between adjacent bolts was four times and seven times as large as the diameter of a bolt.

TEST METHOD

Figs.3 and 4 show an apparatus for the shear test of bolted joints. The tension load was applied to the both ends of a specimen with a hydraulic jack, and the slip between the main member and the side members were measured. The tension load was increased monotonously until the specimen failed, and the load-slip curves of the failed joint was analysed.

ULTIMATE LOAD AND YIELD LOAD OF A BOLTED JOINT SUBJECTED TO THE
SHEAR LOAD PARALLEL TO THE GRAIN

DESCRIPTION OF SPECIMEN

1) SPECIMEN HAVING A SINGLE SHEAR BOLT

Fig.1 shows the kinds of specimens having a single shear
bolt. They were divided into following five types.

WD: double shear bolted joint having a main member and side
members of glued-laminated wood.

SD: double shear bolted joint having a main member of
glued-laminated wood and steel side plates.

SI: double shear bolted joint having a main member of
glued-laminated wood and a steel plate which was
inserted in the center of the main member.

WS: single shear bolted joint having two members of
glued-laminated wood.

SS: single shear bolted joint having a member of
glued-laminated wood and a steel plate.

W D   S D   S I   W S   S S
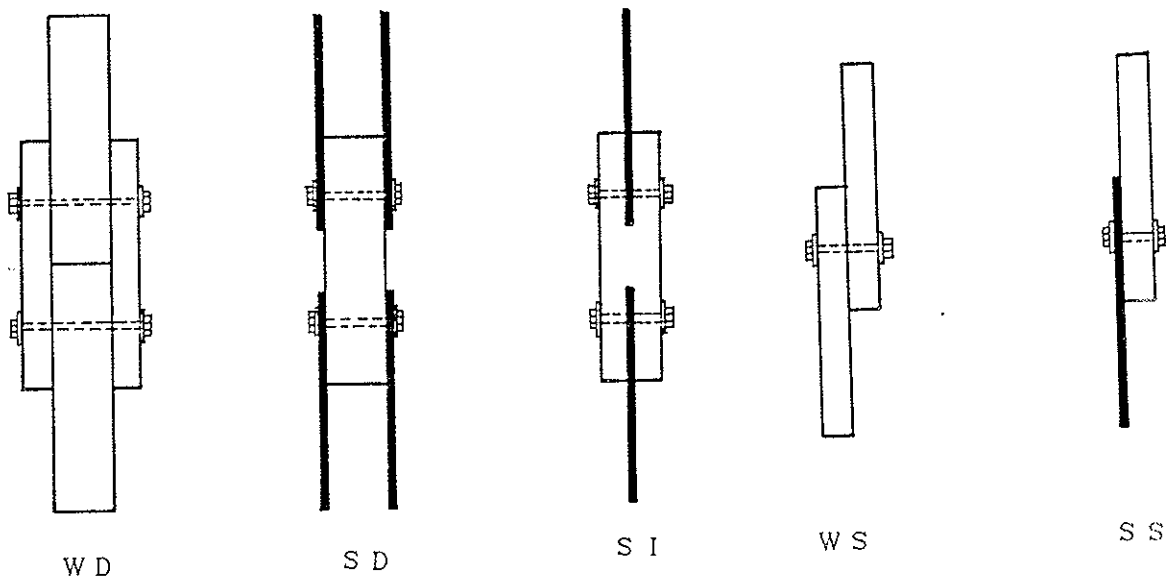
Fig.1 Types of the specimens Subjected to the shear load
parallel to the grain
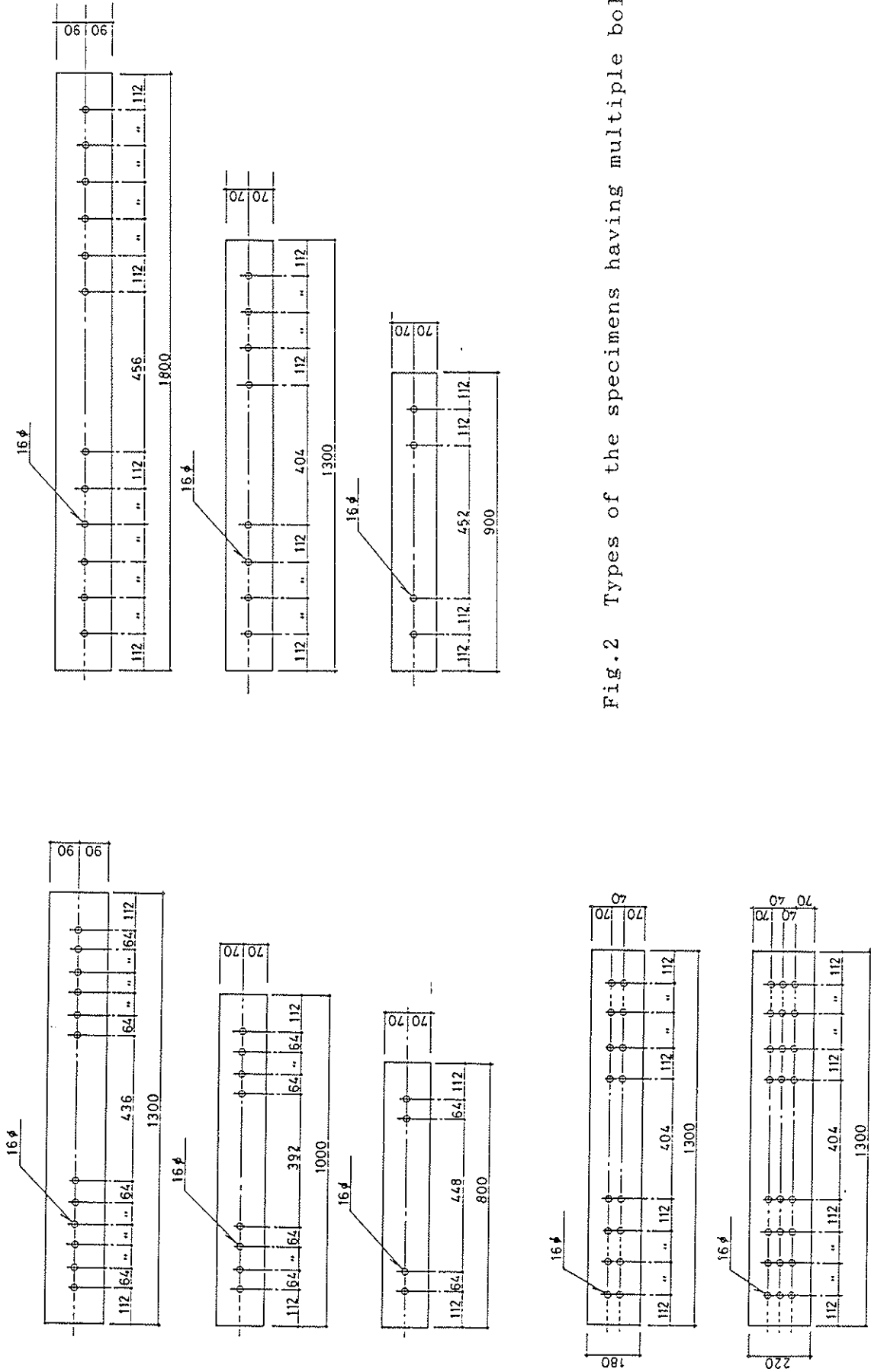
Fig.2 Types of the specimens having multiple bolts
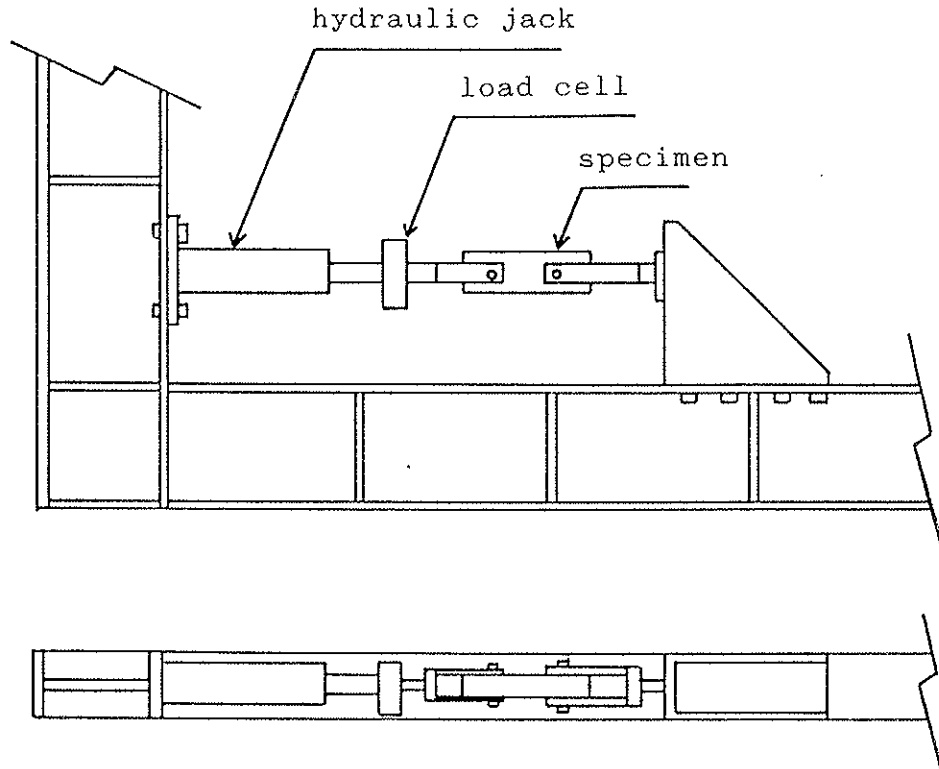
Fig.3 Apparatus for the shear test of the bolted
joints having a single bolt
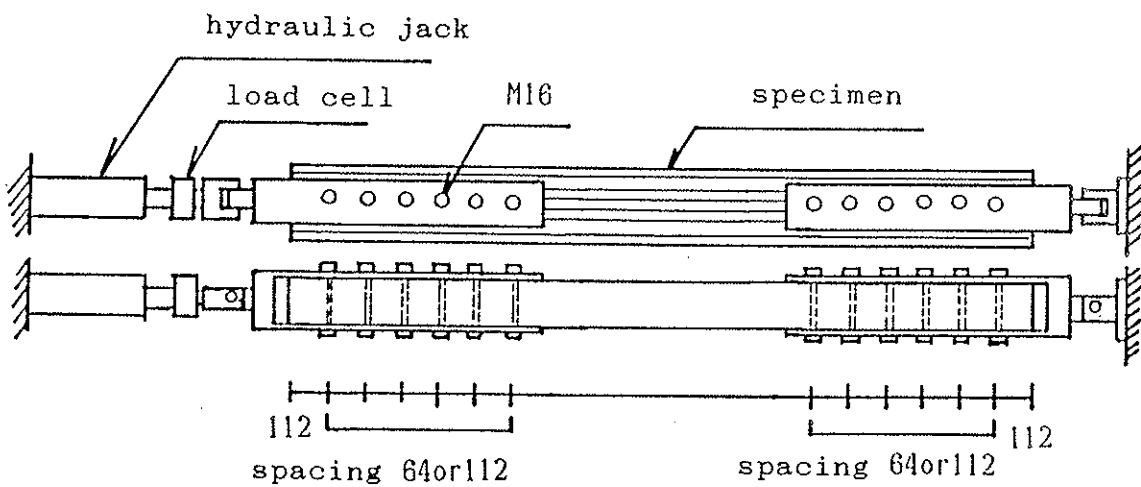
Fig.4 Apparatus for the shear test of the bolted joints
having the multiple bolts

COMPARISON OF THE CALCULATED VALUES OF THE YIELD   LOAD   WITH   THE
EXPERIMENTAL RESULTS.

The yield models as shown in Fig.5 give the following for-
mulae for the yield load of each joint [1].

(1) Double shear bolted joint having a main member and side
    members of glued-laminated wood.

$$\frac{P_y}{2 \cdot f_e \cdot d \cdot l} = \min \begin{cases} \alpha \beta \\[4pt] \dfrac{1}{2} \\[8pt] \sqrt{\dfrac{2\alpha^2\beta^2(1+\beta)}{(2\beta+1)^2} + \dfrac{2\beta\gamma(d/l)^2}{3(2\beta+1)}} - \dfrac{\alpha\beta}{(2\beta+1)} \\[12pt] \dfrac{d}{l}\sqrt{\dfrac{2\beta\gamma}{3(1+\beta)}} \end{cases}$$

————————— (1)

(2) Double shear bolted joint having a main member of glued-
    laminated wood and steel side plates.

$$\frac{P_y}{2 \cdot f_e \cdot d \cdot l} = \min \begin{cases} \dfrac{1}{2} \\[8pt] \dfrac{d}{l}\sqrt{\dfrac{2\gamma}{3}} \end{cases}$$

————————— (2)

(3) Double shear bolted joint having a main member of glued-
    laminated wood and a steel plate which was inserted in
    the center of a main member.

$$\frac{P_y}{2 \cdot f_e \cdot d \cdot l} = \min \begin{cases} \dfrac{1}{2} \\[8pt] 2\sqrt{\dfrac{1}{8} + \dfrac{(d/l)^2\gamma}{6}} - \dfrac{1}{2} \\[12pt] \dfrac{d}{l}\sqrt{\dfrac{2\gamma}{3}} \end{cases}$$

————————— (3)

(4) Single shear bolted joint having two members of glued-laminated wood.

$$\frac{P_y}{f_e \cdot d \cdot l} = \min \left\{ \begin{array}{l} 1 \\[4pt] \alpha\,\beta \\[4pt] \dfrac{\sqrt{\beta + 2\beta^2(1+\alpha+\alpha^2) + \alpha^2\beta^3} - \beta(1+\alpha)}{(1+\beta)} \\[8pt] \sqrt{\dfrac{2\beta(1+\beta)}{(2+\beta)^2} + \dfrac{2\beta\gamma\,(d/l)^2}{3(2+\beta)}} - \dfrac{\beta}{(2+\beta)} \\[8pt] \sqrt{\dfrac{2\alpha^2\beta^2(1+\beta)}{(2\beta+1)^2} + \dfrac{2\beta\gamma\,(d/l)^2}{3(2\beta+1)}} - \dfrac{\alpha\,\beta}{(2\beta+1)} \\[8pt] \dfrac{d}{l}\sqrt{\dfrac{2\beta\gamma}{3(1+\beta)}} \end{array} \right.$$

———————————— (4)

(5) Single shear bolted joint having a member of glued-laminated wood and a steel plate.

$$\frac{P_y}{f_e \cdot d \cdot l} = \min \left\{ \begin{array}{l} 1 \\[4pt] \sqrt{2 + \dfrac{2\gamma\,(d/l)^2}{3}} - 1 \\[8pt] \dfrac{d}{l}\sqrt{\dfrac{2\gamma}{3}} \end{array} \right.$$

———————————— (5)

where, P_y : Yield load of a joint (kgf)

d : Diameter of a bolt (cm)

l : Thickness of a main member (cm)

α : Ratio of the thickness of a side member to that of a main member

β : Ratio of the embedding strength of a side member to that of a main member

f_e : Embedding strength of a main member (kgf/cm²)

f_y : Yield point of a bolt (kgf/cm²)

γ : f_y/f_e

Table 1. Comparison of the calculated values of the yield load
with the experimental results (in average)

| SPECIMEN | SPIECIES | diameter of a bolt (cm) | l/d | YIELD LOAD (kgf) | | | ULTIMATE LOAD (kgf) |
				EXPERIMENT	THEORY	RATIO	
WD	spruce	16	2	1793	1930	0.93	1817
	spruce	16	4	3705	2910	1.27	4432
	spruce	16	8	3733	4054	0.92	4712
	D. Fir	16	4	3821	3598	1.06	4855
	D. Fir	16	8	5106	4727	1.08	6041
	spruce	20	4	4621	4547	1.02	6167
	spruce	20	8	5285	6334	0.83	7340
	D. Fir	20	4	5254	5619	0.94	5333
	D. Fir	20	8	6284	7387	0.85	6840
ID	spruce	16	2	1660	1930	0.86	1743
	spruce	16	4	3727	3860	0.97	3727
	spruce	16	8	5209	4614	1.13	5783
	D. Fir	16	4	4745	4907	0.97	4745
	D. Fir	16	8	5443	6083	0.89	5740
	spruce	20	4	4448	6032	0.74	4448
	spruce	20	8	7885	8951	0.88	8700
	D. Fir	20	4	6919	7667	0.90	6919
	D. Fir	20	8	8412	9505	0.89	8412
SD	spruce	16	2	1880	1930	0.97	1880
	spruce	16	4	4056	3860	1.05	4056
	spruce	16	8	6312	5733	1.10	7478
	D. Fir	16	2	2904	2801	1.04	2904
	D. Fir	16	4	4997	5601	0.89	4997
	D. Fir	16	8	7318	6918	1.05	7747
	spruce	20	2	2953	3016	0.98	2953
	spruce	20	4	7477	6032	1.24	7667
	spruce	20	8	9192	8958	1.03	11236
	D. Fir	20	2	3671	4376	0.84	3671
	D. Fir	20	4	8296	8752	0.95	8296
	D. Fir	20	8	11656	10809	1.08	13075
WS	spruce	16	2	1448	799	1.81	1848
	spruce	16	4	2039	1599	1.28	2592
	spruce	16	8	2258	2029	1.11	3416
SS	spruce	16	2	2237	1930	1.16	2436
	spruce	16	4	2813	2309	1.22	3161
	spruce	16	8	3016	2869	1.05	3655

Table 1. shows the comparison of the calculated values of the yield load with the experimental results. The embedding strength of spruce and douglas-fir was assumed to be 377kgf/cm² and 547 kgf/cm² from the embedding test as shown in Fig.6, and the yield point of a bolt was assumed to be 5,000 kgf/cm² from the relation between the moment and strain obtained from the bending test of a bolt according to JIS Z 2204(See Fig.6). The yield load of a bolted joint subjected to the shear load parallel to the grain calculated from the formulae (1) to (5) agreed comparatively well with the experimental results.
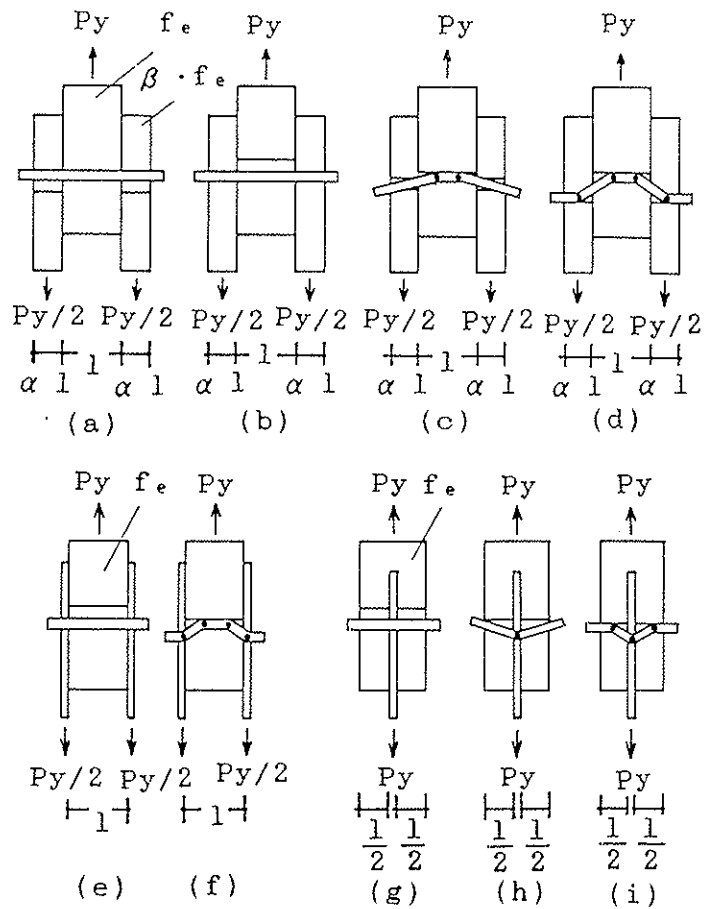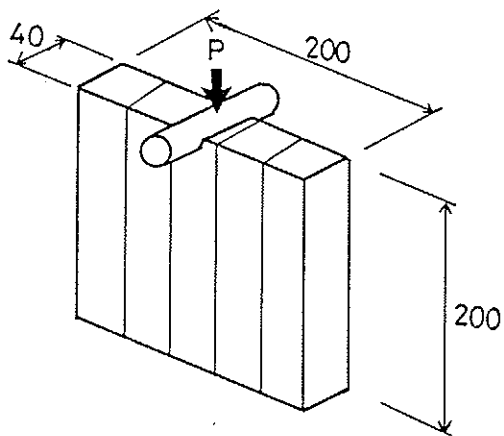
Fig.5 Yield models for the bolted joints

Fig.6 Embedding test
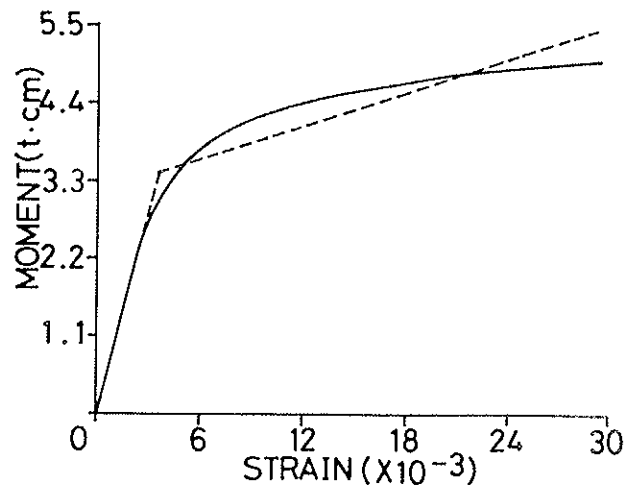
Fig.7 Relation between the moment and the strain in bending test of a bolt

-8-

INFLUENCE OF THE END DISTANCE ON THE MAXIMUM LOAD

Fig.8 shows the relation between the end distance and the maximum load in the specimen having a main member of glued-laminated wood of spruce and steel side plates subjected to the shear load parallel to the grain. In the specimen whose ratio of the thickness of a main member to the diameter of a bolt (l/d) was four, the maximum load increased in proportion to the end distance in case that the end distance was less than four times as large as the diameter of a bolt, and the maximum load did not increase any more when the end distance was greater than four times as large as the diameter of a bolt. In the specimen whose ratio of l/d was eight, the maximum load increased in proportion to the end distance in case that the end distance was less than ten times as large as the diameter of a bolt, and the maximum load was almost constant when the end distance was greater than ten times as large as the diameter of a bolt. These results indicate that the maximum load depends more on the embedding strength of the wooden member than the shear strength in case that the end distance is large enough, while the maximum load depends more on the shear strength of the wooden member than the embedding strength when the end distance is comparatively small.

PREDICTION OF THE ULTIMATE LOAD

Figs.9 to 11 shows the relation between the ratio of l/d and the quotient of the maximum load divided by the products of the embedding strength of the wooden member and the projected area of a bolt "Pmax/(fe·d·l)". In the specimen having the steel side plates, the value of "Pmax/(fe·d·l)" was almost constant as shown in Fig.9 regardless of the ratio of l/d when the ratio of l/d was smaller than eight, while the value of "Pmax/(fe·d·l)" decreased with the increase of the ratio of l/d as shown in Figs.10 and 11 in the specimen having the wooden side members and that having wooden main member and steel plate inserted in the center of a main member. This means that the ultimate load of the bolted joint having the steel side plates whose ratio of l/d is smaller than eight can be estimated with the products of the embedding strength of the wooden member and the projected area of

a bolt, and for other types of joint it is necessary to consider more accurately the distribution of the embedding stress in wooden members.
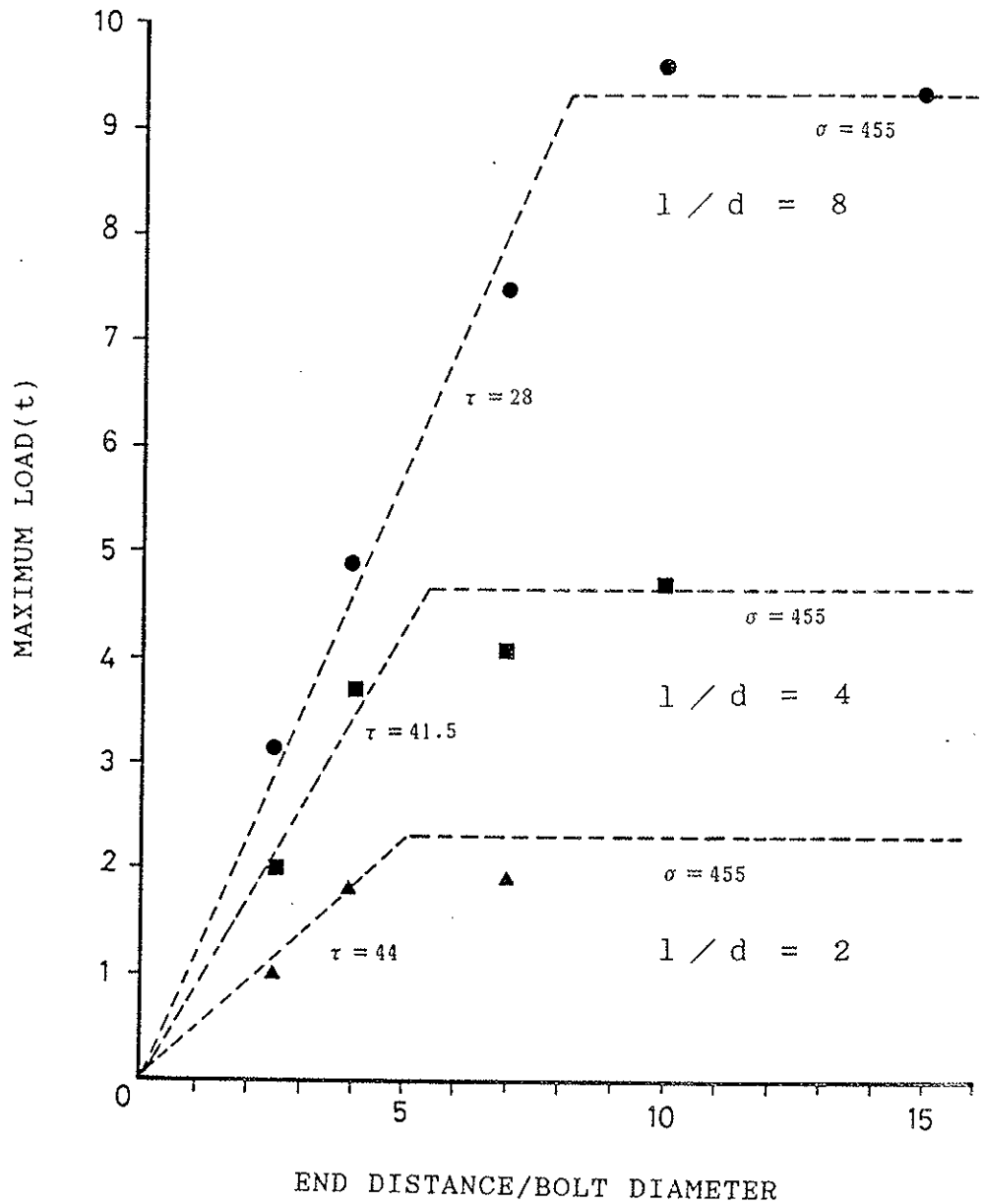
Fig.8   Relation between the maximum load
and the end distance
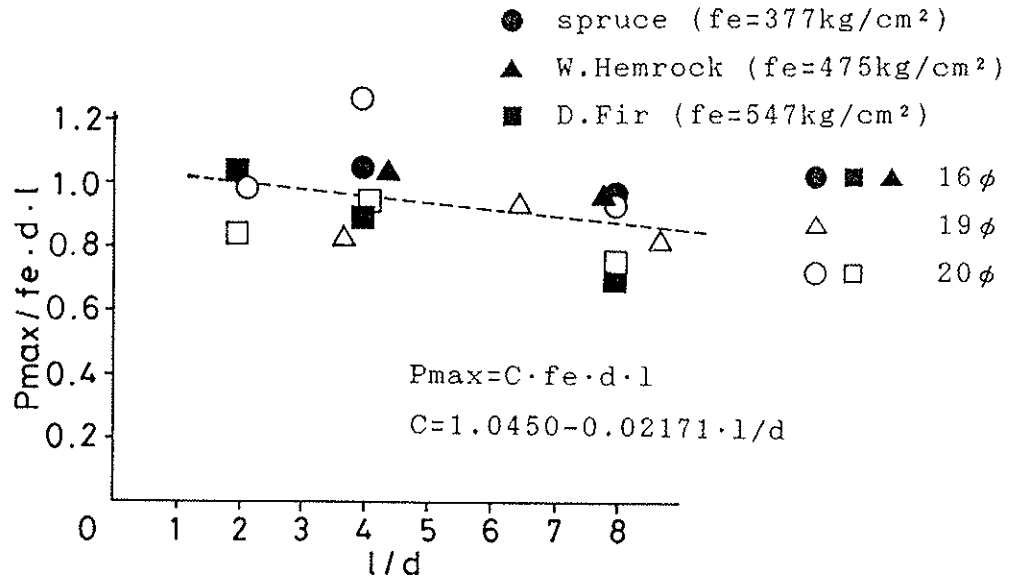
Fig.9 Relation between the value of Pmax/(fe·d·1)
and the ratio of 1/d (steel side plates)
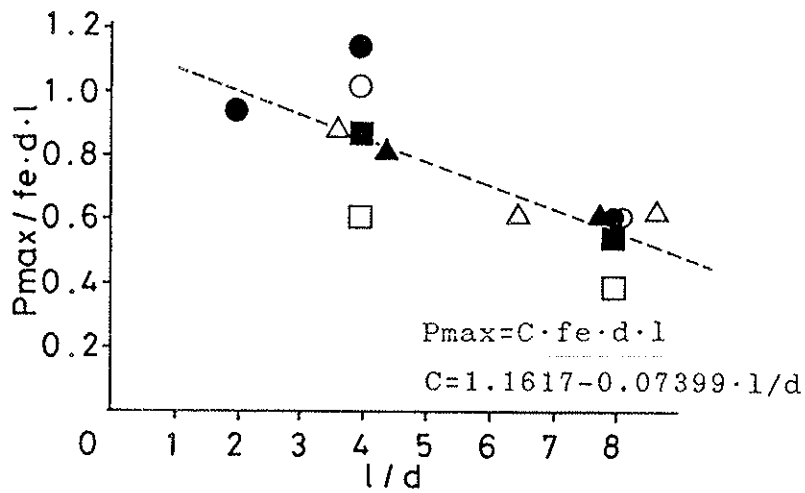
Fig.10 Relation between the value of Pmax(fe·d·1)
and the ratio of (wooden side member)
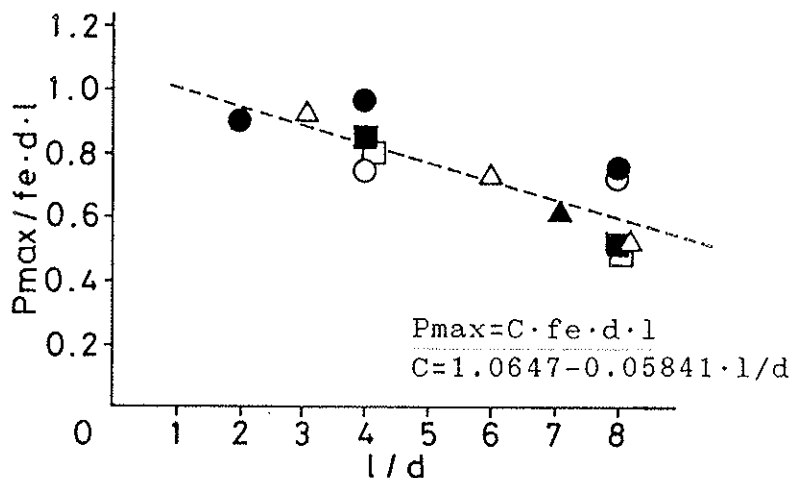
Fig.11 Relation between the value of Pmax/(fe·d·1)
and the ratio of 1/d (steel plate inserted)

INFLUENCE OF NUMBER OF BOLTS ON THE ULTIMATE SHEAR LOAD

Figs.12 to 14 show the relation between the number of bolts and the ultimate load per bolt of the specimen whose ratio of l/d was four, six and eight. In case that the ratio of l/d was four, the ultimate load per bolt decreased with the increase of the spacing between adjacent bolts. In the specimen whose ratio of l/d was six, the ultimate load per bolt decreased as shown in Fig.13 with the increase of the number of bolts in both specimens whose spacing between adjacent bolts was four times and seven times as large as the diameter of a bolt. In the specimen whose ratio of l/d was eight and the spacing between adjacent bolts was four times as large as the diameter of a bolt, the ultimate load per bolt decreased as shown in Fig.14, while in the specimen whose ratio l/d was eight and the spacing between adjacent bolts was seven times as large as the diameter of a bolt, the decrease of the ultimate load per bolt with the increase of the number of bolts was very small.

The relation between the number of bolts and the rate of the decrease of the ultimate load per bolt was obtained from the experimental results by the least square method as shown in Figs.15 and 16 respectively. Fig.17 shows the relation between the number of rows of bolts and the ultimate load per bolt when the number of bolts in a row was four. In case that the ratio of l/d was eight, the ultimate load per bolt decreased remarkably with the increase of the number of rows of bolts, and the ultimate load per bolt of the specimen having three rows (twelve bolts in total) was about a half of that of the specimen having one single bolt.
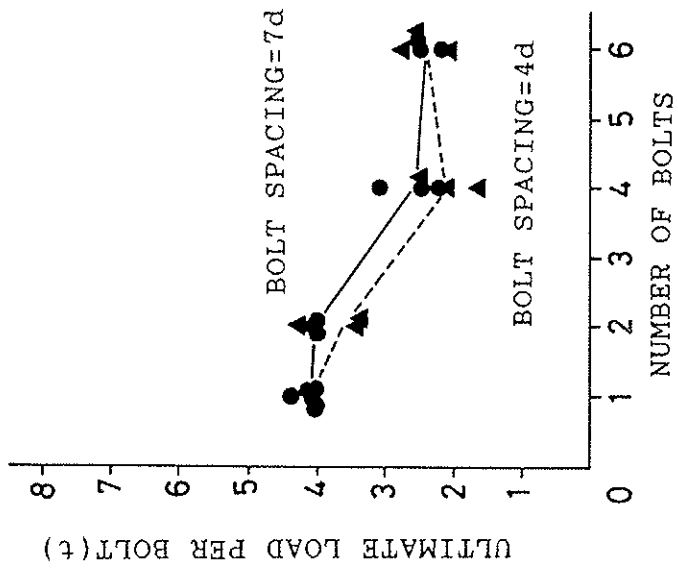
Fig 12. Relation between the number of bolts and the ultimate load per bolt (l/d=4)
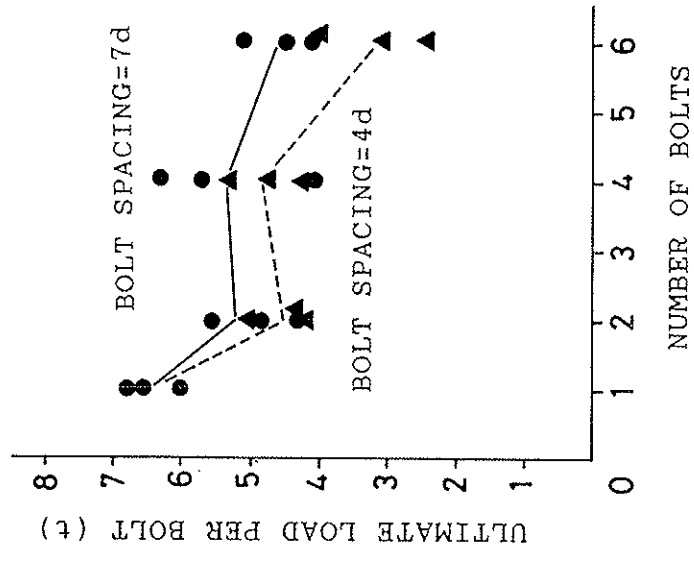
Fig 13. Relation between the number of bolts and the ultimate load per bolt (l/d=6)
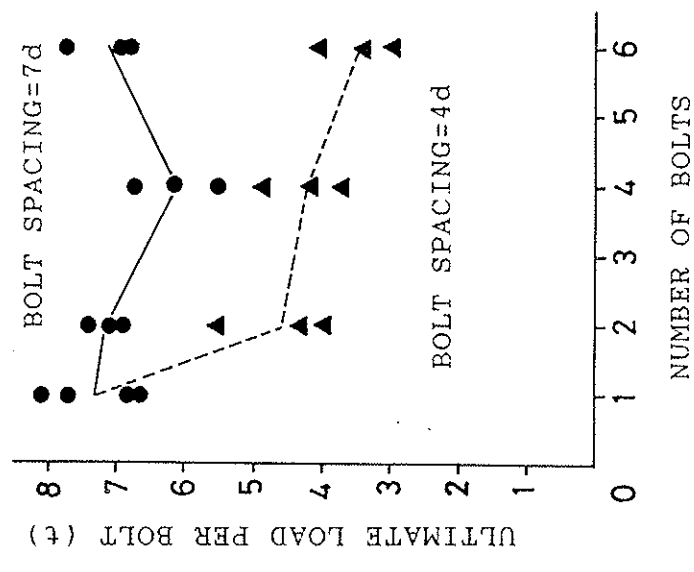
Fig 14. Relation between the number of bolts and the ultimate load per bolt (l/d=8)
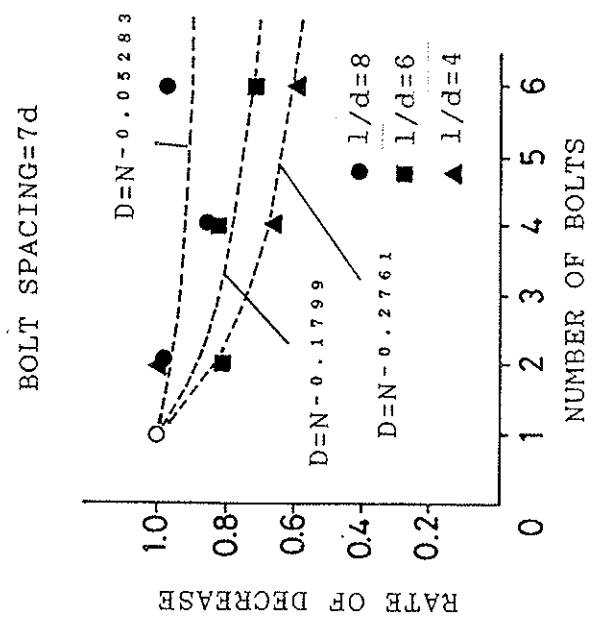
Fig 15. Relation between the number of bolts and the decreasing ratio of the ultimate load per bolt
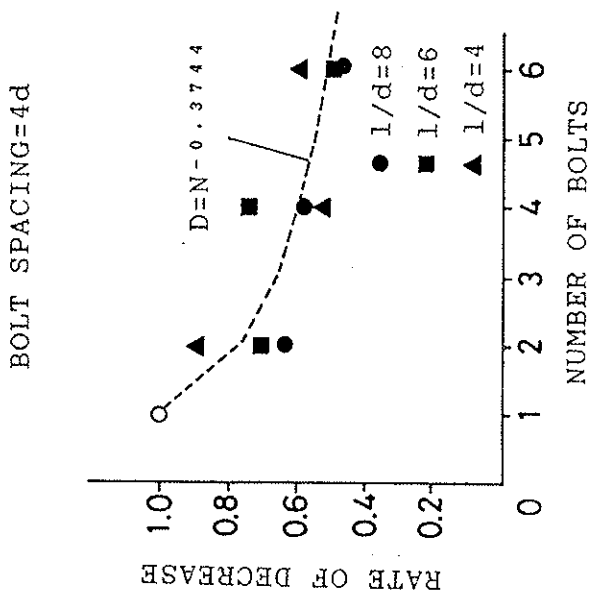
Fig 16. Relation between the number of bolts and the decreasing ratio of the ultimate load per bolt
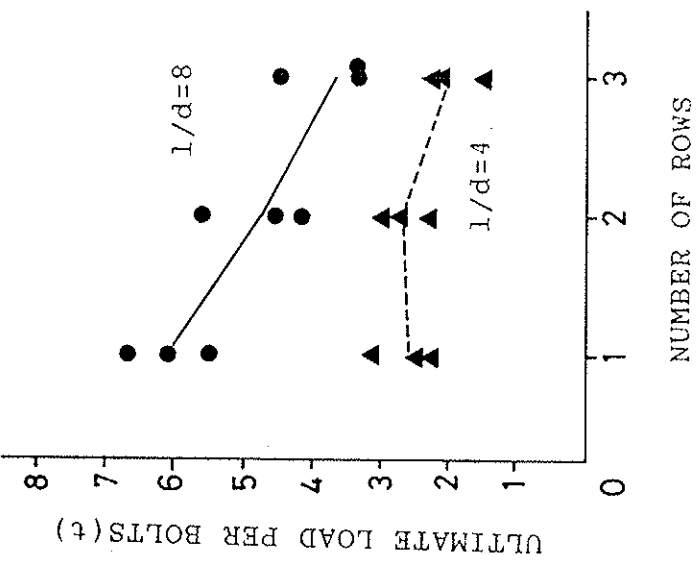
Fig 17. Relation between the ultimate load per bolt and the number of rows (one row includes four bolts)

ULTIMATE LOAD OF A BOLTED JOINT SUBJECTED TO THE SHEAR LOAD PER-
PENDICULAR TO THE GRAIN

DESCRIPTION OF SPECIMEN

The specimen included a main member of glued-laminated wood
of spruce, douglas-fir and ezomatu-todomatu and steel side
plates. The ratio of the thickness of a main member to the
diameter of a bolt was four, eight and ten. The diameter of a
bolt was sixteen millimeters and twenty millimeters. The end dis-
tance of a joint varied from four times to twenty-five times as
large as the diameter of a bolt, and the edge distance varied
from two and a half times to ten times as large as the diameter
of a bolt.

TEST METHOD

Some specimens were subjected to the shear load perpen-
dicular to the grain by tension as shown in Fig.18, and others
were subjected to the shear load by bending as shown in Fig.19.
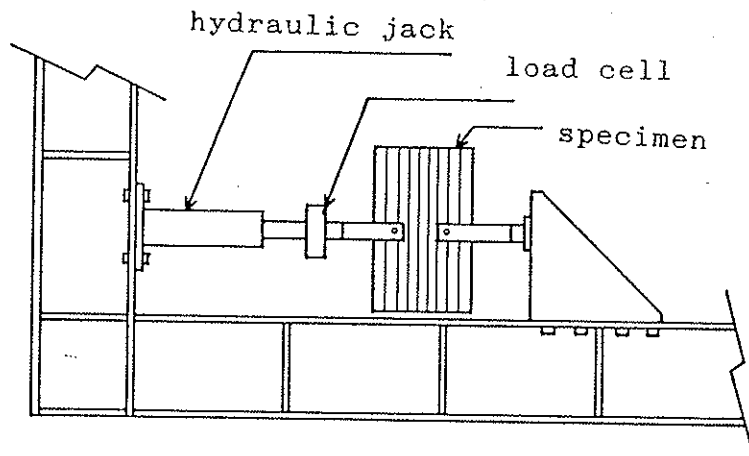
Fig 18. Shear test of the
bolted joints per-
pendicular to the
grain by tension
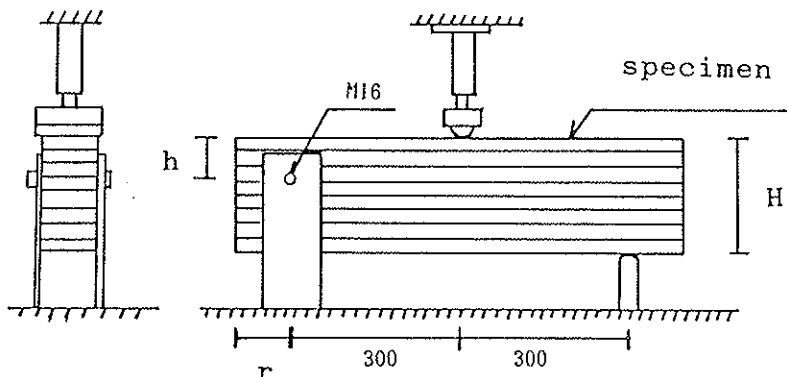
Fig 19. Shear test of the
bolted joints per-
pendicular to the
grain by bending

ESTIMATION OF THE ULTIMATE LOAD

Assuming the distribution of the tension stress perpendicular to the grain in the plane AA' in Fig.20 is expressed by the following function,

$$\sigma = \sigma_m \{ C_1 \cosh(tx/r) + C_2 \sinh(tx/r) \}$$

$$\text{———————— (6)}$$

where, σ : tension stress perpendicular to the grain at the point of x (kgf/cm^2)

σ_m : maximum tension stress perpendicular to the grain of a member (kgf/cm^2)

C_1, C_2 : constant

t : variable

and $\sigma = \sigma_m$ when x=0, and $\sigma = 0$ when x=r, the tension stress perpendicular to the grain is expressed as follows,

$$\sigma = \sigma_m \{ \cosh(tx/r) - \coth(t) \cdot \sinh(tx/r) \}$$

$$\text{———————— (7)}$$

where, r is the end distance of a joint in centimeter.

$$\sigma = \sigma_m \{ \cosh(tx/r) - \coth(t) \sinh(tx/r) \}$$
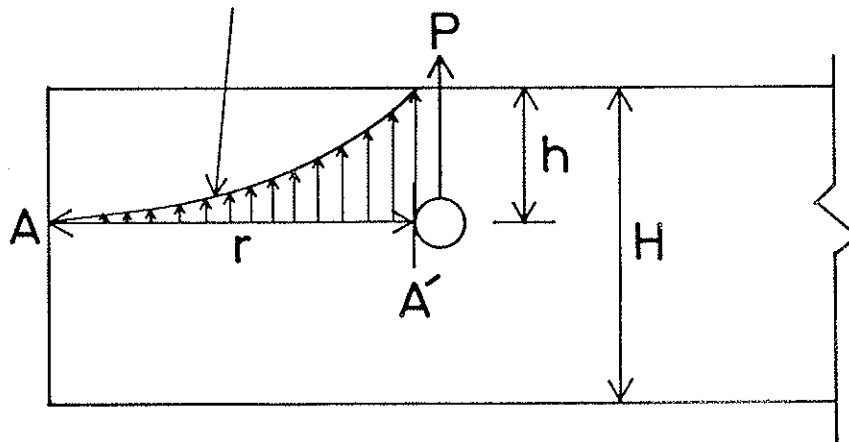
Fig 20.   Assumption of the distribution of the
          tension stress perpendicular to the grain

If we assume the shear load applied to the bolted joint is distributed equally both ends of the bolt hole, the ultimate load per thickness of the wooden member P in kgf/cm is obtained as follows by integrating the expression (7).

$$P = \frac{2 \sigma_* r (\cosh(t) - 1)}{t \sinh(t)} \qquad\qquad (8)$$

where, t is the variable according to the edge distance h in centimeter and the height of a beam H in centimeter. By assuming t is expressed by the following formula,

$$t = \frac{\alpha r}{h} (1 - h/H)^{\beta} \qquad\qquad (9)$$

the values of α and β obtained from the experimental results by use of the least square method were $\alpha = 1.88$ and $\beta = 0.311$ in case that the value of σ_m was 30kgf/cm².

COMPARISON OF THE CALCULATED VALUES WITH THE EXPERIMENTAL RESULTS

Table 2. shows the comparison of the shear strength of a bolted joint per thickness of a member calculated from the formulae (8) and (9). The values calculated from the formulae (8) and (9) agreed well with the experimental results in case that the end distance was comparatively large, but the calculated values for the specimen whose end distance was extremely small (especially four times as large as the diameter of a bolt) was about two thirds of the experimental results. This means the formulae (8) and (9) predict practically well the ultimate load of a bolted joint subjected to the shear load perpendicular to the grain, however further study should be necessary to predict more accurately the ultimate load of a bolted joint whose end distance is small.

The ultimate load per thickness of a main member was almost constant when the ratio of l/d was smaller than eight, and the ultimate load per thickness decreased in case the ratio of l/d was ten. This means the formulae (8) and (9) are applicable only for the joint whose thickness of a main member is less than eight times as large as the diameter of a bolt.

Table 2. Comparison of the calculated values of the ultimate load per thickness with the experimental results of the bolted joints subjected to the load perpendicular to the grain (steel side plates)

r (cm)	h (cm)	H(cm)	ULTIMATE LOAD (kgf/cm)		
			EXPERIMENT	THEORY	RATIO
10.4	4	*	161	126	1.28
5.6	6.4	*	147	138	1.06
10.4	6.4	*	183	186	0.98
24.16	6.4	*	219	204	1.07
39.2	6.4	*	197	204	0.96
10.4	11.2	*	220	251	0.88
13	8	*	195	233	0.84
39	8	*	224	255	0.88
5.6	6.4	22.4	189	143	1.33
10.4	6.4	22.4	223	200	1.12
23.2	6.4	22.4	257	226	1.14
39.2	6.4	22.4	263	227	1.16
5.6	11.2	22.4	262	160	1.63
10.4	11.2	22.4	328	269	1.22
23.2	11.2	22.4	374	407	0.92
39.2	11.2	22.4	466	439	1.06
10.4	16	22.4	452	295	1.53
39.2	16	22.4	656	690	0.95
5.6	11.2	44.8	176	158	1.11
10.4	11.2	44.8	225	259	0.87
39.2	11.2	44.8	360	389	0.93
5.6	22.4	44.8	280	166	1.68
10.4	22.4	44.8	345	300	1.15
5.6	6.4	12.8	213	147	1.45
10.4	6.4	12.8	247	214	1.16
39.2	6.4	12.8	264	253	1.04

* Tension load was applied at the both ends of the specimen (H→∞)

r: end distance
h: edge distance
H: depth of a beam

CONCLUSION

    The results of this study lead to the following concluding statements:

1. The yield load calculated from the formulae (1) to (5) agreed comparatively well with the experimental results. However further study on the evaluation of the embedding strength of wood and the yield moment of the bolt would be necessary.

2. The maximum load of the bolted joints depends more on the embedding strength of the wooden member than the shear strength in case that the end distance is large enough, while the maximum load depends mainly on the shear strength of the wooden member in case that the end distance is comparatively small.

3. In the joint having the steel side plates whose ratio of the thickness of a main member to the diameter of a bolt was smaller than eight, the ratio of the maximum load parallel to the grain to the products of the embedding strength of the wooden member and the projected area of a bolt "Pmax/(fe·d·l)" was almost constant regardless of the ratio of l/d, but the value of "Pmax/(fe·d·l)" decreased in the increase of the ratio of l/d in other types of joints.

4. In the joint whose ratio of l/d was eight, the number of bolts did not influence a lot on the ultimate load in case that the number of bolts in a row was not greater than six . In the joint whose ratio of l/d was four and six, the ultimate load per bolt decreased in the increase of the number of bolts as shown in Fig.15. In the joint whose spacing between adjacent bolts was four times as large as the diameter of a bolt, the ultimate load per bolt decreased in the increase of the number of bolts regardless of the ratio of l/d as shown in Fig.16. The ultimate load per bolt of the joint decreased in the increase of the number of rows, and that of the joint having three rows (twelve bolts in total) was about a half of the ultimate load of the joint having one single bolt.

5. The ultimate load per thickness of the joint perpendicular to
   the grain calculated from the formulae (8) and (9) agreed
   comparatively well with the experimental results. However
   these formula tend to underestimate the ultimate load of the
   joint whose end distance is small comparing with the edge
   distance, and they are not applicable for the joints whose
   ratio of l/d is greater than eight.

REFERENCES

[1] LARSEN, H.J., DESIGN OF BOLTED JOINTS, CIB-W18/12-7-2,
    October 1979.

[2] SUGIYAMA, M., YASUMURA, M., and OKUTOMI, S., STRENGTH OF
    BOLTED JOINTS IN GLUED LAMINATED TIMBER SUBJECTED TO DOUBLE
    SHEAR LOAD, Summary of Technical Paper of Annual Meeting
    1984, Architectural Institute of Japan, October 1984.

[3] YASUMURA, M., NAKAMURA, N., and SUGIYAMA, H., EXPERIMENTAL
    AND THEORETICAL ANALYSIS OF BOLTED JOINTS IN GLUED
    LAMINATED TIMBER, Summary of Technical Paper of Annual
    Meeting 1983, Architectural Institute of Japan, September
    1983.

[4] YASUMURA, M. and SAKAI, H., INFLUENCE OF NUMBER OF BOLTS ON
    SLIP STIFFNESS AND STRENGTH OF THE BOLTED TIMBER JOINTS,
    Summary of Technical Paper of Annual Meeting 1987,
    Architectural Institute of Japan, October 1987.

[5] YASUMURA, M. and SAKAI, H., STRENGTH OF THE BOLTED TIMBER
    JOINTS PERPENDICULAR TO THE GRAIN, Summary of Technical Paper
    of Annual Meeting 1987, Architectural Institute of Japan,
    October 1987.

INTERNATIONAL COUNCIL FOR BUILDING RESEARCH STUDIES AND DOCUMENTATION

WORKING COMMISSION W18A - TIMBER STRUCTURES

MODELLING THE LOAD-DEFORMATION BEHAVIOUR OF CONNECTIONS WITH PIN-TYPE FASTENERS UNDER COMBINED MOMENT, THRUST AND SHEAR FORCES

by

I Smith
University of New Brunswick
Canada

MEETING TWENTY
DUBLIN
IRELAND
SEPTEMBER 1987

MODELLING THE LOAD-DEFORMATION BEHAVIOUR OF CONNECTIONS WITH PIN-TYPE
FASTENERS UNDER COMBINED MOMENT, THRUST AND SHEAR FORCES.

Ian Smith, PhD., PEng., F.I.W.Sc.

Department of Forest Engineering, University of New Brunswick

Abstract

This paper gives an initial theoretical consideration of how to

utilize data collected by the author and coworkers, on the behaviour

of connections with a single pin-type fastener, to predict

load-deformation behaviour of multi-fastener connections subjected to

two dimensional combinations of moment, thrust and shear forces.

Based on application of this theory, it is tentatively concluded that

a combination of linear elastic and limit type analyses can be used to

design frames with pin-type fastener connections.

August 1987

1. Introduction

Previous work by the author and coworkers reported to CIB-W18 concentrated on the behaviour of connections with a single fastener subjected to short-term lateral loading, (4, 5, 9, 10). This reflected an initial need to focus on the reference or characteristic properties to which modification factors are applied in design. Emphasis has now begun to shift to definition of the modification factors. Three recent CIB-W18 papers have dealt with the influence of the number of rows of fasteners upon the ultimate capacities of axially loaded connections, (6, 7, 8). What emerged from these was that existing knowledge (practical and theoretical) is relatively reliable when pin-type fastener connections fail in a ductile manner, by crushing the wood under each fastener or by simultaneous development of a plastic hinge(s) in each fastener and crushing failure of the wood beneath it. Less confidence should be placed in present knowledge when brittle fracture governs the load capacity of any connection. Much remains to be done on this topic which is important in, for example, design of heavy trusses with spliced tension chords. Concern over design of axially loaded connections is, however, only one manifestation of a broader requirement for reliable design of pin-type fastener connections subjected to arbitrary combinations of moment, thrust and shear forces.

This paper gives an initial theoretical consideration of how to utilize data collected by the author and coworkers, on the behaviour of connections with a single pin-type fastener, to predict load-deformation behaviour of multi-fastener connections subjected to two dimensional combinations of moment, thrust and shear forces.

2. Theory

The theory presented below is applicable to spliced timber connections with fasteners such as nails or bolts. It is assumed that the load-slip response for an arbitrary lateral loading of a connections with only one fastener is described by an equation of the form, (1):

$$[1] \quad P = [K_2 + K_3 (\delta - \delta_0)] [1 - \exp(-K_1 (\delta - \delta_0)/K_2)]$$

where: P = load at slip δ

δ_0 = initial take up (e.g. due to the tolerance in a bolt hole)

K_1 = initial tangent stiffness

K_2 = intercept of final tangent on load axis

K_3 = final tangent stiffness

A graphical definition of these terms is given in Figure 1.
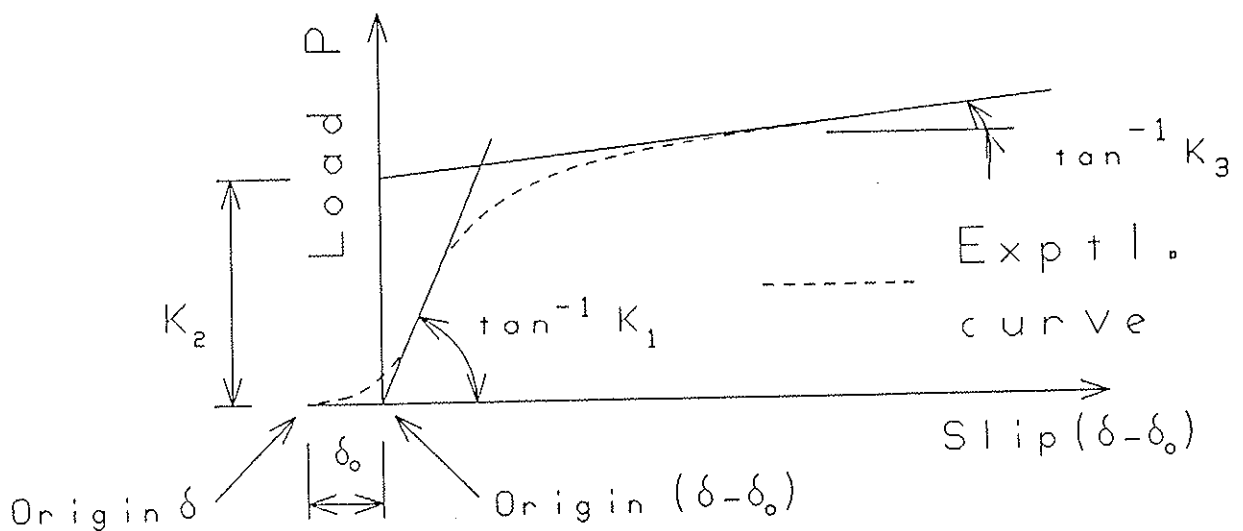
Fig. 1 Definition of constants

Now, considering a connection such as that shown in Figure 2, deformation of that connection at a given load level can be completely defined in terms of translations u and v, and rotation θ. If it is assumed that the gusset is rigid and each fastener has the same load-slip characteristics, to a first order approximation:

$$[2] \quad P_{x,i} = \Phi_i \, [K_{2x} + K_{3x} \, | \, \delta'_{x_i} \, |] \, [1 - \exp(-K_{1x} \, | \, \delta'_{xi} \, | / K_{2x})]$$

$$[3] \quad P_{y,i} = \psi_i \, [K_{2y} + K_{3y} \, | \, \delta'_{yi} \, |] \, [1 - \exp(-K_{1y} \, | \, \delta'_{yi} \, | / K_{2y})]$$

where:

$P_{x,i}$ = load component in x-axis direction for ith fastener

K_{1x} = K_1 for loading in x-axis direction

K_{2x} = K_2 for loading in x-axis direction

K_{3x} = K_3 for loading in x-axis direction

$| \delta'_{xi} | = | u - \theta y_i | - \delta_{0x}$

δ_{0x} = δ_0 for loading in x-axis direction

Φ_i = state variable

If $(u - \theta y_i) > 0$ and $| \delta'_{xi} | > 0$ then $\Phi_i = 1.0$

If $(u - \theta y_i) < 0$ and $| \delta'_{xi} | > 0$ then $\Phi_i = -1.0$

If $\quad | \delta'_{xi} | < 0 \quad$ then $\Phi_i = 0.0$

$P_{y,i}$ = load component in y-axis direction for ith fastener

K_{1y} = K_1 for loading in y-axis direction

K_{2y} = K_2 for loading in y-axis direction

K_{3y} = K_3 for loading in y-axis direction

$| \delta'_{yi} | = | v + \theta x_i | - \delta_{0y}$

δ_{0y} = δ_0 for loading in y-axis direction

ψ_i = state variable

If $(v + \theta x_i) > 0$ and $| \delta'_{yi} | > 0$ then $\psi_i = 1.0$

If $(v + \theta x_i) < 0$ and $| \delta'_{yi} | > 0$ then $\psi_i = -1.0$

If $| \delta'_{yi} | \quad < 0 \quad$ then $\psi_i = 0.0$

x_i, y_i = coordinate pair for ith fastener

Notation:

$-\bigoplus-$ = fastener location prior to loading

C = centroid of connection prior to loading
(gusset and connected members)

C' = centroid of connection in connected member
under load

Moment = M = M' + Qe

Thrust = N

Shear = Q
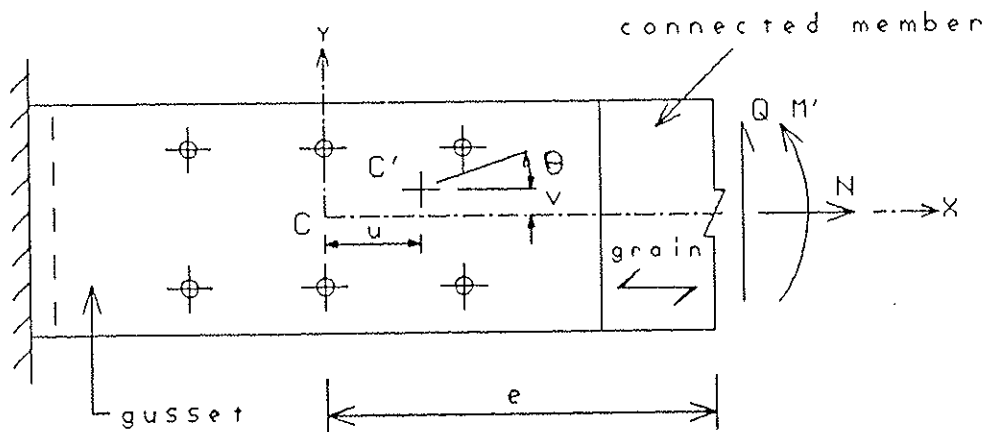
Fig. 2 Notation: displacements u, v and θ

Summing forces in the x-axis and y-axis directions, taking moments
about centroid C and neglecting second order terms yields:

$$[4] \quad N = \sum_{i=1}^{n_f} P_{x,i}$$

$$[5] \quad Q = \sum_{i=1}^{n_f} P_{y,i}$$

$$[6] \quad M = - \sum_{i=1}^{n_f} (P_{x,i}\, y_i - P_{y,i}\, x_i)$$

where: n_f = number of fasteners in the connection.

Equations [2] through [6] can be used to find the u, v and and θ

values associated with a particular combination of forces N, Q and M. A

computer program employing a modified Newton-Raphson technique has been

used by the author for this purpose.

It should be noted that displacements u, v and θ, as defined above,

are localized movements relative to the gusset.

3. Application of the theory

3.1 Influence of thrust and shear forces on moment-rotation

relationships, and interaction of displacements u, v and θ

Because of the non-linear nature of the load-slip responses for

fasteners the N-u, Q-v and M-θ relationships are not independent unless N

or Q or M acts alone, even if we neglect geometric non-linearity. Figures

5 and 6 show how the M-θ relationships, for the nailed connection in Figure

3 and the bolted connection in Figure 4 respectively are influenced by the

application of non-zero N and Q forces. Constants K_{1x}, K_{2x}, K_{3x}, δ_{0x}, K_{1y},

K_{2y}, K_{3y} and δ_{0y} used to generate Figures 5 and 6 represent a short-term

behaviour as measured during a test to failure at a cross-head movement of

2.5mm/min, (3). Considering the nailed connection, Figure 5, it can be

seen that if a moment is applied in combination with thrust and/or shear

forces, the rotation θ at a given moment is greater than when only the

moment is applied. As might be expected the general trend is that

enhancement of the rotation is proportional to the thrust and shear forces.

Note that for the nailed connection $\delta_{0x} = \delta_{0y} = 0.0$. From Figure 6 (bolted

connection) it can be seen that the interactions between displacements u, v

and θ are more complex when δ_{0x} and δ_{0y} are non-zero.

Using the bolted connection in Figure 4 as an illustration, design

charts such as those shown in Figures 7 to 9 can be used to estimate

translations u and v and rotation θ under a specified combination of M, N

and Q. Table 1 shows values extracted from these charts.

Notation :

⊕ head-side ⎤
              ⎦ nail location
⊕ point-side ⎤

⟵ direction of grain
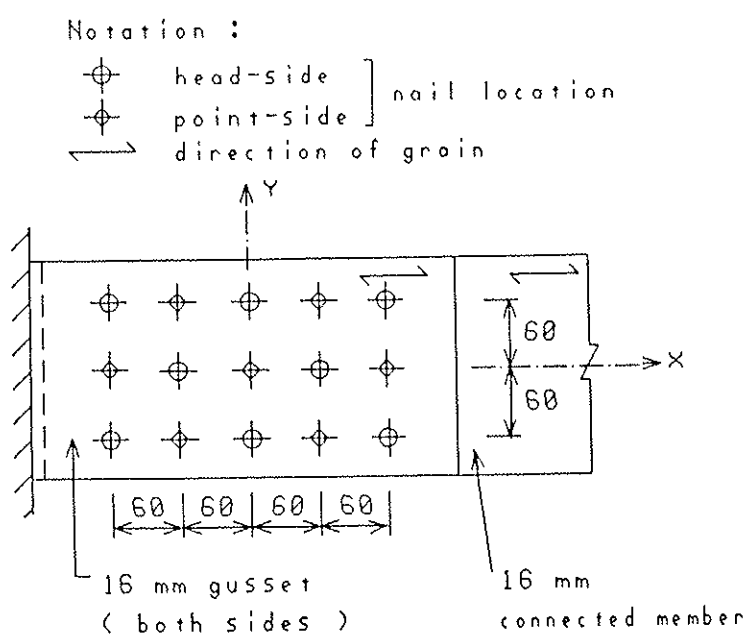
Fastener constants :

$K_{1x} = K_{1y} = 2975$ kN/m

$K_{2x} = K_{2y} = 0.6785$ kN

$K_{3x} = K_{3y} = 84.06$ kN/m

$\delta_{0x} = \delta_{0y} = 0.0$

↑ Y

60
60

→ X

|60|60|60|60|

16 mm gusset
(both sides)

16 mm
connected member

Fig. 3 15 Nail connection: Canadian spruce (375 Kg/m³, 9.3%m.c.)
2.65 mm Common wire nails in Double Shear

Notation : ⊕ bolt location

⟵ direction of grain
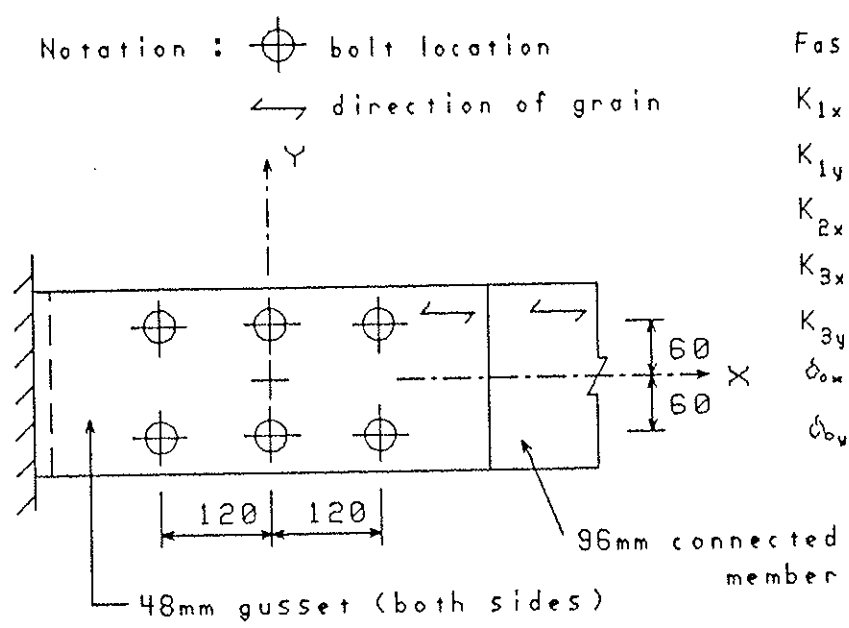
Fastener constants :

$K_{1x} = 23011.0$ kN/m

$K_{1y} = 9721.0$ kN/m

$K_{2x} = 31.10$ kN, $K_{2y} = 20.02$ kN

$K_{3x} = 762.0$ kN/m

$K_{3y} = 712.0$ kN/m

$\delta_{0x} = 1.10$ mm

$\delta_{0y} = 0.77$ mm

↑ Y

60
60

→ X

|120|120|

96mm connected
member

48mm gusset (both sides)

Fig. 4 6 Bolt connection: Canadian spruce (375 Kg/m³, 8.6%m.c.)
M16 Black hexagon head bolts in Double Shear
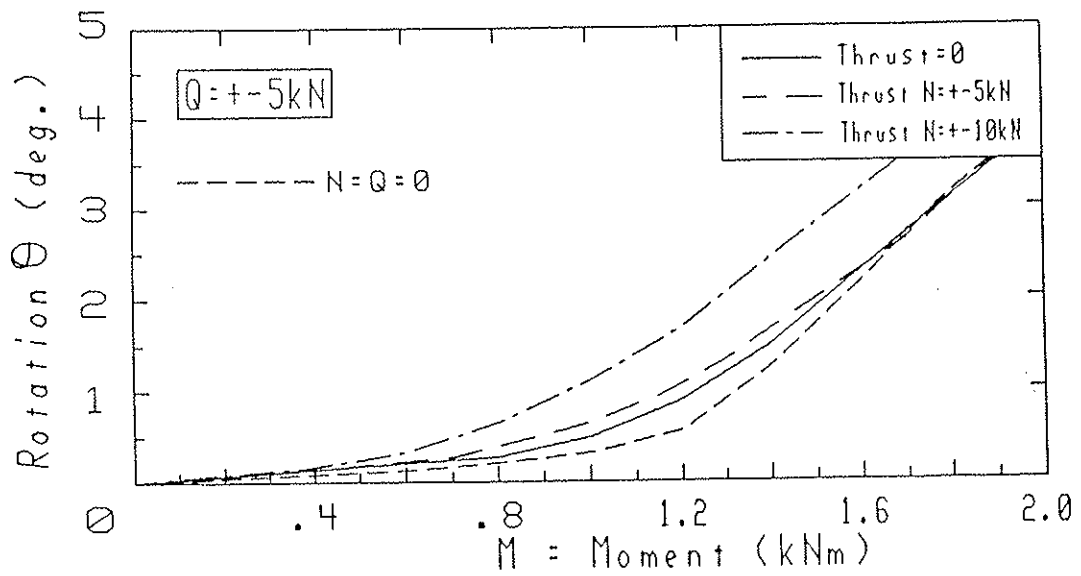
Fig. 5   Influence in N and Q on Rotation-Moment relationship
         (15 nail connection)
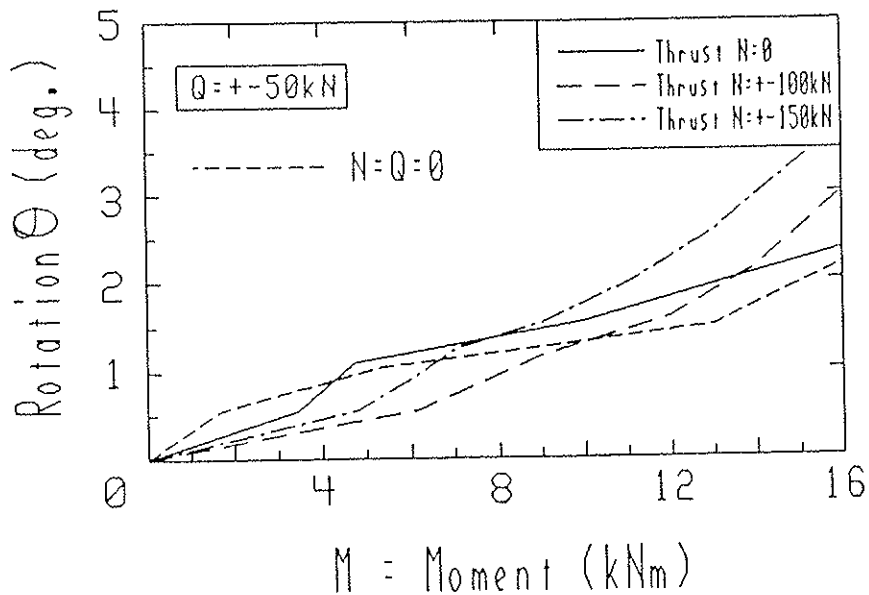
Fig. 6   Influence of·N and Q on Rotation-Moment relationship
         (6 bolt connection)

SLIP PARALLEL TO GRAIN
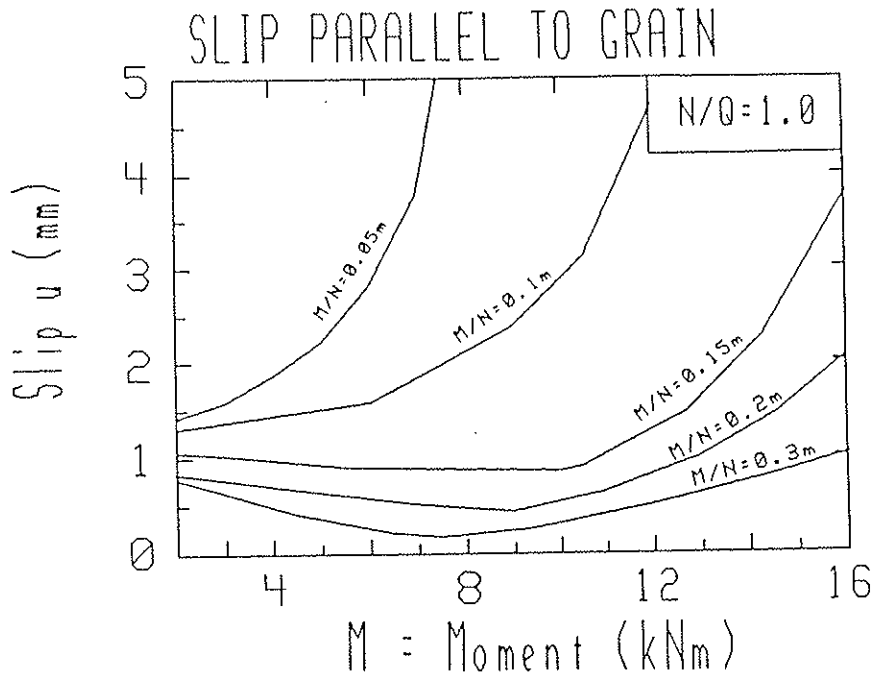
Fig. 7   Typical Design Chart-estimation of u
(6 bolt connection)

SLIP PERPENDICULAR TO GRAIN
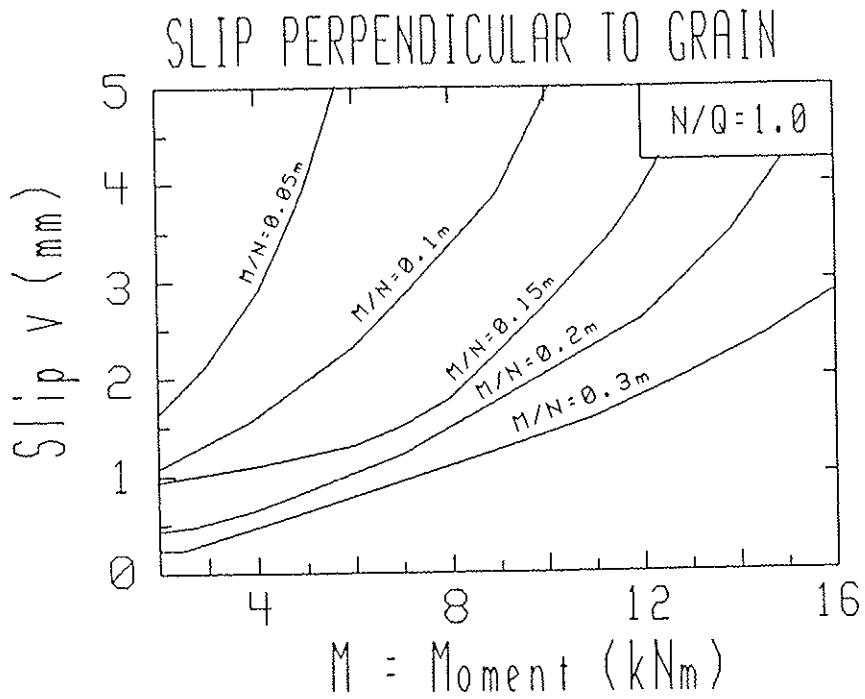
Fig. 8   Typical Design Chart-estimation of v
(6 bolt connection)

ROTATION ABOUT GROUP CENTROID
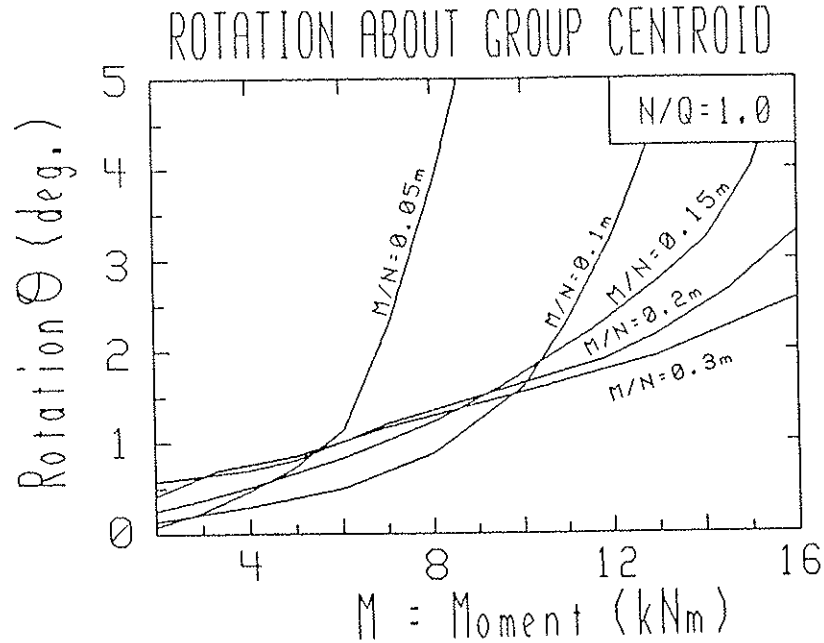
Fig. 9   Typical Design Chart-estimation of θ
         (6 bolt connection)

Table 1.   Estimation of u, v and θ for Six Bolt Connection

	M = 6 kNm N = Q = 30 kN	M = 6 kNm N = Q = 40 kN	M = 6 kNm N = Q = 60 kNm	M = 6 kNm N = Q = 0.0
u(mm)	0.57	0.90	1.71	0.0
v(mm)	1.05	1.32	2.12	0.0
θ(deg.)	1.05	0.89	0.50	1.12

3.2 Deflections in structures containing pin-type fastener connections

Three simple beam type structures are used below to illustrate

considerations in predicting deflections in structures containing pin-type

fastener connections.

Ex. 1   Beam with connections subject to moment only

   (Figures 10a, 10b and 11):

Mid-span displacement Δ_c is given by:

[7] $\Delta_c = \Delta_{Ej} + \Delta_{Gj} + \theta\ell$

where: Δ_{Ej} = elastic bending displacement due to deformation of the

   beam.

$$= \frac{PL}{96E_j I_j} (15L\ell - L^2 - 18\ell^2)$$

Δ_{Gj} = elastic shear displacement due to deformation of the beam

$$= \frac{1.2\ PL}{4G_j A_j} = \frac{0.3\ PL}{G_j A_j}$$

θ = rotation in connection either side of the joint

   = f (M = PL/4)

If: E_j = 9700 N/mm², G_j = 650 N/mm², A_j = 6992 mm²

and I_j = 19.727 x 10⁶ mm⁴, then

Δ_{Ej} = 5.362 x 10⁻³ P and Δ_{Gj} = 59.41 x 10⁻⁶ P (where both are in mm if P

is in N).

As can be seen in Figure 11, up to a load level of about P = 1 kN the

component of Δ_c due to deformation in the connections is approximately

equal to the components associated with beam deformation. Beyond this load

level connection deformations begins to dominate the displacement equation.

Ex. 2   Beam with connections subject to moment and shear

   (Figures 10a, 10c and 12).

Mid-span displacement Δ_c is given by:

[8] $\Delta_c = \Delta_{Ej} + \Delta_{Gj} + (\theta_1 + \theta_2)\frac{\ell}{2} - v_1 + v_2$

12

b) Ex.1 - Moment Only

c) Ex.2 - Moment and Shear

d) Ex.3 - Moment, Thrust and Shear

a) Connection Detail (15 nails each side of joint)

38 x 184 NO.1 Grade S-P-F

38 x 184 NO.1 Grade S-P-F (both sides)

$K_{1x} = K_{1y} = 3300$ kN/m , $K_{2x} = K_{2y} = 0.75$ kN
$K_{3x} = K_{3y} = 90$ kN/m , $\delta_{ox} = \delta_{oy} = 0.8$

Symmetric

Fig.10 Simple Beam Type Structures with Pin-type Fastener Connections
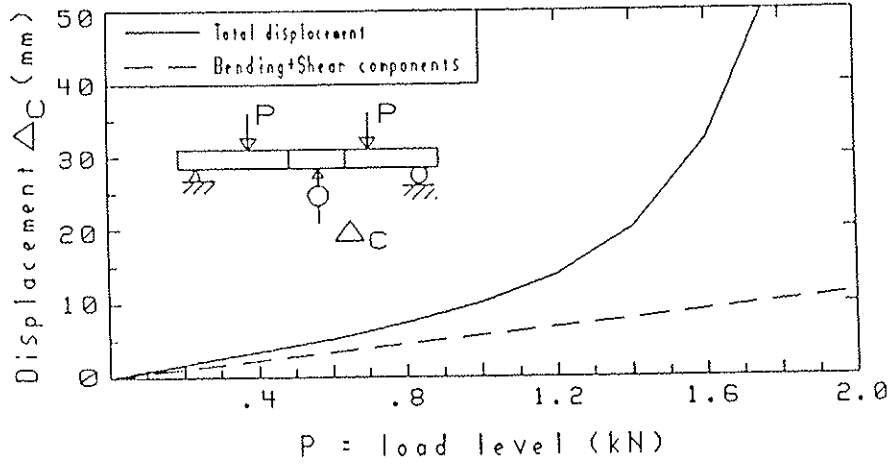
Fig. 11 Ex. 1- Beam with connections subject to Moment Only
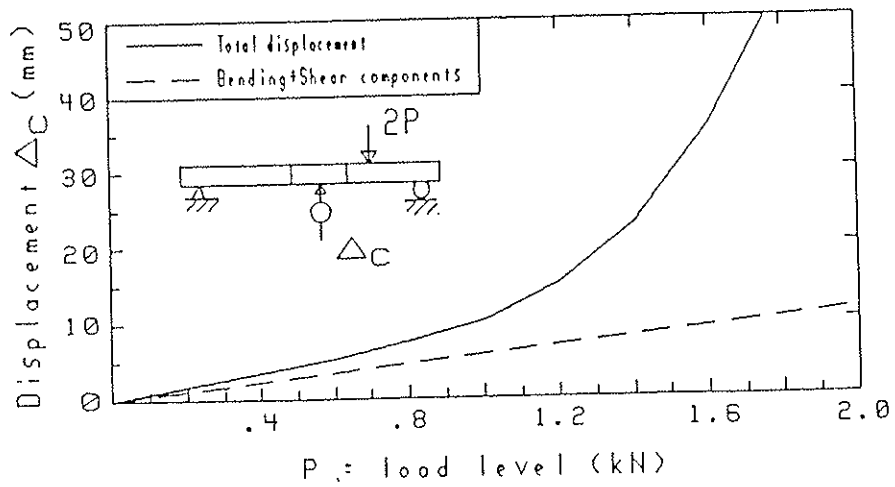
Fig. 12 Ex.2- Beam with connections subject to Moment and Shear

where: $\quad \Delta_{Ej} = \dfrac{PL}{96E_jI_j} (15L\ell - L^2 - 18\ell^2) \qquad$ (as Ex. 1)

$\Delta_{Gj} = \dfrac{0.3\ PL}{G_jA_j} \qquad$ (as Ex. 1)

$\theta_1 \quad$ = rotation in connection 1

$\quad = f\ (M = \dfrac{P\ell}{2}\ ,\ Q = \dfrac{P}{2})$

$\theta_2 \quad$ = rotation in connection 2

$\quad = f\ (M = \dfrac{P\ [L - \ell]}{2},\ Q = \dfrac{P}{2})$

$v_1 \quad$ = vertical translation in connection 1

$\quad = f\ (M = \dfrac{P\ell}{2},\ Q = \dfrac{P}{2})$

$v_2 \quad$ = vertical translation in connection 2

$\quad = f\ (M = \dfrac{P\ [L - \ell]}{2},\ Q = \dfrac{P}{2})$

Substituting the same geometric and material beam properties as in Example 1: $\Delta_{Ej} = 5.362 \times 10^{-3}\ P$ and $\Delta_{Gj} = 59.41 \times 10^{-6}\ P$ as before.

Comparing Figures 11 and 12 it can be seen that the total displacement is approximately the same for the beams in examples 1 and 2 at all load levels. [For a solid beam, i.e. no joint at mid-span, the solutions for examples 1 and 2 would be exactly the same].

Ex. 3 Cantilever with connections subjected to moment, thrust and shear (Figures 10a, 10d and 13).

Tip displacement Δ_A is given by:

[9] $\quad \Delta_A = \Delta_{Ej} + \Delta_{Gj} + \theta_1 e + (\theta_1 + \theta_2)\ \ell + v_1 + v_2$

where: $\Delta_{Ej} = \dfrac{PL \cos \phi}{E_j \ I_j} \left[-\dfrac{\ell^3}{3L} + \dfrac{3\ell^2}{2} + \dfrac{3e\ell}{2} - \dfrac{e\ell^2}{2L} + \dfrac{e^2\ell}{2L} + \dfrac{e^3}{6L} \right]$

$\Delta_{Gj} = \dfrac{1.2 \ P \cos \phi}{G_j \ A_j} \left[2 \ \ell + \dfrac{e}{2} \right]$

$\theta_1 = $ rotation in connection 1

$= f \ (M = P \cos \phi \ (L - \ell), \ Q = P \cos \phi)$

$\theta_2 = $ rotation in connection 2

$= f \ (M = P \ \ell \cos \phi, \ Q = P \cos \phi)$

$v_1 = $ vertical translation in connection 1

$= f \ (M = P \cos \phi \ (L - \ell), \ Q = P \cos \phi)$

$v_2 = $ vertical translation in connection 2

$= f \ (M = P \ \ell \cos \phi, \ Q = P \cos \phi)$

Substituting $\phi = 45°$, and the same geometric and material beam

properties as in example 1:

$\Delta_{Ej} = 57.43 \times 10^{-3} P$ and $\Delta_{Gj} = 0.635 \times 10^{-3} P$.
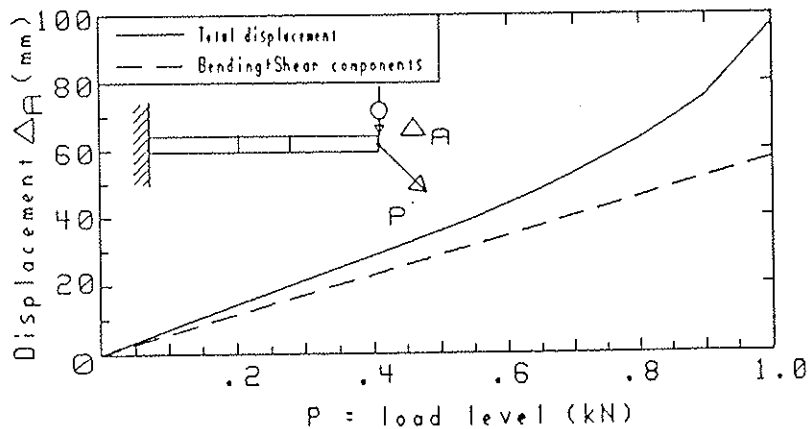
Fig. 13   Ex. 3- Cantilever with connections subject to
Moment, Thrust and Shear

From Figure 13 it can be seen that the proportion of the cantilever's

tip displacement due to deformation in the connections is relatively small.

This is because the tip displacement is mainly a result of the bending

deformation in the proportion of the cantilever adjacent to the

built-in-end.

4. Discussion

Verification of the theory, Section 2, using a direct method of measuring displacement u, v and θ under various combinations of forces M, N and Q, would require relatively complex instrumentation of specimens. The beam type structures of examples 1 to 3, Section 3.2, offer an experimentally much simpler, indirect, alternative. It is intended to check the validity of the theory in section 2 using a coordinated series of tests on beams with either nailed or bolted connections. This will indicate whether it is necessary to make refinements to the theory. Possible refinements include, an improved method for modelling initial take up δ_0, and use of fastener specific values for constants such as K_1, K_2, K_3 and δ_0 within a connection. The latter modification would reflect the existence of random variations in load-slip responses.

Based on the studies in the previous section, other unreported analyses by the author, and work on truss connections by Lau (2), tentative conclusions can be drawn concerning design of two dimension frames with pin-type fastener connections. First, for static type serviceability calculations, linear elastic frame analyses using spring elements, or 'fictitious' members to represent connections will give accurate predictions of deformed shapes of structures. This is especially true if suitable secant stiffness properties are used rather than initial tangents. Second, for static type ultimate capacity calculations, a type of limit analysis allowing for development of plastic hinges at connection locations will give accurate predictions.

Future papers will explore the validity of the theory presented in this paper, and develop the limit type analysis referred to above.

5.   Conclusions

Based on this paper, the following general conclusions are drawn concerning pin-type fastener connections:

(1) Because of the non-linear nature of the load-slip responses for pin-type fasteners, load-deformation relationships for individual degrees-of-freedom (translations u and v or rotation θ) are not independent, except when one force component acts alone. Interaction of displacements is significant in nailed connections at high load levels only, but can be significant at all load levels in bolted connections.

(2) Linear elastic frame analysis techniques using spring elements, or 'fictitious' members to represent connections ~~will~~ *can* give accurate static deflection type serviceability checks in design.

(3) Limit type frame analysis allowing for development of plastic hinges at connection locations will give accurate ultimate capacity checks in design.

References

1. HILSON, B.O., WHALE, L.R.J., POPE. D.J. and SMITH, I. (1987). "Characteristic properties of nailed and bolted joints under short-term lateral load: Part 3 - Analysis and interpretation of embedment test data in terms of density related trends". Journal of the Institute of Wood Science, December.

2. LAU, P.W.C. (1987). "Factors affecting the behaviour and modelling of toothed metal-plate joints". Canadian Journal of Civil Engineering, Vol. 14, 183-195.

3.   SMITH, I. (1982). "Interpretation and adjustment of results from short-term lateral load tests on whitewood joint specimens with nails or bolts". TRADA Research Report RR5/82.

4.   SMITH, I., WHALE, L.R.J., ANDERSON, C. and HELD, L. (1984). "Mechanical properties of nails and their influence on mechanical properties of nailed timber joints subjected to lateral loads". CIB-W18 Paper No. 17-7-1.

5.   SMITH, I. and WHALE, L.R.J. (1985). "The influence of the orientation of mechanical joints on their mechanical properties". CIB-W18 Paper No. 18-7-2.

6.   SMITH, I. and STECK, G. (1985). "Influence of number of rows of fasteners or connectors upon the ultimate capacity of axially loaded timber joints". CIB-W18 Paper No. 18-7-3.

7.   STECK, G. (1984). "Notes on the effective number of dowels and nails in timber joints". CIB-W18 Paper No. 17-7-2.

8.   STECK, G. (1986). "Effectiveness of multiple fastener joints according to national codes and Eurocode 5 (Draft)". CIB-W18 Paper No. 19-7-3.

9.   WHALE, L.R.J., SMITH, I. and HILSON, B.O. (1986). "Behaviour of nailed and bolted joints under short-term lateral load - conclusions from some recent research". CIB-W18 Paper No. 19-7-1.

10. WHALE, L.R.J. and SMITH, I. (1986). "The Derivation of design clauses for nailed and bolted joints in Eurocode 5". CIB-W18 Paper No. 19-7-2.

INTERNATIONAL COUNCIL FOR BUILDING RESEARCH STUDIES AND DOCUMENTATION

WORKING COMMISSION W18A - TIMBER STRUCTURES

PROPOSED CODE REQUIREMENTS FOR
VIBRATIONAL SERVICEABILITY OF TIMBER FLOORS

by

Y H   Chui
Timber Research and Development Association
United Kingdom

I   Smith
University of New Brunswick
Canada

MEETING TWENTY
DUBLIN
IRELAND
SEPTEMBER 1987

PROPOSED CODE REQUIREMENTS FOR

VIBRATIONAL SERVICEABILITY OF TIMBER FLOORS

by

Y H Chui
Timber Research and Development Association
United Kingdom

I Smith
University of New Brunswick
Canada

Abstract

This paper proposes how vibrational serviceability requirements for timber floors can be incorporated into a design code. Simple expressions are presented for estimating the fundamental natural frequency and the mean magnitude of the response caused by human footfall impact. These two parameters have been identified as the two governing parameters for assessing a prospective design solutions. Limits are also given for these parameters for ensuring satisfactory floor designs.

May 1987

Introduction

Timber floors have been traditionally designed based on the 'working stress' method. Because of their relatively light weight, timber floors sometimes exhibit excessive vibrations which cause undue disturbances and discomfort to their users. This problem has been precipitated in the recent past by the adoption of higher elastic moduli and more refined design techniques which lead to more flexible and lighter floor systems.

Present major national design codes (1, 2, 3) provide no criteria for ensuring acceptable vibrational performance although the static deflection limits do provide an indirect control over the problem. The draft Eurocode 5 (4), which forms the basis of a future common unified code for the European Community, specifies a lower bound limit of 5 Hz for the fundamental natural frequency as the vibration criterion. Work by the first author (5) revealed that the magnitude of the vibrational response caused by human footfall is usually the more critical parameter and that it, as well as the fundamental natural frequency, should be limited.

The recommendations for code input proposed in this paper are based on test work by TRADA. The study also covered the development of methods for predicting vibrational behaviour of timber floors. The following proposes the controlling parameters and sets out simplified equations for calculating their values.

Controlling Criteria

The common practice of ensuring acceptable vibrational performance of any structure is to impose a bound limit for its natural frequencies. The effect of the magnitude of the vibration is often overlooked. This is justifiable for heavy structures made of steel or concrete which often have low fundamental natural frequencies as well as low vibrational response magnitude. This is because both these parameters are inversely proportional to the mass of the structure.

It is possible to show that because of the static deflection limits given in design codes, timber floors are not likely to have low natural frequencies.

The fact that troublesome floors are still sometimes produced indicates that this frequency limit alone is not adequate and that the magnitude of the vibrational response should also be included as an extra criterion. Based on the recommendations of the British Standard BS 6472 (6), the first author (7) has proposed the following two criteria:-

1. the fundamental natural frequency (f_n) should be higher than 8 Hz,

2. the frequency-weighted root-mean-square acceleration (Ar) of the response caused by a normal human footfall impact should be less than 0.45 m/s^2.

Details about the basis of the above are given in reference 7. It is added here that, to ensure acceptable floor performance, criteria 1 and 2 should both be satisfied.

Calculation of f_n and Ar

Having established the criteria for controlling floor vibration, there is a need for a reliable method of predicting at the design stage the meeting of the criteria by a given floor design.

Prediction of either f_n and Ar can be considerably simplified if the design model is assumed to be a one-dimensional beam structure as in present static 'working stress' design, rather than the more appropriate two dimensional rib-plated structure. This simplified approach would inevitably produce less reliable estimates of these parameters. The design expressions given in this section follows the rib-plated approach and are therefore based on a model of orthotropic plate (sheathing) attached to a series of equidistant ribs (joists). In the model the four sides of the structure are assumed simply supported. It can be noticed that the final expressions are more complicated than the corresponding ones based on the single beam approach, but are still easily executable on an electronic calculator.

The expression for estimating the fundamental natural frequency f_n is given in equation 1 (see reference 8 for its derivation).

$$f_n = \frac{\pi}{2a^2} \sqrt{\frac{E_j I_j (n-1)}{\rho_s h b + \rho_j A (n-1)}} \quad Hz \quad \text{------- (1)}$$

where   a = span of joists

E_j = MoE of joists

I_j = second moment of area of joists

n = number of joists

ρ_s = density of sheathing

h = thickness of sheathing

b = width of the floor

A = cross section area of joists

ρ_j = density of joists.

The mean values may be used for joist properties provided there are more than three josits in the system. Although equation 1 applies to floors with all four sides simply supported, it gives very good estimates of f_n for floors with two parallel sides simply supported. This is because the mode shapes of these two types of floor are very similar for the fundamental mode.

In the case where sheathing is rigidly attached to joists using relatively dense nailing or rigid glue the stiffness term $E_j\ I_j$ in equation 1 may be increased due to the composite action between the two components. Guidance on the calculation of the increase in stiffness is given by the authors (8).

The derivation of the expression for estimating the frequency-weighted r.m.s. acceleration Ar is rather more complicated than for f_n . Certain assumptions had to be made in order to simplify the final expression. These assumptions are:-

1.   the response is dominated by the fundamental mode and there is negligible contribution from the higher modes,

2.   the impact causing the vibration is applied at the centre of the floor,

3.   the mass of the person applying the impact is 70kg,

4.   the total duration of the response caused by one impact is taken to be one second.

Based on the above assumption the following expression has been derived (9).

$$A_r = \frac{2000\,K}{m\,\pi\,f_o^2} \qquad m/s^2 \qquad \text{------- (2)}$$

$$\text{where} \quad f_o = \frac{\pi}{2a^2}\sqrt{\frac{E_j\,I_j\,(n-1)}{\rho_s hb + \rho_j A(n-1) + \frac{280}{a}}} \quad Hz \quad \text{------- (3)}$$

$$m = \frac{a}{2}\left(\rho_s hb + \rho_j A(n-1) + \frac{280}{a}\right)\quad kg \text{------- (4)}$$

$$K = \sqrt{\frac{\omega_n\left[(1-e^{-2\delta\omega_n t_1} + (1-e^{-2\delta\omega_n(1-t_1)})(1-2e^{-\delta\omega_n t_1}\cos\omega_n t_1 + e^{-2\delta\omega_n t_1})\right]}{4\delta}}$$

$$\text{--- (5)}$$

in which ω_n = $2\pi f_o$ = angular natural frequency

δ = viscous damping ratio

t_1 = duration of the impulse producing the vibration.

Experimental results (10, 11) indicate that t_1 is normally between 0.05 s and 0.07 s whilst for normal domestic dwellings δ can be taken as 0.03. Assuming δ to be constant, K is therefore a function of f_o and t_1 . A table of K against f_o has been worked out, which is presented in Table 1 for 8 Hz $\leqslant f_o \leqslant$ 40 Hz. This shows the worst value of K at any f_o for $0.05s \leqslant t_1 \leqslant 0.07s$. The design procedure is summarised in a flow chart form shown in Figure 1. It is recommended here that design of wooden floors should follow the procedure shown in Figure 1. The initial stage is identical to present static design, which is obviously to ensure that the structure is structurally safe. The remaining stages involve the checking of both f_n and Ar.

Design Examples

In this section, design examples incorporating the method proposed in previous sections are given for two floors of different sizes. Two floors of plan dimensions 2.4m x 2.4m and 4.0m x 4.0m are chosen. Designing both floors to the British Standard BS 5268: 'Structural Use of Timber: Part 2, Code of Practice for permissible stress design, materials and workmanship' results in the designs shown in the first rows of Tables 2 and 3

respectively. A worked example is given in the Appendix to demonstrate the calculations of both f_n and Ar for the smaller floor. Repeating the calculations yields the f_n and Ar values shown in Table 3 for the larger floor.

Comparison of the calculated values with the criteria given before, shows that both floors would not satisfy the vibrational serviceability requirements proposed here. Both designs are then improved until they satisfy the requirements. All the designs tried are presented in Tables 2 and 3.

From Tables 2 and 3 it can be observed that troublesome vibrational behaviour does not necessarily occur in long span floors. Small sized floors are equally likely to have vibrational problems if they are designed to static criteria only. In fact the Tables show that the small floor is more prone to annoying vibration. This is reflected in the relatively high Ar value in Table 2.

Further unreported studies by the authors indicate that for both British and Canadian situations adoption of the proposals in this paper would only result in increased joist sizes in a small proportion of practical floor arrangements.

Conclusion

It is proposed here that in future design of wooden floors should follow the procedures set out in Figure 1. In order to ensure that a floor is free from excessive vibration which causes discomfort to its occupants, its fundamental natural frequency (f_n) and frequency-weighted acceleration (Ar) of the response due to a human footfall impact shall be higher than 8 Hz and smaller than 0.45 m/s^2 respectively. These two parameters may be satisfactorily estimated using the equations presented in this paper.

References

1. BRITISH STANDARDS INSTITUTION. Structural Use of Timber: Part 2. Code of Practice for permissible stress design, materials and workmanship. British Standard BS 5268: Part 2. London, BSI. 1984.

2. CANADIAN STANDARDS ASSOCIATION. Engineering design in wood (Limit States design). CSA Standard CAN 3-086.1-M84. Rexdale, Ontario, CSA. 1984.

3. CIB Working Group 18. Structural timber design code. CIB Publication 66. 1984.

4. CRUBILE, P. EHLBECK, J. BRUNINGHOFF, H. LARSEN, H. and SUNLEY, J. - Common unified rules for timber structures. Report prepared for the European Communities. 1985.

5. CHUI, Y.H. - Vibrational performance of timber floors and the related human discomfort criteria, Journal of the Institute of Wood Science, June 1986, 10 (5) 183 - 188.

6. BRITISH STANDARDS INSTITUTION. Evaluation of human exposure to vibration in buildings (1 Hz to 80 Hz). British Standard BS 6472. London, BSI. 1984.

7. CHUI, Y.H. - Evaluation of vibrational performance of light-weight wooden floors: Method of assessment of floor vibration due to human footsteps. TRADA Research Report 3/86. Hughenden Valley, TRADA. 1986.

8. SMITH, I. and CHUI, Y.H. - Predicting the natural frequencies of light-weight wooden floors. Proceedings of the IUFRO Wood Engineering Group Meeting, Florence, Italy. 1986.

9. CHUI, Y.H. - Evaluation of vibrational performance of light-weight wooden floors: Design to avoid annoying vibrations. TRADA Research Report 17/86. Hughenden Valley, TRADA. 1986.

10. CHUI, Y.H. - Evaluation of vibrational performance of light-weight wooden floors: Determination of effects of changes in construction variables on vibrational characteristics. TRADA Research Report 2/86. Hughenden Valley, TRADA. 1986.

11. OHLSSON, S. - Floor vibrations and human discomfort. Ph.D. thesis, Department of Structural Engineering, Chalmers University of Technology, Gothenburg, Sweden. 1982.

Appendix: Worked Example

The following shows how f_n and Ar values in Table 2 were calculated.

The floor was initially designed by usual practice to BS 5268: Part 2. The calculation yielded the design shown in row 1 of Table 2. The vibrational serviceability was then checked, assuming the flooring was 22mm thick particleboard with a density of 640 kg/m^3. From BS 5268: Part 2 for SC3 'strength class' timber:

$$E_j = 8.8 \times 10^9 \ \text{N/m}^2$$

$$\rho_j = 540 \ \text{kg/m}^3$$

The following data were also obtained:

$$a = 2.4\text{m}$$
$$b = 2.4\text{m}$$
$$h = 0.022\text{m}$$
$$A = 0.00681\text{m}^2$$
$$\rho_s = 640 \ \text{kg/m}^3$$
$$I_j = 1.194 \times 10^{-5} \ \text{m}^4$$
$$n = \frac{2.4}{0.6} + 1 = 5$$

Substitution of the above data into equation 1 gives:

$$f_n = \frac{\pi}{2 \times 2.4^2} \sqrt{\frac{8.8 \times 10^9 \times 1.194 \times 10^{-5} (5-1)}{640 \times 0.022 \times 2.4 + 540 \times 0.00681 \times (5-1)}}$$

$$= 25.3 \ \text{Hz}$$

> 8 Hz, hence frequency acceptable.

The A_r value was then checked using equations 2, 3 and 4 and Table 1.

$$f_O = 13.7 \text{ Hz}$$

$$m = 197.0 \text{ kg}$$

From Table 1 $K = 43.0$, therefore:

$$Ar = \frac{2000 \times 43.0}{197.0 \; \pi \times 13.7^2} = 0.73 \text{ m/s}^2$$

$$> 0.45 \text{ m/s}^2 \text{ , hence response magnitude unacceptable.}$$

The design was then improved to that shown in row 2 of Table 2. The values of f_O and Ar were calculated as before such that:

$$f_n = 26.5 \text{ Hz}$$

$$Ar = 0.65 \text{ m/s}^2$$

Hence response magnitude was still higher than the acceptable value.

The design was then improved further as shown in row 3 of Table 2. This was found to be satisfactory with the following values of f_n and Ar.

$$f_n = 28.9 \text{ Hz}$$

$$Ar = 0.4 \text{ m/s}^2$$

Acknowledgement

TABLE 1 : K Values

f_0 (Hz)	K
8	38.8
9	41.4
10	44.0
11	45.5
12	45.6
13	44.5
14	42.2
15	38.7
16	34.4
17	35.9
18	45.1
19	52.9
20	58.7
21	62.0
22	62.7
23	61.9
24	65.8
25	67.7
26	67.4
27	65.1
28	69.5
29	72.6
30	74.1
31	74.0
32	72.4
33	69.3
34	72.8
35	76.8
36	77.9
37	76.1
38	71.8
39	74.8
40	80.2

TABLE 2 : Designs of the Floor Sized 2.4m x 2.4m

Joist *				f_n (Hz)	A_r (m/s^2)
Strength Class	Size (mm)	Spacing (mm)	Permissible Span (mm)		
SC3	47 x 145	600	2580	25.3	0.73
SC4	47 x 145	600	2749	26.5	0.65
SC3	47 x 145	400	3025	28.9	0.40

* Design to BS 5268: Part 2

TABLE 3 : Designs of the Floor Sized 4.0m x 4.0m

Joist *				f_n (Hz)	A_r (m/s^2)
Strength Class	Size (mm)	Spacing (mm)	Permissible Span (mm)		
SC3	47 x 194	400	4026	15.1	0.60
SC3	47 x 219	500	4128	16.6	0.52
SC4	47 x 194	400	4188	15.7	0.52
SC4	47 x 219	500	4384	17.3	0.43

* Design to BS 5268: Part 2

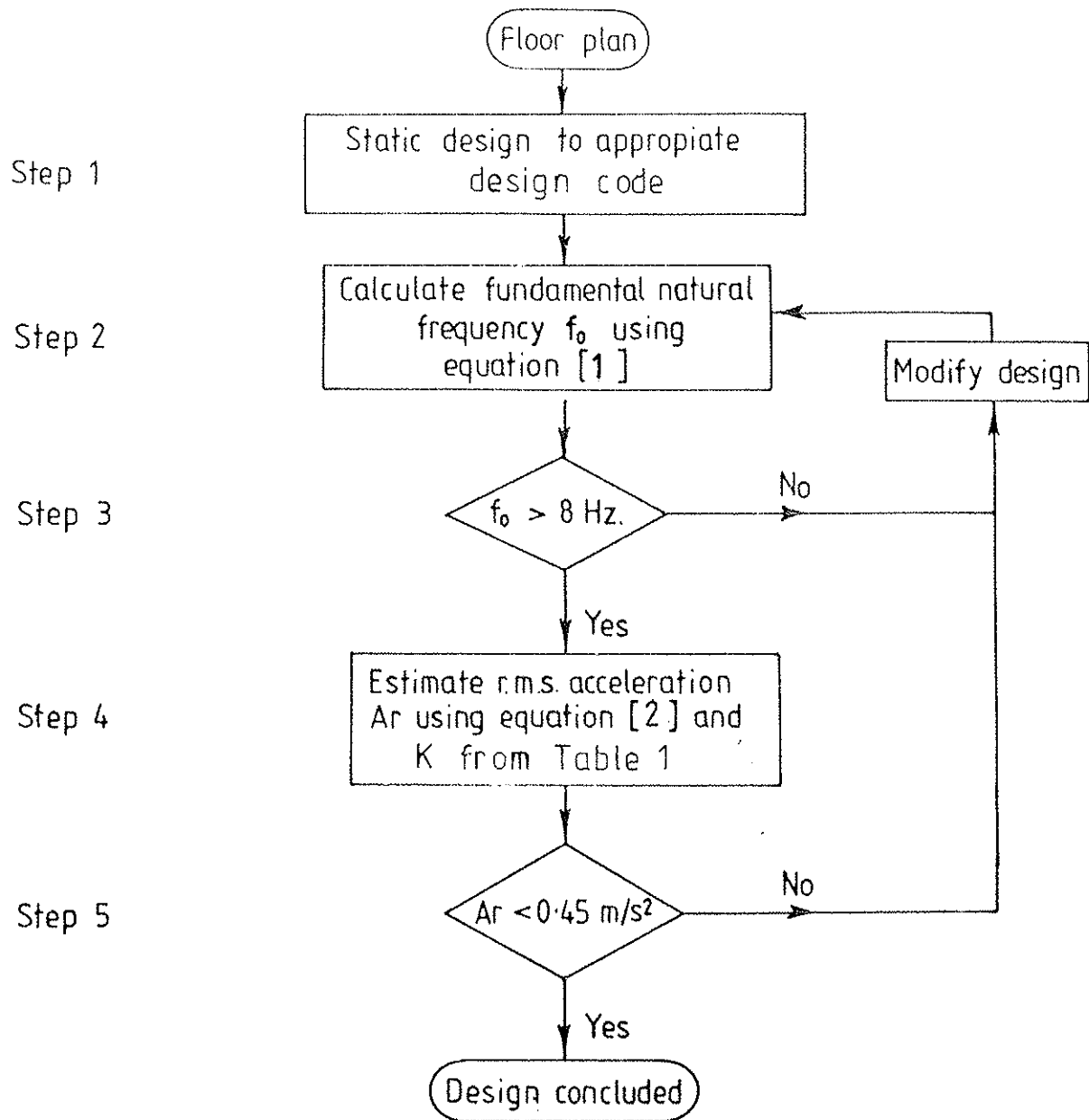FIG.1 . Flow chart for proposed design method

INTERNATIONAL COUNCIL FOR BUILDING RESEARCH STUDIES AND DOCUMENTATION

WORKING COMMISSION W18A - TIMBER STRUCTURES

DRAFT CLAUSE FOR CIB CODE
FOR BEAMS WITH INITIAL IMPERFECTIONS

by

H J Burgess
Timber Research and Development Association
United Kingdom

MEETING TWENTY
DUBLIN
IRELAND
SEPTEMBER 1987

Draft clause for CIB Code
for beams with initial imperfections

DRAFT CLAUSE

5.1.3 Bending

The effective span of flexural members shall be taken as the distance between the centres of areas of bearing. With members extending further than is necessary over bearings the span may be measured between the centres of bearings of a length which would be adequate according to this code; attention should be paid to the eccentricity on the supporting structure.

A beam which is held in position at its ends but is free to deflect about both the major axis and the minor axis should be so proportioned that

$$\frac{\sigma_m}{k_m f_m} \leq 1 \tag{5.1.3a}$$

where σ_m are the bending stresses calculated without regard to initial curvature and deflections, and k_M and k_m are factors depending on the material parameters and the initial twist and curvature. k_m may be put equal to 1 for a beam where lateral displacement of the compression side is prevented throughout its length.

The initial curvature is assumed to be the same as that applied for columns in section 5.1.7, accompanied by a related initial twist such that the value η' in the following expressions is

$$\eta' = \eta \frac{2i}{b} \gamma \frac{h}{b} \pi \sqrt{\frac{EI}{GJ\gamma}} \tag{5.1.3b}$$

where i = radius of gyration about the minor axis

$$\gamma = 1 - \frac{I_y}{I_x} \tag{5.1.3c}$$

For rectangular cross-sections, taking $G = E/16$ and

$$J = \frac{hb^3}{3} \left(1 - 0.63 \frac{b}{h}\right) \tag{5.1.3d}$$

$$\gamma = 1 - \left(\frac{b}{h}\right)^2 \tag{5.1.3e}$$

then $\quad \eta' = \frac{2\pi}{\sqrt{3}} \eta \frac{h}{b} \sqrt{\frac{1 - \left(\frac{b}{h}\right)^2}{1 - 0.63 \frac{b}{h}}} \tag{5.1.3f}$

in which η takes the value applied for columns in (5.1.7b).

k_M and k_m are given by

$$k_M = \frac{\sigma_{m,crit}}{f_m} = \frac{\pi}{z \ell f_m} \sqrt{\frac{EIGJ}{\gamma}} \qquad (5.1.3g)$$

$$k_m = 0.5 \left[(1+n')(1+k_M) - \sqrt{((1+n')(1+k_M))^2 - 4(1+n)k_M} \right] \quad (5.1.3h)$$

The expression for k_M is appropriate for equal end moments. Where other loading conditions apply, π may be replaced by the corresponding figure in Table 3.07 of paper no. CIB-W18 5-10-1.
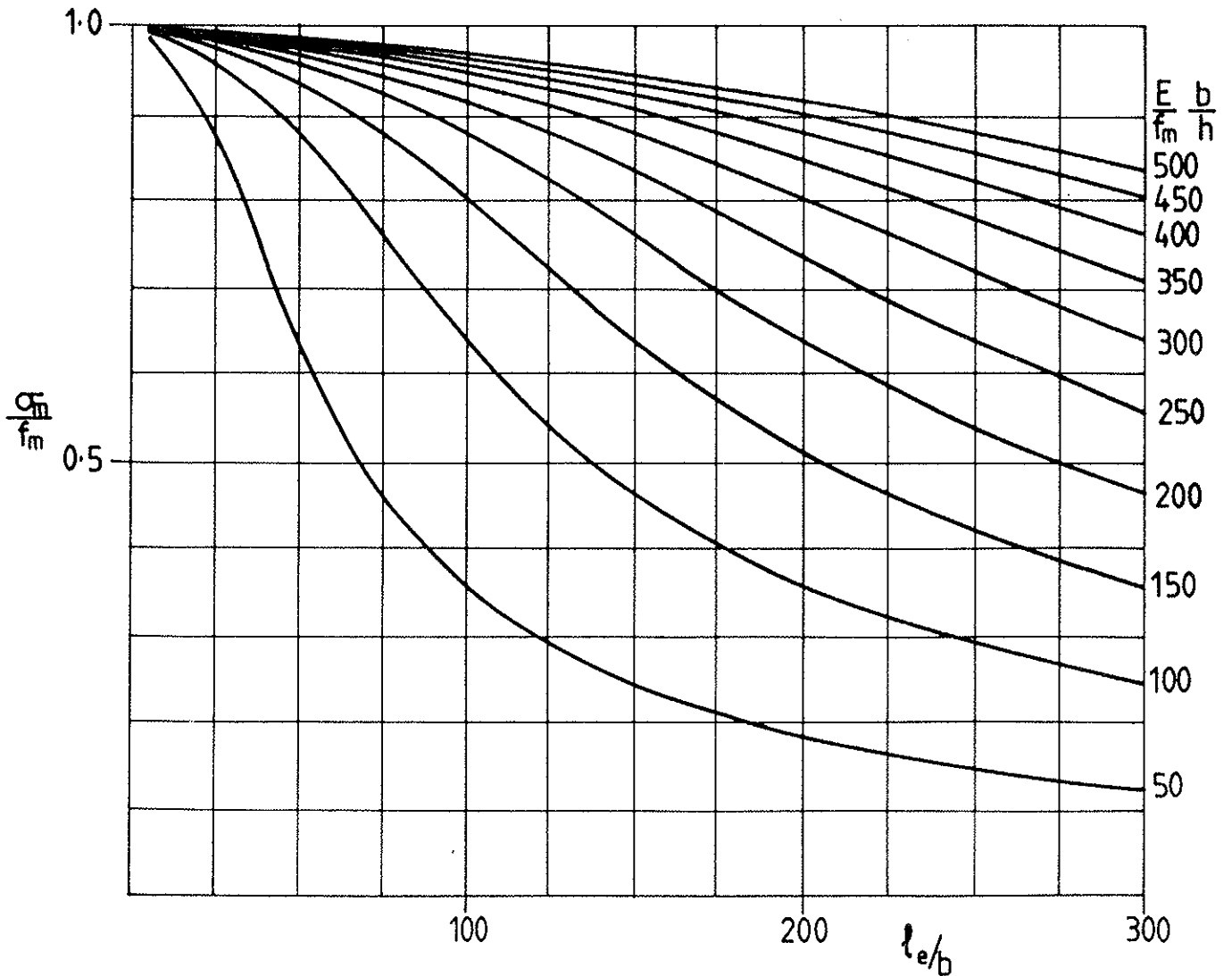

Figure 5.1.3

For rectangular cross-sections with equal end moments, taking $G = E/16$,

$$k_M = \frac{\pi}{4} \frac{b}{\ell_e} \frac{b}{h} \frac{E}{f_m} \sqrt{\frac{1 - 0.63 \frac{b}{h}}{1 - \left(\frac{b}{h}\right)^2}} \tag{5.1.3j}$$

where ℓ_e is the effective length of the beam, and the maximum permissible value of $\frac{\sigma_m}{f_m}$ in (5.1.3a) may be obtained from fig. 5.1.3.

For a number of structures and load combinations ℓ_e is given in table 5.1.3 in relation to the free beam length ℓ.

The free length is determined as follows:

a) When lateral support to prevent rotation is provided at points of bearing and no other support to prevent rotation or lateral displacement is provided throughout the length of a beam, the unsupported length shall be the distance between points of bearing, or the length of a cantilever.

b) When beams are provided with lateral support to prevent both rotation and lateral displacement at intermediate points as well as at the ends, the unsupported length may be the distance between such points of intermediate lateral support. If lateral displacement is not prevented at points of intermediate support, the unsupported length shall be the distance between points of bearing.

Table 5.1.3 Relative effective beam length ℓ_e/ℓ

Type of beam and load	ℓ_e/ℓ
Simply supported, uniform load or equal end moment	1.00
Simply supported, concentrated load at centre	0.85
Cantilever, uniform load	0.60
Cantilever, concentrated end load	0.85
Cantilever, end moment	1.00

The values apply to loads acting in the gravity axis. For downwards acting loads ℓ_e is increased by 2 h for loads applied to the top and reduced by 0.5 h for loads applied to the bottom.

Deflection

If desired, add section from 'BEAMS - DEFLECTION' on page 8 below.

BACKGROUND - DESIGN FORMULAE FOR
MEMBERS SUBJECT TO LATERAL BUCKLING

The graphs shown in the previous paper (Burgess 1986) for a beam without end load were drawn by fixing the value $\phi_v = 0.0001 \, \ell/b$, and this determined the related value of u_o . When extending the study to beam-columns for a more recent paper (Burgess 1987) it became evident that u_o must be fixed as a constant times the ℓ/b ratio if the graphs are to reduce to appropriate values for columns without lateral load when $\sigma_m = 0$.

This is a consequence of the value of u_o usually applied for columns, coupled with the relationship between u_o and ϕ_o . With $u_o = $ constant $x \, \ell/b$, the related value of ϕ_o is found to be independent of ℓ/b and the permissible value of $\frac{\sigma_m}{f_m}$ does not reduce to 1.0 when ℓ/b approaches zero.

In proposing design formulae for beams for the CIB Code, two different approaches are tried. In the first it is supposed that what is needed is a minimum degree of alteration to the Code as it stands, and that there is no need to consider any possible effect of linking the beam design rules with those for beam-columns at some later stage.

After presenting a proposal on these lines the second approach below will show the formulae and graphs arising from an integrated treatment of beams, beam-columns and columns.

FIRST APPROACH

1. Not related to beam-column theory
2. Initial twist $\phi_v = 0.0001 \, l/b$ with related u_o (paper 19-10-1)

Replace page 15 of the CIB Code by the following.

CIB-STRUCTURAL TIMBER DESIGN CODE

k_{inst} is a factor (<1) taking into account the reduced strength due to failure by lateral instability (lateral buckling). k_{inst} is determined so that the total bending stresses, taking into account the effect of initial curvature, eccentricities and the deformations developed, do not exceed f_m . Its value may be found from the formula

$$k_{inst} = 0.5\left[\left(1+(1+\eta')\right)\frac{\sigma_{m,crit}}{f_m} - \sqrt{\left(1+(1+\eta')\frac{\sigma_{m,crit}}{f_m}\right)^2 - 4\frac{\sigma_{m,crit}}{f_m}}\right] \quad (5.1.3b)$$

$$\text{where} \quad \eta' = \frac{b}{h}\left(\frac{I_x}{I_y} - 1\right)\phi_o \quad (5.1.3c)$$

$$\text{and} \quad \frac{\sigma_{m,crit}}{f_m} = \frac{\pi}{Z_x l_e f_m}\sqrt{\frac{E I_y G J}{1 - I_y/I_x}} \quad (5.1.3d)$$

In (5.1.3d) $\sigma_{m,crit}$ is the critical bending stress calculated according to the classical theory of stability. η' allows for an initial twist ϕ_o at mid span, accompanied by an initial lateral deviation from straightness.

k_{inst} may be put equal to 1 for beams where lateral displacement of the compression side is prevented throughout its length and where torsion is prevented at the supports.
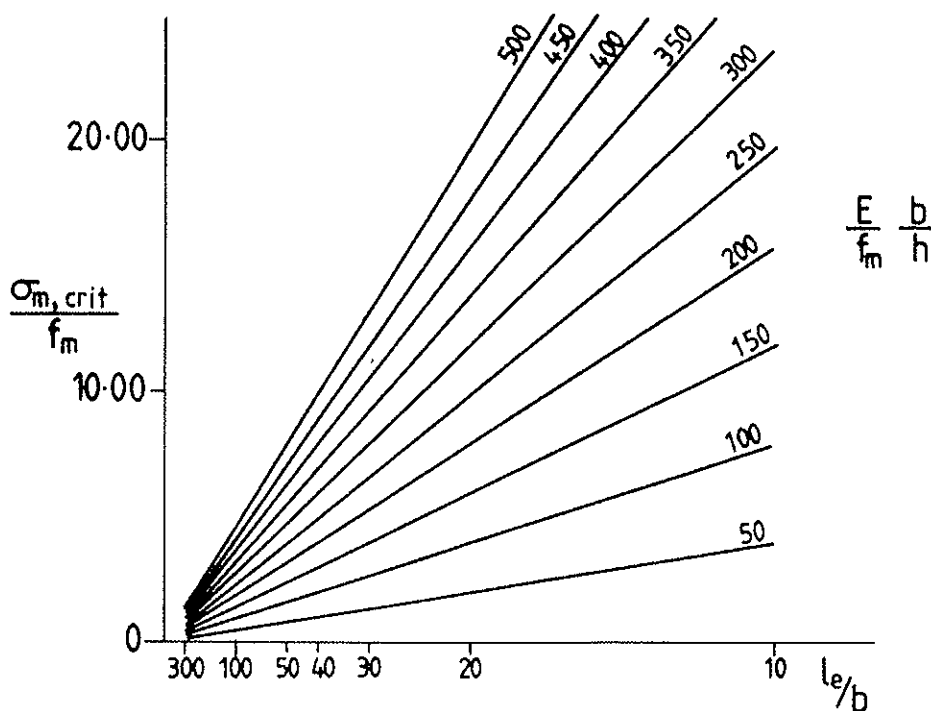

Figure 5.1.3.

For a beam with rectangular cross-section

$$\eta' = \frac{h}{b}\left(1 - \frac{b^2}{h^2}\right)\phi_o$$

Taking $\phi_o = 0.0001\,\ell/b$, $\dfrac{\sigma_{m,crit}}{f_m}$ may be determined from fig. 5.1.3 which is based on the following formula with $\dfrac{E_{0,mean}}{G_{mean}} = 16$.

$$\frac{\sigma_{m,crit}}{f_m} = \frac{\pi b^2}{\ell_e h}\frac{E_{o,d}}{f_{m,d}}\sqrt{\frac{G_{mean}}{E_{o,mean}}}$$

where ℓ_e is the effective length of the beam. For a number of structures and load combinations ℓ_e is given in table 5.1.3 in relation to the free beam length ℓ.

The free length is determined as follows:

a) When lateral support to prevent rotation is provided at points of bearing and no other support to prevent rotation or lateral displacement is provided throughout the length of a beam, the unsupported length shall be the distance between points of bearing, or the length of a cantilever.

b) When beams are provided with lateral support to prevent both rotation and lateral displacement at intermediate points as well as at the ends, the unsupported length may be the distance between such points of intermediate lateral support. If lateral displacement is not prevented at points of intermediate support, the unsupported length shall be the distance between points of bearing.

For the rectangular cross-section, the lateral deflection of the centre of the beam at its centre-line may be calculated as

$$\frac{4.26}{10^6}\frac{\ell^2}{i_y}\frac{\dfrac{\sigma_m}{\sigma_{m,crit}}}{1 - \dfrac{\sigma_m}{\sigma_{m,crit}}}$$

SECOND APPROACH

     - integrated treatment of beams, beam-columns and columns.

In the following formulae, η has the meaning applied in the CIB code; it is a constant which multiplies the value of λ and does not mean the product as in the British code.

<div align="center">

Tentative design formulae
for members subject to lateral buckling
</div>

The formulae given apply only to a member with a cross-section which is symmetrical about both the major and the minor axis. The symbol I without a subscript refers to bending about the minor axis, and Z refers to bending about the major axis.

The value of η' to be used in the following expressions should be calculated from

$$\eta' = \eta \, \frac{2i}{b} \, \gamma \, \frac{\ell}{b} \, \pi \sqrt{\frac{EI}{GJ\gamma}}$$

where i = radius of gyration about the minor axis

$$\gamma = 1 - \frac{I_y}{I_x}$$

For rectangular cross-sections, taking $G = E/16$ and

$$J = \frac{hb^3}{3}\left(1 - 0.63\,\frac{b}{h}\right)$$

$$\gamma = 1 - \left(\frac{b}{h}\right)^2$$

then $\eta' = \dfrac{2\pi}{\sqrt{3}} \, \eta \, \dfrac{\ell}{b} \sqrt{\dfrac{1 - \left(\frac{b}{h}\right)^2}{1 - 0.63\,\frac{b}{h}}}$

BEAMS - STRENGTH

For a beam which is held in position at its ends but is free to deflect about both the major axis and the minor axis, the maximum permissible value of the applied bending stress may be found from

$$k_m = \frac{\sigma_{m,max}}{f_m} = 0.5\left[\left(1+(1+\eta')\right)\frac{\sigma_{m,crit}}{f_m} - \sqrt{\left(1+(1+\eta')\frac{\sigma_{m,crit}}{f_m}\right)^2 - 4\frac{\sigma_{m,crit}}{f_m}}\right]$$

OR

$$k_M = \frac{\sigma_{m,crit}}{f_m} = \frac{\pi}{z\ell f_m}\sqrt{\frac{EIGJ}{\gamma}}$$

$$k_m = \frac{\sigma_{m,max}}{f_m} = 0.5\left[\left(1+(1+\eta')k_M\right) - \sqrt{\left(1+(1+\eta')k_M\right)^2 - 4k_M}\right]$$

The above expressions are derived for equal end moments. Where other loading conditions apply, π' in the expression for k_M may be replaced by the appropriate figure from paper no. CIB-W18 5-10-1.

For rectangular sections, with G = E/16

$$k_M = \frac{\sigma_{m,crit}}{f_m} = \frac{\pi}{4}\frac{b}{\ell}\frac{b}{h}\frac{E}{f_m}\sqrt{\frac{1-0.63\frac{b}{h}}{1-\left(\frac{b}{h}\right)^2}}$$

The value of E should incorporate any reduction factor applied in column design.

BEAMS - DEFLECTION

The lateral deflection of the centre of the beam at its centre-line may be calculated as

$$\eta\frac{2i}{b}\ell \cdot \frac{\frac{\sigma_m}{\sigma_{m,crit}}}{1-\frac{\sigma_m}{\sigma_{m,crit}}}$$

where i = radius of gyration about the minor axis.

For a beam of rectangular cross-section the corresponding expression is

$$\frac{\eta\ell}{\sqrt{3}} \cdot \frac{\frac{\sigma_m}{\sigma_{m,crit}}}{1-\frac{\sigma_m}{\sigma_{m,crit}}}$$

For either expression, $\sigma_{m,crit}$ should be calculated without a reduction factor (load factor) for E, and using the 'mean' or 'minimum' value of E as appropriate.

BEAM-COLUMNS - STRENGTH

The following expressions apply to members subject to axial compression and to bending about the major axis, which are free to bend also about the minor axis.

Such a member which is held in position at its ends but is otherwise free to buckle and twist should be so proportioned that:

$$\frac{\sigma_m}{k_m f_m} + \frac{\sigma_c}{k_c f_c} \leq 1$$

This gives a conservative approximation. For rectangular sections with $\frac{h}{b} \geq 4$ or for other bisymmetrical sections with $\frac{I_x}{I_y} \geq 16$, a more accurate solution may be obtained using the following expression if $\ell/b \geq 50$:

$$\frac{\sigma_m}{f_m} + \frac{\sigma_c}{f_c} + \frac{\frac{\sigma_m}{f_m}\eta' + \frac{\sigma_c}{f_c}\frac{f_c}{f_m}\eta\lambda}{1 - \frac{\sigma_c}{\sigma_E} - \frac{\sigma_m}{\sigma_{m,crit}}} \leq 1$$

If $\frac{h}{b} < 4$ or $\frac{\ell}{b} < 50$, the following expression should not exceed unity; the first term is for bending about the major axis and the last term for bending about the minor axis.

$$\frac{\frac{\sigma_m}{f_m} + \frac{\sigma_c}{f_c}\frac{f_c}{f_m}\frac{b}{h}\eta\lambda}{1 - \frac{\sigma_c}{\sigma_{E,x}}} + \frac{\sigma_c}{f_c} + \frac{\frac{\sigma_m}{f_m}\eta'\left(1 - \frac{\sigma_c}{\sigma_E} + \frac{\sigma_m}{\sigma_{m,crit}}\right) + \frac{\sigma_c}{f_c}\frac{f_c}{f_m}\eta\lambda\left(1 - \frac{\sigma_c}{\sigma_\phi} + \frac{\sigma_m}{\sigma_{m,crit}}\right)}{\left(1 - \frac{\sigma_c}{\sigma_E}\right)\left(1 - \frac{\sigma_c}{\sigma_\phi}\right) - \left(\frac{\sigma_m}{\sigma_{m,crit}}\right)^2}$$

where σ_ϕ is the critical longitudinal stress for twist buckling about a point at a distance $\frac{\ell}{\pi}\sqrt{\frac{GJ\gamma}{EI}}$ from the centroid.

$\frac{\sigma_c}{\sigma_\phi}$ may be found from

$$\frac{\sigma_c}{\sigma_\phi} = \frac{\sigma_c}{E}\left[4 \cdot \frac{\left(\frac{\ell}{h}\right)^2 + 1}{1 - 0.63\frac{b}{h}} + \frac{12}{\pi^2}\left(\frac{\ell}{b}\right)^2\left\{1 - \left(\frac{b}{h}\right)^2\right\}\right]$$

BEAM-COLUMNS - DEFLECTION

$\ell/b \geqslant 50$ and $I_x/I_y \geqslant 16$

The lateral deflection of the centre of the beam-column at its centre-line may be calculated as

$$u_1 = \eta \frac{2i}{b} \ell \; \frac{\frac{\sigma_c}{\sigma_E} + \frac{\sigma_m}{\sigma_{m,crit}}}{1 - \frac{\sigma_c}{\sigma_E} - \frac{\sigma_m}{\sigma_{m,crit}}}$$

where i = radius of gyration about the minor axis.

For a beam of rectangular cross-section the corresponding expression is

$$u_1 = \frac{\eta \ell}{\sqrt{3}} \; \frac{\frac{\sigma_c}{\sigma_E} + \frac{\sigma_m}{\sigma_{m,crit}}}{1 - \frac{\sigma_c}{\sigma_E} - \frac{\sigma_m}{\sigma_{m,crit}}}$$

$\ell/b < 50$ or $I_x/I_y < 16$

$$u_1 = \eta \frac{2i}{b} \ell \; \frac{\frac{\sigma_m}{\sigma_{m,crit}}\left(1 + \frac{\sigma_m}{\sigma_{m,crit}}\right) + \frac{\sigma_c}{\sigma_E}\left(1 - \frac{\sigma_c}{\sigma_\phi}\right)}{\left(1 - \frac{\sigma_c}{\sigma_E}\right)\left(1 - \frac{\sigma_c}{\sigma_\phi}\right) - \left(\frac{\sigma_m}{\sigma_{m,crit}}\right)^2}$$

or for a rectangular cross-section:

$$u_1 = \frac{\eta \ell}{\sqrt{3}} \; \frac{\frac{\sigma_m}{\sigma_{m,crit}}\left(1 + \frac{\sigma_m}{\sigma_{m,crit}}\right) + \frac{\sigma_c}{\sigma_E}\left(1 - \frac{\sigma_c}{\sigma_\phi}\right)}{\left(1 - \frac{\sigma_c}{\sigma_E}\right)\left(1 - \frac{\sigma_c}{\sigma_\phi}\right) - \left(\frac{\sigma_m}{\sigma_{m,crit}}\right)^2}$$

BEAMS - GRAPHS FOR RECTANGULAR CROSS-SECTIONS

To introduce the theory allowing for initial imperfections into the CIB code requires replacing Fig. 5.1.3 of the code by graphs making it easier to use the formulae for beams (strength) given above.

At first sight it appears that one or other of the following sets of curves will be needed:

(1) For each $\frac{h}{b}$ ratio, a set of curves for different $\frac{E}{f_m}$ values showing $\frac{\sigma_m}{f_m}$ plotted against $\frac{\ell}{b}$ as shown in Figure 1 for $\frac{h}{b} = 8$.

For $\frac{h}{b} = 4,5,6,7$ and 8, five such graphs would be needed.

or (2) For each $\frac{E}{f_m}$ value, a set of curves for different $\frac{h}{b}$ ratios, such as those shown in Figures 2 to 6 for $\frac{E}{f_m} = 2000, 1600, 1200, 800$ and 400. This requires five graphs even with such a coarse interval in the $\frac{E}{f_m}$ values.

However, if Figure 3 is successively overlaid on Figures 4 and 5 it is found that the curve in Fig.3 for $\frac{E}{f_m}$ = 1600 with $\frac{h}{b}$ = 8 also closely fits that for $\frac{E}{f_m}$ = 1200 with $\frac{h}{b}$ = 6 (Fig.4) and that for $\frac{E}{f_m}$ = 800 with $\frac{h}{b}$ = 4 (Fig.5)

In each case the value $\frac{E}{f_m}\frac{b}{h}$ = 200, and further trials similarly give the prospect of finding a set of curves which will cater for the whole range of this factor.

The trial curves shown in the diagrams are artificially forced to meet the vertical axis at $\frac{\sigma_m}{f_m}$ = 1.0 as explained in an accompanying paper, by making use of the formula

$$ 1 = \frac{\sigma_m}{f_m}\left(1 + \frac{\eta'}{1 - \frac{\sigma_m}{\sigma_{m,crit}}}\right) - \eta' \tag{1} $$

A similar procedure will be applicable if the last term $-\eta'$ is omitted so that the axis is met below the value 1.0.

The denominator of the second term in the bracket is

$$ 1 - \frac{\sigma_m}{\sigma_{m,crit}} = 1 - \frac{4}{\pi}\frac{\sigma_m}{f_m}\frac{f_m}{E}\frac{l}{b}\frac{h}{b}\sqrt{\frac{1 - \left(\frac{b}{h}\right)^2}{1 - 0.63\frac{b}{h}}} \tag{2} $$

and by trial plotting it is found that the curves obtained are not very sensitive to changes in η' or in the square root term. Both of these are therefore set at constant values derived as the average of five figures for $\frac{h}{b}$ = 4, 5, 6, 7 and 8. The resulting curves are shown in Figure 7 for a range of 50 - 500 in $\frac{E}{f_m}\frac{b}{h}$ with intervals of 50.

Laying Figure 7 over Figures 2 to 6, it can be seen that the diagram is valid for design use over the whole range of timber sizes and properties. In making the comparison it should be borne in mind that the original values of η and the related η' are not determined with great precision, so that small discrepancies are unimportant, especially if they are on the conservative side.

The equation plotted for different values of $\frac{E}{f_m}\frac{b}{h}$ is

$$1 + \eta' = \frac{\sigma_m}{f_m}\left[1 + \frac{\eta'}{1 - \frac{\sigma_m}{f_m}\left(\frac{f_m}{E}\frac{h}{b}\right)\frac{4}{\pi}\frac{\ell}{b}\alpha}\right] \qquad (3)$$

with $\eta' = 0.11336$

and $\alpha = \sqrt{\dfrac{1 - \left(\frac{b}{h}\right)^2}{1 - 0.63\frac{b}{h}}} = 0.9586$

For a given value of $\frac{E}{f_m}\frac{b}{h}$, this may be solved to give the maximum permissible value of σ_m as

$$\frac{\sigma_{m,max}}{f_m} = \frac{1}{2}\left(\frac{\pi}{4\alpha}\frac{b}{\ell}\frac{E}{f_m}\frac{b}{h} + 1\right)(1+\eta') - \sqrt{\left\{\frac{1}{2}\left(\frac{\pi}{4\alpha}\frac{b}{\ell}\frac{E}{f_m}\frac{b}{h}+1\right)(1+\eta')\right\}^2 - \frac{\pi}{4\alpha}\frac{b}{\ell}\frac{E}{f_m}\frac{b}{h}(1+\eta')} \quad (4)$$

By solving (1) the same equation may be expressed as

$$\frac{\sigma_{m,max}}{f_m} = \frac{1}{2}(1+\eta')\left(\frac{\sigma_{m,crit}}{f_m} + 1\right) - \sqrt{\left\{\frac{1}{2}(1+\eta')\left(\frac{\sigma_{m,crit}}{f_m}+1\right)\right\}^2 - (1+\eta')\frac{\sigma_{m,crit}}{f_m}} \quad (5)$$

but of course for inserting a particular value of $\frac{E}{f_m}\frac{b}{h}$ this would have to be broken down into the form shown by (4).

REFERENCES

Burgess, H.J. (1986) - Possible code approaches to lateral
buckling in beams.
CIB-W18 paper no.19-10-1,Florence,September 1986

Burgess, H.J. (1987) - Lateral buckling theory for rectangular section
deep beam-columns.
CIB-W18 paper no.20- 2 - 1,Dublin,September 1987

CIB (1983)   - CIB Structural timber design code. Sixth
edition, January 1983

Larsen, H.J. (1975) - The design of timber beams. CIB-W18 paper
No. 5-10-1, Karlsruhe, October 1975

$$\frac{h}{b} = 8$$

Figure 1.

$$\frac{E}{f_m} = 2000$$
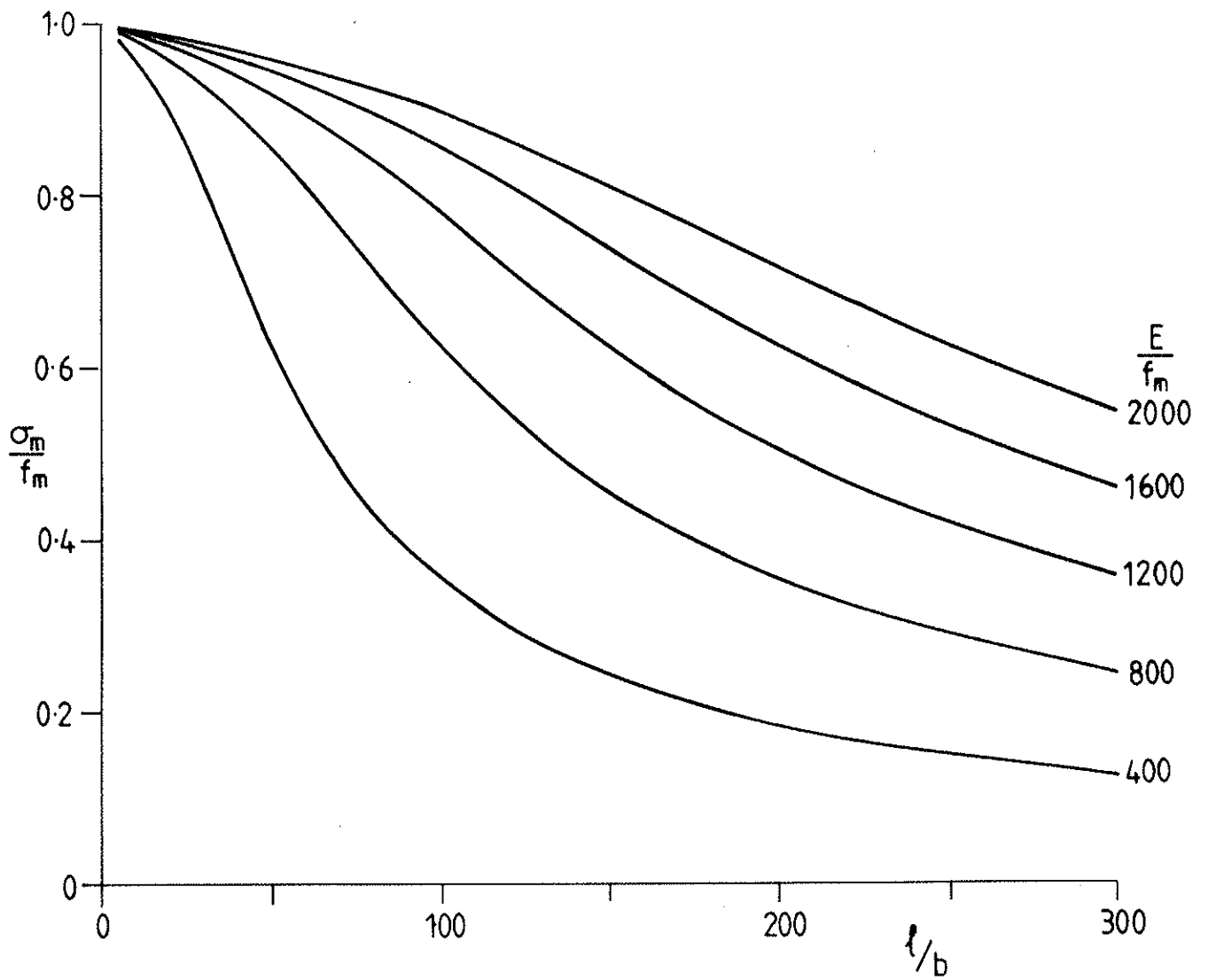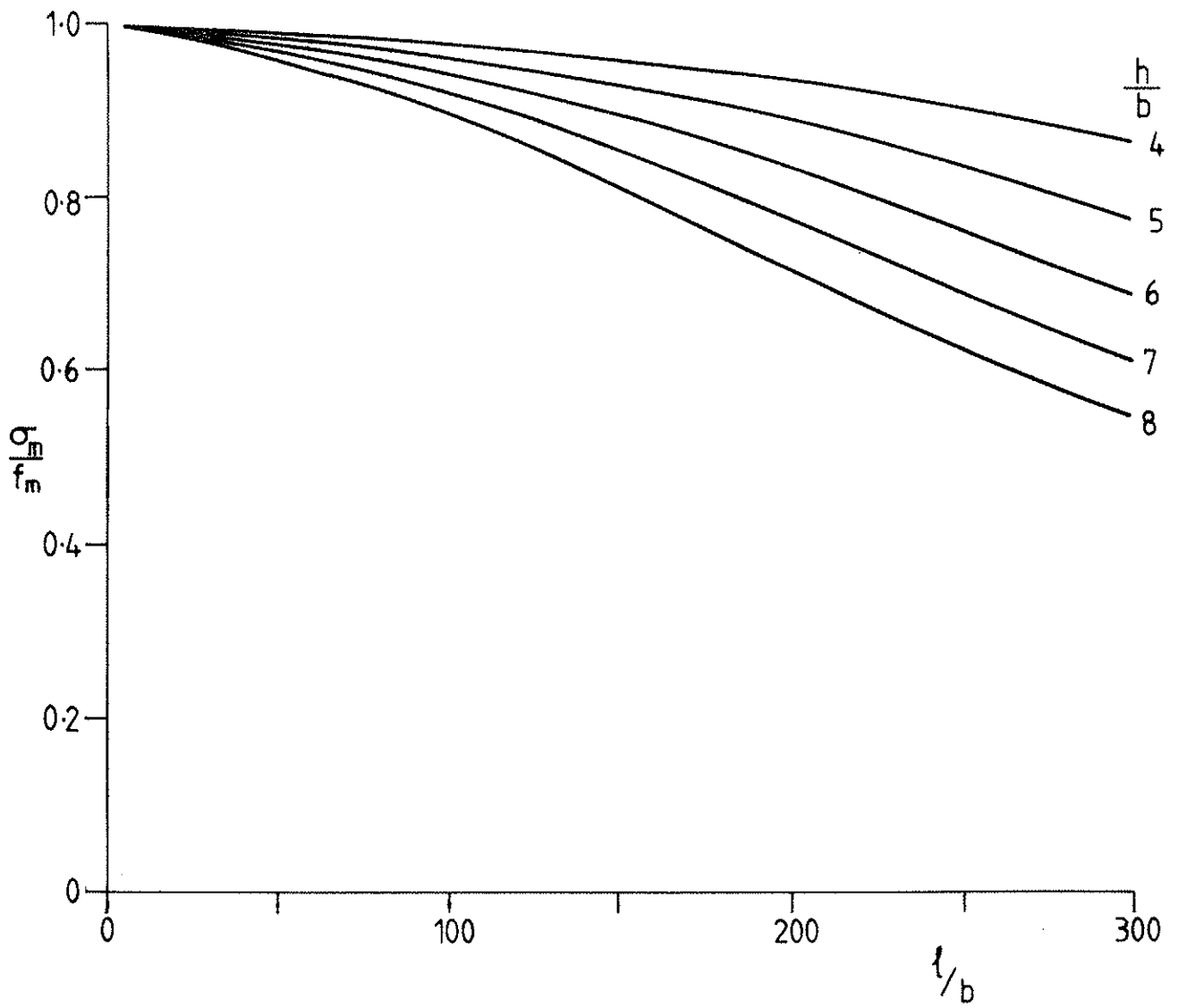

Figure 2.

$$\frac{E}{f_m} = 1600$$
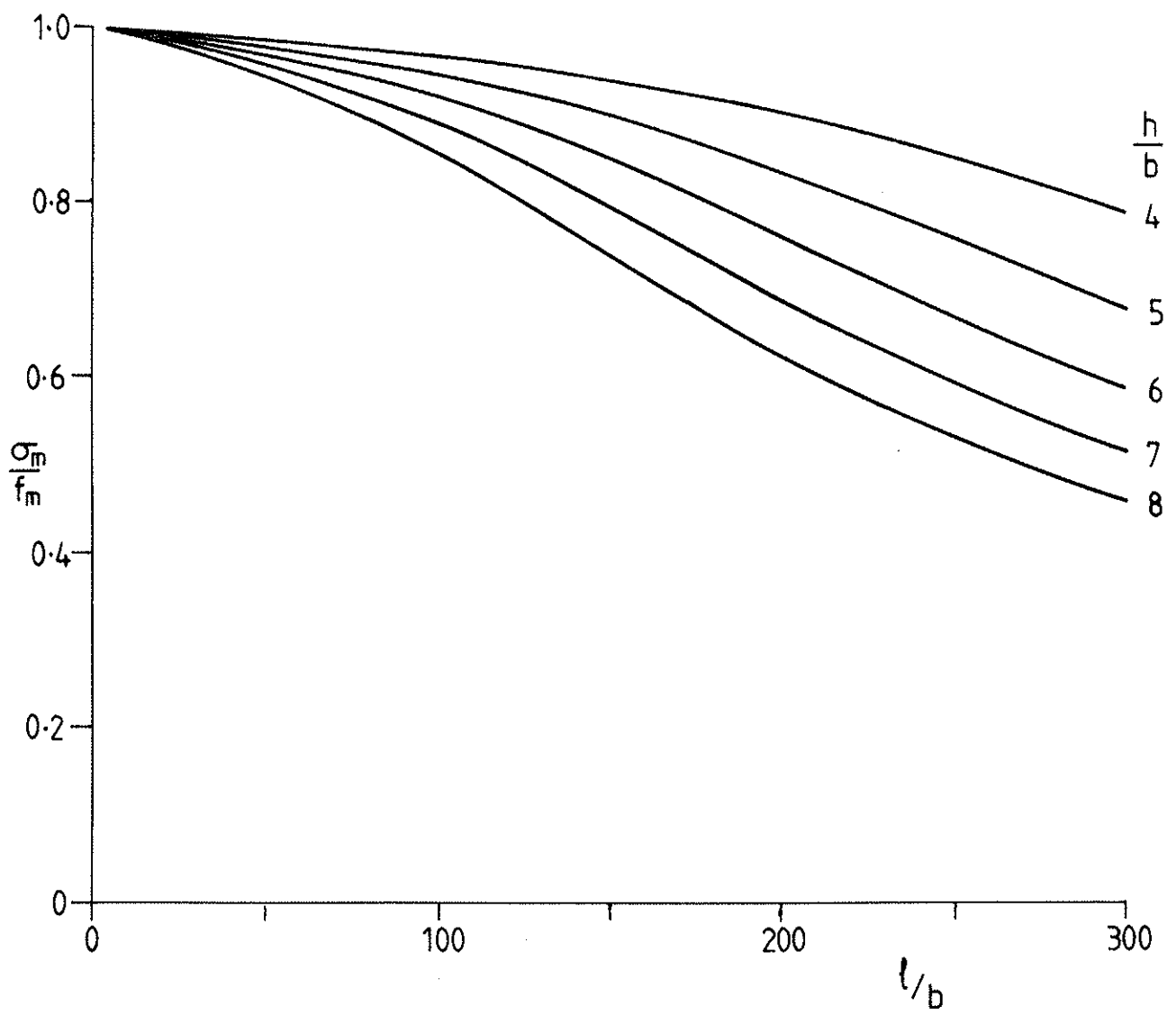
Figure 3.

$$\frac{E}{f_m} = 1200$$

Figure 4.

$$\frac{E}{f_m} = 800$$
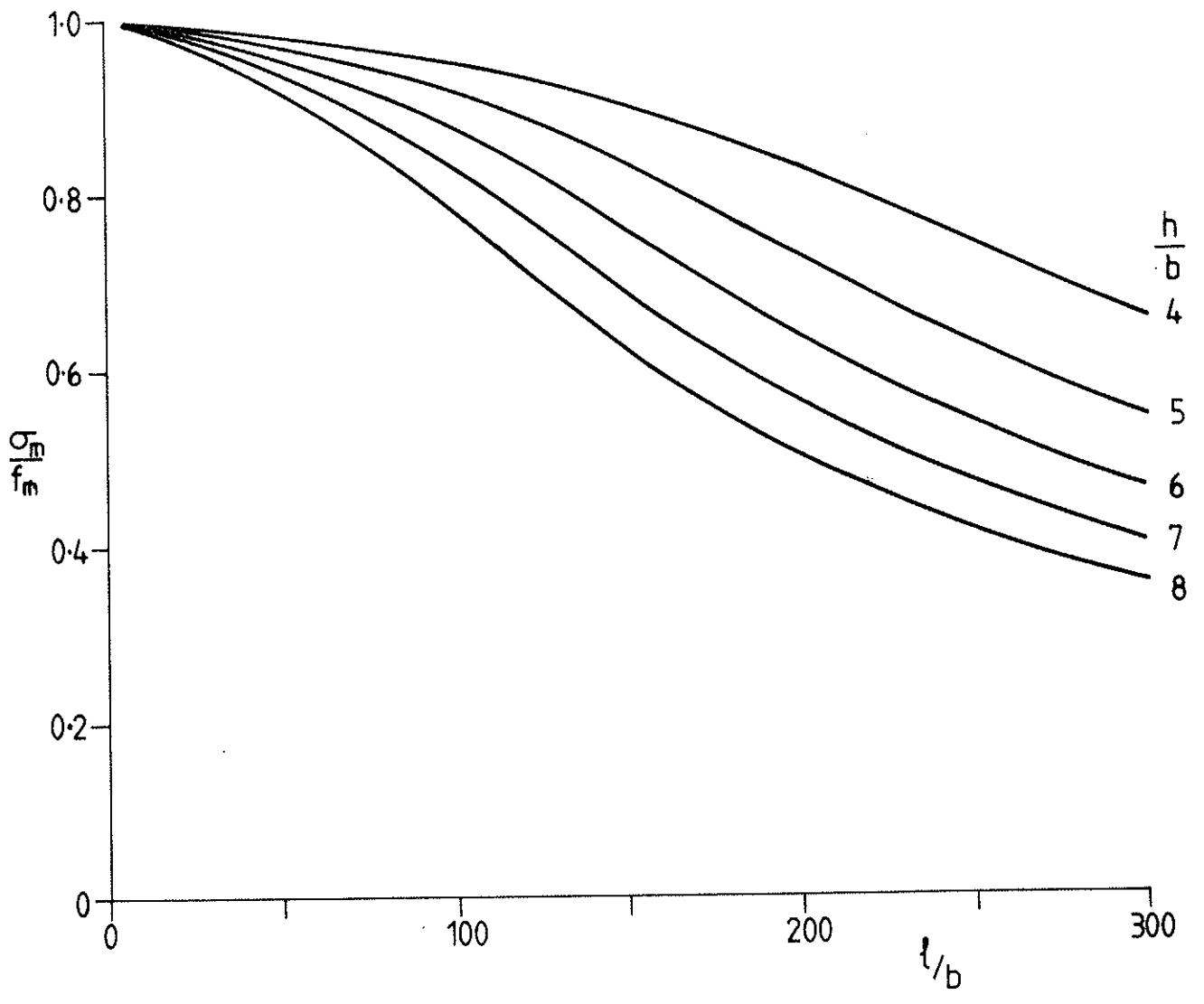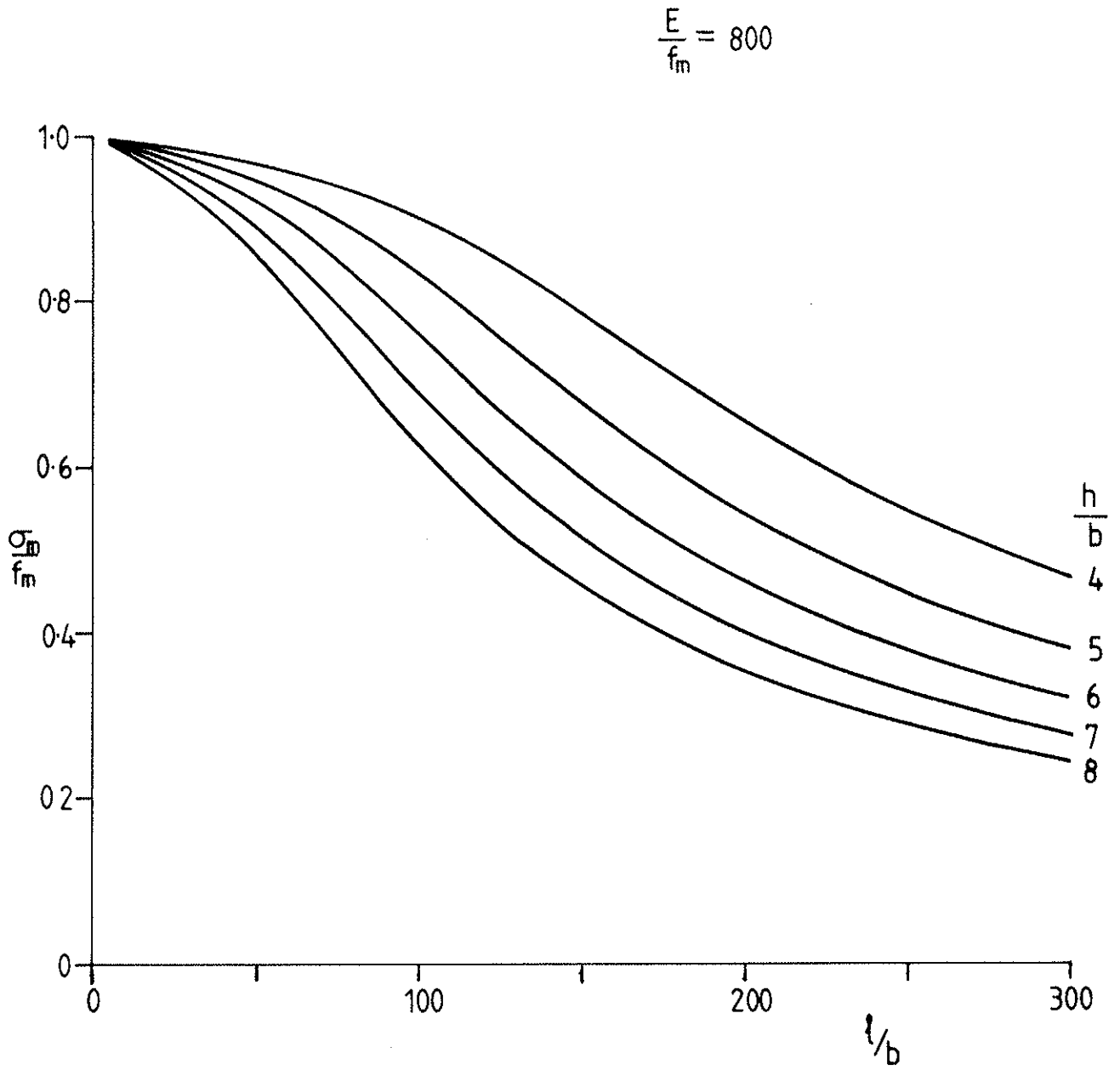
Figure 5.

$$\sqrt{\frac{1-\left(\frac{b}{h}\right)^2}{1-0\cdot63\,\frac{b}{h}}} = \quad \begin{array}{l} n' = 0\cdot 11336 \\ 0\cdot 9586 \end{array} \Bigg\} \begin{array}{l} \text{average values for} \\ \frac{h}{b} = 4,5,6,7 \text{ and } 8 \end{array}$$
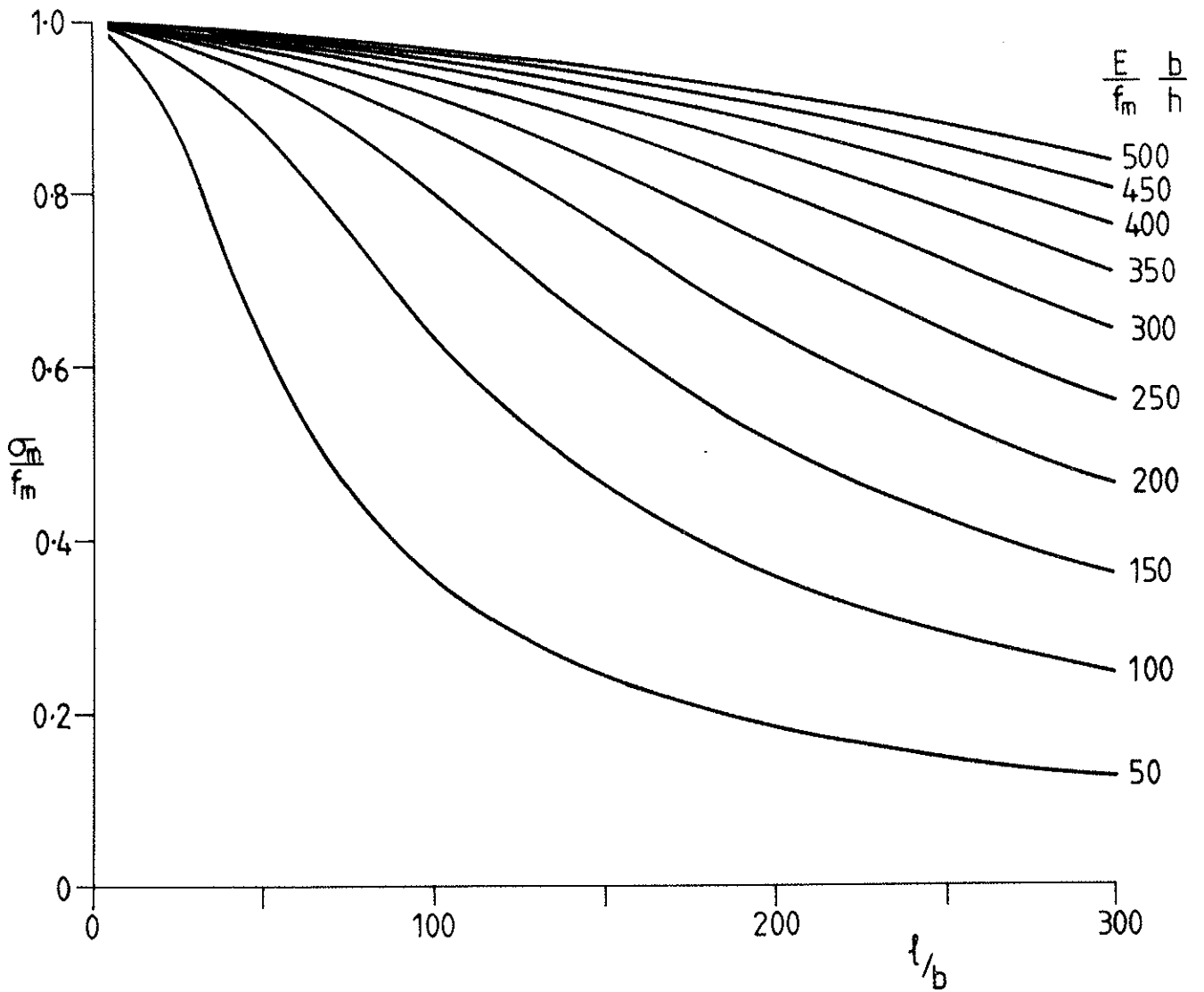
Figure 7.

INTERNATIONAL COUNCIL FOR BUILDING RESEARCH STUDIES AND DOCUMENTATION

WORKING COMMISSION W18A - TIMBER STRUCTURES

SPACE JOISTS IN IRISH TIMBER

by

W J Robinson
Forest Products Department
Institute for Industrial Research and Standards
Ireland

MEETING TWENTY
DUBLIN
IRELAND
SEPTEMBER 1987

INTRODUCTION

Irish forests annually produce a considerable quantity of small sawlogs which would not normally be used in building construction other than perhaps for stud partitions. These small sawlogs however could be used structurally by using them as chords in a ' box ' or ' I ' beam or any similar system.

Space joists are just such a system which use two timber chords separated by a metal lattice. (See FIG 5). Besides being used as floor or roof joists these members are suitable for use in A frames and portal frames and indeed any frame combination of column and beam.

OBJECTIVES

Space joists were fabricated in a number of spans with the viewpoint of producing load-span tables. For any 1 configuration two spans were manufactured – one for the theoretical design span based on SS imported timber and one for the theoretical design span based Irish M75 timber. The theoretical spans based on SS imported timber are slightly higher than those based on Irish M75 and it was hoped that the test series might justify using spans higher than those obtainable from theoretical calculation and possibly as high as the SS imported whitewood spans.

However after the initial few test results it was clear that the joists for both spans were failing the load tests on a deflection criterion.This necessitated a change of emphasis in the stated objectives.

It was therefore decided that the testing should proceed but with the desired aim of producing a design criterion rather than load-span tables for a limited number of joist sizes. Based on this approach load-span tables could than be produced for other member sizes than those under test. The test methodology used in this new objective remained as before.

A decription of the test method is given in Appendix A along with comments on the acceptance criteria.

FABRICATION

The timber used in the manufacture of the space joists was Irish M75 (a machine grade). The nearest competitor in the Irish domestic market to Irish M75 is Imported whitewood SS grade. The grading rules used are essentially those as set out in BS 4978 : 1973. The relevant design stresses for these two grades are given in Table 1.

The space joists were fabricated in the United Kingdom under instruction from the system owners. Some difficulty was found in pressing home the punched metal plates (generally in timber greater than 72 mm in thickness). The timber tended to bow outwards under the applied pressure and once this pressure was removed the timber reverted to its original shape thereby forcing the teeth of the punched metal plates out slightly. Impact embedment by a mallet solved this problem and under inspection only a few plates were not fully embedded.

TABLE 1: DESIGN STRESSES* FOR IRISH M75 & SS IMPORTED TIMBER

TIMBER	Bending	Tension	Comp. Pll	Comp. Perd	Shear Pll	Emean	Emin
M75 (Irish)	6.6	4.6	6.4	1.45	0.98	9000	5500
SS (Imported)	7.3	5.1	8.0	1.55	0.86	10000	5700

* Units N/mm2

TEST RIG.

The initial test rig consisted of load application through a series of wires and pullies (this tended to produce a series of point loads on the joists). After 3 tests this arrangement was changed so that load was applied as a uniformly distributed load (U D L) by means of an air bag and the wire / pully system was abandoned. A fuller description of the test rigs is given in Appendix B.

TEST RESULTS

The 24 hour deflections results are shown graphically in figures 1 to 4.

All joists passed the strength test and generally reached a load factor in excess of 3.

TEST COMMENTS

The test load was obtained by assuming that the joists were spaced at 600 mm centres and were carrying a total floor load of 2.0 KN/M^2 (1.5 superimposed and 0.5 dead).

In beam 16 the preload was repeated with approximately a 24 hour gap between the tests. The 24 hour test was extended to approximately 160 hours. The deflection over the extra 136 hours was approximately the same as that over the 24 hours. Only over the last 60 hours of the test did the rate of deflection decrease substantially.

Figures 1 to 4 show the 24 hour test deflections only. For clarity the preload deflections and the return curve for load release have been omitted.

Triangular joints were also taken from several joists and were subjected to a point loading. Deflection was measured and from these readings the deflection due to nail slip was calculated and a nail slip curve was drawn as an indication of the nail properties.
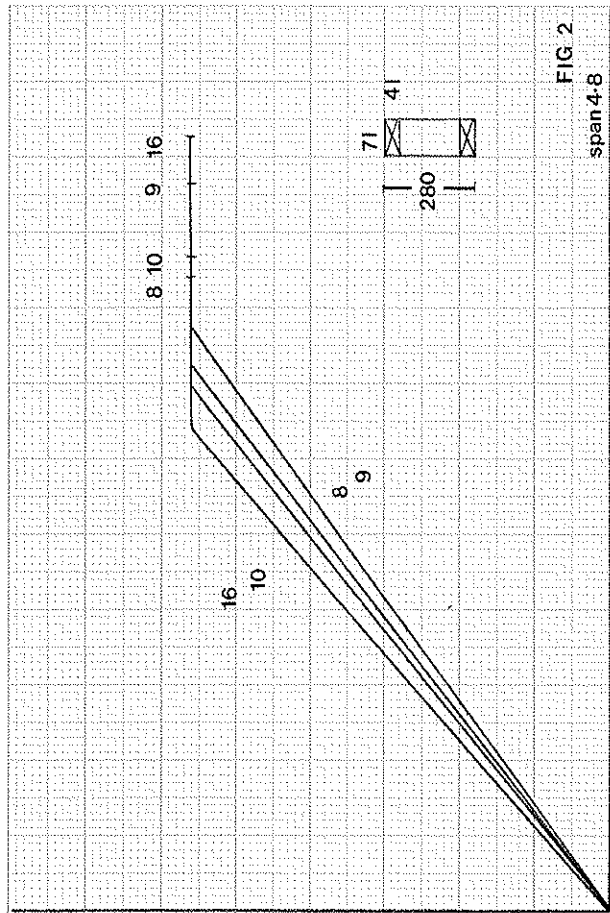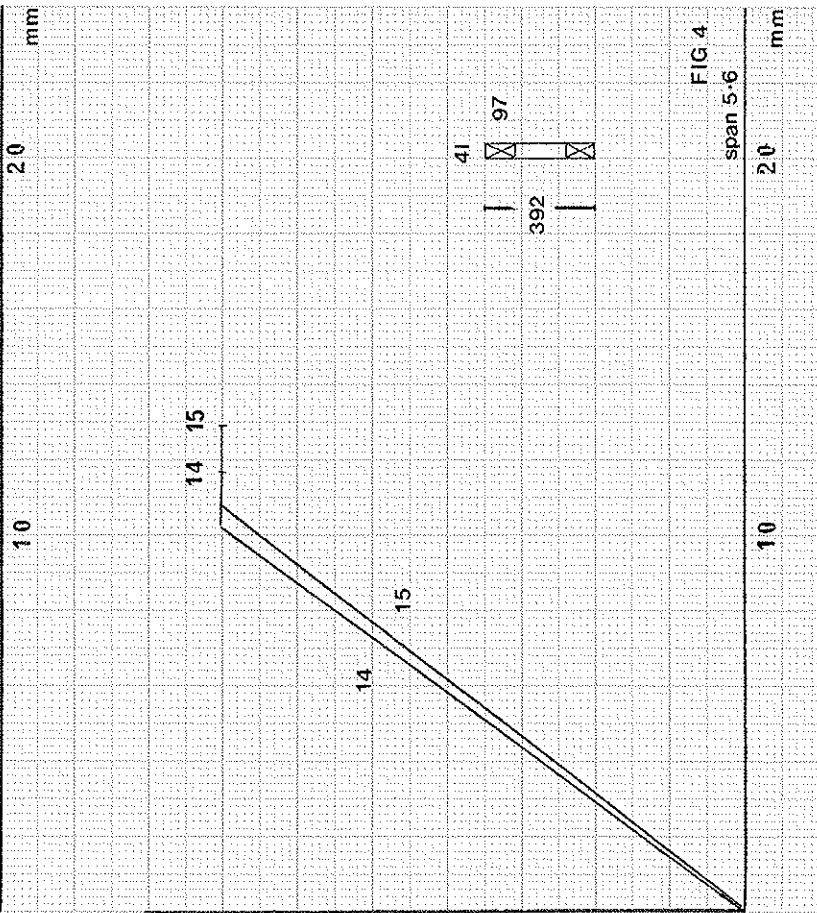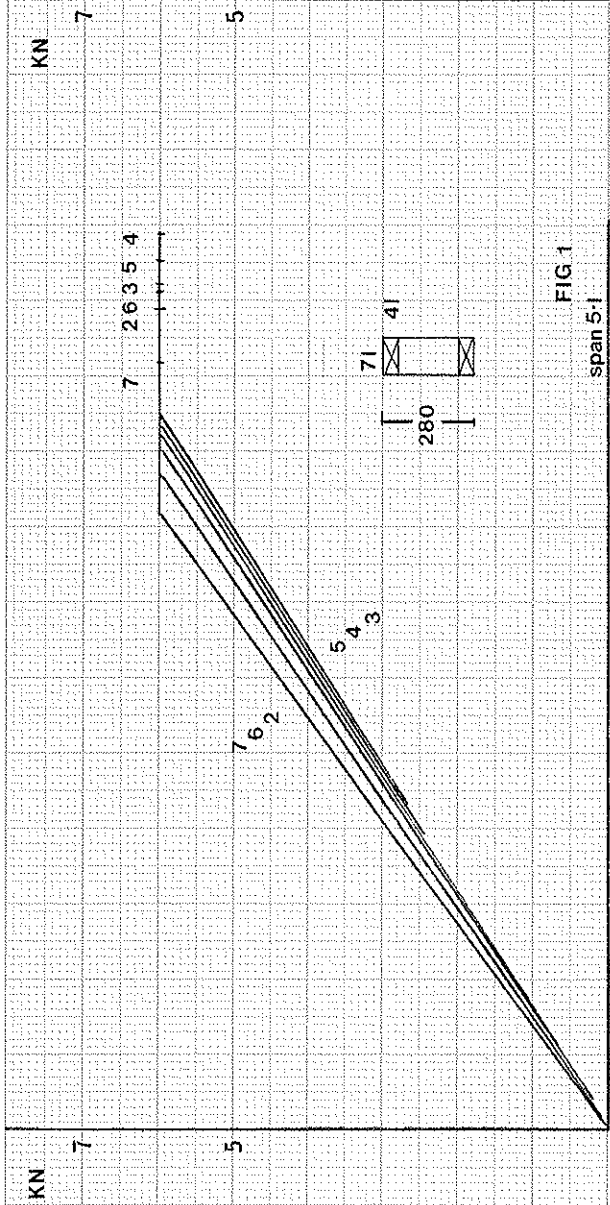
FIG. 1
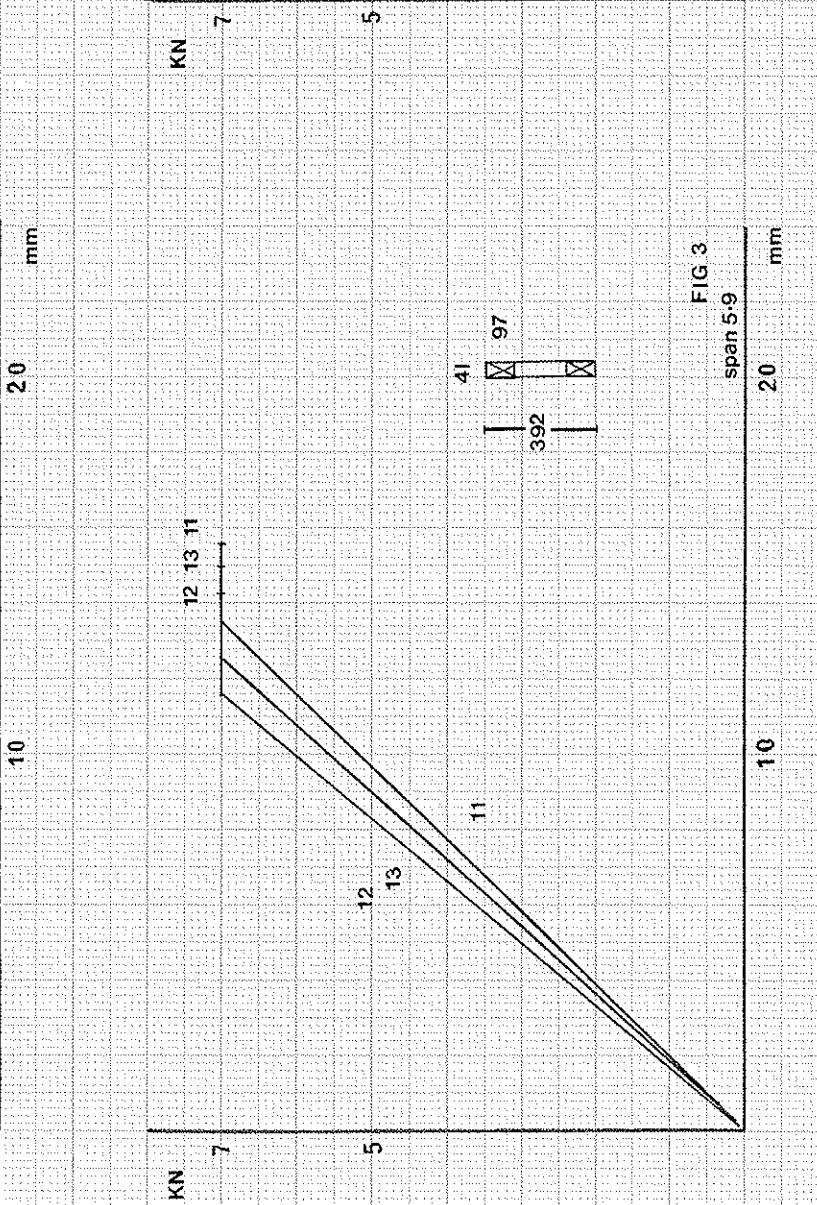span 5-1

FIG. 2
span 4-8

FIG 3
span 5-9

FIG 4
span 5-6

DESIGN CRITERION

The joist sections were analyised both as Box beams and as a pin jointed lattice girder. The theoretical deflections and stresses were similar for both cases and therefore it was decided that the design procedure should be based on the simpler Box beam method.

The design proceedure adopted was based on BSCP 112 the code in force at the time of testing. This code sets limits on the combination stress index - the limits are essentially 0.9 for bending and compression and 1 for bending and tension. The axial forces are based on the central bending moment divided by the distance between the centres of the timber chords. The design bending stresses are derived from secondary bending moments based on the relevant chord loading between the node points. The secondary bending moment coefficent will be dependant on the degree of continuity of the timber chord - a value of o.85 was considered reasonable. Deflection calculations for the final design procedure are based only on the timber sections.

The calculation of nail slip was standardised by rationalising the geometry of the space joists so that the node points were considered to be at a centres of 610 mm. This made little difference to the theoretical deflection calculations. The theoretical deflection in mm due to nail slip was found to be approximately equal to 1.25 times the span in metres (using a typical slip value of 0.18 mm).

It was thought that as the nail slip would be different at each section joint or node point because each joint is subject to a different load a relationship between nail slip and the overall stress levels in the joists might exist. The slip value of 0.18 mm was taken as the slip for a joist under maximum load (ie the stress combination ratio was 1) . A nail slip factor was then obtained from the nail slip curve. This factor was designated Ks and was simplified to the following equation ;

$$Ks = 0.4 + (R - 0.5) \times 1.2$$

Where R is the combined stress index and has a maximum value of 1 for a fully stressed joist. It can be assumed that only relatively highly loaded joists will be checked for deflection.

As in the case of similar structures the long term deflection has been allowed for by multiplying the theoretical deflection by a factor .A value of 1.3 was taken in this case and this was justified to some extent by the test results in joist 16 and from the evidence of a permanent set in joists 2 and 3 . However further investigation of the long term deflection is warranted into this aspect of the design . The final deflection equation is therefore ;

$$1.3 \times (\frac{5\ W\ L^4}{384\ EI} + 1.25\ Ks\ L)$$

Table 2 shows the average test deflections and the theoretiacl deflections. The theoretical deflections show reasonable agreement with the test deflections although it would be desirable to have tested more joists in these and other spans.

TABLE 2

Span (M)	Bending Deflection	Ks	Nail Slip Deflection	Average Test Deflection	Theoretical Deflection
4.8	11.3	0.9	5.1	17.1	16.4 X 1.3 = 21.3
5.1	14.4	1.0	6.2	21.9	20.6 X 1.3 = 26.8
5.6	9.6	0.46	2.9	12.2	12.5 X 1.3 = 16.2
5.9	11.8	0.5	3.3	15.0	15.1 X 1.3 = 19.6

CONCLUSIONS

The deflection of the space joists is represented by the following equation ;

$$1.3 \times \left(\frac{5 \, W \, L^4}{384 \, EI} + 1.25 \, Ks \, L \right)$$

Where $Ks = 0.4 + (R - 0.5) \times 1.2$

R is the combined stress ratio index and has a maximum value of 1 for a fully stressed joist. It can be assumed that only relatively highly loaded joists will be checked for deflection.

W is the uniformly distributed load (KN/M)acting on the joist.
L is the span of the joist in metres.
The E value is taken as the mean value and the I value is based only on the timber sections.

The performance of the joists is improved if the main axis of the timber chords is perpendicular to the vertical plane (as in Figures 3 & 4).

The position and the design of the splice plates (particularily the tension plates in the bottom chord)is important to the structural integrity of the joist. To maintain the same overall factor of saftey in the design it may be necessary in some cases to design the splice plates for the secondary bending moments due to the chord loading. While these secondary moments are usually small particularily in the case of the bottom chord they can represent a significant portion of the total stresses acting on the plates.

As deflection is the main criterion for the joists the use of a precamber will increase the effective joist span. The use of any precamber should be clearly stated in design tables and in any design specification.

APPENDIX A

DESCRIPTION OF TEST METHOD

The test method involved 3 different processes.

(1) Preload

A load equal to the long term design load was applied and maintained for a period of 30 minutes before it was released. The deflection of the joist was measured before and after the load was released and again at the end of 15 minutes.

(2) Deflection Test

Immediately following the preload test the long term design load was again applied. This was maintained for a period of 24 hours before being released. The long term load was applied generally over a period of 30 and 45 minutes and deflection readings were taken as follows:

A. 15 minutes after the application of the long term design load.
B. At regular intervals during the 24 hour period.
C. At the end of the 24 hour period.
D. 15 minutes after the release of the long term design load.

(3) Strength Test

After the completion of the 24 hour test the long term design load was re-applied as under the deflection test. This load was then increased at approximately the same uniform rate until an appropiate saftey factor was reached (this varied from 2.5 for 1 joist tested to 2 for 5 or more joists tested) where upon the load was held for 15 minutes. Where appropiate the load was further increased until failure or instability was reached.

TEST ACCEPTANCE

The usual criterion for the acceptance of the above tests are;

1. The deflection of a joist at the end of the 24 hour period must not exceed 0.8 times the amount specified in the design. (0.8 X 0.003 times the span).

2. The rate of increase in deflection should tend to decrease during the 24 hour period.

3. The joist should sustain the appropiate load (the long term design load times the appropiate factor for the number of joists tested) for 15 minutes.

Given the excessive deflections experienced the 24 hour deflection test was used as a guide for determining a design method rather than as a straight forward acceptance / failure criterion as described above.

DESCRIPTION OF TEST RIG

The first 3 joists were tested on a converted truss test rig. Load was applied only to the upper chord which was restrained at 600 mm centres.
This proved unsatisfactory for a number of reasons. The self weight of the pullies and cables were too high a percentage of the total test load (approximately 40 %) and therefore no accurate zero load datum could be established. The load over a period of time tended to relax as the joist deflected and this necessitated numerous ajustments in the load application which in any case was not a true U D L.

Due to the above the test rig was altered - so that the load was applied by an air bag rather than through pullies and cables . The air was forced into the bag under pressure and this resulted in the bag expanding and reacting against a steel ' I ' beam and the test joist. The ends of both these members were enclosed in a ' force ring ' of hollow steel sections and steel bars with their end reactions cancelling eachother out. Details of this test rig are shown in figure 6.

Load was measured by load cells and deflection gauges were placed at the supports at the joist centres and under the splice positions. The advantages in using this rig were;

The applied load was a true U D L.
Zero applied load can easily be obtained.
Load application is accurate.
Load application is more stable and therefore adjustment is less frequent.
The test area is clear of cables etc and observation of the test is easier.
An improvement in the time taken to set up the diferent joists for testing.
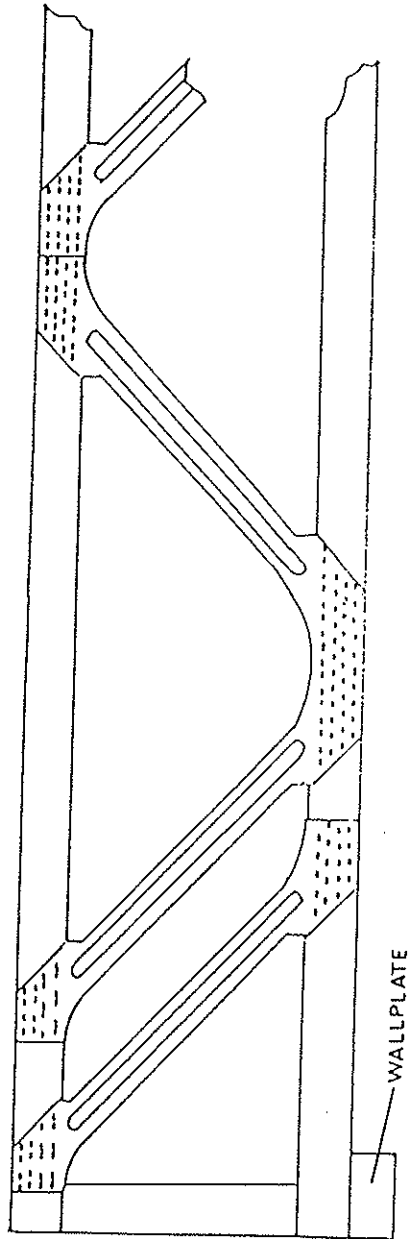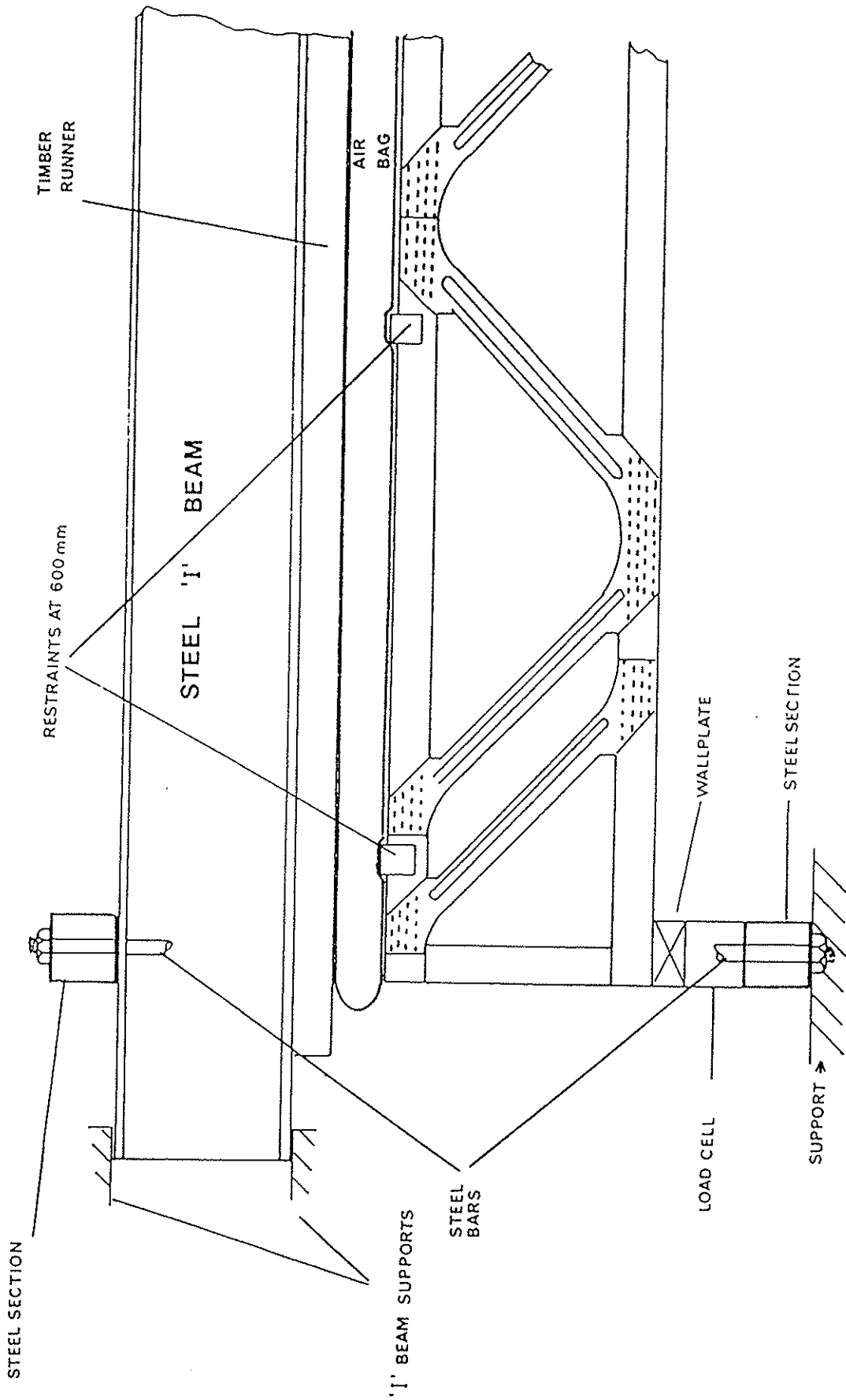
WALLPLATE

END DETAIL

FIG 5

TIMBER RUNNER

AIR BAG

STEEL 'I' BEAM

RESTRAINTS AT 600 mm

STEEL SECTION

'I' BEAM SUPPORTS

STEEL BARS

WALLPLATE

STEEL SECTION

LOAD CELL

SUPPORT

FIG 6

-10-

INTERNATIONAL COUNCIL FOR BUILDING RESEARCH STUDIES AND DOCUMENTATION

WORKING COMMISSION W18A - TIMBER STRUCTURES

COMPOSITE STRUCTURE OF TIMBER JOISTS AND CONCRETE SLAB

by

T   Poutanen
Finland

MEETING TWENTY
DUBLIN
IRELAND
SEPTEMBER 1987

Composite structure of timber joists and concrete slab

by

T. Poutanen

M.Sc. (dipl.eng.) Director, Insinööritoimisto Tuomo Poutanen Ky, Omenapolku 3A, SF-33270 TAMPERE

Specialist lecturer, Tampere University of Technology

Abstract

Two composite structures of timber joists and concrete slab, PB-stab and TP-slab[1] developed by the author and manufactured in Finland since 1979 and 1985 are presented, the design basis and a design method is described, some experience is discussed.

Key words

Composite structure, timber joist, concrete slab, nail plate

Contents:

1. Introduction

Timber has been utilized together with mineral materials thousands of years ago. E.g. timber brushwood has been used as a reinforcement of clay, mortar, concrete or masonry. Timber joists have been used as an opening beams of brick or stone walls or as a reinforcement of brick or stone structures.

---

[1] The structures are called here according their Finnish initials "timber-concrete-slab" (puu-betoni-laatta) and "steel-timber-slab" (teräs-puu-laatta).

Nowadays it is not common to connect timber and concrete or any other mineral material to the same structural unity. The reason is in the author's opinion mainly the following:

• There are many poorly known things, e.g. shrinkage of concrete, deformation created by temperature and moisture which have frightened usual designers to utilize the composite behavior.

• Among some designers timber structures may have a bad reputation due to the poor durability caused by unskilled and/or negligent moisture control.

• Designers have usually specialized only on one material (which they favor). Timber concrete composite structures require knowledge of two materials.

Composite timber joists concrete slabs have been utilized earlier e.g. in U.S.A. as bridges and in Sweden as small house walls and floors since 1971. (The Swedish system, called EW-element, has been a great source of ideas to the author.) The connection between joist and concrete has been achieved by nail, stable or bolt. Some tests have been made to utilize contact by grooving the joist edge adjacent to concrete.

The author has worked with nail plate connector. It has some advantages:

The nail plate is an effective timber connector with the low ratio of prize/stiffness and prize/strength. The nail plate is a reliable connector, though it is stiff, it is ductile. It is possible to use the nail plate with any joist cross sections, also small joist breadth 50...38 mm which usually leads to little joist costs is possible. The nail plate can be utilized to increase the shear strength in joist by using the large nail plates at joist ends. It is possible to have a gap between joist and concrete which brings many advantages:

• The possible moisture in concrete can not be transported into timber and many harms e.g. moisture deformation in timber and risk of timber damage are eliminated.

• Timber is saved on the gap area. This takes place with no practical loss of strength or stiffness because the neutral axis is located in the gap.

• The gap increases the total structural depth. Timber joists are usually available in limited depths, so the maximum span is increased.

• The gap makes the force to transfer from the joist to the concrete softly. The stress peaks created by the constraint forces are less than in the case of no gap.

• The gap makes space to pipes and wires across joists.

2. PB-slab

PB-slab ("timber-concrete"-slab) fig.1 (in the appendix) is suited to concrete element industry. Production happens in the following way:

The nail plates are pressed into timber joists, a part of the nail plate ≈45 mm exceeds timber edge.

Concrete, 40...70 mm, is poured on horizontal mould, central reinforcement is used.

The joists with nail plates are pressed into the wet concrete making a gap of ≈20 mm between joist and concrete, the nail plates will get into concrete ≈25 mm.

After concrete is hardened, the element is lifted and transported to building site. The structural connection between elements is usually achieved by welding in steel anchors. The connection through joists with nails is sometimes used. The element seam is filled with plastic or mineral mortar.

PB-slab is mainly used as a wall element. Concrete is usually as an outer surface. In buildings where humidity is high, e.g. barns, concrete is inside. Horizontal applications (floors, ceilings) are also utilized in some extent. Concrete may be on the lower or upper surface, usually on the lower surface.

3. TP-slab

TP-slab ("steel-timber-concrete"-slab) Fig. 2 (in the appendix) is suited to trussed rafter and prefabricated timber house industry. TP-slab is used at present only as horizontal structures (floors). Concrete is on the upper surface. Production happens in the following way:

The nail plates are pressed into the timber joists on plant. The joists (with the plates) are transported to building site. They are adjusted to their position. Above the joist there will be spread timber battens and a .4 mm steel sheet which is punched 12 mm into nail plates using a lath and a mallet. Concrete 25...50 mm is cast on the sheet. The steel sheet works as a working platform, mould and reinforcement. A reinforcement mesh is not usually needed. According to experience reinforcement is not needed for strength but to force width of cracks little.

Alternatively, the joists, the battens and the steel sheets are connected together on plant to form an element which is transported to building site. Only concrete casting takes place on site. Or even concrete may be cast on plant.

While concrete is cast temporary support is needed at the middle of the span. The support is utilized to get a camber of appr. span/800.

4. Nail plate

The nail plate used in BP- and TP-slap is especially developed for the purpose, fig.3 (in the appendix). In BP- and TP-slab nail plates the stiffness and the shear strength are most important. Spikes are not punched on the gap area which increases plate shear- and compression strength. To make the plate still stronger the gap area is slightly corrugated. The part of the nail plate which is poured into concrete is cut in spike form. These spikes have anchoring barbs to ensure the connection in concrete. The plate is corrosion protected with zinc 350 g/m^2.

The nail plates are usually pressed only to the other side of the joists. As a high strength or stiffness is needed the nail plates are pressed on both sides. The high strength of the nail plate allows a gap of 20...50 mm between timber and concrete i.e. the nail plate can transfer the shear force from timber to concrete over the gap. The nail plates have width 100...180 mm (usually 120 mm) and length 150...300 mm (usually 300 mm) and they are located 400...600 mm (usually 600 mm) apart.

5. Joist

Usual sawn timber of cross section 38...75*100...225 mm^2, 400...1200 mm apart with finger joints or nail plate splices can be used. LVL-joists (laminated veneer lumber, e.g. KERTO-LVL) have turned out to be good due to several reasons:

• LVL-joists are strong and stiff.

• LVL-timber has (apparently) small and slow moisture deformation.

• LVL-joists are available in the large variety of cross sections and lengths.

Glue lam joists are also possible. Only Scandinavian softwood (Picea abies, Pinus sylvestris) has been used so far.

6. Design method

6.1 General

The analysis is simplified assuming that the slab is made up of several two dimensional composite joist-

concrete "beams" i.e. the real three dimensional behavior is neglected. This assumption is justified because nearly always in practice the slab length (or span) is larger or at least of the same magnitude as the slab width. This means that the three dimensional action is small.

These subbeams have the structural form of a vierendel beam which is made of joist (timber beam) and concrete (a part of concrete slab) connected together with the nail plates. The vierendel beam can be analyzed with the general theory of composite beams with a partial interaction. Natterer, Kessel and Hoeft /2/ have demonstrated the theory to the case of timber joists and concrete slab. Girhammar /1/ has developed the theory to consider the nonlinear behavior of the connector, he has also handled the buckling of a wall. The theories /1/ and /2/ require an uniform contact between joist and concrete and they are well suited to the hand calculations of simple cases.

The nail plate connector is different. The connection is not uniform and the support and/or load conditions are often complicated. That is why the author uses the finite element theory.

Further, the finite element theory is sometimes necessary because TP-slab and PB-slab may be connected to the other structures to create the same structural unity, e.g. TP-slab is cast over the bottom chord beams of a timber frame. In this case the interaction between the slab and the frame has a big effect both on the frame and the slab which means that the total structure has to be analyzed as one unity.

The author has developed a finite element program for trussed rafters. This program is general enough to suit to PB- and TP-slab. The following modifications are made:

• The concrete member is replaced by its elastic and strength values.

• The connection between concrete and nail plate is completely stiff (the spring value is very high).

• If concrete is under tension and cracks approximations are needed. A satisfactory assumption for the strength analysis is that the concrete is idle at the tension zone and the tension forces lie completely on reinforcement. The deflection analysis creates problems, the (skilled engineering) interpolation between two extreme analysis boundaries has been used.

The design of TP- and PB-slab means in practice the material selection and the definition of deflection and strength (sometimes also estimation of crack width). The strength analysis consists of:

• Definition of timber stress (compression or tension and bending, shear and compression perpendicular).

• Definition of nail plate stress (shear, compression), the highest stresses are usually at joist ends.

• Definition of needed reinforcement if concrete is under tension.

Concrete has usually excess compression strength and it seldom becomes dimensioning.

6.2 Constraint forces
6.21 General

As the timber or the concrete structures are designed separately it is assumed that there are no constraint forces. But the timber concrete composite structures have constraint forces: the concrete shrinkage, the temperature deformation between timber and concrete and the moisture deformation in timber.

The constraint forces are created by the strain difference $\Delta\varepsilon$ between concrete and joist. This strain difference causes internal stresses in concrete and timber and deflection in the total structure. The size of the stresses and the deflection depends on stiffnesses and geometry and they can not be analyzed simply. However, two extreme cases can be defined easily:

Case 1: If the structure is prohibited from deflecting and the stiffness difference between the concrete and the joist is large (A_cE_c and A_tE_t is of different magnitude) the strain deformation takes place completely in the weaker part (concrete or joist, usually joist), assuming the strain difference is $\Delta\varepsilon$ then the stress

$\sigma = E\Delta\varepsilon$. This case represents the maximum value of the stress, the other part has ≈ 0 stress (also deflection is 0).

Case 2: If the concrete and the joist have a little flexural stiffness ($I_cE_c \approx 0$, $I_tE_t \approx 0$) and the structure is free to deflect the strain and stress in concrete and the joist is ≈ 0. The strain difference $\Delta\varepsilon$ causes only deflection. The structure bends to constant curvature:

$$R = \frac{\Delta h}{\Delta\varepsilon} \qquad (1)$$

$$v = \frac{l^2}{4R} \qquad (2)$$

where

R = radius of curvature

Δh = difference between concrete and joist center axes

$\Delta\varepsilon$ = strain difference (between joist and concrete)

l   = span

v = deflection

In practice the deflection is less than the case 2 and the stress is less than the case 1. (A rough estimation is that the strain is $\Delta\varepsilon/3$ and the deflection is v/3, these values apply to the approximate excess action by the strain difference in the most structures in practice.)

6.22 Shrinkage of concrete

The Finnish concrete code advises that 25...50 mm thick standard concrete, cast on 0.4 mm steel sheet, has the total shrinkage of 0.023%...0.049% depending upon climate conditions. This is bigger than the ultimate tensile strain and the concrete should crack from shrinkage. However, we know from experience that cracks do not usually occur. This can be explained with the fact that the areas cast at the same time have been little and they have been free to shrink. On the other hand cracks are produced if concrete has large shrinkage or the concrete is poorly cured after casting e.g concrete dries too quickly after casting (concrete is not covered with a plastic film on hot and/or sunny climate). According to some tests these cracks do not seem to decrease strength further the slab may be watertight in spite of cracks (at least against little water pressure i.e. the cracks do not extend through the slab and/or they are very narrow).

6.23 Temperature deformation

The concrete has temperature deformation $10^{-5}/°C$ and timber respectively $0.5 \cdot 10^{-5}/°C$ parallel to grain. Assuming the temperature difference amplitude is $\pm 40°C$ the strain difference $\Delta\varepsilon$ caused by temperature is $\pm 0.02\%$.

6.24 Moisture deformation

Timber has moisture deformation parallel to grain $7\ 10^{-5}/\%$ (strain $7\ 10^{-5}$ per 1 % change of moisture content). Under indoor climate conditions (e.g. standard living houses with no air dampening) timber has the moisture content variation between $\approx6...12\%$ in Finland. So, the strain amplitude $\Delta\varepsilon$ is $\pm0.021\%$. The strain difference from completely dry to completely wet is $\approx0.3\%$. Both in TP- and BP-slab timber moisture content has varied from dry to wet ($\approx6...\approx25\%$) without creating any detectable harm to the structure (though the calculative stresses are high).

Oil treated timber has ≈0 moisture deformation which gives a chance to utilize composite structures at places where the timber is subjected to direct water.

6.25 Constraint forces in design

Timber fails at $\approx0.2...0.5\%$ tension strain. The ultimate compression strain is appr. twice as much as that. The ultimate tension strain in concrete is $\approx0.01\%$ and the ultimate compression strain is $\approx0.3...0.5\%$. Concrete has a little tension strain capacity but this is not any problem in practice because cracks are allowed and forces are transferred to reinforcement. The steel has a high strain capacity ($5...20\%$). In practice concrete compression strain never becomes dimensioning due to the high strength and stiffness. So, in practice, the strain difference becomes dimensioning mainly in timber tension and the connectors get some excess stress.

By controlling timber moisture content during casting it is possible to get a prestressing effect (at least theoretically) e.g. it is possible to compensate the concrete shrinkage and get appr. unstressed structure by having the timber moisture content $\approx3...6\%$ higher during casting than in the final structure.

Timber tension is the major reason for failure in PB- and TP-stabs. Under controlled climate conditions the approximate maximum strain from temperature and moisture is less than 10% out of the timber tension strain capacity. One could assume that the constraint forces have such a little effect that they can be included to the safety factor. This thinking has been adopted in the present Finnish PB-slab approval.

On the other hand the constraint forces are real and they apparently reduce the potential strength and the strain difference causes excess deflection. The type approval of the Swedish EW-element prescribes that the constraint forces are considered assuming that the strain difference $\Delta\varepsilon$ between timber and concrete is $\pm0.02\%$ and its effect is added to all the other loads both in the strength and deflection analysis. This strain includes the effect caused by shrinkage, moisture and temperature (if they do not exceed their common values in construction). This applies to the allowable stress design. (If the limit state design method is used the strain ($\pm0.02\%$) must be multiplied in the failure analysis with the load factor $1.3...1.6$ depending upon the safety system and the number of other actions in the same load case.) This method looks good and in practice it means roughly the reduced potential composite behavior strength of $\approx10\%$.

6.3 Test-analysis comparison

Many tests have been done both with PB- and TP-slab. A typical TP-slab was tested recently by Technical Research Centre of Finland /4/. The slab size was $2350*6000\ mm^2$, the concrete was 50 mm thick, standard K30 quality, steel thickness was 0.5 mm, no reinforcement mesh was used. The battens were $48*48\ mm^2$ 600 mm apart, the slab had 5 joists $48*198\ mm^2$ 485 mm apart, the slab was loaded with 4 line loads.

The analysis applies to the load level of $F=1.59\ kN$ per joist ($\approx2.2\ kN/m^2$, $R=3.18\ kN$).

The following elasticity values were used:

Concrete elasticity E_c=29000 MPa, got from strength with equation E_c=5000√33. Timber elasticity E_t=13000 MPa, got from elasticity measurement before concrete casting. Nail plate stiffness k=8 N/mm^3, got from experience.

The analysis is based on a model shown in fig 4. Black nodes represent stiff joints, white ones represent the semirigid joints between timber and plate.
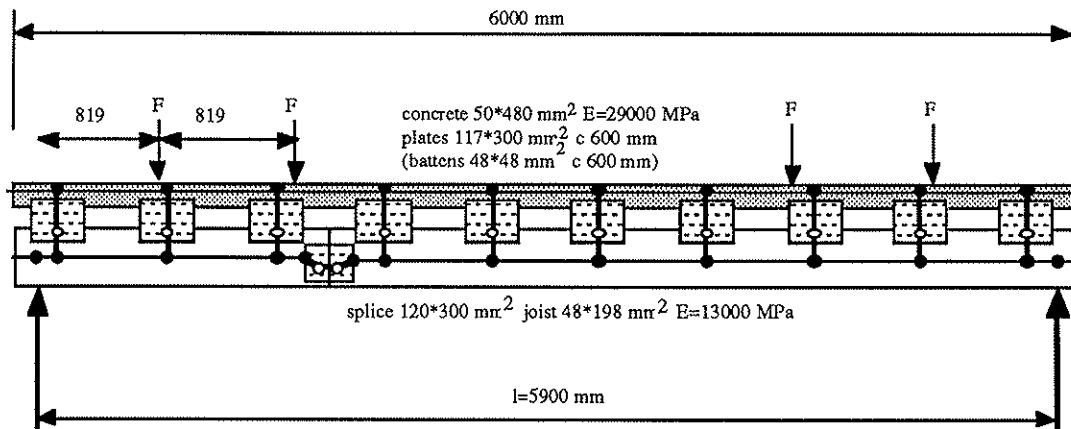

Fig. 4, Finite element model for TP-slab analysis

The analysis gives the result shown in table 1 (case 0, representing the same stiffness values as measurement) there are given results also from 4 other analyses:

Case 1: Timber elasticity is reduced ≈25%, E_t=10000 MPa

Case 2: Nail plate stiffness is reduced 50%, k=4 N/mm^3

Case 3: Strain difference $\Delta\varepsilon$ between concrete and timber is 0.02% (e.g. timber dampens ≈3%)

Cases 1,2 and 3 are calculated adding the effects to the case 0 simultaneously, i.e. the case 3 has E_t=10000 MPa, k=4 N/mm^3, $\Delta\varepsilon$=0.02%. The case 4 represents noncomposite behavior k≈0 meaning no (very little) shear force between joist and timber but having a vertical force to make the same deflection to the concrete and the joist, E_t=13000 MPa, $\Delta\varepsilon$=0, the nail plate splice has been replaced with stiff (finger) joint and concrete thickness 50 mm has been changed to 30 mm to represent the flexural stiffness better. The concrete has a little flexural stiffness, so the joist carries nearly all the load. The results are presented in the table 1, CSI denotes the compound stress index of timber (f_t=7 MPa, f_b=11 MPa), v denotes deflection and σ_{cu}, σ_{cl}, σ_{tu}, σ_{tl} stress in concrete and timber upper and lower edge in mid cross section.

	measurement	case 0	case 1	case 2	case 3	case 4
σ_{cu} (MPa)	-1.5	-1.60	-1.78	-1.87	-2.45	
σ_{cl} (MPa)	0	+0.08	+0.26	+0.39	+1.18	
σ_{tu} (MPa)	+0.6	+0.41	+0.52	+0.39	-0.89	
σ_{tl} (MPa)	+3.2	+3.41	+3.30	+3.42	+4.08	≈12
CSI (%)		42	41	42	47	≈110
v (mm)	7.3	6.6	7.6	8.9	12.6	≈40

Table 1, Measurement and analysis results of TP-slab

7. Experience

PB-slab is mainly used as a wall element. In this application the structure is sound, concrete carries the compression force and the joist gives the buckling support. In this case both tests and analyses show that the wall carries a very high compression load.

TP-slab is mainly used as a floor structure where besides strength and stiffness also deformation stability, dynamics, acoustics, fire and moisture resistance are important. In all these factors TP-slab is better than conventional timber floors. According to Olsson /4/ the common timber joist floor: 48*198 T30 c600 with a particle board sheeting is not satisfactory at 3500 mm span but the same joists connected to 25 mm or 50 mm concrete are satisfactory with 6000 mm span.

Both PB- and TP-slabs have performed well during 9 and 3 years, no damage has occurred, neither has any complaints about serviceability (deflection, cracks, dynamics, acoustics, etc.) reported.

8. Summary

As timber and concrete is connected to the same structural unity excess stresses occur due to the strain caused by shrinkage, temperature and moisture. These stresses, of course, reduce the potential benefit by the composite behavior. Though, under controlled climate conditions or using the oil treatment the advantage due to composite behavior still is significant. In a typical case strength increases 2...3-times and stiffness 5...10-times compared to noncomposite behavior. Other benefits are gained, too.

9. References

1. Natterer J., Kessel M.H, Hoeft M.: Konstruktion und Bemessung von Holz-Betong-Verbunddecken (Construction and Design of Composite Timber Concrete Slabs), unpublished paper, 1987

2. Girhammar U. A.: RABO-väggelement teoretisk och experimentell studie av sammansatt element av trä och betong (RABO-element Theoretical and Experimental Study of Composite Element of Timber and Concrete) Research report 1980:30 Luleå Technical University

3. Test report no RTT64555, Technical Research Centre of Finland, 1987

4. Olsson S., Svikt svängningar och styvhet hos bjälklag, dimensioneringmetoder (Flexibility, Swing and Stiffness at Floors), Statens råd för byggnadsforkning, Stockholm, 1984

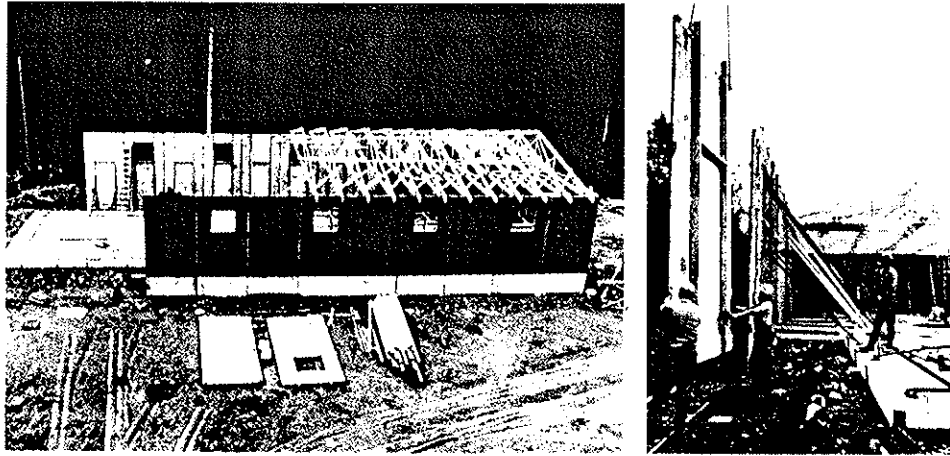5. Poutanen T., Model For Trussed Rafter Design, CIB-W18/18-14-2, Beit Orein, 1985

Fig. 1, BP-slab used as wall element of industrial hall

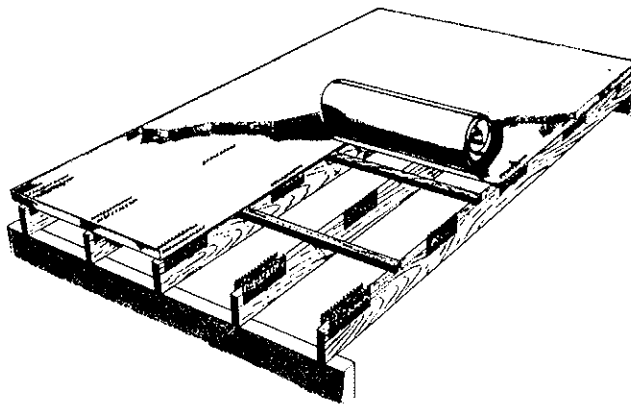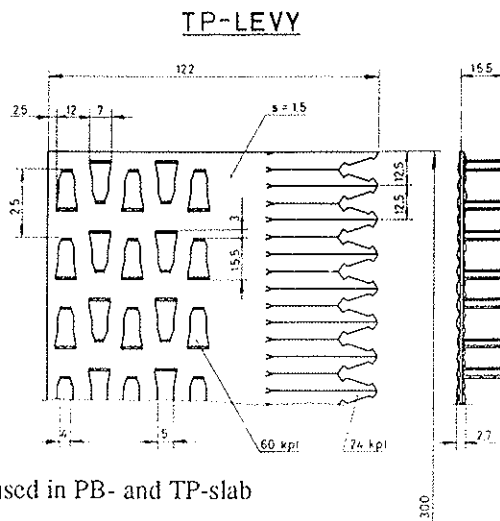Fig. 2, Principle of TP-slab

TP-LEVY

Fig. 3, Nail plate used in PB- and TP-slab

INTERNATIONAL COUNCIL FOR RESEARCH STUDIES AND DOCUMENTATION

WORKING COMMISSION W18A - TIMBER STRUCTURES

CLASSIFICATION SYSTEMS FOR STRUCTURAL WOOD-BASED
SHEET MATERIALS

by

V C Kearley and A R Abbott
Timber Research and Development Association
United Kingdom

MEETING TWENTY
DUBLIN
IRELAND
SEPTEMBER 1987

CLASSIFICATION SYSTEMS FOR STRUCTURAL WOOD-BASED SHEET MATERIALS

INTRODUCTION

The majority of applications in the U.K. requiring the use of a structural wood-based sheet material have, traditionally, been met by one of the many types of plywood available. However, recent advances in wood-panel technology have resulted in an increasing use of particleboard and other wood-based composite panels for structural applications, particularly in less onerous environments where durability is not a prime requirement.

The choice of an appropriate board material in the U.K. is complicated by the fact that the majority of panels are imported and originate from a large number of sources with little U.K. control over their specification. Thus we can do little more than accept or reject each board type for use on an almost ad-hoc basis.

With such a wide variety of board types available, a means of simplifying design and specification would be beneficial. This is particularly important if a complicated and confusing situation is not to be "built into" the new Eurocode 5 from the start.

DESIGN DATA FOR STRUCTURAL SHEET MATERIALS

The present edition of BS 5268 : Part 2 : 1984 includes fourteen tables of structural plywoods (covering 136 different species/lay-up/thickness combinations) and four thicknesses of tempered hardboard. This causes problems with the design and specification of structures and components, particularly those involving the use of plywood, since a design using one of the 136 possible plywoods should be rechecked if substitution of another plywood is desired. In practice, substitution is all too common, and even non-structural boards are used, giving timber products in general a poor image, and an unfairly bad reputation.

The revision of BS 5669 : 1979 'Specification For Wood Chipboard' is at an advanced stage. When issued it will include specifications for various grades of chipboard, flakeboard and cement-bonded particleboard. Part 5 of the current draft is entitled 'Code of Practice for the Selection and Application of Particleboard for Specific Purposes', and is intended to give guidance on suitable applications for various types and grades of particleboard. It appears likely therefore that at some future date further particleboards will be added to the materials included in BS 5268 : Part 2.

The next amendments to BS 5268 and the revised version of BS 5669 are likely to include improved marking requirements for boards. Whilst this should improve the users awareness of what products are, or are not, permissible, it is only part of the solution.

The situation therefore is approaching one in which the designer will be faced with a plethora of wood-based sheet materials, not all of which will be suitable for all applications. In the past, the simpler timber codes, giving only solid timber and glulam stresses, have been fairly unrestrictive with regard to climate, service conditions and considerations such as creep. The newer codes, which include sheet materials, are seeking to take such factors into account. Commercial availability, or otherwise, is another aspect strongly influencing final choice, although this is hardly amenable to codification.

In addition to the confusion that is likely to occur with the range of materials in BS 5268 : Part 2, other materials continue to be introduced under 'type approval' arrangements. In the U.K., for example, the Agrement system has been used for this purpose. If this process were to continue in a piece-meal fashion, as each product is accepted for broader applications, a vast number of slightly differing specifications could be foreseen. It has therefore been suggested in the U.K. that, to avoid the worsening confusion and growing risk of inappropriate specification, a system be produced under which all wood-based sheet materials intended for structural use can be classified and specified on a common basis.

A report by Soothill(1), made an initial study of the subject, and proposed a grouping system for wood-based sheet materials on a similar basis to the strength class system adopted for solid timber in BS 5268 : Part 2, except that boards could have a different rating for different properties. Plywood

was excluded from this system, since it was felt that its inclusion would lead to uneconomic under-estimates of certain properties. The main reason for this is that the ratios between various properties for plywoods are often very different from those of other types of board. This highlights the fundamental problem faced by anyone attempting to produce an all-embracing classification system. However, it is essential that structural plywood be included in any future system if it is to receive widespread acceptance from manufacturers, specifiers and users alike.

Furthermore, because of the large variety of board types and constructions and the need to include other performance factors such as durability and moisture resistance ratings, it is obvious that any viable system will be more complex than a corresponding solid wood classification system.

ALTERNATIVES

As mentioned above, there are problems associated with a simple strength class type of system. The variation in interrelationships of different properties for different board types makes such a scheme difficult to define and implement. For example, for particleboards the ratio between modulus of elasticity in bending and shear modulus is typically about 3, whereas for many plywoods this ratio can be in excess of 10. In general, there is no common correlation between any two properties for all board types.

An alternative approach might be to adopt performance rating, as used in North America. In such methods, panels are submitted to tests designed to simulate in-service loads and conditions for a specific application, e.g. flooring. The panels are then given a rating for that application. One problem associated with this type of system is that there are fundamental differences in loading and environmental conditions between North America and Europe. This would therefore require specialised testing of panels intended for each market.

Another objection is that the performance rating system does not allow the board to be used for alternative purposes where design stresses are required. Although this system is popular in North America it has met with considerable resistance in Europe.

Another suggested approach is to adopt a combined system, where performance rating is used for the larger market areas such as flooring and sheathing, whilst design stresses are made available for special designs. This system seems to combine the problems of both the others which may well outweigh the benefits to be gained. It would also be difficult and time consuming to implement.

Alternative approaches might be developed based around each major end-use e.g. flooring, wall sheathing etc., with only properties related to that end use being included in the required assessment. This would in many instances require an assessment of durability, appearance and stability under changing environmental conditions. This is, in effect, similar to the Agrement approval system, but would be carried out under a properly codified and approved system.

Other, yet to be defined, systems may be possible, but considerable effort may be required to define and specify any system for use in the U.K. as the majority of panels are imported and these originate from a large number of sources. It is unlikely that European or U.K. specifications can be imposed on overseas producers aiming their products at a range of markets and therefore the system should contain a method of rapidly assessing imported boards produced to foreign specifications.

CLASSIFICATION PROJECT

To develop proposals for a classification system for wood-based sheet materials, a programme of work, part sponsored by the Department of the Environment, has recently started at TRADA. The following are its stated aims:-

1) To review the implication of completed programmes, and to further develop existing work carried out at other establishments, for a more unified approach to the classification of structural wood-based sheet materials in Europe.

2) To develop a classification system in the context of BS 5268 and Eurocode 5 with the intention that it should be suitable for the full range of structural boards available in Europe and form the basis for harmonization of European standards relating to panel products.

3) To identify a limited range of tests for materials and components that will enable any particular board type to be assessed in accordance with the new system.

4) To undertake a selective programme of materials testing and performance testing on components, with the aim of refining certain tests and collecting comparable information on representative materials. To include measures of variability and the influence of important effects such as durability and dimensional stability.

The project is aimed towards the classification of structural panel products according to their mechanical and physical properties, but will also consider related aspects such as durability and reaction to moisture.

The initial stages of the project will involve a review of work already carried out on classification and component testing, a study of systems used in other countries, and liaison with other organizations and individuals in the construction and related industries.

To conclude, an interim report will be produced outlining the proposed classification system. This will relate to as wide a range of wood based sheet materials as possible and will take into account important end uses such as sheathing, flooring and common structural components, e.g. built-up I-beams. Feedback from the industry will be sought at all stages prior to the full development of the system.

REFERENCE.

1) Soothill, C. A unified approach to the classification, specification and characterisation of particleboards and fibreboards.
Unpublished TRADA report. June 1984

INTERNATIONAL COUNCIL FOR BUILDING RESEARCH STUDIES AND DOCUMENTATION

WORKING COMMISSION W18A - TIMBER STRUCTURES

SOME NOTES ABOUT TESTING NAIL PLATES SUBJECTED TO MOMENT LOAD

by

T Poutanen
Finland

MEETING TWENTY
DUBLIN
IRELAND
SEPTEMBER 1987

Some notes about testing nail plates subjected to moment load

by

T. Poutanen

M.Sc. (dipl.eng.) Director, Insinööritoimisto Tuomo Poutanen Ky, Omenapolku 3A, SF-33270 TAMPERE

Specialist lecturer, Tampere University of Technology

Abstract

The present nail plate tests are aimed to be momentfree. However, there may occur a big moment which is demonstrated in the paper. The definition of a moment loaded joint is cleared up. Some discussion is made how the nail plate joint could be tested under the moment load.

Key words

Test, nail plate, moment load

Contents

1. Introduction

In the CIB-conference 19, Florence, Italy the author was asked to write a paper about testing nail plate joints subjected to moment load. This paper is a preliminary reply to the request. A research project has been established under the leadership of the author lasting 30.4.1989 having the aim to define guidelines for design of the moment loaded nail plate joint. However, three suggestions will be made and offered for a discussion. A more thorough report will be published later.

2. Definition

Some definition is made to clear up the basic concept of moment loaded nail plate joints . The concept is not completely the same as the one of Norén /3/. The difference lies on the location of force F_p. The reason for having a different concept is to have the analysis model equal to the joint model. Norén's concept sees the problem from the joint design of view and serves better the joint design. As the author can see, both concepts give the same results if they are applied at the same conditions (e.g. the plate rotation is considered).

When two (or more) timber members are connected with a nail plate there occur many types of "joints" (junctures, connections, scarfs, seams etc.) which represent the different degree of integrity. All these joints are called here "joints" as suggested by Norén /1,3/. The joints are made up of the following elementary actions (forces and/or moments):

a. Friction force F_{fxy} from member x to y

b. Compression force F_{oxy} from member x to y

c. Plate force F_{pxz} from member x to plate z

d. Moment from member x and to plate z due to rotation (difference) M_{rxz}

The actions a,b and c (F_{fxy}, F_{oxy} and F_{pxz}) create a moment which depends upon the reference point. The moment d (M_{rxz}) is invariant and does not depend upon the selected measure system (reference point and/or coordinate). "The nail plate joint subjected to the moment load" is mainly understood as a joint loaded by the moment d (M_{rxz}). However, the eccentricity moment by actions a,b and c is often bigger than the moment d. The figure 1 illustrates the forces a,b,c and d in a heel joint with a wedge.

The elementary actions create (at least) four type of logical compositions which may be called "joints":

1. The compression and the friction force (a,b) occur simultaneously and they may occur without the plate force and the moment (c,d). The vector sum of the compression and the friction force is called contact force, (F_{cxy} contact force from member x to y) and it creates a contact joint (between member x and y). The contact force can not occur in all directions, only in those which create compression. The contact joint can transfer the moment only via eccentricity. Norén /1,3/ calls this joint "timber/timber joint", tt-joint.

2. The plate force (c) and the moment (d) occur simultaneously and they may occur without the contact force. The plate force and the moment creates a plate joint (between member x and plate z). The plate joint can have a force of any size (below strength limit) in any direction, the joint can transfer the moment via eccentricity and rotation. Norén /1,3/ calls this joint "plate/timber joint", pt-joint.

3. The composition of the plate joint and the contact joint is called a timber joint (between members x and y).

4. All the members connected to the same nail plate create a joint.

Fig. 1, A nail plate heel joint and its actions (forces and moments)

An important assumption is how the size and the location of the contact force (F_c) is defined. The author uses a method where F_c is defined (by size and location) in the analysis of the total structure utilizing the action-displacement equation of the contact. This seems to perform well if the gap in the real joint corresponds to the analysis assumption. In order to get a good similarity between the analysis and the reality the nonlinear behavior of the contact has to be considered (probably), too.

3. Moment in present nail plate tests

The present nail plate tests are interpreted as momentfree. However, these tests may include a big moment, especially M_r (moment due to plate timber rotation) and M_p (plate eccentricity moment) occurring simultaneously. This is shown by the following exercise:

Firstly, the standard grip strength test parallel to grain /4/ shown in fig. 2 (left and middle) is studied.
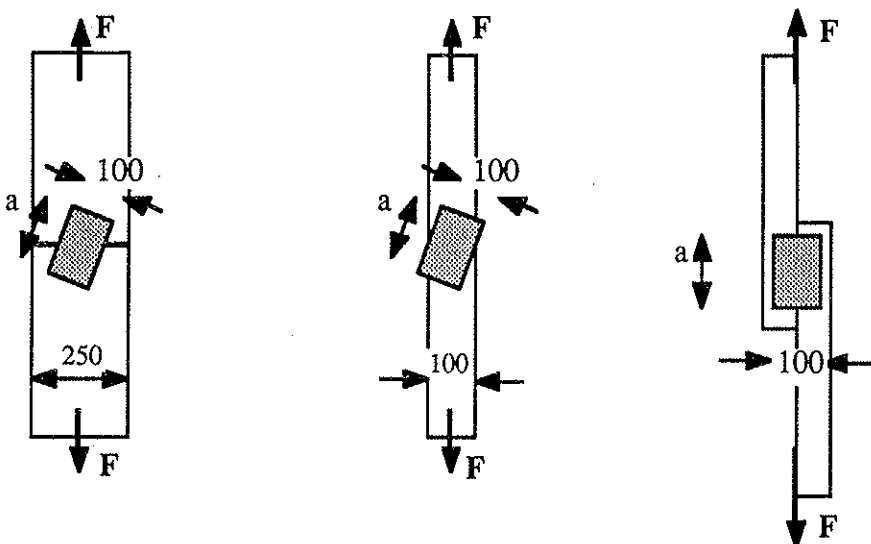
Fig. 2. Test samples used in the moment load study

The average grip stress $\tau_F=F/2A$ is defined. Also the total maximum grip stress τ_{F+M} which is the vector sum of τ_F and τ_M (the grip stress caused by the moment $\tau_M=r*M/2I$, i.e. calculated from elastic distribution) is defined. The ratio $k=\tau_{F+M}/\tau_F$ is calculated. k applies here the maximum value of τ_{F+M}/τ_F occurring in one of the corners of the effective area. This ratio k may be used as a measure of the moment compared to the force.

The following things are kept constant:

Timber breadth (48 mm), gap (3 mm) large enough not to create contact, plate breadth (100 mm), force timber angle ($\beta=0°$).

The following things are varied:

Timber depth, 100 and 250 mm, in case of 250 mm timber is large enough to stay under the plate, in case of 100 mm a part of plate may exceed the timber edge.

Plate length 100, 150 and 200 mm, denoted as small (s), medium (m) and large (l),

force plate angle, $\alpha=0°$, 22.5°, 45°, 67.5°, and 90° (in case of 0° and 90° eccentricity is 0 and k=1).

The results, k versus angle α, are shown in the fig. of 3.
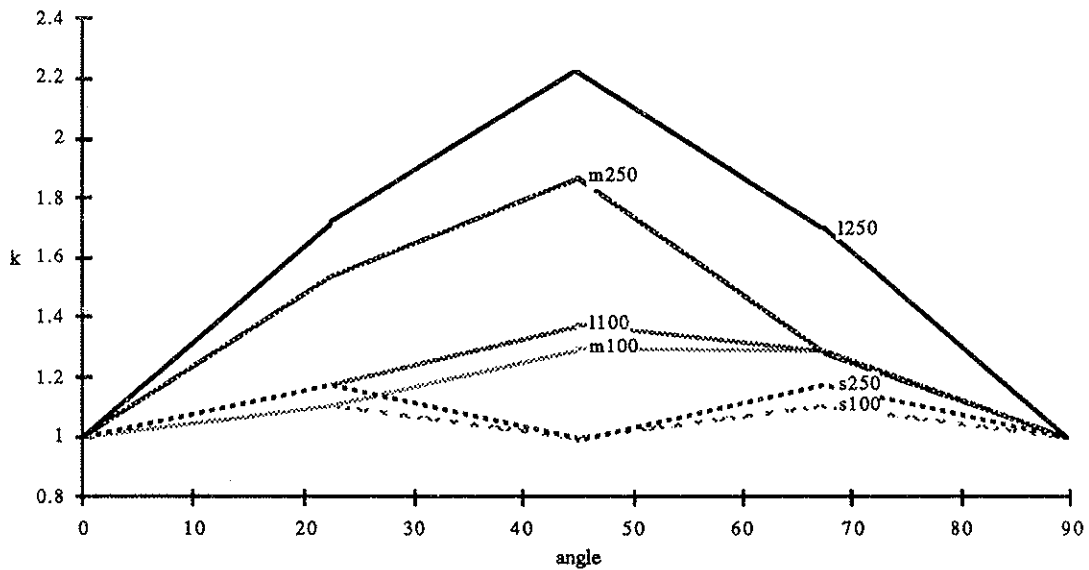
Fig. 3. The grip stress results, ratio $k=\tau_{F+M}/\tau_F$ versus angle $\alpha=0°...90°$, the different plate sizes are denoted as s (small, 100 mm), m (medium, 150 mm) and l (large, 200 mm) and the timber sizes 100 (mm) and 250 (mm)

Secondly, the standard shear test /4/ is studied (fig. 2, right). Only plate length is varied a=50...400 mm, $\alpha=\beta=0°$ and ratio k is calculated. The results are shown in the fig. 4. If the plate is short (b/a$\approx\infty$), the case can be calculated by hand, k=3, if plastic stress distribution is assumed k=2 (if no edge reduction is applied).
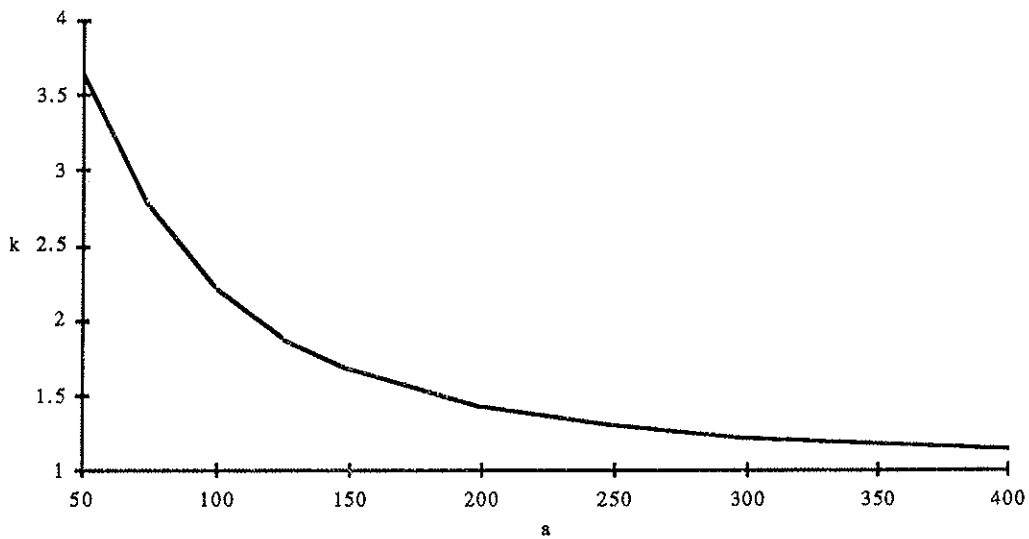
Fig. 4. The shear test results, (grip stress in shear test) ratio $k=\tau_{F+M}/\tau_F$ versus plate length a=50...400 mm.

It can be seen from fig. 3 and 4 that the unexpected joint moment may create high excess stresses.

4. Suggestions

4.1 Edge reduction

The present method for defining the effective plate area (A) in most countries is: An area which is closer than 5 mm to timber edge is not counted, however if the timber has a tension force the reduction (the measure from the timber edge) is at least 10 mm measured in a force direction. It is very obvious that the effective area must be calculated reducing a constant measure e.g. 0 or 5 mm from the timber edge. I.e. the rule of the tension force and 10 mm is wrong and it must be abolished. There are (at least) three reasons to this:

• A moment loaded nail plate may have a part of the plate under tension and a part under compression, the tension and compression sides must not have a different method for the effective area definition, otherwise the calculation becomes to diffuse.

• Calculation is simpler if the effective area depends only on geometry and not on loads. E.g. the different load cases may lead to a different force direction which leads to the different effective area (in the present method).

• Large nail plates resist lower grip strength per effective area than little ones do. This is partly due to the size effect (failure tends to follow the weakest link), partly due to the fact that the adjacent spikes harm each other's strength (especially the spikes in a large plate penetrate less effectively into timber). The grip strength per unit area should be as invariable as possible. If no edge reduction is made large plates give the least strength per unit area. This is true, as the author can see, with all the present nail plates. If any (positive) edge reduction is applied the disharmony is increased. The least variation in grip strength per effective unit area between the different plate sizes is got with the least edge reduction.

So, the effective area in a nail plate joint must be calculated by applying a constant edge reduction which is not larger than 5 mm (0 mm is simple and may be good) i.e. the effective area depends only upon geometry, not upon loads.

4.2 Tests with moment load

It is obvious that testing a nail plate under the moment load must include mainly grip strength testing by M_p (the moment caused by timber plate rotation difference). Other moments (eccentricity moment by plate, compression and friction) are simpler. All the moments that occur in a joint influence upon each other and it is necessary to know the effect of each moment separately. However, the knowledge of strength and stiffness of M_p is most important. Other moments can probably be calculated with elementary static and they need none or little testing.
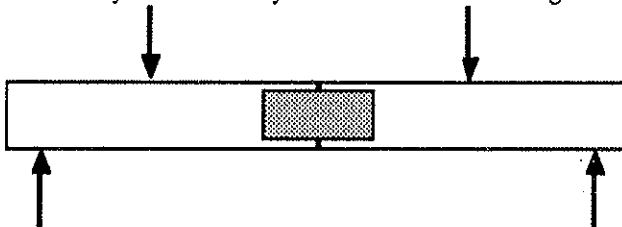
Fig. 5. Moment testing of a nail plate with a beam test

A nail plate can be tested with a beam test with pure bending. Though this represents a common case in practice the beam test can not be used as a general moment test due to several disadvantages:

• The beam test represents a case of F=0, e=∞ , the other combinations of F and e need to be tested, too.

• The beam test does not measure pure M_p behavior but composite M_p and M_c (the moment due to rotation and contact) behavior. If a large gap is used, not to make a contact, the plate buckling on the compression side leads to early failure (prefailure, strengthening and stiffening detected later in most cases due to the contact) and the whole M_p behavior is not got.

The author does not see any other way than testing the nail plate with the eccentric force. The basic principle is shown in fig. 6.
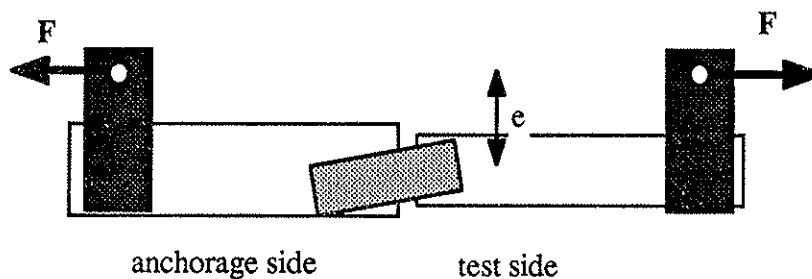
alternative 1
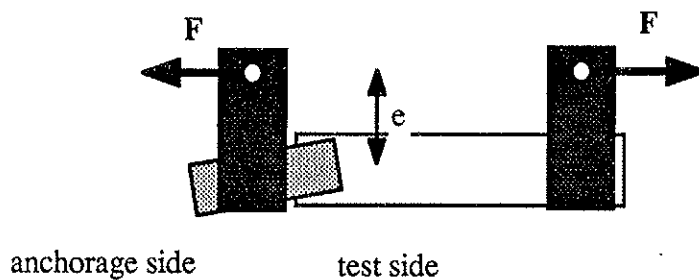
alternative 2

Fig. 6. The recommended moment test

The force would be applied to the test sample through special clamps which create the wanted eccentricity. There is one problem. The joint has two plate joints which are not symmetrical (if angle≠0°,90°) and the different subjoint has a different eccentricity (and moment). Due to the interpretation of the test results it is necessary to test only the one subjoint. This means that the other subjoint serves only the anchorage of plate to testing apparatus, alternative 1 in fig. 6. It probably is possible to anchor the testing apparatus directly to the plate by cutting the teeth or bending them down to the holes, alternative 2 in fig. 6.

4.3 Alteration procedure

The timber is a large source of strength deviation. Besides the timber density and moisture, the annual

ring size and pattern influence results. Because the results have to be presented at standard conditions (density, moisture etc.), which seldom exist in practice, an alteration procedure is used. Various alteration methods have been developed mainly for moisture and density. We have bad experience from these methods: They have been developed with certain plate types and conditions and they are apparently applied beyond their field of relevance.

However, the alteration procedure is needed. If no alteration is applied, (e.g. it is claimed that density, moisture etc. has to stay inside the prescribed limits, otherwise the results are rejected) the testing becomes expensive and complicated and the good test results need good luck (how closely the prescribed conditions are reached).

In the suggested method appr. half of the timber (the timber to have the prescribed properties) is saved, this gives the opportunity to make far more (nearly double) tests at the same expense because the major costs are created by the timber.

The principle of comparative tests can be applied: Simultaneously with the current test another test, reference test, with a previously tested wellknown joint is done using the same timber (different ends of the same cut). This method gives all the same information as the present testing method but also a reliable reference to the prior knowledge. This reference is not disturbed by any alteration. This method also gives information about the alteration procedure of the current joint.

5. References

1. Norén B.: Design of Joints with Nail Plates - Principles, CIB-W18/19-7-7, Florence, Italy 1986

2. Norén B.: Shear Tests for Nail Plates, CIB-W18/19-7-8, Florence, Italy 1986

3. Norén B.: Design of Joints with Nail Plates, CIB-W18/14-7-1, Warsaw, Poland, 1981

4. RILEM/CIB-3TT, Testing Method for Joints with Mechanical Fasteners in Load-Bearing Structures, Annex A Punched Metal Plate Fasteners, CIB-W18/15-7-1, Karlsruhe, Germany, 1982

INTERNATIONAL COUNCIL FOR BUILDING RESEARCH STUDIES AND DOCUMENTATION

WORKING COMMISSION W18A - TIMBER STRUCTURES

MOMENT DISTRIBUTION IN TRUSSED RAFTERS

by

T Poutanen
Finland

MEETING TWENTY
DUBLIN
IRELAND
SEPTEMBER 1987

Moment distribution in trussed rafters

by

T. Poutanen

M.Sc. (dipl.eng.) Director, Insinööritoimisto Tuomo Poutanen Ky, Omenapolku 3A, SF-33270 TAMPERE

Specialist lecturer, Tampere University of Technology

Abstract

The paper presents 10 trussed rafters with nail plate joints and their moment distribution based on 4 different analysis models. The trusses have been tested in full scale. The test results are shown and the comparison between the analyses and the models is made.

Key words

Trussed rafter, moment distribution, nail plate

Contents:

1. Introduction

A truss test procedure was developed in the theses /1/. This procedure was developed further in the theses /2/ and 10 trusses were tested in full scale. All the trusses were quality control trusses, they came from different plants and they were selected at random from a current production lot.

It was not realized to pay attention to joint gaps. The importance of the joint gap was revealed afterwards while analyzing the results (e.g. the rafter 6 had apparently gaps with eccentric contact in several joints). These trusses were used as reference trusses in the study /3/, which included the definition of the moment distribution with 3 models: continuous beam, pin joint frame and rigid frame. The results have been copied into this paper. The author has developed an analysis model for trusses /4/, the results of this

model are presented (also presented in /2/ in slightly different form). The author is continuing the study of the moment distribution in trussed rafters. A more thorough report will be published later.

2. Test procedure
2.1 General
All the trusses were loaded on the top chord with hydraulic cylinders 600 mm apart. The force in each cylinder was divided into two points, so the true load was made up of point loads ≈300 mm apart (the hinged cylinder head was ≈400 mm long and it had contact pins at both ends). Each cylinder supplied a lateral support (600 mm apart) to the top chord.

Both support reaction forces were measured with an electronic gauge. All the trusses, except one, were symmetric by geometry and loading. So the symmetry could be used to control the measurement error.

The measurement cross sections were defined to the locations which were expected to be the most interesting from the point of view of analysis. The restrictions from truss geometry, defects and test rig had to be considered. Defected cross sections were rejected. Due to the principle of utilizing symmetry in error control the selected cross sections had to be defectfree on the both sides of the truss. At top chords measurements could be done only between cylinder heads. The measurements were done at cross section edges, in some few cases at faces.

There were appr. 10 measurement cross sections in each truss.

The measurement in each cross section consisted of the recording of the strain in the upper and the lower edge ε_1 and ε_2 (sides 1 and 2). For the purpose there were glued steel pins with holes. A mechanical measuring apparatus, length 100 mm, (in some few cases 200 mm) with an electronic recording connected directly to a registration computer was used.

The testing includes a sensitive human factor in adjusting the measuring apparatus to the pins. The human error was minimized with the following procedure:
• One and the same person always adjusted the apparatus to the pins.
• The measuring apparatus was always in the same position as to the pins.
• The measuring was done twice in two cycles, if the difference between the cycles was larger than a prescribed value the measuring was repeated the third time etc.
• The measurement in each cycle was repeated 10 times in 0.3 sec intervals, the computer calculated the average value which was considered to be the measurement value.

2.2 Moment measurement
The moment measurement was based on the fact that the normal force (N) in each member is not sensitive to the analysis model, i.e. all the (reasonable) analysis models give the same result with high accuracy (as far as the force is concerned). This applies to rafters which have the structural form closely to truss (not e.g. frame). All the test rafters were clear trusses by basic structural form (however, one had large chords with high stiffnesses creating a small excess error). The normal force was defined by the author's design program /4/ using approximate timber and joint stiffness values.

The following derivation is presented (equations are different in /1/ and /2/ but giving the same results):

$$\sigma_1 = E^* \varepsilon_1 \tag{1}$$

$$\sigma_2 = E^* \varepsilon_2 \tag{2}$$

$$\sigma_1 = \frac{N}{A} - \frac{M}{W} \tag{3}$$

$$\sigma_2 = \frac{N}{A} + \frac{M}{W} \tag{4}$$

by eliminating A and W from 3 and 4 and considering 1 and 2:

$$M = N \frac{h\,(\varepsilon_2 - \varepsilon_1)/6}{\varepsilon_1 + \varepsilon_2} \tag{5}$$

where

A= cross section area (=b*h)

W= section modulus (=b*h²/6)

b= breadth

h= depth, measured in each cross section

N= normal force, got from analysis

M= moment, positive if side 2 has tension at positive N

E= modulus of elasticity, assumed to be constant over the cross section

ε_1= strain in upper edge, measured

ε_2= lower , measured

σ_1= stress in upper edge

σ_2= lower

2.3 Error estimation

The error of the moment M consists of the error of N, h, ε_1 and ε_2. The error of M was got by estimating the errors $\Delta N, \Delta h, \Delta\varepsilon_1$ and $\Delta\varepsilon_2$. A little computer program was used to calculate the effect of the different error combinations (positive and negative) on M. The error of N and h is small and may be neglected (though in the error study of /2/ the error of N, ±0.1 kN, and h, ±0.5 mm, was assumed). The major error is created by the ε-measurement. The actual ε-measurement is got from the ε-recording at the current load level and the zero load level. At both load levels the ε-measurement error was assumed to be the measurement difference between the recording cycles. By experience we know that the maximum error in ε could be as little as ±0.004%. The error is presented in the appendixes 11...20, the measurement values in each cross section are denoted by a circle (or ellipse). The circle center, marked with a cross, denotes the measurement value and the radius denotes the error. As seen in the figures and clearly understood from the equation 5 the relative error is small if the force (N) is high.

3. Analysis models

3.1 Continuous beams

The model continuous beams have widely been used in the past and partly nowadays, too. The moment distribution is defined by calculating the chords as continuous beams over nondeflecting joints, i.e. chords

are analyzed separately from the other structure. The members between the chords (diagonals and verticals) as well as and apexes are assumed to be hinged. The chord splices are assumed to be stiff.

3.2 Pin joint frame

The model pin joint frame is the same as continuous beams but the deflection of chords is considered. In this case the deflection is calculated assuming the joint slip to be as nil.

3.3 Rigid frame

The model rigid frame is a standard frame analysis with completely stiff joints (force and moment), the joint eccentricities are not considered.

3.4 Semirigid joints with eccentricities

The model semirigid joints with eccentricities is described in /4/. The nail plate joint stiffness value $k=10$ N/mm^3 has been used, the possible contact has been considered (initial gap 0.2 mm and foundation modulus $K \approx 30$ N/mm^3, parallel to the grain and $K \approx 15$ N/mm^3, perpendicular to the grain), the eccentricities (plate, timber and contact eccentricity) have been considered. The excess (or cut) moment due to the compression (or tension) force is considered (the analysis is based on the second order theory). The semirigid behavior of the chord splices is considered.

4. Results

The results of the models 1,2 and 3 are presented in the appendixes 1...10. The test results have been marked with a cross. The cross represents the mean measured moment value observed at the different load levels and at the different sides of the rafter.

The results of the model 4 are presented in the appendixes 11...20, the actual moment measurements and the errors (circle size) are presented, too.

In all the cases (appendixes 1...20) the moment (M) is presented as a ratio to support reaction (R=sum of all vertical loads), i.e. the moment M (Nm) is got by multiplying the value in the figure with the support reaction R (kN).

The presentations of the appendixes 1...10 and 11...20 are comparable with two exceptions: The moment values in the appendixes 11...20 include the second order effect by the force and the joint moments are presented at plate edges (while presented in the joint centers in the appendixes 1...10).

5. References

1. Leivo M., Naulalevyrakenteiden kuormituksesta ja analysoinnista (Trussed Rafter Testing and Analysis), diploma theses, Tampere University of Technology, 1983.

2. Laasonen M., NR-kattotuolien momenteista ja taipumista (Trussed Rafter Moments and Deflections) diploma theses, Tampere University of Technology, 1986

3. Leivo M., Laasonen M.: NR-suunnitteluohjelmistojen kartoitus (Rewiev on Trussed Rafter Design Programs), information bulletin, Technical Research Centre of Finland, 1987

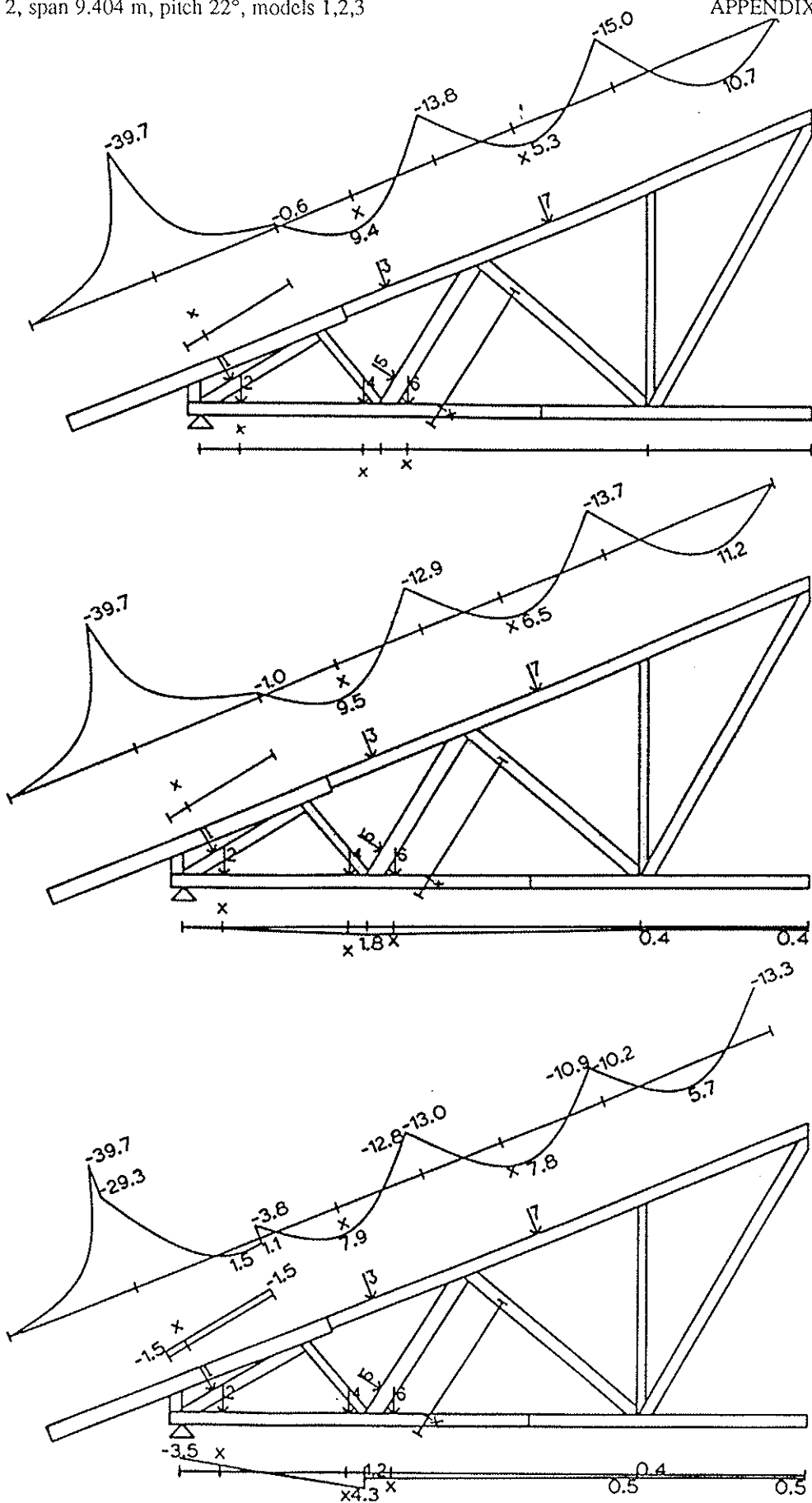4. Poutanen T., Joint Eccentricity in Trussed Rafters, CIB-W18/19-14-3, Florence, Italy, 1986
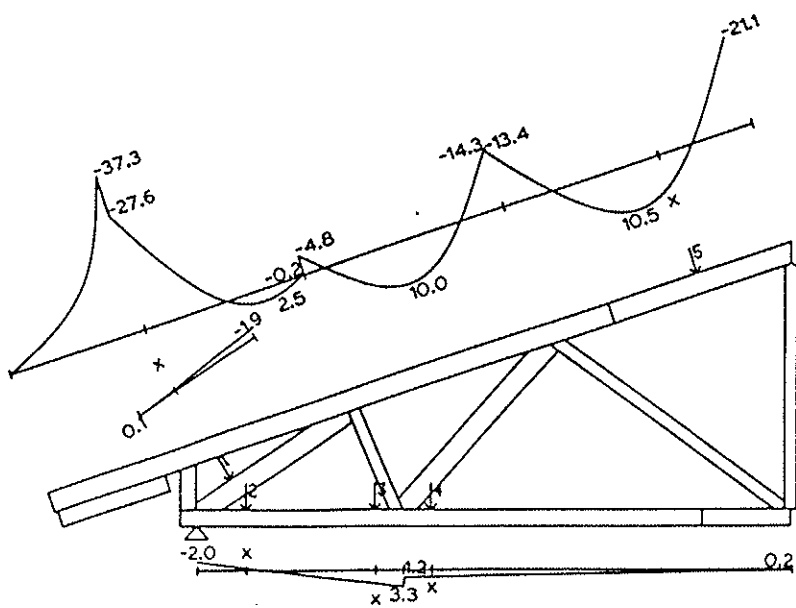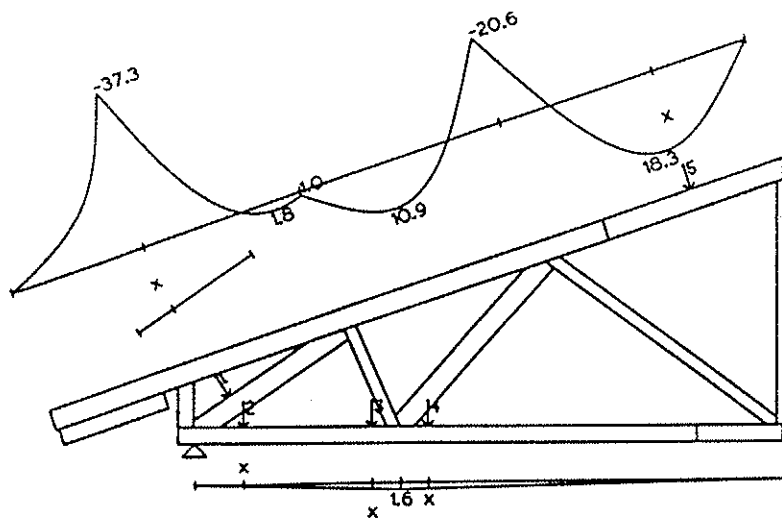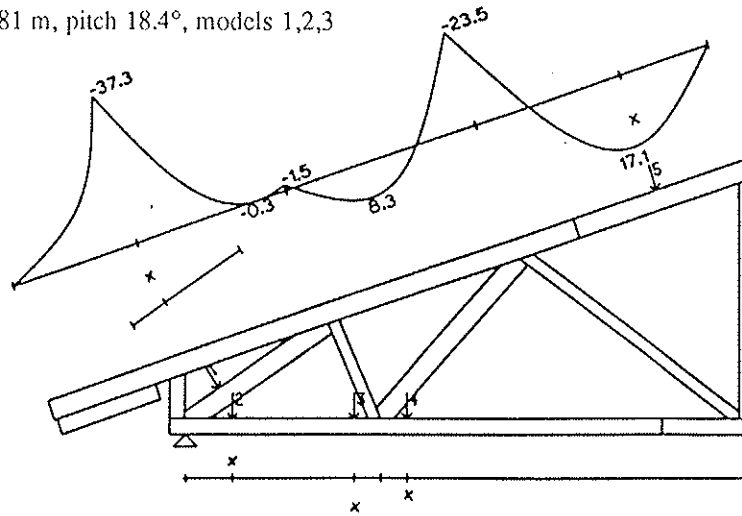
Rafter 1, span 8.06 m, pitch 18.4°, models 1,2,3
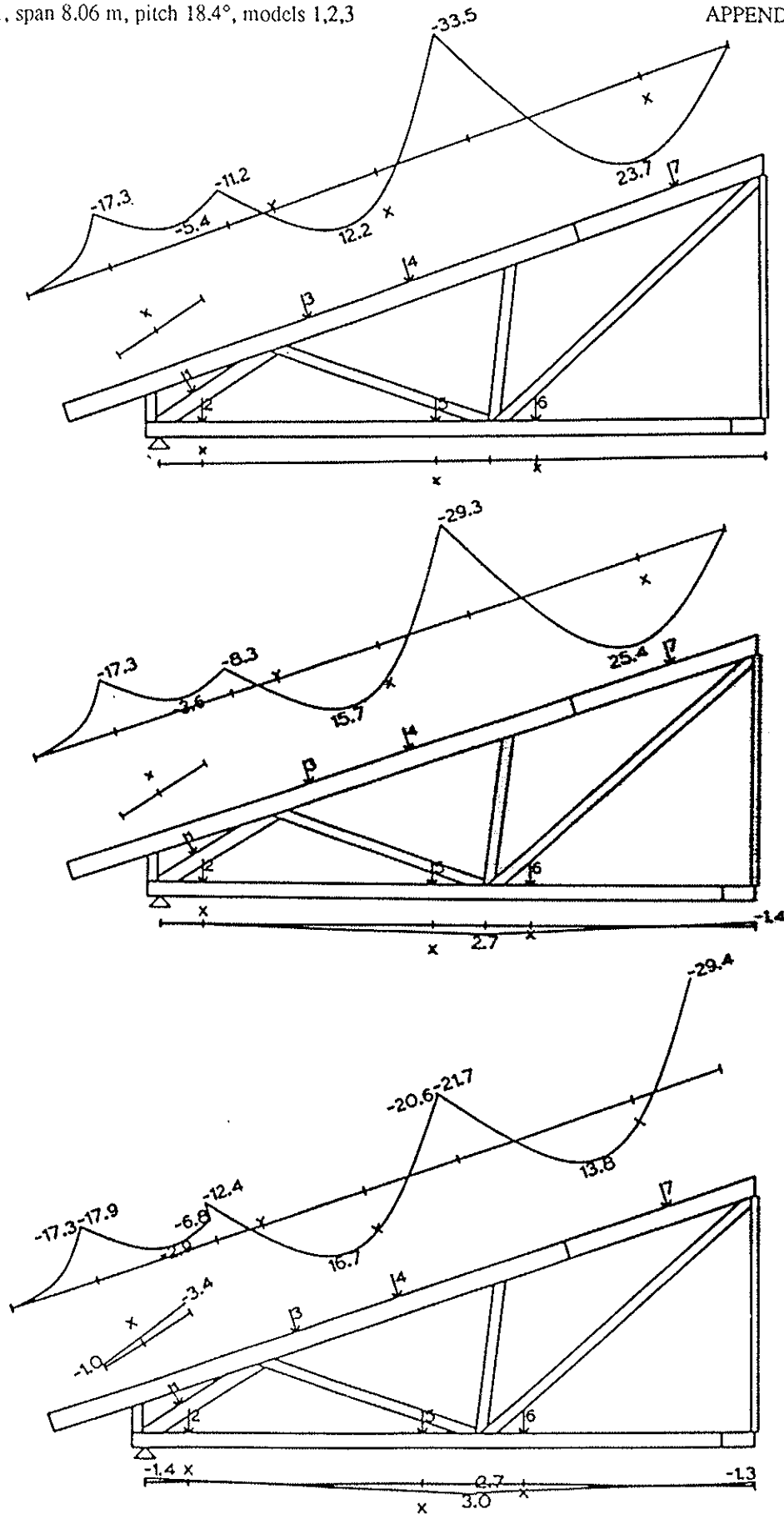
Rafter 2, span 9.404 m, pitch 22°, models 1,2,3
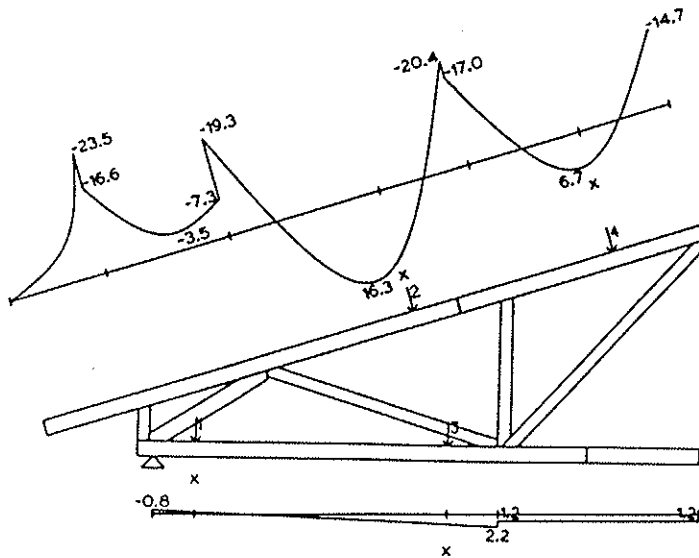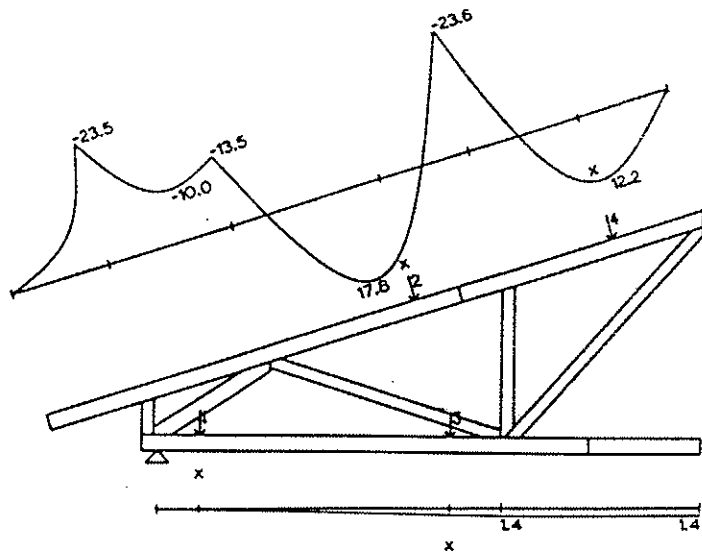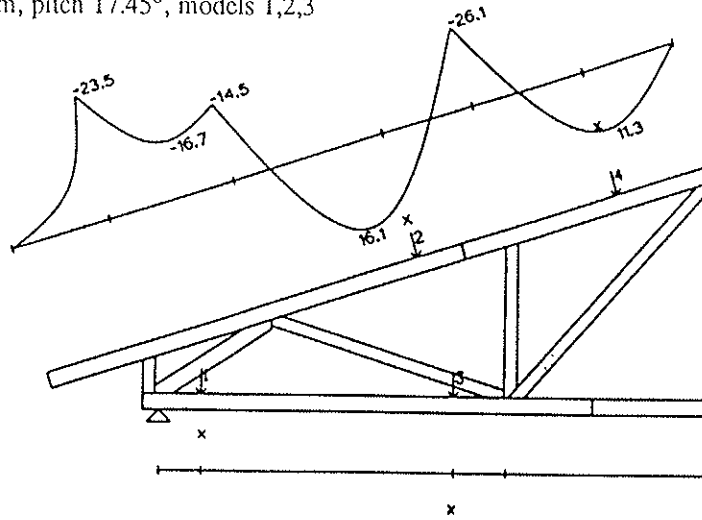
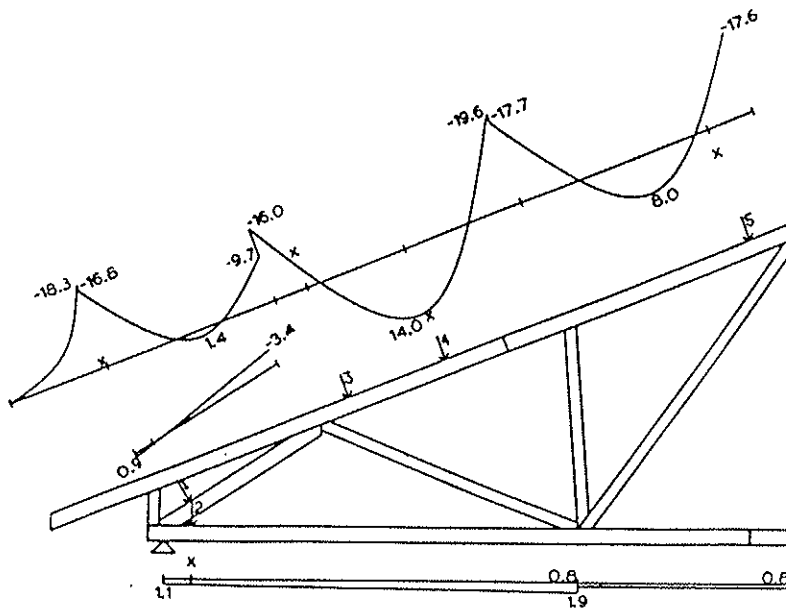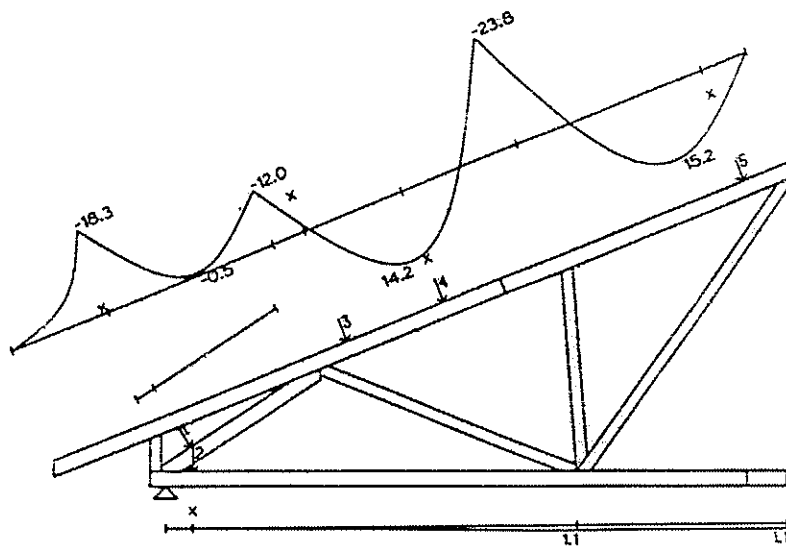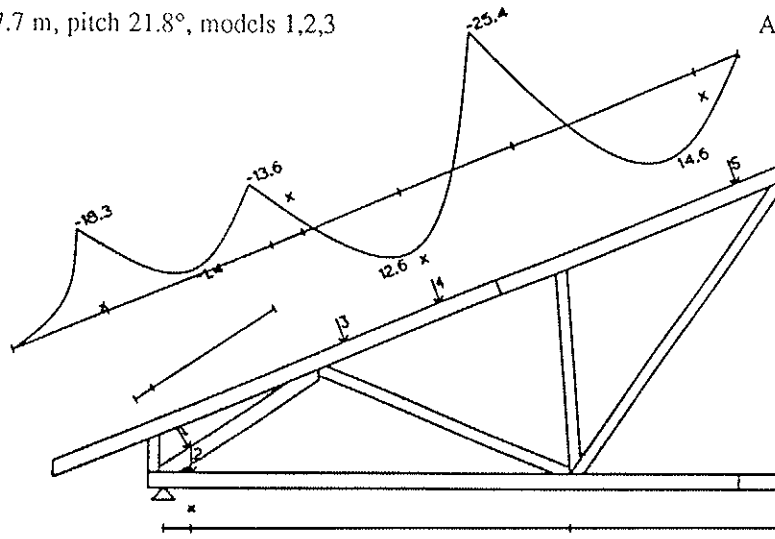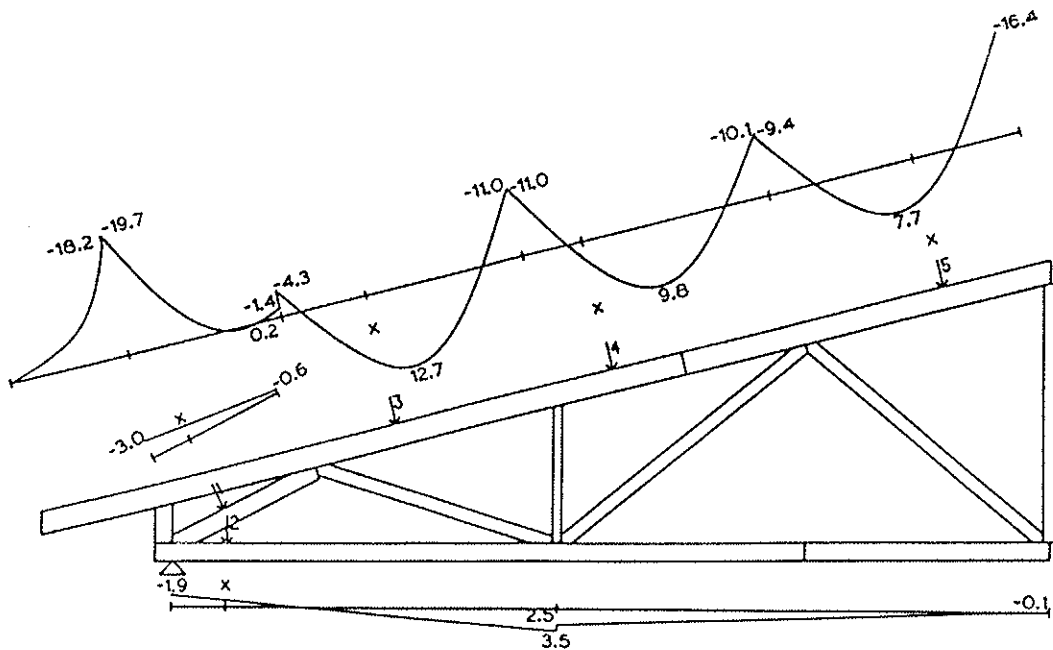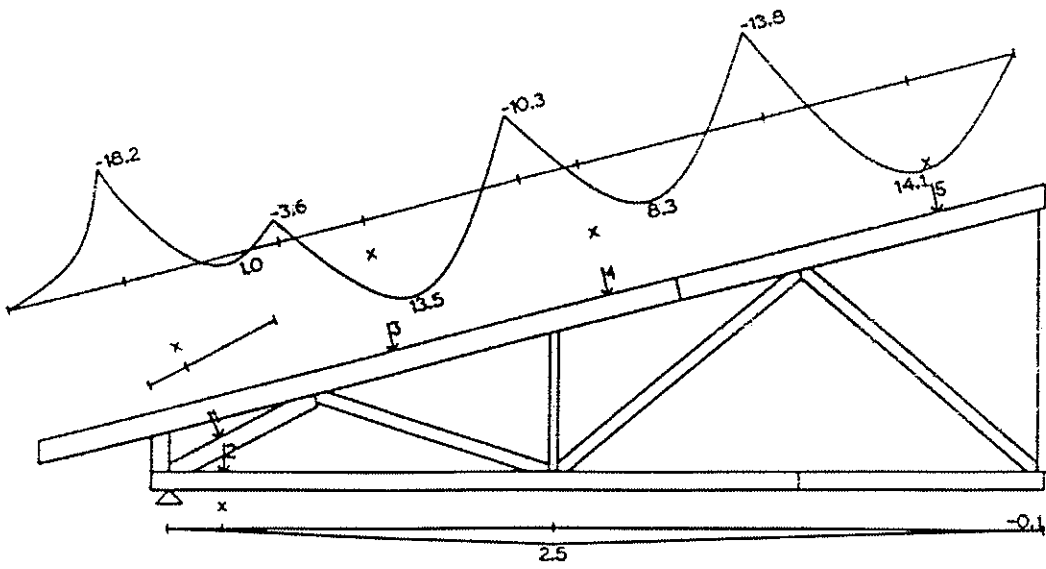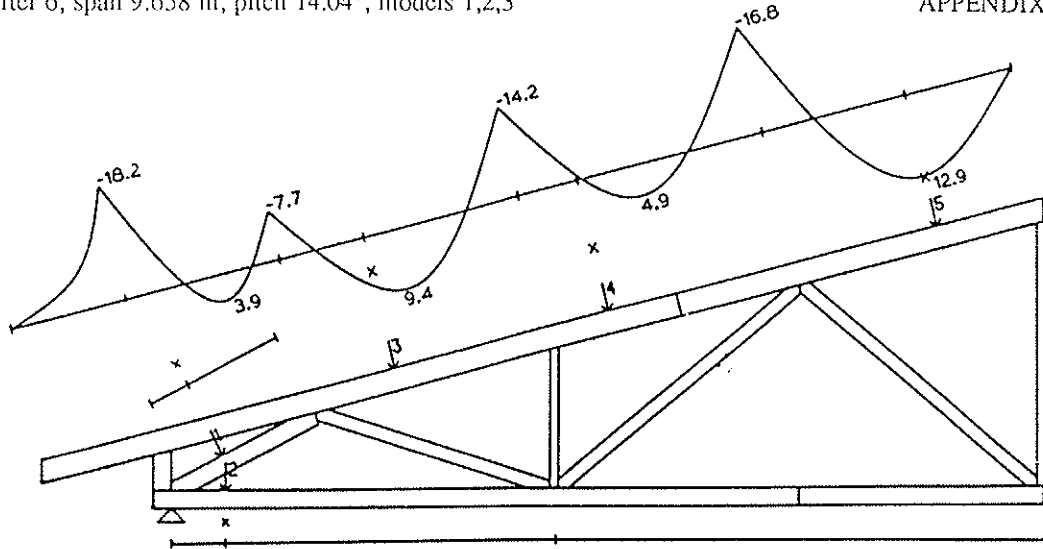Rafter 3, span 6.81 m, pitch 18.4°, models 1,2,3   APPENDIX 3

Rafter 4, span 6.8 m, pitch 17.45°, models 1,2,3

Rafter 5, span 7.7 m, pitch 21.8°, models 1,2,3
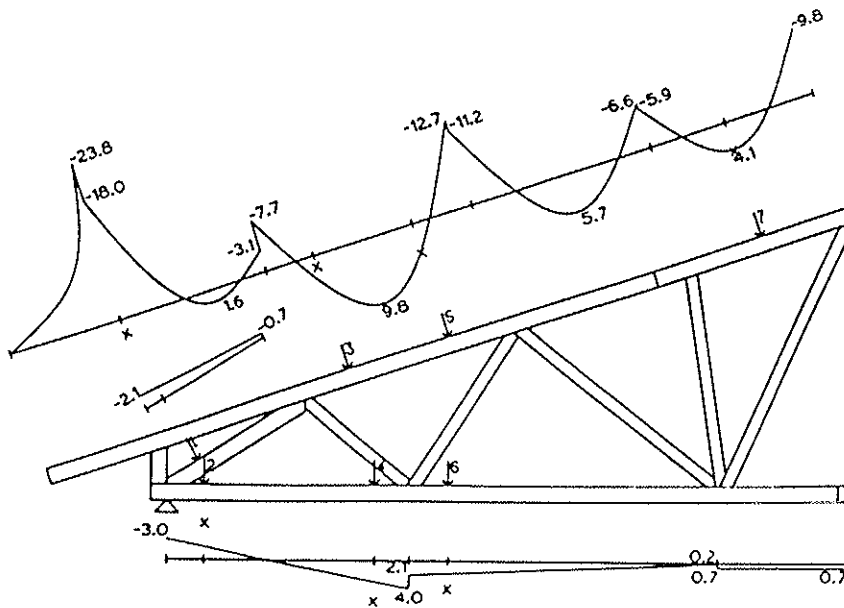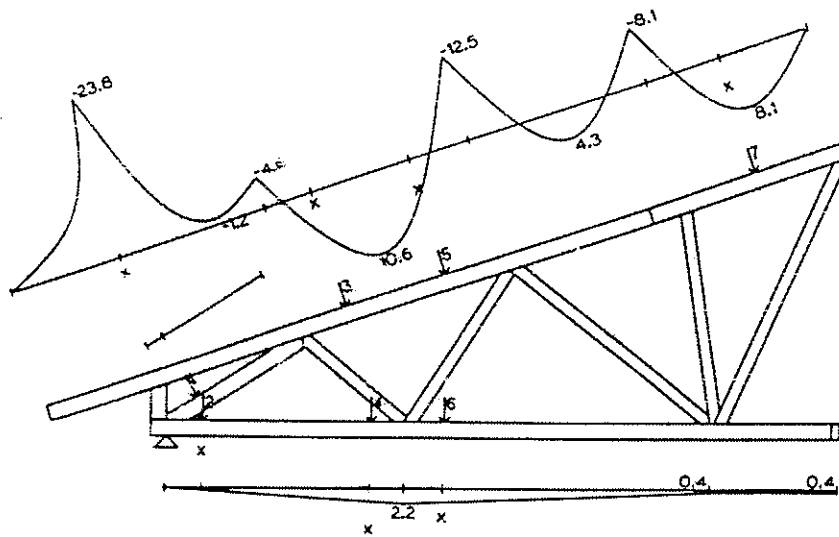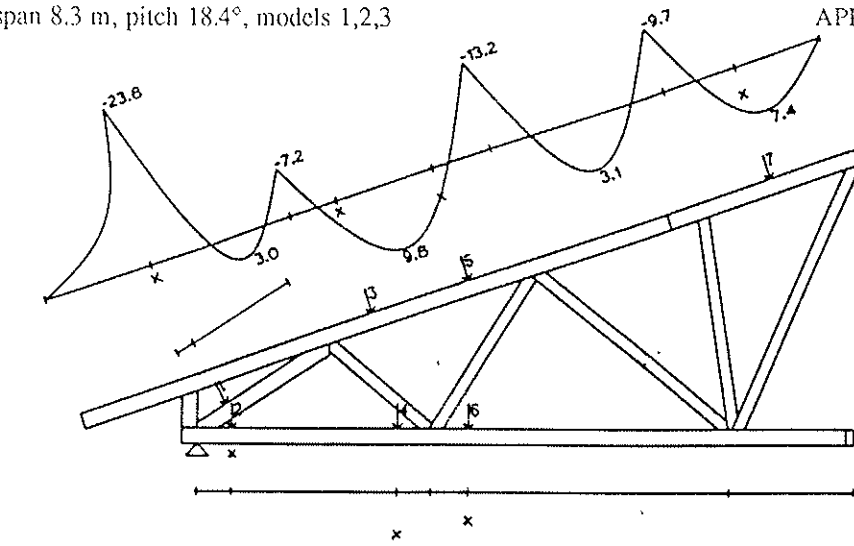
Rafter 6, span 9.658 m, pitch 14.04°, models 1,2,3

Rafter 7, span 8.3 m, pitch 18.4°, models 1,2,3   APPENDIX 7

Rafter 8, span 9.4 m, pitch 11.2°, models 1,2,3   APPENDIX 8

Rafter 10, span 7.66 m, pitch 26.57°, models 2,3
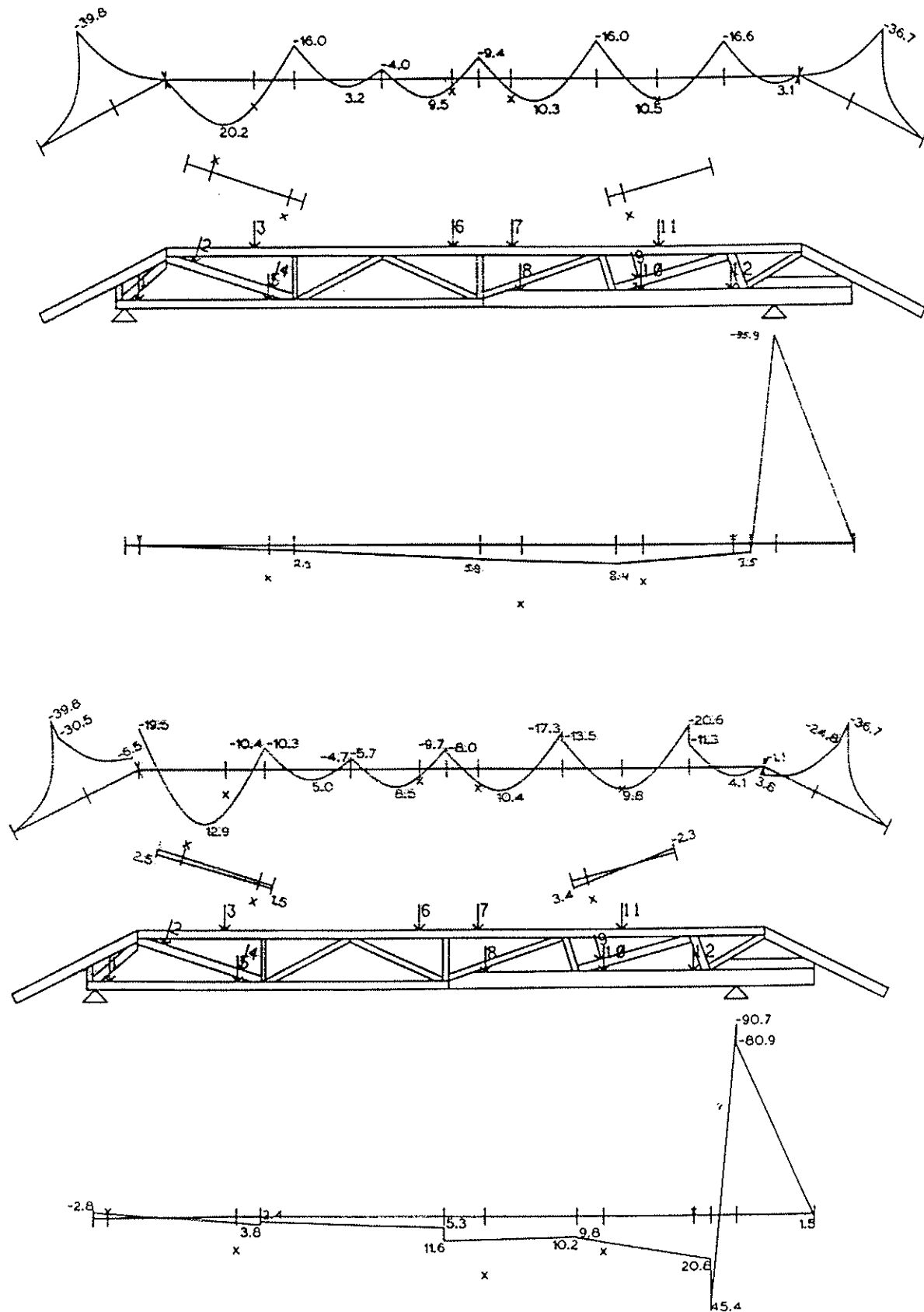
Rafter 1 ,span 8.06 m,pitch 18.4 ,load cases 1,2,3   APPENDIX 11
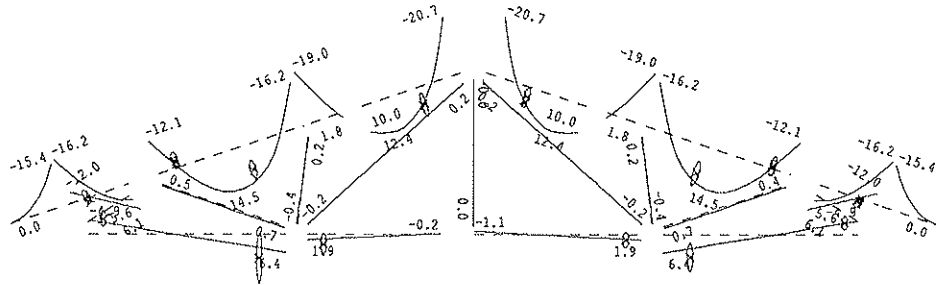
Support reaction 28.27 kN

Support reaction 42.65 kN

Support reaction 53.93 kN

Rafter 2 ,span 9.404 m,pitch 22 ,load cases 1,2,3   APPENDIX 12

Support reaction 24.64 kN
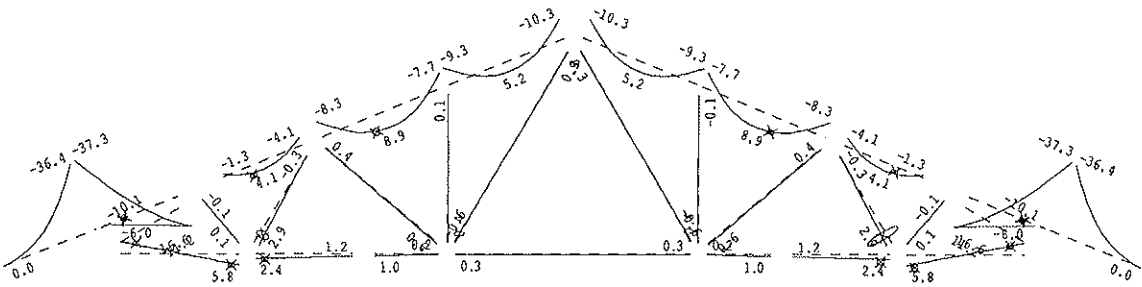
Support reaction 35.15 kN
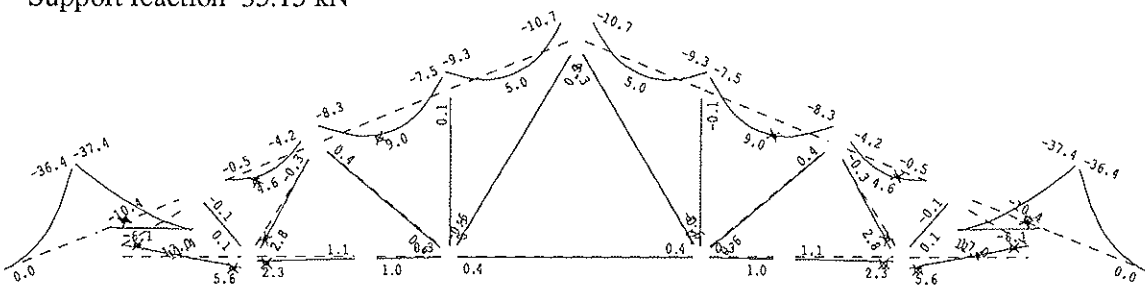
Support reaction 48.27 kN

Rafter 3 ,span 6.81 m,pitch 18.4 ,load cases 1,2,3

Support reaction 22.70 kN

Support reaction 33.91 kN

Support reaction 46.83 kN

Rafter 4 ,span 6.8 m,pitch 17.45 ,load cases 1,2,3,4   APPENDIX 14

Support reaction 16.42 kN

Support reaction 23.10 kN

Support reaction 32.50 kN

Support reaction 41.05 kN

Rafter 5 ,span 7.7 m,pitch 21.8 ,load cases 1,2,3
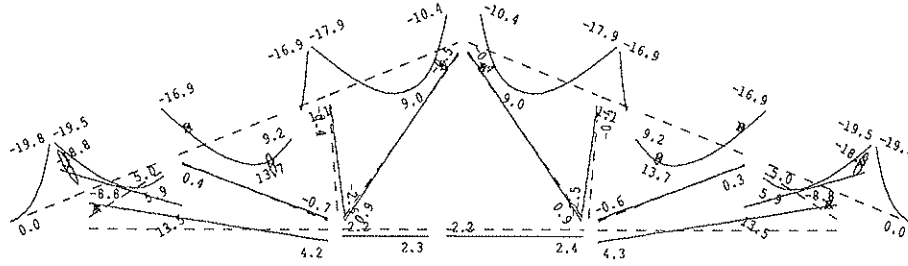
Support reaction   17.09 kN
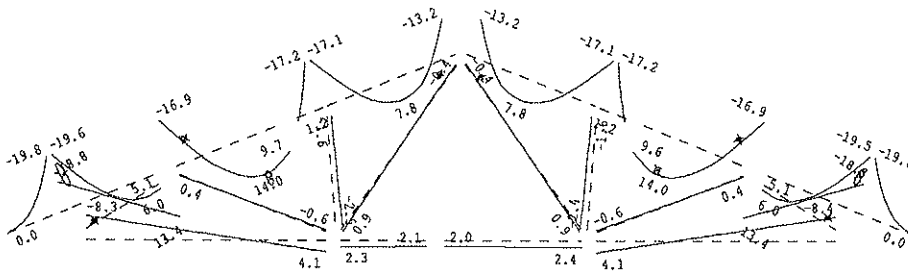
Support reaction   25.59 kN
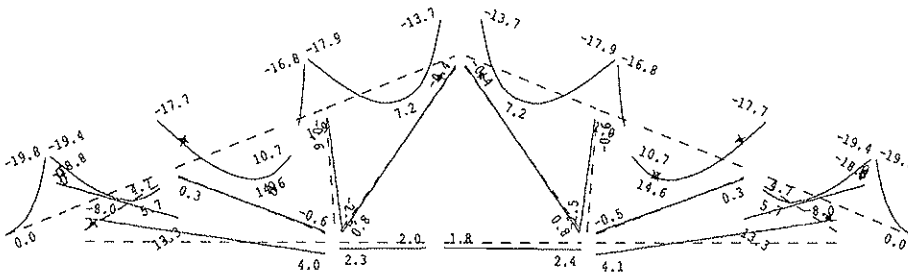
Support reaction   34.39 kN

Rafter 6 ,span 9.658 m,pitch 14.04 ,load cases 1,2,3
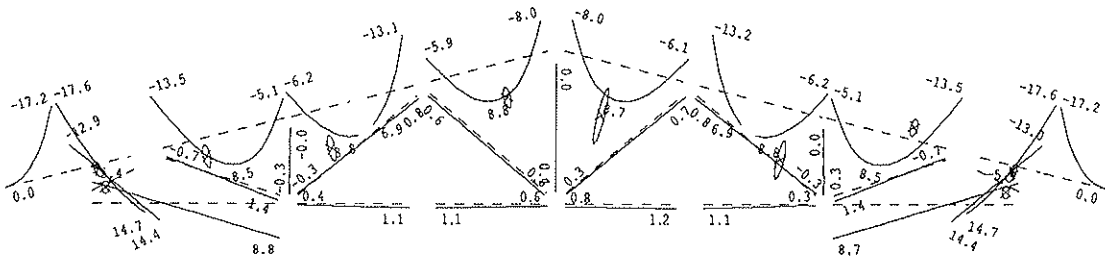
Support reaction 19.29 kN
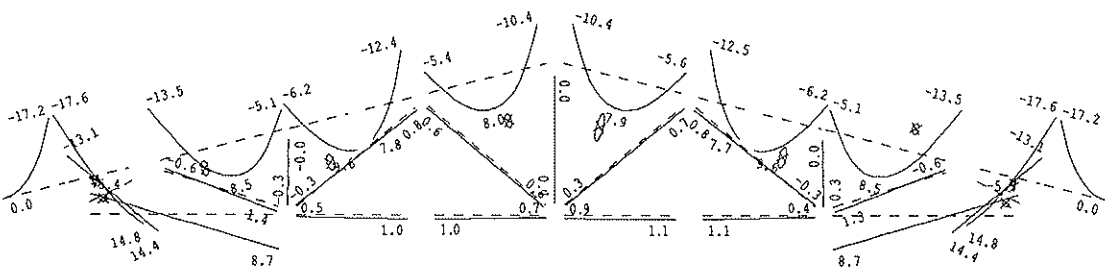
Support reaction 30.40 kN
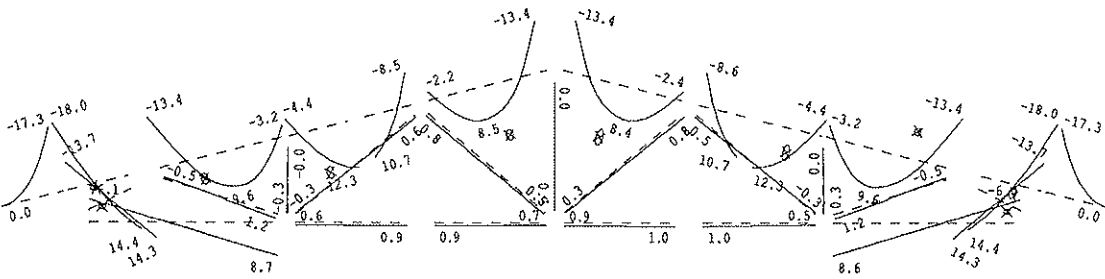
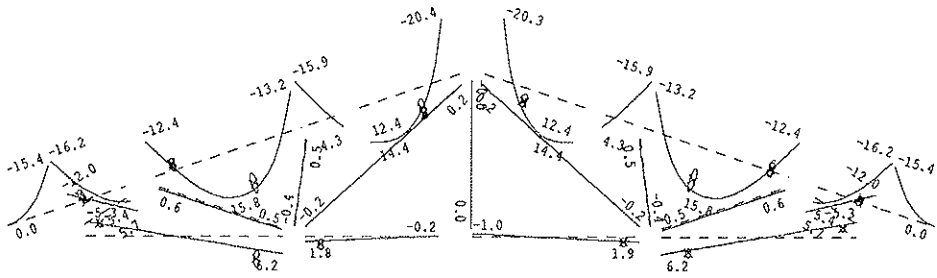Support reaction 41.59 kN

Rafter 7 ,span 8.3 m,pitch 18.4 ,load cases 1,2,3   APPENDIX 17
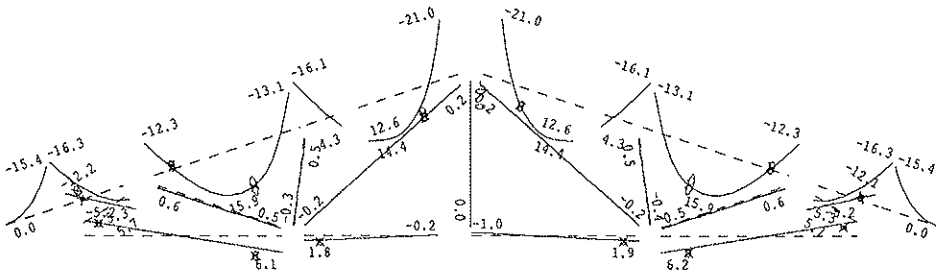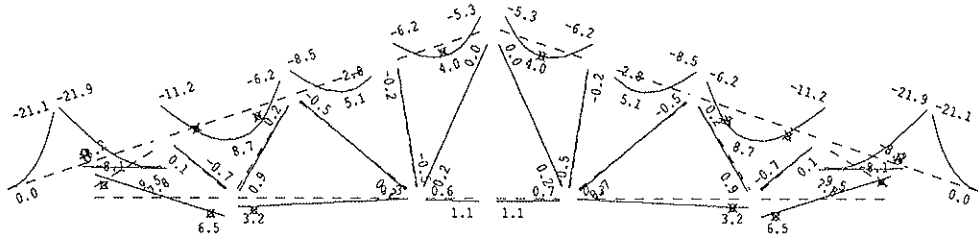

Support reaction 21.60 kN
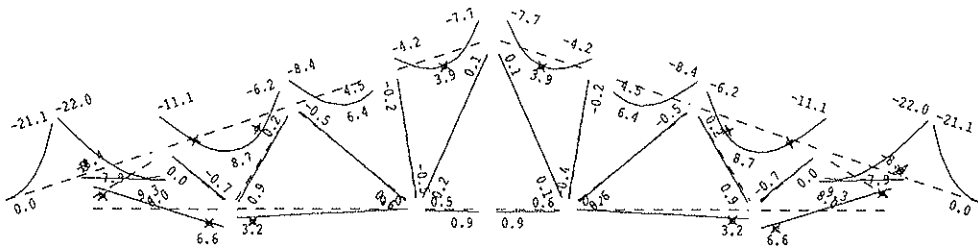
Support reaction 32.50 kN
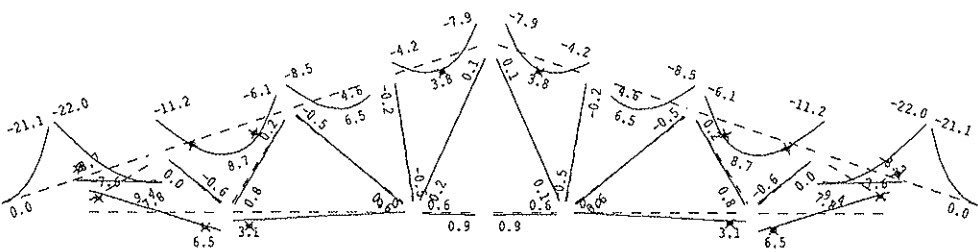
Support reaction 42.41 kN

Rafter 8 ,span 9.4 m,pitch 11.2 ,load cases 1,2,3

Support reaction 20.00 kN

Support reaction 29.71 kN

Support reaction 39.50 kN

Rafter 9 ,span 9.51 m,pitch 21.8 ,load cases 1,2,3
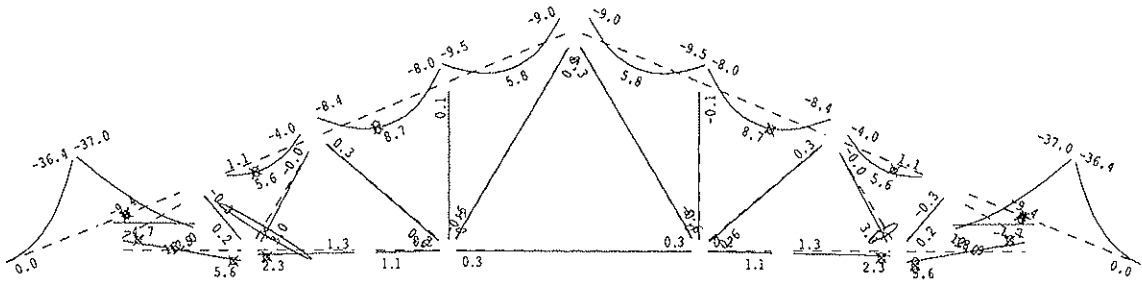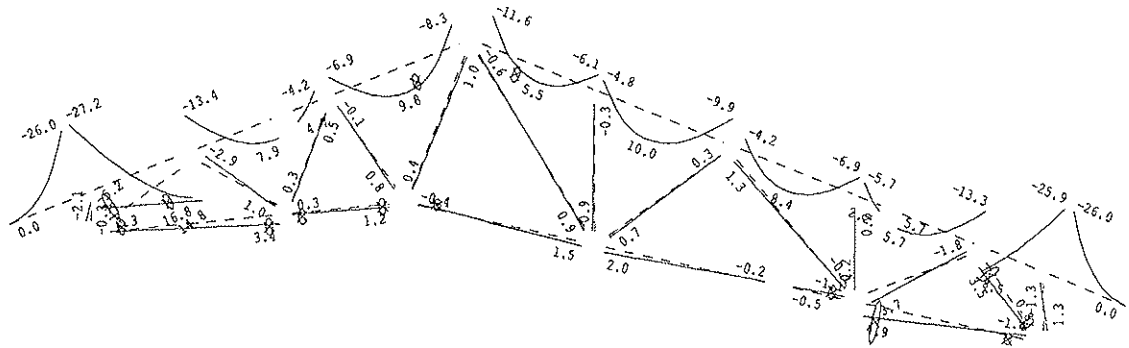

Support reaction 19.69 kN
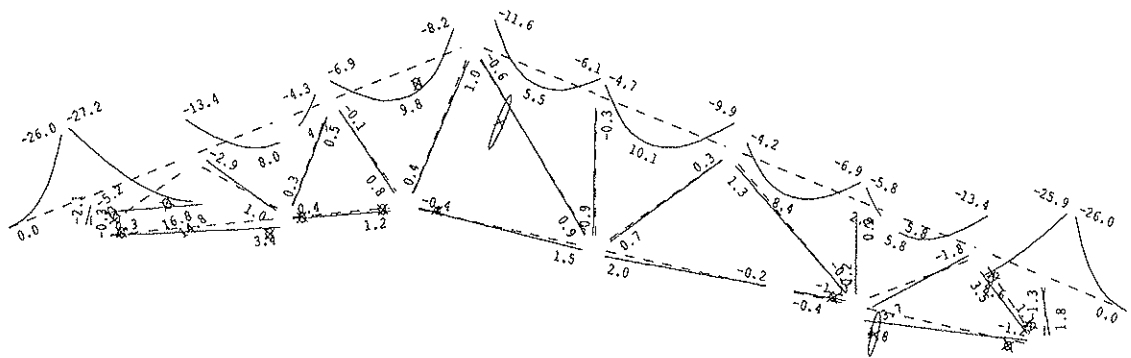
Support reaction 29.39 kN
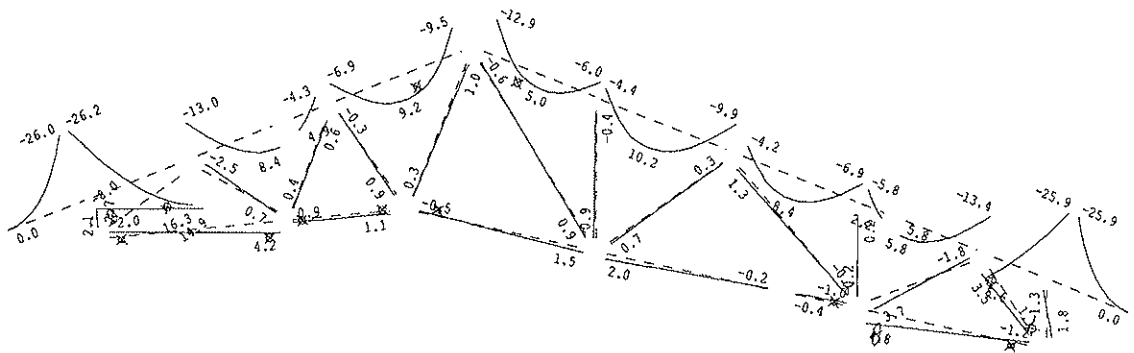
Support reaction 40.09 kN

Rafter 10 ,span 7.66 m,pitch 26.57 ,load cases 1,2,3   APPENDIX 20
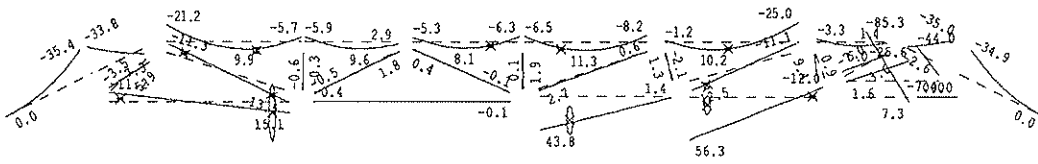
Support reaction 12.90 kN
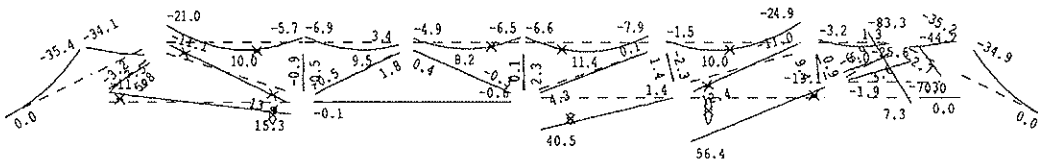
Support reaction 26.01 kN
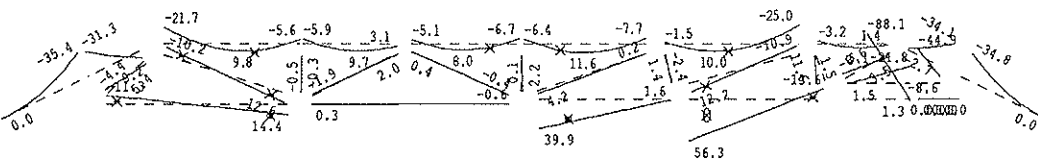
Support reaction 50.33 kN

INTERNATIONAL COUNCIL FOR BUILDING RESEARCH STUDIES AND DOCUMENTATION

WORKING COMMISSION W18A - TIMBER STRUCTURES

PRACTICAL DESIGN METHODS FOR TRUSSED RAFTERS

by

A R Egerup
United Kingdom

MEETING TWENTY
DUBLIN
IRELAND
SEPTEMBER 1987

PRACTICAL DESIGN METHODS FOR TRUSSED RAFTERS.

Introduction.

Since 1973 the CIB W18 truss group has discussed design methods for trussed rafters.During that time millions of trusses have been produced.These have generally been very satisfactory, due mainly to the industry. Relatively few failures are due to actual errors in design, but errors are very often caused by faulty workmanship, faulty materials or lack of lateral support. The design is satisfactory mainly because of the vast experience of the designers in the truss industry. In many countries a considerable number of full-scale tests of standard trusses are carried out and form a basis for the design. What, then, is the reason for concern about the design of trussed rafters?

The real problem in most countries is in ensuring that the industry performs according to common design rules to obtain the required safety for the structure. In this way the industry can compete on equal terms, producing a structure with the required factor of safety and at the same time giving an optimum structure with minimum use of resources.

Existing Design Methods:

Existing design methods fall into two categories:

1. Simplified Methods and

2. Complex Methods.

Simplified methods often give the "right" result whereas complex
methods often give a conservative solution. This can be proved by
mathematics or energy methods and can be seen, for example, for
different types of finite elements. The simplified method, such
as moment coefficients, can more easily be adjusted to, say,
full-scale tests by "adjusting" the moment coefficients or the
buckling lengths.

A complex method, for example a finite element model, is very
rigid and members are more inter-related so that it becomes
difficult to adjust to full-scale testing.

The difference in the two types of method is that the complex
method takes more effects into account. Most people agree that a
design method for trussed rafters must be based on a complex
finite element model (frame model), but so far no one model has
proved satisfactory over the whole range of trusses. Why does a
complex model not give the right answer? This is because the
model is still simplified and does not take all effects into
account. Among the more important effects are:

    1. Slip in joint

    2. Rotational stiffness in joints

    3. Non-linear behaviour

    4. Strength distribution in joints and members

    5. Real buckling length

    6. Redistribution of stresses
       in a non-determinant structure
    7. Probability of failure in a non-determinant structure

    8. Interaction formula

It is very difficult to take all these effects into account in a
day-to-day design method where speed is an important factor for
the industry. For example, the strength distribution along
members related to a failure criterion can only be determined
with a probabalistic method which will be very time-consuming.
The non-linear behaviour of the model is different for trusses
with low pitches and high pitches, mainly because of different
slip behaviour in the heel-joint.

As a failure criterion, the inter-action formula has proved to be
very poor for determinant structures.

A complex model which takes all important effects into account is
impossible to work with. However, a combination of a complex
model and full-scale testing will often take all the effects into
account in a more simple way and produce a reliable design.

The existence of ever more powerful micro-computers and the new science information technology make possible the production of designs for commonly-used trusses by using a data base system. The data for the full range of trusses will be produced partly by calculations and partly by using full-scale tests. A data-based programme can be used to retrieve the relevant values of a required truss.

The data-base system will be a convenient and fast procedure for the truss industry to work with and will ensure optimum structures complying with safety systems, as well as providing authorities with a possibility for efficient control.

INTERNATIONAL COUNCIL FOR BUILDING RESEARCH STUDIES AND DOCUMENTATION

WORKING COMMISSION W18A - TIMBER STRUCTURES

BEHAVIOUR FACTOR OF TIMBER STRUCTURES IN SEISMIC ZONES

by

A   Ceccotti and A   Vignoli
University of Florence
Italy

MEETING TWENTY
DUBLIN
IRELAND
SEPTEMBER 1987

BEHAVIOUR FACTOR OF TIMBER STRUCTURES IN SEISMIC ZONES

by   A. CECCOTTI and A. VIGNOLI

Department of Civil Engineering - University of Florence

SUMMARY

The ideas pertaining to the definition of the structural behaviour factor for the structures' design in seismic zones are re-examined. A method of evaluating the behaviour factor of plane timber structures composed of rigid (glued) joints or seimi-rigid joints (i.e. dowels) is presented. Behavioural laws relating to the timber's structural elements and their joints under cyclic loads were obtained experimentally.

Accelerograms, applied to the base of the structures, were pulled out on the basis of their response spectrum as defined by the italian draft proposal CNR-GNDT. The acceleration values corresponding to the elastic field limit and the point of collapse (i.e. A_y, A_u) were obtained using a direct integration technique with a DRAIN-2D non-linear analysis computer program. The behaviour factor was definied as the ratio between A_u and A_y. The values of this coefficient in the case of semi-rigid joints can even be ten times greater than the values obtained for rigid joints. At the conclusion of the research a critical analysis of the results was carried out, indicating suggestions for further research.

1. INTRODUCTION: STRUCTURAL RESPONSE TO EARTHQUAKES

1.1 Characteriscs of Seismic Input

In the study of structural behaviour, seismic actions can be regarded as random dynamic motions of the foundation soil. Typical records of one component of ground (i.e. acceleration) during a medium magnitude earthquake are shown in Fig. 1a; but the details of the motion can never be reproduced identically even if a quake of the same general characteristics occured in the same site. Therefore, the essential properties of seismic input are not well described by the actual records. In recent years the "response spectrum" has been often used to satisfy this need.

A "response spectrum" is definied as the response of an
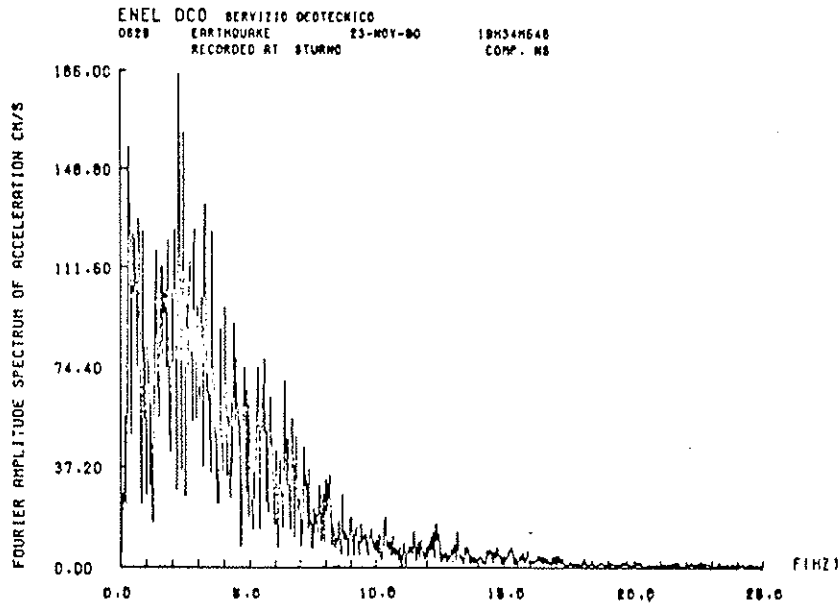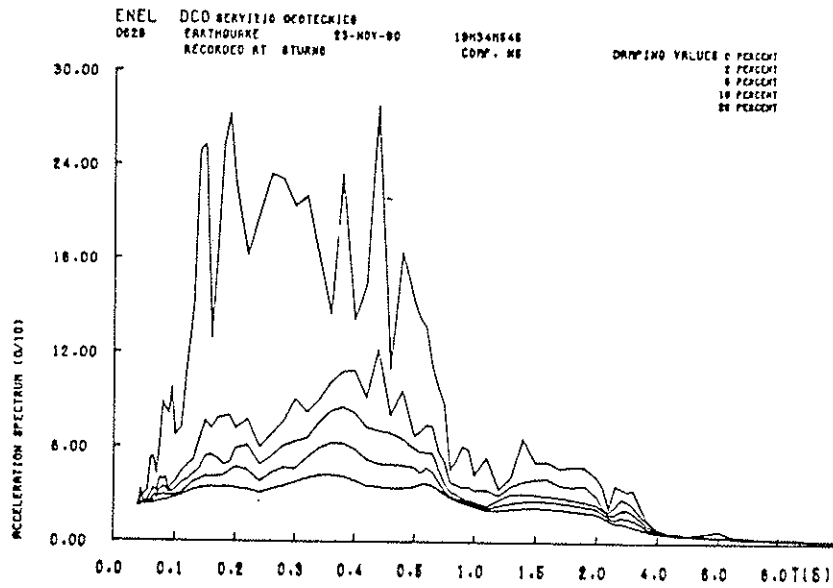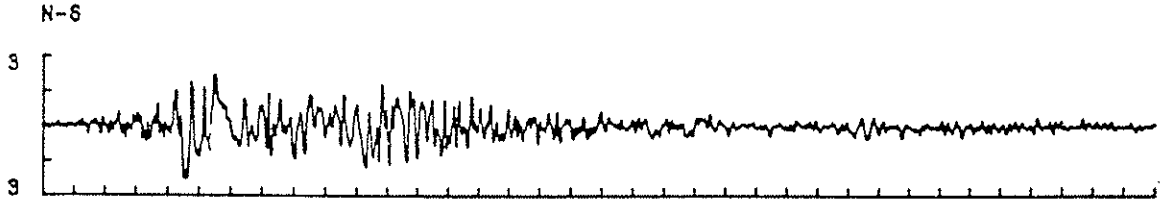
Fig. 1 - Campania-Lucania Earthquake: Sturno N-S Accelerogram a); Acceleration Response Spectra b); and Fourier Spectrum c).

elementary oscillator (Fig. 2) varying its own frequency with a given damping, subjected to the seismic motion under consideration. Following this definition, acceleration, velocity and displacement spectra can be plotted. All available earthquake responses in a given seismic area are then "smoothed" to obtain the standard spectrum, used for structural design. As an example, the acceleration response spectrum of the earthquake of Fig. 1a are shown in Fig. 1b. It is useful too to know the Fourier spectra which summarizes the "frequency content" of the earthquake (Fig. 1c).
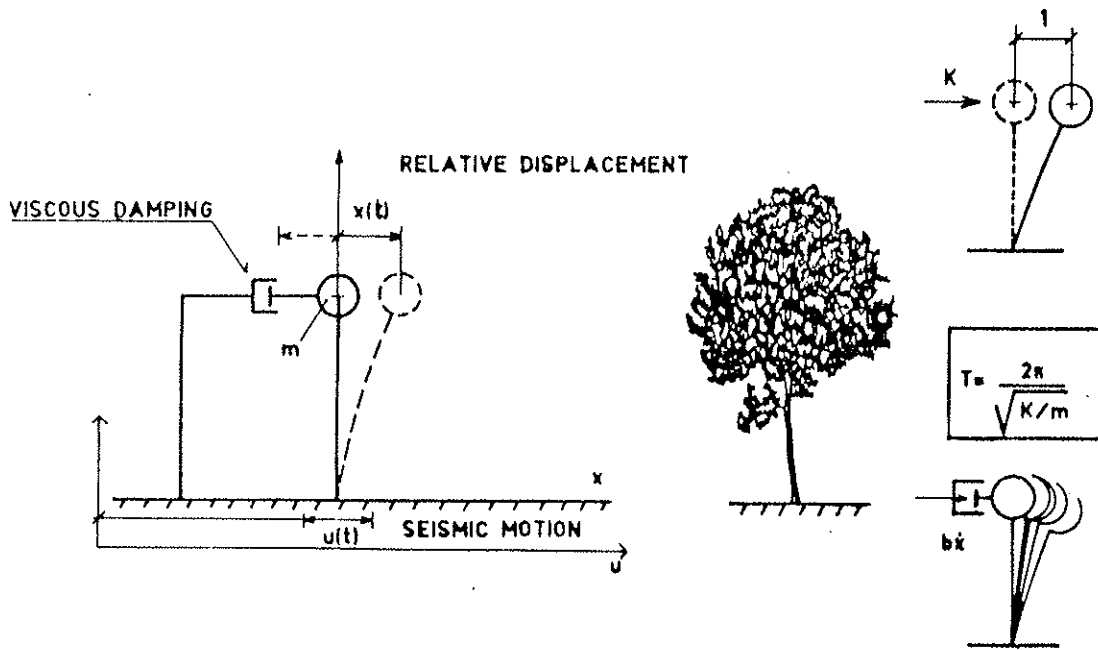
Fig. 2 - Elementary Oscillator and Seismic Action (Diagrammatic)

1.2 Structural Behaviour; Ductility

Strong accelerations and consequent inertia forces connected to the elastic responses even under a moderate earthquake very often overcome the elastic limits of a structure. Therefore, during the seismic motion, the structure "softens", varies its own period of oscillation, dissapates kinetic energy and, thanks

3

also to the cyclic character of the input action, "has time" to invert its motion prior to collapse. Thus, the capacity of the structure to develope plastic deformations without breaking becomes an essential part of its capacity to resist a seismic input.

This structural property is characterized by "ductility", which is conventionally defined as the ratio between the ultimate value x_u of an appropriate response parameter (e.g. horizontal displacement) in the "actual" elastic-plastic behaviour and the value x_y of the same parameter at the limit of elasticity. This ratio can be shown (Fig. 3) to be equal to the ratio between the forces, F_{el} and F_u respectively, that correspond to x_u in the elastic-plastic behaviour and in an ideally, indefinitely elastic behaviour.

1.3 Approximate Assessment of Non-linear Response

The maximum displacement of a single-degree-of-freedom system effected by an earthquake is approximately proportional to the earthquake's intensity, even if it can create "plastic zones". The above simplifying hypothesis is overstated, but it provides useful qualitative results, even if the problem can be studied without it.
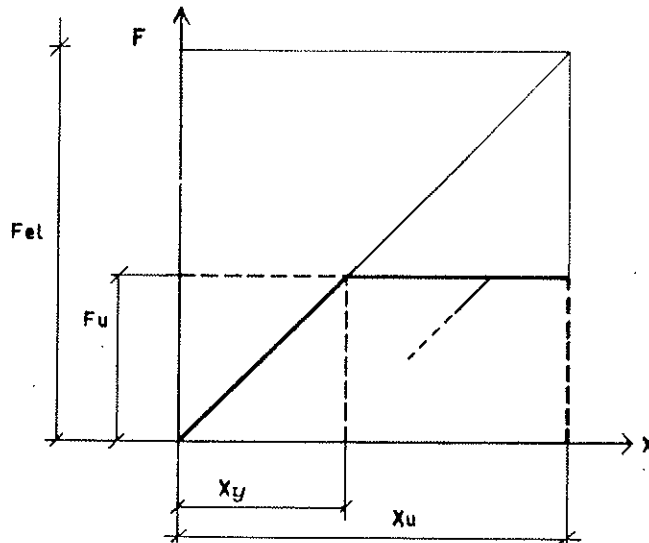
Fig. 3 - Conventional Load-Displacement Diagrams

The Fig. 4 illustrates this criterion. In Fig. 4a the response spectra relative to three different intensities; A_1, A_2, A_3, correspond to the same accelerogram's shape.

4

a)

$A_2 = 2A_1$
$A_3 = 3A_1$

$R(T) = \dfrac{0.862}{T^{(2/3)}}$

b)

$x_2 = 2x_1$
$x_3 = 3x_1$

c)
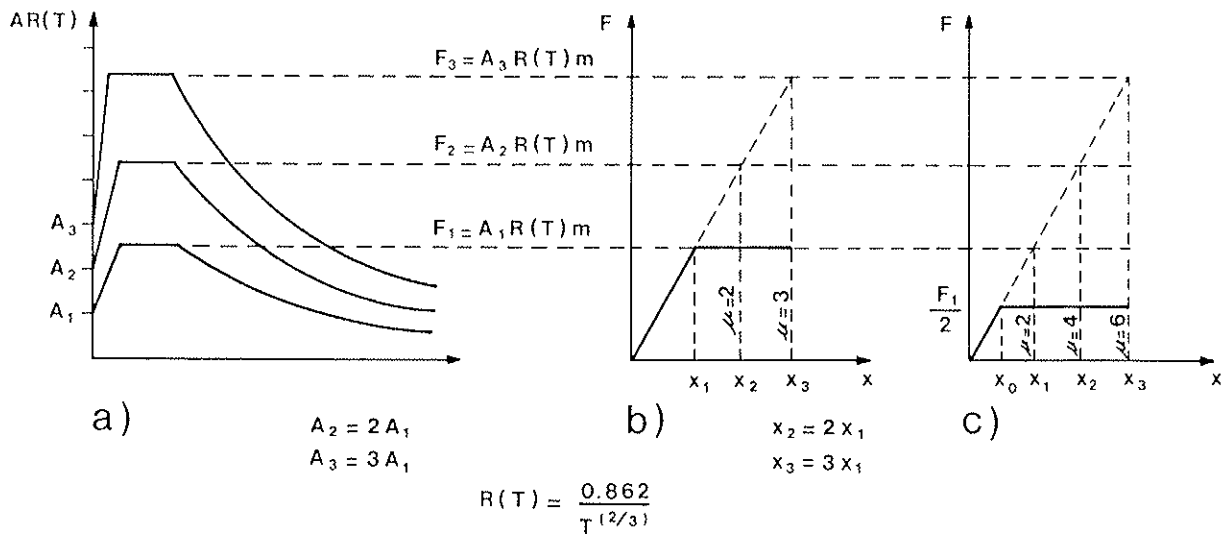
Fig. 4 -   Approximate Assessment of Non-Linear Response (Diagrammatic, from /2/)

The three earthquakes affect the single-degree-of-freedom structure with unitary mass m and stiffnes K (Fig. 2). In the three cases:
a - a structure with total elastic behaviour; b - a structure with a yield limit of F_1 (Fig. 4b); c - a structure with a yield limit of $F_1/2$ (Fig. 4c).

The displacements (x_1, x_2, x_3) caused by the three earthquakes are always proportional to the intensities A_1, A_2, A_3. The displacements can be calculated, based on the initial stiffness of the structure, following this formula:

$$x = AR(T)m/K \qquad (1)$$

The structure shown in Fig. 4b was designed in such a way that it reached the yield limit during the A_1 earthquake. The displacement corresponding to the yield limit is (in this case) $x_y = x_1$. One can see from Fig. 4b that the earthquake $A_2 = 2A_1$ requires a ductility of $\mu = 2$, and the quake $A_3 = 3A$, requires a ductility of $\mu = 3$.

The structure represented in Fig. 4c has a yield limit half of the prior case. This structure was designed to withstand a seismic event $A_1/2$ in the elastic phase. Since the absolute displacements produced by ⟨the three earthquakes equal those of

5

the prior structure and its x_y is half that of the preceding structure, the ductility requirements are doubled. Violent earthquakes force the structure to enter the plastic phase much more as the earthquake increases, relative to seismic action that procuces the yield point.

In spite of the above, structures have an intrinsic capacity to withstand a certain degree of plasticization without serious disconnectedness that provoke collapse.

Given the hypothesis that the available ductility of the two structures, whose diagram load-displacement is shown in figures 4b e 4c is $\mu_D = 3$ and $\mu_D = 6$, both structures reach the collapse point with the same intensity A_3 earthquake. These two structures then give the same guarantee against collapse even if designed at two different resistance levels. The smaller resistance of structure c is compensated by its greater deformability in the plastic field.

Given the preceding arguments it is possible to formulate a design criterion based on the plastic capacity of structures with already established seismic collapse acceleration:

1. A normalized response spectrum R(T), whose shape reflects the dynamic characteristics of the soil, is given. This spectrum also covers the uncertainties relative to the frequency content of a forseen event.
2. The value A_u of the collapse acceleration is given.
3. The available ductility μ_D is defined.
4. Following the design spectrum, the structure's yield resistance is designed:

$$A_u R(T)/\mu_D \qquad (2)$$

The above criterion is clarly derived from the simplified hypothesis regarding non-linear response. The criterion is only valid in the realm of the hypothesis which approximates the reality of the non-linear dynamic behaviour.

Moreover, the analysis conducted up to this point is applicable to elements or structures that show behaviour comparable to that of the simple element. The use of this analysis for more complex structures is not simple because the plastic zones caused by the earthquake appear and avolve along the structure, depending on: stiffness and resistance ratios between the elements, the modal shapes excited during vibrations. The terms, "required ductility" and "available ductility", defined as displacement ratios can be referred either to each section or element, but not to the entire structure.

6

1.4 Structural Behaviour Factor

The structural response to earthquakes can be solved by the numerical integration of the general equation of the dynamic equilibrium, considering the behavioural laws pertainig to the sections and joints in the non-linear field. In this case, as widely demonstrated in /2/, it is always possible to apply the simplified rule for the evaluation of the design spectrum with a fixed value of the "required ductility" μ using the elastic response spectrum devided by the "behaviour factor" $q(T, \mu)$. This coefficient is defined by the ratio between the collapse acceleration (A_u) and the acceleration that produces the design stress (A_y):

$$q = A_u/A_y \qquad (3)$$

We underline that the structure is designed in such a way that the sections reach the yield point when stressed by the acceleration A_y.

This design criterion is appropiate for buildings prone to seismic actions. This collapse acceleration value A_u and the structural behaviour factor value q related to the structure's typology are defined by following the national seismic standards.

The design acceleration is then calculated as $A_y = A_u/q$, then the elastic analysis of the structure is conducted. The design of sections is then carried out so that the sections' resistance to the yield point equals the stress calculated by the above (2) formula.

When an earthquake's intensity is smaller than A_y, the structural response obviously remains in the elastic field; otherwise the plasticization effects the structure's response.

Following commonly used technical standards, the definition of a (forfait) value for this reduction coefficient is based only on the structural typology. This forfait value already presumes an even greater ductility reserve.

2. OBJECTIVES

Timber used for construction, unlike small timber samples which contain no faults, shows a linear-elastic behaviour when stressed parallel to the fibers up to the point of collapse.

This linear-elastic response depends on the species and quality of timber. Despite these two variables there is always a

brittle failure. On the other hand ductility and the capacity of dissipating energy can be recuperated in the joints. The same thing happens when the structure is stressed transversally to the fibers.

Recently, GNDT Commission of CNR (Italian National Research Council) submitted a new proposal for rules dealing with buildings in seismic zones to public scrutiny. Actually, the theoretical and experimental knowledge of timber structures is not comparable to that of steel and reinforced concrete structures; therefore choosing the behaviour factor values q has not been yet standardized. The same Commission that prepared the GNDT-CNR standardized proposal for seismic zones, prudently chose a coefficient value q = 1 for all timber structures, and q = 2 value for timber and plywood frameworks.

In reality, the standard typologies for timber structures show an efficient response to earthquakes. The Commission's cautious choice was based on two facts: the limited knowledge of the joints behaviour under cyclic loads compared to that of other materials, and the limited available data for a set of standards based on the limit states design.

The objectives of the present research is to quantify the variation of the structural behaviour factor using numerical simulation methods (see /6/). Timber structures with simple static schemes were tested. Different behavioural laws obtained experimentally were given to the joints. Seismic actions with different frequency content values, obtained from the same response spectrum were simulated.

3. METHODS

3.1 The Geometrical Characteristics of The Model

Two types of simple glue-laminated portals: base restrained (T_o = 0.26 sec) and base hinged (T_o = 0.52 sec) were numerically simulated. The sections dimensioning was conducted with a vertical service load of 10 kN/m placed on the beam, and a horizontal service load of 0.3 kN/m acting on the colums. The horizontal load simulated the wind effect that, according to the actual standards, is more dangerous than seismic actions. The DIN standard /7/ values for glue-laminated first class European whitewood timber sections were used as reference values for the possible service stress values. In order to use a one-dimensioning-design for the two different structural schemes, the worst situation for

the two structures was considered section by section. Consequently, the base restrained portal had over-dimensioned sections at the beam-column joints, and the base hinged portal had over dimensioned base sections. The final dimensions are shown in Fig. 5.

The joints were: rigid-glued, or semi-rigid, assembled with mechanical fasteners like dowels. The dimensioning of dowels in semi-rigid joints was conducted following DIN standards. This procedure was based on the service due to the load conditions described above. The beam column was composed of about 60 dowels of $\varnothing$8 mm with resistant double sections. The dowels formed a double ring centered at the crosspoint between the beam and the column's axis, Fig. 6.
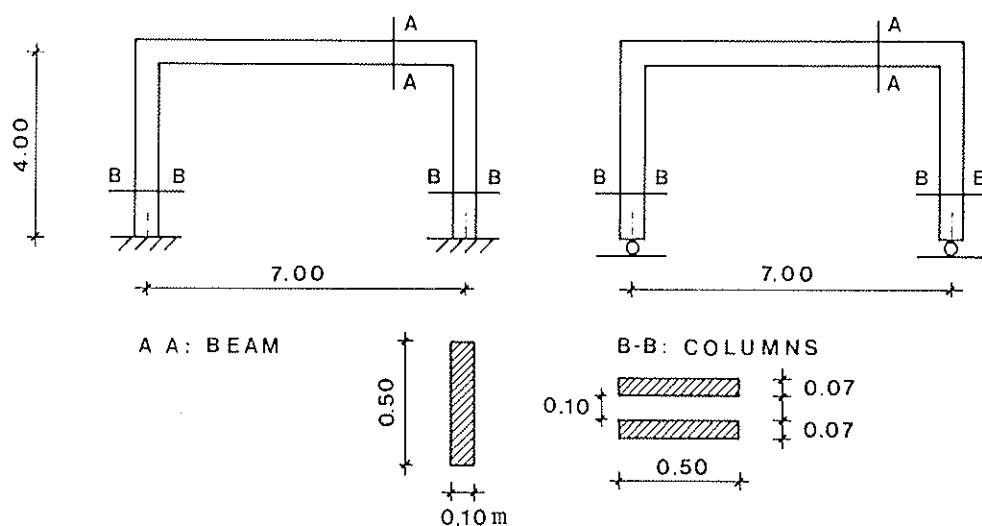
Fig. 5 - Dimensions of Model Studied
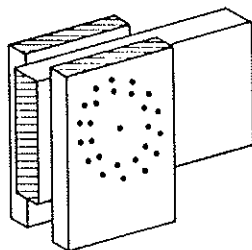
Fig. 6 - Types of Joint with Dowels Used for The Beam Column
Connections

9

3.2 Mechanical Characteristics of The Model

3.2.1 - A series of experimental tests were previously conducted, at the University of Florence Civil Engineering Department (/8/), in order to assess the behaviour of the connections and more specifically the behaviour of the dowels when stressed. The tested connections were similar to designed connections but reduced in size with single section resistant dowels. These joints were stressed with displacement control cyclic loads. A special test device (Fig. 7) was used to stimulate only the bending action without the influence of the shear and/or axial forces (/9/). Actually due to the large ratio between the full-scale structure's and the section's dimensions the contribution of the shear to the total load, supported by each dowel, is negligible compared to that of the bending moment. The joint behaviour under cyclic quasi static actions is like the one shown in Fig. 8 with the relevant skeleton curve. The behaviour of each dowel, no matter its position, demonstrated nearly the same behaviour due to the 90° crossed fiber arrangement. For this reason the ratio between the dowel's load and the timber's relative local displacement can be considered invariable.
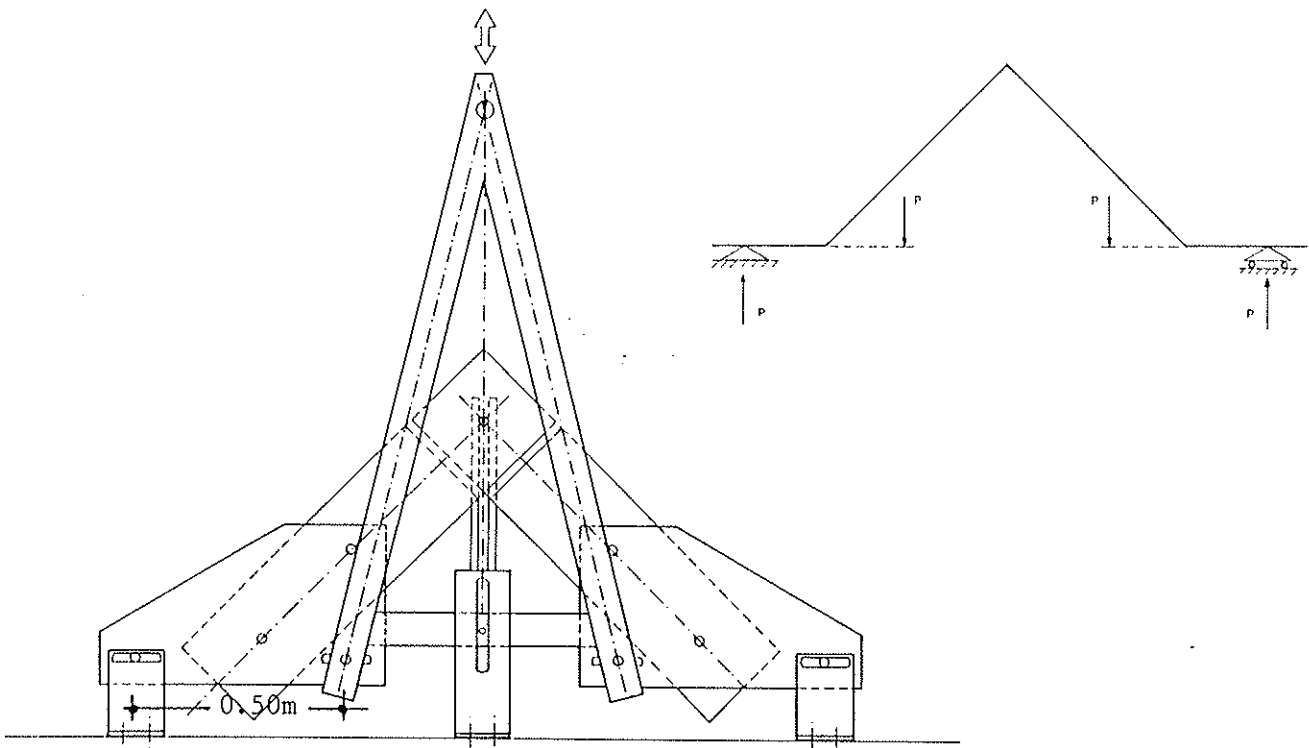
Fig. 7 -   Load Device for Cyclic Testing (from /8/) and Relevant
            Theoretical Scheme
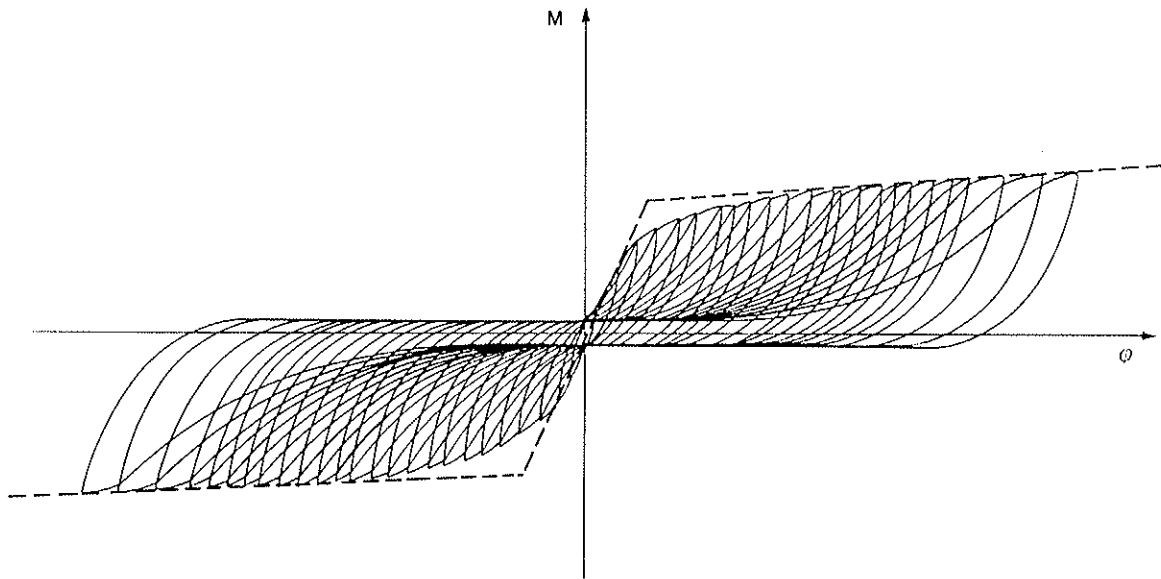
Fig. 8 - Moment-Rotation Law's Shape for Joint with Dowels (from /8/)

3.2.2 - The skeleton curve relationship between the moment and the designed joint's rotation was then constructed (Fig. 9). The improving coefficients, described in the technical literature (i.e. /7/) for the resistant dounble section dowels, compared to those used in the tested joint were also taken into account.

The joints' behaviour under cyclic loads was described, as in /6/, by a bilinear law (Fig. 10) that obviously can not express the real behaviour. Even if exact values can not be obtained by this law, it allows one to have a reasonable idea of the approximate values and above all of the general tendencies of the structural behaviour. A rigid behaviour was chosen for the glued joints (Fig. 9).
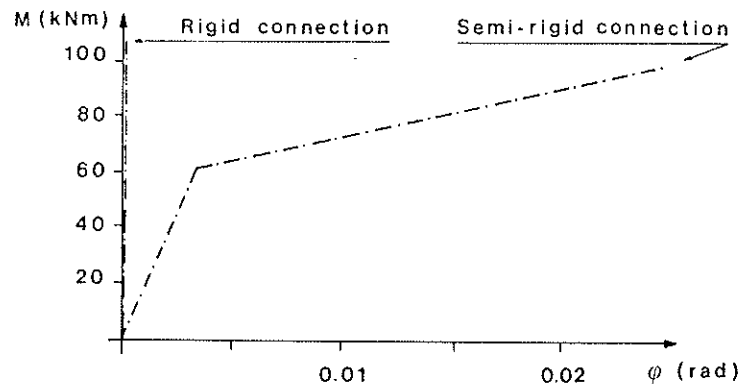
Fig. 9 - Moment-Rotation Laws Chosen for The Studied Model's Joints

11

A linear-elastic law was chosen for the basic material and used until the characteristic strength values under instantaneous loads were reached: - 30 MPa for bending, tension and compression; - 2.4 MPa for shear stresses.

The elastic instability of the colums in the frame plane was taken into account by means of an appropriate strength reduction.

The chosen value of 15000 MPa for the timber's elastic modulus was higher than the usual one for static loads, as shown in /10/. The viscous damping coefficient of the basic material was chosen 5% of the critical damping. The studied cases are summarized in Fig. 11.
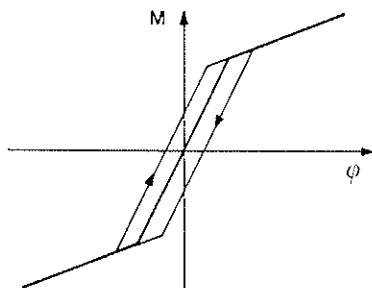
Fig. 10 - Behavioural Laws for Cyclic Loads, Used for Semi-Rigid Connections

Rigid connections   Semi-rigid connections
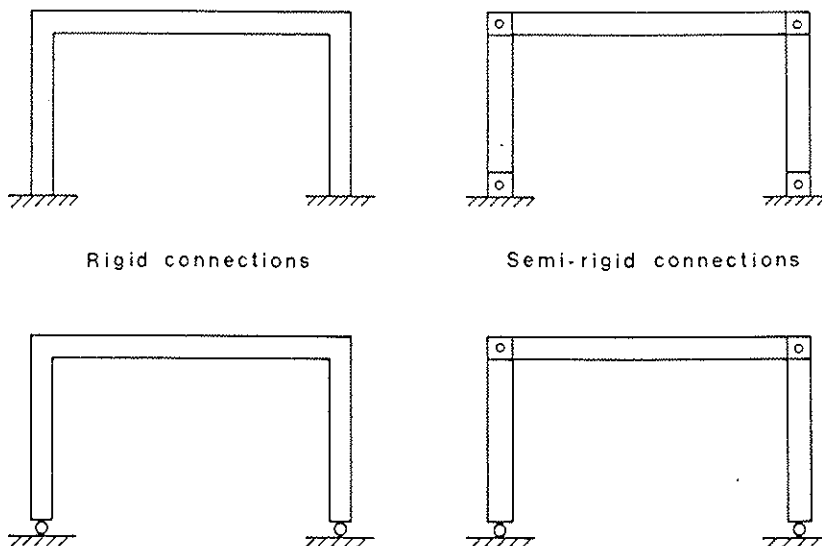
Fig. 11 - The Various Cases Studied

3.3 Numerical Simulations

The numerical simulation was conducted with a non-linear dynamic analysis computer program (DRAIN-2D) which uses the direct integration method. The tested portals supported their own weight and a vertical load of 10 kN/m applied to the beam. Six accelerograms were applied to the base of the portals:

a. Two of them were the North-South, and South-Est/North-West components of the Tolmezzo recordings, (Friuli, 1976).

b. Four of them were obtained using the SIMQKE program drawn out from the elastic response spectrum which correspond to the S_1 ground as reported in the CNR-GND standards for zones prone to seismic events.

These accelerograms demonstrate different frequency contents as shown in the Fourier analysis of Fig. 12. The maximum acceleration values (A_y), that corresponds to the elasticity limit, and the maximum acceleration value (A_u) that causes collapse, were assessed for: each structural scheme, each type of connection, and for each foreseen accelerogram shape. The occurance of the collapse mechanism depended on the types of the connections:

a. In the case of structures with rigid joints, given the timber's elastic-brittle behaviour, this mechanism corresponded to the collapse of the most stressed section.

b. In the case of smi-rigid joints plasticity is concentrated in the connections; the collapse takes place when a section breaks down and when the beam's displacement goes beyond the fixed value of $1/20^{th}$ of the portal's height.

The computer program takes into account the mechanical non-linearities and the P-delta effect in the columns.

3.4 Assessment of The q Value

The structural behaviour factor's value was calculated using the formula $q = A_u/A_y$; A_y indicates the acceleration corresponding to the elastic response limit; A_u represents the acceleration that produces collapse.

4. ANALYSIS OF THE RESULTS

The most important results pertaining to A_y, A_u, and q are shown in Fig. 13-14-15-16. The reference frequency content, also called dominant frequency ($\bar{f}$), was assessed for each accelerogram's shape, calculating the weighted average of the three
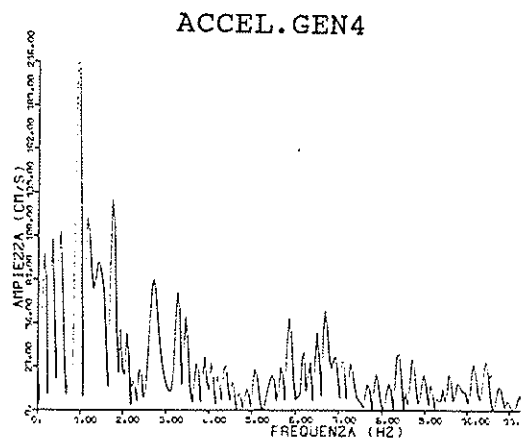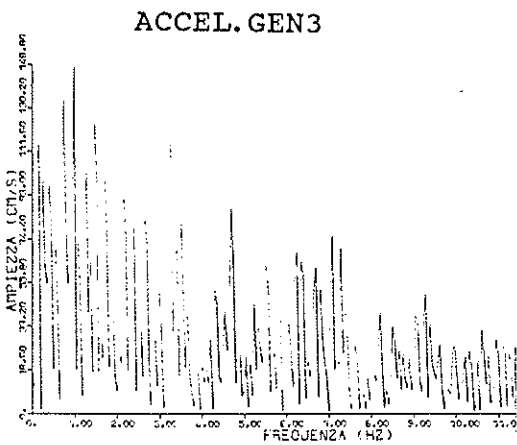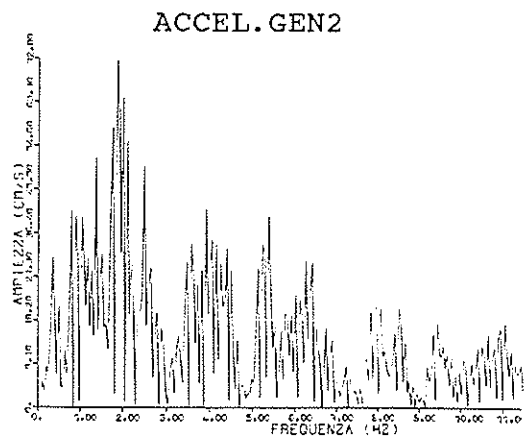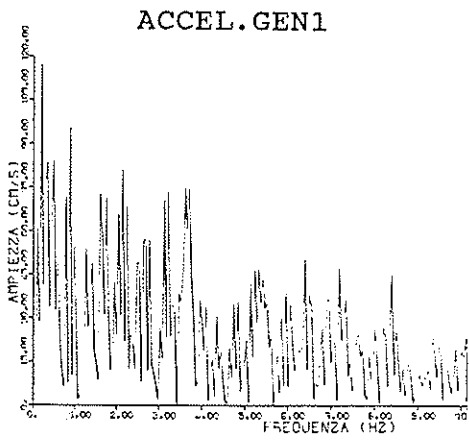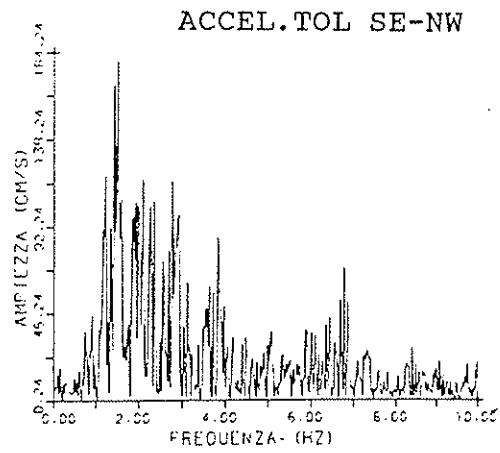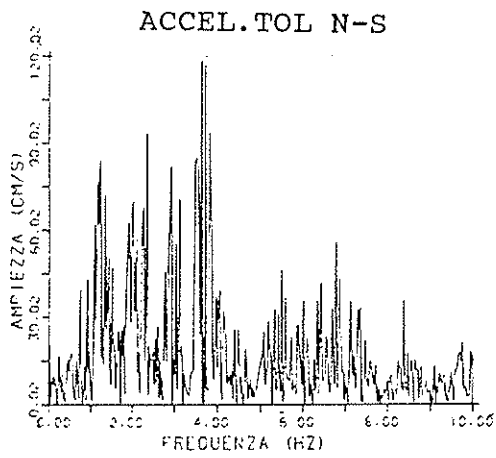
Fig. 12 - Fourier Spectra for The Chosen Earthquakes

14

frequencies whose Fourier's spectrum showed the highest energy content.

In the case of rigid joints the break down occurred when the most stressed sections (i.e. the beam's sections in base-hinged portals and the columns' inferior sections in base-restrained portals) collapsed. In the case of semi-rigid joints the collapse occurred when the joints reached unacceptable large deformations.

4.1 The Influence of Different Accelerograms

The influence of the accelerograms's shape and frequency content on the A_y and A_u values is fundamental. This confirms, as already outline in /2/, the necessity to repeat this kind of analysis for a wide range of different frequency content accelerograms.

4.2 The Influence of Different Types of Connections

4.2.1 The Structural Behaviour Factor - Given the kind of law chosen for the basic material, the structural coefficient value equals 1, for rigid joints schemes, but it is much greater than 1 for semirigid joints. The coefficient's average value is greater than 11 for schemes with two hinges at the base, it is greater than 8 in the scheme with restrained joints at the base.

4.2.2 Collapse Acceleration - In the case of semi-rigid joints, the collapse acceleration ranges from one to six times greater than in the case of rigid joints.

4.3 The Influence of Different Static Schemes

4.3.1 The Structural Behaviour Factor - The static scheme with two semi-rigid joints and two perfect hinges demonstrates tendencially greater "q" coefficient values compared to that of the scheme with four semi-rigid joints. Despite this fact, the ratio between the structural coefficients of the two schemes showed a notable variability between 1 and 2.

This variability seemed to be essentially connected to the accelerograms' frequency content.

4.3.2 Collapse Acceleration - The collapse acceleration value of the structure with four semi-rigid joints was always equal or greater than the case of the two semi-rigid joints and two hinges. Apart from the different accelerogram shape and
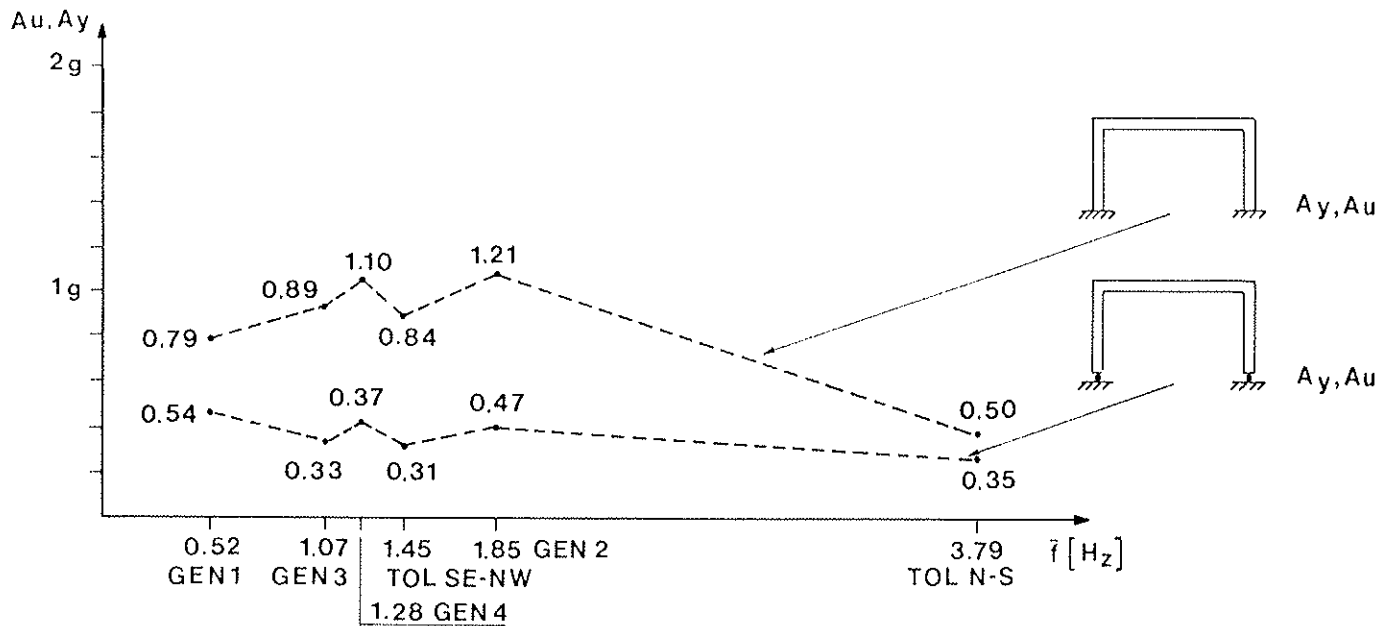
Fig. 13 - A_y, A_u for Frames with Rigid Connections Versus Earthquake Dominant Frequency ($\bar{f}$)
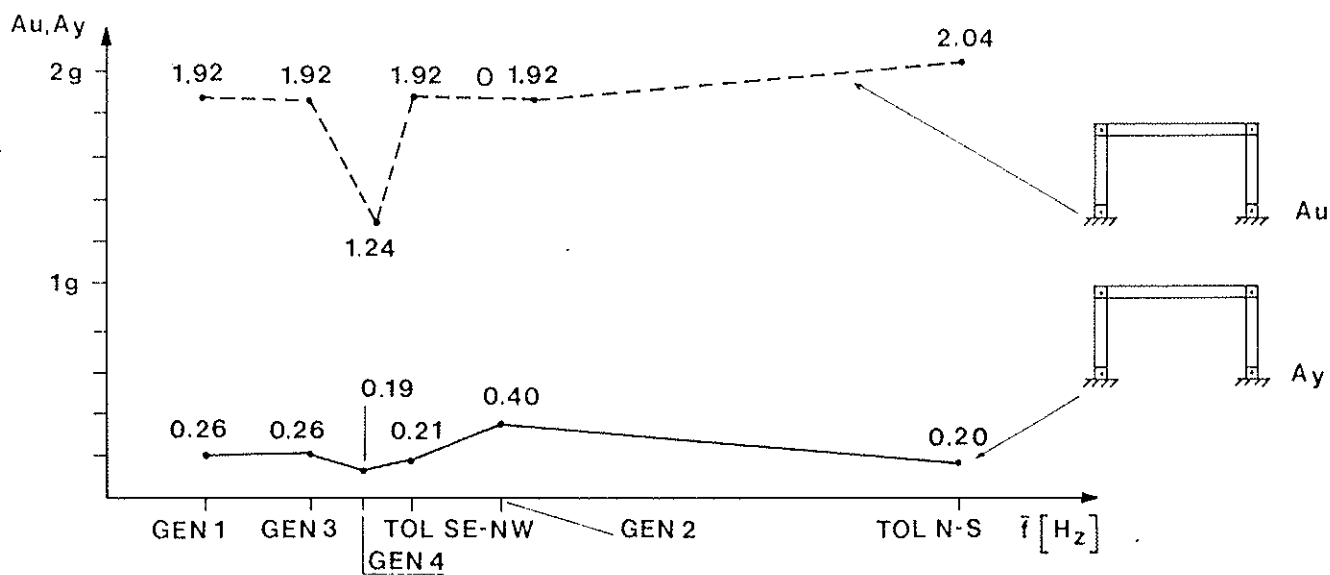
Fig. 14 - A_y, A_u for Base Restrained Frame with Semi-Rigid Connections Versus Earthquake Dominant Frequency ($\bar{f}$)
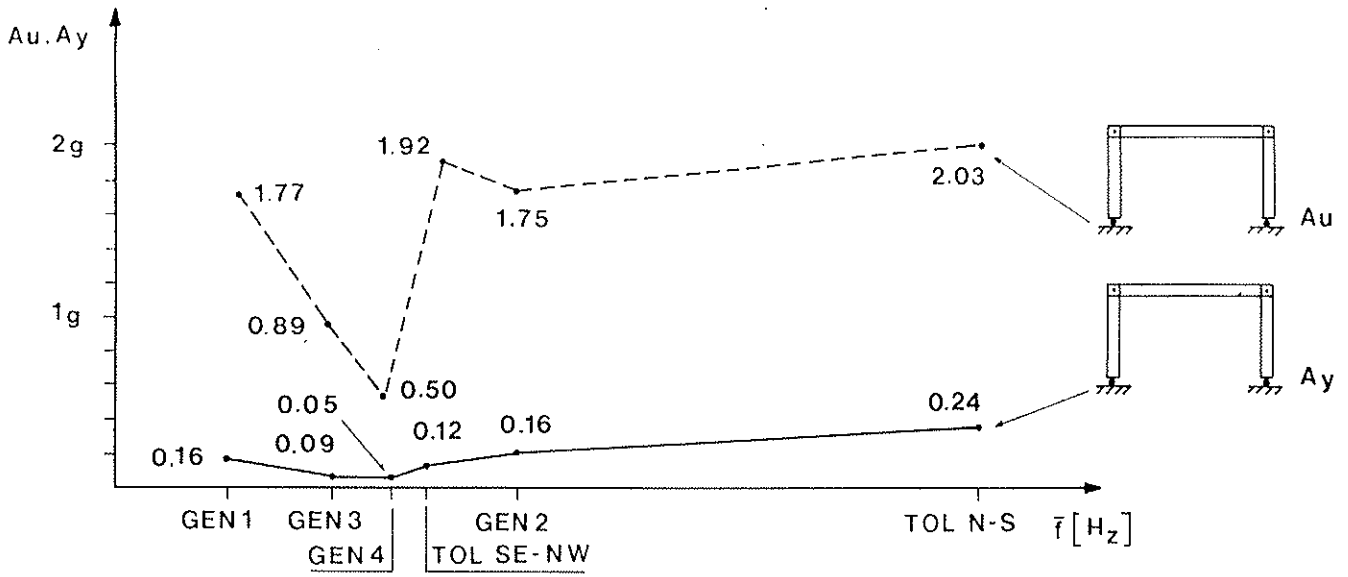
Fig. 15 - A_y, A_u for Base Hinged Frame with Semi-Rigid Connections Versus Earthquake Dominant Frequency ($\bar{f}$)
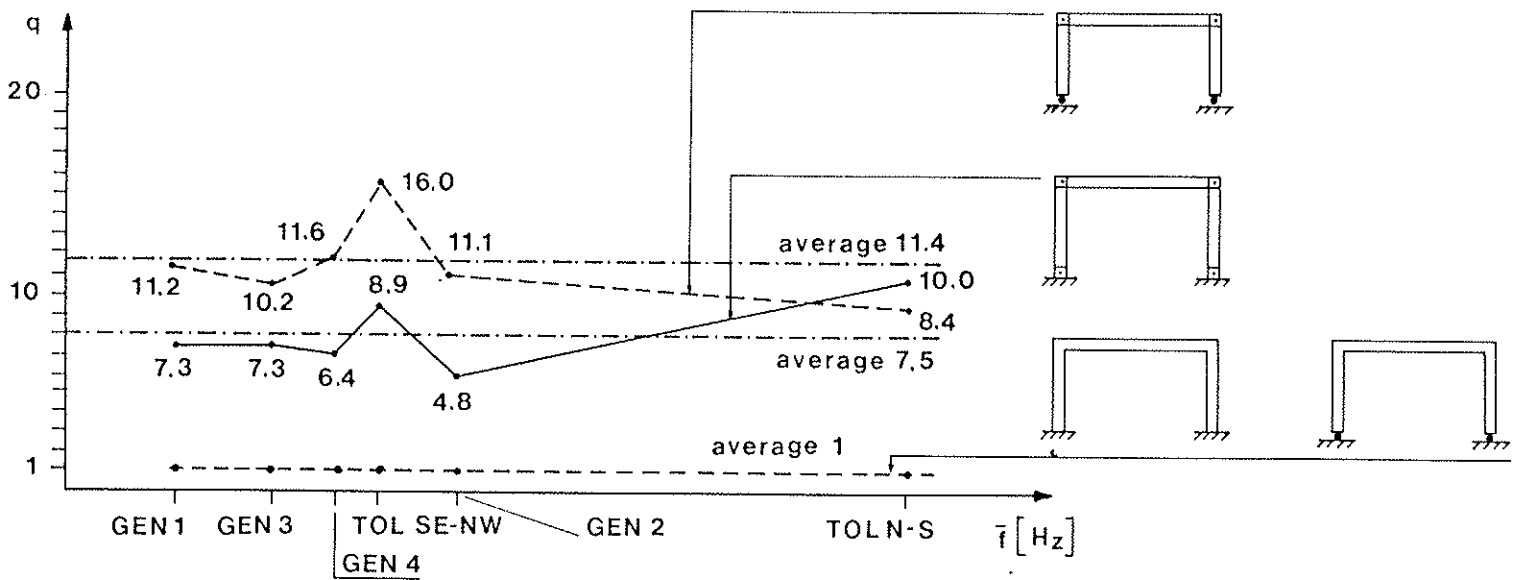
Fig. 16 - Behaviour Factor "q" Versus Earthquake Dominant Frequency ($\bar{f}$)

dimensioning, this result is due to the greater stress redistribution capacity of the four-semirigid joint scheme. This capacity increases the "final resistence" of the structure.

4.4 Considerations: Rigid Connections Response

Where q = 1, the collapse limit value was almost always much greater than 0.35 g, except for the Tolmezzo SE-NW and GEN 3 accelerogram's shapes. However, in these cases the collapse limit value was greater than 0.3 g. These results show acceptable structural seismic resistance.

5. CONCLUSIONS AND SUGGESTIONS FOR FURTHER RESEARCH

The conducted analysis clearly allows the assessment of the variation tendency of some fundamental quantities depending on the most important constructive factors. More specifically, it can be stated that, in the case of joints with nails or dowels of simple frames, the structural behaviour factor can be ten times greater than the case of glued joints. These results are just an approximate indication of the structural coefficient values for timber structures, because the conducted analysis was limited to a few examples and the joints' behavioural laws were simplified. The methods presented will provide more precise indications for the behaviour factor if more realistic models of the joints' cyclic behaviour are used. Following this procedure, significant indications for the structural behaviour factor can be obtained also for more complex static schemes.

6. REFERENCES

/1/ G. AUGUSTI, A. CECCOTTI, 1985: "Antiseismic rules for timber structures: an italian proposal". CIB-W18 Paper N. 18-102-1, Haifa.

/2/ A. GIUFFRE', G. GIANNINI, 1982: "La risposta non lineare delle strutture in cemento armato". In: "Progettazione e particolari costruttivi in zona sismica", ANCE, Roma.

/3/ A. CECCOTTI, P. SPINELLI, L. UZIELLI, 1983: "Sul comportamento sotto carichi statici e dinamici di travi di legno lamellare incollato di abete rosso e pioppo". La Prefabbri-

cazione, Milano.

/4/ F.J. KEENAN, 1980: "The earthquake resistance of timber construction". In: "International Conference on Engineering for Protection from Natural Disaster". Bangkok.

/5/ CNR-GNDT, 1984: "Norme Tecniche per le Costruzioni in Zone Sismiche". Ingegneria Sismica, Bologna.

/6/ A. CECCOTTI, A. VIGNOLI, 1986: "Connections deformability in timber structures: a theoretical evaluation of its influence on seismic effects". CIB-W18 Paper N. 19-15-1, Firenze.

/7/ DIN 1052, 1969: "Holzbauwerke". Beuth Verlag Gmbh, Berlino.

/8/ A. CECCOTTI, S. GIORDANO, 1987: "Su un dispositivo per prove a carichi ciclici di giunti di legno lamellare incollato". UFIST-DIC, Firenze.

/9/ M. PIAZZA, G. TURRINI, 1986: "Advances in technology of joints for laminated timber - Analysis of the structural behaviour". CIB-W18, Paper N. 19-7-9, Firenze.

/10/ A. CECCOTTI, A. VIGNOLI, 1985: "Full-scale structures in glued laminated timber, dynamic tests: theoretical and experimental studies". CIB-W18 Paper N. 18-15-1, Haifa.

/11/ G.H. POWELL, 1975: "DRAIN-2D Users Guide". Earthquake Engineering Research Center, Report UCB/EERC N. 73-22, University of California, Berkeley.

/12/ E.H. VANMARCKE et al., 1976: "SIMQKE Users Guide". M.I.T. Department of Civil Engineering, Research Report R76-4, Cambridge, Massachussets.

INTERNATIONAL COUNCIL FOR BUILDING RESEARCH STUDIES AND DOCUMENTATION

WORKING COMMISSION W18A - TIMBER STRUCTURES

WOOD MATERIALS UNDER COMBINED MECHANICAL AND HYGRAL LOADING

by

A Martensson and S Thelandersson

Lund Institute of Technology

Sweden

MEETING TWENTY

DUBLIN

IRELAND

SEPTEMBER 1987

WOOD MATERIALS UNDER COMBINED MECHANICAL AND HYGRAL LOADING

by

Annika Mårtensson and Sven Thelandersson

Div. of Structural Mechanics

Lund Institute of Technology

Lund, Sweden

INTRODUCTION

The influence of environment on the performance of wood or wood based materials is significant in many applications. The mechanical properties of wooden materials depend on moisture content and dimensional changes induced by moisture variation often lead to displacements which are greater than those caused by mechanical loading. Moreover, interaction of moisture changes with mechanical loading can lead to excessive deformation of wooden structures.

In composite structures like stressed skin panels, composite beams and layered wooden products, differential swelling or shrinkage produces internal stresses, which can cause degradation as well as distortion of shape. Such effects may accumulate as a result of repeated moisture cycling during the lifetime of the structure, and may contribute significantly to reduce its durability.

In codes for wooden structures, e. g. Eurocode 5, design values of strength and stiffness parameters are made dependent on moisture class and load-duration class. This means that the effect of moisture conditions on basic material properties during the lifetime of the structure is considered in a simple way suitable for practical design. Due to the complexity of the underlying

physical problems, however, a rational basis for description and quantification of these effects is still lacking. Clearly, there is a need for further research in this area, in order to establish a more reliable knowledge base for code specifications.

In addition, environmental effects should enter structural design not only on the "capacity" side, but also on the "loading" side. Moisture and temperature induced deformations are referred to as indirect actions to be considered along with and in combination with other types of loading. It is not quite evident, though, how such actions should be considered in the analysis of wood structures. For instance, if stresses due to restrained shrinkage or swelling are calculated by normal engineering methods, unrealistically high values are usually obtained.

Consider, as a simple example, a wooden element which is drying with the shrinkage fully restrained, Fig. 1. According to linear theory of elasticity, the stress change $\Delta\sigma_i$ due to restrained shrinkage is given by

$$\Delta\sigma_i = E\Delta\epsilon_s \tag{1}$$

where E is the modulus of elasticity and $\Delta\epsilon_s$ is the shrinkage strain that would occur if the element were free to shrink.
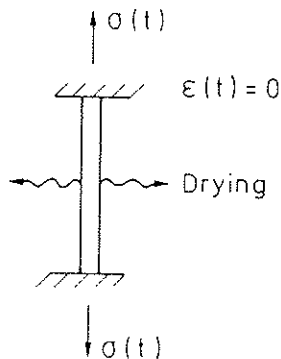
Fig. 1. Drying wood element under full restraint.

Using representative values for $\Delta\epsilon_s$ in moisture class 1 and design values for E it is found that $\Delta\sigma_i$ calculated from Eq (1) may be as high as 50% of the design value of the tensile strength for wood (parallel to the grain) and wood based products. It should be noted that the design value of E is specified in codes under the assumption that a low value of E is unfavourable. When E is used to calculate restraint stresses the opposite is valid, implying that a consistent choice of design parameters would give still higher values of $\Delta\sigma_i$.

Stresses due to imposed deformations may be neglected when they contribute to 'ductile' types of failure as for wood in compression. But for 'brittle' types of failure as for wood or adhesive joints in tension and shear, such stresses can be expected to contribute significantly. Accordingly, it is of importance in many situations to be able to predict stresses induced by moisture variations in an accurate way. A main purpose with the present paper is to contribute to the solution of this problem.

INTERACTION BETWEEN MOISTURE AND STRESS

One of the main difficulties in describing the behaviour of wooden materials is the strong interaction effect between mechanical and hygral loading. This kind of interaction has been found also for other hygroscopic materials as for instance concrete, but it is particularly significant for wooden materials. The term mechano-sorption is often used to describe the phenomena related to combined mechanical and hygral loading of wood [1].

Mechano-sorptive effects were first documented in the early sixties [2-5]. A number of studies of mechano-sorption have been reported since then, dealing with various aspects of the problem. Grossman [1] has summarized the experimental knowledge in a comprehensive review.

The major part of the experiments on mechano-sorption has been performed in bending. These tests have the advantage of being easy to perform and also that the bending mode is the most common one in reality, but the results are difficult to interprete since the stress varies over the cross section and both tension and compression are involved at the same time.

Studies made of the mechano-sorptive behaviour for australian wood species in tension and compression [2], indicate that the mechano-sorptive effect is of quite different magnitude for different loading modes. Hunt [6] studied mechano-sorptive effects in tension and bending on two species of softwood. His conclusion was on the contrary that at low stresses bending and tension gives similar results. This is also supported by recent results by Mohager [7] on Scots pine, indicating that the behaviour in tension and compression is similar, at least for softwoods under low stress. At higher stress levels when nonlinear behaviour can be expected a distinct interpretation of bending tests becomes very difficult.

Constitutive type models for description of the combined effects of mechanical and hygral loading have been proposed by Leicester [8], Ranta-Maunus [9,10], Rybarczyk & Ganowics [11] and Bazant [12], but the applicability of these models under general stress and moisture variations has not yet been demonstrated. A major problem is lack of systematic experimental information. Moreover, experimental data from various sources are difficult to synthesize, due to the large variability in material properties.

SCOPE OF THE PRESENT STUDY

The present paper is part of a greater study which has as its main purpose to develop and evaluate a constitutive model for wooden materials considering environmental effects. The idea is to test the same material under various combinations of stress and strain histories during moisture change. In this first part of the study

tests on structural hardboard in tension are made. In a later pa-
per similar experiments in compression will be reported. Some of
the tests were performed in a conventional way with constant load
during the test period ("creep") while others were performed with
the strain of each specimen prescribed during the test period. In
one of the test series the strain was held constant, which corre-
sponds to the situation shown in Fig. 1 ("quasi-relaxation").

A constitutive model is suggested and quantified on the basis of
test data from the conventional constant load experiments. The
general validity of the model is then checked independently
against the other tests.

The choice of hardboard as a test material was mainly motivated by
the fact that various mechanical and hygroscopic properties of
that particular material including creep at different constant
moisture levels is very well documented through the comprehensive
work by Lundgren [13]. It was also presumed that it should be
easier to control the variability in hardboard than in wood. As
regards mechano-sorptive behaviour, though, only few studies are
found in the literature, all performed in bending. Armstrong &
Grossman [14] found very significant mechano-sorptive effects for
wet-processed hardboard prepared from a mixture of eucalypt
species, whereas Sauer & Haygreen [15] observed more moderate
effects of mechano-sorption in hardboard made from aspen.
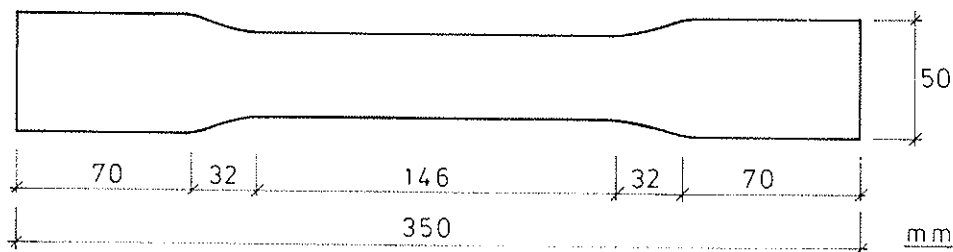
Fig. 2. Test specimen, thickness 6.4 mm.

The working hypothesis at the outset of this study was that the mechano-sorptive effects should be qualitatively similar in hardboard and clear wood, although quantitatively different. Thus the principles of constitutive modelling ought to be the same.

MATERIALS AND METHODS

Test specimens

The tests were made on wet-processed hardboard (from Scots pine, Pinus Sylvestris), which was delivered directly from the factory and kept in a chamber with constant climate, 65 % RH 20°C, until it was used in the tests. The test specimens which were of the shape shown in Fig. 2, were cut from boards of regular size (1400 x 3060 mm^2). From each board 25 pieces were sawn and ten of these were selected. The selection was made on the basis of density and dynamic modulus of elasticity, see Table 1. The latter was obtained by measuring the travelling time of a stress wave. The ratio between the dynamic modulus and the modulus of elasticity was determined to the value 1.1 in tensile loading.

Experimental setup

Strain measurements were made by means of conductive plastic resistance elements. Two gauges were placed on each test piece, one on each side. The average of the reading from the gauges was used as a measure of the deformation of the specimen.

Fig. 3 shows the experimental setup. The measurements from the strain gauges and the load cells were recorded by a personal computer. Loading was arranged with water-cans applied via leverarms. The strain history of the specimens could then be controlled by the computer, which was connected to the valves on
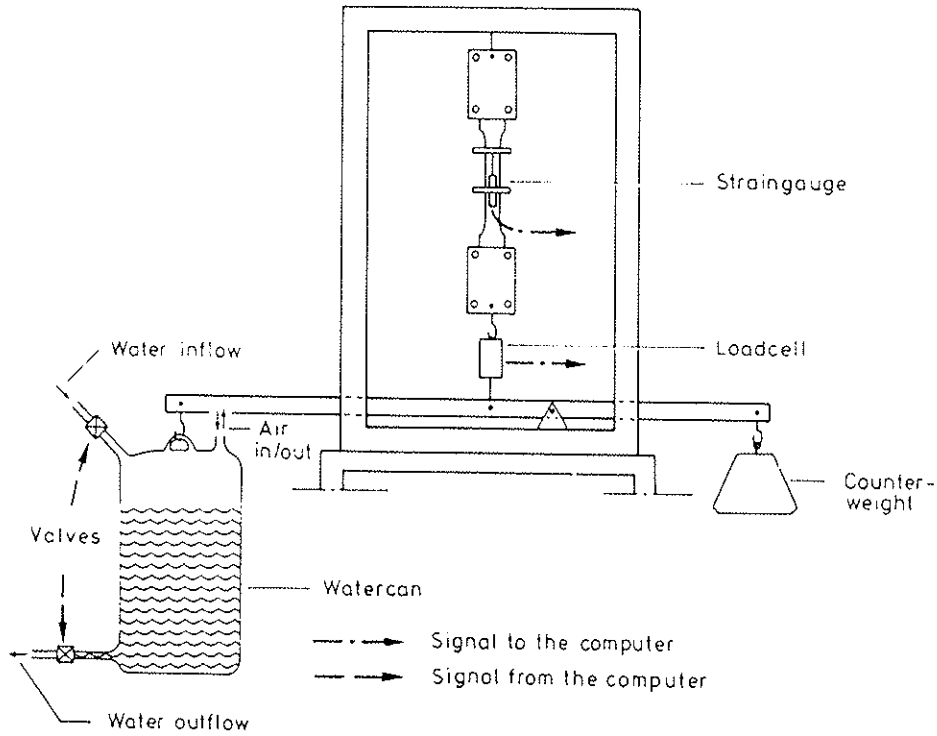
Fig. 3. Experimental setup.

the cans. Whenever the strain reading tended to deviate from the prescribed value the load was adjusted automatically by letting water into or out of the cans.

Moisture control and cycling

The climate chamber in which the tests were made had a total volume of 24 m^3. In all tests the temperature was held constant at 24°C ($\pm$ 0.5°C). The relative humidity in the chamber was controlled by means of salt solutions. In this study two different levels were of interest, 30 % RH and 88 % RH. The maximum deviation from the desired values was of the order $\pm$ 1.5 % RH. In

Table 1. Test plan

Series	Number of specimens	Stress levels (MPa)	Density (kg/m^3)	Dynamic modulus of elasticity (MPa)
A1	6	3.0		
constant stress	2	-	975 - 990	5500 - 6200
A2	3	3		
constant stress	4	8.5	948 - 962	5500 - 6100
	1	-		
B	3	1.6		
constant strain	4	8.5	949 - 965	5300 - 5800
	2	-		
C	4	1.6		
constant stress	4	8.5	969 - 980	5500 - 6100
constant RH	2	-		

tests where the humidity was varied, each cycle comprised one week at 30 % RH and one week at 88 % RH, a period which is sufficiently long to approach equilibrium with the surrounding relative humidity.

In Table 1 the different types of experiments are summarized. The tests can be divided into three groups. In the first group (series A1 and A2) the load was kept constant throughout the test. At the time when the load was applied the specimens were in equilibrium at 65 % RH. The relative humidity was then changed to 88 % (series A1) or 30 % (series A2). Following this the humidity was changed two or three times between 88 % and 30 %. In series B the test pieces were first conditioned to 88 % and then loaded to 1.6 MPa

or 8.5 MPa. The strain attained immediately after this loading was then kept constant for the rest of the four week test period. Also immediately after loading RH was changed to 30 %. The humidity was then changed each week between 30 % and 88 %. In series C both load and climate were kept constant. Two stress levels were used, one at 1.6 MPa and one at 8.5 MPa and the relative humidity was 88 %. One or two test specimens in each test series were kept unloaded and pure swelling and shrinkage were measured on these. One test specimen in each series was used to measure weight changes during the test period.

RESULTS

The main results are presented in Figs. 4 to 8. All graphs show the mean value of measurements from 3-6 test pieces, see Table 1. The variability in the measurements was of the order ± 20 % of the measured values. Despite this variation all specimens react in a qualitatively similar manner.

Figs. 4 and 5 show the behaviour of the specimens in test series A1 and A2. Figs. 4b and 5b give the results of Figs. 4a and 5a respectively, after zero-load correction. This correction was obtained by subtracting the average strain of two non-loaded specimens from the average strain of the loaded specimens. The variation in free dimensional changes between different unloaded specimens was generally small.

Features to note after zero-load correction, Figs. 4b and 5b, are that the strain increases during the first sorption irrespective of whether it is desorption or adsorption. At the beginning of all the following sorption periods an immediate change in deformation occurs, an increase if it is adsorption and a decrease if it is desorption. At low stress levels the strain is then nearly constant after that step change. At the higher stress level, however, the deformation increases during the whole sorption period.
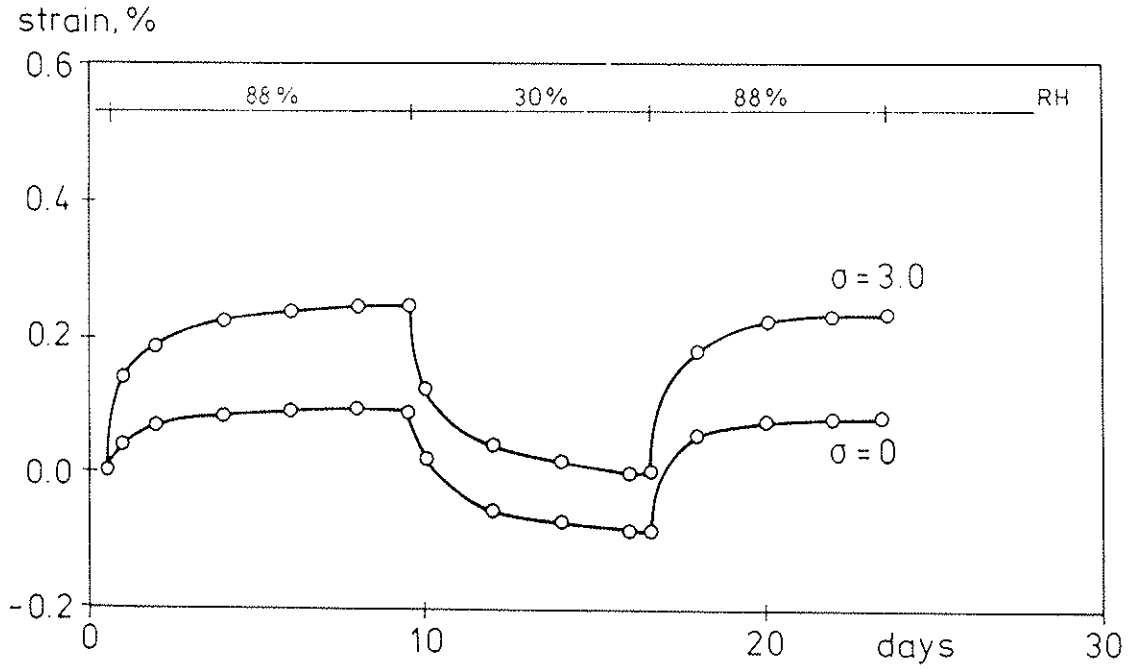
Fig. 4a. Measured strains in test series A1.
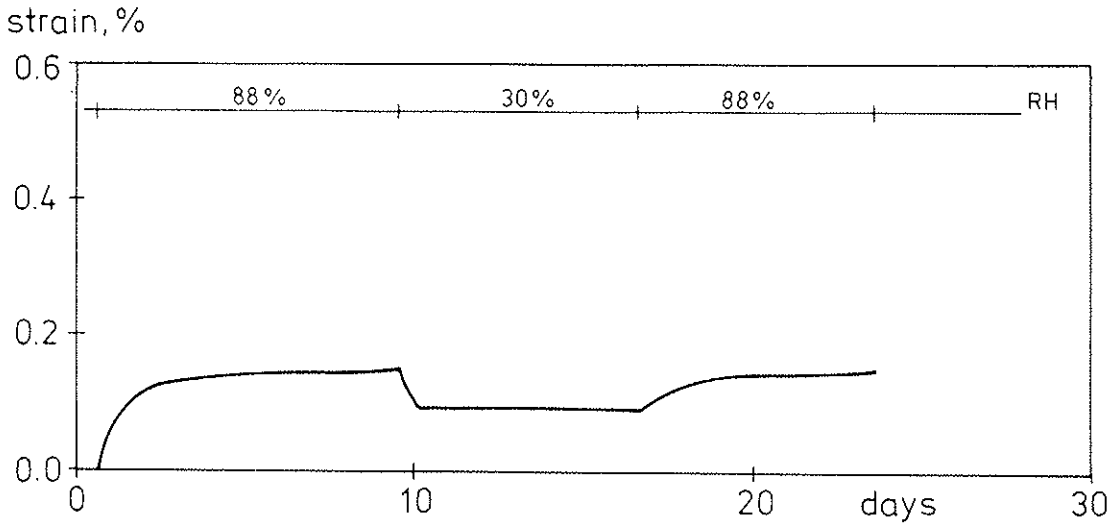
Fig. 4b. Zero-load corrected deformation obtained from the results
in Fig. 4a, σ = 3.0 MPa.
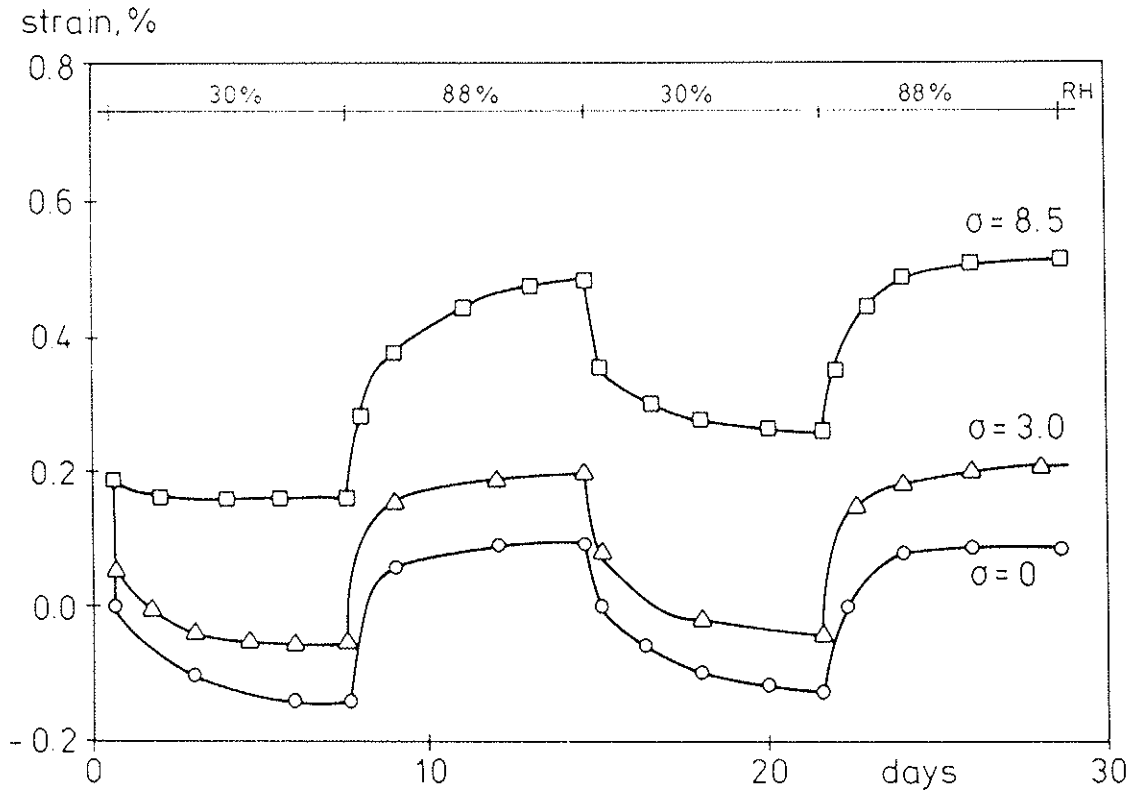
strain,%

Fig. 5a. Measured strains for three different stress levels in
    test series A2.

strain,%
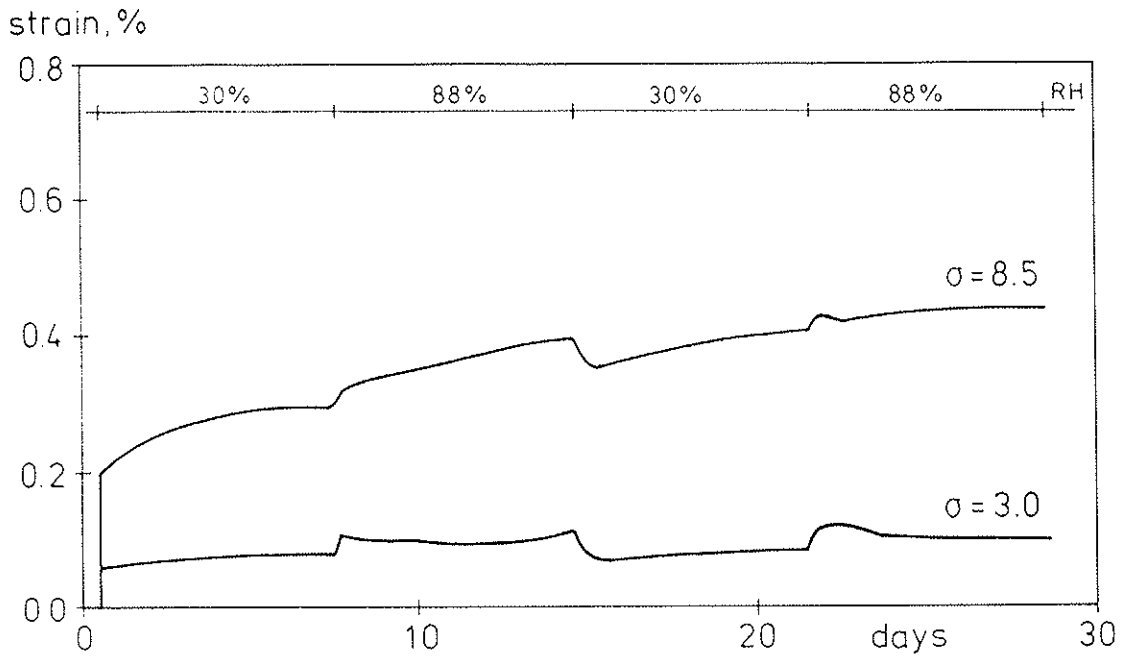
Fig. 5b. Zero-load corrected deformation obtained from the results
    in Fig. 5a.

In test series C the creep was measured during a period of nearly four weeks, with the specimens in equilibrium with a relative humidity of 88 %. At both stress levels the rate of creep is low after four weeks, see Fig. 6. If a comparison is made with the zero-corrected creep curves in Fig. 5b, it can be seen that the effect of mechano-sorption is small at both stress levels.

Fig. 7 shows how the free swelling and shrinkage occurs, and the moisture content variation during the test B. This result shows that the specimens are in equilibrium with the surrounding climate when they reach a moisture content of 6 % at 30 % RH and of 13 % at 88 % RH.

The results from the quasi-relaxation tests (series B) are shown in Fig. 8. In this test series the specimens were loaded after seven days conditioning in a relative humidity of 88 %. The deformation was then kept constant as the humidity varied, cf. Fig. 1. The mechano-sorptive effect is more evident in these tests. An elementary elastic calculation according to Eq. (1) predicts a total stress change of about 10 MPa ($\Delta\epsilon \approx 0.2$ %, $E \simeq 5000$ MPa), whereas the measured change in stress is only 2-3 MPa for the first desorption at both stress levels. In the following re-sorption the change in stress becomes larger but not as large as 10 MPa on any test specimen. During the second desorption the stress level never reaches the magnitude achieved in the first one. Note that during adsorption, the strain of the specimens with low initial stress deviates from the initial strain when the stress becomes zero, due to the inability of the loading equipment to transfer compressive forces.
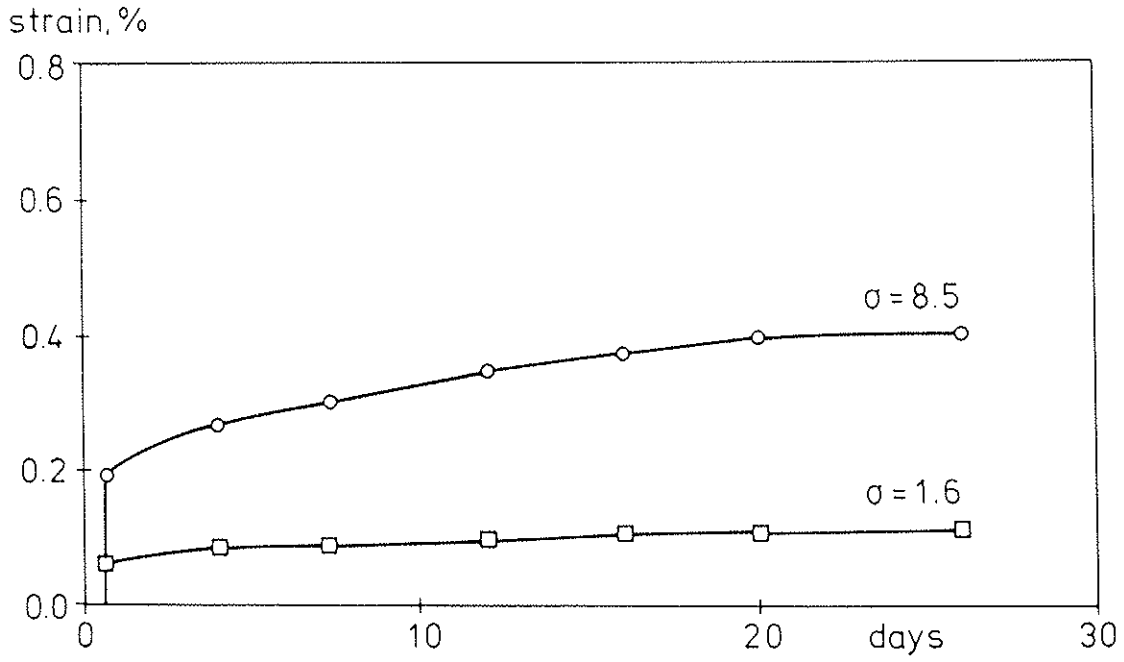
strain, %

Fig. 6. Creep at 88 % RH for two different stress levels.
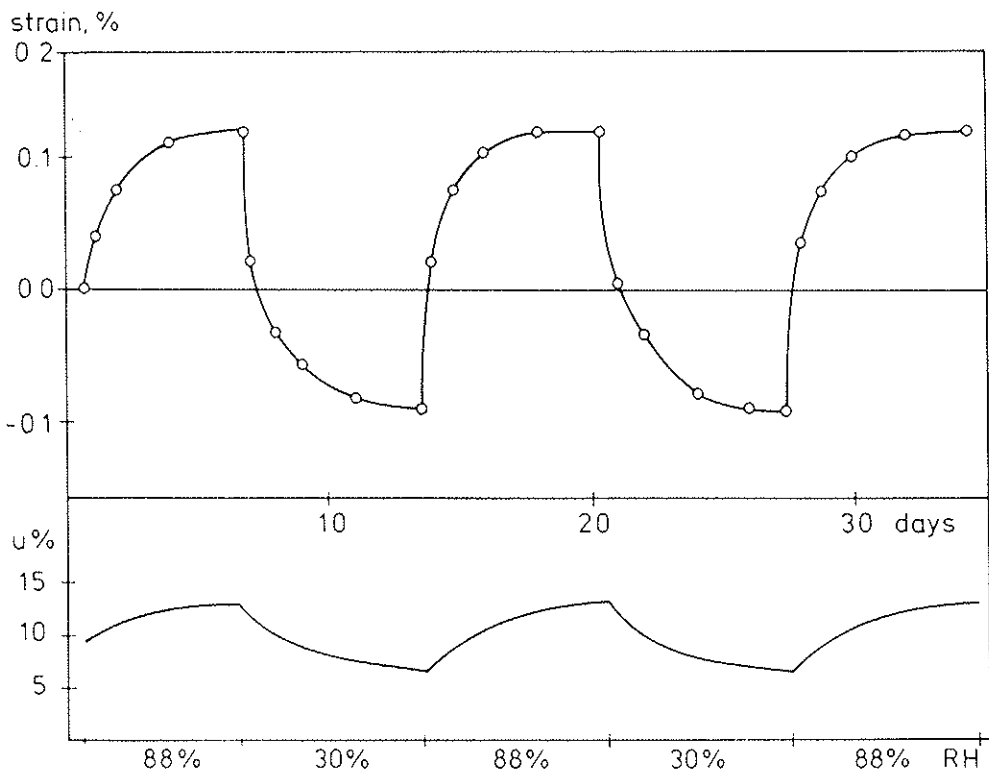
strain, %

Fig. 7. Deformation of non-loaded test specimen in test series B.
The lower figure shows the moisture content variation
during the test.
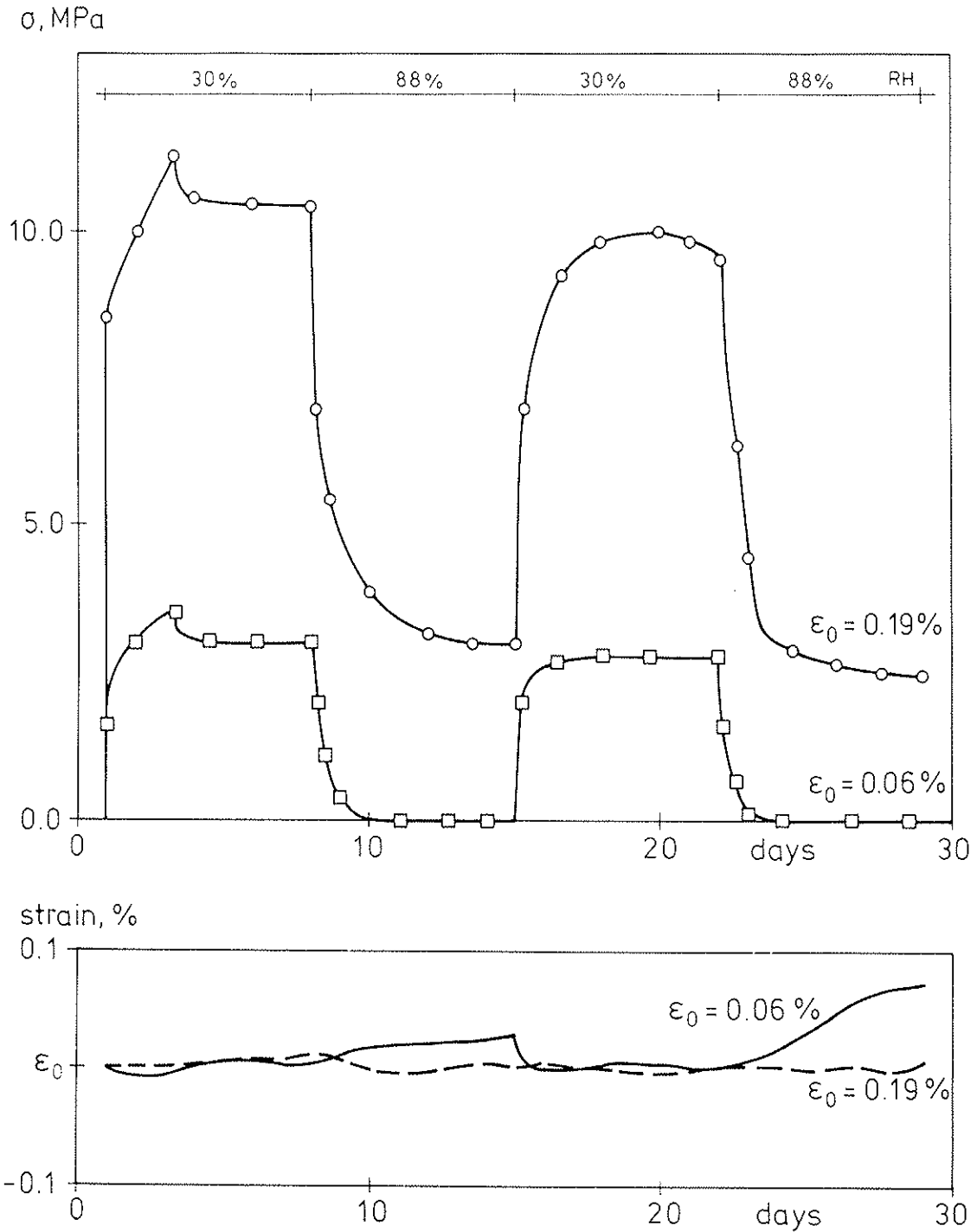
Fig. 8. Quasi-relaxation tests. Prescribed constant strain,
ϵ_0 = 0.06 or 0.19 %, corresponding to initial stres-
ses of 1.6 MPa and 8.5 MPa, respectively. The lower
figure shows the deviation from ϵ_0.

CONSTITUTIVE MODELLING

In conventional engineering analysis the moisture induced strain rate $\dot{\epsilon}_s$ is considered to be a function of the rate of change $\dot{w}$ of the moisture content and possibly of the current moisture content w, i.e. $\dot{\epsilon}_s = \dot{\epsilon}_s(w, \dot{w})$. This strain is then simply added to the mechanically induced strain, assuming that there is no interaction between hygral response and mechanical response.

Since such interaction has been shown to exist in the present case, an alternative way of formulation is preferable. A simple way to describe the interaction is to postulate that the moisture induced strain rate also depends on the current stress state [16,12], i.e. $\dot{\epsilon}_s = \dot{\epsilon}_s(w, \dot{w}, \sigma)$ in the case of uniaxial stress. Assuming that the total strain rate $\dot{\epsilon}_x$ is given as the sum of linear elastic strain rate $\dot{\sigma}_x/E$, creep strain rate $\dot{\epsilon}_c$ and stress-dependent moisture induced strain rate $\dot{\epsilon}_s$, the constitutive equation for uniaxial stress becomes

$$\dot{\epsilon}_x = \frac{\dot{\sigma}_x}{E(w)} + \dot{\epsilon}_c + \dot{\epsilon}_s \qquad (2)$$

The creep strain rate $\dot{\epsilon}_c$ represents basic creep, measured under constant moisture conditions, and will be discussed later. Note that E is assumed to depend on the moisture content w.

To describe the moisture induced strain the following simple formulation will be used.

$$\dot{\epsilon}_s = \dot{\epsilon}_{so} + \kappa \frac{\sigma_x}{\sigma_u} |\dot{\epsilon}_{so}| \qquad (3)$$

where $\dot{\epsilon}_{so}$ is the free moisture induced strain rate, which can be measured on a non-loaded specimen, σ_u is the ultimate stress in uniaxial tension and κ is a material parameter describing mechano-sorptive behaviour.

The formulation of Eq.(3) coincides in principle with the models proposed by Leicester [8], Rybarczyk & Ganowics [11] and later by Bazant [12]. It can be seen as a first linear approximation and cannot be expected to be valid for general moisture and stress histories. General variations of the moisture state may be considered, however, by taking the coefficient κ as a function of the moisture history.

To describe creep, the linear theory of viscoelasticity is employed, see e.g. Pipkin [17]. The creep strain under constant stress and moisture conditions is then given by $\epsilon_c(\sigma, t) = \sigma J(t)$, where $J(t)$ is the creep compliance and t is the time since application of σ. When the moisture content varies, it is important to notice that the higher the moisture content, the faster the creep develops. The effect of moisture content on creep can be described by introducing a material time ξ defined by $d\xi = dt/a(w)$, and a reference moisture state w_r, for which the material time is equal to the real time, i.e. $a(w_r) = 1$. Then, the creep strain during arbitrarily varying stress and moisture is described by the convolution [17]

$$\epsilon_c(t) = \int_0^t J[\xi(t)-\xi(t')]d\sigma(t') \qquad (4)$$

The compliance function J is described by means of a rheologic model consisting of N Kelvin elements, see Fig. 11. The compliance is then given by

$$J(t) = \sum_{n=1}^{N} J_n[1-\exp(-t/\tau_n)] \qquad (5)$$

where τ_n is the retardation time of Kelvin element n and J_n is its equilibrium compliance, to be determined from experimental data.
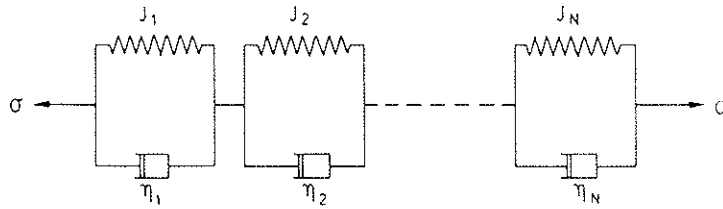
Fig. 9. Generalized Kelvin model. The retardation times are given by $\tau_i = \eta_i J_i$, where η_i is the viscosity of element i.

THEORY VS. EXPERIMENTS

The model according to Eq.(2) was implemented in a finite element program, which was used for theoretical simulations of the experiments. The reference moisture content w_r corresponds to equilibrium at 88 % RH, and the value of $E(w_r)$ was taken from the measurements. The basic creep parameters J_n and τ_n were determined by fitting Eq. (5) to the basic creep curve for $\sigma = 8.5$ MPa in Fig. 6. The moisture dependence of the elastic modulus $E(w)$ and the moisture shift factor $a(w)$ was determined from the comprehensive test data published by Lundgren [13]. Finally, as regards the mechano-sorptive parameter κ, all calculations were performed according to two alternatives. In one set of calculations, mechano-sorptive effects are not considered at all, i.e. $\kappa = 0$ during the whole process. This will be referred to as the conventional model. In the other set of calculations mechano-sorption is included as described below.

Since the experiments indicate that the mechano-sorptive effect is of major importance only during the first moisture cycle, it was assumed that $\kappa \neq 0$ only for the first change in moisture content, irrespective of whether the moisture content increases or decreases. Subsequent changes in moisture content will lead to

mechano-sorptive effects only when the moisture content reaches values not earlier attained. The value of κ was therefore given a constant value different from zero during the first sorption period and was then taken to be zero until the moisture content reaches values not achieved before. In this way mechano-sorption is described by a single material constant, which was determined to the value 0.8 by fitting the model to the test results for $\sigma = 8.5$ MPa in Fig. 5. The tensile strength σ_u was determined to 26 MPa.

The results from the calculations as well as comparisons with the experimental data are shown in Figs. 10 and 11. Fig. 10a refers to that particular experiment (Fig. 5), which was used to determine the parameter κ. When mechano-sorptive effects are included (MS) a good correlation was achieved, showing that the proposed model is able to describe the mechano-sorptive behaviour under constant stress. Comparing with the results from the "conventional model", it is also found that the effect of mechano-sorption is surprisingly small in this case.

Fig. 10b refers to a test under the same conditions as in Fig. 10a but with a lower stress. The strains predicted by the model are somewhat too large. This may indicate that the response is not ideally linear with stress, as is assumed in the model.

Fig. 11 shows the results when the model is applied for the quasi-relaxation tests, cf Fig. 8. Evidently, the model predicts too high restraint stresses during the desorption periods, especially in the case with low initial stress (Fig. 10b). It is surprising that a model, which describes the behaviour under constant load in a reasonably correct way, gives such poor results under similar climatic conditions, the only difference being that the strain is prescribed instead of stress. The results indicate clearly that the mechano-sorptive effect is much more significant under relaxation type conditions than under creep type conditions.
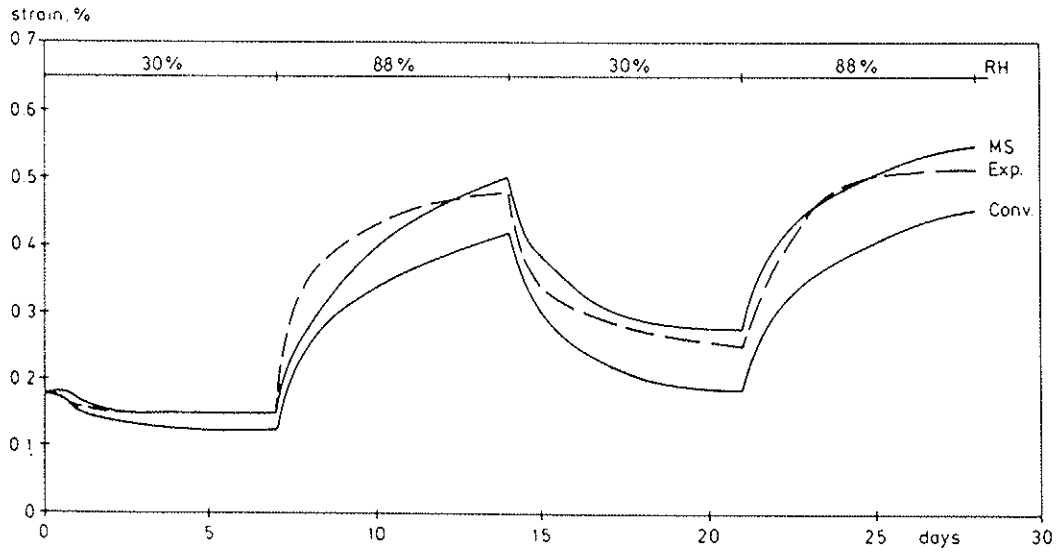
Fig. 10a. Comparison between experimental results from series A2,
and calculations. σ = 8.5 MPa.

Conv = conventional model.

MS = mechano-sorption considered in the model.
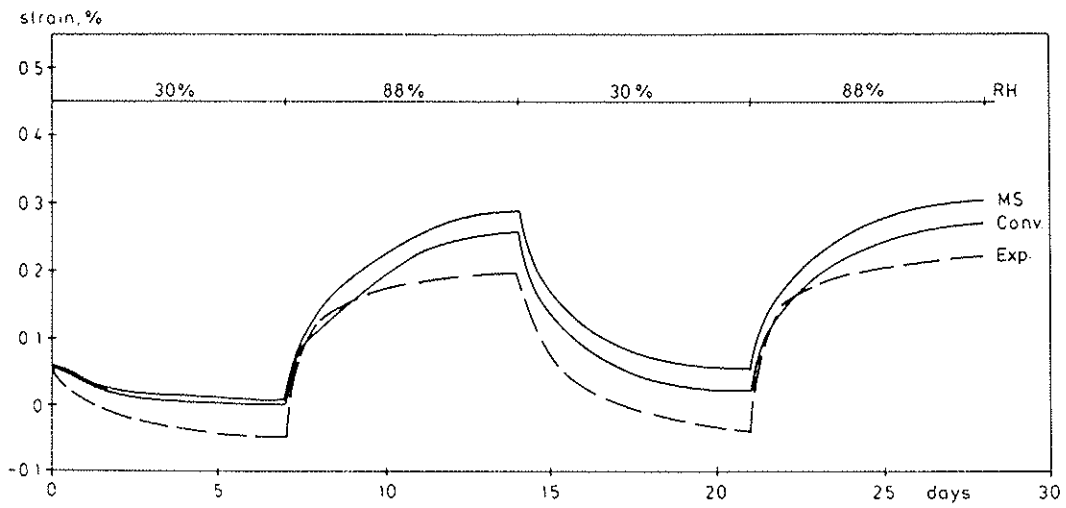
Fig. 10b. Same as Fig. 10a but with σ = 3.0 MPa.
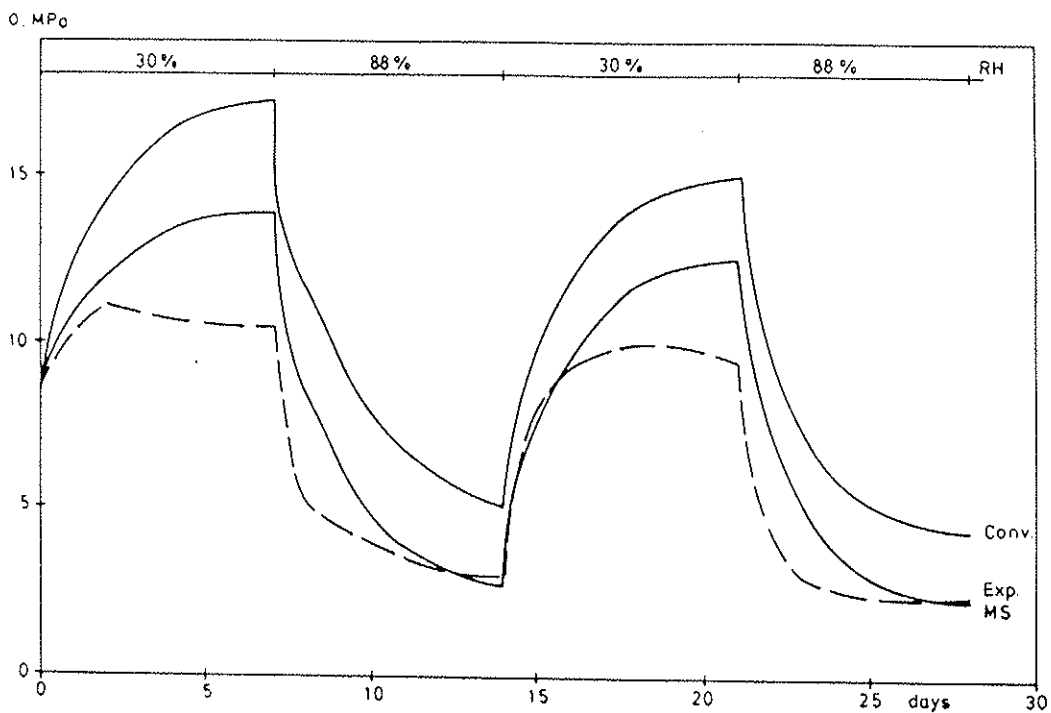
Fig. 11a. Comparison between experiments from series B
(quasirelaxation) and calculations. $\epsilon_o = 0.19\%$.
Conv = conventional model.
MS = mechano-sorption considered in the model.
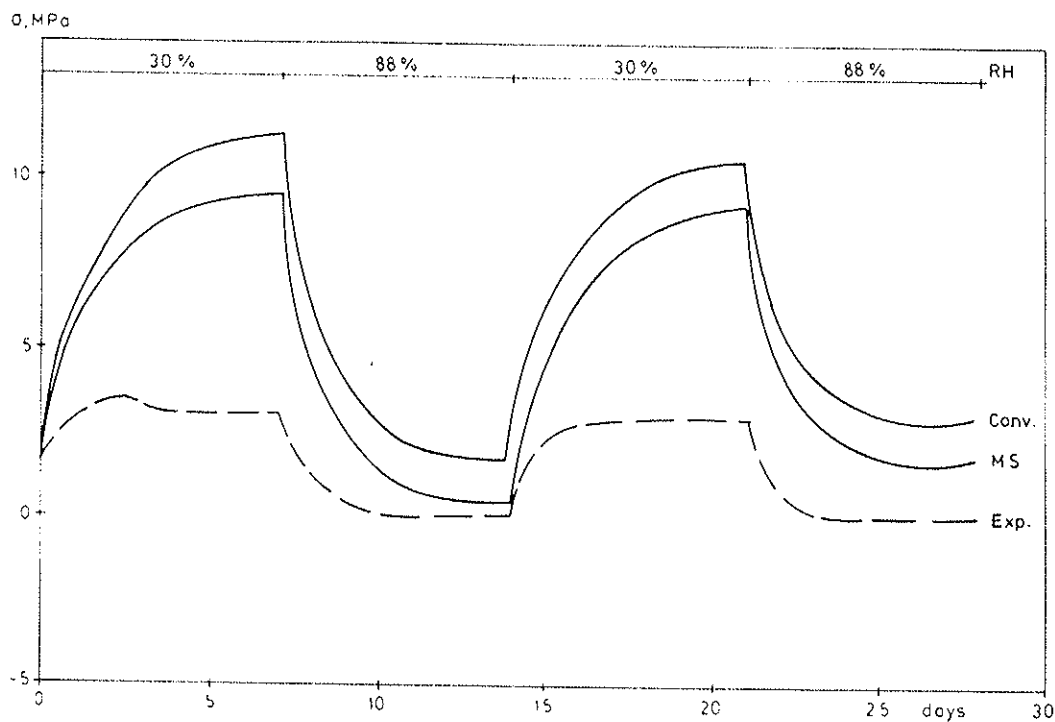
Fig. 11b. Same as Fig. 11a, but with $\epsilon_o = 0.06\%$.

CONCLUDING REMARKS

The following main conclusions can be drawn from the present investigation:

1) Tests on hardboard show that the effect of moisture variations on tensile creep is surprisingly small, in view of the very significant mechano-sorptive effects observed for other wooden materials.

2) The mechano-sorptive effects in the tested hardboard was found to be much greater in relaxation tests under moisture variations. Typically, the initial stress was reduced to 1/3 at the end of the first full moisture cycle.

3) The increase in tensile stress due to restrained shrinkage in wooden materials can be expected to be very moderate and only a fraction of that predicted by linear elastic theory.

4) When a full drying/wetting cycle has been completed, there will be a significant stress change in the opposite direction.

5) A simple constitutive model taking into account mechano-sorptive behaviour was found to give good agreement with creep type experiments when calibrated against these.

6) When the model was checked against relaxation type experiments (using the same material parameters), however, it showed poor agreement.

Based on published experimental evidence, Grossman [1] has given a number of requirements for a model which exhibits mechano-sorptive behaviour. To this list can be added that the model shall be able to predict both relaxation and creep behaviour under varying

moisture conditions. Tests of relaxation type are almost non-existent in the literature, and it would be of great interest if experimentalists could perform such tests for different wooden materials and for different loading modes. For instance, prediction of drying stresses and cracking in timber requires such information for wood under tension in the radial and tangential directions.

REFERENCES

[1] Grossman, P.U.A., 1976: Requirements for a model that exhibits mechano-sorptive behaviour. Wood Sci. Techn. 10: 163-168.

[2] Armstrong, L.D.; Kingston, R.S.T., 1962: The effect of moisture content changes on the deformation of wood under stress. Aust. J. Appl. Sci. 13(4): 257-276.

[3] Christensen, G.N., 1962: The use of small specimens for studying the effect of moisture content changes on the deformation of wood under load. Aust. J. Appl. Sci. 13(4): 242-256.

[4] Hearmon, R.F.S.; Paton, J.M., 1964: Moisture content changes and creep of wood. For. Prod. J. 14(8): 357-359.

[5] Eriksson, L.; Noren, B., 1965: The effect of moisture changes on the deformation of wood with tension in fibre direction. Holz Roh u. Werkst. 23(5): 201-209.

[6] Hunt, D.G., 1986: The mechano-sorptive creep susceptibility of two softwoods and its relation to some other material properties. J. Mat. Sci. 21: 2088-2096.

[7] Mohager, S.,1987: Studies of creep in wood (in swedish). The Royal Institute of Technology. TRITA-BYMA 1987:8, Stockholm.

[8] Leicester, R.H., 1971: A rheological model for mechano-sorptive deflections of beams. Wood Sci. Techn. 5: 211-220.

[9] Ranta-Maunus, A., 1975: The viscoelasticity of wood at varying moisture content. Wood Sci. Techn. 9: 189-205.

[10] Ranta-Maunus, A., 1973: A theory for the creep of wood with application to birch and spruce plywood. Technical Research Centre of Finland, Publ. 4.

[11] Rybarczyk, W., Ganowics, R., 1974: A theoretical description of the swelling pressure of wood. Wood. Sci. Techn. 8: 233-241.

[12] Bazant, Z.P., 1985: Constitutive equation of wood at variable humidity and temperature. Wood Sci. Techn. 19: 159-177.

[13] Lundgren, S.Å., 1967: Board as a building material (in swedish). Dissertation, Nyköping.

[14] Armstrong, L.D.; Grossman, P.U.A., 1972: The behaviour of particleboard and hardboard beams during moisture cycling. Wood Sci. Techn. 6: 128-137.

[15] Sauer, D.J.; Haygreen, J.G., 1968: Effects of sorption on the flexural creep behavior of hardboard. For. Prod. J. 18(10): 57-63.

[16] Thelandersson, S., 1983: On the multiaxial behaviour of concrete exposed to high temperature. Nucl. Eng. Des. 75(2): 271-282.

[17] Pipkin, A.C., 1972: Lectures on viscoelasticity theory. Springer Verlag, New York- Heidelberg- Berlin.

INTERNATIONAL COUNCIL FOR BUILDING RESEARCH STUDIES AND DOCUMENTATION

WORKING COMMISSION W18A - TIMBER STRUCTURES

ANALYSIS OF GENERALIZED VOLKERSEN-JOINTS IN TERMS
OF NON-LINEAR FRACTURE MECHANICS

by

P J Gustafsson
Lund Institute of Technology
Sweden

MEETING TWENTY
DUBLIN
IRELAND
SEPTEMBER 1987

ANALYSIS OF GENERALIZED VOLKERSEN-JOINTS IN TERMS OF NON-LINEAR FRACTURE MECHANICS

P.J. Gustafsson, research associate

Division of Structural Mechanics, Lund Institute of Technology
Box 118
S-221 00 Lund
Sweden

ABSTRACT

The strength of lap joints in pure shear is studied theoretically by a non-linear fracture mechanics approach, taking into account the complete τ-δ curve of the bond line, including its softening branch. Bending effects and peel stresses are not considered.

The purpose is to present a unified method of analysis which incorporates more conventional methods as special cases and which makes it possible to study the significance of various parameters. A joint-characteristic brittleness ratio is introduced. Fracture energy, G_f, defined as the area under the τ-δ curve, is found to be an important parameter. The significance of the shape of the τ-δ curve is studied and the optimal shape is deduced.

The range of application for more conventional methods of analysis is indicated and limiting conditions for application of 1D analysis of overlap joints are proposed. A linear elastic fracture mechanics strength expression is developed and a method for simple calculation of the self-similar stress distribution is proposed. For cases where adherend fracture may occur, it is found that a small increase in adhesive strength may produce a drastic decrease in joint strength.

ANALYSIS   LAP JOINTS   STRENGTH   FRACTURE
FRACTURE MECHANICS   FRACTURE ENERGY   VOLKERSEN
BOND   SHEAR   JOINTS   ADHESIVE   SOFTENING

1. INTRODUCTION

For theoretical strength analysis of adhesive joints, different methods from the sciences of structural mechanics and strength of materials may be employed. These methods include linear elastic fracture mechanics (see e.g. Anderson et al., 1977), elastic and elasto-plastic analysis together with some maximum stress or strain criterion (see e.g. Adams and Wake, 1984), and limit load analysis by means of the theory of ideal plasticity. The applicability of these different approaches is known to depend on the geometry and the physical size of the joint and on the material properties of the adhesive and the adherends. The various methods predict different strength and entirely different sensitivity to changes in joint geometry and material properties.

The purpose of this paper is to present a unified method of analysis which incorporates the above mentioned approaches as different special cases. The approach presented below is essentially inspired by methods for non-linear fracture mechanics analysis of fracture softening solid materials (Hillerborg et al., 1976), (Gustafsson, 1985).

Analysis of the single-lap joint in pure shear forms the base for the study. In order to enable simple numerical calculations by means of existing analytical solutions, (Ottosen and Olsson, 1986), and to facilitate a qualitative interpretation of essential aspects of joint behaviour, some of the simplifying assumptions used by Volkersen (1938) are adopted: the adhesive is assumed to be in a state of pure shear and the adherends are assumed to be in a state of pure tension without any bending effects. Accordingly, peel stress is not considered in the present study.

The theoretical results obtained for the single-lap joint are valid also for the double-lap joint and are also directly applicable to the mechanically analogous joint consisting of overlapping pipes exposed to torque. The substitutions of variables required for application to analysis of overlapping pipes in torsion or tension are given in (Gustafsson, 1987).

2. GEOMETRY AND ASSUMPTIONS

The geometry of the single-lap joint is shown in Fig 1. The adherends are regarded as linear elastic bars in pure tension and the bond line is regarded as a shear medium in which influence of normal stress is neglected. The modulus of elasticity of the adherends is E_1 and E_2, respectively. The change in geometry of the joint during loading is assumed to be small so that geometrical non-linearity may be disregarded. Please note the convention $t_1 E_1/(t_2 E_2) = \alpha \leq 1.0$. The mechanical constitution of the bond line, Fig 2, is defined by a relation between the local shear stress, τ, and the local shear displacement, δ, across the adhesive layer. This relation is regarded as a constitutive relation and may depend on type of adhesive, bond line thickness, curing, loading rate, surface preparation, interphase between

adhesive and adherend, and so on. It is of significance that the constitutive relation comprises the softening branch of the $\tau-\delta$ curve. Existance of a softening branch has been experimentally verified for various adhesives (Wernersson and Gustafsson, 1987).
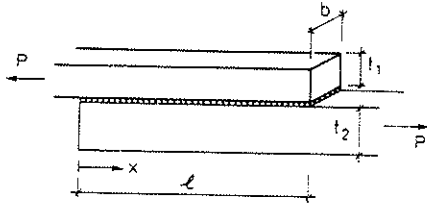
Fig 1. Geometry of single-lap joint.
$t_1 E_1 / (t_2 E_2) = \alpha \leq 1.0$.
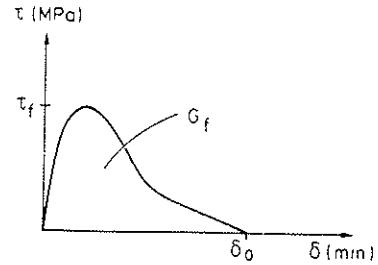
Fig 2. Constitutive relation of bond line.

3. FRACTURE ENERGY

Fracture energy, G_f, of a bond line is defined as the energy required to bring one unit area of the bond surface from its unloaded state to its completely fractured state. For the case of pure shear, we get by definition:

$$G_f = \int_0^\infty \tau \, d\delta \qquad (1)$$

i.e. G_f corresponds to the area under the $\tau-\delta$ curve. This fracture energy, G_f, must be distinguished from the critical energy release rate, G_c, used in linear elastic fracture mechanics. While G_f represents the energy required to bring a fixed unit area to complete separation, G_c represents the energy dissipated during movement of a distinct tip of a sharp crach.

G_f may be determined from the $\tau-\delta$ curve and may also be experimentally determined from the total work done by the external load during testing of a joint. This latter method demands that energy is dissipated only in the bond line and that a gradual and stable performance can be recorded also when the load is decreasing during increase in displacement. It is also required that peel stresses must be avoided, but not that the shear stress is uniformly distributed. It may also be possible to determine G_f indirectly by fitting theoretical load carrying capacity to test results.

4. NORMALIZED CONSTITUTIVE RELATION

It is suitable to normalize the constitutive relation, τ versus δ, by dividing τ by τ_f and δ by G_f / τ_f, with τ_f defined in Fig 2. $\tau-\delta$ curves which after normalization to τ/τ_f versus $\delta/(G_f/\tau_f)$ coincide

are referred to as τ-δ curves with the same shape. This shape may be described by a function g:

$$\frac{\tau}{\tau_f} = g \left[\frac{\delta}{G_f/\tau_f} \right] \qquad (2)$$

Thus the constitutive relation of the bond line is uniquely defined by the two variables τ_f and G_f and by the shape function g. The significance of these variables shall be studied later on in this paper. Idealized examples of normalized constitutive relations are shown in Fig 4. The peak value of these curves is 1.0 and also the area under each curve is 1.0.

5.   BRITTLENESS RATIO AND STRENGTH FUNCTION FOR JOINT

The load carrying capacity of a joint is defined as the maximum load, P_{max}, during gradual increase in joint displacement. This means that no special fracture criterion for a joint, based on for instance stress, strain or energy release, is introduced in the present analysis.

P_{max} may be influenced by the nine variables that define joint geometry and material properties: E_1, E_2, t_1, t_2, b, ℓ, τ_f, G_f and g. Thus a total of ten variables are involved. As E_1, E_2, t_1 and t_2 enter the present one-dimensional analysis only through the normal stiffness of the adherends, $E_1 t_1 b$ and $E_2 t_2 b$, and as P_{max} and normal stiffness must be proportional to b, the number of variables is reduced from ten to seven:

$$\frac{P_{max}}{b}, \ t_1 E_1, \ t_2 E_2, \ \ell, \ \tau_f, \ G_f, \ g$$

During analysis of structures with insignificant change in geometry during loading, similitude in the performance of different structures may be utilized for generalization of computational results. Keeping ℓ, τ_f, g and load, P/b, constant, a proportional increase in strain and deformation in all parts of the joint at unchanged force in all cross-sections of the adherends and at unchanged stress in all parts of the bond line is obtained if $t_1 E_1$, $t_2 E_2$ and $1/G_f$ are decreased proportionally. For all values of the load P/b the absolute value of the global tangential stiffness of the joint, d(P/b)/du, is decreased accordingly and by the same factor of proportionality. However, this also means that the value of P/b corresponding to d(P/b)/du = 0, i.e. P_{max}/b, is not influenced by the proportional change in $t_1 E_1$, $t_2 E_2$ and $1/G_f$. Where calculation of P_{max}/b is concerned, consequently these three variables may be reduced to two: $t_2 E_2/(t_1 E_1)$ and $1/(G_f t_1 E_1)$ or alternatively α (= $t_1 E_1/(t_2 E_2)$) and $1/(t_1 E_1 G_f)$.

For further reduction of the six variables now remaining, dimensional analysis may be applied. Two dimensions, force and length, are involved resulting in 6 - 2 = 4 non-dimensional variables. Defining normalized load carrying capacity as

$P_{max}/(\tau_f b \ell)$, the following general relation for the strength of the lap joint is obtained:

$$\frac{P_{max}}{\tau_f b\ell} = f\left[\frac{\ell^2 \tau_f^2}{t_1 E_1 G_f} \quad , \quad \alpha, \quad g\right] \tag{3}$$

For joints with constant α and g, this strength function may be written:

$$\frac{P_{max}}{\tau_f b\ell} = f\left[\frac{\ell^2 \tau_f^2}{t_1 E_1 G_f}\right] \tag{4}$$

This relation shows that the normalized mean shear stress at failure is governed by the ratio $(\ell^2 \tau_f^2)/(t_1 E_1 G_f)$. This important ratio is below called the brittleness ratio of lap joints, or more briefly the brittleness ratio. High values of the brittleness ratio correspond to brittle fracture and low values correspond to ductile fracture. The transition from ductile to brittle characteristics is gradual and it is probable that a majority of joints may be referred to the transition region. It may be instructive to note that the brittleness ratio of lap joint is of similar character as the slenderness ratio of a column.

The ratio $(\ell^2 \tau_f^2)/(t_1 E_1 G_f)$ depends on the absolute size of the joint through ℓ, its geometrical shape through ratio ℓ/t_1, stiffness of the material in the adherends through E_1 and on the properties of the bond line through the ratio τ_f^2/G_f. For some different bonds, experimental values of the bond line characteristic ratio τ_f^2/G_f are given in (Wernersson and Gustafsson, 1987). The material property ratio $E_1 G_f/\tau_f^2$ has the dimension of length and for constant E_1/E_2 this ratio may be regarded as an intrinsic material property of the joint. The corresponding material length parameter used in linear elastic fracture mechanics analysis of solid materials is $(K_c/\sigma_y)^2$, where K_c is the critical stress intensity factor and σ_y the yield stress. Ratio ℓ^2/t_1 can be directly compared with the experimentally deduced "joint factor", $\sqrt{t}/\ell$, (Marian, 1954).

6. STRENGTH ACCORDING TO LEFM AND SELF-SIMILAR STRESS DISTRIBUTION

6.1 Strength according to LEFM

It is appropriate to develop a linear elastic fracture mechanics (LEFM) expression for the strength of a one-dimensional (1D) lap joint as defined by the basic assumptions in section 2. LEFM basically requires that fracture takes place as a progressive movement of a fracture region of constant shape and size and that this region is very small compared with relevant dimensions of the structure. Presuming ℓ is large, during 1D analysis these demands are fulfilled even if there is no pre-existing sharp crack in the joint and even if no stress singularity is predicted. If ℓ is large, only the ends of the bond line are active and during a movement dx of the fully developed self-similar fracture region of

constant size the same amount of energy is dissipated as totally required for complete fracture of a bond line of area bdx. This means that the energy, G_c, dissipated during movement of the active fracture region of constant size is equal to G_f.

Assuming that the fully developed fracture region is very small compared to ℓ, the change in compliance of the joint, dC, during movement of the fracture point from x = 0 to x = dx, Fig 1, is:

$$dC = \frac{dx}{E_1 t_1 b} - \frac{dx}{E_1 t_1 b + E_2 t_2 b} \tag{5}$$

The corresponding change in potential energy, dW, is:

$$dW = - \frac{1}{2} P^2 dC \tag{6}$$

When the load, P, has reached the value necessary for movement of the fracture region - dW = $G_f$bdx, giving:

$$P_{max} = \sqrt{2 (1 + \alpha)} \ \ b \sqrt{t_1 E_1 G_f} \tag{7}$$

This LEFM expression for the strength of a 1D-overlap joint may be written in the form of the general strength function, (3):

$$\frac{P_{max}}{\tau_f b \ell} = \sqrt{2 (1 + \alpha)} \ / \ \sqrt{\frac{\ell^2 \tau_f^2}{t_1 E_1 G_f}} \tag{8}$$

From (7) and (8) it is evident that LEFM predicts no influence of local shear strength, τ_f, shape of τ-δ curve, g, and overlap length, ℓ. Consequently the strength of a brittle lap joint is not increased by increase in adhesive strength, τ_f, but is instead proportional to the square root of the area under the τ-δ curve, $\sqrt{G_f}$.

6.2 Stress distribution in progressively moving fracture region

The constant stress distribution within a self-similar fracture process region moving along a crack path is in general governed only by properties of the material and type of loading. However, in 1D analysis of joints this stress distribution becomes dependent also of the thickness of the adherends. Starting from Eq. (7) the gradient of the relative displacement, dδ/dx, can be found (Gustafsson, 1987):

$$\frac{d\delta}{dx} = - \sqrt{\frac{2(1+\alpha)}{t_1 E_1}} \ \sqrt{\int_0^\delta \tau(\delta)d\delta} \tag{9}$$

This somewhat remarkably simple explicit expression for the gradient of the relative displacement makes it easy to calculate incrementally the self-similar stress distribution corresponding to an arbitrary non-linear τ-δ curve. If the value of δ corresponding to τ = 0 is denoted δ_0 (see Fig 2), then, for conveniency, one may assume x = 0 in the point were $\delta = \delta_0$ and

$\tau = 0$ and use this point as the starting point for the incremental calculation of the relative displacements. The corresponding stresses may then be obtained from the actual $\tau-\delta$ curve. Thus, knowing $\tau(x)$, $\tau(x + \Delta x)$ is obtained from

$$\tau (x + \Delta x) = \tau (\delta + \Delta\delta) \tag{10}$$

where

$$\Delta\delta \approx \Delta x \frac{d\delta}{dx} \tag{11}$$

In Fig 3 an example of a self-similar stress distribution in a brittle joint is shown. This example is valid for the shape of the $\tau-\delta$ curve shown in Fig 4b). The diagram in Fig 3 indicates also how the self-similar stress distribution may be normalized and thus being made valid for, for instance, joints with different α.
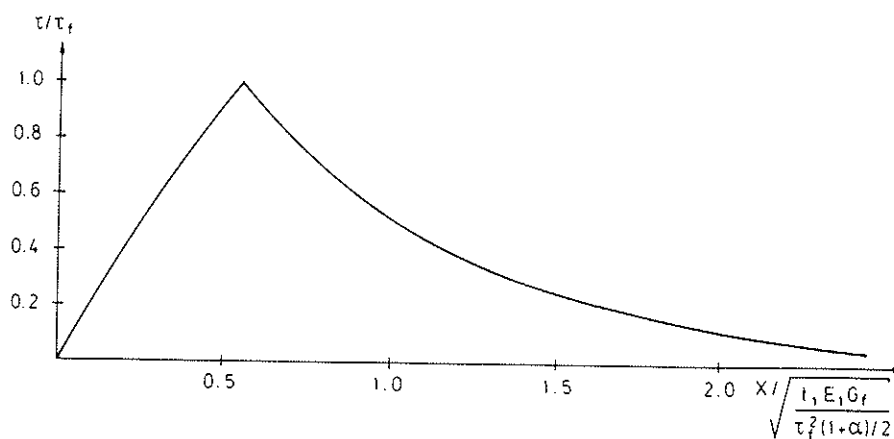
Fig 3. Stress distribution in a fracture region moving along the bond line during fracture of a brittle joint. Const. prop. according to Fig 4b).

From (9) it follows that for $\tau-\delta$ vurves with a finite slope when $\delta \rightarrow 0$, τ reaches zero only asymptotically during increase in x. In spite of this, for the actual bi-linear $\tau-\delta$ curve Fig 3 shows that the absolute length of the major part of the active shear stress transferring area is about $2\sqrt{t_1 E_1 G_f/(\tau_f^2(1+\alpha)/2)}$. The theoretically shortest possible length of a fully developed self-similar shear stress transferring area is $\sqrt{t_1 E_1 G_f/(\tau_f^2(1+\alpha)/2)}$. This shortest possible length is obtained for the pile-shaped $\tau-\delta$ curve shown in Fig 4d). In addition to estimation of length of fracture region, the self-similar shear stress distribution gives a possibility to compare and illustrate the performance of different types of adhesives.

7. GENERAL PROPERTIES OF THE STRENGTH FUNCTION

Without need for numerical calculations, some general properties of the general strength function, (3), for 1D lap joints may be

found by application of results obtained during non-linear fracture mechanics analysis of fracture softening solid materials (Gustafsson, 1985). These properties also show hos more conventional methods of strength analysis form special cases or limiting values. In order to abbreviate formulas, in this section the notation $\bar{\tau}_{max}$ is used for $P_{max}/(\tau_f b\ell)$ and the notation λ is used for the brittleness ratio $\ell^2\tau_f^2/(t_1E_1G_f)$. For all values of the ratio α ($= t_1E_1/t_2E_2 \leq 1.0$) and for all shapes, g, of the $\tau-\delta$ curve, the following is found:

$$\bar{\tau}_{max} \to 1.0 \qquad\qquad \text{when} \quad \lambda \to 0 \qquad\qquad (12)$$

$$\bar{\tau}_{max} \to \sqrt{2(1 + \alpha)/\lambda} \qquad\qquad \text{when} \quad \lambda \to \infty \qquad\qquad (13)$$

$$\frac{d\ (\bar{\tau}_{max})}{d\lambda} \leq 0 \qquad\qquad \text{for all } \lambda \qquad\qquad (14)$$

$$\frac{d\ (\bar{\tau}_{max})}{d\lambda} \geq - 0.5\ \frac{\bar{\tau}_{max}}{\lambda} \qquad\qquad \text{for all } \lambda \qquad\qquad (15)$$

The numerical results shown in Fig 5 illustrate the above relations. From (12) and (13) it is evident that a small value of the brittleness ratio corresponds to ductile fracture and limit load analysis by ideal plasticity and that a large yalue of the brittleness ratio corresponds to fracture through propagation of a fracture process region and limit load analysis by linear elastic fracture mechanics. From (12) and (13) it is also evident that entirely different material property parameters govern P_{max} when λ is small and large, respectively. Thus, for small λ P_{max} is proportional to τ_f but independent of G_f, whereas for large λ P_{max} is proportional to $\sqrt{G_f}$ but independent of τ_f. It is also interesting that the two assymptotical values of P_{max} are both independent of the shape, g, of the $\tau-\delta$ curve. In the region of λ corresponding to transition between ductile and brittle fracture, both τ_f, G_f and g has influence on P_{max}.

(14) and (15) may be derived from the trivial assumption, for solid materials and joints verified by a large number of numerical calculations, that P_{max} never decreases when τ_f or G_f is increased at constant values of all other variables. Validity of (12) - (15) requires that failure takes place in the bond line and accordingly not in the adherends.

As one result of (12) - (15) a theoretical upper bound for the strength of the joint is found:

$$\bar{\tau}_{max} \leq \text{Min} \begin{cases} 1.0 \\ \\ \sqrt{2\ (1 + \alpha)/\lambda} \end{cases} \qquad\qquad (16)$$

This upper bound statement, illustrated by Fig 5, is valid for all α, g and λ. Thus, if a curve shape, g, can be found such that $\bar{\tau}_{max}$ coincides with the upper bound for all α and λ, then this shape of the $\tau-\delta$ curve must be optimal. In fact, such an optimal shape exists and is found to be the pile-shaped curve shown in Fig 4d).

A lower bound statement of equal simplicity as the upper bound statement has not been found. Of course, if the ascending branch of the τ-δ curve is known a lower bound of $\bar{\tau}_{max}$ may be obtained by numerical calculation of the load that corresponds to the first occurrence of peak stress, τ_f , in any point along the bond line. Accordingly, calculation of P_{max} by means of a maximum stress or strain criterion, taking into account the actual linear or non-linear ascending branch of the τ-δ curve, gives a value of P_{max} which is less than or equal to the load carrying capacity of the joint.

8.   CALCULATION OF STRENGTH AT DIFFERENT SHAPES OF τ-δ CURVE

Applied calculations of the strength of lap joints are carried out for the four shapes of the τ-δ curve shown in Fig 4. These four shapes allow analytical calculation of strength and stress distribution. For other curve shapes, calculations may be carried out numerically.
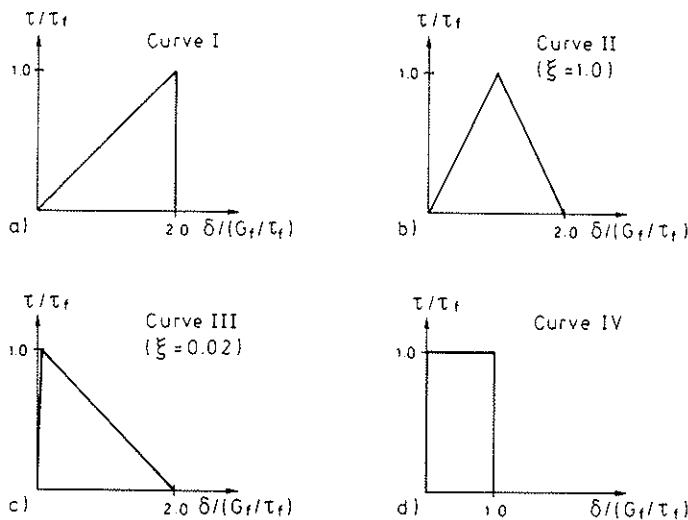
Fig 4. Different shapes of τ-δ curve.

Curve I is linear up to peak stress and has then a sudden drop to zero stress. Though Volkersen (1938) didn't define the properties of the shear stress medium after peak stress, curve I corresponds closely to the assumption made by Volkersen. By substitution of variables and introduction of fracture energy, G_f , the result of Volkersen gives the following expression:

$$\frac{P_{max}}{\tau_f b \ell} = \frac{(1 + \alpha) \sinh \omega}{\omega (\alpha + \cosh \omega)} \tag{17}$$

where

$$\omega = \sqrt{\frac{1 + \alpha}{2}} \; \sqrt{\frac{\ell^2 \tau_f^2}{t_1 E_1 G_f}} \qquad\qquad (18)$$

For bi-linear τ-δ curves, i.e. curves II and III, provided $\alpha = 1.0$ an analytical solution presented by Ottosen and Olsson (1986) may be utilized. The shape of different bi-linear τ-δ curves is here defined by ξ, which denotes the normalized shear displacement when $\tau/\tau_f = 1.0$. For curve II $\xi = 1.0$ and for curve III $\xi = 0.02$. Substitution of variables and introduction of fracture energy in the same manner as in the case of curve I gives the following expression for joints with $\alpha = 1.0$ and with a bi-linear τ-δ curve:

$$\frac{P_{max}}{\tau_f \, b\ell} = \sqrt{\frac{2}{(2-\xi)} \Big/ \frac{\ell^2 \tau_f^2}{4 t E G_f}} \quad \sin \sqrt{\left(\frac{x_p}{\ell}\right)^2 \frac{\ell^2 \tau_f^2}{t E G_f} \frac{2}{(2-\xi)}} \qquad (19)$$

x_p is the point where $\tau = \tau_f$ and may obtained by iterative solution of:

$$\text{tgh} \sqrt{\left[\frac{1}{2} - \frac{x_p}{\ell}\right]^2 \frac{\ell^2 \tau_f^2}{t E G_f} \frac{2}{\xi}} \; - \; \sqrt{\frac{\xi}{2 - \xi}} \; \text{tg} \sqrt{\left[\frac{x_p}{\ell}\right]^2 \frac{\ell^2 \tau_f^2}{t E G_f} \frac{2}{(2 - \xi)}} = 0$$
$$(20)$$

For the pile-shaped τ-δ curve, curve IV, the following result can be obtained (Gustafsson, 1987):

$$\frac{P_{max}}{\tau_f \, b\ell} = \begin{cases} 1.0 & \text{when} \quad \dfrac{\ell^2 \tau_f^2}{t_1 E_1 G_f} \leq 2 \, (1 + \alpha) \\[3mm] \sqrt{2 \, (1+\alpha)} \Big/ \sqrt{\dfrac{\ell^2 \tau_f^2}{t_1 E_1 G_f}} & \text{when} \quad \dfrac{\ell^2 \tau_f^2}{t_1 E_1 G_f} \geq 2 \, (1 + \alpha) \end{cases} \qquad (21)$$

Comparison with (16) shows that Eq. (21) coincides with the upper bound relation and from (21) it is also evident that the pile-shaped τ-δ curve gives an abrupt transition between the ductile or plastic relation (12) and the linear elastic fracture mechanics relation (8) or (13). Relation (21) illustrates also that an increase in adherend stiffness $t_2 E_2$ ($\geq t_1 E_1$) at constant adherend stiffness $t_1 E_1$ may result in a reduction of P_{max}.

In Fig 5 normalized joint strength, $P_{max}/(\tau_f b\ell)$, versus brittleness ratio, $\ell^2 \tau_f^2/(t_1 E_1 G_f)$, is shown for joints with $\alpha = 1.0$. The four curves in Fig 5 correspond to the four τ-δ curves in Fig 4. Fig 5 indicates that the numerical results are all in agreement with the general properties of the strength function of 1D overlap joints, discussed in section 7. Fig 5 also shows that the three apparently very different τ-δ curves I, II and III don't produce very different joint strength provided that the peak stress, τ_f, and the area under the τ-δ curve, G_f, are the same. Curve IV yields a more significant deviation in the intermediate range of $\ell^2 \tau_f^2/(t_1 E_1 G_f)$.

Although curves I-III don't produce very different joint strength, it is important to note, as shown by Ottosen and Olsson (1986),

that gradual softening of an adhesive may have great influence on the load carrying capacity of a joint. Thus, if τ_f would drop abruptly to zero when peak stress, τ_f, is reached, for joints with a high brittleness ratio, from (7) it is for the bi-linear $\tau-\delta$ curves found that the joint strength would be reduced by the factor $\sqrt{\xi/2}$. For curve II this corresponds to a 30 % reduction in joint strength and for curve III to a 90 % reduction.
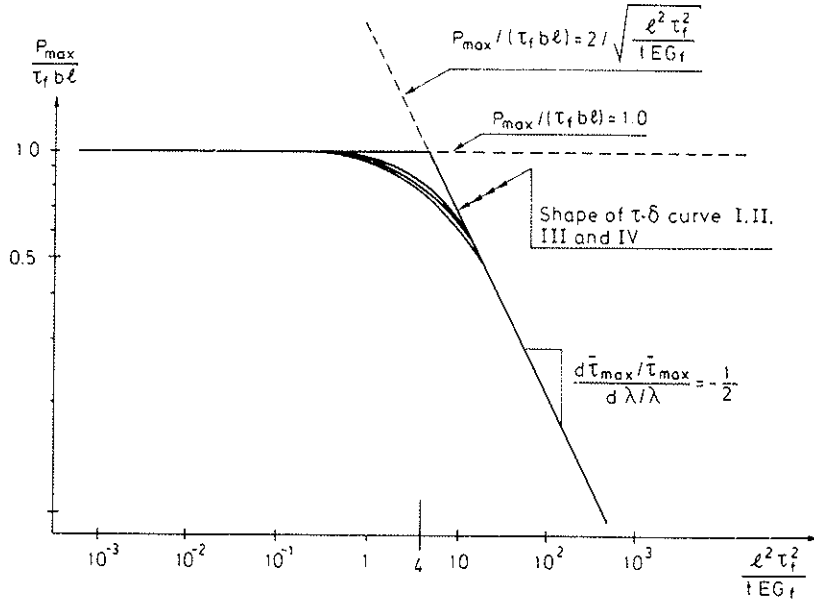
Fig 5. Normalized joint strength, $P_{max}/(\tau_f\,b\ell)$ $(=\bar{\tau}_{max})$, versus brittleness ratio, $\ell^2\tau_f^2/(tEG_f)$ $(=\lambda)$. Curves shown are valid for joints with $\alpha = 1.0$, i.e. with $t_1 E_1 = t_2 E_2$.

By Fig 5 it is possible to approximately estimate when simplified strength formulas may be expected to give engineering accuracy and when it is necessary to apply the more general method of calculation:

$$\left\{ \begin{array}{ll} P_{max} \approx \tau_f\,b\ell & \text{when } \dfrac{\ell^2\tau_f^2}{t_1 E_1 G_f} \leq 0.1\ (1+\alpha) \\[3ex] P_{max} = \tau_f\,b\ell\ f\left[\dfrac{\ell^2\tau_f^2}{t_1 E_1 G_f}\,,\ \alpha,\ g\right] & \text{in general} \qquad\qquad (22) \\[3ex] P_{max} \approx \sqrt{2\ (1+\alpha)}\ b\ \sqrt{t_1 E_1 G_f} & \text{when } \dfrac{\ell^2\tau_f^2}{t_1 E_1 G_f} \geq 10\ (1+\alpha) \end{array} \right.$$

In section 9 requirements for the tacitly assumed validity of the 1D analysis are discussed.

In Fig 6 a comparison with test results from (Marian, 1954) is shown. The test results are valid for Redux adhesive light metal joints of various overlap length, ℓ, and adherend thickness, t $(= t_1 = t_2)$. As τ_f and G_f of the actual bond line are not reported, these two parameters have been estimated from the test results by means of a non-linear least square method. The

theoretical curve in Fig 6 corresponds to curve I in Fig 4a). With slightly different values of τ_f and G_f, one may expect τ-δ curves II and III to give almost the same good agreement.
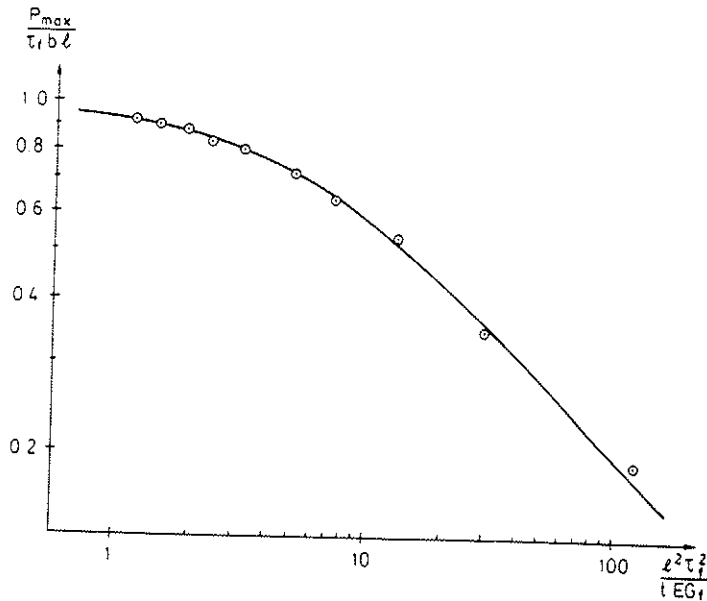
Fig 6. Strength of lap joints. Test results (Redux adhesive - light metal joints) from (Marian, 1954) compared with theoretical curve valid for τ_f = 40 MPa and EG_f/τ_f^2 = 22 mm.

9. REQUIREMENTS FOR 1D ANALYSIS AND REMARK ON 2D ANALYSIS

In one-dimensional analysis of overlap joints, adopted in the present study, it is assumed that peel stresses are negligible and that the adherends are in a state of pure tension without any bending or shear effects. This means that the length of the active shear stress transferring part of the bond line must be large compared to the thickness of the adherends. This infers two requirements: one with respect to the geometrical slenderness of the joint and one with respect to the length of the active part of the bond line in the geometrically slender joints (compare Fig 3). Thus, one may expect the 1D analysis to be accurate if the following inequalities are satisfied for large values of the numbers A and B.

$$\frac{\ell}{t_2} \geq A \tag{23}$$

$$\frac{1}{t_2} \sqrt{\frac{t_1 E_1 G_f}{\tau_f^2 (1 + \alpha)/2}} \geq B \tag{24}$$

As a rough estimate A = 10 and B = 4 may be suggested. Typically, these requirements suggest that a steel joint with long and thin adherends and with a weak and ductile adhesive may be suitable for 1D analysis, whereas a short and thick wooden joint with a strong and brittle adhesive may not be suitable for quantitative 1D

analysis. However, even in cases where the requirements for quantitatively accurate 1D analysis are not satisfied, qualitative results and knowledge obtained by 1D analysis regarding for instance the significance of different parameters may be very useful.

In addition to the above important requirements, in 1D analysis it must also be assumed that the difference in lateral straining of the two adherends is insignificant. When applied to overlapping pipes exposed to tension or torsion, it must furthermore be assumed that possible volume change of the bond line during shear deformation is of minor importance.

In the case of 2D analysis, influence of geometrical shape of joint, defined by ℓ/t_1 and t_1/t_2, must be considered separately and thus not only through the brittleness ratio and α, respectively. Thus, in analogy with the strength function (3), for the case of 2D analysis:

$$\frac{P_{max}}{\tau_f \, b\ell} = f \left[\frac{\ell^2 \tau_f^2}{t_1 E_1 G_f} \, , \, \alpha, \, g, \, \frac{\ell}{t_1} \, , \, \frac{E_1}{E_2} \right] \tag{25}$$

Here g represents the shape of the 2D constitutive relation of the bond line, which in the case of path independency may be written $(\bar{\sigma}_\perp, \bar{\tau}) = g \, (\bar{\delta}_\perp, \bar{\delta})$ where $\bar{\sigma}_\perp$ and $\bar{\delta}_\perp$ is the normalizied stress and relative displacement, respectively, perpendicular to the bond line. General properties of (25) are analogous to those of (3), though not identical. In Eq. (25) geometrical non-linearity is not considered and isotropic adherend materials with given values of Poisson's ratio are assumed.

10. INFLUENCE OF SHEAR FRACTURE IN ADHERENDS

10.1 Discussion

For wooden adherends and fibre reinforced composite adherends, failure may not develop in the adhesive but instead in a thin layer of the adherend material close to the bond line. Such a shear failure is assumed to develop if τ_f is greater than the shear strength, τ_{fr}, of the adherend material. Just as the bond line, the adherend layer has a τ-δ curve and accordingly a fracture energy. For simplicity, in this discussion it is, however, assumed that the fracture energy of the adherend material is negligible as compared to the fracture energy of the bond line. This may be a reasonable assumption for many adhesives and non-metallic adherends.

The negligible fracture toughness of the adherend material means that the local shear stress immediately drops to zero when τ_{fr} is reached. If τ_f is greater than τ_{fr} this means, in turn, that only a part of the ductility, and accordingly only a part of the fracture energy, of the bond line is utilized. This is illustrated in Fig 7 where the effective fracture energy is represented by the shaded area and where the effective τ-δ curve is represented by

the curve enclosing the shaded area. The reduction in effective fracture energy that results from $\tau_f > \tau_{fr}$ is of particular signficance for brittle joints as for such joints P_{max} is directly governed by the fracture energy. It can also be noticed that the limit case $\tau_f = \tau_{fr}$ corresponds to an abrupt change in effective fracture energy. Accordingly a small increase in τ_f may produce a sudden and drastic decrease in load carrying capacity of brittle joints.

From the above discussion one may conclude that adhesives stronger than the adherend should be avoided in the presumably common case when the fracture energy of the bond line is great as compared with the fracture energy of the solid material in the adherends. Taking into account also joints with a low brittleness ratio, the ideal adhesive should be strong, but still not as strong as the adherend with low fracture energy. At this point it must be remarked that certain adhesives under the action of long-term load lose a significant part of their strength. Of course, in this case it may be favourable to choose an adhesive with a strength at short time loading greater that the strength of the adherend material.

<u>10.2 A test</u>

Where wooden joints are concerned, the above conclusion may seem remarkable since fracture in the wood is usually taken as a positive sign of a good and suitable adhesive of high quality. However, in order to attain some verification of the theoretical conclusion a small test series was carried out. 3 x 3 centrically loaded single-lap joints with wooden adherends (Pinus Silvestris) and with $\ell = 160$ mm and $t_1 = t_2 = 20$ mm were tested. Three of the specimens were joined by polyurethane and three by resorcinol/phenol and three specimens were made of solid wood without any bond line. The solid specimens were sawn in one piece from larger pieces of wood and accordingly, in contradiction to the first 2 X 3 specimens, not sawn into two adherends subsequently joined by adhesive. The τ-δ curves of the actual bond lines, see (Wernersson and Gustafsson, 1987), are shown schematically in Fig 8: the two bond lines have approximately the same G_f, but in the event of adherend fracture the effective fracture energy of the weak polyurethane bond line may become significantly greater than that of the strong resorcinol bond line. In the present tests, in all cases adherend fracture developed and in Table 1 the results are indicated. Clearly, the actual very limited test series appears to support the above discussion. The weaker polyurethane bond line with a greater effective fracture energy produces a stronger joint than the resorcinol bond line which has negligible effective fracture energy in the case $\tau_f > \tau_{fr}$ and produces about the same joint strength as the solid type of specimen. The theoretical discussion as well as the test results also suggest that in certain cases a structural member can be made stronger if sawn into two pieces which then are joined together by means of a suitable adhesive.
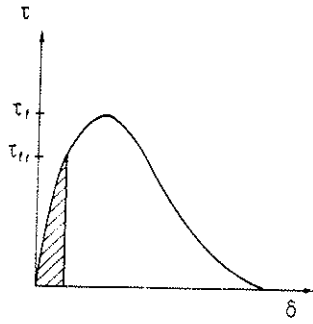
Fig 7. Simplified effective fracture energy when $\tau_f > \tau_{fr}$.
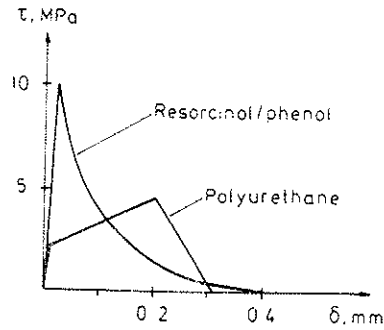
Fig 8. Schematic $\tau-\delta$ curves for two adhesive bond lines.

BOND	$\dfrac{P_{max}}{b\ell}$, MPa
Solid wood	1.4
Resorcinol/phenol	1.3
Polyurethane	2.1

Table 1.
Strength of joints. Mean values from three tests.

11. CONCLUSIONS

From the above study of 1D joints in pure shear, the following conclusions may be drawn.

* By means of a non-linear fracture mechanics approach, taking into account the complete $\tau-\delta$ curve of the bond line, it is possible to analyse the strength of joints with different characteristics in a unified manner. The joint strength may be described as a function of a brittleness ratio which also characterizes the joint and its fracture performance.

* Fracture energy, G_f, is an important parameter which depends on both the ascending and descending branch of the $\tau-\delta$ curve.

* For ductile joints the strength, τ_f, of the bond line is the governing strength parameter while for brittle joints the strength is determined by G_f. In the intermediate range both τ_f, G_f and the shape of the $\tau-\delta$ curve have influence.

* The unified theory makes it possible to estimate when more conventional methods of strength analysis are applicable. It is also estimated when the 1D analysis is applicable.

* A linear elastic fracture mechanics expression for the strength of 1D joints can be obtained. The self-similar stress distribution in the fracture process region can be calculated for an arbitrary non-linear τ-δ curve in a simple manner.

* If adherend fracture may occur, a small increase in adhesive strength may produce a drastic decrease in joint strength.

ACKNOWLEDGEMENT

REFERENCES

Adams, R.D., and Wake, W.C., 1984, "Structural Adhesive Joints in Engineering", Elsevier Applied Science Publishers Ltd.

Anderson, G.P., Bennett, S.J., and DeVries, K.L., 1977, "Analysis and Testing of Adhesive Bonds", Academic Press, Inc.

Gustafsson, P.J., 1985, "Fracture Mechanics Studies of Non-Yielding Materials Like Concrete: Modelling of Tensile Fracture and Applied Strength Analyses", thesis, Report TVBM-1007, Div. of Build. Mat., Lund Inst. of Techn., Sweden.

Gustafsson, P.J., 1987, "Analysis of Generalized Volkersen-Joints in Terms of Non-Linear Fracture Mechanics", Report TVSM-7036, Div. of Struct. Mech., Lund Inst. of Techn., Sweden. In preparation.

Hillerborg, A., Modéer, M., and Petersson, P.-E., 1976, "Analysis of Crack Formation and Crach Growth in Concrete by Means of Fracture Mechanics and Finite Elements", Cement and Concrete Research, Vol. 6, pp. 773-782.

Marian, J.E., 1954, "Lim och limning", Strömbergs, Stockholm, Sweden. In swedish.

Ottosen, N.S., and Olsson, K.-G., 1986, "Hardening/Softening Plastic Analyses of an Adhesive Joint", accepted for publication in J. of Enginering Mechanics, ASCE.

Volkersen, O., 1938, "Die Nietkraftverteilung in zugbeanspruchten Nietverbindungen mit konstanten Laschenquerschnitten", Luftfahrtvorschung, Band 15, pp. 41-47.

Wernersson, H., and Gustafsson, P.J., 1987, "The Complete Stress-Slip Curve of Wood-Adhesives in Pure Shear", to be presented at EUROMECH 227, "Mechanical Behaviour of Adhesive Joints", Saint-Etienne, France.

INTERNATIONAL COUNCIL FOR BUILDING RESEARCH STUDIES AND DOCUMENTATION

WORKING COMMISSION W18A - TIMBER STRUCTURES

THE COMPLETE STRESS-SLIP CURVE OF WOOD-ADHESIVES IN PURE SHEAR

by

H   Wernersson and P J   Gustafsson
Lund Institute of Technology
Sweden

MEETING TWENTY
DUBLIN
IRELAND
SEPTEMBER 1987

THE COMPLETE STRESS-SLIP CURVE OF WOOD-ADHESIVES IN PURE SHEAR.

H. Wernersson, res.assistent., and P.J. Gustafsson, res.associate.
Division of Structural Mechanics, Lund Institute of Technology
Box 118
S-221 00 Lund
Sweden

ABSTRACT

A test method and test results regarding the complete stress-slip curve of adhesive bond lines in pure shear are presented. The test program concerns the bond between wooden adherends (Pinus Silvestris) and comprises the adhesives PVAc, polyurethane and resorcinol/phenol, tested after different curing time, 4 and 16 days, and at various rates of deformation, 1 mm/min - .0625 mm/min. The test set-up might be described as a further development of the thick adherend test and is designed in order to enable a stable test performance also during strain softening and fracture. The test set-up is also designed at the purpose of achieving pure shear, i.e. zero peel stress, uniform stress distribution and avoidance of adherend fracture.

It is found possible to obtain a complete $\tau-\delta$ curve of a bond line. The deformation capacity of a bond line during plastic hardening and softening is found to be very large as compared with the first linear elastic deformation. From the test results, $\tau-\delta$ curve, peak shear stress, τ_f, fracture energy, G_f, and a bond line characteristic ratio, τ_f^2/G_f, is evaluated. Characteristic differences between the performance of the different adhesives are found. In some cases, curing time and rate of deformation are found to have a significant influence on the performance of the bond line.

JOINTS	ADHESIVE	STRENGTH	FRACTURE	ENERGY
STRESS-SLIP	SHEAR	WOOOD	TEST	RATE OF LOADING
CURING	TESTMETHOD	SOFTENING	BOND	FRACTURE

1. INTRODUCTION

Within the field of adhesive science a number of theoretical models for strength evaluation of joints has been proposed, see e.g. (Adams and Wake, 1984). These models, whether they are based on continuum mechanics or fracture mechanics, numerical or analytical, all demand relevant material properties.

The test method to be described in this paper can be regarded as a further development of the thick adherend test. The aim is to determine the complete stress-slip curve of adhesive joints in shear. A test program including PVAc, polyurethane and resorcinol/phenol is carried out to find some typical properties of adhesives used as wood connectors.

When testing lap joints, load and sometimes also relative motion of the adherends are recorded. These tests are usually simple to accomplish but the test result is valid only for the specific test piece and it is difficult to make conclusions about the behaviour of a joint with different geometry.

To make more general conclusions from a test and to estimate the response of other joints, information about fundamental material properties of the different parts of the joint is required. Different methods for evaluating these properties of an adhesive are conceivable. One is to measure the strain distribution along the bond line followed by a backward calculation of a likely material model. This method may seem difficult to use as it is complicated to make accurate strain measurements in the very thin glue line (Sharpe and Muha, 1974, Asundi, 1987).

Another method is to cast blocks of the adhesive from which bulk specimens can be machined. This is, however, a doubtful method if the curing process is dependent of the adherend material or if the interface between adhesive and adherend may influence the properties of the bond line. Where the elastic properties at small strains are concerned, recent research (see e.g. Jeandrau (1986)) has shown that adhesive properties in a thin film and in bulk are similar, but it is still very uncertain whether the properties are similar in a state of large strain, shear slip and fracture. Hence, it may seem more appropriate to determine the properties of a bond line rather than the properties of the adhesive in bulk.

To evaluate the shear properties of a bond line the two most common methods are the napkin ring test (ASTM E 229-70) and the thick adherend test (ASTM D 3983-81). If the adherends are isotropic the napkin-ring test gives a fairly uniform stress distribution around the glue line. For testing of the complete stress-slip curve of the bond area between wood adherends, the method is believed to be less suitable due to difficulties in specimen preparation, and also due to the possibility of fracture in wood and also due to the demand of a stable preformance of the test set-up especially during fracture and softening of the bond line. The thick adherend test may be more appropriate for determination of the actual stress-slip curve and the test method described below may be regarded as a further development of the thick adherand test.

2. TEST METHOD

The aim of the test is to determine the shear stress, τ, as a function of shear deformation, δ. Special effort is made to determine the complete τ-δ curve of the bond line, i.e. also the softening or descending branch when the stress is decreasing as the deformation increases. Testing brittle adhesives this infers special requirements on the test set-up and the testing machine. It has to be stable and stiff and, if it is a closed-loop machine, it must also be fast. The machine used is a servo-hydraulic, cloosed-loop, MTS 810, a testing machine primarily constructed for advanced dynamic testing.

The test set-up is shown in Figure 1. It consists of two steel parts connected by the wooden test specimen and a steel ball placed in a notch. The width of the steel parts is 20 mm.

As the aim of the test is to load the glue line in pure shear, consequently peel stresses must be avoided. This is achieved by anti-symmetric loading on the symmetric wooden test piece. Perfect anti-symmetric loading requires that the steel parts are infinitely stiff compared with the wooden test piece and that the connection between steel and wood is perfect. If ideal anti-symmetry could be achieved, the peel stresses would be identically zero along the bond line. The possibility to achieve peel stresses identical to zero represents a fundamental difference between the present test method and the thick adherend test.

Loading is done in compression to simplify the test set-up and to avoid lashes which can induce instabilities during testing.
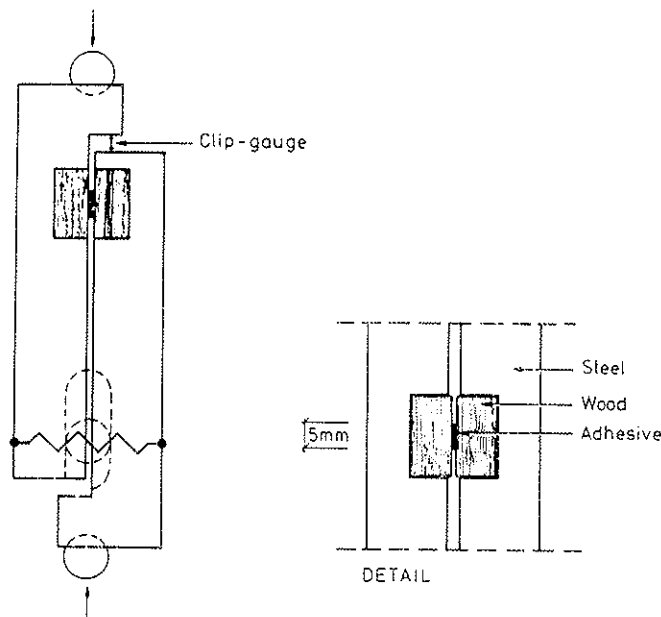
Figure 1. Test set-up.

Moment across the glue line is avoided primarily by letting the line of action of the force act through the symmetry axis of the glue line. To reduce any influences of excentricities a steel ball is placed in a notch in the steel piece and a rubber band is tightened to keep it steady. The ball counteracts bending, torsion and peel of the bond during testing as well as during previous handling.

The slip is measured by two clip-gauges placed according to Figure 1. The deformation of the clip-gauges also controls the testing machine, i.e. the tests are carried out at constant rate of deformation. Notice that the recorded deformation is not the shear deformation of the bond line but that of the whole joint.

As shown in Figure 1, the glue line is only 5 mm. Besides that a short joint gives a uniform stress distribution, the purpose is to reduce the possibility of wood failure. To control the length of the glue line a 0.1 mm PTFE- film is used. The film is removed just before testing.

To reduce influence of possible boundary effects, e.g. due to lower hydrostatic pressure at the edges of the glue line during curing, the test piece is made with duble length and after curing it is cut to desired test size, $20*20*22$ mm^3.

The test pieces are prepared as follows:

a. Two wooden pieces with dimension $11*20*40$ mm^3 is sawn and the surfaces toward the glue line is polished with sand paper.

b. The PTFE-film is attached.

c. The adhesive is applied according to instructions from the manufacturer and the pressure is applied with lever and weight.

d. The test pieces are cured in climate room of 20°C, 65% RH.

e. The test pieces are cut to required size, with a bond area of $5*20$ mm^2.

f. The test pieces are attached to the steel parts with fast curing epoxy.

g. The test set-up is placed in the testing machine, the PTFE-film is removed and the two clip-gauges are attached.

k. The test is run.

Quality and characteristics of a bond line depends of a number of different factors. The variables studied in the test program are type of adhesive, curing time and rate of deformation. The adhesives tested are 1-component PVAC (CASCO 3304), 1-component polyurethane (CASCO 1809) and 2-component resorcinol/phenol (CASCO 1703). The curing times are 4 and 16 days. Rates of deformation are 1 mm/ min, 1 mm/ 4 min and 1 mm/ 16 min. For each testing condition six tests

are made. Properties the wood (Pinus Silvestris) like density, moisture and angle to the R- or T-direction of the fibres, are recorded but has not been attemted to be held constant. Further, the curing condition and amount of glue are noted.

The choice of adhesives is no attempt to find the most common glues. However, as regards essential features of their mechanical behaviour, they are believed to be representative for various kinds of wood adhesives on the market.

3. EVALUATION

A typical test result is shown in Figure 2. The curve does not show the load versus deformation for the bond line but for the total joint. Deformations outside of the bond must be subtracted. It is also seen that the very first part of the curve is vertical and that the load does not reach zero at the end of the curve. This is due to the force in the clip-gauges and must also be corrected for.
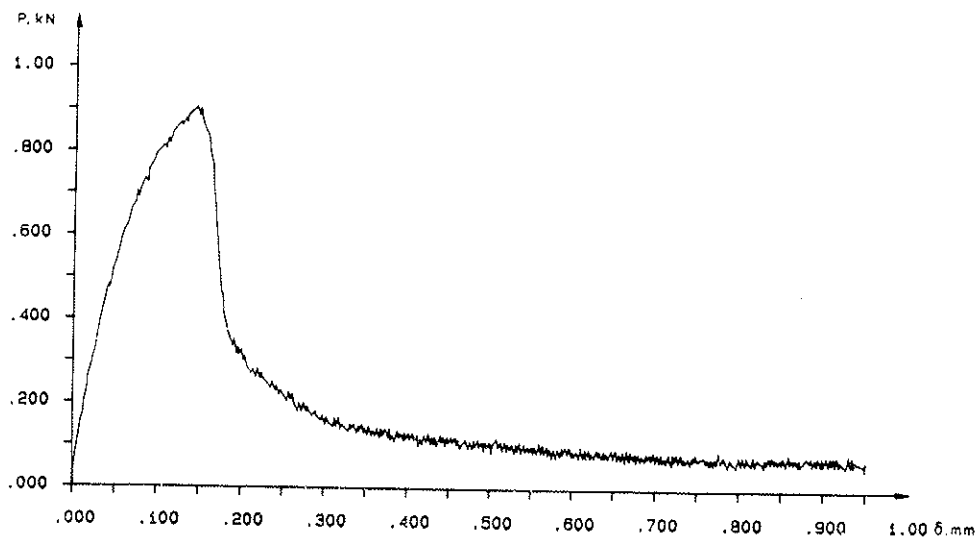
Figure 2. Example of recorded load versus displacement in the clip-gauges.

To estimate the additional deformations, six comparative tests were made on specimens of solid wood, i.e. a solid wood piece were cut in half except for a lap of 5 mm in the middle. A typical result from these tests are shown in Figure 3. As the ascending branch of the $\tau-\delta$ curve must be corrected for the additional deformations outside the bond line during loading while the descending branch must be corrected for the additional deformations during unloading, the preformance of the solid specimens were recorded for both loading and unloading. The mean values of the stiffness of the solid specimens during loading and unloading, respectivly, were used for correction of the deformation recorded during test of the bond line specimens.
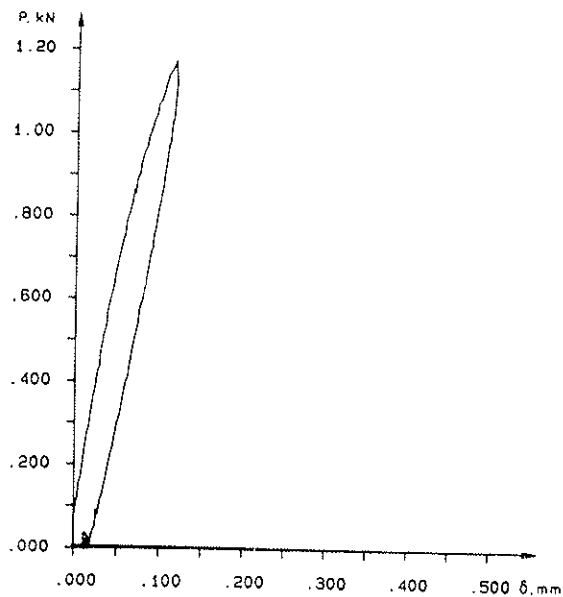
Figure 3. Loading and unloading of test-piece of solid wood

The force in the clip-gauges is easiest measured by the test machine when they are adapted and removed. As the test results are recorded digitaly, the compensations for the above mentioned effects can be done on a personal computor.

A crucial step in the evaluation process is the calculation of the local stress in the bond line. The present test method has been designed at the purpose of achieving an almost uniform shear stress distribution along the the bond line and during the evaluation it is assumed that the local shear stress can be calculated as the load divided by the bond area. This assumption is further discussed below.

4. RESULTS

As a major result from the test program it was found possible to obtain the complete τ-δ relation of an adhesive bondline. The results from the test are summarized in Figures 4, 5, 6 and in Table 1. Except for resorcinol/phenol, Figure 6, the curves represent mean curves of six tests. Som of the resorcinol/phenol specimens fractured in a sudden and brittle manner and consequently the complete τ-δ curve could not be recorded. Occurrence of brittle failure may be due to limited performance characteristics of the testing machine.

In Table 1 the parameter G_f is specified. G_f is the fracture energy, i.e. the area below the τ-δ curve. The fracture energy must be distinguished from the critical energy release rate, used in linear fracture mechanics, see e.g. (Gustafsson, 1987).
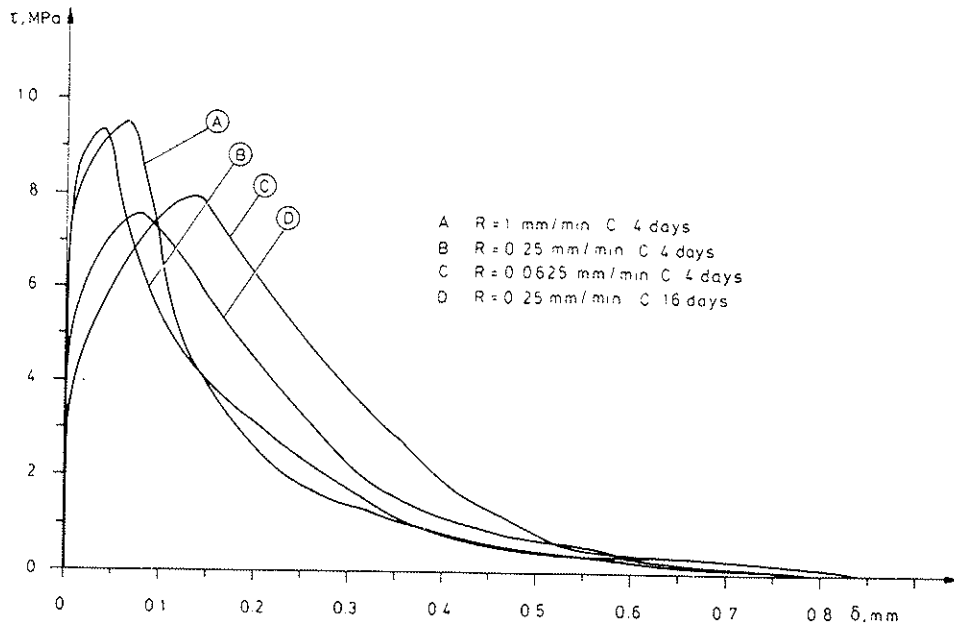
Figure 4. $\tau-\delta$ curves for PVAc, tested at different rate of
deformation (R) and after different curing time (C).

All curves show a very stiff behavior at small stresses in the
elastic region. Due to the uncertainties in subtracting additional
deformations, the slope of the first steep part of the $\tau-\delta$ curve is
difficult to determine accurately and the test method is not
suitable for determination of the elastic shear modulus of
adhesives. On the other hand, the linear elastic deformation of a
bond line seems to be very small as compared with the deformation
during plastic hardening and softening.
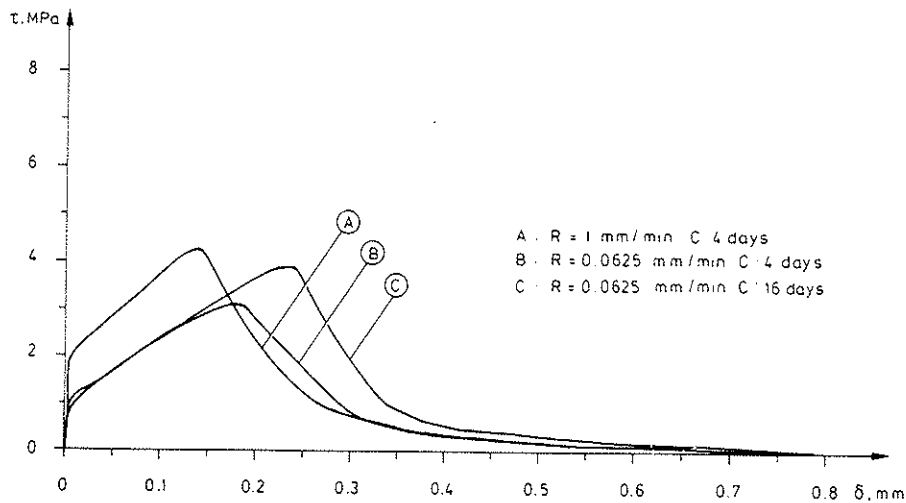
Figure 5. $\tau-\delta$ curves for polyurethane, tested at different rate of
deformation (R) and after different curing time (C).

In Figure 4-6 the deformation is given as relative motion of the adherend surfaces. If this would be transformed into shear strains, it is notable that the strains at the peak shear stress are of a magnitude of 100% for PVAc and polyurethane.

Figure 7 shows normalized τ-δ curves for the three different adhesives with equal deformation rate and curing time. It is shown that the predominant deformation occurs in the plastic region and for PVAc and for resorcinol/phenol the major deformations occurs in in the softening region.

Like for most polymeer materials, properties of adhesives may be dependent on the rate of deformation. A decreased deformation rate was expected to give a lower strength and increased deformation at peak stress. The tests confirmed this behaviour, except for the curves A and B of PVAc. The two curves are similar and any significant difference is hardly possible to confirm statistically.

The three different adhesives have different curing mechanisms. PVAc cures by emitting solvents to the wood material, polyurethane cures by a reaction with moisture in the adherends and resorcinol/phenol cures by a chemical reaction between the two components. This may explain the different response on increased curing time. PVAc shows a tougher response and lower strength, polyurethane indicates no difference in toughness but in strength while resorcinol/phenol indicates no difference in strength but a more brittle behaviour.

In Table 1 the standard deviation of each test series is given. For peak shear stress, τ_f, as well as for fracture energy, G_f, the coefficient of variation is of the magnitude of 10 % for PVAc and
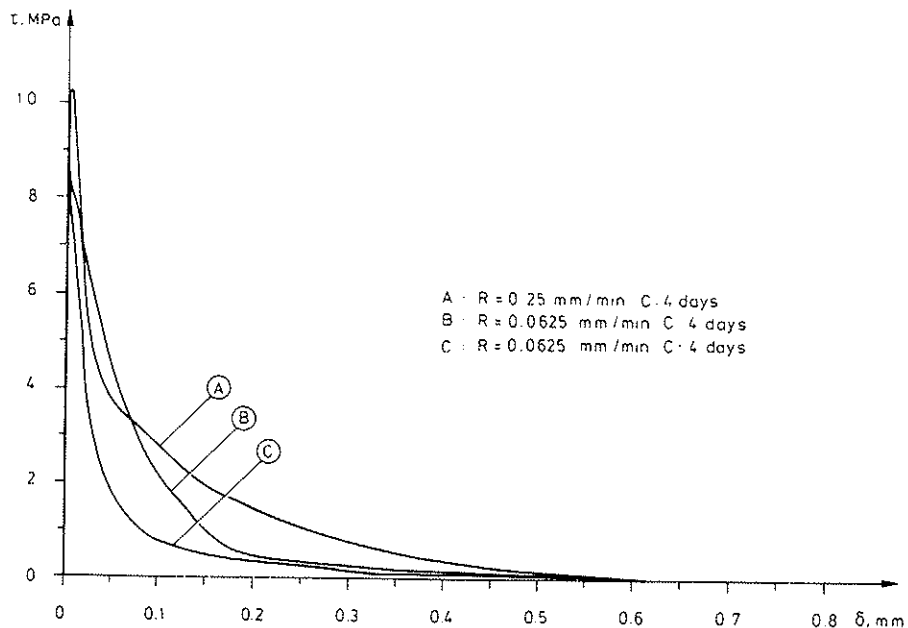
Figure 6. τ-δ curves for resorcinol/phenol, tested at different rate of deformation (R) and after different curing time (C).
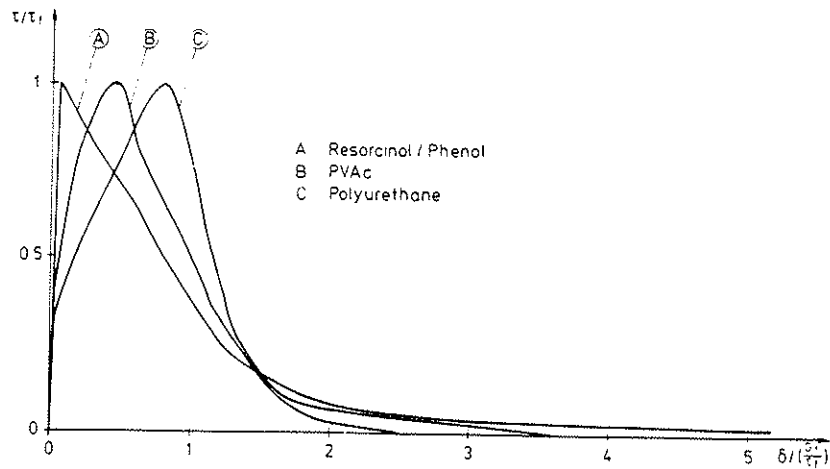
Figure 7. Normalized $\tau-\delta$ curves for PVAc, polyurethane and resorcinol/phenol adhesives. R= .0625 mm/min, C= 4 days.

resorcinol/phenol and of 35 % for polyurethane. Here it must be noted that the sensitivity in load carrying capacity, P_{max}, of a lap joint to deviations in τ_f and G_f, respectivly, is different. According to the analysis presented in (Gustafsson, 1987), if failure occurs in the bond line, P_{max} is at the most propotional to τ_f and $\sqrt{G_f}$, repectively. Consequently the effect of a deviation in G_f is much less than the effect of a deviation in τ_f, a 20 % deviation in G_f corresponding to a $\sqrt{1.2}$ -1.0 = 10 % deviation in τ_f.

The controled size of the bond area and the presumably very small peel stresses in the bond line implied that the failure, with a few exceptions, occured within the bond line. In a few cases, i.e. at the brittle failures of resorcinol/phenol and for PVAc tested at the highest rate of deformation, the failure occured partly in the wood adherends. In those cases the wood failure was limited to late wood.

Ratio τ_f^2/G_f, indicated in Table 1, has the dimension of stress/deformation and may be interpreted as a general measure of the stiffness of the bond line, a high value corresponding to stiff and "brittle" characteristics and a low value corresponding to a ductile performance. Table 1 shows that resorcinol/phenol has brittle characteristics, in particular after a long time of curing. The polyurethane bond lines are much more ductile, in particular at the lower rate of deformation. While the value of ratio τ_f^2/G_f is found to be about ten times higher for resorcinol/phenol than for polyurethane, PVAc is found to be in the intermediate range of ductility. For PVAc the test result suggest that a long curing time and a low rate of deformation produce a decrease in the general stiffness of the bond line. However, decrease in the rate of deformation from 1 mm/min to 0.25 mm/min was not found to have any significant influence on the τ_f^2/G_f. Ratio τ_f^2/G_f forms a part of the

Adhesive	Conditions	τ_f [MPa]	G_f [kNm/m^2]	τ_f^2/G_f[GPa/m]
PVAc	R= 1 mm/min C= 4 days	9.35 ± .87	2.04 ± .56	42.9
	R= .25 mm/min C= 4 days	8.96 ± .62	1.82 ± .23	44.1
	R=.0625 mm/min C= 4 days	7.84 ± .91	2.36 ± .44	26.0
	R= .25 mm/min C= 16 days	7.46 ± .89	1.92 ± .27	29.0
Poly- urethane	R= 1 mm/min C= 4 days	4.21 ± 1.43	1.01 ± .39	17.5
	R=.0625 mm/min C= 4 days	3.02 ± 1.31	0.68 ± .28	13.4
	R=.0625 mm/min C= 16 days	3.83 ± .98	1.04 ± .28	14.0
R/P	R= .25 mm/min C= 4 days	10.3 ± .94	1.06 ± .17*	100.1
	R=.0625 mm/min C= 4 days	8.51 ± .65	0.71 ± .06***	102.0
	R=.0625 mm/min C= 16 days	8.53 ± 1.37	0.36 ± .02**	202.1

Table 1. τ_f and G_f for different adhesives at different rate of
deformation (R) and after different curing time (C).
*. Only 2 stable tests.
**. Only 3 stable tests.
***. Only 4 stable tests.

brittleness ratio of lap joints, $(\tau_f^2/G_f)/(tE/\ell^2)$, see (Gustafsson,
1987),where the numerator characterizes the bond line and where the
denominator characterizes joint size and geometry and stiffness of
the adherends.

5. CONCLUDING REMARKS AND CONCLUSIONS

It is important to state that the adhesives tested are not comparable in a design situation as they have totally different creep properties and strength in long-term loading. Resorcinol/phenol is a structural adhesive whereas the other two are usually not regarded as structural adhesives in wood design. On the other hand, the parameters tested are important for strength evaluation of joints. Knowledge or consideration of the complete τ-δ curve is believed to be essential when new or improved adhesives are to be developed.

In the evaluation of the test results a uniform shear stress distribution was assumed. A non-uniform stress distribution may influence the recorded τ-δ curve and the value of τ. G is calculated from the total work of fracture and should not be influenced by a non-uniform stress distribution. It is probable that the stress distribution along the bond line is significantly non-uniform during its first linear elastic deformation. Therefore and also by other reasons, see above, the present test method is not estimated as suitable for determination of slope of the first steep part of the τ-δ curve. Where PVAc and polyurethane are concerned there is little doubt about the accuracy of the assumption of a uniform stress distribution after start of plastic yielding. For resorcinol/phenol the presented method might have underestimated τ and the steepness of the first part of the descending branch of the τ-δ curve. However, if the specimen is analysed as a one-dimensional lap joint and the brittleness ratio of the joint calculated, being less than about 0.1 for all specimens tested, the computational results presented in Figure 5 in (Gustafsson, 1987) suggest that τ may be accurately determined also for the resorcinol/phenol. On the other hand, it is of course very doubtful whether the present specimen can be analysed as a one-dimensional lap joint. For a brittle adhesive such as resorcinol/phenol it would therefore be appropriate to verify the method of evaluation by a finite element analysis of the performance of the specimen.

From the test series several conclusions can be drawn:

* Adhesive bond lines expose gradual softening, i.e. the stress does not drop abruptly to zero when peak stress is reached, and it is possible to obtain the complete τ-δ curve of an adhesive bond line.

* The deformation of the bond lines in the elastic region appears negligible as compared to the deformation after start of yielding, see Fig 7.

* For PVAc and polyurethane the shear strains are very large at peak stress and may be estimated to be in the order of 100 %.

* Characteristic differences in the preformance of the adhesives tested are evident both through the shape of τ-δ curve and through the bond line characteristic ratio τ_f^2/G_f.

* For all adhesive tested it appears that a decrease in rate of deformation gives a decrease in peak stress, τ_f. For polyurethane and resorcinol/phenol the same is found with respect to both the fracture energy, G_f, and ratio τ_f^2/G_f.

* For resorcinol/phenol an increase in curing time gave a decrease in G_f and increased "brittleness" of the bond line, τ_f^2/G_f. For PVAc and polyurethane the influence of curing time is less significant.

* The fracture energy of wood adhesive bond lines appears to be in the order of magnitude of 1 kNm/m^2.

ACKNOWLEDGMENT

REFERENCES

Adams, R.D., Wake, W.C., 1984, "Structural Adhesive Joints in Engineering", Elsevier Applied Science Publishers Ltd.

Asundi, A., 1987. "Deformation in Adhesive Joints Using Moiré Interferometry", International Journal of Adhesion and Adhesives. vol 7 no 1, pp 39-42.

Gustafsson, P.J., 1987, " Analysis of Generalized Volkersen Joints in Terms of Non-Linear Fracture Mechanics". to be presented at EUROMEC 227, "Mechanical Behaviour of Adhesive Joints", Saint-Etienne, France.

Jeandrau, J.P., 1986, "Intrinsic Mechanical Characterization of Structural Adhesives", International Journal of Adhesion and Adhesives. vol 6 no 4, pp 229-231.

Sharp, W.N., and Muha, T.J., 1974, "Comparison of Theoretical and Experimental Shear Stress in the Adhesive Layer of a Lap Joint Model", Procedings of Army Symposium on Solid Mechanics, pp 23-44.

INTERNATIONAL COUNCIL FOR BUILDING RESEARCH STUDIES AND DOCUMENTATION

WORKING COMMISSION W18A - TIMBER STRUCTURES

DEVELOPMENT OF A GDR LIMIT STATES DESIGN CODE
FOR TIMBER STRUCTURES

by

W   Rug and M   Badstube
Academy of Building of the GDR
Institute for Industrial Buildings
German Democratic Republic

MEETING TWENTY
DUBLIN
IRELAND
SEPTEMBER 1987

DEVELOPMENT OF A GDR LIMIT STATES DESIGN CODE FOR TIMBER STRUCTURES

By W. Rug and M. Badstube
Academy of Building of the GDR,
Institute for Industrial Buildings
Berlin, 1987

1. Introduction

The state of the research work performed with regard to the
future timber design code by adapting the limit states method
has been reported hitherto by the authors in references /1/
and /2/.
The papers as to /1/ and /2/ include - inter alia - the
research program for the period from 1986 to 1988 as well
as first results and findings concerning the standard strength
of visually sorted structural timber and glued laminated tim-
ber and concerning the adaptation factors.
In compliance with the objective of the research program,
the work performed in 1986 (see reference /3/) has been fo-
cussed on studies and investigations concerning the strength
of mechanically sorted glued laminated timber and structural
timber. Other activities were accomplished to examine the
influence of the moisture and of the depth of girder on the
flexural strength of glued laminated timber.
The report following hereinafter covers the results and fin-
dings of said studies and investigations.

2. Strength of Mechanically Sorted Glued Laminated Timber (GLT)

2.1. Test Procedure

New grades of glued laminated timber have already been de-
scribed in /1/ and /2/. The layers have been sorted mechani-
cally according to the modulus of elasticity (bending) and
to the knottiness. The timber was classified into three
strength grades.
Figure 1 shows the general design of the glued laminated
timber.
The design of the individual grades of glued laminated timber
which have been sorted visually and mechanically is shown
in Table 1.
The investigations covered 5 test series (see Table 2) of
mechanically sorted glued laminated timber. Each test series
included 12 beams.

./..

With the exception of the test series V_2 and V_5, the key-dovetailing of layer 1 was located at the tension side of the beams within the test zone. The test series V_2 and V_5 did not have any key-dovetailing within the test zone. The key-dovetail skew notch (in German: KZV) between the 1st and 2nd layer amounted to ≥ 250 mm. With all other layers it was at choice (see also Table 2).

With a view to providing a zone being free from transverse forces, a four-point loading was selected for the test design of the glued laminated timber girders (see Table 2). The ratio of the effective span to the test-sample height was 15. The length of the test zone was about four times the height.

Taking into consideration the stipulations included in /5/, the tests have been performed under the following conditions :-

relative air humidity: $\varphi = 65 \pm 5\ \%$

temperature: $T = 20 \pm 2\ ^{\circ}C$

time of loading until failure: $t_B = 5 \pm 2$ min.

The loading was effected continuously until failure.

The dimensions of the beams are included in Table 2.

As a result of the individual tests, the following particulars (parameters) have been determined :-

1) moisture of timber u of the corresponding glued laminated timber beam by means of a moisture meter

2) apparent specific gravity ϱ of the beam by weighing according to /11/

3) flexural strength R_m

4) deformation u_z at mid-beam (see Table 2) by means of measuring rod and level

5) modulus of elasticity in bending E_m with a ratio of $\frac{E_m}{G} = 15$ according to the data included in /6/.

2.2. Test Evaluation

The results and findings of the tests summarized in Table 2 can be derived from Table 3. Inter alia, mean values and 5 % quantiles of the flexural strength and the modulus of elasticity in bending of the GLT girders are being indicated there.

The quantile values are derived from Weibull distributions according to /9/. One can see that the flexural strength and the modulus of elasticity in bending increase with an increasing GLT quality (Table 3: see the results of V_4, V_3, V_1).

Thus, the increase in strength for $R_{m,5\%}$ amounts to :-
    19 % with GLT 5 (V_3) as compared with GLT 6 (V_4)
    42 % with GLT 4 (V_1) as compared with GLT 6 (V_4)
    19 % with GLT 4 (V_1) as compared with GLT 5 (V_3).

The increase in flexural strength with an increasing GLT quality is more significant than the increase of the modulus of elasticity in bending. In this connection, the key-dovetailing doesn't have any disadvantageous influence on the increase.

By a comparison of the tests performed with and without key-dovetailing in layer 1, information can be provided concerning the effect of the key-dovetailing on the flexural strength of glued laminated timber (see Table 3: compare V_2 with V_1 and V_5 with V_4).

As compared with the tests performed with key-dovetailing (V_1), the tests performed with GLT 4 without key-dovetailing in layer 1 of the test zone resulted in increased strength values which are higher by 34 % for R_m and by 12 % for $R_{m,5\%}$.

When using GLT 6, the tests without key-dovetailing (V_5) as compared with those performed with key-dovetailing (V_4) resulted in increased strength values being higher by 35 % for R_m and by 11 % for $R_{m,5\%}$ (see Table 3).

The strength of mechanically sorted glued laminated timber is higher than with comparable visually sorted glued laminated timber (see Figure 2) as follows :-

- flexural strength being higher by 6 % as related to R_m
- flexural strength being higher by 19 % as related to $R_{m,5\%}$.

The failure of the GLT girders is initiated by the rupture of the 1st layer in the key-dovetailing area to an extent of about 80 % and in the layer cross-section with large knots only to an extent of about 20 %.

3. Strength of Mechanically Sorted Structural Timber

Reference /4/ deals with the investigations performed by Apitz as a bending test until failure by using 354 test samples of structural timber with various cross-sectional heights selected from various quality grades. In this connection, the author has determined the knottiness and the modulus of elasticity in bending with each board. These tests were statistically interpreted and evaluated according to /9/ with regard to a mechanical sorting by three strength grades.

The result of said evaluation is included in Table 4.

As compared with the sorting according to visual criteria, mechanically sorted structural timber provides minor scattering in terms of the strength and increased strength values (see Figure 3). However, in the case of mechanically sorted timber the increase in strength diminishes with a reduction of the quality grade and/or strength grade; this phenomenon must still be further studied and investigated.

4. Standard Values of the Design Strength

Taking into consideration the latest results and findings of recent tests and experiments, the standard values of the design strength and of the modulus of elasticity in bending of structural timber and glued laminated timber indicated in table 7 of reference /1/ have been further exactly defined (see Table 5). In this connection, the values for the flexural stress and strain are verified by our own separate tests. All other values have been defined for the time being in accordance with the international state of knowledge and information,

in particular according to /12/ and /13/. With regard to the other stresses and strains, specific studies and investigations will be accomplished as well within the next years.

A comparison of the values for mechanically sorted timber with the values for visually sorted timber demonstrates an increase in flexural strength by 14 to 33 % with structural timber and by 20 to 28 % (33 %) with glued laminated timber. The mean modulus of elasticity is higher by 4 to 12 % with mechanically sorted timber.

The quantities of timber to be economized as a result of this will still be determined by accomplishing separate investigations after having defined the material factor $\gamma_{m,o}$.

5. Investigations Concerning the Adaptation Factors "Depth of Girder" and "Moisture of Timber" with Glued Laminated Timber Subjected to Bending Stress and Strain

In the case of the adaptation factors "cross-sectional height" and "moisture of timber" as indicated in /1/, the international state of knowledge and information has been followed.

The adaptation factor "cross-sectional height" $\gamma_{m,2}$ for glued laminated timber subjected to bending stress and strain corresponds to the applicable code /14/ as well as to the Swiss Code /15/. Concerning glued laminated timber, the decrease in strength commences beyond h = 300 mm.
In reference /1/, three moisture grades are indicated for structural timber and glued laminated timber. A reduction of the strength occurs from a timber moisture rate of ≥ 18 %.

The stipulations indicated hereinbefore should be verified or possibly corrected accordingly for bending stress and strain by performing appropriate tests and experiments.

5.1. Test Procedure

The load scheme and the test procedure corresponded to the particulars indicated in para 2.1. hereinbefore. The tests

./..

have been performed by using test beams of grade 6 of glued laminated timber (in German: BSH 6 - see Table 6). The adaptation factor "cross-sectional height" was verified with depths of girder h = 192, 288 and 608 mm (see Table 2, V_4, and Table 6, V_4 and V_7).

Due to the connection or relation between moisture of timber and flexural strength which is still obscure, in particular within the range of the moisture of timber of u $\geq$ 15 %, the authors investigated the strength of GLT girders with a moisture of timber of u = 15, 18, 24 % (see Table 2: V_4, and Table 6: V_8, V_9).

The moisture of timber was achieved by storing the GLT girders in a humidity chamber.

A typical distribution of moisture over the cross-section is demonstrated in Figure 4.

All values are formed from mean values of 12 test samples. One can see that after 146 days of storage with a climate of T = 20°C and φ = 95 % only the boundary zones are containing the required moisture of timber. Within the heart, the mean moisture of timber is about 18 %.

The loading until failure was only performed when the layer 1 of the GLT girder concerned had achieved the required moisture of timber.

5.2. Test Evaluation

The results and findings are shown in Table 7.

The tests performed for determining the adaptation factor "cross-sectional height" with the depths of girder of h = 192, 288 and 608 mm (Table 3: V_4, and Table 7: V_6, V_7) do not reveal any decrease in strength for $R_{m,5\%}$.

Accordingly, thus the adaptation factor - up to a depth of girder of h = 608 mm - is: $\gamma_{m,2}$ = 1.

The tests performed for determining the adaptation factor "moisture of timber" with the moistures of timber of u = 15, 18 and 24 % (Table 3: V_4, and Table 7: V_8, V_9) do not reveal

./..

any decrease for $R_{m,5\%}$ with u = 18 % as compared with u = 15 %, but they reveal a decrease of 7 % with u = 24 %.

The adaptation factor for a moisture of timber of u ≤ 18 % is $\gamma_{m,1,1}$ = 1 whereas for a range of the moisture of timber of u = 18 % up to u = 24 % it is as follows :-

$$\gamma_{m,1,1} = \frac{R_{m,5\%}(V_9)}{R_{m,5\%}(V_4)} = \frac{23.6}{25.5} = 0.93$$

A comparison of the test series V_4 (16 girders) with the combined values of the test series V_4, V_6 and V_8 (36 girders of grade 6 of glued laminated timber with h = 288 mm and u ≤ 18 %) shows that the $R_{m,5\%}$-value of the combined series deviates only by 1 % from the $R_{m,5\%}$-value of the series V_4.

The density distribution according to Weibull for GLT 6 (36 girders) is shown in Figure 5.

Thus, the values indicated in /1/ are verified (see Table 7).

However, a new classification of the categories of structures/ buildings and of the pertinent climatic conditions has been accomplished which considers the adaptation inertia of cross sections of different sizes and/or the influence of certain types of utilization on the moisture of timber accordingly (see Table 8).

6. Summary / Further Research Activities

Girders of structural timber and of glued laminated timber sorted mechanically according to the modulus of elasticity in bending and to the knottiness have been investigated and the standard strength was determined.

The comparison of mechanically sorted timber with visually sorted timber shows increased strength values being higher by 14 to 25 % (33 %) for mechanically sorted timber. The mean modulus of elasticity is by 4 to 12 % higher with mechanically sorted timber.

./..

Furthermore, investigations have been accomplished concerning the influence of the depth of girder and of the moisture of timber with girders of glued laminated timber being subjected to flexure (bending).

No influence on the flexural strength was determined with depths of girder up to 600 mm.

No decrease in flexural strength can be determined with a moisture of timber up to 18 %. The flexural strength decreases by 7 % within the range of the moisture of timber between 18 and 24 %.

Future research activities will be focussed on :-

1) The influence of the key-dovetail skew notch on the flexural strength of glued laminated timber.

2) The influence of the key-dovetail length on the tensile strength of layers of boards.

3) The possibilities of increasing the strength of glued laminated timber girders.

4) The determination of the material factor for glued laminated timber and structural timber.

At the same time, the realization of the research program as described in /1/ will be continued.

7. References (Bibliography)

/1/ Rug, W.; Badstube, M.
New Developments of Limit State Design for the New GDR
Timber Design Code; Academy of Building of the GDR,
Institute for Industrial Buildings, CIB-W18-Paper
19-102-4, Florence 1985

/2/ Badstube, M.; Rug, W.
"Forschungsarbeiten auf dem Gebiet der Bemessung nach
Grenzzuständen in Vorbereitung auf den neuen DDR-Standard
Holzbau" (Research Activities in the Field of Limit States
Design in Preparing the New GDR Timber Design Code)
Holztechnologie (Timber Technology), Leipzig 27 (1986),
pp. 281-336

/3/ Badstube, M.; Rug, W.
Erarbeitung von ingenieur-theoretischen Grundlagen für
den Standard "Holzbau; Tragwerke, Berechnung nach Grenz-
zuständen" (Preparation of Engineering-Theoretical Funda-
mentals for the Code "Timber Construction; Loadbearing
Members, Limit States Design"); Academy of Building of
the GDR, Institute for Industrial Buildings; Research
Report, Berlin 1986

/4/ Apitz, R.
"Ermittlung von Festigkeitswerten für Vollholz bei der
Beanspruchungsart Biegung durch Versuche" (Determination
of Strength Values for Solid Timber with the Bending Type
of Stress and Strain by Tests)
Wismar Engineering College, Research Report, 1982

/5/ "Testing Methods for Plywood in Structural Grades for
Use in Load-Bearing Structures"
Joint committee RILEM/CIB-3TT, Testing methods of timber
Mater. Constr., Paris 11 (1978) - pp. 445-452

/6/ Krabbe, E.
"Elastizitätszahlen von Fichtenholz in Abhängigkeit von
der Holzfeuchtigkeit" (Moduli of Elasticity for Spruce-
Wood Depending on the Moisture of Timber)
Bauen mit Holz (Construction by Using Timber), Karls-
ruhe 85 (1983), pp. 218-220

/7/ Apitz, R.
Beitrag zur Bestimmung der Festigkeitskennwerte von Bau-
holz bei Biegebeanspruchung für eine Bemessung nach der
Methode der Grenzzustände (Paper Concerning the Determi-
nation of the Strength Parameters of Structural Timber
Subjected to Bending Stress and Strain for a Design by
Adopting the Limit States Method)
Wismar Engineering College, Grade "A" Dissertation,
Wismar 1985

/8/ Apitz, R.
Vorschlag von Festigkeitsklassen für Nadelschnittholz
und Möglichkeiten der Sortierung (Proposed Strength
Grades for Sawn Coniferous Timber and Sorting Possibi-
lities)
Holztechnologie (Timber Technology), Leipzig 27 (1986) 6,
pp. 299-300

/9/ RGW-Norm ST-RGW 877-78 / DDR-Norm TGL 38 791/03:
Angewandte Statistik, Bestimmung der Schätzwerte und
Konfidenzgrenzen für Parameter der Weibullverteilung
(CMEA Code ST-RGW 877-78 / GDR Code TGL 38/791/03:
Applied Statistics, Determination of the Estimated
Values and Confidence Limits for Parameters of the
Weibull Distribution)

/10/ GDR Code TGL 117-0767, 1963, "Bauschnittholz, Güte-
bedingungen" (Sawn Structural Timber, Quality Conditions)

/11/ GDR Code TGL 25 106/03, 1979, "Prüfung von Holz, Bestim-
mung der Rohdichte und Raumdichtezahl" (Testing of Timber,
Determination of the Apparent Specific Gravity and Volume
Density Coefficient)

/12/ CIB-W18-Code: CIB-Structural Timber Design Code, 6th edi-
tion, January 1983, CIB-Report 1983, Publication 66,
Working Group W 18, Timber Structures

/13/ Larson, H.J.
Eurocode 5, Timber Structures
CIB-W18-Paper/18-1-2, Orn 1985

/14/ Vorschrift 174/85: Holzbau, Tragwerke; Berechnung; Bau-
liche Durchbildung (1. Änderung von TGL 33 135/01)
(Specification 174/85: Timber Construction, Loadbearing
Members; Calculation; Structural Design (1st Modification
to TGL 33 135/01)
Mitteilungsblatt der Staatlichen Bauaufsicht (Bulletin
of the State Building Supervision Authority), Berlin
9 (1985) 10/11, pp. 82-84

/15/ Swiss Code SIA 164: Holzbau (Timber Construction)
Schweizer Ingenieur- und Architekten-Verein (Swiss
Association of Engineers and Architects), Zurich 1981

/16/ GDR Code TGL 25 106/02, 1979: "Prüfung von Holz, Bestim-
mung des Feuchtesatzes bei physikalisch-mechanischen
Prüfungen" (Testing of Timber, Determination of the
Moisture Rate with Physico-Mechanical Tests)
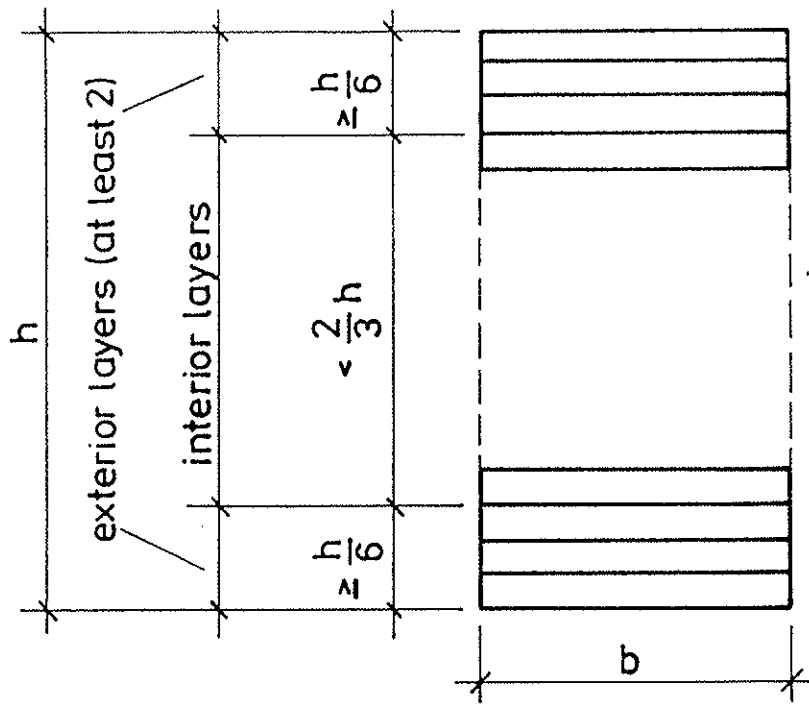
Figure 1: Design of glued laminated timber

Weibull density

density [y-axis]: 0,040, 0,036, 0,032, 0,028, 0,024, 0,020, 0,016, 0,012, 0,008, 0,004

x-axis: 20, 30, 40, 50, 60, 70, 80 R_m [N / mm^2]

$R_{m\,5\%} = 28,5$ N / mm^2

$R_{m\,5\%} = 33,9$ N / mm^2

$\bar{R}_m = 44,6$ N/mm^2, s = 10,3 N/mm^2, v = 23,1%, E$_m$ = 12 180 N/mm^2

$\bar{R}_m = 47,6$ N/mm^2, s= 9,37 N/mm^2, v= 19,7%, E$_m$ = 13 232 N/mm^2

92 samples

24 samples

——— visually sorted GLT 1
— — — mechanically sorted GLT 4
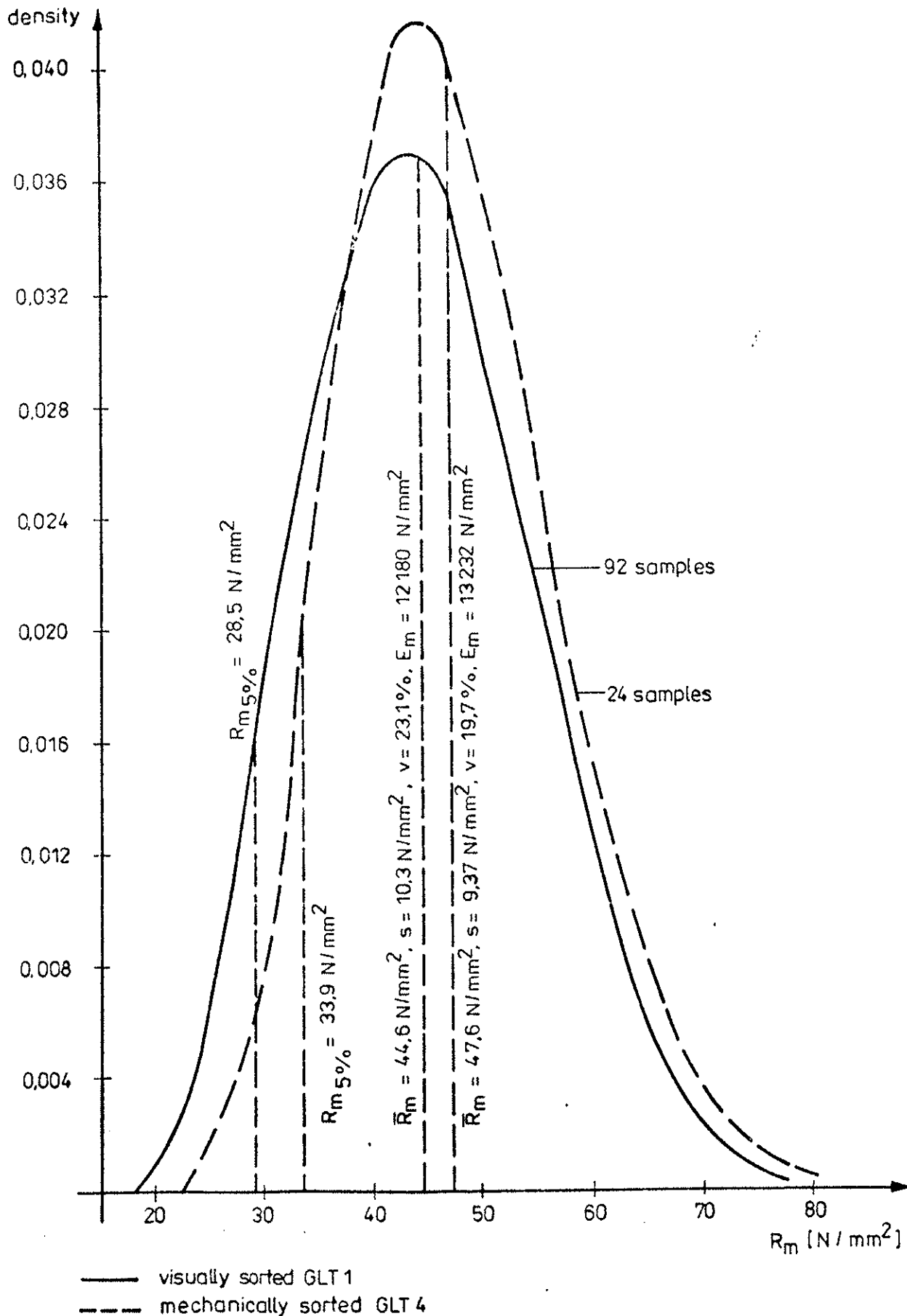
Figure 2 : Comparison of mechanically and visually sorted GLT;
bending failure strength.
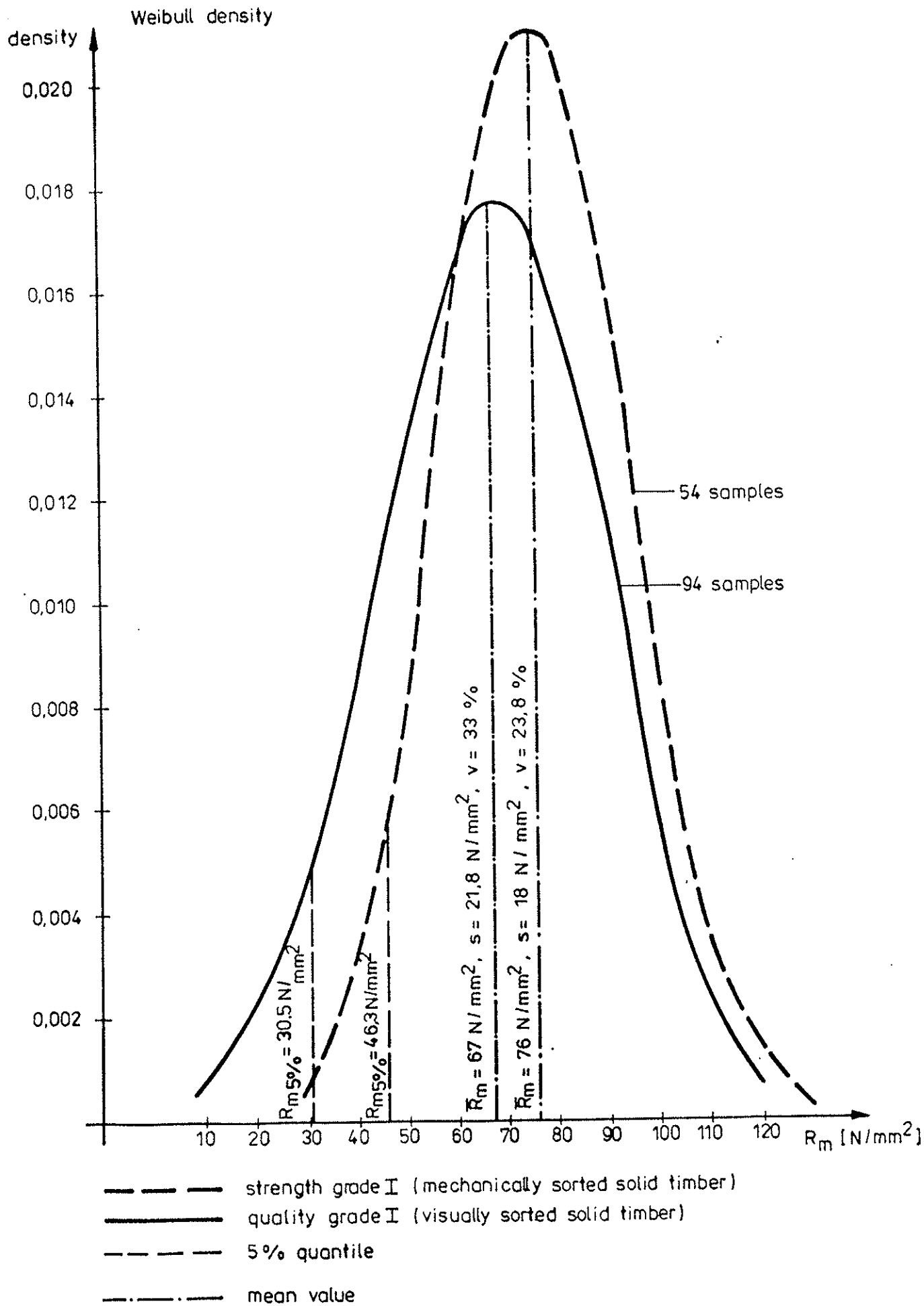
Figure 3 : Comparison of mechanically and visually sorted
structural timber of the strength grade I and/or
quality grade I (bending failure strength)

24,7	22,3	21,0	22,1	25,4	25,0
23,5	20,5	20,1	20,9	22,2	26,4
21,6	20,3	18,0	17,4	19,1	21,2
21,1	19,0	17,8	18,1	19,0	21,2
22,1	19,9	18,1	18,4	20,3	22,2
22,0	21,9	20,8	21,3	23,1	25,1

heart
ū ~18 %

layer 1
(tension)
ū = 22,4%

192

97
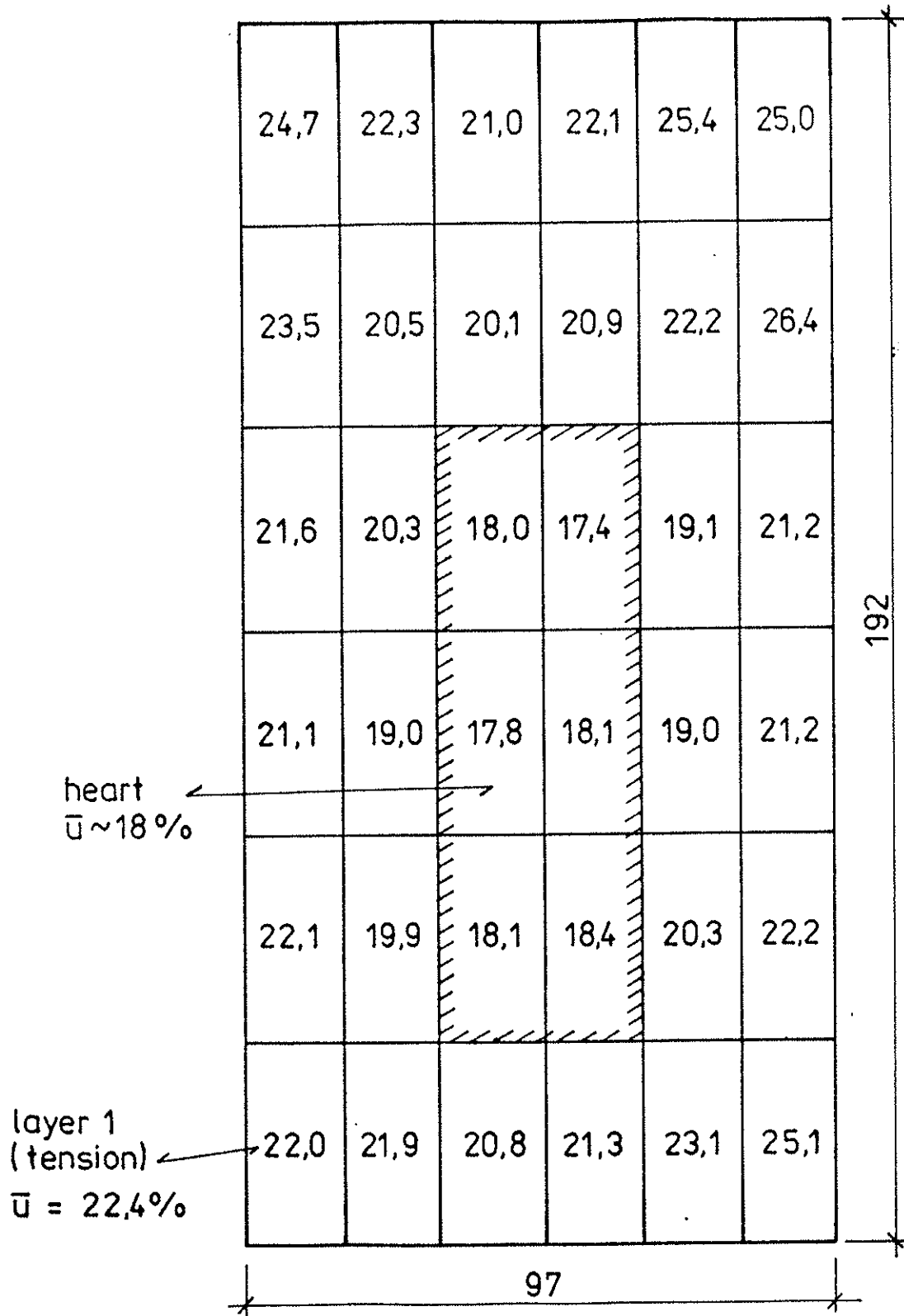
Figure 4 : Moisture distribution u (%) over the cross section
of GLT after 146 days of storage with a climate of
T = 20°C , ƒ = 95 %
(mean values from kiln- drying tests acc. to /   /
of 12 girders)
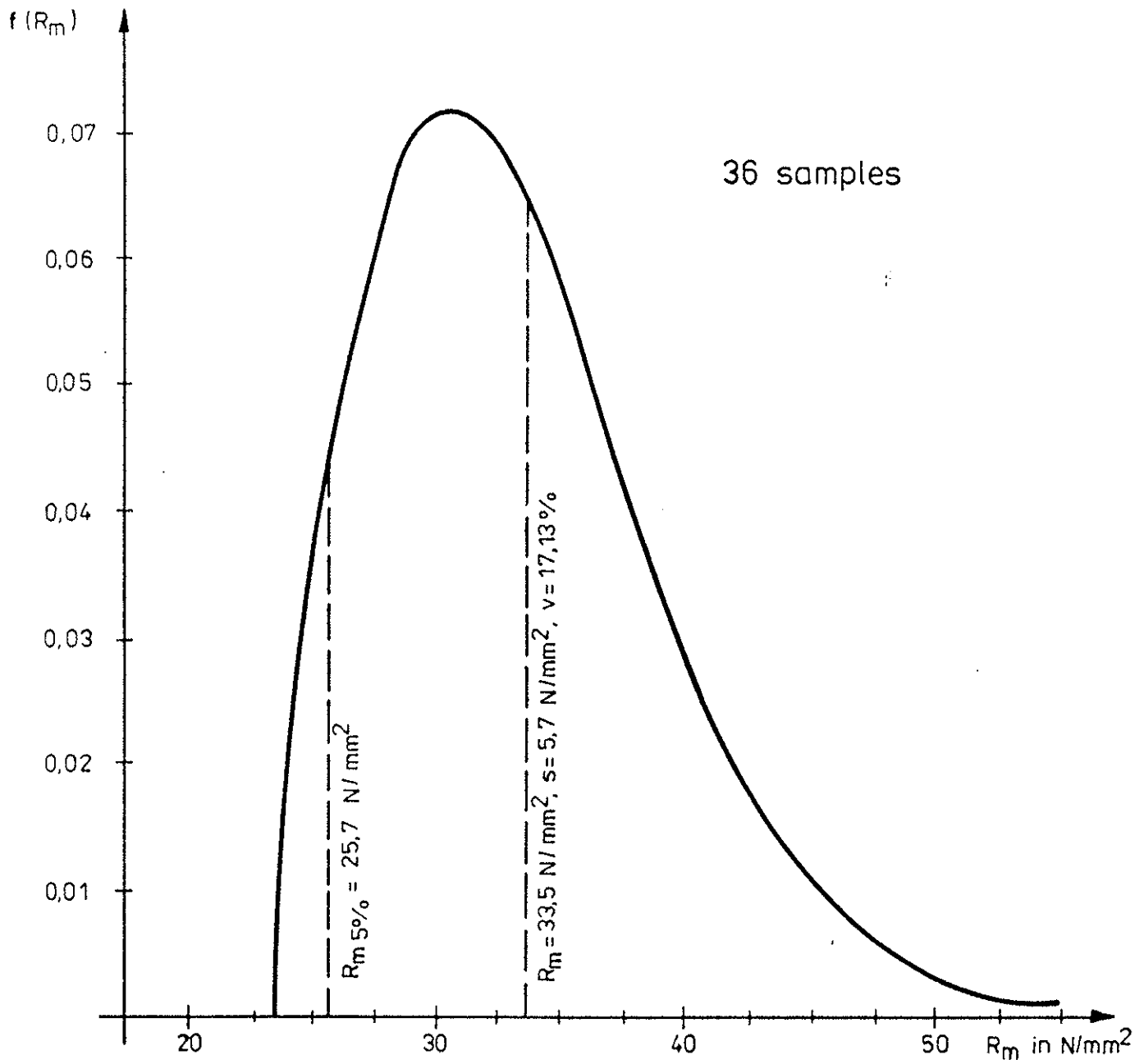
Figure 5 : Density function of the Weibull distribution of the
flexural strength of mechanically sorted glued
laminated timber (BSH 6) with h ≤ 288 mm,
u ≤ 18 %

GLT grade		GLT 1	GLT 2	GLT 3	GLT 4	GLT 5	GLT 6
sorting of layers		visually	visually	visually	mechani-cally	mechani-cally	mechani-cally
exterior layers	kind of timber	NSH GK II	NSH GK II	NSH GK	NSH F I	NSH F II	NSH F II
	KZV (mm)	≥ 250	≥ 250	≥ 0	≥ 250	≥ 250	≥ 250
interior layers	kind of timber	NSH GK II	NSH GK III	NSH GK II	NSH F III	NSH F II	NSH F III
	KZV (mm)	≥ 250	≥ 0	≥ 0	≥ 0	≥ 0	≥ 0

designations:

BSH	=	glued laminated timber (GLT)
NSH	=	sawn coniferous timber
KZV	=	key-dovetail skew notch
GK	=	quality grade acc. to /10/
F	=	strength grade acc. to /1/

Table 1 :   Design of the grades of glued laminated timber

Table 2 : Tests for determining the strength of mechanically sorted glued laminated timber

designations:

PB = test zone (TZ)
BSH = glued laminated timber (GLT)
F = strength grade
KZ = key-dovetailing (KD)
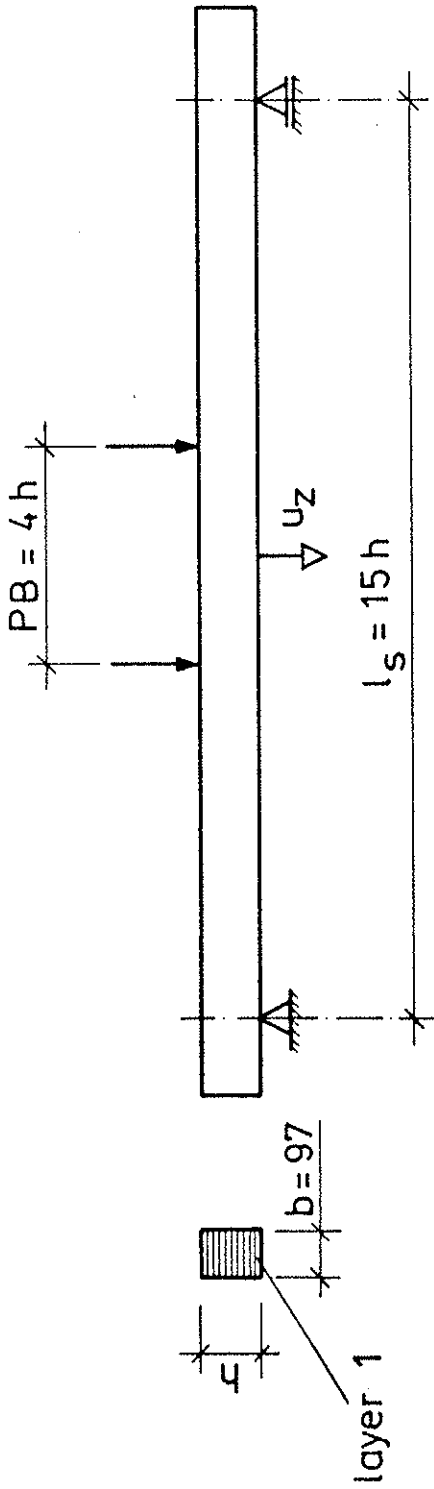
12 GLT girders for each test series

test series	GLT grade acc. to Table 1	l_s [mm]	h [mm]	u [%]	particularities	test aim
V1	BSH 4	2 880	192	≤15	KD in TZ, layer 1	standard values of strength
V2	BSH 4	2 880	192	≤ 15	no KD in TZ, layer 1	
V3	BSH 5	2 880	192	≤ 15	KD in TZ, layer 1	
V4	BSH 6	2 880	192	≤ 15	KD in TZ, layer 1	
V5	BSH 6	2 880	192	≤ 15	no KD in TZ, layer 1	

test series	GLT grade acc. to Table 1	$\bar{\rho}$ $\left(\frac{kg}{m^3}\right)$	$\bar{u}$ (%)	$\bar{R}_m$ $\left(\frac{N}{mm^2}\right)$	s_R $\left(\frac{N}{mm^2}\right)$	$v_R = \frac{s_R}{R_m}$ (%)	$R_{m,5\%}$ $\left(\frac{N}{mm^2}\right)$	$\bar{E}_m$ $\left(\frac{N}{mm^2}\right)$	s_E $\left(\frac{N}{mm^2}\right)$	$v_E = \frac{s_E}{E_m}$ (%)	$E_{m,5\%}$ $\left(\frac{N}{mm^2}\right)$
V1	4	502	10,8	40,6	4,0	9,8	36,1	12646	904	7,2	11155
V2	4	525	11,1	54,6	7,9	14,5	40,6	13818	1054	7,6	11879
V3	5	507	10,3	37,9	4,3	11,5	30,4	12395	767	6,2	11077
V4	6	504	11,2	33,3	5,3	15,8	25,5	10909	968	8,9	9568
V5	6	515	10,2	45,1	9,4	20,8	28,3	11876	1228	10,3	9915

designations:

ρ = density
u = moisture of timber

R_m = flexural strength
s = standard deviation
v = variation coefficient

E_m = modulus of elasticity in bending

Tabelle 3 : Results of the bending tests with mechanically sorted glued laminated timber (quantile values from Weibull distribution acc. to /9/)

Table 4 : Results of the bending tests with mechanically sorted structural timber (sawn coniferous timber)

kind of timber (spruce) (pine) (larch)	strength grade	number of samples	mean moisture u [%]	mean apparent specific gravity ϱ [%]	dimensions, mm	$\bar{R}_m$ [N/mm²]	s_R [N/mm²]	v_R [%]	$R_{m\,5\%}$ [N/mm²]	E_m [N/mm²]	s_E [N/mm²]	v_E [%]	$E_{m\,5\%}$ [N/mm²]
NSH*	I	54	9,82	0,569	30,69 x 90,34 x 1350	75,93	18,04	23,76	46,34	13958,4	1345,1	9,64	12373
NSH	II	155	9,32	0,49	30,6 x 90,53 x 1350	54,104	20,23	37,39	27,75	11630,63	1807,38	15,54	9195,4
NSH	III	100	9,37	0,468	30,5 x 90,4 x 1350	45,38	17,68	38,96	19,84	9871,33	2114,52	21,42	6720,04

* sawn coniferous timber

Table 5 : Standard values of the design strength and of the modulus of elasticity in bending for structural timber and glued laminated timber, in $\dfrac{N}{mm^2}$

(listed from our own tests for R_m^n and acc. to / I, /, /, / /, /, / /)

	softwood (spruce, pine, larch)												round timber	hardwood (stalk oak, sessile oak, red beech)
	sawn structural timber						glued laminated timber							
	quality grade			strength grade			grade							
	I	II	III	I[1]	II[1]	III[1]	1	2	3	4[2]	5[2]	6[2]		
flexure $\bar{E}_m$	12000	11000	10000	13500	11500	10000	12500	11500	11000	13500	12350	11500	12000	15000
E_m^n	8500	7800	7100	12000	9000	7000	9000	8000	7800	11500	11000	10000	8500	10750
R_m^n	28,5	24,0	21,5	38,0	28,5	24,0	28,5	24,0	21,5	38,0	30,0	26,0	26,5	43,0
tension $R_{t,0}^n$	18,0	14,5	13,5	24,0	18,0	14,5	18,0	14,5	13,5	24,0	20,0 -	17,0	14,5	27,0
$R_{t,90}^n$	0,5	0,45	0,4	0,6	0,5	0,45	0,5	0,45	0,4	0,6	0,5	0,4	0,4	0,7
compression $R_{c,0}^n$	26,0[3]	21,0	19,0	30,0	26,0	21,0	26,0	21,0	19,0	30,0	27,0	25,0	22,8	34,0
$R_{c,90}^n$	8,0[3]	7,5	7,0	11,0	8,0	7,5	8,0	7,5	7,0	11,0	8,0	7,5	7,0	12,0
shearing-off $R_{v,0}^n$	2,50[3]	2,25	2,0	2,3	2,5	2,25	2,5	2,25	2,0	2,8	2,75	2,5	2,5	5,0
shear from transverse force $R_{v,90}^n$	3,50[3]	3,00	2,5	3,8	3,5	3,0	3,5	3,0	2,5	3,8	3,4	3,5	3,25	6,5

1) mechanically sorted structural timber

2) mechanically sorted layers of boards

3) These values are adopted from the specifications of CIB-W18-Code, Jan. 1983 / / and / /.

designations:

PB = test zone (TZ)
BSH = glued laminated timber (GLT)
KZ = key dovetailing (KD)

$PB = 4h$

$l_s = 15 h$

U_z

$b = 97$
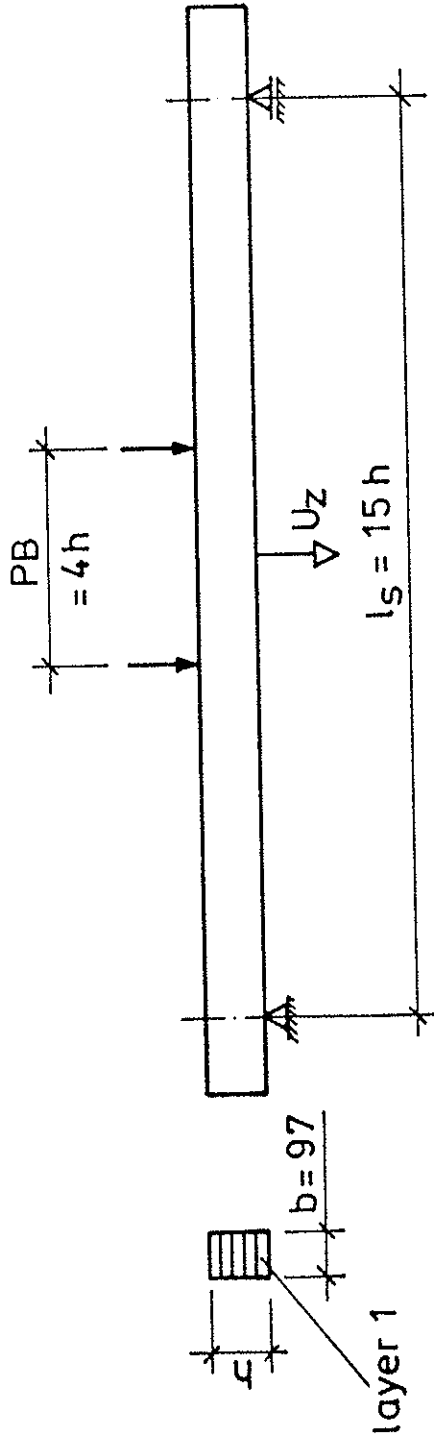
layer 1

test series	GLT grade acc. to Table 1	l_s [mm]	h [mm]	u [%]	particularities	test aim
V 4	BSH 6	2880	192	≤ 15	KD in TZ, layer 1	standard values of strength
V 5	BSH 6	2880	192	≤ 15	no KD in TZ, layer 1	
V 6	BSH 6	4320	288	≤ 15	KD in TZ, layer 1,2	adaption factor "cross-sectional height"
V 7	BSH 6	9120	608	≤ 15	KD in TZ, layer 1,2,3	
V 8	BSH 6	2880	192	18	KD in TZ, layer 1	adaption factor "moisture of timber"
V 9	BSH 6	2880	192	24	KD in TZ, layer 1	

Table 6 : Bending tests with mechanically sorted glued laminated timber

test series	GLT grade acc. to Table 1	$\overline{\rho}$ $\left(\frac{kg}{m^3}\right)$	$\overline{u}$ (%)	$\overline{R}_m$ $\left(\frac{N}{mm^2}\right)$	s_R $\left(\frac{N}{mm^2}\right)$	$v_R = \frac{s_R}{\overline{R}_m}$ (%)	$R_{m,5\%}$ $\left(\frac{N}{mm^2}\right)$	$\overline{E}_m$ $\left(\frac{N}{mm^2}\right)$	s_E $\left(\frac{N}{mm^2}\right)$	$v_E = \frac{s_E}{\overline{E}_m}$ (%)	$E_{m,5\%}$ $\left(\frac{N}{mm^2}\right)$
V4	6	504	11,2	33,3	5,3	15,8	25,5	10909	968	8,9	9583
V5	6	515	10,2	45,1	9,4	20,8	28,3	11876	1228	10,3	9915
V6	6	512	10,8	37,2	6,3	17,0	26,8	12273	1340	10,9	10069
V7	6	507	9,9	35,8	5,9	16,4	26,0	12799	641	5,0	11760
V8	6	532	17,9*	29,9	2,7	9,0	26,2	10183	925	9,1	8695
V9	6	540	22,4*	28,2	2,6	9,2	23,6	9869	1060	10,7	8488
V4+V6+V8		516	13,3	33,5	5,7	17,1	25,7	11121	1378	12,4	9138

designations:

ρ = density
u = moisture of timber
R_m = flexural strength
s = standard derivation
v = variation coefficient
E_m = modulus of elasticity in bending

* in the tension boundary position

Table 7: Results of the bending tests with mechanically sorted glued laminated timber (quantile values from Weibull distribution acc. to /9/)

Table 8 : PROPOSAL FOR MOISTURE GRADES AND ALLOCATED CLIMATIC CONDITIONS

Moisture grade		Classification of the category of buildings/structures (=b/s) and climatic conditions	Moisture of timber	Relative air humidity at 20°C	Remarks	k_e
1	1.1	– enclosed b/s with heating (properly ventilated; no rooms with moisture sources) – enclosed b/s slightly heated (properly ventilated; no rooms with moisture sources)	$u \le 12\%$	$\varphi \le 65\%$		1.0
	1.2	– enclosed b/s without heating (properly ventilated; with rooms having weak moisture sources) 1) – compound units made of glued laminated timber and square-sawn timber being subjected to service conditions acc. to moisture grade 2, but being provided with a hydrophobic (water-repellent) coat	$12 \le u \le 18\%$	$65 \le \varphi \le 85\%$	1) grain storages; factory halls and assembly bays of the metal-working industries	
2	2.1	– enclosed b/s with rooms having moisture sources 2) – free-standing b/s made of medium to large-size timber sections such as square-sawn timber and glued laminated timber compound units – compound units made of boards and laths/battens being subjected to service conditions acc. to moisture grade 1.2 – roofed-over b/s being open on all sides with unprotected compound units	$10 \le u \le 26\%$	$\varphi > 85\%$	2) e.g. baths, swimming-pool halls, weaving mills, foodstuffs factories, industrial and water-supply humidity rooms; buildings with wet rooms, such as tanneries, laundries etc. In case of doubt, the classification will be accomplished acc. to the magnitude of permanently acting air humidity, by coordination with the state building supervision authority concerned	0.93

Table 8 (continued): PROPOSAL FOR MOISTURE GRADES AND ALLOCATED CLIMATIC CONDITIONS

Moisture grade		Classification of the category of build-ings/structures (=b/s) and climatic conditions	Moisture of timber	Relative air humidity at 20°C	Remarks	k_e
2	2.1			$\rho > 85\%$		0.93
	2.2	– small-sized components of free-standing b/s such as laths/battens, boards, planks – compound units made of glued laminated timber and square-sawn timber being sub-jected to service conditions acc. to moisture grade 12, but serving for the roofing-over of fertilizer halls, in particu-lar for urea – building/structures with wet rooms having a permanent air humidity of 95%				
3		– compound units in water	>30			0.8